VRIJE UNIVERSITEIT BRUSSEL
FACULTEIT VAN DE WETENSCHAPPEN

DEPARTMENT OF GEOLOGY

THE QUATERNARY STRATIGRAPHY AND ENVIRONMENTS OF OLDUVAI GORGE – TANZANIA, BASED ON FOSSIL SOILS AND RELATED DATING

By

Dalaly Peter KAFUMU

Thesis submitted in fulfillment for the requirements for the Degree of Doctor of Philosophy

Promotor: **Prof. Dr Roland Paepe**

BRUSSELS, MARCH 2000

Dedication

This work is dedicated to my loving mother **Misozi Kulebelwa** and my elder brother **George Manyanda** for their contribution to prepare me as a child to attain this highest academic achievement.

This work is also dedicated to my family, my wife **Mchikirwa**, my 2 daughters, **Misozi** and **Mwanahawa** and my 2 sons, **Kafumu** and **Idofe** for their constant prayers and support to finish this work.

Faculteit van de Wetenschappen
Vrije Universiteit Brussel
Pleinlaan 2, B – 1050 Brussel
☎ 02/6293357
℔ 02/6293389
email : rdespieg@vub.ac.be

Brussel, 14 maart 2000.

Onze Referentie: WE/Y/2000/077/RDS

Aan Prof. Prof. E. Keppens
CHRO

Geachte professor,

Hierbij deel ik u mee dat het FB in zijn vergadering van 13 maart 2000 de examencommissie voor het doctoraat van de heer Peter D. Kafumu als volgt heeft samengesteld:

Prof. E. Keppens, voorzitter
Prof. P. Pasteels, secretaris
Prof. em. R. Paepe, promotor
Prof. C. Susanne
Prof. J. Hus
Prof. em. D. Roggen
Dr. E. Van Overloop
Dr. A. Boven
Prof. G. Stoops, UG
Prof. J. Thorez, ULg

Mag ik u verzoeken mij zodra mogelijk de datum van de besloten verdediging mee te delen ?

Met oprechte hoogachting,

Prof. Dr. J. Lemonne,
Decaan Faculteit Wetenschappen.

CC. Leden van de examencommissie
Prof. D. Tourwe, CDO
Promovendus

FACULTEIT VAN DE WETENSCHAPPEN

PROMOTIE

de heer Peter Dalaly KAFUMU

verdedigt op

VRIJDAG 12 MEI 2000 OM 14U30

een oorspronkelijk proefschrift en een stelling ter verkrijging van de academische graad van

DOCTOR IN DE WETENSCHAPPEN

in het Auditorium 4G110
Gebouw G - 4e verdieping
Campus Oefenplein

TITEL VAN HET PROEFSCHRIFT

The Quaternary Stratigraphy and Environments of Olduvai Gorge - Tanzania, based on fossil soils and related dating

STELLING

The presence of ruby in marble host rocks can not be considered as a sufficient criterion for prospection

Brussel, 4 mei 2000.

Professor Jacques LEMONNE,
Decaan van de Faculteit van de Wetenschappen

Examencommissie

Prof. Dr E. Keppens (VUB) – Chairman
Prof. Dr P. Pasteels (VUB) – Secretary
Prof. Dr R. Paepe (VUB) – Promotor
Prof. Dr J. Hus (VUB) – Member
Prof. Dr N. Roggen (VUB) – Member
Dr A. Boven (VUB) – Member
Dr E. Van Overloop (VUB) – Member
Prof. Dr C. Suzanne (VUB) – Member
Prof. Dr J. Thorez (UL) – Member
Prof. Dr G. Stoops (RUG) – Member

ACKNOWLEDGEMENTS

Though it is not possible to mention all people who I am deeply indebted for their guidance and help they gave during the research, but the few named here will represent them all.

First I am grateful to acknowledge to my Promotor Prof. Dr Roland Paepe for his keen guidance he gave to me throughout this study. His guidance and instructions in the field in Tanzania was indispensable for the completion of this study. He was willing to teach and instruct me all aspects of theoretical and practical Quaternary environmental geology. This will remain a greater treasure to me. I am also thankful to him for sponsoring most of the field work campaigns performed in Tanzania. He spent with me in the field and at home many hours with great humility and patience discussing or correcting the text. He was always ready to sacrifice his valuable time to guide this academic work. *"Thank you Prof. Dr R. Paepe"*.

I am grateful to the Government of Belgium through the Belgian Administartion for International Development and Cooperation, A.B.O.S (B.A.D.C) for offering me a scholarship to undertake this study. The scholarship covered my stay in Belgium and some funds were directed to cover the field works in Tanzania. Special thanks should go to Mrs. Sabine Meyssen, Mr. Ben Schutz and Mrs. Marianne Degrugillier of A.B.O.S. who were responsible for my good and healthy stay in Belgium. They took care of my family and me with tender and generosity, always with a smile. I am also indebted to the Leviers s.a. Company of Belgium for providing me with additional funds to undertake fieldwork in Tanzania.

I must thank Dr E. Van Overloop the Director of IFAQ in which context this research began in 1994. Her financial and moral support in Brussels and in the field (in Tanzania) will not be forgotten. I must thank her for providing me the Infra Red Spectrometry (PIMA) instrument and software for the mineralogical analysis. I will specifically remember the good 1997 field supervision and support in Tanzania, together with Prof. Dr R. Paepe, which helped me very much to complete my fieldwork. Agatha and Emma should also be thanked for their inspiration to me during this same fieldwork. I am also grateful to Mr. H. Goossen of the Geological Survey of Belgium who helped me in the Short Wave InfraRed (SWIR) spectrometry mineral analysis.

I am thankful to Prof. Dr J. Hus for his supervision and guidance on some part of the laboratory work of this study. His review and correction of the text enabled this work to be completed.

I am grateful to Prof. Dr G. Stoops of the University of Gent for supervising and instructing the laboratory work done in his laboratory. His guidance enabled me to complete a large part of the laboratory work of this study. His close and critical review of this work and especially the generous help to read and correct the text is highly appreciated. This precious help made possible this study to be completed.

Thank you to Prof. Dr P. Pasteels of Geochronology laboratory (VUB) and Prof. Dr Vereecken of the Metallurgical engineering laboratory (VUB) for allowing me to use their laboratories to perform some stereo and scanning electron microscopic mineral examinations respectively. Dr A. Boven and Dra N. Punzulan are specifically thanked for their close supervisions during the laboratory works I conducted in the Geochronology laboratory.

I am indebted to Prof. Dr J. Klerkx of the Royal Museum for Central Africa for allowing me to undertake some ASS analysis in his Laboratory under the supervision of Dr Luc Andre of the Geochemical and Mineraology Laboratory. Dr M. Kaseba of IFAQ computer laboratory is also thanked for introducing me to the Intergraph and Corel draw computer software that helped me to complete most of the sections and map drawings of this study.

Many thanks are extended to my employer the Permanent Secretary of the Ministry of Energy and Minerals. Whom through the Commissioner for Mineral Resources Mr. G. Mwakalukwa, the Assistant Commisioner for Geology Mr. P. M. Kenyunko and the Assistant Commissioner for Mines Mr. S. Mohamed gave me transport facilities throughout the fieldwork in Tanzania. I must acknowledge Mr. C. Mng'ong'o, Mr. Nassoro and Mr. Woria motor drivers from the Ministry of Energy and Minerals for their professional and safe driving in the rough field terrain of Tanzania. The Tanzania Commission for Science and Technology and the Antiquities Unit of Tanzania are thanked for offering me the necessary permits to be able to work in Olduvai Gorge, Manonga-Wembere Valley and Holili localities in Tanzania. Thank you to the Antiquities Staff in Olduvai Gorge specifically Mr O. Kileo and Mr. G. Olle-Moita who provided a nice field guidance and living environment in Olduvai Gorge.

Deep appreciation is extended to the ambassador of the United Republic of Tanzania in Belgium H.E. Mr. Ali Karume and the entire office of the Embassy in Brussels. His personal efforts and that of his office helped us to live a better life in Belgium. I must also acknowledge the S. Jenga, C. Tungaraza and F. Mwanuzi families, Mr. D. Mwanauta, Mr. E. Massawe, Mr. S. Ulomi, Mr. Y. Kajia, Ms. J. Mawalla, Ms. F. Mneney and Dr M. Abbu Tanzanian who live or lived in Belgium.

They created a conducive Tanzanian environment in a foreign land. Their willingness to come together and share some time as Tanzanians was instrumental to a successful completion of this study.

I am deeply indebted to Mr. Jack Van Basil, secretary to the King of Belgium who helped my family with all immigration arrangements to be able to come to Belgium to join me. Gratitude is extended to Rev. Fr R. Rahouns, Mr. M. Kabue and all residents of the Saint Rafael House for their brotherly community life. I will always remember their prayers and Christian community love which maintained our (my family) spiritual life with renewed commitment to our Lord Jesus Christ. Such graces made our stay and indeed this study a success. I am deeply grateful to Mr. F. N. Petro, Mr. D. Singo and Sister O. Jory who took care of our family matters in Tanzania. Thank you very much.

My final but not least acknowledgement goes to my family that is, my wife Maria Magdalena Mchikirwa, my daughter Illuminata Mwanahawa and my sons Benedicto Kafumu and Berenardo Idofe who endured the pain of leaving their land to come to live with me in Belgium. It is very hard to live in Belgium but they did it for me, I thank them a million for that. I am grateful to my daughters Immakulata Misozi, Ritta Ledaiwe and Lucia Kang'hwa who have to remain in Tanzania enduring the pain of family separation for three years with great love. Indeed my whole family has to undergo such a crisis so that I can complete this study. I deeply thank them all.

Kafumu P. D.
Brussels, 1st March 2000.

The Lord is my shepherd;... Even though I walk through the valley of the shadow of death I will fear no evil.
(Psalm 23:1,4)

ABSTRACT

This study reports research results and interpretations based on field geological-stratigraphical-litological-palaeosol sequential studies of Tertiary-Quaternary deposits of **Olduvai Gorge** (main work), **Manonga-Wembere Valley** and **Holili,** (annex work) localities in Tanzania. It is also based on laboratory studies (micromorphology, mineralogy, geochemistry and magnetic susceptibility). Special emphasis is placed on the study of palaeosol levels frequently found in these sedimentary sequences.

Geology and stratigraphy

In all the three areas, Pliocene-Pleistocene sediments are laid down unconformable on a Precambrian basement complex. A huge unconformity exists between the Precambrian rocks (granite, quartzite and gneiss) and the Pliocene-Pleistocene sediments. The basement is a remnant planation surface, which was formed at the beginning of the Tertiary, often represented by isolated granite kopjes, quartzite and gneiss inselbergs and hills sticking out from the present plain level.

In **Olduvai Gorge** the study revisits the stratigraphy and reveals numerous sediments and palaeosol levels (not earlier reported). These levels and beds are within the earlier recognized general Bed I, II, III, IV, Masek and Ndutu Beds. Bed I (2.2Ma – 1.75Ma) contains at least 43 lithological (clay, sands, gravel, mudstone, limestone and marls) units including palaeosol levels. Bed II (1.75Ma – 1.15Ma) is also a zone of abundant geological depositional environments composed of clay, sand-gravel bed complexes, tuff (ash fall or ash flow), limestone and palaeosol levels. Bed III (1.15Ma – 0.6Ma) is a complex volcano-sedimentary depositional environment marked by lacustrine marly sequences, clay layers, sand-gravel beds and calcarenaceous sediments itercalated by red-brown palaeosol levels. Bed IV and Masek Beds (0.6Ma – 0.4Ma) are not distinguishable in the field and therefore grouped together and names adapted from previous workers. The zone contains about 4 palaeo-Vertisols each developed on a clay layer. Ndutu Bed (0.2Ma and younger) is represented by a series of 7 palaeo-Vertisol levels (similar to the ones in Masek Beds), mudstone, claystone and limestone from bottom to top.

Gravel and sand beds across the profile have the highest magnetic susceptibility (MS) values compared to clay, marls, calc-sediments or tuff lithologies. Magnetic susceptibility values of palaeosol levels in sandy units are usually lower than the background values of the sand layers. Palaeosols that developed on clay units have higher MS record than the clay background values.

The general MS pattern shows an increasing trend across the stratigraphy from older to younger units. The mineralogical signatures also reflect the general stratigraphical characterization. The lower (Bed I and Lower Bed II) stratigraphical unit show higher clay minerals and carbonate concentrations, the middle (Bed II and Bed III) indicate slightly low clay minerals and carbonates abundance and the upper parts of the profile (Masek/Bed IV) show higher concentrations of clay and carbonate minerals.

Based on field and some micromorphological studies 57 palaeosol levels are mapped. They are grouped into (a) Red-brown to dark gray palaeosols which are probably palaeo-Alfisols or Ultisols, occur in Upper Bed I, Middle Bed II and Bed III. (b) Olive to gray palaeo-vertisols (Bed I, Masek and Ndutu Beds). (c) Palaeo-Andisols found in Bed I and Bed II are observed to develop on ash fall/flow tuffs and (d) Palaeo-Aridisols are gray to olive palaeosol levels, seem to have developed on sand levels mainly in upper Bed II. Red to brown palaeosols (Alfisols/Ultisols?) are slightly richer in FeO-Fe_2O_3 and MnO values than other palaeosol levels. Total soil silica/sesquioxide mole ratios of both palaeo-Alfisols and palaeo-Vertisol resemble modern Alfisols and Vertisols.

Micromorphological studies indicate that gray-olive palaeosols (Vertisols, Aridisols and Andisols) contain numerous calcite nodules, calcite coatings/hypocoatings and infillings with rare Fe-Mn hydr(o)xide coatings and nodules. Clay coatings are rare or absent. They commonly show a granostriated or monostriated b-fabric and porphyric c/f related distribution of the basic components. The red-brown and dark gray palaeo-Alfisols contain multiple micromorphological features (red-yellow clay coatings and clay coating fragments, Fe-Mn oxide nodule and coatings with some calcite coatings and in-fillings) that are usually seen, imprinted on one another. Palaeo-Aridsols are regarded to be formed in semi-arid palaeoclimates, while palaeo-Vertisols were formed in alternating wet and dry conditions of the Pleistocene Epoch. The red to brown palaeo-Alfisols are assumed to have developed during wet/humid palaeoclimates in Olduvai Gorge during the Pleistocene.

The **Manonga-Wembere Valley** geology comprises of Pliocene-Pleistocene lacustrine gravel, sands and calcareous-clay deposits and Holocene mbuga clays and alluvial sand. The micromorphology of palaeosol levels from Manonga-Wembere Valley show strong clay illuviation of red to yellow clay coating and clay coating fragments with Fe-Mn (hydr)oxide coatings. The clay coating fragments occur as accumulation of oriented clay-coating fragments in a red to yellow groundmass resembling clay illuviation fronts found in present day warm and humid (Meditterranean) climates.

Manonga-Wembere Valley palaeosol levels are therefore assumed to represent a wet and humid climate and environment during the Pliocene-Pleistocene times. Kaolinite and illite clay minerals together with gibbsite and some zeolites (analcime and stilbite) dominate the mineralogy of these palaeosol levels.

The geology and stratigraphy of **Holili** begins with the Precambrian basement rocks and then covered by lava flows (basalt) of the Kilimanjaro volcanic episode. Then a soil (palaeosol) developed on the basalt. The landscape (palaesol) was finally covered in succession by tuffaceous mudstone and calcareous tuffaceous grit. A hominid tool, fossil leaf impressions of *angiosperm dicotyledon* flowering plants and animal remains (tooth, horn and canon bone) were recovered in Holili Pleistocene deposits.

Palaeoclimatic and palaeoenvironmental variability

The palaeoclimatic and palaeoenvironmental variability in **Olduvai Gorge, Manonga-Wembere** and **Holili** localities as deduced from facies, magnetic susceptibility, mineralogy, geochemistry, micromorphology and palaeosol occurrences and cyclicities seem to be linked to the global causes of climatic changes. 400ka Gravel beds cyclicity (at about 2.2Ma, 1.76Ma, 1.4Ma, 1.00Ma 0.65Ma and 0.2Ma), 40Ka and 10Ka palaeosol cyclicity are observed in Olduvai Gorge. The climatic variability of Olduvai Gorge during the Quaternary is found to correlate with that of Greece (Mediterannean). This is evidence that the climate of Olduvai Gorge during the Quaternary also followed global trends. In Olduvai Gorge hominids and other animal fossil remains are frequently found on palaeosols levels or closely associated to palaeosol levels. Long periods of 400Ka marked by gravel bed complexes are generally wet periods. Gravel bed complexes that mark significant short periods of drought in this study are correlated to FAD and LAD of *Australopithecus boisei, Homo habilis* and *Homo erectus* hominid species in Olduvai Gorge. Likewise in Manonga-Wembere Valley and Holili deposits animal fossil remains occurrences are associated to palaeosol levels.

Future research

For future research a complete micromorphological study of all possible palaeosol levels will be helpful in discerning more the climatic variability. Future hominid search would be more successful if palaeosol levels were mapped and followed over long distances. New Ar-Ar dating of the basalt and tuff in Manonga-Wembere Valley and Holili areas would provide better age estimates of the deposits.

Samenvatting

Deze studie beoogt een palaeoclimatologische interpretatie van de opeenvolging van palaeobodems in Tertiaire-Quartaire afzettingen van de Olduvai Gorge, Tanzanië, binnen het kader van een verfijnde stratigrafische analyse van deze klassieke Hominid Site. Manonga-Wembere Valley en Holili localiteiten werden eveneens onderzocht in dat algemeen verband. In de drie gebieden liggen sedimenten van het Plioceen-Pleistoceen discordant op het Precambrisch basiscomplex.

Olduvai Gorge afzettingen beslaan de laaste 2.2Ma, en op basis van vroegere stratigrafische-geochronologische studies, kunnen als volgt opgesplitst worden: Bed I (2.2Ma – 1.75Ma), Bed II (1.75Ma – 1.15Ma), Bed III (1.15Ma – 0.6Ma), Bed IV en Masek (0.6Ma – 0.4Ma) welke, op basis van onze studie, niet van elkaar te onderscheiden vallen en moeten bijeengebracht worden tot één enkele stratigrafische eenheid. Aan top komt het Ndutu Bed voor (0.2Ma – 0Ma), met dus een hiaat tussen 0.4Ma en 0.2Ma.

Behalve gedetailleerde veldwaarnemingen, steunt onze interpretatie op mikro-morfologische, mineralogische, geochemische en magnetische analysen.

Een totaal van 57 paleobodems werd geïdentificeerd en ze werden in de stratigrafische sekwentie geplaatst: (a) "Red-brown to dark gray palaeosols" vermoedelijk palaeo-Alfisols of palaeo-Ultisols, (b) "Olive to gray palaeo-Vertisols", (c) "Palaeo-Andisols" and (d) "Palaeo-Aridisols. Type (a) bodems komen in Upper Bed I voor, alsook in Middle Bed II en Bed III, (b) in Bed I, Masek en Ndutu Beds, (c) in Bed I en Bed II, maar enkel boven vulkanishe lagen, terwijl type (d) aan top van zandige lagen ontwikkeld werd vooral in Upper Bed II.

Deze waarnemingen geven aanleiding tot volgende interpretatie: type (a) bodems worden aan vochtig klimatische voorwaarden, (b) aan alternerende droge en vochtige toestanden, (c) aan een bepaalde lithologie gebonden; (d) zou op een semi-aried paleoklimaat wijzen. Een algemene interpretatie kan gegeven worden in het raam van de astronomische factoren, aan de oorzaak van een cyclische evolutie van het klimaat. De 400ka cyclus komt goed tot uiting (~2.2Ma, 1.76Ma, 1.4Ma, 1.00Ma, 0.65Ma en 0.2Ma). Dit wordt verder bevestigd door de korrelatie met het Middellandse-Zee gebied. Palaeobodem interpretatie is ook belangrijk, i.v.m. het feit dat fossielen van Hominiden en andere vertebraten hieraan gebonden zijn.

TABLE OF CONTENTS

CHAPTER ELEVEN

CHAPTER ONE

INTRODUCTION

1 INTRODUCTION

1.0 GENERAL INTRODUCTION

Quaternary continental and marine deposits of volcanic and sedimentary origins extensively cover Tanzania. The deposits occur in many-isolated place all over the Country. In the review of literature a comprehensive descriptive revision of the Quaternary deposits of Tanzania (chapter 4) is presented.

This study presents the Quaternary geology and attempts to reconstruct the Quaternary environments and climates of three selected Quaternary localities in Tanzania, namely, Olduvai Gorge (Serengeti plains) & Holili (Mount Kilimanjaro volcanic fields) both located in NE Tanzania and Manonga-Wembere valley in Central Tanzania, (figure 1.1). The palaeoclimatic-palaeoenviromental study of the Quaternary deposits is based on the geology, stratigraphy and palaeosol occurrences in the sedimentary lithosequences. Olduvai Gorge is the main area of study, while Manonga-Wembere Valley and Holili localities are treated as minor (annex) study areas.

Palaeosol levels and positions are strong indicators of climatic and environmental fluctuations and cyclicities of the past (Paepe & Ilunga 1990, Paepe & Van Overloop 1994). They are stable palaeolandscapes with stable stratigraphical positions, which provide sufficient information for reconstructing Quaternary palaeoclimates (Mahaney 1980, Paepe & Van Overloop 1990, and Allen & Wright 1989). In brief, sedimentary sections with palaeosols are good study areas of the past climate and environments.

Palaeosol are more true record of the regional climate than pollen sequences, which seem to show considerable variation over a short time range in the stratigraphy. The study of palaeosols is thus not only one of the best means to reconstruct past environmental conditions but also needed for the prediction of the resistance to change and response time of various soil features when subject to environmental change, (Arnold, et. al, 1990).

Substantial geological, palaeontological, palaeonthropological, archaeological, palynological and geochemical work (for the palaeoclimatic and palaeoenvironmental reconstruction) has been carried out at Olduvai Gorge, (Hay, 1976, Hay *et al.,* 1977, Hay & Leeder, 1978, Bonnefille & Riollet 1980, Bonnefille 1984, Cerling & Hay, 1986, Manega 1993, to mention only a few). Nevertheless, a clearer picture of Pliocene-Pleistocene–Holocene Climatic and environmental record is still regarded as ambiguous (Manega 1993) and awaits further detailed study.

Occurrences of palaeosols in Olduvai Gorge were long recognised four decades ago. Hay (1967) refers palaeosol levels as hominid occupation levels or living floors. In his stratigraphical study of the area he recognised some of these levels as land laid trachyte tuffs and tuffaceous clays extensively penetrated by root channels. This observation suggested the presence of vegetation on a developed soil at that geological time. Caliche layers and rosettes of gypsum crystals were also recognised as palaeoclimatic features indicating a dry climate during the Pleistocene.

A limited number of stable isotopic studies of pedogenic carbonate concretions, nodules and calcretes were carried out in Olduvai Gorge, (Cerling *et al.,* 1977, Hay & Leeder 1978, and Cerling & Hay 1986) in an attempt to establish a comprehensive palaeoclimatic stratigraphy reliable for a regional and global correlation. These studies fell short of a precise positioning of the palaeosol in the stratigraphy. The first attempt to study the palaeosol *sensu stricto* of the Olduvai Gorge was made by the author, where 38 individual palaeosol levels were mapped (Kafumu 1995) based on field observations and descriptions.

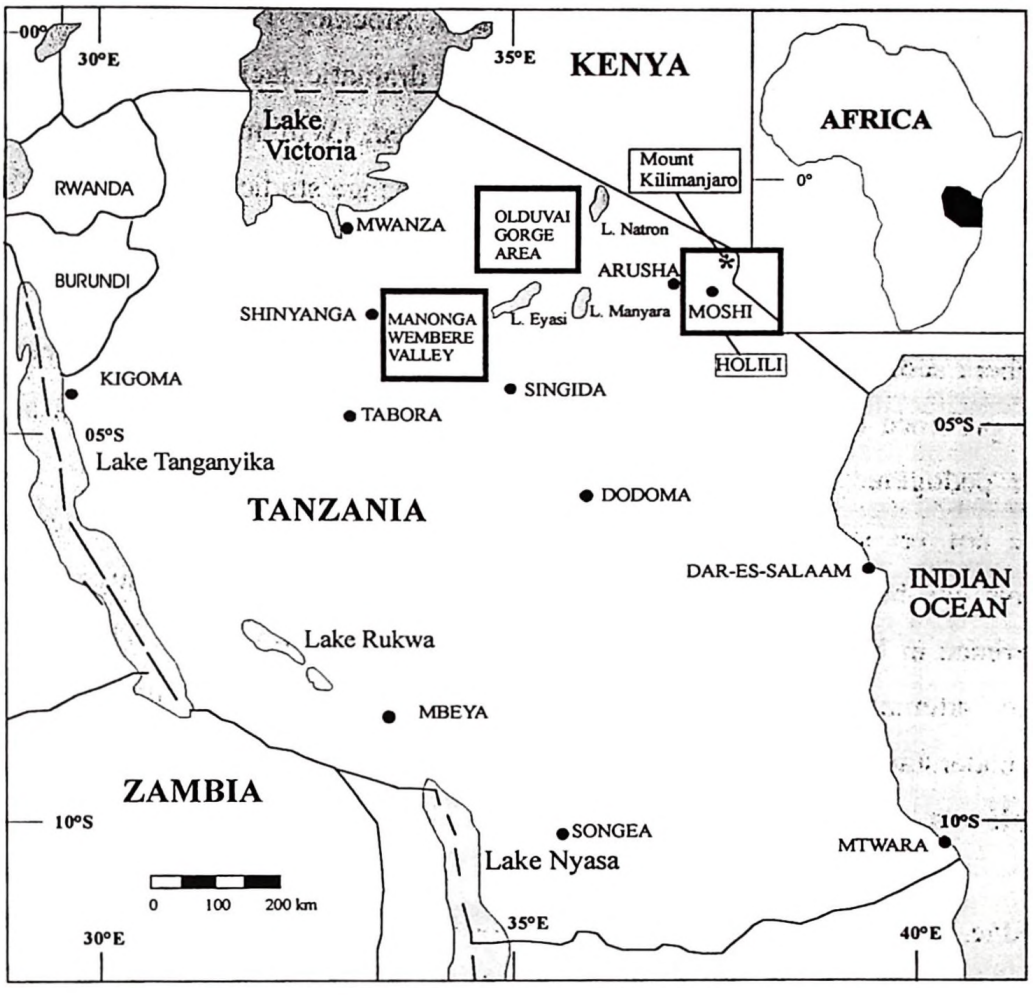

Figure 1.1: Location map of the study area [Olduvai Gorge, Manonga-Wembere and Holili localities indicated by squares].

However, laboratory studies had not yet been undertaken to ascertain the stratigraphical positions and their implications to the Quaternary climates and environments of East Africa. This research is therefore a more detailed follow up of a preliminary field study of the palaeosols in the area conducted by the author for a M.Sc. degree at the Free University of Brussels.

In Manonga-Wembere basin, evidence of Pliocene–Pleistocene–Holocene Climatic and environmental changes were long identified based on palaeontological and geological studies. For instance, there is evidence of Palaeolake shoreline regressions and

transgressions indicated by great extensions and reductions of fresh water conditions, (Stockley 1930, Grace & Stockley 1931, Wayland 1934, Stockley 1947, Barth 1989). Sedimentation regime changes indicated by presence of dramatic facies changes from fine sediments to sands over long distances are also reported, (William & Eades 1938, Grantham *et al.,* 1945, and Verniers 1997). Finally, faunal change studies (Handley 1956, Stewart 1997, Van Damme & Gautier1997) indicate climatic variations.

Manonga–Wembere sediment are Lake beds with clear evidence of pedogenesis, which is, indicated by presence of extensive clayey red beds (this study). The red beds are associated with pedogenic calcareous concretions and nodules. The aspects of the pedogenesis are not yet studied in detail. Mineralogical studies indicated weathering products minerals like brown paragonite and brown montimorillonitic clays, suggesting palaeosol occurrence in Manonga–Wembere sediments (Mutakyahwa 1997). This study is a deliberate attempt to contribute to the Tertiary–Quaternary climatic and environmental understanding of the Manonga–Wembere deposits by studying some of these palaeosol levels.

To my knowledge, little studies have been conducted to indicate the palaeoclimatic and palaeoenvironmental changes of the Kilimanjaro basin deposits. However, Quaternary glacial climates have been studied on the snow (glacial) cover peak of the Kilimanjaro Mountain (Downie & Wilkinson 1972). Extensive volcanic rocks of several volcanic episodes emanating from several volcanic centers (Wilkinson *et al.,* 1986) represent Kilimanjaro volcanic field. Distinct red colored alluvial sandy clays with secondary calcareous limestone sediments frequently intercalates these deposits, (Sampson 1953, and Kanza 1985). The red coloured deposits are sometimes recognised to be of pedogenic origin, (Downie & Wilkinson 1972). Again this study sets out to point out some of the palaeoclimatic and palaeoenvironmental elements in these sediments. In this way their implications to the Pliocene-Pleistocene-Holocene Climates will be highlighted.

It is therefore evident from the above discussions that there have been attempts to reconstruct the palaeoclimatic and palaeoenvironmental evolution of Olduvai Gorge,

Manonga–Wembere and Holili areas, mainly based on sedimentation regimes, faunal changes, hominid cultural evolution, some stable isotopic and pollen studies (mainly in the Olduvai Gorge). Studies based on palaeosol sequences in East Africa and Tanzania in particular is rare, unlike in southern Africa where palaeosol developed in sediments have been extensively studied. These studies indicate cyclicities related to climatic and environmental fluctuations of the Quaternary (Watson *et al.*, 1984, Botha *et al.*, 1992 and Botha & Fedoroff, 1995).

This research will serve as an initial detailed palaeosol stratigraphical study in East Africa. It is a contribution to the establishment of a palaeosol traverse in Africa together with other studies in the Democratic Republic of Congo (Ilunga 1982 & Yamba 1993) Uganda (Musisi 1992) and South Africa (Botha *et al.*, 1992).

1.1 BACKGROUND OF THE RESEARCH

1.1.1 The palaeoclimatic Deep-Sea sediments and ice core records

The past two decades have seen a great deal of research directed to the study of Pliocene-Pleistocene-Holocene climatic and environmental long-term and short-term changes. Records in the continents did come from pollen studies of Lake Sediments, loess sequences and ice core isotopic studies from ice caps in the Polar Regions. More importantly from deep-sea sediments studies, (Paepe 1966, Zagwijn & Paepe 1968, Zagwijn, 1974, 1985, Dansgaard 1969, 1971, Paepe & Van Hoorne 1967, West 1980, Shackleton *et al.*, 1990, Crownly & North 1991, Bater 1994, Feng 1996, Kemp *et al.*, 1997, Paepe 1970 and references therein). These studies have resulted in a long distance correlation of Quaternary palaeoclimatic and environmental changes of the globe.

The past climatic cycles preserved in the deep-sea sediments and in the ice caps have clearly been established by the Oxygen Isotope Stages (OIS) (Shackleton *et al.*, 1976) showing continuous cyclic climatic variations. Today standard curves have been widely published. The curves indicate a global response of the climatic and environmental

changes. These studies have indicated climatic fluctuations of 23Ka, 41Ka & 100Ka cyclicities consistent to the Milankovitch solar insolation temperature curve.

1.1.2 The palaeoclimatic land records

Land records (continental – apart from the ice cores and the loess sediments of China) of palaeoclimatic variation of the Quaternary Period have been discrete in the sense that the continental sediments are not continuous. Less continuous sedimentation can (have) be (been) encountered, (except in the loess of China). Even in places (African Rift System, Lake sediments) where continuous sedimentary sections are encountered, methods and study conventions have provided a difficulty in isolation and resolution of the palaeoclimatic pulses due to rapid short facies variations of sediments.

There is also lack of methods to set up geochemical/isotopic parameters comparable to those of the deep-sea and ice caps (Paepe & Van Overloop, 1994). In this respect long distance correlations have been somehow difficult to achieve from continental sedimentary records due to none transference of one formation to another.

However, the presence of palaeosol levels in most sedimentary sequences has provided an alternative as a reliable tool of global palaeoclimatic studies in the continents. Palaeosols are fossil soils, which witness the presence of vegetation on a soil of the past. Palaeosols are therefore imprints of the climate and the environment of the past as they remind us of the past atmosphere (climate), biosphere (animals and plants) and the lithosphere (rocks-crust) in a continuous interaction to form a pedosphere (soil). Palaeosols represent land surfaces of the past that separate periods of sedimentation and stability of the landscape. For this reason it is normal to continuously trace them into areas where sedimentation occurred under totally different conditions.

Studies carried out by IFAQ scholars since 1977 on palaeosols of the land time series can indicate climatic cycles comparable to those of the deep-sea sediments and ice core records. The basic concept in this assumption lies in the fact that the astronomically

enforced climatic change affects the atmosphere, which in turn simultaneously affects the ocean, the land and the ice caps (glaciers). There exist a continuous exchange of CO_2 and H_2O between the ocean, the land and the icecaps (Figure 1.2), which leaves imprints of temperature and precipitation within deep-sea sediments, land palaeosols and ice cores. These temperature fluctuations can be read from $CaCO_3$ and CO_2 of deep-sea sediments, $CaCO_3$ and CO_2 in palaeosols in land sections and CO_2 in ice cores.

A palaeosol is considered as a Member in lithostratigraphicalal classification in which it is a perfect marker horizon that can be extended from one Formation to another. A palaeosol can form on different sediments and rocks of the same age under the same influence of climate. For example, a soil can form on continental sandy, clayey or eolian sediments to sediments of marine origin and weathered rocks of different types. This means that the same palaeosol can be followed from typical loess section into a purely terrace sequence (Paepe *et al.,* 1990) or even sequences alternating with marine or sedimentary deposits and further on to igneous and volcanic rocks of different age and types. This constant transference from one type of formation to another is an important characteristic of a palaeosol, which is often a strong argument in favour of a global palaeosol traverse.

Palaeosols show broader regional and global similarities than the other sediments because under the influence of the same (globally enforced) climatic conditions (regardless of their origin) were subjected to the same pedogenic processes that build up palaeosol levels suitable for regional or global correlations (Paepe 1993). Thanks to the presence of these palaeosols in the continental sediments, several studies have been able to point out to global climatic variations.

This concept led to the establishment of a global palaeosol study traverse that was perceived and developed by Paepe, (1966, 1970 and 1974), Paepe and Ilunga, (1990) and Paepe *et al.,* (1984, 1990, & 1996). The global palaeosol traverse was furtheron pursued by IFAQ research students under the guidance of R. Paepe in the Loess plateau of China,

the Mediterranean, and in Rift valley of East Africa. Paepe & Van Overloop (1994), describe these studies which formed the global geosoiltraverse as follows:

"...New observations made at numerous sites by the Simo-Belgian Research Group on the Loess Plateau of China (Haesaerts, et al., 1994 in Press), enabled to establish a complete, however, composite section in which the geosoil (paleosoil) sequence correlates with the OIS deep-sea sequence (figure 2). It is a composite section on which the upper part of the Quaternary covering a timespan of 1.2Ma was recorded At Site Huangling (NE of Xian, N3,39 – E119,42) from the present until GRAVEL BED D (or L15 in earlier Chinese publications) and the lower part of the Quaternary from 1.2Ma down till 2.6Ma was recorded at Site Jiacun (due West of Xian; N34,22 – E107,14) as of geosoil S15 in earlier Chinese publications until GRAVEL BED F, below L36 of earlier Chinese publications..."

The explanation above suggests a complete land record of the Quaternary palaeoclimatic variations comparable to those of the deep-sea records. It is important to note here that the Chinese continental Loess deposits and its palaeosol sequences has for a long time provided an alternative proxy data to understand the global climatic changes for the last 2.5Ma. For example magnetic susceptibility of the loess and the palaeosols has been used as a proxy indicator for the palaeoclimatic changes during the Quaternary Period. Susceptibility curves in the loess of China when transformed into time series show remarkable correlation to the Deep-Sea oxygen isotope records. Many researchers today are convinced that magnetic susceptibility provides an independent measure of time (Kukla 1987 & Kukla *et al.*, 1988).

Other significant palaeosol studies from continental deposits have yielded encouraging results. For instance, studies in the Mediterranean area as again best described by Paepe & Van Overloop (1994) her below:

"...On the Northern Plateau around Sparta (N37.05 – E22.27) in the Southern Peloponesu (Greece), the site of Affision East wall produced another composite section (Paepe et al., 1994 in press) similar to that of China for the whole Quaternary, Pleistocene and Holocene together, no longer in the monsoon but in the etesian belt of the Eastern Mediterranean, a similar belt (Figure 2). In this section at almost the same latitude as the Chinese Loess Belt, same type GRAVEL BEDS are extremely well developed and serve as even better marker beds than in the Loess record of China. The contact between the two sections, the upper

Afission Road and the lower Afission East Wall, is made at GRAVEL BED B (corresponding with L6 of the Chinese record as seen above) occurring between 670 and 620Ka... "

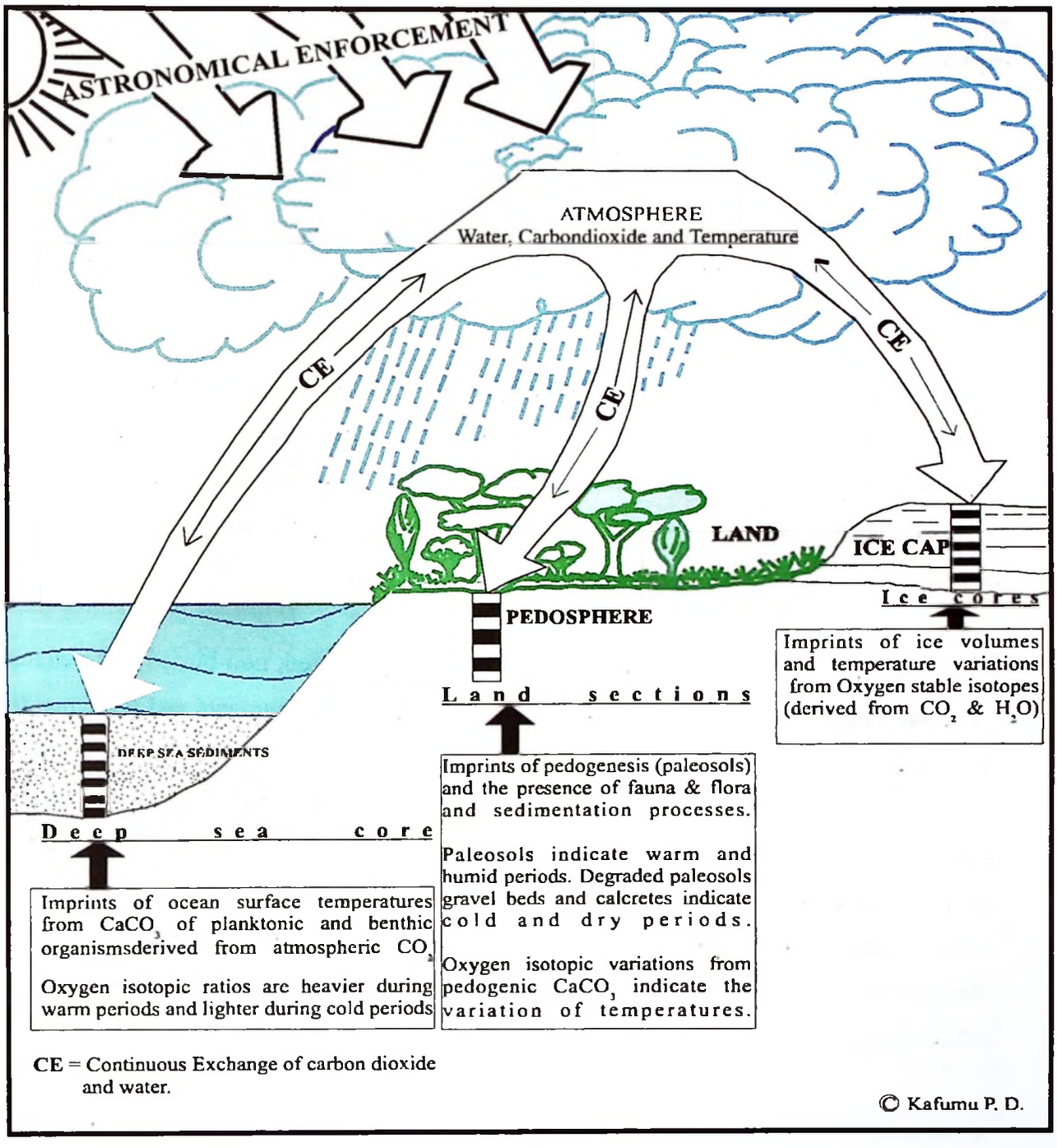

Figure 1.2: Deep sea sediment, ice (core) caps and land sediments paleoclimatic Records; All enforced by the same climate, (artistic impression).

In the Western part of the Rift System of Africa several studies did recognise limited palaeosol sections which can be correlated to those of Greece, China as well as the established OIS stages of Shackleton *et al.*, (1990). Paepe & Van Overloop (1994) further explains:

"...The West African Rift provided the location for a number of studies in the Ruzizi Plain (S2,30 – E28,58) in Zaire (DRC) (Ilunga, 1984) in the Elizabeth National Park (S0,13 – E29,53) in Uganda (Musisi, 1991) and again in Zaire namely in the Rutshuru Plain (Yamba 1993) in between the aforementioned sites. The sections can be compared with Ilunga's (1984) which shows a striking resemblance with those of Greece..."

However, similar studies have been done by Alam (1994) in Bangladesh (Asia) and the results are similar. It can then be summarized that these studies have opened a new approach on global palaeoclimatic record as registered in the positions and cyclicities of paleosoils in the continental sediments. The positions and cycles of palaeosols represent the global palaeoclimatic variations with a synchronous nature.

Based on the position of the palaeosols in the landscape buried, non-buried and exhumed palaeosol can be distinguished and used to scan the past environments and climates. It is therefore possible to read from palaeosol-sediment sequences of various landscapes and vegetation cover (the environment) over time (Van Overloop & Paepe, 1998) using sediment characters, paleomagnetism, magnetic susceptibility, (Heller & Liu, 1982, 1984 & 1986, and Hus & Han 1992) and isotopic parameters, in order to express the environmental variation through time. Palaeoclimatic and palaeoenvironmental cycles obtained from palaeosols can be readily correlated to deep-sea oxygen isotope variations (Shackleton *et al.*, 1990) and ice core isotopic records, (Dansgaard *et al.*, 1971).

If the palaeosol sequences can be recognised, their cyclicities modeled and transformed into time series, the author believes that they can provide an independent global measure of climatic change through time. This is a subject of intense research still to be pursued in the future.

The present study in Tanzania is another effort to register more new sites for the complete land records of the palaeoclimatic variation of the Quaternary, based on palaeosols.

1.1.3 The two Schools of Thought

It seems important to review some important palaeoclimatic and palaeoenvironmental thinking and arguments, which have dominated this field since the 20th Century. During this time of rapid expansion of palaeoclimatic and palaeoenvironmental geo-scientific knowledge, two schools of thought have existed. On one hand those who advocate that during glacial times in high latitude areas the tropic responds by becoming more wet and in interglacial times the tropic became dry. In other words the glacial periods are regarded as equivalent to Pluvial (wet and rainy times) and the Interglacial as equivalent to Interpluvials periods (dry and cold). The pioneers of this school (theory) were Clark and Cole (1957) who first correlated Tropical Africa palaeoclimates to that of Europe. Many other studies followed (Nillson 1963, Clark, 1965, McCall *et al.*, 1967,). This theory dominated most of the 1950's and 60's.

On the other hand, the advocates of the global palaeoclimatic synchronous response, started to dominate during the 1980's through studies carried out by IFAQ scholars. They propound that when it cools down (glacial period) in the high latitude areas, the Tropical area responds by being drier and cooler and interglacial correspond to wetter and warmer climates in the Tropics. Clear evidence favoring this argument started to emerge in the 1970's (Paepe 1966, 1970 & 1974, Kendall 1969, Grove and Goudie 1971 and Williams, 1975), Ilunga 1882 and Paepe *et al.*, (1984). Paepe *et al.*, 1990) and Paepe & Van Overloop (1994) could show migration of landscape by observing mixed landscape signals in sediments due to migrations of vegetation cover during climatic fluctuations. For instance during the growth of boreal ice caps vegetation shrank towards the Equator and expanded more from the equator when ice caps melted.

The Young Dryas recorded in Europe about 11,000BP enhanced desertification all over the Globe. There was polar desert in Belgium, (Paepe 1966, 1967, 1970, Paepe, *et al.*, 1990 and Paepe & Van Overloop 1990) and the Sahara desert expanded (Petit-Marie, 1990). Sea surface temperatures (SST) during the last glacial stage were 5°C lower than today in the equatorial areas, (Beck *et al.*, 1997 and Webb *et al.*, 1997). Modeling shows that such an effect would enhance cooling and sometimes accompanied by aridity in the low latitude tropical areas (Kennedy, 1998)

This fact is also evident from coral record from Barbados (Guiderson *et al.*, 1994). Ocean core records from Western Equatorial Atlantic, (Curry & Oppo, 1997) suggest that during the LGM (last glacial maximum) tropical temperatures were significantly below the present day values. Modeling by Weaver *et al.*, (1998) predicted tropical temperatures during the LMG to be 6.2^0C lower than today, while Ganopolski *et al.*, (1998) observes 4.6^0C cooler climates in the tropics during the LGM. All these studies point to the fact that when it cools in the Polar Regions the Equator cools also and vise versa.

Other recent studies have reported a series of short to long-term climatic fluctuations during the last Glacial-Interglacial cycle in low latitude areas, for example sediment cores from Arabian sea were successfully correlated to ice core studies from Greenland. For example, on one hand, laminated organic-carbon-rich bands of sediment cores from Arabian Sea reflecting strong monsoon-induced biological productivity correlated to the mild interstadial climatic events in ice cores from Greenland regions. On the other hand, lower south-west monsoonal intensity indicated by bioturbated organic-carbon-poor bands were correlated with intervals of high latitude atmospheric cooling, (Schulz *et al.*, 1998). The above study indicates that glacial periods (cooling) in Greenland correlates to mild (drier) with reduced biological productivity, while interglacial periods relate to times of wet climates associated with strong biological activities in the tropics. The study by Schulz *et al.*, 1998, is once again another proof to synchronous responses of climate of the high latitude areas to that of the Tropics.

There is more clear evidence today than before for a general relationship between low latitude climatic variability in sea sediments and the rapid temperature fluctuations of high northern latitude that are recorded in the ice cores. There is also firm evidence of Late Pleistocene aridity in many parts of Tropical Africa, (see chapter 1.1.4) this is in contrast to the belief that high latitude glacial periods were equivalent to low latitude pluvial periods. The Pluvial/Interpluvial equivalency to Glacial/Intergalacial is now viewed by many as scientifically incorrect and obsolete.

1.1.4. Quaternary Palaeoclimates in the Great Lakes Region of East Africa

Quaternary long distance correlations based on climatic changes in the Sub-Saharan Africa, South of the Equator have remained elusive compared to studies in the temperate World (especially Europe). However, earlier (1970's) studies of palaeolake shore lines in East Africa showed that Lake levels rose at the start of the Holocene after a long period of low levels and high salinity. Grove & Goudie, (1971) found that Lakes Victoria and Albert were low for an unknown time just before 12,500BP, while Lake Rudolf was low before 12,000BP and was higher thereafter. Lake Victoria level rose rapidly at the close of the Young Dryas and probably reached the Nile outlet shortly after 10,000BP, (Kendall 1969). Lake Levels also rose in the nearby Magadi-Manyara-Natron basin, (Roberts *et al.,* 1994). Lake Manyara palaeolake shore line was at its highest during the last Interglacial from 127Ka – 115Ka (Somi, 1993).

There is also indication from studies of fossil fish evolution that East African climate changed dramatically over the last 14,000years BP and during the Last Glacial age, this region experienced arid conditions. Work in Lake Victoria basin show that the Lake (Victoria) dried out shortly before 12,400BP, (Johnson *et al.,* 1996). A study of fossil stromatolites indicate that similar arid episode occurred in the Northern Tanganyika basin about 2,500BP, (Casanova & Hillaire-Marcel 1992). Stager *et al.,* (1997), from diatoms record of Lake Victoria, reports four distinct Holocene climatic pulses bounded by sudden transition, (11,400 – 10,100BP) a variably dry phase, (10,000 – 7,200BP) a

humid, (7,200 – 2,200BP) more seasonal phase and (2,200 – 0BP) relatively arid phase, with a dry 'little ice age' event at 600 – 200BP.

At 18,000BP the water balance of Lake Tanganyika basin reflects glacial conditions. There were also lower SSTs in the Indian Ocean and the related lower availability of global atmospheric moisture during cooler climatic phases, (Bergonzini *et al.,* 1997). A pollen study by Bonneffile *et al.,* (1992) in Tropical East Africa could infer glacial climates comparable to those of the Temperate World. Multivariante analysis of pollen time series data from peat deposits in Burundi for the last glacial period show that there was a decrease of temperature of about 3°C to 5°C with an accompanied decrease of mean annual rainfall of about 30% (Bonnefille *et al.,* 1990).

Direct evidence of Late Glacial Tropical African aridity comes from Quaternary extensive dunes and eolian activity in parts of Angola, Zambia, Mozambique, Zimbabwe and Democratic Republic of Congo, (Williams, 1975). For example, eolian studies in Central Equatorial Africa show that maximum aridity did occur during ice growth phases following interglacial maxima (sub-stage 5e/5d, 5c/5b and 5a/4 boundaries) and the latest Holocene. Maximum humidity occurred during deglaciation (6/5e, 5d/5c, 5b/5a and 2/1 boundaries) Wet periods occurred consistently at times of high summer insolation, (Pokras & Mix, 1985). These records appear to reflect nearly synchronous global climatic changes.

Other recent studies coming from terrestrial sediments in the Great Lakes Region of Africa, (Ilunga, 1982, Musisi 1991, Yamba 1993, Bonnefille *et al.,* 1995, De Menocal 1995, Harrison & Mbago 1997, Kennedy 1998, and others), suggest dry and humid phases of palaeoclimatic and palaeoenvironmental changes in the area. The phases are highly correlatable to the high latitude glacial and interglacial events respectively. In other words these studies have supported the global synchronous effect of past climatic changes. Such research evidence leads us to a safe conclusion of the synchronous glacial (dry & arid) conditions in both high latitude and low latitude areas.

Following the above review it is clear that there is much more evidence the global climatic change is one big system, which responds synchronously. However, the above researches are far from conclusive regarding the complete Pliocene-Pleistocene-Holocene climatic and environmental changes in Tropical Africa. More research is still needed to provide a more complete picture.

It is under this preamble that this study sets out to investigate the sediments in the East African Rifts as an attempt to fill in the pieces of this climatic past puzzle. The present study in Olduvai Gorge, Manonga Wembere and Holili areas in Tanzania is therefore another effort to register more evidence of the land record of palaeoclimatic/palaeoenvironmental variation of the Quaternary Period. The study is based on the geology, stratigraphy and palaeosol occurrences and sequences.

1.2. OBJECTIVES OF THE STUDY

The general main objective of this study is to try to understand more the Quaternary stratigraphy, climates and environments of the Olduvai Gorge beds (hominid site) – NE Tanzania. Two other areas, (Holili – Kilimanjaro and Manonga-Wembere Valley – Central Tanzania) are treated as additional research areas (annex) to accompany the major work at Olduvai Gorge.

1.2.1. Olduvai Gorge

The Pliocene-Pleistocene-Holocene sediments of Olduvai Gorge are well known for their records of both hominid evolution and palaeoenvironments where these hominids lived, (Kappelman 1984). Kappelman, (1984) identifies at least 22 fossil levels which Hay, (1976) indicates that the levels (animal & hominid occupation) are in fact located on palaeosol levels. Discrete sampling and subsequent laboratory studies of pedogenic carbonate nodules and concretions from some of the palaeosol levels were undertaken by, Cerling *et al.*, (1977), Hay & Leeder (1978) and Cerling & Hay (1986), across the Olduvai Gorge composite section. In all the foresaid studies, little efforts were directed

into a proper identification and positioning of the palaeosols into the lithostratigraphy. The palaeosol types and positions in the stratigraphy would (will) be very helpful (see explanations on chapter 1.2.2) in recognizing short-term climatic impulses for the purpose of regional and global correlation.

Based on these studies attempts to make long distance correlations were made. For example, Cerling & Hay (1986) on their study of isotopic composition of palaeosol carbonates, identified 3 distinct time periods of climatic changes in the Lower Pleistocene and made the following remark:

"...We are not yet able to say whether the climatic record of Olduvai Gorge is one of regional or global significance, our data suggest that Olduvai Gorge had at least three distinct climatic changes at about 1.67Ma, 1.3Ma and 0.6Ma..."

This remark indicates a long time scientific desire to discover the globally enforced Quaternary climates and environments. Also, earlier Cerling *et al.*, (1977) attempted successfully to correlate Olduvai Gorge palaeoclimatic changes to those of Lake Turkana in Kenya. Kappelman (1986) based on habitat indicators attempted to correlate continental and marine Pliocene-Pleistocene climates and environments of East Africa. Again a palynological study by Bonnefille (1984) indicated some Quaternary climatic changes consistent to those of Kappelman (1984), Cerling *et al.*, (1977) and Cerling & Hay (1986). Reading through such works I was inspired that based on palaeosols studies, I can contribute to this debate.

1.2.2. Manonga-Wembere Valley

In Manonga-Wembere basin little studies have been conducted to reconstruct the Pliocene-Pleistocene-Holocene climates and environments. Nevertheless, several fossil localities earlier dated as Middle Pleistocene were found and collected by C. Grace in 1929 at a now obsolete village name of Tinde, today known as Ibole in Igunga District, Tanzania (Grace & Stockely 1931). Other studies (Hopwood 1931, Teale 1931 and William & Eades 1939,) followed later to map in detail the geology of the area. Apart

from this brief and old studies the Manonga-Wembere valley was largely unexplored. This fact inspired Terry Harrison to launch a palaeontological expedition in 1992 – 1994 to study the palaeoenvironments of the area based on paleontology, (Harrison & Mbago 1997).

The detailed stratigraphy of Verniers (1997) as a result of this expedition, mapped approximately 70m thick sediments with widespread thin to thick palaeosols. The palaeosols contain various types and contents of pedogenic calcareous concretions and nodules forming up to 80% of the palaeosol levels. Verniers, (1997) does not map out the palaeosol levels, but only gives a brief mention. In situ fossil levels are also closely related to palaeosol levels as Harrison (1997) offers an account:

"...Fossil in situ levels are restricted to a light gray calcareous clay impregnated with a honey comb-like calcareous matrix and light gray to white clays immediately above and below this layer. Just above the fossil horizon is a distinctive bright red clayey layer...It seems likely the diagenetic process involved in the formation of this local bed were responsible for conditions suitable for the preservation of the fossil remains..."

The above quotation underlines the fact that the honey comb-like calcareous fossiliferous layer is bounded (above and below) by a pure un-impregnated light gray to white clay. Just above this bounded fossil layer lies the palaeosol (bright red clayey layer). The fossils were deposited in a sub-aquatic environment of a shallow lake. When the lake retreated, sub-aerial exposure of clays led to the formation of the palaeosol above it. Through the action of capillarity up from the lower water table, calcium carbonate could concentrate in a narrow band just below the palaeosol. Harrison (1997) further suggests that the increased calcium carbonate concentration led to a perfect fossil preservation of animal remains.

These palaeosols are distinct marker horizons in the Manonga-Wembere deposits, closely associated with the fossil levels. In fact there is so much evidence of Pliocene-Pleistocene-Holocene pedogenesis in this area indicated by presence of extensive red beds. The red beds are associated with calcareous nodules & concretions, rootlets and

twig infillings. It is therefore safe to expect that detailed studies of palaeosol levels would serve as a good Quaternary environmental and climatic key elements in the area. This study will once again dwell on the study of some of these palaeosol levels, which have largely been unexplored, as an attempt to identify the palaeoclimates and palaeoenvironments of the area.

1.2.3. Holili calcareous deposits

Another annex area, that is considered briefly in this study is the Holili calcareous grit deposits near Taveta (Tanzania-Kenya border) on the foot of the giant mount Kilimanjaro. The same palaeosol study approach is adopted as discussed in chapter 5. Briefly, this area is least studied. Only brief geological reviews can be found (Downie & Sampson 1953, Downie *et al.*, 1953-1957 Wilkinson *et al.*, 1986 and Kanza 1985). The literature indicates presence of palaeosol levels within the volcano-sedimentary deposits of Kilimanjaro area, as indicated by the following quotation;

> *"...Red soils – South of Kirua are extensive alluvial deposits of sand clay and conglomerate with secondary limestone, all distinctly red in color. Similar deposits have a widespread but irregular on the lower slopes of Kilimanjaro, west of Shira and East of Mawenzi but are not shown on this map. In places they reach thickness of 200 feet. Fringes of duricrust surround all outcrops of Precambrian rocks, which may be highly calcareous in places. Surface limestone is present on some of the parasitic in the Shira zone and locally elsewhere..."* (Downie *et al.*, 1953-1957).

The above description suggests presence of palaeosols in sedimentary sequences of Kilimanjaro area. Again as said before this study intends to point out some of the stratigraphical, palaeoclimatic and palaeoenvironmental elements (from Holili sediments) and their significance to the Quaternary climates and environments.

In light of the foresaid review of related literature, it is my belief that palaeosol levels can best map out the Quaternary climates and environments, in turn enabling us to pick out some of the climatic changes and cycles. This is because palaeosols have stable

stratigraphicalal positions and marker beds that can be traced over long distances, (chapter 1.2.2).

1.2.4. Specific objectives of this study

1. **A regional and detailed geological mapping shall be carried out to be able to establish and present the geology and stratigraphy of the studied areas.**

2. **The research shall recognise and describe palaeosol levels and identify their stratigraphical positions in Olduvai Gorge deposits (main work), Manonga-Wembere Valley deposits and Holili calcareous grit deposits, (minor work),** (Based on detailed field observations and mapping)

3. **The palaeosols and other lithological units shall be examined and described in the laboratory for a possible identification and classification,** (Based on laboratory examinations and measurements).

4. **An attempt to set up a Quaternary palaeosol stratigraphy and climatic-environmental changes of the areas shall be carried out,** (Based on lithostratigraphical Member classification and palaeosol sequence categorisation).

5. **This stratigraphical evolution shall be correlated to known global palaeoclimatic and palaeoenvironmental variation curves known in other parts of World,** (Based on palaeosol sequences and cyclicities identified in objective 3 above).

6. **A possible correlation between the palaeoclimatic-palaeoenvironmental variation (in 4 above) and the occurrence of fossil man (hominid) in Olduvai Gorge,** (based on the association of archaeological levels and palaeosol levels).

1.3. METHODS OF THE STUDY

This chapter provides a brief description and explanation of the field and laboratory methods, which were employed in this study. The methods are 1. **A review of related literature**. 2. **Field work in Tanzania.** and 3. **Laboratory methods.**

1.3.1. Literature review

This is a review of the related literatures of first the global views of palaeoclimatical and palaeoenvironmental studies of the globe throughout 5 last decades. Secondly, a review of previous research works done in Eastern African Rift systems and specifically in the study areas.

The data set reviewed included reports, books and journal publications in the fields of geology, archaeology, paleontology, stratigraphy, paleoclimatology & paleoenvirometology and chronostratigraphy. Other data sets were, geological & geomophological maps and aerial photographs. The literature review was conducted in the Quaternary Geology, Geochronoloy & Geography sub-libraries and Main library of the Free University of Brussels. Other libraries consulted were the Geological Survey of Belgium, the Royal Museum for Central Africa-Tervuren, the University of Gent and the Catholic University of Louven.

One month (December 1996) and two weeks (August 1998) were spent at the Geological Survey of Tanzania-Dodoma and the Ministry of Energy and Minerals-Dar-es-salaam libraries in Tanzania collecting and consulting relevant literatures (books, research reports, journal publications, geological & topo-sheet maps and aerial photos).

Review of literatures also included the learning and familiarization to the VUB-Intergraph computer software facilities under the assistance of Dr M. K. Kaseba. This process enabled me to accurately and easily draw diagrams cross-sections and maps. Using the same software it was also easy to analyze, interpret and correlate sections.

1.3.2. Field methods

Fieldwork campaigns were carried out in the three areas of study, that is Olduvai Gorge & Holili in NE-Tanzania and Manonga-Wembere Valley in Central Tanzania. There were two field seasons (a total of three months) that were undertaken. The first fieldwork campaign was carried in summer 1997, (i.e. July through September 1997) The second field season was in summer 1998, (i.e. July through August of 1998).

1.3.2.1.Geological and geomorphological field mapping

A regional geological and geomophological mapping was conducted to be able to recognise the general geologic and geomorphological features of the areas and make synthesis of the geological evolution. Aerial photographs, satellite imagery and topographic sheets heavily assisted this fieldwork.

The mapping was carried out in the summer of 1997 field season, three field sessions were conducted in Olduvai Gorge and Manonga-Wembere areas. The first session took place during the last two weeks of July 1997. This was a general geologic and geomorphologic mapping of the Olduvai Gorge area and detailed mapping and description of geological sections along the Olduvai Gorges (see chapter 5). During the mapping of the sections, detailed measurements, drawings, descriptions and photographing were made. Also in the coarse of mapping, samples were taken for laboratory works.

More than 50 palaeosol levels were mapped on a more than 60m composite section. Sampling for representative different lithological units was done, in which a total of 100 samples were collected. Prof. Dr Paepe and Dr E. Van Overloop supervised this field session.

1.3.2.2. Lithostratigraphical – palaeosol field studies

A systematic lithological recognition was performed. It was a lithostratigraphical and palaeosol mapping of the sections. Palaeosol levels were recognised carefully measured and described.

Lithostratigraphical studies were undertaken in the second field session, which took place during the first three weeks of the month of August 1997, geological mapping, detailed measurements, drawings, descriptions and photographing were made at Holili locality in the Kilimanjaro area. A total of 5 samples including some animal and plant fossils were collected in this area, (see chapter 9.2). A brief work was also conducted in Manonga-Wembere Valley, in which the geology of the area was reviewed (chapter 9.1). General geological work was also continued in Olduvai Gorge area. This work (Olduvai Gorge) concentrated the correlation of various units at a large-scale context. This enabled me to understand better the general geology of the Olduvai Gorge basin.

The third fieldwork session in this season was conducted during the two first weeks of the month of September. This was the continuation of the detailed work (measurements, drawings, descriptions and photographing) on the Olduvai Gorge sections. Additional 60 (rocks, palaeosols and sediments) samples were collected. Prof. Dr R. Paepe the promotor of this work supervised this fieldwork session.

Summer 1998 was the second season of the fieldwork campaign in Tanzania. There were two fieldwork sessions that lasted for three weeks each. In the first session, Holili and Olduvai Gorge stratigraphy were revisited. 8 new oriented palaeosol samples were collected and 10 palaeosol levels (earlier sampled) were re-sampled in Olduvai Gorge sections. Geological mapping also continued in the Holili area.

The second fieldwork session during this time was directed to the study of the Manonga-Wembere sediments. During this session geological mapping, detailed measurements,

drawings, descriptions and photographing were undertaken. 8 palaeosol levels were recognised and sampled, (see chapter 9.1).

1.3.3. Laboratory methods

Three laboratory methods were employed to study the stratigraphy of Olduvai Gorge; they include 1. Mineralogical and geochemical analyses of sediments 2. Magnetic susceptibility measurement and interpretation and 3. Micromophological examinations of palaeosols.

1.3.3.1. Mineralogical and geochemical studies

Mineral contents of the samples were determined at the Geological Survey of Belgium Laboratory. The determinations were carried out using a modern Short Wave Infrared Reflectence (SWIR) Spectrometer instrument under the guidance of Mr. Hendrix the technician of the Geological Survey of Belgium. Prof. Dr R. Paepe supervised the whole laboratory study process. Some electron scanning microscopic examinations of sand grains from Olduvai Gorge locality were performed at the Metallurgical Engineering Laboratory of Prof. Dr Vereecken at the VUB. Also stereo microscopic examination of sand grains were carried out in the Geochronology Laboratory of Prof. Dr Pasteels at the VUB. Some major elements geochemical analyses were carried out at the Royal Museum for Central Africa laboratory in Tervuren with the help of Prof. Dr J. Klerkx.

1.3.3.2. Magnetic susceptibility measurements

Samples were prepared in the Quaternary Geology Laboratory at the VUB, (the laboratory of Prof. Dr Paepe) and then the measurements of the magnetic susceptibility were carried out at the Physics Institute '*Centre Physique du Globe*' Laboratory in Dourbe. Prof. Dr J. Hus supervised the work.

1.3.3.3. Micromorphological studies

Soil thin sections were prepared and micropedological features (micromorphology) were studied using a polarized microscope. The studies were carried out in the Mineralogy, Petrology and Micropedology Laboratory of the Geological Institute at Gent State University, under the supervision of Prof. Dr G. Stoops.

CHAPTER TWO

THE QUATERNARY PERIOD

2 THE QUATERNARY PERIOD

2.0 THE PERIOD OF HUMAN CIVILISATION

The Quaternary Period is the most recent in geological period (fig 2.1) which is characterized by three essential facts. First, is the latest and shortest in time and it is the uppermost layers of the earth's surface which, is still in dynamic interaction and development with the environment, (i.e. the interaction between the biosphere, atmosphere and the lithosphere. The second fact is the appearance of man, for the first time an animal appears on earth able to prepare tools for a determined use. This is the period related to the humankind development and civilization. The third fact is the growth of huge glaciers, which spread over wide areas of the world. Glaciers advanced further than they were ever before. This fact has led to the subdivision of the Quaternary Period into glacial and interglacial epochs.

During this Period (especially the last 10,000years) human use of land, water, minerals and other natural resources has increased tremendously. Further increase in population and economic activities will intensify this need still further. The chemical composition of air, water and soil are changing as a consequence the structure and the functions of the natural ecosystem are also changing very fast. These changes will influence the global climate as a result, threaten the natural ecosystem upon which life depends. This is the period of humankind civilization, in which, all of us live and move. It needs to be studied for the protection of the environment to guarantee a safe future of humankind.

The geoscientific community having understood this fact has drawn most of its efforts to study this important geological period with the major concern of protecting humankind. In other words Quaternary environmental research has therefore became a very important aspect of scientific research for understanding the earth's environment, as Paepe & Van Overloop (1994) explains;

"... a hundred years ago active environmental geology was restricted to geo-technical problems alone (engineering geology). Emphasis and scope of environmental geology was most local well site geology and not regional environmental impact and its consequences to humankind. Indeed the society's demands were far more fewer as population density was lower, quality of life aspects were restricted, energy consumption and spatial occupation was restricted. As more people steadily live on small space more respect for quality of life and spatial occupancy has become new targets in geological research. In defining the environment, geology takes the charge of understanding the climatic circumstances of sedimentation that took place and how fossils both plants and animals were living. This eventually has led to the reconstruction of the past in the palaeogeographic maps and scenes of the global environment. Such mystery and imagination in the past has remained an idyllic scene of geological past without much of a practical application to benefit the future of mankind..."

Therefore a couple of international research programs and projects have highlighted some new possibilities by reconstructing the global paleoclimatic changes and use it to model the future climates. For example, IMAGE (1998) CLIPMAP (1981), PAGES (1998a & 1998b) & UNESCO (1997) projects have since their establishment initiated, funded and guided research endeavors with much broader view of understanding the climatic changes of the Quaternary Period for the benefit of humankind and the future of the planet earth. The present research is within this perspective of contributing to the understanding of the Global past climate (using palaeosols) as a key to understanding past and future climatic changes.

2.1 THE EPOCHS OF THE QUATERNARY PERIOD

The Quaternary is a division in geological time scale (figure 2.1) in the Cenozoic Era right after the Tertiary Period. It began about 2.6Ma ago and has continued to the present time. The Period is divided into Pleistocene Epoch (Ice Age), which is the earliest and

longest part of the period and the Holocene Epoch (Post Glacial). The Holocene began about 10,000BP and extended to the present.

2.1.1 The Pleistocene Epoch

The Pleistocene named by the British geologist Charles Lyell (Lyell 1839), immediately follows the Pliocene in the geological time scale extending from the beginning of the Quaternary to about 10,000 years ago. This Epoch was defined based on the proportions of extinct to living shellfish living species in the fossil record. In fact the strata containing 90% to 100% of living species were assigned in this Epoch. The Pleistocene was most notably characterized by the spreading of glacier ice over more than a quarter of the earth's land surface.

However, the boundary between the Pliocene Epoch (Tertiary Period) and the Pleistocene Epoch (Quaternary Period) is still an ongoing controversial issue and still remains a vital problem to choose an appropriate Tertiary-Quaternary boundary. In the developed world (specifically Europe and the USA) the Tertiary-Quaternary boundary is generally accepted between the 2.4Ma and 2.6Ma range, (Zagwijn 1974, Nikiforova 1978, Johnson 1988, Lutgen & Turbuck 1989). This boundary is mainly based on the Late Pliocene climatic change.

The formal Tertiary-Quaternary boundary as accepted by INQUA is based on the Calabrian stratotype of Santa Maria de Catanzaro and la Castella sections of Southern Italy. The first appearance of cold related foraminifera and calcareous plankton species in these sections indicating the arrival of a cold period was taken as the boundary between the Tertiary and the Quaternary (Pliocene/Pleistocene boundary). The date assigned to this boundary is the top of the Olduvai subcron with an age of 1.79Ma (Berggen *et al.*, 1995).

Many scientists now accept the age of 2.6Ma (West 1980 and Johnson 1988) as the Tertiary-Quaternary boundary, based on the climatic change at the end the Pliocene. The

Matuyama-Gauss magnetostratigraphical time boundary, which is at about 2.58Ma is sometimes used to mark this boundary in the Western World. In East Africa there is still more controversy on this boundary but several researches have pointed out to the range between 2.4Ma – 2.0Ma, (Howell et. al 1987, Musisi 1991 and Manega 1993).

Moreover, this boundary is still much in dispute as demonstrated by the following three quotations below.

"...Following a decade of study and discussions by the International Union for Quaternary Research (INQUA) subcommission 1a (Pliocene/Pleistocene Boundary) on stratigraphy and International Geological Correlation Program Project 41 (Neogene/Quaternary Boundary) a draft proposal on the choice of the boundary stratotype for the Pliocene/Pleistocene boundary was submitted and approved by the INQUA Commission on stratigraphy and the Sub-commission on Quaternary Stratigraphy of the ICS in 1983 (see review by Pasini and Colalongo, 1982), and published 2 years later (Aquirre and Pasini 1985) together with the announcement (Bassett 1985) that the content of the proposal had been formally ratified by the IUGS executive as the GSSP for the base of the Pleistocene. The 'golden spike' was placed at the base of a claystone unit conformably overlying the sapropelic marker bed e in the Vrica section of Calabria in southern Italy. This level has been shown to lie at or near the top of Olduvai (C2n) Subchronozone. Current attempts to relocate the Pliocene/Pleistocene boundary to coincide with the late Pliocene climatic change at ca. 2.6Ma are judged here to be inappropriate and to ignore stratigraphical first principles..." (Berggren *et al.*, 1995).

"...Quaternary described as a sub-era is the most recent of all geological time and includes the Pleistocene and the Holocene Epochs. It began about 2Ma ago and continues to the present day..." (Walter & Trotman, 1995).

"...Quaternary Period of geological time that began 1.64Ma years ago and still in process. It is divided into the Pleistocene and Holocene..." (Lafferty & Rowe, 1997).

Today this debate rages on with a handful of geo-scientists maintaining that the Pliocene-Pleistocene boundary is at the 1.8Ma mark and others accepting the 2.6Ma boundary. Who is right? This is the controversy at large.

This work will however adapt the 2.6Ma Pliocene-Pleistocene boundary in all the discussions presented in the chapters to come. Going back to the Pleistocene Epoch, this is sometimes called the age of man because the earliest humans are believed to have appeared.

Southwestern Sahara and Sahel were driest during glaciation and stadials but wetter than present during interglacials and interstadials (Pokras & Mix, 1985) during the Pleistocene Epoch. It was a dynamic Epoch marked by the appearance of a super animal (man) who later over-populated and changed the face of the earth by his discoveries and innovations, especially during the later part of the Holocene Epoch. Today the environment is so much intangled by man's activities, so much that scientists are wondering on what is going to be the future climate considering man's activities in the climatic equation.

This fact has divided geoscientists into two camps. Those who believe that man's activities (e.g. Industrial gas emissions, deforestation etc) will shift the climatic equation in such a way that a global warming will be eminent. This is a stance of the short-term conceptual thinkers such as climatologists, ecologists, geographers etc. On the other hand geologists (geoscientists *per se*) with their extended concept of time generally do not take the later view. They believe that climatic changes are largely externally controlled by cosmic-astronomical influences. The internal influences (volcanic activities, man made effects etc) are temporal, they are too weak to change the general trend caused by astronomical causes. Their effects would usually be accommodated or cancelled out within the general trend.

Paepe & Van Overloop (1994) suggest that the Greenhouse syndrome is rather a global warning and not a global warming. The same astronomically enforced global climatic changes are going to befall the planet as it happened in past geological times. As we are at the end of a current interglacial moving to the next glacial, the decay of the climate is a natural trend (Paepe & Van Overloop 1994).

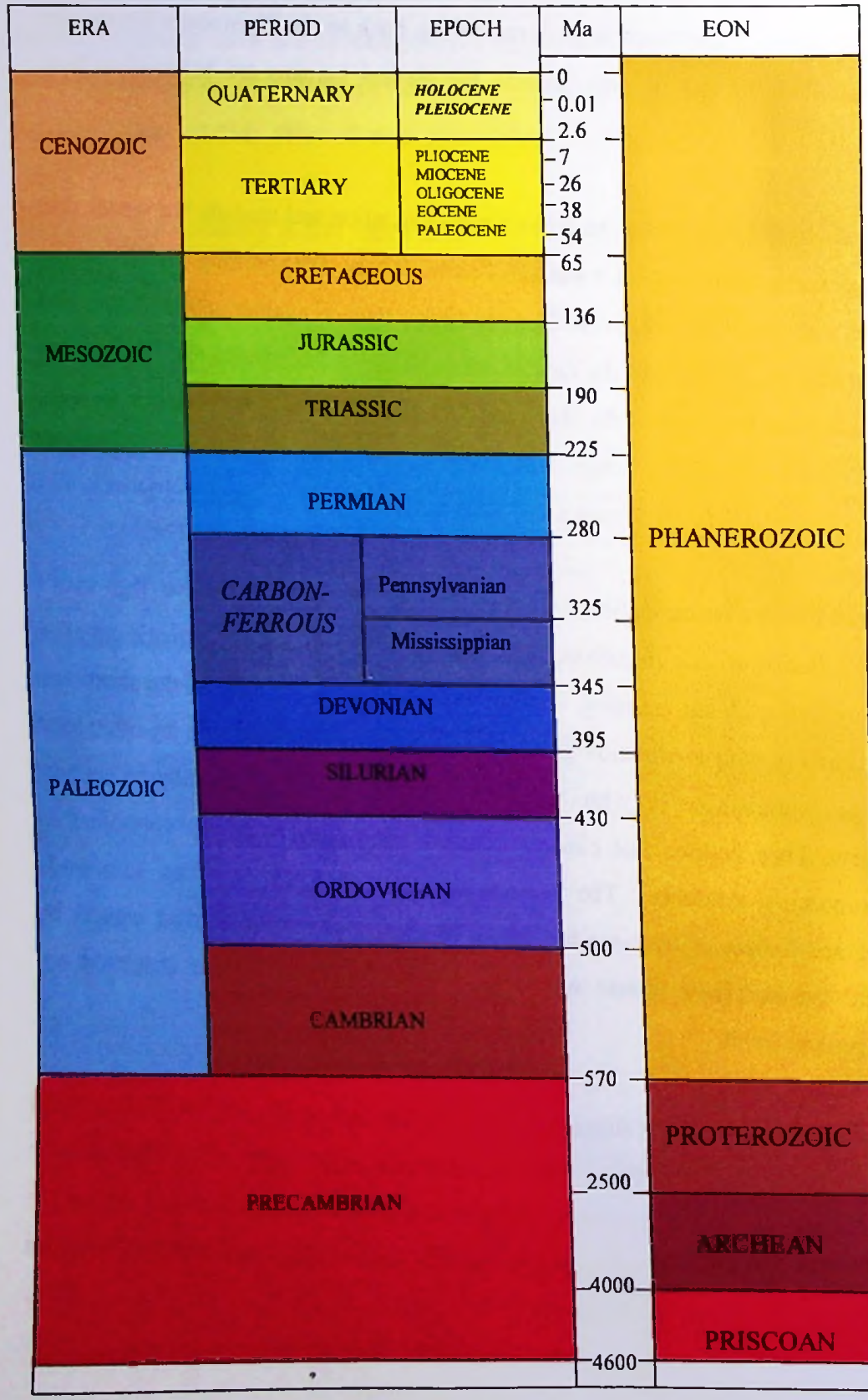

Figure 2.1: The Geological Time Scale

This period is likely to be accompanied by drought and desertification, higher frequency of floods and storms and ultimately the decay of temperature in a full-blown glacial epoch.

2.1.2. The Holocene Epoch

During the Holocene beginning about 10,000BP melting ice (McCabe & Clark 1998) caused the sea level to rise 20m or more drowning large areas of land and broadening most continental shelves and especially during the climatic optimum (about 5000BP) when the sea level was at its highest. Many animals (mammals) became extinct the beginning of the Holocene. Little explanation has been offered on this massive extinction, but many scientists do suggest a climatic change might have been responsible.

This Epoch was a warm period and has already lasted for 10Ka, which is a standard interglacial time span. This time has been used as a model interglacial time frame in many modeling studies of the past and future global climatic changes. In this respect all time intervals with similar duration and climates as that of the Holocene Epoch are termed or regarded as interglacial times, (for example, the Eamian Interglacial in NW Europe).

The Holocene Epoch has fairly been studied in recent years. For example, Paepe & Van Overloop (1994) indicate 4 short-term climatic cycles of 2.5Ka each, based on palaeosols studies (Holocene soils – HS) in Greece. These cycles are; 10Ka – 7.5Ka (HS1 – HS2), 7.5Ka – 5.0Ka (HS3 – HS7), 5.0Ka – 2.5Ka (HS8 – HS11) and 2.5Ka – 0.0Ka (HS12 – HS20). The palaeosol cycles are consistent to the 2.5Ka cycles (Pre-Boreal & Boreal, Atlantic, Sub-Boreal and Sub-Atlantic respectively) based on CO_2 contents in the ice cores, (Ruddiman et. al, 1986) and archaeological periods, (Mesolithic, Neolithic, Bronze Age and Historical times respectively). It is important to notice here that these short-term cycles can not be resolved by the Milankovitch curve. This fact has prompted a lot of high-resolution paleoclimatic researches to be able to pick these short-term changes.

2.2. GENERAL REVIEW OF THE CAUSES OF THE PLEISTOCENE ICE AGES

Ice Ages are periods in the earth's history when a significant, extended cooling of the atmosphere and ocean took place. The earth last entered a significant ice age about 2.4 million years ago, at the beginning of the Quaternary period. The most recent one was at about 15,000BP where most of Northern Europe was covered by ice (Walter & Trotman). Great ice sheets extended to about 40°N – 45°N covering about all of Canada and Europe north of the Alps, (Dasch, 1996). Although continental ice sheets withdrew from North America and Europe about 6,800 years ago (the climatic optimum), at the end of the Pleistocene epoch, many scientists believe that the Quaternary Ice Age is not over yet.

Evidence of earlier ice ages also exists. Since the time of the earliest recorded life on earth about 3.6 billion years ago. Old Ice ages occurred at average of about every 150 million years, and last a few million years (Lafferty & Rowe, 1997 and Figure 2.2). Seven Ice Ages are so far known, as given in the table 2.1 below.

Table 2.1: The Ice Ages, which occurred during the geological evolution of the world. (After; Lafferty & Rowe, 1997)

ICE AGE	TIME RANGE	LENGTH	INTERVAL BETWEEN ICE AGES
Pleistocne	2.5Ma – 0.001Ma	2.4Ma	247.5Ma
Permo-Carboniferous	330Ma – 250Ma	80Ma	100Ma
Ordovician	440Ma – 430Ma	10Ma	130Ma
Verangian	615Ma – 570Ma	45Ma	155Ma
Sturtian	820Ma – 770Ma	50Ma	60Ma
Gnejso	940Ma – 880Ma	60Ma	860Ma
Huronian	2,700Ma – 1,800Ma	900Ma	

Ancient Ice Ages were longer than the Quaternary ones. The longest of the ancient ice ages (excluding the first one) in recent geological times was probably the Permo-

Carboniferous, (fig. 2.2) which began about 300 million years ago and affected all southern hemispheres land. This period is marked by a significant change in marine life, where many corals and trilobites became extinct and deserts were widespread (Lafferty & Rowe, 1997). Still earlier, about 440 million years ago, another giant ice sheet extended from Brazil to North Africa and all the way across Yemen and Saudi Arabia. Paleomagnetic measurements indicate that the South Pole then lay in West Africa. About 600 million years ago, yet another great glacial age occurred. Layers of tillite rocks consisting of hardened glacial drift provide evidence of these ancient ice ages.

Although the causes of old Ice Ages and during the Quaternary are still a subject of controversy, an argument based on astronomical observations of the galaxy has gained credibility in recent years. The earth and its solar system are located accentrically within one limb of the Milky Way galaxy. The galaxy completes one rotation about once every 300 million years, taking the solar system through denser and thinner regions of interstellar dust and through changing gravity and magnetic fields. Two disturbing phases appear to exist for each full circle, so that every 150 million years a very slight change takes place in the solar system's galactic environment, which possibly alters the earth's climate.

Other earth-based processes are also suggested as possible causes of climatic changes. For example continental drift which changes the earth's geography. These changes occurred about 60Ma ago, when a warm equatorial seaway called Tethys separated the northern landmass (Laurasia) from the southern one (Gondwanaland), bringing warm swirling currents to all the oceans, (Dasch 1996). The old southern lands began drifting northward, however, so that Africa, Arabia and India successively collided with Eurasia. Finally Australia separated from Antarctica, allowing a cold current to circle the globe. One by one the land blocked the former equatorial seaways. Each ocean was now isolated and connected with polar latitudes by great swirls of cold current. The galaxy's rotation and the favorable geographic-oceanographic setting due to continental drift can initiate a chain reaction of cooling and warming climates.

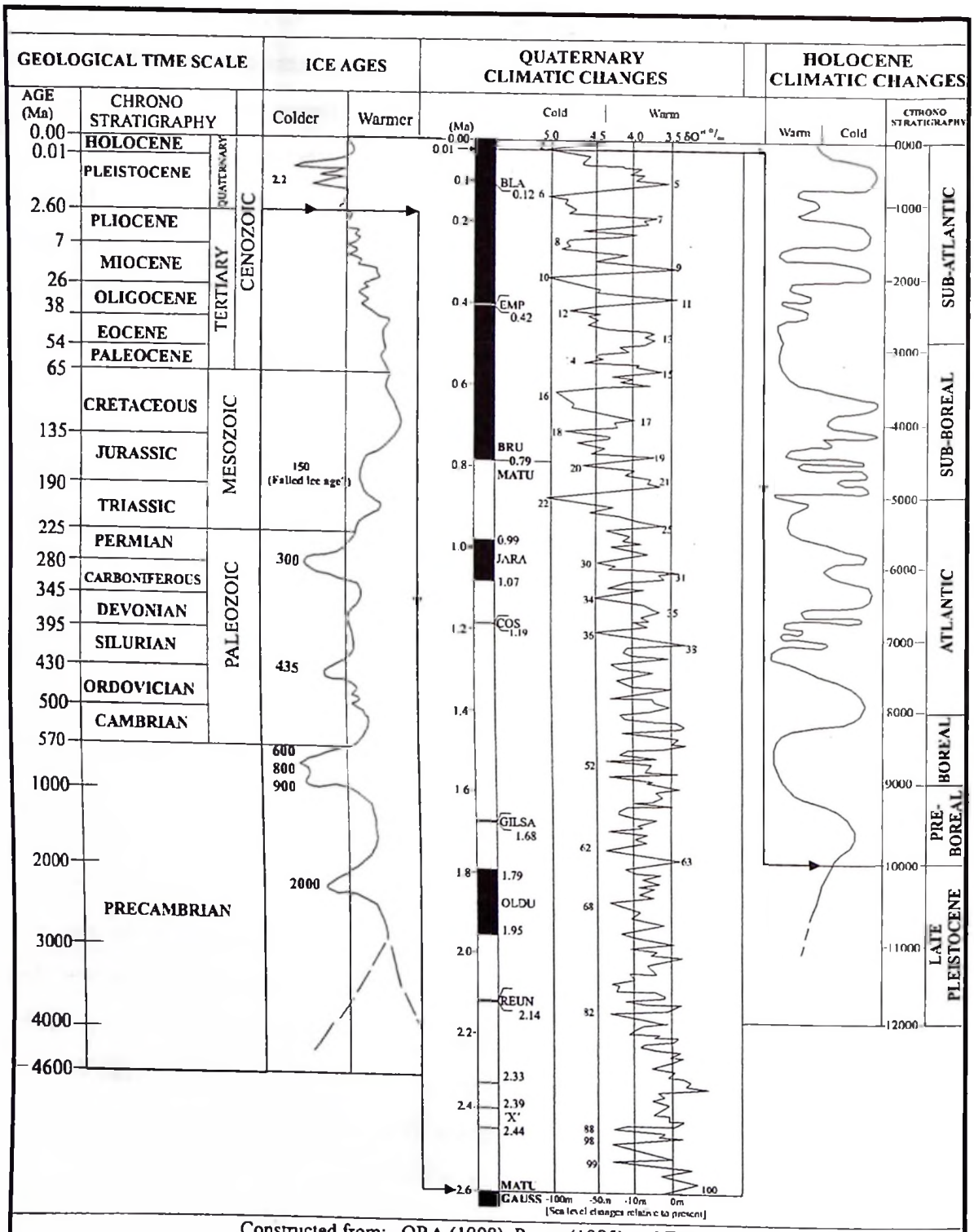

Constructed from: QRA (1998), Paepe (1985) and Frake (1979).

Figure 2.2: The Geological Time Scale, ancient Ice Ages, Quaternary and Holocene climatic changes

Within each Ice Age there exist remarkable fluctuations known as glacials and interglacials of cold and warm phases that correspond to cycles of about 100,000 years. It is widely believed that earth's orbital effects cause the cycles. These glacial and interglacial cycles were first recognised by Croll (1864) and then worked out by Milankovitch (1941), a Yugoslav scientist who showed that the cycles correspond to three variables in the earth's orbit. He calculated the radiation input at different latitudes as a function of time and hence he inferred temperature changes as a function of time.

Most important of these variations is the eccentricity cycle of 93,408 (100,000) years, this is the variation of the orbit from its almost circular path. This affects the spin rate of the earth-moon system, which increases when the earth and the moon are closer to the sun. The lower the spin rate, the stronger is the earth's magnetic field, which, in turn tends to screen off the incoming particles of high energy from the sun, thereby cooling the climate. The second of the orbital cycles is the change in the tilt of the earth's equatorial plane, the obliquity, in relation to its orbital plane over a period averaging 41,000 (40,000) years. About 25% of the glacial and interglacial temperature variations are due to this change. The third orbital phenomenon is the 25,920 (25,000) years precession cycle, which is similar to the wobble of the spinning top, (Lowe & Walker, 1987 and figure 2.3).

Since the Milankovitch discovery it has been shown again and again by research that the earth's climate during the Quaternary has been characterized by a succession of cold and warm periods known as glacial-interglacial cycles. The periodicity of these cycles corresponds to those of the earth's orbital parameters as mentioned above (i.e. precession-23Ka, obiquity-41Ka and accentricity-100Ka). The astronomical theory of climate in which the orbital variation are taken to drive the climatic changes has been successful in explaining many features of the paleoclimatic record, (Hays *et al.*, 1976, Howard 1977, Berge 1978, Imbrie, T. & Imbrie, J. 1980, Imbrie *et al.*, 1984, Paepe *et al.*, 1990, Muller & MacDonald 1995, Paillard 1998, and Van Ovaloop, 1998).

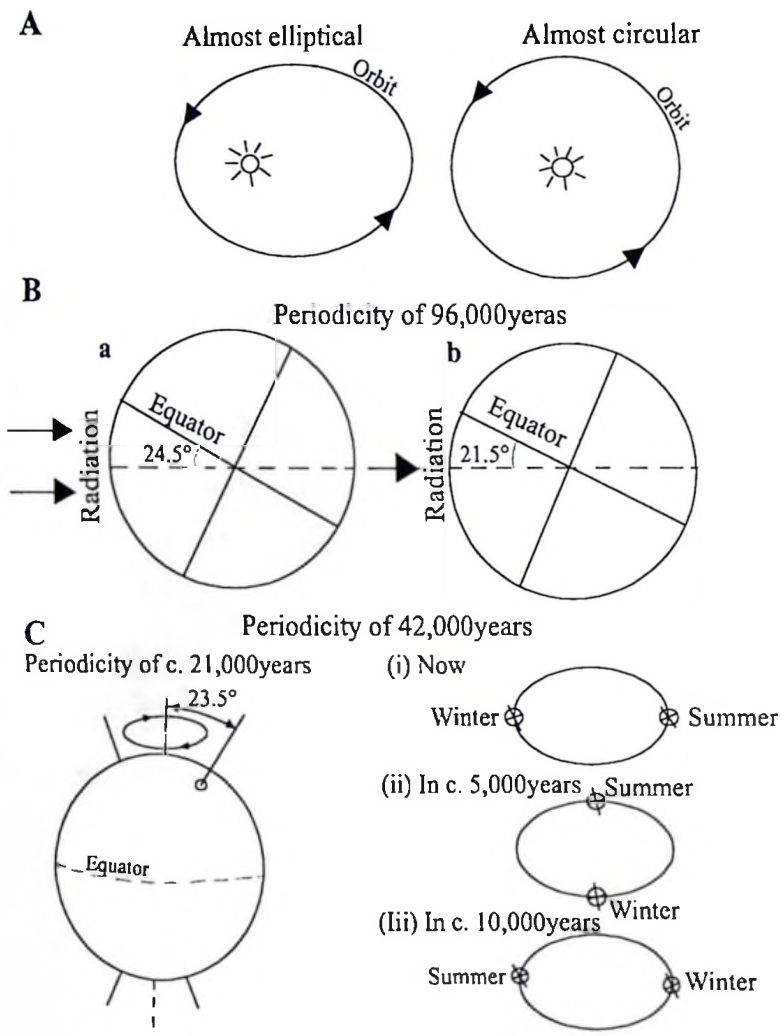

Figure 2.3: Astronomical enforcement of climate. [Orbital and axial variations affecting receiption of solar radiation on the earth's surfacc: A = Eccentricity of the orbit. B = Obliquity or axial tilt. C = Precession of the aquinoxes (right) resulting from wobble of the earth's axis.] (From Lowe and Walker, 1987).

Another element involved in the climatic change apart from the precession cycle is the geographic positions. Besides the blocked seaways of the present ice age, most of the Northern Hemisphere is land that generates a continental climate, whereas the Southern Hemisphere is encircled by a continuous seaway that provides far more maritime climates. For example, a study by Blunier *et al.*, (1998) indicates that Arctic warming

events around 36Ka and 4Ka lag their Antarctica counterparts by more than 1Ka. If the land and sea were uniform in both hemispheres, the precession effect would be canceled out.

Many recent studies indicate that Milankovitch's cycles do not fully account for the timing of events in the recent glacial/interglacial cycle, (McCabe & Clark 1998). Some researchers propose that other large-scale influences, including feedback from change in ocean currents, (Crowley & Kim, 1996 and Mann et. al, 1998) are equally important. These short-term oscillations have been tentatively linked to solar influences and/or ocean circulation patterns. The exact causes of these short periodicities remain unknown, (Stager *et al.*, 1997).

The Quaternary Ice Age is a series of glacial/interglacial cycles which can be recognised by sedimentation regimes, table isotope studies, floral & faunal changes, palaeosol sequences and many other scientific parameters as discussed earlier in chapter 1. This study will exploit the presence of palaeosols in sedimentary sequences as a tool to picking the climatic changes of the Quaternary geological past.

CHAPTER THREE

THE STUDY AREAS

3 THE STUDY AREAS

3.0 GENERAL INTRODUCTION

This chapter provides background information on the studied areas. The information is given in terms of location, physiography and climate. Olduvai Gorge is the main area of study, while Manonga-Wembere Valley and Holili localities are treated as minor (annex) study areas. Olduvai Gorge (Serengeti plains) & Holili (Mount Kilimanjaro volcanic fields) both located in NE Tanzania and Manonga-Wembere valley in Central Tanzania (figure 1.1 – chapter 1).

3.1 OLDUVAI GORGE

Olduvai Gorge is among the most important hominid sites in the world, which has also yielded abundant animal fossils and fossil traces. The uniqueness of Olduvai Gorge both as a scientific study area and its natural beauty has been expressed by different people since its discovery. For instance, Prof. Simpson wrote:

" ...There is no spot on earth more fascinating and more deeply significant for all of us than Olduvai Gorge. It has, to begin with, extraordinary scenic beauty. In one-direction stretches the great, open Serengeti Plain, broken here and there by hills that are massifs of old, weathered rock piercing the younger sediments. In the opposite direction is the rifted Balbal depression and, beyond it, the towering slopes of Ngorongoro Caldera... " (Simpson, 1967).

Hillary Clinton when she visited the Olduvai Gorge in 1997 had this to say:

"...I spent few hours in one of the World most important archaeological sites, the Olduvai Gorge in Northern Tanzania...Walking through this archaeological gold mine was nothing short of extraordinary... In the walls of the gorge we could see layers of geological development, which correspond with biological changes in the development of humankind. As much as the reservoir of scientific information the gorge is yielding I was moved by the massage of humanity imbedded in its walls. The Olduvai Gorge offers a lesson that no matter how different human being are on the surface; ultimately we come from the same place. We share a common ancestral home. And in the end no matter our gender, the tone of our skin or the God we believe in – no matter the wide oceans or expanses of land that separate us we are part of the same human family..." (Clinton, 1997)

Olduvai means OLDUPAI (wild sisal in Masai language). OLDUPAI is a sisal-like plant species *'Sansevieria ehrenbergiana'*, which is widespread in the area. The word Oldupai was mis-pronounced as OLDUVAI by Prof. Kattwinkel of German in 1911 (Leakey *et al.*, 1976). Prof Kattwinkel was studying butterflies of the Serengeti plains when he accidentally entered the gorges. From that time this area has been known as OLDUVAI GORGE.

Olduvai Gorge area is well known for its continuous sedimentary deposits. Nearly two million years of deposit were laid down in an orderly sequence, each new layer above the earlier one without many disturbances (Hanbay & Bygott 1992). This unique geological sequence of Pleistocene deposits, which are exceedingly rich in fossil fauna as well as long stages of earlier stone age culture (Leakey 1967) has attracted multitude of international and local scientists to study this Quaternary sequence. The area has therefore, continuously been studied since this time (1911) to the present time.

3.1.1 Location and accessibility

Olduvai Gorge area is located in the Ngorongoro conservation area. The Ngorongoro conservation area is located in the Arusha region of Northern Tanzania, southeast of the Serengeti National Park. It is within 2°30`S – 3°30`S latitudes and 34°50`E – 35°55`E (figure 3.1) (WCMC, 1998). The Olduvai Gorge area is about 200km from Arusha Town.

The area can be reached using the Arusha-Musoma road of which the first 90km stretch to Makuyuni is a tarmac road part of the "great north road" across Africa, from Johannesburg (South Africa) to Cairo (Egypt). The rest stretch (from Makuyuni) is all weather gravel road. This former stretch runs though the Gregory (Manyara-Natron) rift, Karatu Township and enters the Ngorongoro conservation area, which contains the study area (The Olduvai Gorges).

3.1.2 Physiography

The area is divided into two distinctive physiographic/geomorphologic zones. The eastern part is a volcanic massif-highland (3000m above sea level) composed of extinct volcanic cones (Oldeani, Lemagruti, Sadiman, Ngorongoro and Olmoti), developed along a NE-SW Eyasi rift, (Figure 3.1). This highland is known as the Ngorongoro highlands. The western zone is flat lowland (1600m above sea level), occasionally pierced by inselbergs of an old peneplain. This is the northeastern part of the vast Serengeti plains.

The Olduvai Gorge is long erosion canyon formed by running water in this part of the Serengeti. The gorge has exposed spectacular Quaternary geological sequence. The gorge has two tributaries, the Main Gorge and the Side Gorge. The main gorge is 55km long, containing most of the hominid sites and the side gorge is 45km long. The latter contains the Laetoli *Australopithecus afarensis* footprints. Both gorges have a maximum depth of 130m running generally from west to east and draining their waters into the Albalbal depression. The catchment area for the main gorge is the western side of Lakes Ndutu and Masek and that of the side gorge is the Sadimani volcanic mountain chain.

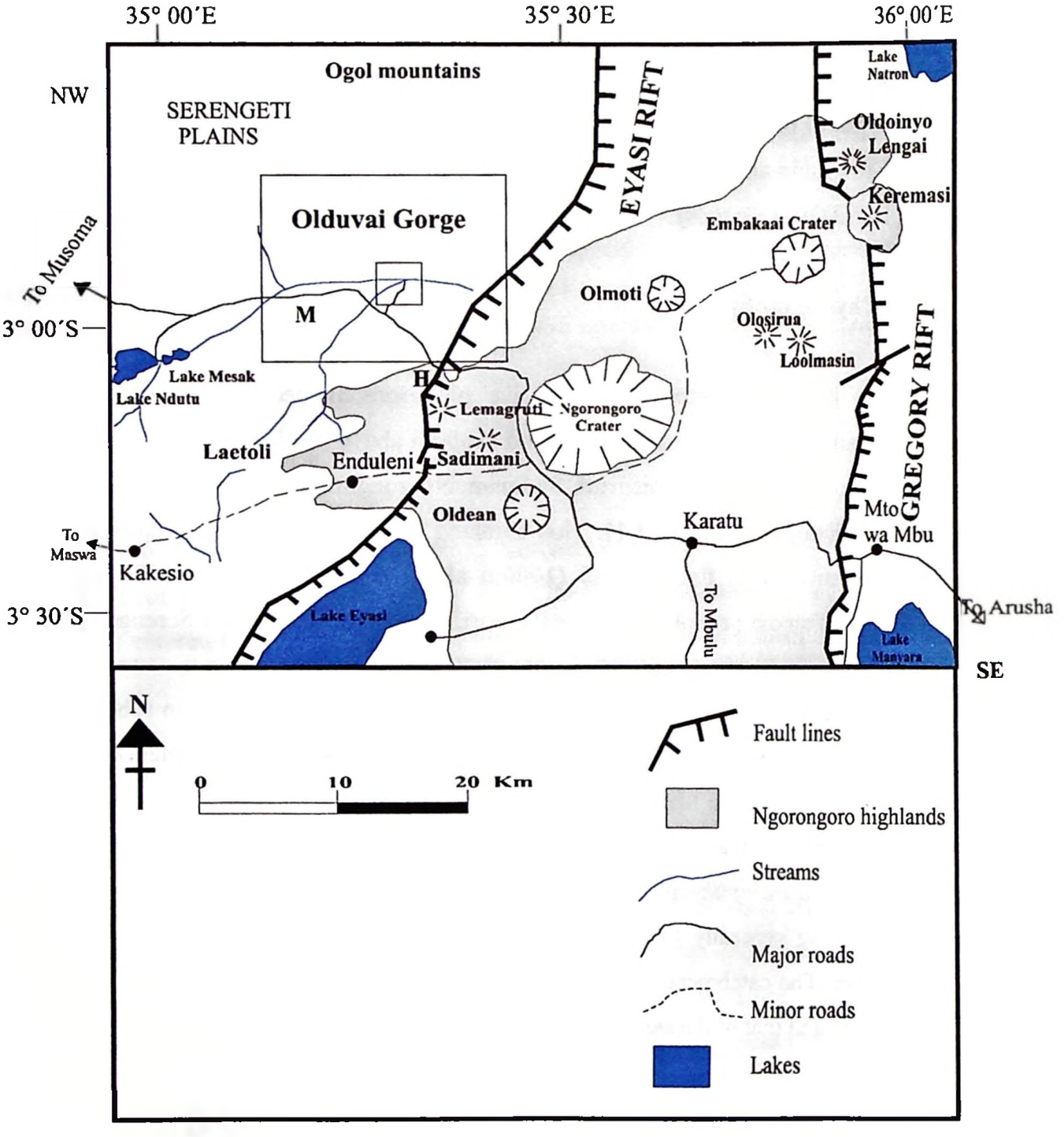

Figure 3.1: Location map Olduvai Gorge and Ngorongoro highlands.

3.1.3 Climate and environment

Climate - Rainfall and temperature

Because of the great geomorphologic variations there is a great variation in the climate of the area. The climate of the area therefore varies from semi-arid to wet tropical climate with two distinctive wet and dry seasons per year.

The wet/rainy season is between the months of November to May and the dry season is from June to October. In the highlands it is generally moist and humid tropical climate. These areas receive more rainfall due to their high relief. The annual rainfall is between 700mm and 1700mm. The mean annual temperature of the highlands and its neighborhood is between 10°C and 25°C, however.

The Lowlands including the Ngorongoro crater floor has a semi-arid climate. Annual rainfall in these areas is below 500mm and during the dry seasons it is a very dry desert environment. The average annual temperature of the lowlands is 25°C. The hottest month (August) has average temperature of 32°C while the coldest month (May) has average temperature of 18°C to 20°C.

Environment - Soil, flora and fauna

As a result of wet climate the soils of the Ngorongoro highlands are dark to dark-red, developed on volcanic rocks and ashes. This type of soil is very fertile. Scrub heath and remains of thick montane forests with shrubs and few grasses thus cover the area. Fertile soil and reasonable rainfall support this thick vegetation cover. The typical vegetation of this area includes tree species like, *Acacia lahai, Acacia seyal, Croton macrostachyus, Nuxia congesta, Celtisafricana, Albizia gummifera* etc. This forest canopy of the steep slopes of the highlands is mixed with shrubs (climbers and herbs) like *Crotalaria agatiflora, Veronica auriculifera, Pterolobium stellatum* and *Senecio hadiensis* (Hanby and Bygott, 1992).

The plains (Serengeti and Salei) including, the Ngorongoro crater floor are covered by white to gray soils grading to dark clay soils in areas with stagnant water bodies. Soils rich in carbonates are also very common. The white-gray soils were derived from volcanic ash falls and pyroclasts, while calcrete soils are result of in situ weathering of old lakebeds. Mainly grass and few shrubs cover this area. The typical flora of the Olduvai Gorges is the yellow-green succulet spear-like leafed Oldupai flora *'Sansevieria ehrenbergiana'*. Others are *Aloe volkensii, Acacia mellifera*, etc. The plains are open grasslands covered by typical grass species like, *Cynodon dactylon, Digitaria macroblephara* and *Andropon greenwayi* (Kafumu, 1995).

This area has a large concentration of fauna; thanks to the floral abundance the area (Serengeti Plain and Ngorongoro crater) has the highest concentration of wildlife on earth. There is a large population of wild animals (table 3.1).

Table 3.1: Representative large fauna of the Olduvai Gorge area (Source: WCMC, 1998b).

Type	Name	Scientific name	Population
Herbivores	Wildebeest	*Cannochates taurinus*	7,000 (Ngorongoro Crater), 1.7million (Serengeti Plains)
	Buffalo	*Syncerus caffer*	4,000
	Zebra	*Equus burchelli*	4,000 (Ngongoro Crater), 260,000 (Serengeti Plains)
	Eland	*Taurotragus oryx*	3,000
	Grand gazelle	*Gazella granti*	3,000 (Ngorongoro Crater) 470,000 (Serengeti Plains)
	Thomson gazelle	*Gazella thomsoni*	3,000
	Mountain reedbuck	*Redunca fulvorufula*	
	Water buck	*Kobus ellipsiprymnus*	
	Dik-dik	*Rhychotragus kirk*	
	Black rhinoceros	*Diceros bicornis*	10
	Elephant	*Loxodonta africanus*	29 (Ngorongoro Crater)
Carnivores	Lion	*Panthera leo*	68 (Ngorongoro Crater)
	Spotted hyna	*Crocuta crocuta*	
	Cheetar	*Acinonyx jubatus*	
	Wild dogs	*Lycaon pictus*	
	Golden cat	*Felis aurata*	
	Leopard	*Panthera pardus*	
Birds	Ostrich	*Struthio camelus*	
	Kori bustard	*Choriotis Kori*	
	Eagles	*Aquila verreauxii*	
	Vulture	*Neophron percnopterus*	
	Sunbird	*Nectarinia reichenoswi,*	

3.2 MANONGA-WEMBERE VALLEY

The word Manonga means 'shells' in sukuma language. The sukuma people gave the name *Manonga* to the river, which seemingly contained a lot of fresh water snails and bivalves. Wembere is a Swahili translation of Ibhembele/Mabhembele in sukuma language. Ibhembele/Mabhembele literally means water adapted tall grass floral species, which flourish in the swampy soils of the lowland environments of the eastern part of the area, "the Wembere steppe".

The Manonga-Wembere Valley is a drainage system made up of the Manonga River in the northern part and the Wembere swamp in the south. The area had received considerable attention in the 1920's – 40's. For example, several fossil localities earlier dated as Middle Pleistocene were found and collected by C. Grace in 1929 at a now obsolete village name of Tinde, today known as Ibole (Stockely, 1930). Other several studies (Hopwood 1931, Teale 1931 and William & Eades 1939,) followed later to map in detail the geology of the area.

Mineral exploration for gold and basemetals became common during the 1980's. There was also geological mapping of QDS 100 and QDS 120, which covers part of the Wembere steppe in the 1990's (Petro and Mafwimbo, 1994 and Petro and Hakika, 1994). The results of these studies are not yet published. Terry Harrison launched a paleontological expedition in 1992 – 1994 to study the paleoenvironments of the Manonga river valley based on paleontology and the results have been published (Harrison & Mbago 1997).

3.2.1 Location and accessibility

Manonga-Wembere Valley is located in Central Tanzania within Latitudes 3°45`S to 4°10`S and longitudes 33°00`E to 3°00`E (figure 3.2). This area can easily be reached. One can approach the area from Singida across the Sekenke fault or from Mwanza, Shinyanga through Nzega or from Tabora by quite good mouram-gravel roads. Locally

the Manonga-Wembere area is accessible during the dry season due to its flat-vast plain geomorphologic characteristics. During this time most of the ephemeral rivers and streams are dry and the remotest areas can practically be reached by car. But during the rainy season the area is muddy and with numerous active rivers, streams and gullies making it impassable.

3.2.2 Physiography

The following account is mainly based on the authors field observations and experience (born and grew in the area – domicile home area and spend 3 years from 1993 in gold exploration in the area). The area is basically a low-lying flat land with low relief elevations of between 1000m to 1300m (a.s.l) broken here and there by remnant of ancient inselbergs of old Precambrian rocks. The Manonga-Wembere basin lies in the Singida, Shinyanga and Tabora regional administrative areas. It consists of two drainage systems – The Manonga river drainage system and the Wembere swamp drainage system.

The Manonga river valley is a sag basin related to the Lake Victoria down warping (sag) basin. The drainage system flows from west to east drawing its water into the Kitangiri Lake near the Eyasi basin. The catchment areas include the Isaka highlands in Kahama district in the neighborhood of Isaka settlement. Several notable tributaries bring significant volumes of water into the Manonga Valley. They include the Mwadui, Kishapu and Shinyanga catchment areas (figure 3.2). During the rainy season the ephemeral Manonga River discharges large amounts of water flowing well above bridge levels. It is sometimes dangerous to human life and property. In the rainy seasons of 1997 (El Nino effect), the violently rushing Manonga River tributary water near the village of Mbutu drowned several people who were trying to cross the river.

The Wembere swamp drainage system, contain the Wembere River flowing from southwest towards the Lake Kitangiri. The two systems (Manonga and Wembere) meet just before entering the lake. The Wembere steppe-swampy area has varied catchment areas consisting of the Iramba Plateau in the east and the Mngazi-Itumba-Susujanda

granite highs in the west (figure 3.2). This basin is related to the east African fault system. It is probably the continuation of the eastern arm (Bahi-Kilimatinde fault). The rift system seems to be intercepted by the east west down warping (Manonga Valley) before joining the southern part of the Eyasi rift.

The Iramba Plateau is the eastern elevated block of the fault system marked by the Sekenke fault line. The Mngazi-Itumba-Susujanda granite high is the western block of the elevated faulted block. It is marked by several alluvial fans all along the fault zone of which some of them are diamondiferrous. The two elevated blocks acts as the main catchment areas supplying water to the central Wembere graben which in turn slowly empties the water into the Kitangiri Lake.

3.2.3 Climate and Environment

Climate - Rainfall and temperature

Manonga-Wembere Valley is hot and dry with average annual rainfall of between 700mm – 900mm during the rainy season. There are two distinct climatic seasons in the area, the dry and the rainy season. June to November is the dry season and the Months of January to April are the rainy season. During the dry season the area is very dry and most of the rivers are also dry. The mean annual temperature in the area is between 20°C to 27°C.The Wembere swamp was a permanent swamp until the 1970's, when for the first time it dried out in 1973. The 1997- El Nino rainfall (>1700mm per year) caused the swamp to attain the 1961 levels. Since then it has again become (at least for now) a permanent water body.

Environment - Soil, flora and fauna

The basins (especially the Manonga valley) are composed of fertile black clay cotton soils which support cotton growing, the major cash crop in the area. The Sukuma people are famous for cotton production. To the east (Wembere) the soils are white to dark-gray mbuga soils usually not suitable for agriculture.

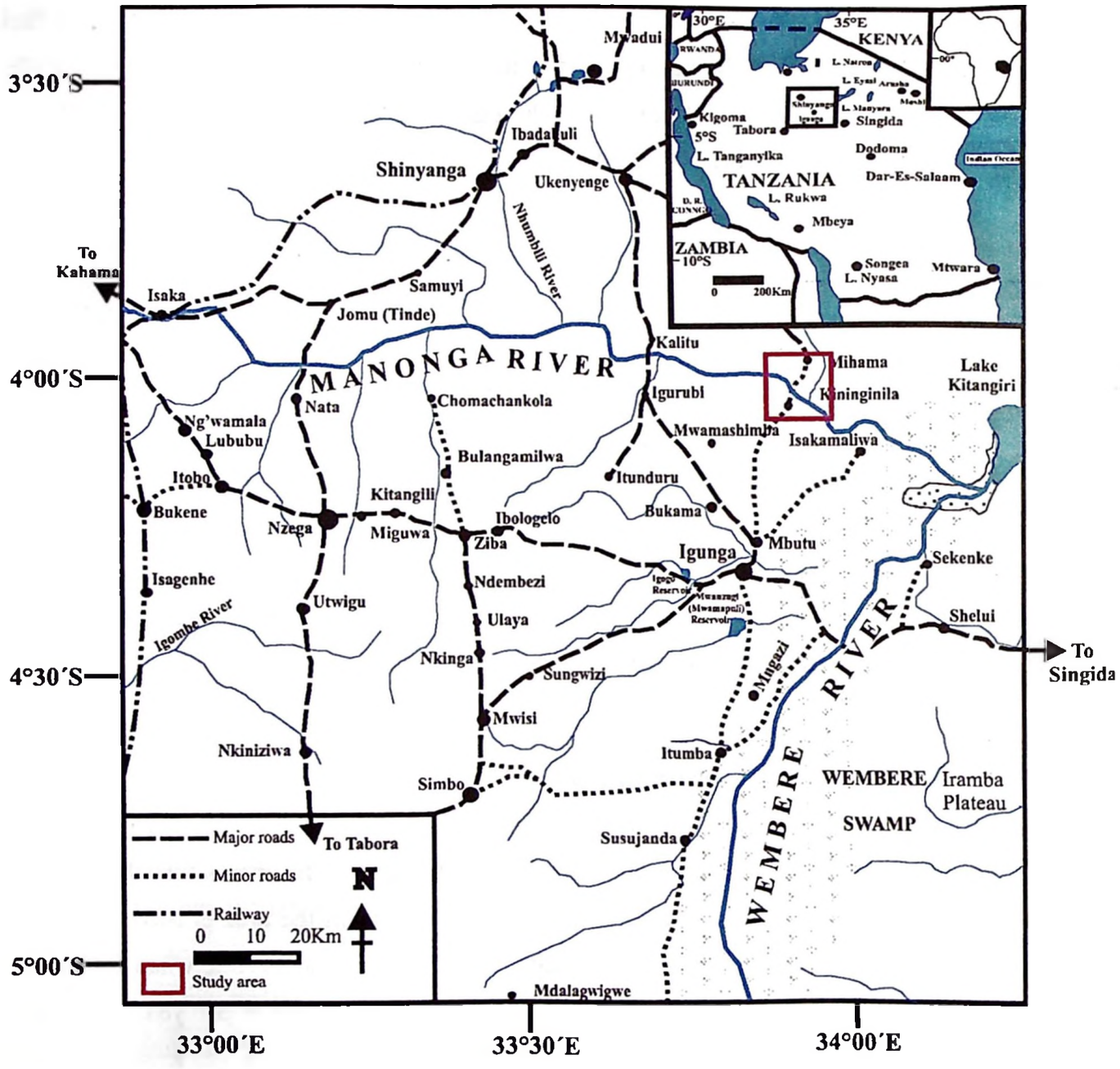

Figure 3.2: Location map of the Manonga-Wembere Valley (Red squre indicates the study locality - Kininginila).

However, the plains are rich in grass suitable for cattle raring. Manonga-Wembere valley area contains the highest concentration of cattle in Tanzania. Thorn bushes shrubs and short grasses dominate the flora. The common tree species of the thorn bushes include the *Acacia-commiphora-Lanea* floral association mainly concentrated in the Manonga river valley (Harrison and Mbago, 1997). The highlands surrounding the Manonga-Wembere valley are covered by dark red to brown fertile soils. These soils support the miyombo woodland with tree species like, *Julbernardia, Isoberlinia,* and *Brachystegia* (Harrison and Mbago, 1997). The Wembere plain is mainly open lowland comparable to the Serengeti Plain. It is sometimes considered as the southern extension of the Serengeti. Typical short grass flora includes *Digitaria macrobleaphara, Andropogon greenwayi* and *Sporobolus ioclados*. This type of grass is designed to provide enough food for grazing wildlife and domestic animals. The grasses are adapted to fast growing during the rainy seasons; they rapidly put an abundance of leaf and seeds providing forage for the animals and for the next future floral boom (the following next season).

The fauna of the Manonga Wembere valley was once (1960's and 70's) abundant grazing mainly around the shores of the Wembere swamp, that is eastern part of the Manonga River Valley, the Iramba Plateau and the margins of the western elevated fault block. Thes areas were rich in fauna (and flora) including the endangered white and black rhinoceros. In the mid-sixties we used to graze cattle among huge herds of wildlife in the Wembere plains. Lions were much more abundant sometimes attacking our cattle during the day. Today there is scarce game. Occasionally lions are heard roaring during the night and especially during the rainy seasons.

Due to population expansion accompanied by extensive hunting the animals have continuously been reduced to small numbers and some have been extinct in the area. Some still live in the forests west of the Wembere swamp concentrated mainly around Mwamampuli dam near Igunga Town. Here and there in the Wembere plains zebras, giraffes, wildebeests, Thomson gazelles, grand gazelles and the small (dik-dik) are common in the areas during the rainy season. The large fauna of the area is summarized in table 3.2.

Table 3.2: Common large fauna of the Manonga-Wembere valley (Own experience – Scientific names are from Fitzpatrick, 1999)

Name	Swahili name	Sukuma name	Scientific name
Elephant	Tembo	Mhuli	*Loxodonta africanus*
Buffalo	Nyati	Mbogo	*Syncerus caffer*
Wildebeest	Nyumbu	Mbushi	*Connochaetes taurinus*
Zebra	Pundamilia	Ndhulu	*Equu burchelli*
Hippopotamus	Kiboko	Ngubh'o	*Hippopotamus amphibius*
Giraffe	Twiga	Nhiga	*Giraffa camelopardalis*
Giant eland	Pofu	Mboku	*Taurotragus derbianus*
Eland	Kongoni	Nimba	*Taurotragu oryx*
Kudu	Tandala mkubwa	Nhandala	*Tragelaphus strepsicerosx*
Antelope?	Tandala	Nhandala	*Gazzella ...?*
Grant's gazelle	Swala granti	Lala nhale	*Gazella granti*
Thomson's gazelle	Swala tomi	Lala	*Gazella thomsoni*
Wild (black) pig	Nguruwe mwitu	Ngurubhe/njemu	*Potamochoerus porcus*
African rabbit	Katita sungura	Lung'wando masanga	*Poelagus marjorita*
Hare	Katiti sungura	Lung'wando kabhumbu	*Lepus crawshayi*
Stripped hyena	Fisi	Mbiti mlhulhu	*Hyaena hyaena*
Lion	Simba	Nshimba	*Panthera leo*
Wild dog	Mbwa mwitu	Mhuge	*Lycaon pictus*
Leopard	Chui	Nsubhi	*Panthera pardus*
White tailed mangoose	Mkia mweupe	Keye	
Warthog	Ngiri	Nghili	*Phacochoerus aethiopicus*
Cheetah	Duma	Nsubhi mondo	*Acinonyx jubatus*
Dik-dik	Dikdik	Subhuya/Digidigi	*Madoqua kirk*
Mole	Panya buku	Fuko	
Porcupine	Nungunungu	Nhunghu	*Hystrix africaeaustralis*
Wild rat	Panya pori/ndezi	Ngoso	*Thryonomys sp.*
Dwarf mangoose	Nguchiru mdogo	Njololo/Nghala	*Helogale parvula*
African hedgehog	Kalunguyeye	Jilunghuminghwa	*Atelerix albiventris*
Civet	Fungo	Nhungo	*Viverra civetta*
Spotted hyena	Fisi	Mbiti	*Crocuta crocuta*
Aardwolf	Fisi mdogo	Mbiti mlhulhu	*Proteles cristatus*
Common jackal	Mbweha	Jidevwe	*Canis aureus*
Serval	Paka mwitu	Nyilili	*Felis serval*
Wild cat	Paka shume	Kimbhulu	*Felis lybica*
Spring hare	Abunuasi	Huuna/mendegere	*Pedetes capensis*
Yellow mangoose	Kicheche	Lonzwe	*Galerella sanguineus*
African Baboon	Nyani	Nghuku	*Papio anubis*
Servet (green) monkey	Ngedere/tumbiri	Nthumbili	*Cercopithecus aethiops*
Golden jackal	Mbweha	Jidevwe	*Canis mesomelas*
Aardvark/ant eater	Muhanga	Naga	*Orycterepus afer*
Scaly anteater	Kakakuona	Ngakakubhona	*Manis temminckii*
Squirrell		Kanono	
Small spotted genet	Paka mwitu	Nyilili	*Genetta tigrina*
Honey bedger	Nyegere	Negele	*Mellivora capensis*
Tortoise (land turtle)	Kobe	Gulumati	
Caracal	Simba mdogo	Nshimba mangu	*Felis caracal*
Mole	Panya buku	Fuko	
Klipspringer	Mbuzi mawe	Nghulughulu	*Oreotragus oreotragus*
Rock hyrax	Pimbi	Mphimbi	*Procavia capensis*
Variety of snakes	Nyoka	Nzoka	*Reptiles*
Ostrich	Mbuni	Nongu	*Struthio camelus*
Variety of other birds	Ndege	Nhoni	*Eves*
Duiker	Minde	Mphongo	*Cephalopus spadix*
Impala	Swala pala	Mphala	*Aepyceros melampus*
Common mangoose	Nguchiru	Njololo /Nyalukala	*Herpestes sanguineus*
Banded mangoose	Nguchiru	Njololo /Nyalukala	*Mungos mungo*

3.3 HOLILI CALCAREOUS DEPOSITS

This area is part of the Kilimanjaro volcanic field located at the southern foot of the mountain near Holili at the Tanzania-Kenya borderline. The area contains thick volcanic calcareous grit deposits, which are presently worked out for brick by local communities.

A fossil bone (fragmented by mining activity) was unearthed by the artisan miners and was collected and brought to the Geological Survey in Dodoma by a geologist, Mr F. Mbawala who was working in a project to evaluate the economic potential of the gritstone for commercial production of bricks. In his memo to the Assistant Commissioner for Geology about this found Mr. Mbawala wrote:

"...Fossil bones from the lower beds of Pleistocene calcareous tuffaceous grits at Holili are suitable for absolute age determination of Holili bulding stone deposits,...They could be hominid skeletal remains of Pleistocene times affected by pa hoe hoe (violent volcanic eruption) disaster...The skull remains to be discovered in the locality..." (Mbawala, 1995).

Having examined the bones the author was convinced that this area could yield sufficient fossil mammal bones and including probably hominid remains and their associated cultures. The author organized a field trip in summer 1996 for a brief field mapping and examination. In this field trip the area was geologically mapped and some new discovery of fossil leaves, wood and hominid tools associated with chopped bones and tooth was made. The area was then included in this study for further research.

3.3.1 Location and accessibility

Holili area refered in this study lies between latitude 3°18`S to 3°22`S and longitude 31°37`E to 37°42`E within the Kilimanjaro Mountain volcanic field. This volcanic field is a mountain massif rissing abruptly from the plateau country at about 2,000m a.s.l and ends up on the Kibo Uhuru peak of 5,896m a.s.l, the highest point on the African Continent (figure 3.3). The area can be reached from Moshi or Same towns using the Dar-Es-Salaam – Arusha highway. Holili is 35km away from Moshi Town towards Same

Town. Branching off to the left after 25km towards Himo along the Himo – Mombasa road 10km from the junction you arrive at Holili settlement at the Tanzania-Kenya border near Taveta Town in Kenya.

3.3.2 Physiography

The area is a gently undulating topography of between 1,000m to 1,600m above sea level relief dissected by ephemeral streams. These highly incised streams form steep gorges of up to 20m high cliffs. The drainage pattern runs from NW to SE towards Kenya. The catchment area is the Kilimanjaro highlands of Rombo and Marangu north of the area.

3.3.3 Climate and environment

Climate – Rainfall and temperature

The area has two sets of wet-rainy seasons: November to December (called, *Mvua za vuli* in Swahili) and March to May (known as *Mvua za masika*). The driest months are August and October. The areas contain variable rainfall range, which decreases rapidly with altitude. The lower altitude belts of the mountain (<1800m a.s.l) is usually inhabited by humans and receives precipitation of between 1700mm to 2000mm per annum. The upper forest zones rising to the peak of the mountain is a protected zone gazetted by the Government of Tanzania as a National Park in 1973 (WCMC, 1998a). This area was also inscribed as a World Heritage Site in 1989.

The National Park Forest zone covers altitudes between 1800m and 2500m a.s.l and receives a mean annual precipitation of between 1300mm and 2300mm. The rainfall drops to about 500mm per annum at altitudes above 2700m a.s.l. Above 4,600m altitude the area is a desert with mean precipitation lower than 200mm per annum. Temperatures are very variable in this area ranging from 10°C to 25°C in the areas inhabited by people while as one goes higher temperature drops to freezing polar temperatures.

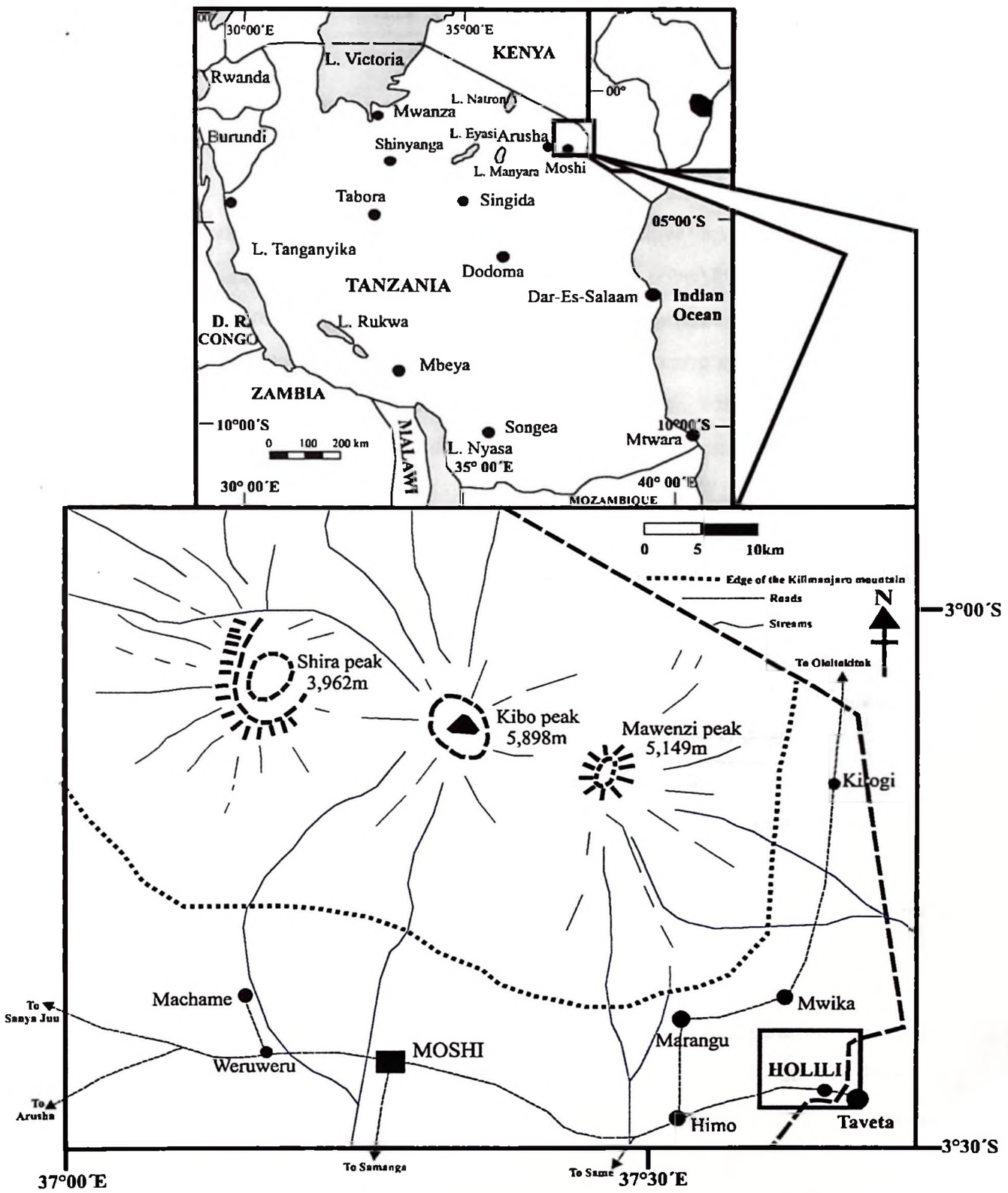

Figure 3.3: Location of the Kilimanjaro mountain volcanic field [Holili locality is in the SE edge of the field]

Environment – Soil, flora and fauna

The lower flank of the mountain is covered by fertile black to red soils derived from volcanic lava, tuffs and agglomerates. This type of soil is very suitable for coffee and banana production. The higher forest belt (Kilimanjaro National Park) is essentially a montane wet forest with a variety of flora trees like, *Podocarpus spp.*, *Ocotea usambarensis* and *Myrica salicifolia*. Others are fern trees species like *Cyathea spp.* and *Lobelia gibberoa*. *Juniperus procera* and *Olea spp.* dominate the drier slopes. The upper belts' flora varies a great deal, of which some are only restricted to the Kilimanjaro area. Such flora includes heath and shrub species like, *Protea kilimandscharica*, *Stoeba kilimandscharica* and *Philippia trimera*. The fauna of the Kilimanjaro area is much recorded above the tree (forest line) includes animal species as summarized in table 3.3.

Table 3.3: Some of the fauna of the Kilimanjaro National Park (Source: WCMC, 1998a).

Name	**Scientific name**
Grey duiker	*Sylvicapra grimmia*
Eland	*Taurotragus oryx*
Bushbuck	*Tragelaphus scriptus*
Red duiker	*Cephalophus natalensis*
Buffalo	*Syncerus caffer*
Elephant	*Loxodonta africana*
Leopard	*Panthera pardus*
Mountain reedbuck	*Redunca fulvorufula*
Tree hyrax	*Dendrohyrax validus*
Abbott's duiker	*Cephalophus spadix*
A variety of birds	

CHAPTER FOUR

THE GENERAL GEOLOGICAL SETTING AND THE REGIONAL QUATERNARY GEOLOGY OF TANZANIA, "A general review".

4 THE GENERAL GEOLOGICAL SETTING OF TANZANIA

4.0 INTRODUCTION

This chapter discusses in brief the geological setting of Tanzania followed by a review of the Quaternary deposits/sediments in terms of their composition and spatial distribution over the country.

4.1 THE GENERAL GEOLOGY OF TANZANIA

The general geology of Tanzania includes rocks of Precambrian to Holocene geological times. The stratigraphy is subdivided into 14 chronostratigraphical units (Teale 1936, Wade 1937, Quennell *et al.*, 1956, UNDP 1991 and Jenga 1998) and grouped into 5 (Archean, Proterozoic, Paleozoic, Mesozoic and Cenozoic) chronolithostratigraphicalal division of the geological time scale (figure 4.1b). The chronostratigraphicalal units of Tanzania are briefly summarized below and as per figure 4.3.

4.1.1 Archean rocks (3.2Ga – 2.5Ga)

The Priscoan and the Lower Archean eons are not represented in Tanzania, thus the oldest rocks known to date in Tanzania are the Upper Archean, the *Dodoman* (3.2Ga – 2.8Ga) system composed of granites, schists and pegmatite forming the Tanganyika Craton. These rocks occupy the central part of Tanzania, (Dodoma, Singida, Iringa and parts of Tabora and Arusha). *Nyanzian* (2.8Ga – 2.5Ga) rocks forming the Greenstone Belts of Tanzania overlie the Dodoman system. The later is composed of high-grade banded iron formations (BIF), green schist and amphibolite facies. The *Nyanzian* are also

highly granitized forming the granite kopjes and hills observed all across these areas, (figure 4.1a_{1-2}). They are the host rocks for most gold deposits of Tanzania. These rocks occur in the northern part of the Country (Shinyanga, Mwanza and Musoma). Overlying the Nyanzian rocks are the *Kavirondian* conglomeratic arkosic feldspathic grits and quartzite rocks. The Kavirondian rocks lie unconformably on the Nyanzian rocks. Their spatial distribution is only in the Musoma Mara region extending into Kenya, (figure 4.3).

4.1.2 Proterozoic rocks (2.5Ga – 0.57Ga)

Two rock zones are recognised in the Proterozoic, the older Lower Pretorozoic rocks constituting of high-grade metamorphic rocks (granulites, migimatites, marbles, amphibolites and pegmatites) mapped as *Usagaran, Ubendian* and *Ukingan* Systems. Usagaran rocks are part of the Mozambican orogenetic belt found in the eastern part of the Country stretching from Mozambique to Ethiopia. This orogeny formed the Uluguru and Usambara Mountain Ranges, (figure 4.1a_3).

The *Ubendian* and Ukingan are the SW cratonic accretion rocks. These rocks are composed of mainly shales, low-grade schists, phyllites and quartzites and some granite. The Karagwe-Ankolean system, which is oldest, contains granites with cassiterite of economic importance.

Bukoban and Buanji rocks overlie the former and extend to the Paleozoic. These rocks occupy the NW Tanzania (figure 4.3). Major plutonic bodies (gabbro, diorite, granodiorites, syenites, eclogite, etc.) were also emplaced during the Upper Proterozoic and Lower Paleozoic. They often intrude country rocks all over the country (Examples: Mbozi ferrosyenite complexes in Mbeya region, gabbro complexes of Bassuto, Arusha region, Zanzui ring structured body in Shinyanga region and the Iringa meta-anothositic complexes).

Figure 4.1a: Archean landscape. **1-2.** Granite kopjes around Mwanza town. These granite bodies are a result of a later granitization event which affected the high grade Nyanzian metamorphic rocks. The spherical shape of the granite boulders is due exo-foliation type of weathering. **3.** The Usambara mountai ranges near Same town in Kilimanjaro region.

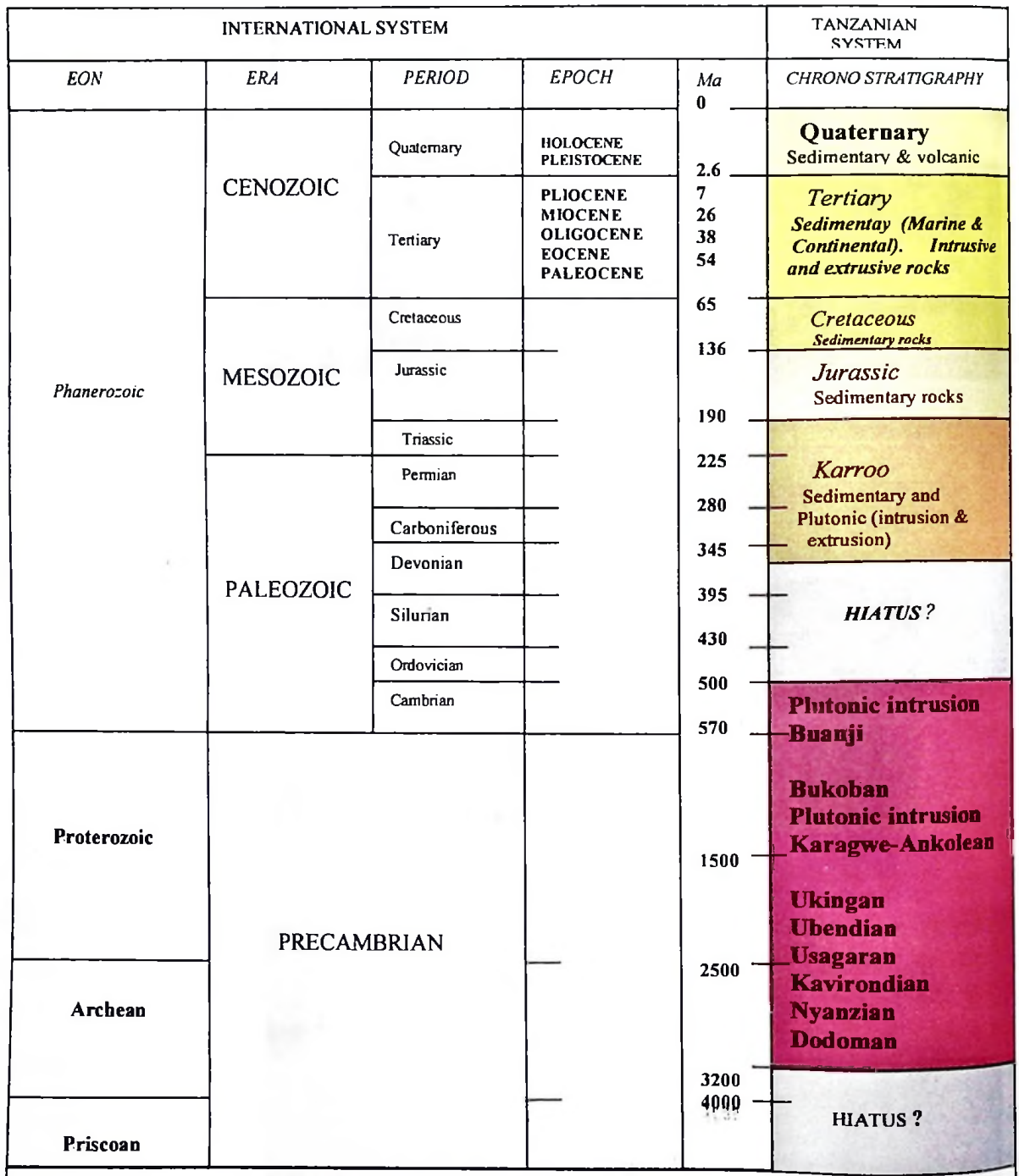

Figure 4.1b. Chronostratigraphical classification of Tanzania

4.1.3 Paleozoic rocks (0.34Ga – 0.19Ga)

Karroo rock system represent Paleozoic rocks in Tanzania. They occupy the upper part of the Paleozoic Era (Carboniferous and Permian) and extend to Lower Mesozoic (Triassic). A huge hiatus of (150Ma) exists between the Bukoban and the Karroo systems. Karroo

rocks are continental sediments mainly composed of shales, siltstone and sandstone. There is also a marked volcanic activity in the Karroo Period, where kimberlites and carbonatite bodies were emplaced. The Karroo rocks are the main host rocks for coal. Karroo sediments cover the eastern part of the country (figure 4.3) running parallel to the Usagaran system.

4.1.4 Mesozoic rocks (190Ma – 65Ma)

These are *Jurassic* and *Cretaceous* rocks in Tanzania. They are composed of continental-estuarine-marine sediments mainly limestone, claystone, shale and siltstone occupying the eastern part (figure 4.3) of the country. The Upper Mesozoic also contains significant intrusive and extrusive rocks (kimberlite, carbonatite and other related rocks). These bodies (kimberlite and carbonatite) are a source of diamond and pyrochloral minerals respectively.

4.1.5 Cenozoic sediments (65Ma – 0Ma)

The *Cenozoic* rocks are well represented in Tanzania. These sediments are divided into two parts, the lower part-*Tertiary* and the upper part-*Quaternary*. The Lower Cenozoic is mainly clay, sand, limestone and gravel, formed along the coastal strip and along lake and river systems. This period also marks the beginning of rifting in East Africa. In the later part of the Cenozoic (Pliocene-Pleistocene) rifting had already created a series of lakes responsible for the formation of much Quaternary sedimentary piles in the rift areas. Three parts of the rift system are recognised in East Africa (figure 4.2). They are the southern part, which formed Lake Nyasa basin, the western part consisting of Lakes Tanganyika and Rukwa basins. And the eastern part with Lakes Manyara, Eyasi, and Natron basins. Rifting was accompanied by widespread volcanism. These areas are therefore the home of thick volcano-sedimentary sequences of archaeological importance. The Quaternary sediments that form the upper part of the Cenozoic sediments of Tanzania are widespread in the country. Their composition and distribution are further discussed in section 4.2, (figure 4.4).

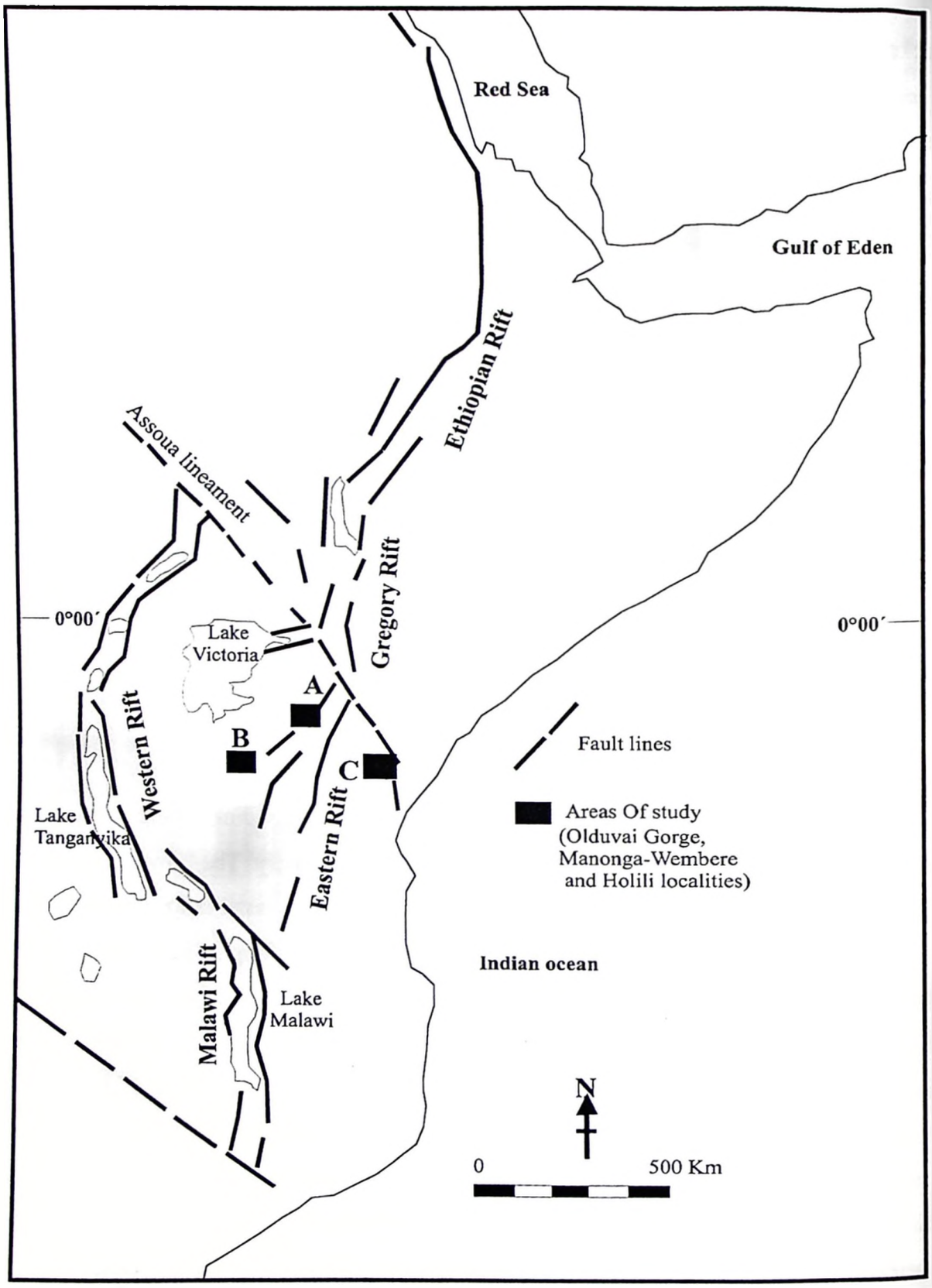

Figure 4.2: The Eastern African Rift system (Study areas; A = Olduvai Gorge, B = Manonga-Wembere Valley and and C = Holili)

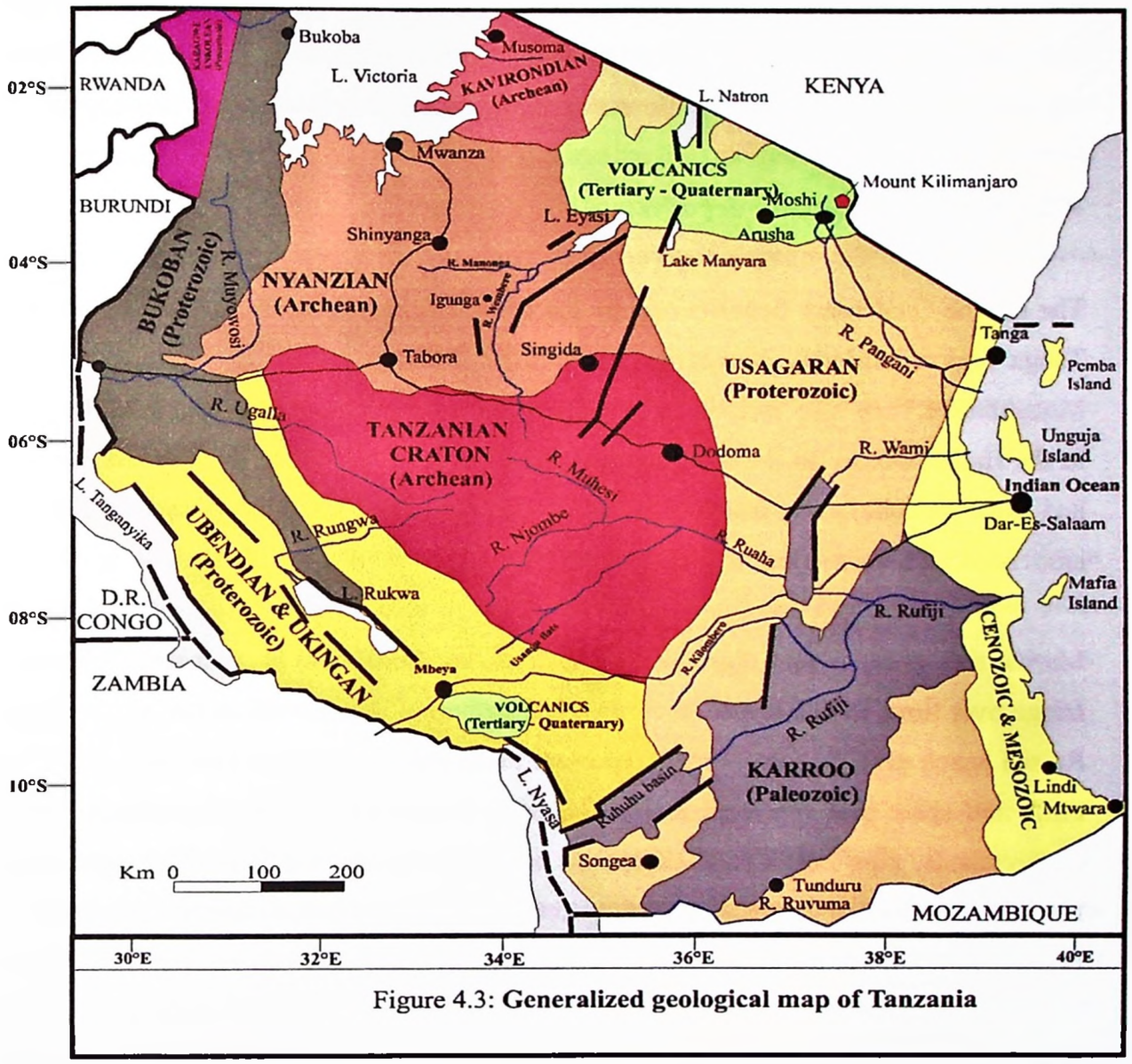

Figure 4.3: **Generalized geological map of Tanzania**

4.2 QUATERNARY DEPOSITS OF TANZANIA – A GENERAL REVIEW

This chapter discusses the general Quaternary geological setting of Tanzania. It gives a short inventory descriptive list of the main Quaternary deposits of Tanzania. This is a general review of the Quaternary geology of Tanzania. The list is not exhaustive but serves the purpose of highlighting the extensive presence of Quaternary deposits in the country, (figure 4.4).

Their importance to the global paleoclimatic studies and commercial significance are specifically pointed out. These deposits indicate a countrywide spatial distribution and are generally grouped into two main groups, the marine and the continental deposits. Figure 4.4 forms the basis of the discussion in the proceeding sections of this chapter.

4.2.1 Marine Quaternary deposits

The marine Quaternary deposits occupy the coastal fringe along the Indian Ocean, from Tanga region bordering Kenya in the North to Mtwara and Lindi regions bordering Mozambique.They also include the coastal fringes of Unguja, Pemba and Mafia Islands in the Indian Ocean. In the Mainland marine deposits occur up to 30m above sea level and as far as 50km away from the present coastal line. The marine deposits are typically associated with the evolution of the coastal area.

Marine transgression and regression cycles (sea level changes) have shaped the coastal fringe over time. In this respect their spatial distribution is restricted to the coastal fringe. Raised beach sands and coral reefs represent these deposits. Present sand beaches ridges, cliffs and spits, also represent them. The main composition of the deposits is clay to clayey sands, pure beach sand composed of mainly quartz and heavy minerals. Other marine deposits are composed of fossilferous limestone and coral reefs of sandy to nodular limestone textures.

Several elevated beach terraces at Mikindani settlement near Mtwara, along Dar-Es-Salaam coast, Lindi and Mtwara towns, (Stockely, 1937) are typical examples of raised beaches. In fact all along the coastal line such paleo-beaches can be observed. Also extensive sand deposits form most of the coastal plains. To elaborate this point several sediment localities are reviewed here below.

4.2.1.1 Dar-Es-Salaam coast

Dar-Es-Salaam area is one of the best localities where the evolution of the coastal shoreline can be studied. It offers scenery coastal features of both geological and geomorphologic interest. As such some studies have exploited this fact. For instance, Somi, (1993) based on paleomagnetic and stable oxygen isotope studies along the Dar-Es-Salaam coast, observed rapid sea level rise during the beginning of the Holocene Epoch.

In the field (this study) it was observed that at Wazo Hill north of Dar-Es-Salaam City a reef limestone have attained an elevation of over 100m above sea level and dips at 8° WNW. At Kunduchi south of Wazo Hill the coral reefs are at about 30m above sea level. These (at Wazo Hill and Kunduchi) reef cliffs represent two different episodes of sea regressions forming different lines of coral formation, Wazo Hill being higher and older than Kunduchi. Werth (1915) in Dar-Es-Salaam earlier recognised these reef levels as upper and lower levels of coral formation on the coast of Tanzania.

Several authors date these raised reef cliffs from Upper Miocene to Upper Pleistocene, (Handely 1955, Prasad *et al.,* 1981 and Kaaya 1985). Moreover, there occur later reef limestones (younger than Upper Pleistocene) which are more flat low lying and tilted seawards. They are closer to the present coastal line and lie more to the east. Two such levels were observed during the field, the Oysterbay coral reef in the City, (figure 4.4Aa-b) lying at about 0 to 5m above sea level and the Mtongani-Tegeta ridges with reef lines attaining 5m to 10m heights above sea level. It was observed in the field that the upper part of the Oyster Bay reefs (above 0m) have been affected by pedogenesis and forms red soils, (figure 4.4Ba-b).

The ridges form lines parallel to the present coastal line. They are separated by sand dunes or silt sand deposits, usually in areas of high-energy seawater activity where corals can not develop. These are typical coastal line developments forming raised Pliocene-Pleistocene-Holocene inlets and reef barrier or back reef material.

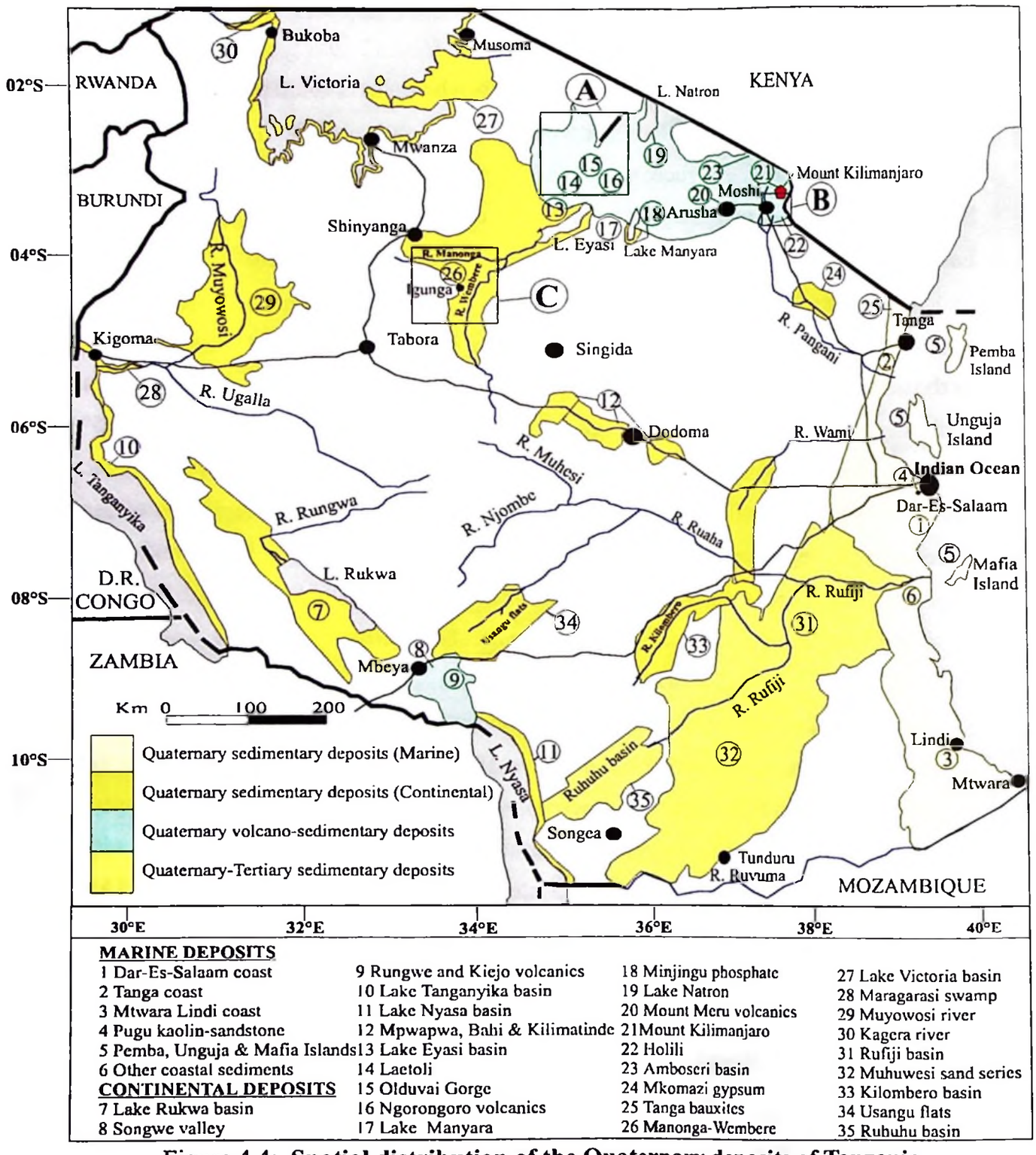

Figure 4.4: **Spatial distribution of the Quaternary deposits of Tanzania [A = Olduvai Gorge area, B = Holili area and C = Manonga Wembere Valley]**

The ridges form the coastal platforms, which are observed in many areas along the coast of Tanzania. Several reef terraces can be recognised along the coast representing different time frames of coral formations in the coastal evolution. These raised coral reefs and beach areas have not yet been studied in detailed, hence they are potential scientific areas of study of the past and present climates and environments.

The economic potential of the coastal areas lies in the use of the limestone (from raised beaches) as a source of building materials (gravel and sands) and limestone as the main raw material in the production of Portland cement in the country. Wazo-Hill-Twiga cements factory relies on this important source of raw material. Another important economic potential is the tourism industry, where the beaches in Dar-Es-Salaam City are clustered by tourist hotels for a good sea view and a sand beach rest and relaxation for tourists.

4.2.1.2. Tanga coast

The Tanga Quaternary deposits resemble those of Dar-Es-Salaam. They are composed mainly of clayey sands and fossiliferous limestone formed by coral growth. Stockely, (1937) described that Pleistocene sediments occurred in the coastal fringe between Tanga and Dar-Es-Salaam. Haligan, (1956) recorded raised reefs at 6m and 30m above sea level, indicating raised coral reefs and beaches all along the Tanzania sea board. The Quaternary limestone at Tanga forms an important part of raw materials for the Tanga and Tanga-Simba Portland cement factory.

4.2.1.3. Lindi and Mtwara coastal deposits

Quennell, *et al.*, (1986), described Mikindani beds near Mtwara as superficial deposits consisting of reddish-brown sands, gravely clay and loam. These deposits attain a thickness of more than 100m. A dispute existed during the 1950's and 60's as to their origins as marine or continental. Stockely, (1943) believed that they were largely fluviatile and elluvial superficial deposits.

Figure 4.4A: Dar-Es-Salaam coast along the Indian Ocean. **a:** A general view. **b:** Oyster Bay coral reefs at 0-5m above sea level.

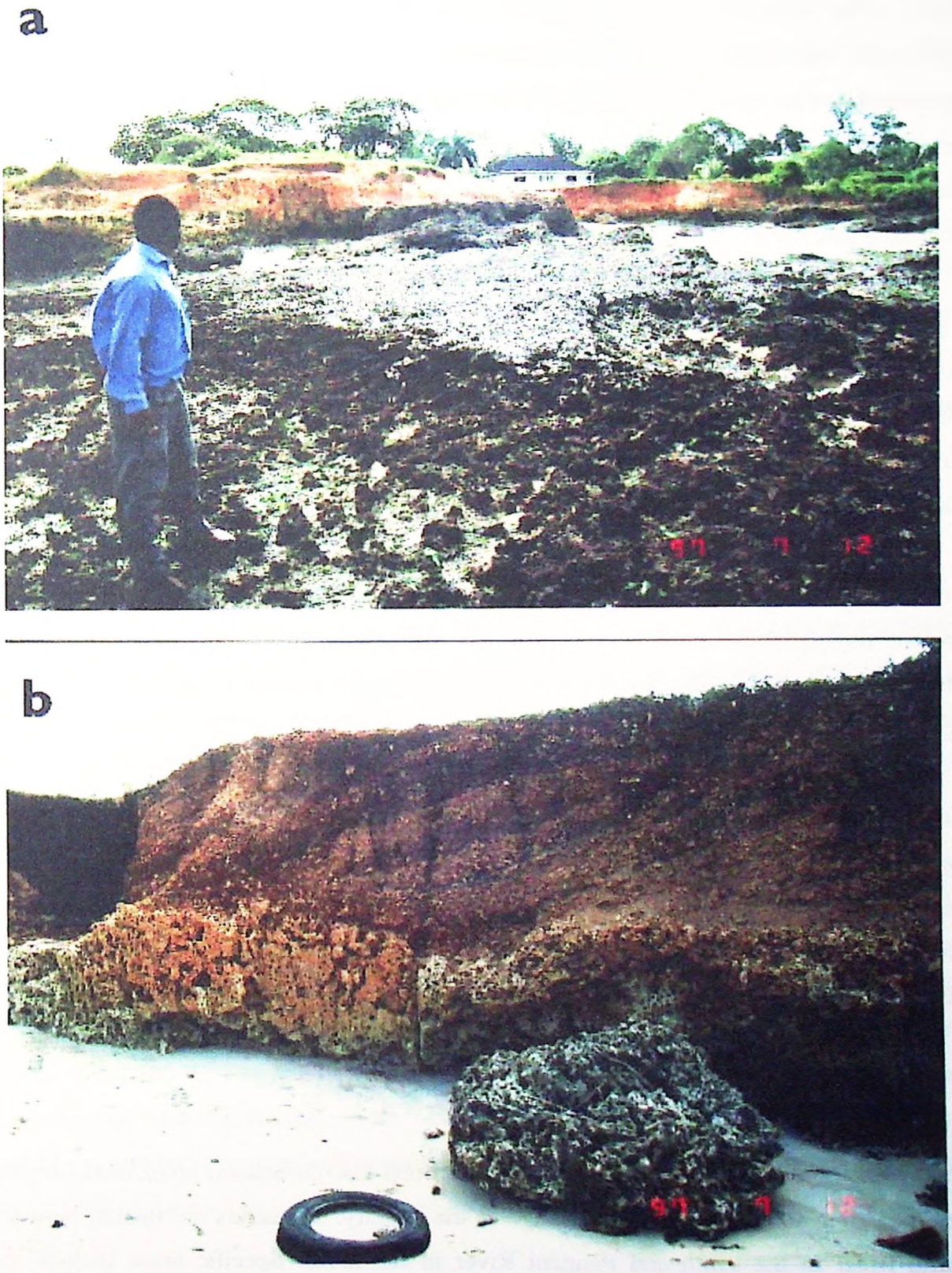

Figure 4.4B: Oyster Bay coral reefs: **a:** Coral reefs – coastal sea floor (foreground – black). The coastal banks are affected by pedogenesis and form red soils (background). **b:** Red Holocene soils forming on Oyster Bay coral reefs.

Today these deposits are generally accepted as of marine origin with intercalation of continental sediments due to transgressions and regressions. The reason behind this agreement is that the deposits indicate a widespread transgression and regression of the sea involving a relative sea level rise to about 800m during the Quaternary. At Lindi Stockely, (1937) recognises limestone found at 15m above sea level. He described them as coastal limestone reefs of Pleistocene age.

As indicated before these deposits (Mikindani beds) reach a thickness of about 80m – 100m and represent the southern coastal deposits of Tanzania. There are also limestone platforms of up to 12m heights along the Mtwara coast. Several authors (Bornhardt 1900, Aemes & Kent, 1955 and Stockely, 1943) refer to these deposits as of Tertiary to Pleistocene in age.

In the Makonde Plateau (Mtwara Region) at an obsolete village of Wanyamao near the present day Dihimba settlement, 15km SW of Mikindani marine deposits can be observed. Stockely (1948) described these deposits as calcareous of marine origin. The age of these deposits are assumed to be Pliocene to Pleistocene.

Local people use these deposits for building purposes as sources of lime burning (white wash); gravel and sands extensively use these deposits. Little studies have been directed to study these huge deposits, but their potential for paleoclimatic and environmental studies lie hidden as a white elephant for the future. These deposits have been targets of coastal oil and gas exploration missions in Tanzania.

4.2.1.4. Other coastal (clayey-sand series) sediments

Vast white sands outcrop over large sections around Dar-Es-Salaam and Coastal region and extending all along the coastal fringe of the country. The sands are thicker between Rufiji River in the south and Pangani River in the north. Specific areas include the Mjimwema-Gezaulole-Kimbiji strip south of Dar-Es-Salaam extending southwards and Mbweni-Mbuju-Bagamoyo strip north of the city, extending to Tanga region. Localities

on the Dr-Es-Salaam-Morogoro road cuts (Kimara-Mbezi-Kibaha) west of the city are spectacular scenes one can not miss to see on a trip to Dodoma. Huge erosion cliffs along the road around Kimara and Mbezi areas are clearly observed.

The deposits are loose to semi consolidated clayey sands. The clays forming the cementing material. In some places the sands occur as mixed clay, sandy silt, sand and pebbles. Several red clayey layers intercalate these white sands. The red layers were recognised at Mbezi section as palaeosols. The pebbles are mainly rounded quartz, quartzite and gneiss particles sometimes mixed with angular feldspars, (Kent *et al.*, 1971) while the sandy fraction constitute of heavy minerals like magnetite, garnet, zircon and rutile. Clay is composed of illite and montmorillonite. The palaeosols indicate clay distratification and bioturbation with some mottling.

The age of the sands is again uncertain many authors assigning them to Mio-Pliocene to Recent, meaning the age stretches from the Tertiary (Miocene-Pliocene) to Quaternary (Pleistocene-Holocene). It would be an interesting work to date these sands using the modern thermoluminescence method. Their economic importance lies in their extensive use in the building and construction industry. They are used as a source of sand fraction for brick-cement and mortar.

4.1.2.5. Pugu kaolin-sandstone

Pugu kaolinitic sand deposits are located 16km SW of Dar-Es-Salaam. It is a hill outcrop of about 300m. Pugu hills are part of an uplifted block forming a prominent NNE strike and a dip of 10° W. The composition of the deposits is mainly white sands at the top and underlain by white kaolinised sandstones. Sometimes the deposit is fine and soft sandy or pebbly in texture. The sand and pebbles are usually cemented by kaolin. The kaolin form up to 60% of the rock volume (Bongole, 1994)

The origin and genesis of the deposits indicate a mixed deltaic to marine sedimentation, evident from a rhythmic succession of arkose kaolinized sandstone to fine quartz-

feldspathic kaolinitic marine sandstone. The deposits are sometimes interbedded by gray to reddish clays. A field observation by the author revealed that the gray to reddish zones represent old palaeosols levels worth for a detailed paleoclimatic study. The age assigned to the deposits is from Miocene to Pliocene. Some Authors (Bongole 1994) refer to them as Mio-Pliocene sands. Other workers (Kent *et al.*, 1971 and Mutakyawa, 1987) refer to them as Lower to Middle Miocene in age.

The author describes these deposits under the Quaternary deposits of Tanzania (after a brief examination in 1998) as he believes they probably extend further into the Pleistocene. There is also a very close correlation between these deposits to the extensive coastal clayey sand deposits described in section 3.1.4 above. The deposits might be the lower part of the extensive Miocene-Pliocene-Pleistocene sands along the coast.

Drill hole Data from BP Shell Petroleum Company indicate that Pugu kaolin sandstone overlie Lower Miocene strata (Quennell *et al.*, 1956), but the upper boundary of the deposits have not yet been observed by earlier workers opening a possibility of extending to the Quaternary. A 10m thick overburden referred to as superficial cover may be Holocene in age (Mushi 1979). Also the dating criterion used by all authors is of relative nature (faunal and facies correlation), which are not conclusive as the absolute dating methods like radiometric dating and thermoluminescence.

The nature of the deposits in terms of origin and composition which is related to the sea transgression and regression due to sea level changes presents them as a huge scientific study platform for the global paleoclimatic variations back into the Miocene and Pliocene Epochs. The Pugu kaolinitic sandstone were worked (mined) for kaolin since the 1940's to the present time, (Harris, 1981). The clay byproduct is used to produce tiles and bricks while the sand is used for building purposes.

4.1.2.6. Unguja, Pemba and Mafia Islands

In Zanzibar Isles (Unguja and Pemba) and Mafia Island the Quaternary deposits are mainly limestone, clays and sands forming a thin layer overlying thick Miocene marine to esturine-deltaic (loams, sandy clay with gravel beds) deposits. The older deposits dominate over the younger Quaternary deposits, (Stockely, 1928). These deposits include the present (Holocene) white sands along the beaches of the Islands. In fact the Quaternary deposits of Zanzibar Isles and Mafia Island need an extensive revision.

4.2.2 Continental Quaternary deposits

The continental deposits are mainly composed of lacustrine fluviatile and volcanic or volcano-sedimentary sediments. They occur in many isolated places all over the country and especially along the rift valley system of East Africa as river terraces (river beds, paleo-flood plains and paleo-streams), lake basins (lakeshores and paleolakes) and volcanic tephras (lava flow, ash flow tuffs or ash fall tuffs). Tanzania posses a great variety of Quaternary rocks which are found in all parts of the country, (Pickering, 1960). Some of the typical localities are reviewed here below.

4.2.2.1. Localities in the western part of the Rift Valley System

Locality areas include Lake Rukwa basin, Songwe basin, Kiejo & Rungwe volcanics and Lake Tanganyika basin. The deposits are always volcano-sedimentary mixtures of Tertiary to Quaternary in age. Some examples are described in the following paragraphs.

Lake Rukwa basin.

The sediments are located around the present Day Lake Rukwa. Rukwa basin is believed to be a deep filled trough of up to 1500m thick sediments of Cretaceous to Quaternary age. The Quaternary deposits are the upper part of the sediment filling this deep trough. They are about 80m thick composed of sands and clays overlying diatomaceous shale.

The beds are found to contain a high proportion of volcanic ash (Quennel *et al.*, 1956). In the SE part of the trough the deposits are mainly volcanic tuffs, gravel and pebble beds with evidence of folding and faulting. The gravel and pebble zones are the main host rocks for alluvial gold which has been economically mined since the 1920's (Harris 1981).

Preliminary gravity, magnetic, seismic and the geological distribution data of the basin suggest that the sediments may contain oil and gas. In recent years the basin have been prospected for oil and gas. There have been also efforts during the 1990's to study the paleoclimatic evolution of the basin through drill cores from the lake, (Massola, 1996).

Songwe Valley deposits

The Songwe deposits are located in the southern part of the country (Mbeya region) in the Songwe Valley, (figure 4.5). The deposits were mapped for the first time by Teale & Oates, (1935) as pink to white banded crystalline limestone of secondary origin. In some places the limestone form caves, which contain Holocene phosphate guano deposits. The limestone is composed of travertine deposited from thermal springs.

Spurr, (1954) distinguished two types of travertine deposits. The first type is the vertically banded deposit formed by Hot Springs oozing from elongated vents parallel to the rift fracture lines, the walls of which were constantly raised and broadened by the deposition of the travertine. The second type is the horizontally banded porcellanous limestone material deposited on top of the vertical travertine deposits. These deposits were deposited during the extension of a lake, which existed in the area. The travertine deposits are regarded as Pleistocene to Holocene.

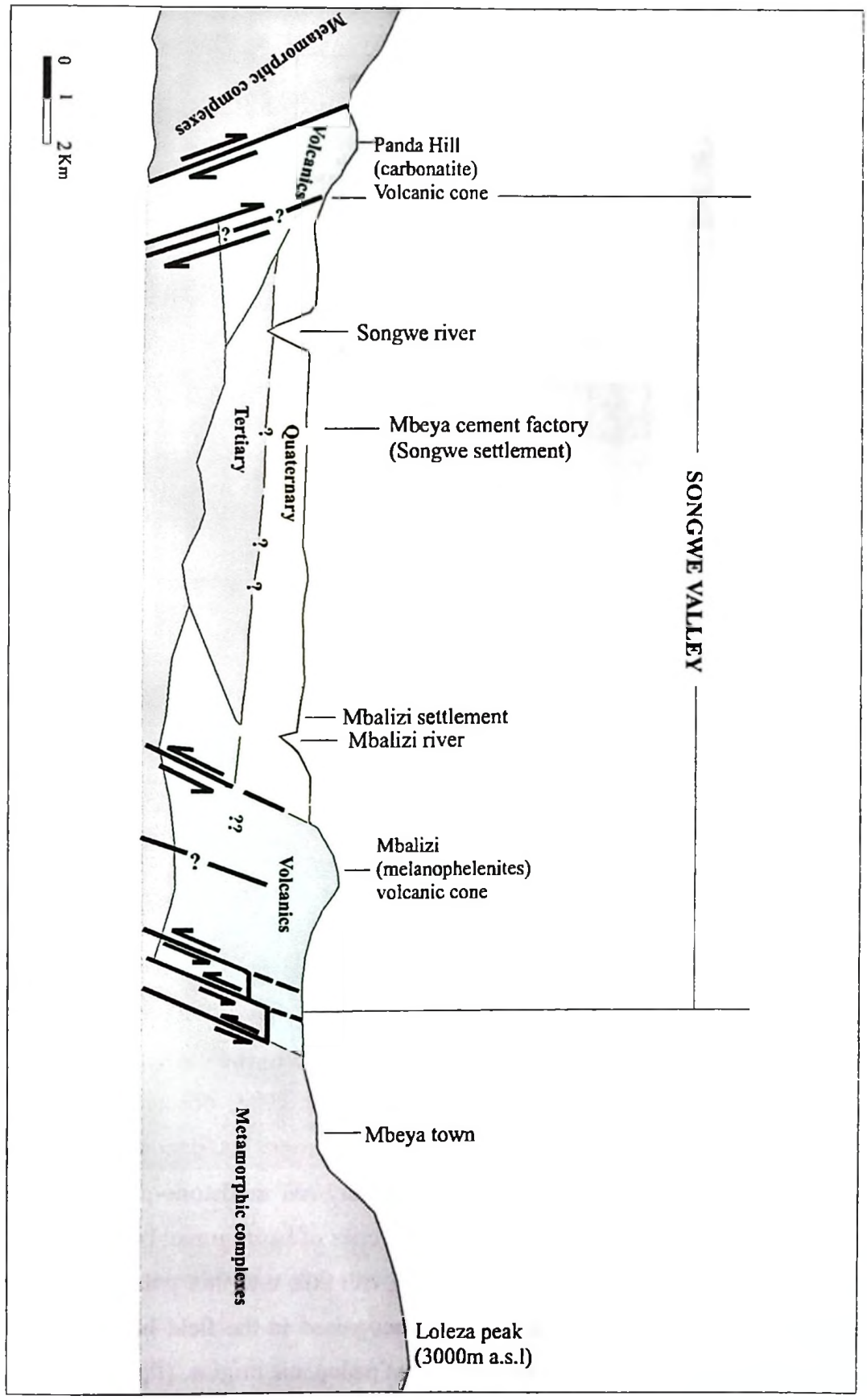

Figure 4.5: Idealized geologic section and geomorphorlogic position of Songwe Valley

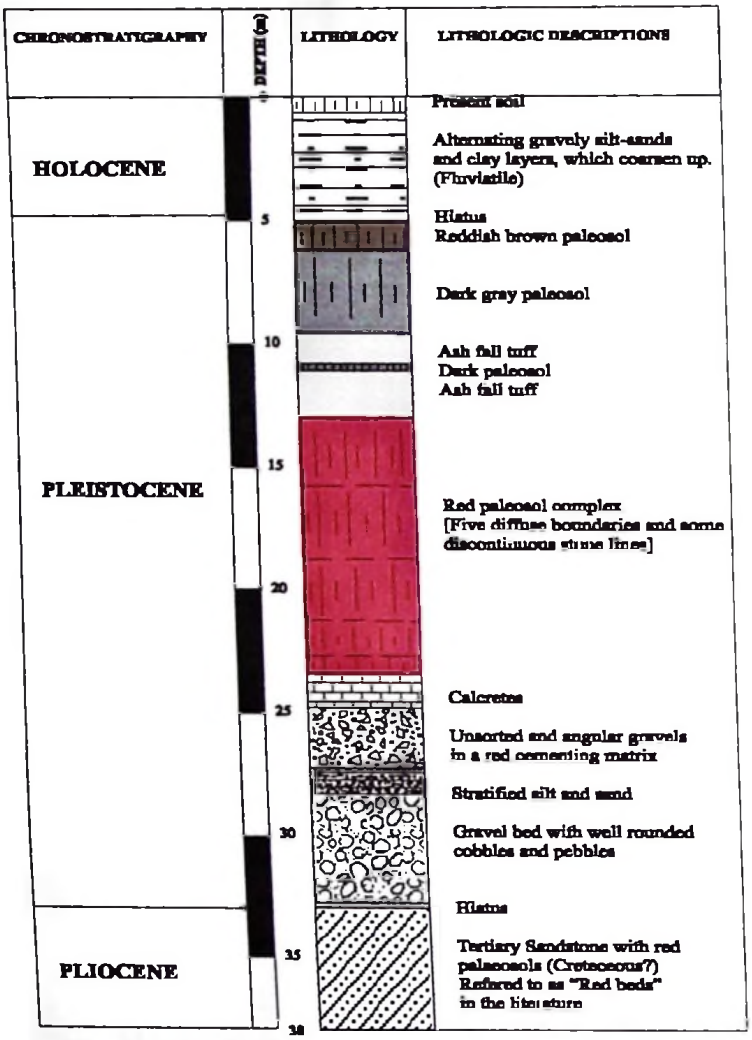

Figure 4.6: Chronolithostratigraphic classification of Songwe Valley deposits (A composite section) [Also see figures 4.6a-c]

The travertine deposits are today the basic raw material for the Mbeya-Tembo cement factory. It also provides the raw materials for cut and dimension stone industry of the country. Local people also burn the travertine for lime. In the eastern part of the basin, (figure 4.6a-B) along the Songwe River the author (in 1994) observed 10 – 20m thick volcano-sedimentary along the Songwe River cut outcrops. The deposits are of Holocene to Pleistocene age lying unconformably on Tertiary red sandstone-palaeosol basement, (figure 4.6c-B). The deposit from bottom are a series of basal gravel bed, (figure 4.6c-A), thick red palaeosol and alternating silty sands, ash falls and thin palaeosol levels at the top (figure 4.6). The palaeosol levels were recognised in the field based on root traces stonelines and carbonate nodular concretions of pedogenic origins, (figure 4.6b-A&B).

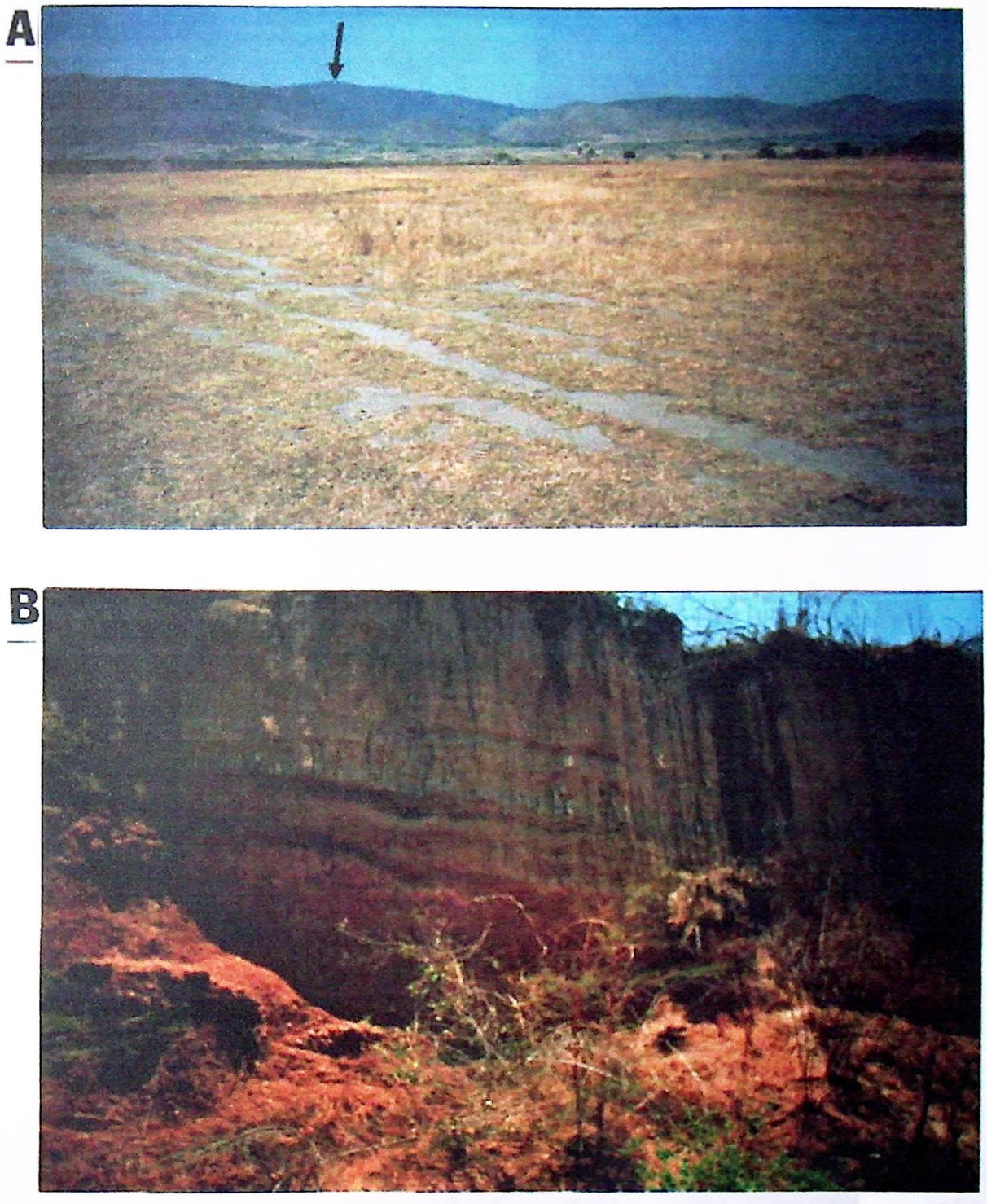

Figure 4.6a: Songwe Valley locality. **A:** Songwe Valley. In the background Panda Hill cabornatite volcanic cone can be seen – indicated by the arrow. **B:** Songwe Valley deposits as observed in the Songwe riverbanks.

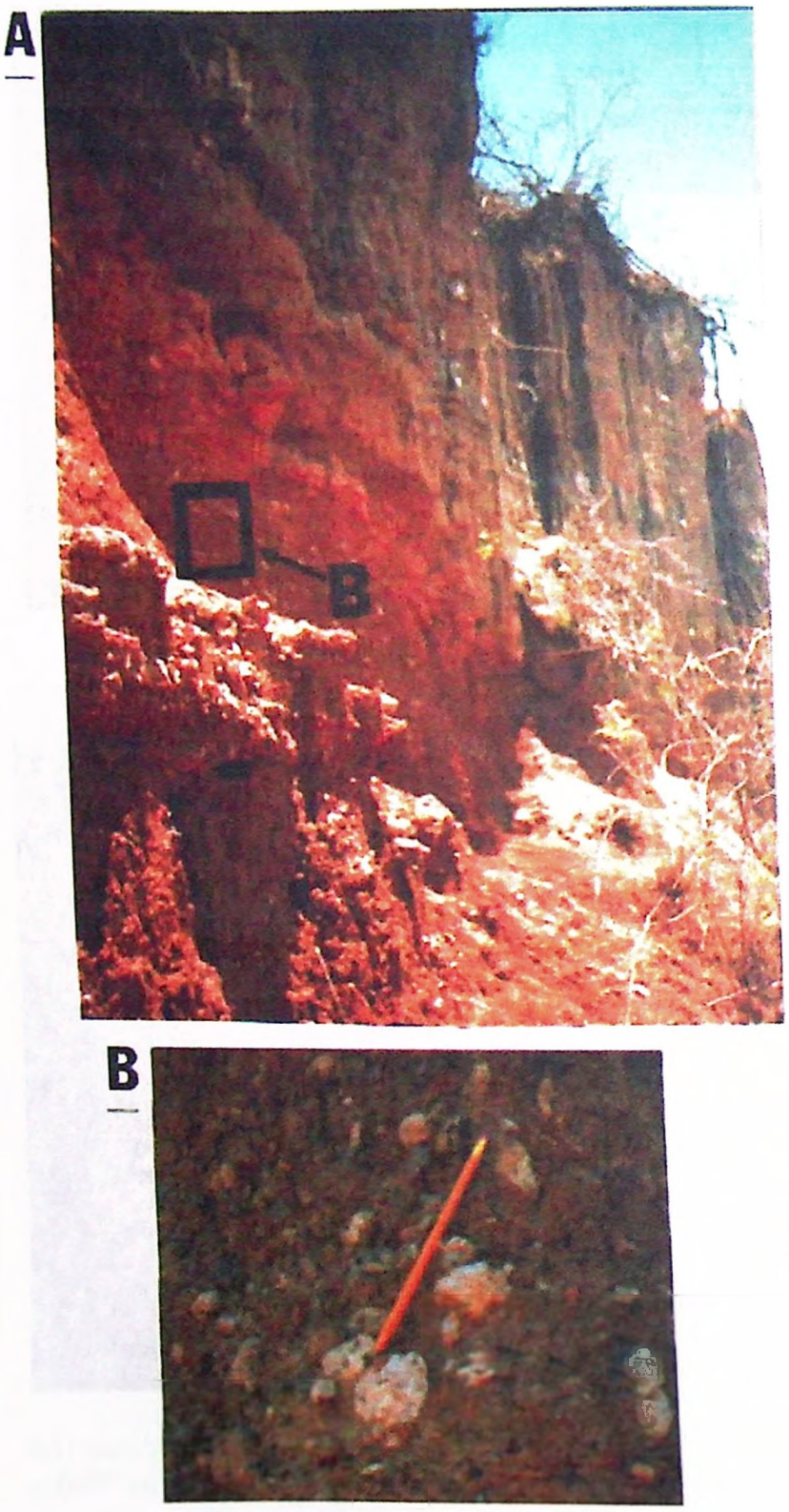

Figure 4.6b: Songwe Deposits. **A:** Red palaeosol complex. **B:** Close up showing carbonate concretions in the red palaeosols.

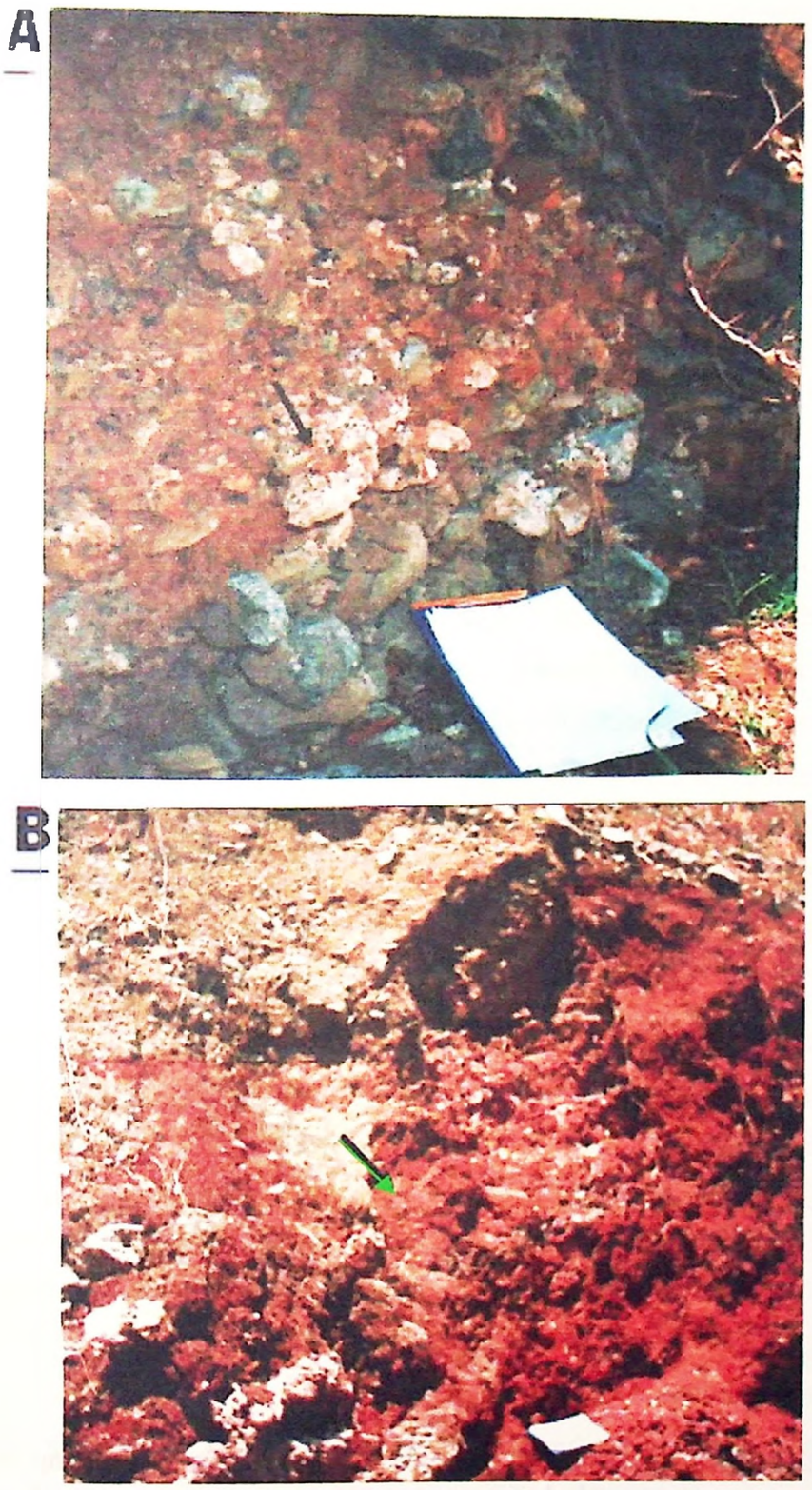

Figure 4.6c: Songwe Valley deposits. **A.** Gravel bed with rounded pebbles and cobbles lying unconformably on Tertiary red palaeosol. **B.** Tertiary red palaeosols (in the literature are refgered to as "Teratiary red beds".

Rungwe and Kiejo volcanics

The Rungwe volcanic rocks occur in Rungwe District (Southern Tanzania – figure 4). They are a series of basaltic-trachytic-phonolitic lava and tuff flows of varying ages ranging from Tertiary to Holocene, (Harkin, 1954). The typical locality for the rocks is in the Rungwe Mountains near the Rukwa-Nyasa rift junction and the Rukwa fault. The age of the rocks was regarded by Stockely, (1948) as Pliocene to Holocene but mainly Pleistocene and having a total thickness of 500 – 600m.

The Rungwe volcanic field has been recognised to have three phases of volcanic episodes. The oldest episode occurred in the Tertiary – 8.6Ma to 5.6Ma (Ebinger *et al.*, 1989). They are represented by the eleveted Mbeya and Mbaka highlands of the Ufipa and Eliton plateaus. The second phase of volcanic eruptions is recorded in the Pleistocene Epoch – 2.2Ma to 1.6Ma. The Pleistocene volcaics are mainly observed in Tukuyu and Katete in Karonga depressions (Ivanov *et al.*, 1998). The third phase is believed to have occurred in the Holocene – 0.52Ma to 0.00Ma (Harkin, 1955, Bolousov *et al.*, 1974 and Ebinger *et al.*, 1989). These younger volcanic rocks and sediments form the Rungwe, Uporoto, Ngozi and Kiejo pumice and ash falls.

The Quaternary volcanic rocks therefore blanket (cover) a large part of Nyasa and Rukwa troughs including the Uporoto Mountains. The Kiejo crater which erupted about 1800AD (Harkin, 1955) is responsible for a continuous emanation of CO_2 gas of commercial value. There were efforts to develop this gas deposit for industrial and domestic use, but unfortunately to date the CO_2 gas lie unexploited in the crater.

Lake Nyasa basin deposits

Little is known about the Quaternary deposits of Lake Nyasa. Nevertheless along the present shoreline Holocene clay mud flats related to the rise and fall of lake-level can be observed. There is also evidence (from satellite imagery) of rapid rise of the lake level in recent years. The study of Lake Nyasa shoreline fluctuations can provide best means of

understanding the climates and environments of the Quaternary in tropical Africa during the Holocene.

Ruhuhu basin deposits

Ruhuhu is part of an extensive basin consist one of the several important coalfields of Tanzania. (Mckinlay, 1954). The coal deposits belong to the Permian to Lower Triassic Karroo Formations. Quaternary sediments of Pleistocene to Holocene age overlay the extensive Karroo sediments of Paleozoic to Mesozoic age. The basin is tectonically active since the Tertiary (Stockley, 1932b). Holocene calcareous deposits are found in present-day hot springs in the area. Other quaternary deposits of the Ruhuhu basin include fluatile sand and clay sediments found along the Ruhuhu river.

Lake Tanganyika basin deposits.

Numerous occurrences of lakebeds within the drainage basins are remnants of Lake Tanganyika transgressions over greater areas in geological times. Pikering 1960 reported that the 1878 – 79 lowering level of Lake Tanganyika exposed lakebeds at Kungwe bay south of Kigoma. Due to their stratigraphical positions the deposits are believed to be of Quaternary age, although detailed studies are lacking. The deposits are mainly composed of sands to silty sands intercalated with limestone layers mainly of lacustrine origin. It is evident from basin research that the Late Miocene until Mid Pleistocene, large patterns of sedimentation within the Tanganyika basin was primarily controlled by tectonism. In contrast, from the Mid Pleistocene to the present, sedimentation in Lake Tanganyika seems to have responded dramatically to climatic changes as suggested by repeated patterns of lake level fluctuations (Lezzar *et al.*, 1996). Recently the Lake basin has received considerable attention to study its paleoclimatic records. For instance basin and lake surface temperatures studies indicate reduction in precipitation in the basin during the Last Glacial Maximum (Bergonzini *et al.*, 1997).

Malagarasi and Muyowosi sediments

The Malagarasi and Muyowosi sediments are fluviatile-riverine deposits related to the Malagarasi and Muyowosi river systems. The deposits are mainly gravel-sand-clay series of Pleistocene to Holocene in age. While the Muyowosi deposits lie unconformably on the Tertiary Nyanza shales, the Malagarasi sediments are underlaid by the Malagarasi sandstone of Tertiary in age (Quennell *et al.*, 1956 and Harris, 1981). The present plain level is covered by mud flats related to the seasonal flooding of the plains.

4.2.2.2. Localities in the eastern part of the Rift Valley System

Along the eastern arm of the Great Rift Valley of East Africa is a home of much quaternary deposits of Tanzania. The locality areas include Mpwapwa, Bahi and Kilimatinde conglomerates in Central Tanzania, Lake Manyara-Eyasi-Natron basins, the Serengeti plains and the Kilimanjaro volcanic areas in Northern Tanzania.

Mpwapwa, Bahi and Kilimatinde deposits

These deposits are grouped together because they occupy the central part of the East African Rift System of Tanzania. The Bahi depression west of Dodoma contains Quaternary deposits composed of white clayey sands of Holocene age intercalated with red oxidized clays. 'Mbuga' white calcareous soils are widespread in the area. According to Harris, (1981) the 'Mbuga' are formed in present day areas of internal drainage, which are flooded during each rainy season. The 'Mbuga' sediments are composed of black sandy clayey sediments with swelling properties. Beneath this layer calcareous to gypsitic deposits accumulate.

The economic potentials of the deposits include the presence of extensive saline groundwater and seepage of which the local people use to produce table salt. Bahi swamp was extensively explored by the Geological survey during the 1950's for evaporite minerals. During this time uranium and strontianite minerals were reported (from

borehole data). Uraniferous strontianite are therefore known to exist at 75m depth in the Bahi sediments (Harris, 1981 and United Republic of Tanzania, 1998). The gypsum and strontianite mineral economic potential is not yet explored since then. The Bahi basin is now heavily used for irrigated rice production for local consumption.

Other economic industrial minerals like gypsum occur in the 'Mbuga' sediments in Itigi area and Msagali area near Kongwa. Near Dodoma Municipality a series of fluvial and eluvial sediments were reported by James, (1954) as composed of quartz grains in a hard clayey matrix, correlated to the Kilimatinde gravely deposits. Sometimes the deposits are conglomerates showing false bedding and washout, (Pickering, 1960).

In Mpwapwa area near Kongwa, and Mvumi limestone are found as superficial deposits. Fawley, (1955) believed that these calcareous deposits were Pleistocene in age. These deposits are a possible source for limestone burning for lime. For instance National Housing Corporation (NHC) for lime presently works out the limestone at Mvumi.

The Kilimatinde cemented deposits are about 40m thick ferrugineous cement deposits and silcretes of elluvial and alluvial origins. The deposits are mainly sands cemented by clay, lime or silica. The sand particles are either quartz derived from quartz veins or relicts of gneiss or granite. Locally iron staining and patchy laterite cement can be observed (Pickering & Teale, 1937). The silcretes and laterites indicate that the deposits were formed during a dry climatic condition of the Pleistocene Period, (Krenkel 1925, Teale & Wade 1937,). The spatial distribution of the sediments includes Manyoni and Itigi Districts. A well-exposed outcrop can be observed along the Central Railway line at the Kilimatinde fault of which the section is referred to as "Kilimatinde cement" due to their cemented texture. The deposits are considered to be of Pleistocene age (Teale, 1937).

Lake Eyasi Rift basin deposits.

Lake Eyasi rift is covered by extensive volcano-sedimentary Quaternary deposits, which are regarded as Pliocene to Holocene in age. This area is within the volcanic province of Tanzania. It is the middle part of the eastern part of the Rift Valley System. Widespread earth movements associated with faulting and a complex interplay of volcanic activity characterizes the basins. Eyasi rift is one of the two major rift systems, which are recognised in Northern Tanzania. The rift systems are the Eyasi rift and the Manyara-Natron (Gregory) rift.

The NE-SW Eyasi rift is the Oldest which began during the Tertiary (Shackleton, 1978). The rifting initiated volcanic Olmoti, Ngorongoro, Sadiman, Oldeani and Lemagruti) activities along the rift lines (figure 5.3a – chapter 5) going along side erosion of the fault ridges and volcanic highs and consequently deposition in the basins. In this respect the deposits of these areas are mixed sedimentary and volcanic sediments deposited in alternating cycles of stable landscape and active volcanic phases. The stable phases would deposit sediments (fluvial and lacustrine) including the formation of palaeosols in between sedimentation phases. Active faulting and volcanism marked the active phases characterized by the formation of volcanic cones and deposition of mainly volcanic rocks. The Eyasi rift basin covers, 1. Lake Eyasi basin, 2. Serengeti plains (this includes Olduvai Gorge and Ndutu/Masek drainage systems, 3. Vogel river drainage system (including Laetoli area) and 4. The Ngorongoro area (an elevated volcanic highland).

This area consists of two distinct geomorphologic parts, the Low lands (Serengeti plains and Lake Eyasi basin) and the Ngorongoro highlands, (a series of volcanic cones, which were developed on the Eyasi rift fault line), (see chapter 3 and 5).

Lake Eyasi/Laetoli basin deposits

The deposits are located in the southern part of the rift basin. They include the lake Eyasi basin deposits and the Laetoli deposits. The Lake Eyasi basin deposits are composed of lacustrine clayey silts, sands and calcareous sediments often intercalated by significant

tephra layers-tuffaceous clays (Manega, 1993). The large part of the tuffaceous clays are nephelinitic in composition and were earlier termed as Ngaloba beds (Pikering, 1960).

The Laetoli deposits are subaerially deposited yellow-orange or pale gray fine tuff (Hay, 1986). The deposits are a series of thick ash fall-tuff deposits, in which numerous hominid and other animal footprints lie, especially in upper most part of the deposits (see chapter 5).

Both the Lake Eyasi basin and Laetoli deposits are considered to be part of an extensive Vogel river drainage series. Stratigraphicalally these deposits have a total thickness of more than 120m and are divided into two lower (Laetoli beds) and upper (Eyasi & Ngaloba beds) units (figure 4.7). The Laetoli beds per se are Pleistocene (4Ma – 2.5Ma) in age, while the Ngaloba/Eyasi deposits are Pleistocene (2.5Ma) and younger in age, (Quennell *et al.*, 1956, Leakey *et al.*, 1976, Hay 1986 and Agnew & Demas 1998).

<table>
<tr><th>Chronostratigraghy</th><th>Formation</th><th>Rock types</th></tr>
<tr><td>Upper Pleistocene</td><td rowspan="2">Ngaloba
(Lake Eyasi Basin)</td><td>Eolian sediments – tuffs, silts and sands.</td></tr>
<tr><td>Middle Pleistocene</td><td>Tuffaceous clays</td></tr>
<tr><td>Lower Pleistocene</td><td rowspan="2">Laetoli</td><td>Ash, clays and tuffaceous clays</td></tr>
<tr><td>Pliocene</td><td>Trachytic to phonolitic lava flows</td></tr>
</table>

Figure 4.7: Chronostratigraphy of Eyasi basin deposits (After; Quennell *et al.*, 1956)

Laetoli locality (deposits) is very famous for its numerous animal footprints including those of hominids. 16 sites have so far been studied and an estimated 18,000 prints representing 17 families of animals in an area of about 800 square meters have been found on a 3.5Ma years tuff layer, (Agnew and Demas 1998). This is unusually the highest concentration of foot print tracks so far known in the world.

The foot print tracks were made and preserved during the Pliocene Epoch about 3.6Ma ago. Studies show that the Laetoli tuff originated from the now extinct Sadimani volcano in the Ngorongoro highlands about 19km east of Laetoli. The preservation of the footprints is related to the active phases of the volcano together with the composition of the ejected volcanic materials. Agnew & Demas (1998) proposes:

"...Sadiman volcano began belching clouds of ash, which settled in layers on the surrounding Savanna. At one point of the volcano's active phase, a series of eruption coincides with the end of an African dry season. After a light rainfall, the animals that lived in that area left their tracks in the moist ash. The material ejected from Sadiman was rich in the mineral cabornatite, which acts like cement when wet. The ash layers harderned preserving the thousands of animal footprints that covered the area. Shortly afterwards Sadiman volcano erupted again depositing additional layers of ash that burried the footprints and fossilized them..."

In one specific locality footprints, which are assumed to belong to the hominid *Australopithecus aferensis*, (lived in the area) can be observed. These hominids left their footprints in the ashes. About 50 footprints run north in two parallel trails. Paleo-anthropologists believe that the trails were made by three hominids. A large male led the way, while a smaller female walked alongside and a medium sized male stepped in the larger male's footprints. Other animals' footprints including giraffes, elephants and extinct horse 'hipparion' footprints are also seen. The footprint tracks were preserved by burial in 1994. The area is now out of public visit.

This preservation has prompted a huge debate among local geoscientists in Tanzania that was it appropriate to bury the footprints once again at this time? Most scientist (including

the author) have the view that this was a hurriedly decision taken at top most administrative hierarchy of a ministry without involving the appropriate local scientists.

Using a lot of money to preserve the Laetoli footprints by burying seems presently a disadvantage than preservation by establishing a small in situ museum. About the same amount of money could have been used to build an appropriate small shed house with accompanied small infrastructure to protect the fragile footprints from rain, wind and exposure to constant tropical sun temperatures and root action. Then a full time conservator would be placed in the area by the Tanzania authorities to guard and protect the locality.

The public and tourist would be allowed to visit the area on payment. This process would bring some money and especially foreign currency. A large part of this money would be used by the Laetoli museum to further conserve and protect at the same time to continue the scientific research in the area. Preserving the site this way is more advantageous that burrying it to lie iddle in the ground. I hope the Tanzanian government will reconsider in the near future to protect the site in an appropriate way.

Olduvai Gorge deposits

Olduvai Gorge sediments are fossilferous volcano-sedimentary deposits, which occupy most of the Serengeti plains. The deposits are best exposed in the eastern edge of the Serengeti plains (Salei plains) along the Olduvai Gorge cliffs. The deposits have an approximately total thickness of 100m. They are regarded as Pleistocene to Holocene in age (Manega 1993 and Kafumu 1995). At the base of the deposit lie an ignimbrite welded volcanic rock lying unconformable on Precambrian metamorphic quartzo-feldspathic gneiss.

The lower part of the strata is a series of ash fall tuffs intercalated with mainly lacustrine sediments (clays, silts and sands); with one major level of lava flows (trachyte and basalt) breaking the series. The upper part of the Olduvai Gorge is series of mixed lacustrine-fluviatile-tuff sediments. The deposits are essentially clays, silts sands and gravel. They

also include tuffaceous clays and reworked volcanic pyroclasts. These deposits contain a significant number of well-developed palaeosols. The geology and stratigraphy of Olduvai Gorge is explained in detail in chapter 5 of this study.

Ngorongoro Highlands deposits

As said before the Eyasi rifting initiated Olmoti, Ngorongoro, Sadiman, Oldeani and Lemagruti volcanic activities along the rift lines forming extensive volcanic highs composed of volcanic rocks. These rocks are mainly composed of volcanic rocks consists of basaltic and trachytic lava flows with subordinate pyroclasts. Both the trachytic and basaltic lava flows are sometimes interbedded with tuff and agglomerates.

The lava flows and pyroclasts of the volcanic centers have been sufficiently studied (Macintyre *et al.*, 1974, Dawson 1989, and Manega 1993). The lava flows dip radially away from the centers and flow directions have sometimes been affected by faulting (Kafumu 1995). The Ngorongoro Highland extrusive is oldest volcanic rock in the area.

The economic significance of the Eyasi rift area

The Eyasi rift contains the Serengeti National Park, the Ngorongoro Conservation area and the Olduvai Gorge and Laetoli archaeological sites. The areas contain the highest concentration of wild life in the world. These areas are protected as world heritage sites. They are major sources of the much-needed foreign currency for Tanzania.

The Serengeti National Park contains over two million animals – the largest and most spectacular concentration of plain animals anywhere in the world. The park lies to the west of the Ngorongoro crater and covers 15,000 square km area. It is a flat low land lying between 1,400m a.s.l and 1,800m a.s.l (Kafumu 1995) and occasionally pierced by metamorphic rock insebergs (eastern part) and granite kopjes (the central and western parts).

The Ngorongoro crater is another wonder of creation. It is the largest intact crater in the world. It is about 18km in diameter, which is about 160 square km area. The crater floor

is at 1,600m a.s.l and the crater rim lies at 2,300m a.s.l. The Ngorongoro high land rises high above the Serengeti Plains. Over 30,000 animals and numerous varieties of birds live in the crater and the crater rims (WCMC 1998).

The Olduvai Gorge and Laetoli hominid sites also located within this area are famous hominid sites frequently populated by international scientists to study these wonders of nature. The Olduvai Gorge is a deep canyon, which cut though the Pleistocene sediments covering the Serengeti plains leaving a spectacular scene of volcano-sedimentary layers. Olduvai Gorge together with other sites in Kenya (Lake Rudolf and Omo valley), Ethiopia (Afar triangle) is referred to as *"The cradle of mankind"* because it was in this gorge the first discovery of an *Australopithethine* was made by Mary D. Leakey in 1959.

Over 700,000 tourists per year visit the Eyasi rift (Serengeti National Park, Ngorongoro Crater and the Olduvai Gorges) area (Rake, 1990). In this respect its economic contribution to Tanzania is very significant due to immense foreign currency it brings through tourism.

Gregory (Lakes Manyara-Natron) Rift deposits

The lake Manyara-Natron rift system is younger than the Eyasi (Gregory) rift. This rift is characterized by active neotectonic activities characterized by faults, shear zones, volcanic cones & craters and Hot Springs. The Gregory rift dates from Early Pleistocene to Holocene. The onset of this rift system initiated younger volcanic centers like Kremasi and the Oldoinyo Lengai, which is active until today (Temu *et al.*, 1992). Extensive Quaternary volcano-sedimentary deposits cover the basin.

The Quaternary deposits of the volcanic highlands of this area consists of older (Pliocene – Pleistocene) volcanic rocks composed of tuffs, scoria, agglomerate, basalt & trachy-basalt and nephelinite that dates between 1.4 Ma – 2.7Ma (Beloussov *et al.*, 1974). The rocks overlie Precambrian Usagaran basement complex. Younger (Pleistocene to Holocene) volcano-sedimentary deposits comprising of LakeBeds, lava flows, volcanic

ashes and alluvial fans mainly cover the basin floor. The lakebeds contain clays, cherts, limestones and diatomites. K-Ar dates range from 0.2Ma – 2.4Ma (Macintyre *et al.*, 1974) and 8Ka – 20Ka are reported from Lake Stromatolites (Hillaire-Marcel *et al.*, 1986).

Lake Natron is an inland playa lake, which has a substantial accumulation of trona that was economically mined during the 1980's. On the other hand, Lake Manyara basin is a source of phosphate deposits, which is currently mined for the fertilizer raw materials. The phosphate deposit was formed by the leaching of bird quano (Harris, 1981), which accumulated at the top of the Minjingu kopje when it was an Island in the Manyara paleolake. Lake regressions which started during the Last Interglacial (Somi, 1993) and continued today left the phosphatic kopje exposed, 5km east of the present day lake Manyara level. The deposit occurs as alternating phosphatic layers and greenish-olive (bentonite) clays. The Manyara National Park lies in the rift cliff flanks of the Gregory rift scarp and extends down to the rift floor where the Manyara Lake is located. This is one of the rare isolated natural ecosystems of Tanzania. It is a sanctuary of wildlife that forms an important sorce of foregn currence due to tourism.

Kilimanjaro -Arusha volcanic fields and Usambara Mountains

This is the Northern Tanzania (Arusha, Kilimanjaro and Tanga regions) extensive volcanic area dominated by thick volcanic deposits, several paleoslake sediments and Quaternary weathering formations of old Precambrian rocks.

The Northwestern part of this area is an extensive volcanic field containing the highest elevations (Mount Kilimanjaro = 5896m and Mount Meru = 4566m) in the area. The southeastern part is essentially the Usambara Mountains (1500 – 2310m above sea level) composed of Precambrian Usagaran rocks. Quaternary weathering of Usagaran rocks has produced thick latosolic to bauxitic soils. Five representative localities will be reviewed, 1. Mount Kilimanjaro and Meru, 2. Holili calcareous deposits, 3. Lake Amboseri basin deposits 4. Mkomazi gypsum deposits 5. Amani and Lushoto bauxite deposits.

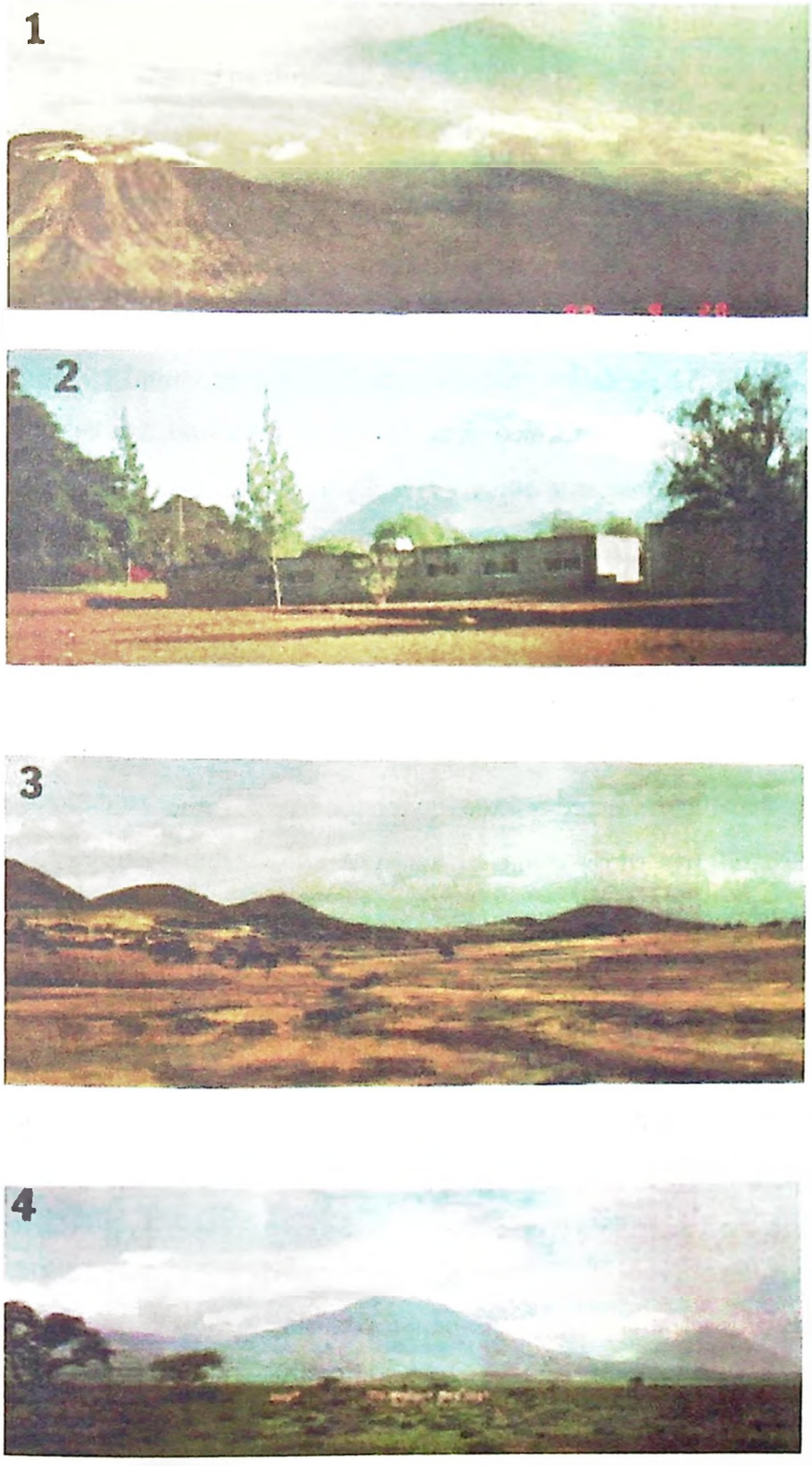

Figure 4.8: The Kilimanjaro volcanic field landscape. **1.** The Kilimanjaro Mountain (Kibo-Uhuru peak-5896m above sea level). Shira peak is seen in the background. **2.** Mount Meru (5466m a.s.l). **3.** Parasitic cones of Arusha area. **4.** Oldoinyo Lengai and Keremasi volcanic cones.

Kilimanjaro-Meru volcanic mountains

Arusha and Kilimanjaro areas are dominated by thick volcanic piles (lava flows, ashes and tuff) of Quaternary age. The area si characterized by volcanic mountains, (figure 4.8_{1-2}). There are Quaternary glacial deposits at the Mount Kilimanjaro Mawenzi and Kibo summits.

The age of both the Kilimanjaro and Meru volcanic activities dates back from 2.49Ma to 0.55Ma (Wilkinson *et al.*, 1986). These major volcanic activities accompanied by minor parastic volcanic eruptions, (figure 4.8_{3-4}) formed thick layers of lava and ash deposits around Meru and Kilimanjaro major volcanic centers (Hecky 1971, Evans *et al.*, 1971, Downie & Wilkinson 1972 and Wilkinson *et al.*, 1986). Rarely the deposits are interapted by fluviatile-palaeosol levels (See Holili calcareous deposits).

The glacial deposits are mainly terminal morains belonging to the last glacial (Downie and Wilkinson, 1972) found on the flanks of Kibo and Mawenzi peaks of the Kilimanjaro Mountain. These deposits have contributed to the understanding of the Pleistocene-Holocene climates and environment of Tropical Africa. The studies have suggested a global climatic response during the Quaternary. For instance during the last glacial maximum known in Europe the climatic snowline was at least 1300m lower than it is now on the Kilimanjaro (Flint, 1959 and Wilkinson 1972). In this regards causative agents of Quaternary climatic and environmental changes in the Tropic are now viewed from a global perspective. Mounts Kilimanjaro and Meru are among important National Parks, sanctuaries of specific wildlife. Each year they also attract a multitude of tourists bringing foreign currency to the Tanzania's economy.

Holili calcareous deposits

Holili Quaternary deposits are thick calcareous grits lying unconformably on a lava flow. They are composed of mainly quartz, gneiss and basalt sand sized grains cemented by calcite or amorphous carbonate materials. The lava is dense or vesicular scoriceous olivine basaltic in composition. The age of the deposit is from Pleistocene to Holocene (Chapter 9).

The stratigraphy of the area consists of basalt laid on a Precambrian pre-existing surface of the Usagaran system. The basalt lava flow was overlaid by by the thick calcareous-tuffaceous grit. This lava flow was weathered (forming a thick red soil) prior to the deposition of the grit. In some places the lower part of the grit sequence is a fossilliferous mudstone (Chapter 9). Due to its hardness and lightness qualities the grit is an excellent building material and hence local communities for bricks work it out.

Lake Amboseri basin

Lake Amboseri basin deposits lie in the Amboseri lake basin mainly lying in Kenya. The area is in the Masai area north of Kilimanjaro mountain. Only the SW tip (10% area) of the basin is in Tanzania. The general stratigraphy of the deposits cover about 100m thickness of sediments (Harris, 1981). The base is essentially clay and silty clay. The clays are then covered by caliche, silty clays and tuffaceous silt (Behrensmeyer & Boaz, 1980). The age of the depositsis believed to be in Pleistocene to Holocene (Quennell *et al.*, 1956). Merchaum is the only economic mineral found in this area. It occurs as banded masses and fills cavities in secondary dolomites and limestones (Harris 1981). The merchaum is worked out for production of tobbacco pipes factory in Arusha.

Mkomazi gypsum deposits

The Mkomazi gypsum sediments are the southern plain deposits of the Kilimanjaro area. They are paleo-playa lake deposits composed of arenaceous clay sand, sandstone and limestone of Pleistocene to Holocene age. The deposit was formed in an inland playa saline lake. Seasonal drought made possible the crystallization of calcium sulfate and carbonate. The type locality is near Mkomazi Township. The gypsum occurs as nodular, platy or powdery gypsum. The nodular gypsum grains are set in clay, the flakes in sand or silt beds with crystals of selenite. The powdery gypsum is weathered material mixed with soil (Harris 1981). This deposit is the main source of gypsum for the Portland cement industry of Tanzania. The deposit is currently worked out by local people and sold to the Tanzania cement industries. The Mkomazi deposits are also considered as the northern extension of the Upper Pangani and its tributaries (800 m.s.l) alluvial plains.

Amani and Lushoto bauxite deposits

In Amani Tanga district and some localities in Lushoto district, bauxite Quaternary deposits are observed. The deposits are a result of appropriate climatic conditions (extensive long chemical weathering), which have affected the Precambrian Usagaran rocks of the Usambara mountain ranges (Harris, 1981). These deposits are believed to have formed during the Quaternary especially in the Holocene Epoch. Recently the deposits have been evaluated for economic purposes but as far as I am aware no economic workings have been put into effect.

4.2.2.3. Other localities

Manonga-Wembere basin

Manonga-Wembere sediments are extensive terrestrial deposits formed in shallow valley and depression laid on a Precambrian peneplain (chapter 9, this study). The old (Precambrian) terrain is represented by granite inselbergs. The base of the sediments which lie on Precambrian basement complex is composed of coarse, poorly sorted granite and gneiss's debris cemented by calcareous-siliceous or ferruginous matrix (Harrison and Mbago 1997). These ferruginous conglomeratic deposits are correlated to the Sekenke conglomerates. The Sekenke conglomerates are observed in the type locality in the Sekenke ridge near Sekenke Township. They are considered to paleolake shoreline accumulations of the Manonga-Wembere beds (Williams and Eades, 1939) and composed of angular to sub-angular quartz and chert pebbles with numerous granite and gneiss rock pebbles cemented by red calcareous clayey materials (Quennell *et al.*, 1956).

The conglomerates are overlaid by white to gray lakebeds (Williams and Eades 1939) composed of fine calcareous clays. The lakebeds are intercalated by red palaeosols formed during periodic lake retreats. Coarse sand and littoral facies, which occasionally interbed the lakebeds, have been formed along the lake paleo-shoreline. The Holocene (upper part) is represented by gravel terraces and 'mbuga' clay cover (Verniers, 1997). The ages of the Manonga sediments therefore range from Pliocene-Pleistocene to

Holocene (Williams and Eades 1939, Quennell *et al.*, 1956, Pickering 1958, Barth 1989 and Petro Mafwimbo, 1994 and chapter 9 – this study). Moreover, Harrison and Mbago (1997) recently suggested an exclusive age of between 5.5Ma to 4.0Ma (Upper Miocene to Lower Pliocene) for the Manonga-Wembere beds based on paleontologic evidence in the Manonga valley.

Other Quaternary sediments considered in this group, are the Songeli-Mtawira beds (Teale 1932a) located in the south of Iramba Plateau south of Singida and very close to the present day Mapela settlement. The deposits are composed of fine bedded marl clay intercalated with gravels (Teale 1932b). The fine bands contain leaf impressions and bone fossils. The age is unknown but probably they are post-Manonga-Wembere (Pleistocene?) as they lie above these deposits.

Lake Victoria basin

Lake Victoria which is a tectonic sag basin (Mbede, 1991) contains up to 100m thick of Quaternary sediments. They overlie Tertiary sediments of Bukoban System and in parts granites of Precambrian age. The Quaternary deposits belonging to this basin form several clay-sand terraces of Pliocene to Pleistocene age. The terraces have been formed at different lake levels during the lake geological evolution. The Quaternary terrace deposits are composed of white fine sand and pale gray clays known as mbuga flats lying on red laterite deposits usually formed on Tertiary peneplained Precambrian surface. The older terraces are covered by present day (Holocene) Lake Victoria terraces mainly consisted of black clay flats lying very close to the lake shore (Stockley, 1947).

The Quaternary deposits of Lake Victoria basin are therefore characterized by lacustrine beach flats (Jenga 1998) which are wave cut plat forms of former lake strewn. Their composition is essentially sand; gravel and pebbles derived from local bedrock. The beach coarse sediments are usually overlaid by calcareous clay-silt facies indicating high level conditions of transgressive phases of the lake. The sands are underlain by laterites

of Pliocene-Pleistocene age, which are products of weathering of older Precambrian rocks.

Usangu flats and Kilombero Valley

Although little reference material was found describing the geology of Usangu and kilombero valleys, nevertheless, their geomorphologic positions made possible to speculate the following. Based on the observations of topographic maps and aerial photographs, Kilombero and Usangu valleys are active basins where loose sand and clay can accumulate. They are essentially mud flats of Holocene age. The mud flat areas are economically important for Tanzania as they are used to grow sugar canes, a raw material for production of sugar.

Rufiji basin

Rufiji basin deposits are riverine sediments associated with the Rufiji River system. The sediments are loose un-banded white to pale gray some times red clay intercalated with coarse unsorted gravel and small boulders (Quennell *et al.*, 1956). These deposits can be observed along the Rufiji River very near to the confluence of Ruaha and Rufiji Rivers upstream. Spence (1957) regarded these deposits as Pliocene to Pleistocene in age and named them Mkindu beds. The lower part of Rufiji basin (downstream towards the sea) consists of flood plain deposits composed of black to gray clay and sand sediments of Holocene age.

Muhuesi sand series

Muhuwesi sand sand deposits are unconsolidated pale brown sands lying on Precambrian basement. On some places they lie unconformably on Karoo rocks (Grantham, 1953). The type locality is the Muhuwesi drainage in Tunduru District. They cover over 2000km^2 area starting from Lumusule river to the North extending southwards to the

Ruvuma River south of Tunduru Township (Quennell *et al.*, 1956). No studies have been undertaken since the 1950's.

Mbemkuru sandstone, sand and alluvial series found in the Mbemkuru and Ruhuu rivers are contemporaneous to the Muhuwesi sand series. They include the Liwale-Upper Lumusule series (Grantham 1953). They are considered as deposits of the same series based on age and textural equivalency.

The genesis of these deposits is still unknown, although it was earlier suggested by Grantham (1955b) as the northward extension of the extensive Kalahari eolian sand system. The sands were assigned a tentative age of Pliocene to Pleistocene. It would be interesting in the future to date the sand bodies by thermoluminacence. Other similar sand bodies are found in the type locality of Mbemkuru in Nachingwea District. Grantham, (1955b) described them as whites to pink sand series of Neogene (Pliocene?) and possibly derived from the Muhuwesi series.

CHAPTER FIVE

OLDUVAI GORGE QUATERNARY GEOLOGICAL AND STRATIGRAPHICAL STUDIES

5 QUATERNARY GEOLOGICAL – STRATIGRAPHICAL STUDIES

5.0 INTRODUCTION

This chapter concerns the Quaternary geological stratigraphical studies caried out in the Olduvai Gorge area. These studies include 1. Field geological and geomorphological studies 2. Lithostratigraphical-palaeosol field studies. The results of these studies are synthesized in an attempt to understand the Quaternary geology and the stratigraphy of the area.

5.1 THE GEOLOGICAL SETTING AND THE STRATIGRAPHICAL BACKGROUND

Olduvai Gorge is a palaeobasin filled by mixed lacustrine and fluviatile sediments intercalated by volcanic sediments. The area was mapped since the early 1900's as deposits containing nearly 2.2Ma of uninterrupted sedimentation (Reck 1914, Pickering 1956, 1957 &1961, Hay 1967 & 1976) after a significant volcanic episode, which occurred towards the end of the Pliocene.

Olduvai Gorge sediments are fossiliferous volcano-sedimentary deposits, which occupy most of the Serengeti plains. The deposits are best exposed in the eastern edge of the Serengeti plains (Salei plains) along the Olduvai Gorge cliffs. The deposits have an approximately total thickness of 100m.They are regarded as Pleistocene to Holocene in age (Hay 1967, 1976, Manega 1993 and Kafumu 1995). At the base of the deposit lays an ignimbrite welded volcanic rock lying unconformable on Precambrian metamorphic quartzo-feldspathic gneiss basement complex (figure 5.1).

The deposits were first described by Reck (1914) in a system of numbering the lithological units from I to VI in an ascending order as Bed I to Bed VI. This stratigraphical nomenclature is still in use today although with some modifications and some name has been introduced specifically in the upper parts of the units.

The Olduvai Gorge deposits are mainly calcareous tuffaceous lacustrine-fluviatile and terrestrial deposits. The compositions of these sediments are essentially limestone, calcareous clay, silt and sand intercalated with gravel. There are also numerous layers composed of ash fall or ash flow tuffs intercalated by numerous palaeosols.

The lower part of the strata (Bed I and Bed II) is a series of ash fall tuffs intercalated with mainly lacustrine sediments (clays, silts and sands); with one major level of lava flows (trachyte and basalt) breaking the series. These sediments have an age estimate between 2.5Ma to 1.60Ma, (Hay 1976). This series lies on a Pliocene-Pleistocene welded ignimbrite, which in turn overlies a Precambrian basement complex (figure 5.1).

The upper part (Bed III, IV Masek and Ndutu beds) of the Olduvai Gorge deposits is a series of mixed lacustrine-fluviatile-tuff sediments. The deposits are essentially clay and claystones, silts sands and gravel. They also include tuffaceous clays and reworked volcanic pyroclasts. These deposits contain a significant number of well-developed palaeosols. The palaeosols are less studied and this study attempts to understand the Olduvai Gorge palaeoenvironments based on palaeosol occurrences, an approach which has been under-estimated in the past in this area. The study aims at offering a better understanding of the numerous geological layers lying in between the broader Bed I – Bed IV units of Reck (1914) and other workers who followed.

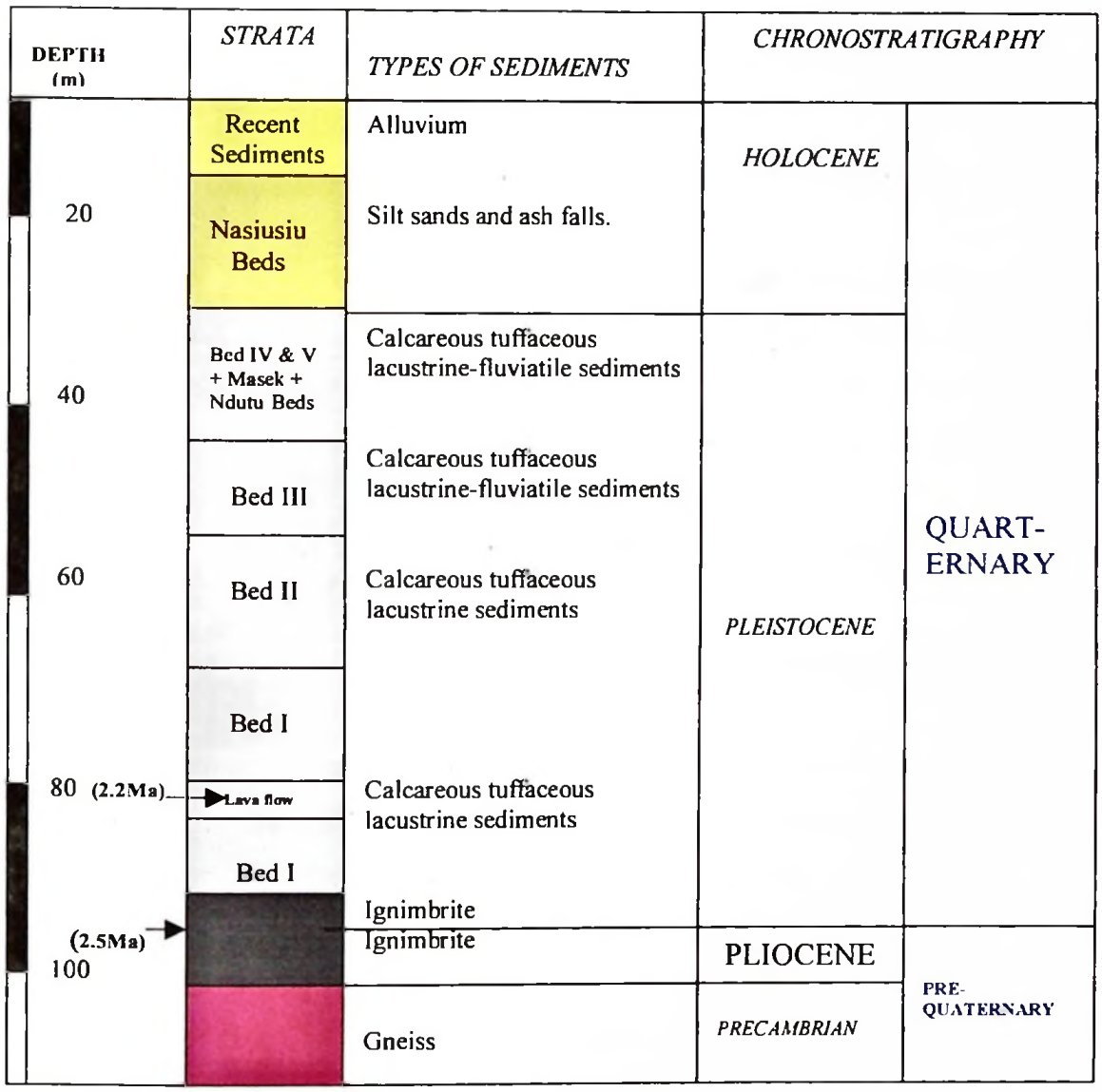

Figure 5.1: A generalized stratigraphical column of Olduvai Gorge locality.

5.2 METHODS OF INVESTIGATION

5.2.1. Geological and geomorphological field studies

A regional geologic and geomorphologic traverse was undertaken from Mto wa Mbu across the Ngorongoro highlands to the Serengeti National Park (table 5.1). Aerial photos, topographic sheets and satellite imagery interpretations heavily assist this geo-traverse mapping. The regional geology is given in figure 5.2. A detailed geological

mapping of the Olduvai Gorge area *per se* was also undertaken and the results are presented in figure 5.6 and subsequent explanation that follow.

5.2.1. Lithostratigraphical – palaeosol field studies

Lacustrine-fluviatile-volcanic sediments of Olduvai Gorge which posses numerous palaeosol levels were mapped, examined, measured and described at 5 sections along the gorge cliff walls. This section reports the results of careful field lithological (sediments and palaeosols) stratigraphicalal vertical measurement and descriptions.

5.3. GEOLOGICAL AND GEOMORPHOLOGICAL STUDIES

5.3.1. Regional mapping

A regional geo-traverse was undertaken (table 5.1) to map the regional geology and indicate the geomorphological features of the area. Based on this an overview of the regional and local geology and geomorphological evolution with some basic interpretations are offered (figure 5.3a, b, c & d).

Table 5.1: Mto wa Mbu – Olduvai Gorge museum geo-traverse.

No	Location	Altitude (m)	Latitude and longitude	Geology
1	(A)Mto wa Mbu	1010	3°22`30``S : 35°51`20``E	Lake Manyara sedimentary deposit
2	(B)Gregory rift cliff near Manyara hotel	1650	3°22`00``S : 35°51`50``E	Lava flow (basalt-trachytes); A fault scarp.
3	(C)20km east of Karatu town	1620	3°19`00``S : 35°40`50``E	Lava flows
4	(D)Karatu town	1600	3°20`30``S : 35°40`50``E	Volcanic lava flows with ashes
5	(E)Ngorongoro crater view	2400	3°15`50``S : 35°34`40``E	Volcanic lava flows of the Ngorongoro eruption
6	(F)Ngorongoro cliff	2600	3°14`52``S : 35°30`20``E	Lava flows and agglomerates of the Ngorongoro eruption
7	(G)Desecrnt route into Ngorongoro crater	2300	3°09`00``S : 35°28`40``E	Lava flow (Ngorongoro)

8	(H)Eyasi rift scarp	1800	3°01`30``S : 35°22`20``E	Lemagruti volcanic lava flows; A fault scarp.
9	(I)Eastern Serengeti Plains	1400	3°00`30``S : 35°20`58``E	Calcareous gray deposits (Olduvai sedimentary deposits)
10	(J)Olduvai Gorge Museum	1450	2°59`30``S : 35°20`54``E	Olduvai Gorge sedimentary lake beds
11	(K)Olbalbal depression	1080	2°59`00``S : 35°27`06``E	Alluvial silts and sands
12	(L)Ngorongoro crater floor	1800	3°10`50``S : 35°32`00``E	Ngorongoro crater sedimentary deposits
13	(M)Serengeti plains	1500	2°59`00``S : 35°16`36``E	Olduvai Gorge sedimentary lake beds

The regional geological setting of the Olduvai Gorge and Ngororngoro areas is closely associated with the East African rifting. Uplifted blocks and grabens, (figure 5.1a) and spectacular volcanic cones, (figures 5.1b and 5.2) along major fault lines of the rift system characterize the area. Most of the basins are filled by mixed lacustrine and fluviatile sediments intercalated with volcanic sediments and rocks. The area contains two (eastern and western) distinct geological and geomorphological parts. The eastern part is a volcanic highland massif (>2700m a.s.l), (figures 5.2 and 5.1c) with rock composition ranging from trachyte-basalt-nepheline-phonolite to carbonatite (Pickering, 1958, 1961 and 1993).

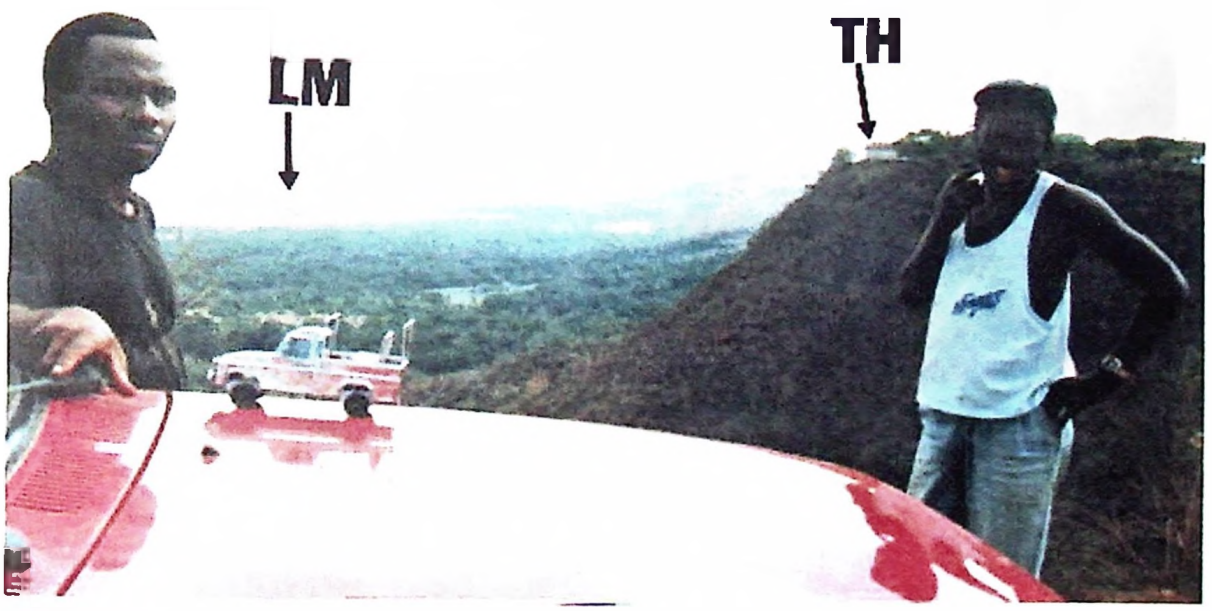

Figure 5.1a: The Greagory rift scarp: The lake Manyara **(LM)** can be seen in the eastern down trow block. Sedimentary deposits belonging to the Lake Manyara depositional regime mainly cover the graben. Lake Manyara touristic hotel **(TH)** is built on the western side up thrown block composed of volcanic lava flows.

Figure 5.1b: The Ngorongoro crater. **1.** Scenery view of the Ngorongoro crater. Crater rim geology comprises of volcanic lava flows and agglomerates. **2.** Sedimentary deposits that are covered by grassland support a multitude of wildlife in the crater floor.

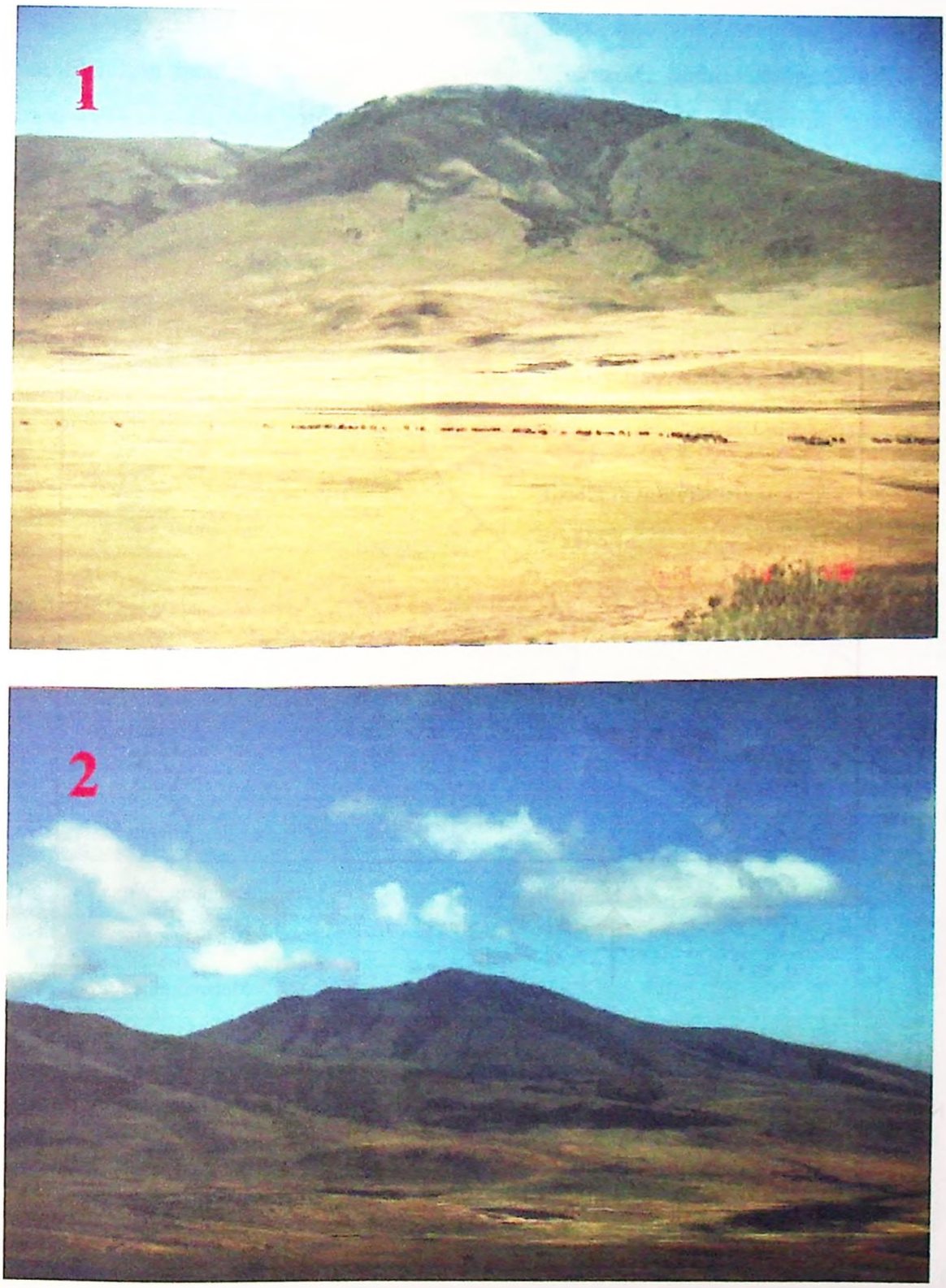

Figure 5.1c: The Ngorongoro Highlands, (Eastern Olduvai Gorge area). **1.** Sadimani volcanic cone. **2.** Lemagruti volcanic cone.

There are numerous volcanic cones, Oldeani, Sadimani (figure $5.1c_1$), Lemagruti, (figure $5.1c_2$), Ngorongoro, Olmoti Olosirua, Loolmasin, Embakaai, Keremasi and Oldoinyo Lengai volcanic cones and craters (figure 5.2). The Ngorongoro crater rims are composed of volcanic rocks (lava flows and agglomerates), (figure$5.1b_1$) and the crater floor is maily covered by Holocene sedimentary deposits, (figure $5.1b_2$).

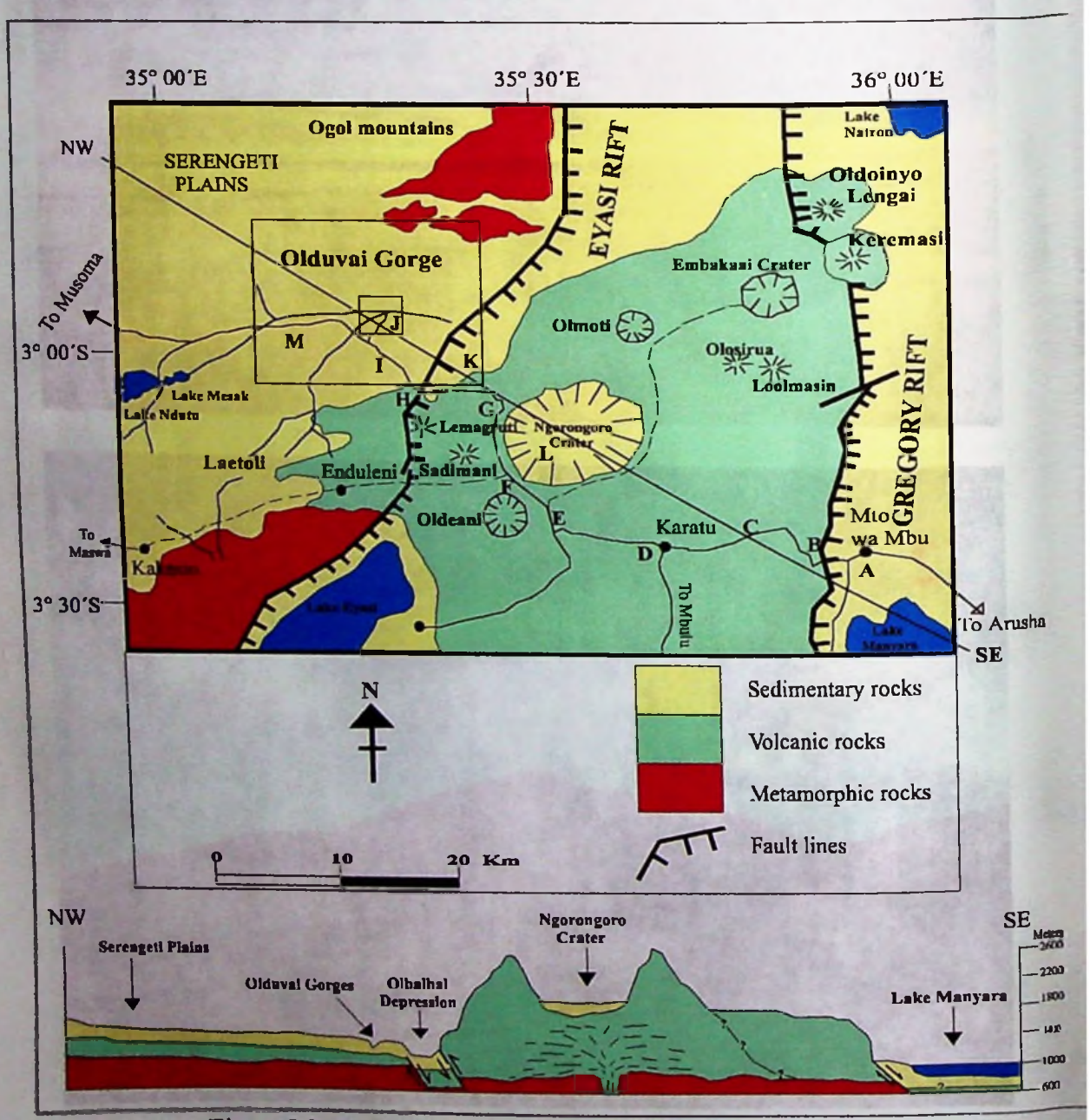

Figure5.2: Location map and the general geology of the Olduvai Gorge and Ngorongoro highlands.

Figure 5.2b: The Olduvai Gorge area - Eastern Serengeti plains. **1.** A view from the Ngorongoro Highland descent [Quartzite-gneiss inselbergs (I) and Lemagruti volcanic lava flows (F) are indicated]. **2.** Detail of the Lemagruti lava flow cliff – Flow direction of the lava is towards the Serengeti Plains (towards the west as indicated by the arrow).

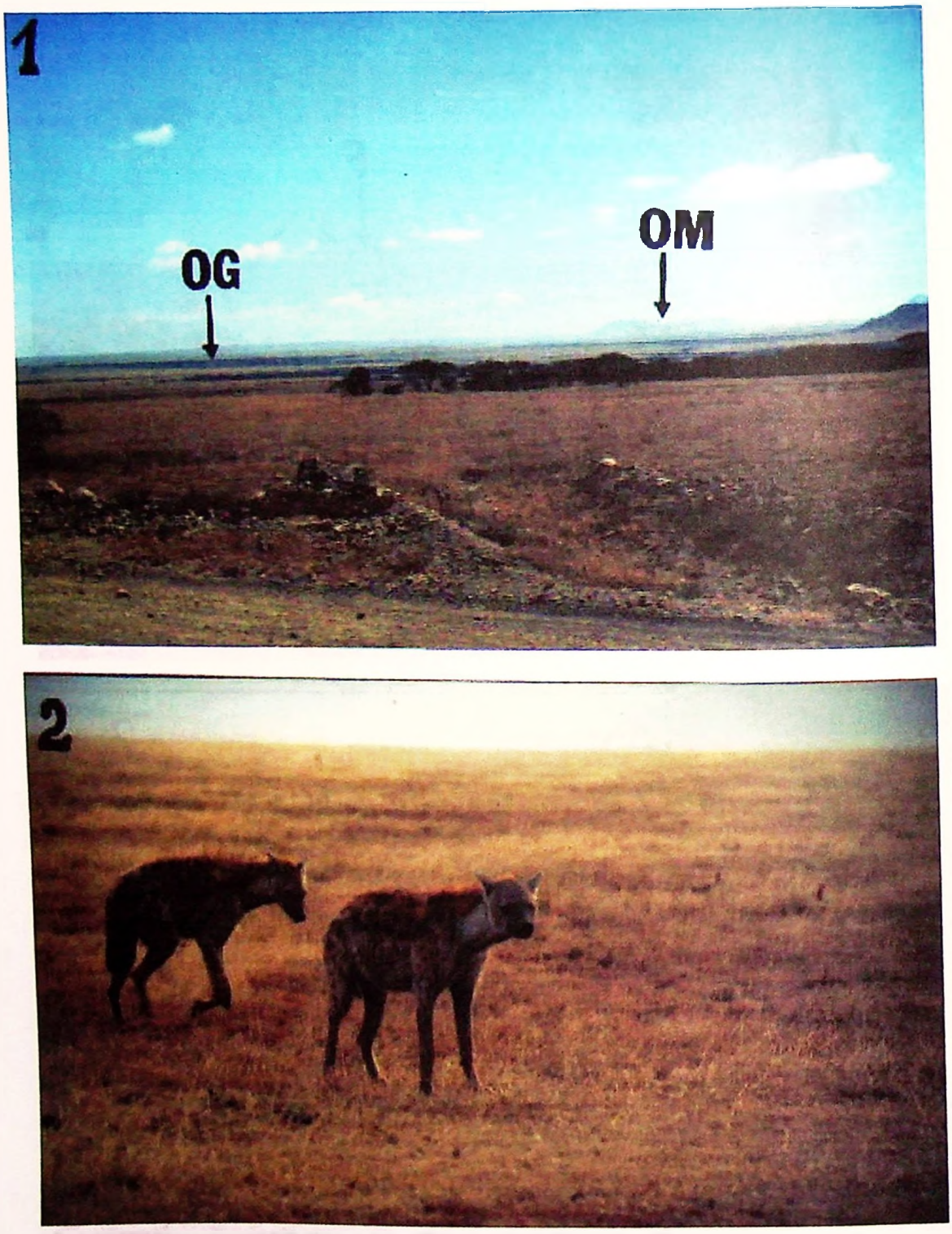

Figure 5.2c: The Serengeti Plains (Western part of the Olduvai Gorge area). **1.** Plains as observed from southeast in which, Ogol Mountains – Precambrian remnants (OM) and Olduvai Gorge (OG) could be seen in the background as indicated by the arrows. **2.** A lone pair of spotted hyenas that is in serch of food is a spectacular view in the open Serengeti Plains. This grassland supports a large number of wildlife.

The lava flow directions of the Ngorongoro highlands are observed to flow radially from each individual cone and towards the lowlying Serengeti plains, (figure 5.2c-1&2).

The western part is the Serengeti plains, (figure 5.2b) mainly covered by calcareous-tuffaceous lacustrine, fluviatile and terestrial deposits refered to as Olduvai Gorge lakebeds. The composition of the deposits is essentially limestone, silts, stratified fossiliferous clay and claystones, sand, sandstone and gravel beds. The sediments also include ash flows and falls belonging to different volcanic episodes. The deposits are wind or water laid. The Olduvai Gorge profile is a typical example of such deposits. A series of volcanic basalts, trachytes and ignimbrites can be recognised especially at the lower part of the sediments. The precambrian basement complex mainly composed of gneisses and quartzites is exposed as inselberghs in the Olduvai Gorge and as Ogol mountains to the north of the gorge.

5.3.2. Implication to the geological and geomorphological evolution (model of emplacement)

Based on field observation, inferences and previous geological works in the area the model of emplacement of the Olduvai Gorge paleo-lake basin and the Ngorongoro volcanic highland massif are presented here below.

During the Early Tertiary, there was a prolonged geological stability which allowed the reduction of large areas of East Africa into peneplains. Inselbergs, hills and mountain ranges preserving remnants of the Late Tertiary (and older) erosion surfaces stood above the Early Tertiary surface and in this geomorphological (large plaination surfaces) context, fracturing of the surface began (Shackleton 1978). The first faulting can be dated to 65Ma, which formed the first NE-SW Eyasi escarpment with the east down faulted and the west upthrown, (figure 5.3a).

In the Olduvai Gorge area the pre-existing Precambrian basement complex underwent a peneplanation process, and vast geomorphologic plains were formed. The relict old rocks

in this area are represented by inselbergs (Olongoidjo hill) in the Serengeti plains and the Ogol Mountains. The plains started to be faulted predominantly along the NE- SW rift direction. This faulting initiated the first phase of volcanic activity along the rift line (Pickering 1993).

This phase of activity resulted into the building-up of trachyte basalt volcanoes, which are dated from Middle Cretaceous up to Early Quaternary interspersed with mainly Pliocene nephilinite-phonolite centers, (figure 5.3b). At about the end of the Pliocene (2.5Ma) the centres grew into huge mountains and their vents were filled with heavy lava and solid rock forcing most of them to collapse into caldera (Ngorongoro) and craters (Oldean and Lemagruti), (figure 5.3c). The growth of these old trachyte-basaltic volcanoes (Ngorongoro, Oldeani and Lemagruti) formed the present highland geomorphology.

The young volcanic cones date way back from Late Pliocene to Holocene. The first phase of this volcanic episode formed the Olmoti and Sadimani centres, joining the already existing older volcanic cones. It is known that the fossil footprints at the Laetolil are preserved on volcanic ash, which came from the Sadiman eruption 3.5Ma ago (Shackleton, 1978). Olmoti and Embakai developed craters during the Quaternary. At the onset of the Quaternary period the Manyara-Natron fault (Gregory rift) (figure 5.3c) was formed. This new fault system initiated a new series of Quaternary volcanism, which are represented by Keremasi and Oldoinyo Lengai volcanic cones (figure 5.3d).

By about 2Ma volcanic activity diminished but erosion and deposition due to new favourable geomorphological conditions created in the area, intensified. In other words there were numerous inland basins and troughs which were now being filled with sediments from denudated volcanic highlands. Probably it was at this time the Olduvai beds started to be formed. The different phases of volcanic eruptions in this area from different volcanic centers could throw large quantities of ashes and tuffs into rivers and lakes all around the area. These are now represented as water laid or wind blown tuffs or ashes in the quaternary geological sequences.

There were spells of diminished volcanic activities and low sedimentation rates where stable landscapes prevailed. Landscapes are now represented palaeosols having a stratigraphical stability. It was at this time, that pedogenesis dominated as a surface activity forming various palaeosol levels. Thus palaeosol levels are observed intercalating the volcano-sedimentary deposits of Olduvai Gorge.

Moreover, the dying out of the Keremasi activity (Hanbay, *et al.*, 1992) marked the beginning of the Holocene (10,000BP), and Oldoinyo Lengai began to erupt sending out large quantities of black volcanic ashes that form dunes of the Serengeti plains. Some nephelinite ashes observed across Olduvai Gorge 60km WSW of Oldoinyo Lengai may have been deposited during this earlier eruption (Hay, 1963). At this time the Olduvai Gorge canyon started to be formed.

The Serengeti and Agata Salei plains are therefore Pleistocene palaeolakes that were filled by sediments and dried out just about 12,000BP, then Olduvai Gorge began to be formed (cutting through the sediments). According to Shackleton, 1978 the lake basin was a result of a rifting regime in the area, which began in the Tertiary about 65Ma and continued to the present time. The present plain morphology was attained about 3.5Ma (Pliocene) in which the area started to be filled with sediments intercalated with tephra and palaeosol layers. As was observed in the field bout 130m thick sediments were finally laid down on a pre-existing Precambrian basement copmlex of the basin floor. The sediment accumulation culminated with probably a pouring of a black ashes and sands from Oldoinyo Lengai volcanic center about 10,000BP to cover the SW of the Agata Salei plain. The ashes and sands started to be spread westward to the Serengeti Plain.

The Oldoinyo Lengai is active until today, it continues slowly day after day to pour out phonolitic-carbonititic lava. Some times strong eruptions can be expected as was observed by Dawson, *et al.*, (1968) in the 1966 eruption where falls of the carbonititic ash were reported up to 130km west of the volcano. The present landscape (figure 5.2 and 5.3d) is a result of a long geological evolution spanning from Early Tertiary until today.

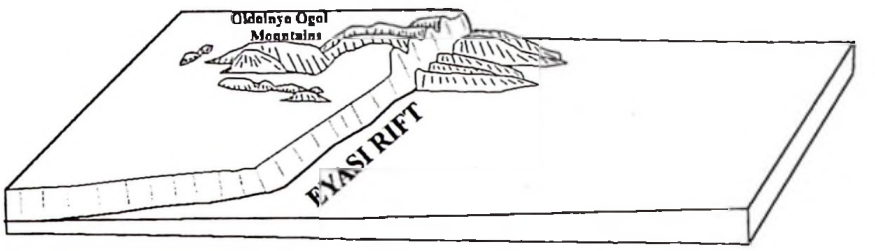

a: Miocene (15Ma to 7ma); The Eyasi rift was formed

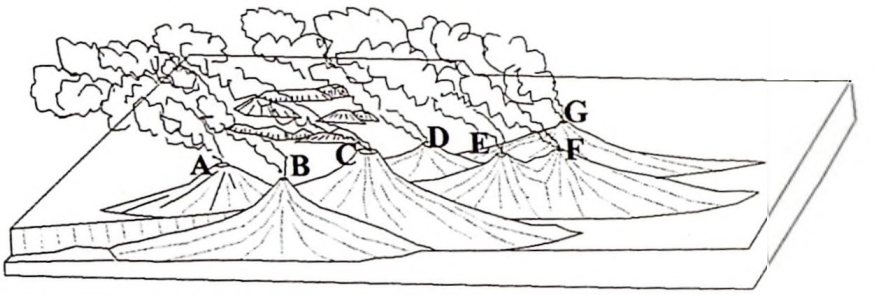

b: Pliocene to Pleistocene (7Ma - 2ma) The formation of volcanoes (A-Lemagruti; B-Oldeani; C-Ngorongoro D-Olmoti; E-Oloirua; F-Loolmasin; G-Embakaai)

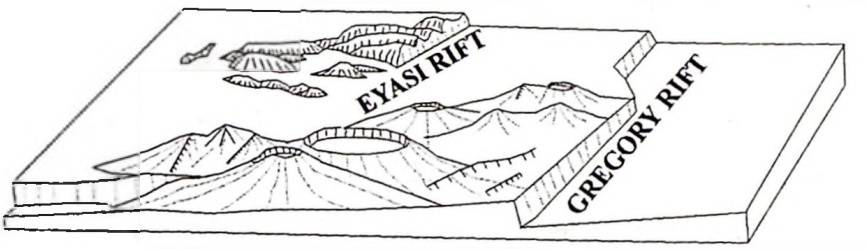

c: Pleistocene to Holocene (2Ma - 10,000BP), Most the volcanoes collapsed, Olduvai Gorge beds were deposited..

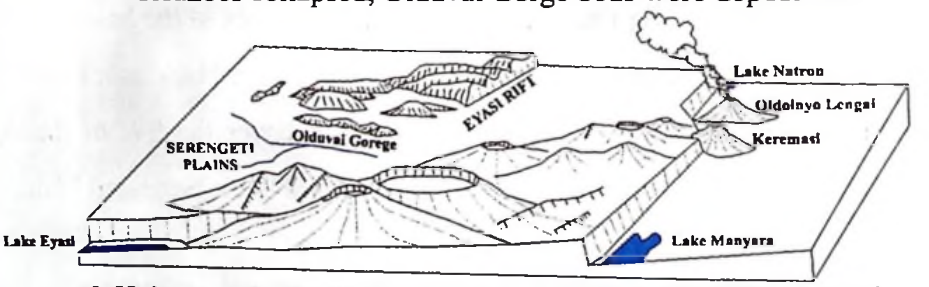

d: Holocene to Present (10,000BP to 0.00BP), Oldoinyo Lengai and Kremasi volcanic centers erupted along the Gregory Rift. The Olduvai Gorges started to be curved in the Serengeti plains.

Figure 5.3a-d: The geomorphological and geological evolution of the Olduvai Gorge and Ngorongoro highlands. (After: Kafumu, 1995).

Following Shackleton, (1978) the geological and geomorphological evolution of Olduvai Gorge area can thus be summarized as according to figure 5.4 and as briefly described here below. The evolution began with a planation of the pre-existing Precambrian rocks during the Tertiary (Miocene). This was a long period of erosion. Then faulting began followed by eruption and deposition of significant lava flows and tuff. Faulting also created Lake Basins, which began to be filled by volcanic, fluviatile and lacustrine sediments often, intercalated by palaeosol levels. Finnaly the basins were filled up and consequently dried out, then the Olduvai river started to be cut out through the sediments eventually curving out the Olduvai Gorges as seen today.

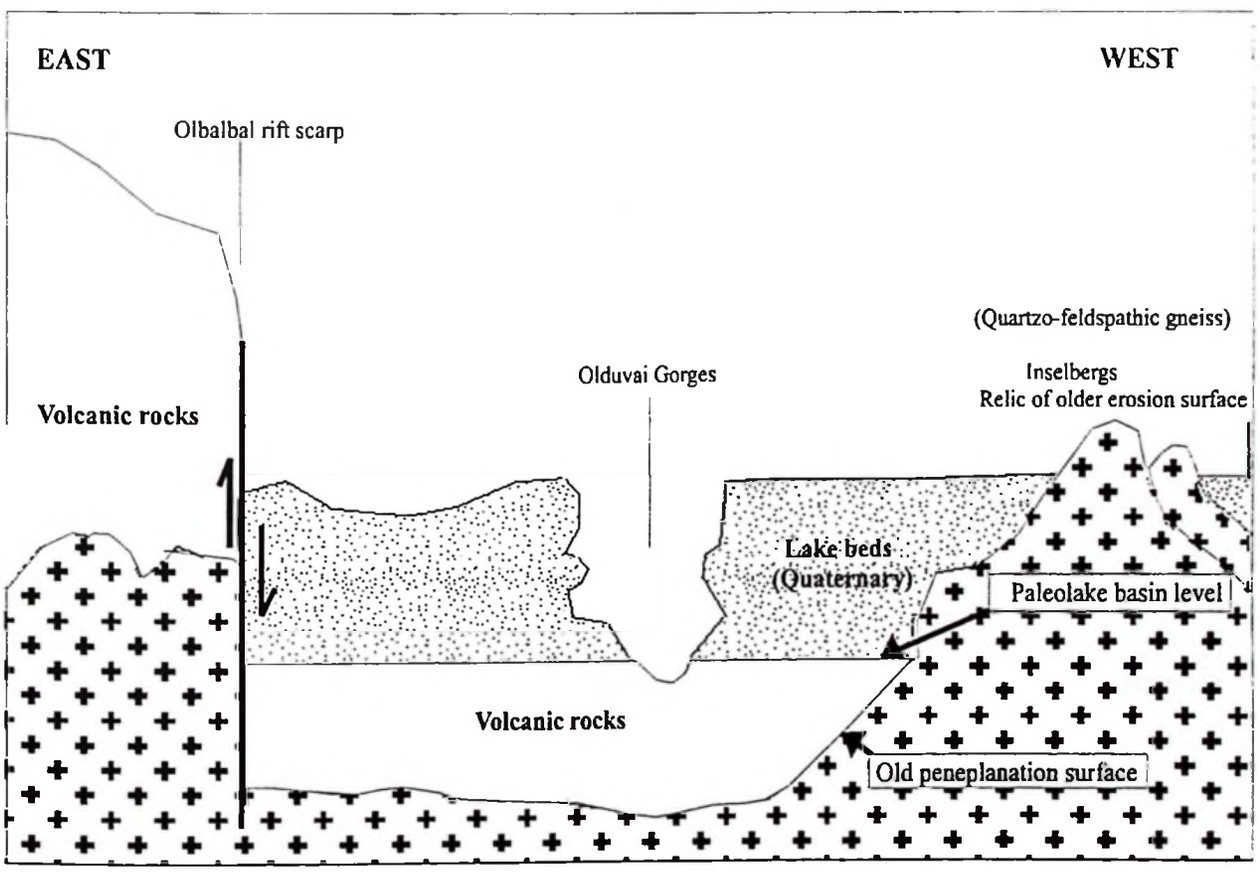

Figure 5.4: Idealized and simplified geological and geomorphological section of Olduvai Gorge paleolake basin. [Peneplanation of the Precabrian metamorhic rocks. Volcanism and sedimentation are triggered followed by the formation of the Olduvai lake basin. Intense sedimentation and filling up of the basin. Finally the Olduvai canyon is curved.]

5.4. DETAILED GEOLOGICAL MAPPING

5.4.1. General geology

The study area which lies within latitudes 35°0`S – 35°28`S and longitudes 2°43`E – 3°4`E was mapped in detail and the geology of the area is then presented in figure 5.5 and 5.6 and briefly discussed here below. The Olduvai Gorge area is mapped as covered by lakebeds lying unconformably on a Precambrian basement complex or on volcanic lava and ignimbrite (see section 5.2.2). In other words the Pliocene-Pleistocene volcanic rocks cover the basement complex and the lakebeds finally rest on the volcanic rocks. The Olduvai Gorge lakebed Formations are classified as Bed I to Bed V from bottom to top (figures 5.5a, 5.5c and 5.5d).

The remnant old Precambrian peneplain outcrop as quartzite-gneiss inselbergs, (figures 5.5b and 5.5e) mainly occur north of the area (Oldongoidjo, Naibor Soit and Agata Kiti hills) and the lakebeds are exposed on the cliff walls of the deep Olduvai Gorge canyon. To the east lies the Olbalbal depression covered by alluvial sand and silts related to the present day sedimentation processes of the Olduvai Gorge drainage system. Black sand (volcanic tephra) covers the southern part of Agata Kiti area (Western Serengeti plains). The sands are believed to have erupted from Oldoinyo Lengai Holocene eruption and covered most of the Salei Plains and started to roll westward towards the Serengeti Plains. To day they form several sand dunes (shifting sands) north of the Olduvai Gorges (figure 5.5).

A detailed lithostratigraphical description and classification of the Olduvai Gorge deposits was undertaken and the results indicate that the E-W crosssection (figure 5.6) show that the Olduvai Gorge Quatenary sediments are are deeply incised by the Olduvai river forming gorges of up to 100m deep. The sediments are intensily faulted with at least 5 fault lines that can be mapped accrosss the section (figure 5.6). The sediments dip

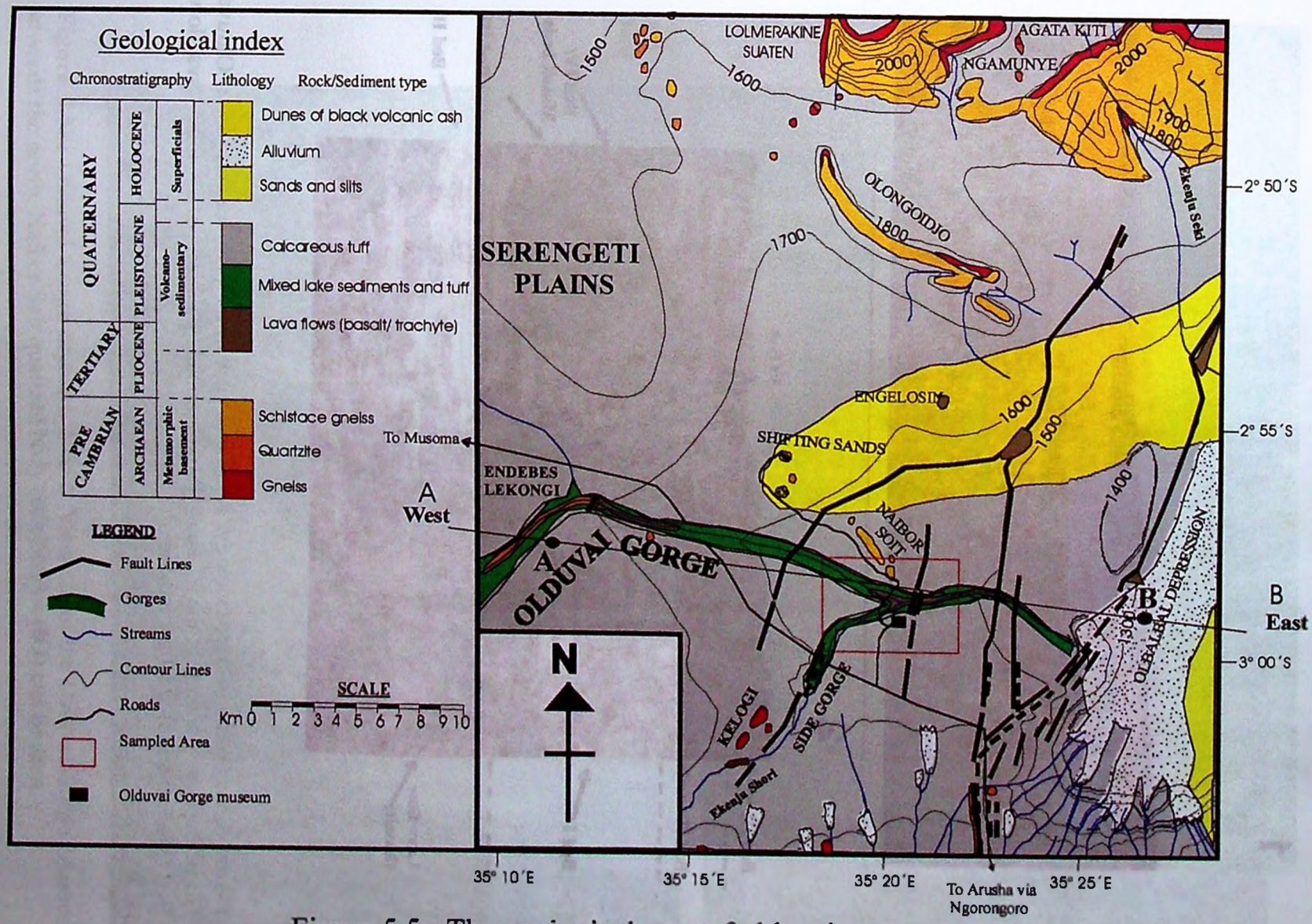

Figure 5.5: The geological map of olduvai gorge area, [A geological East-West section is given in figure 5.6]

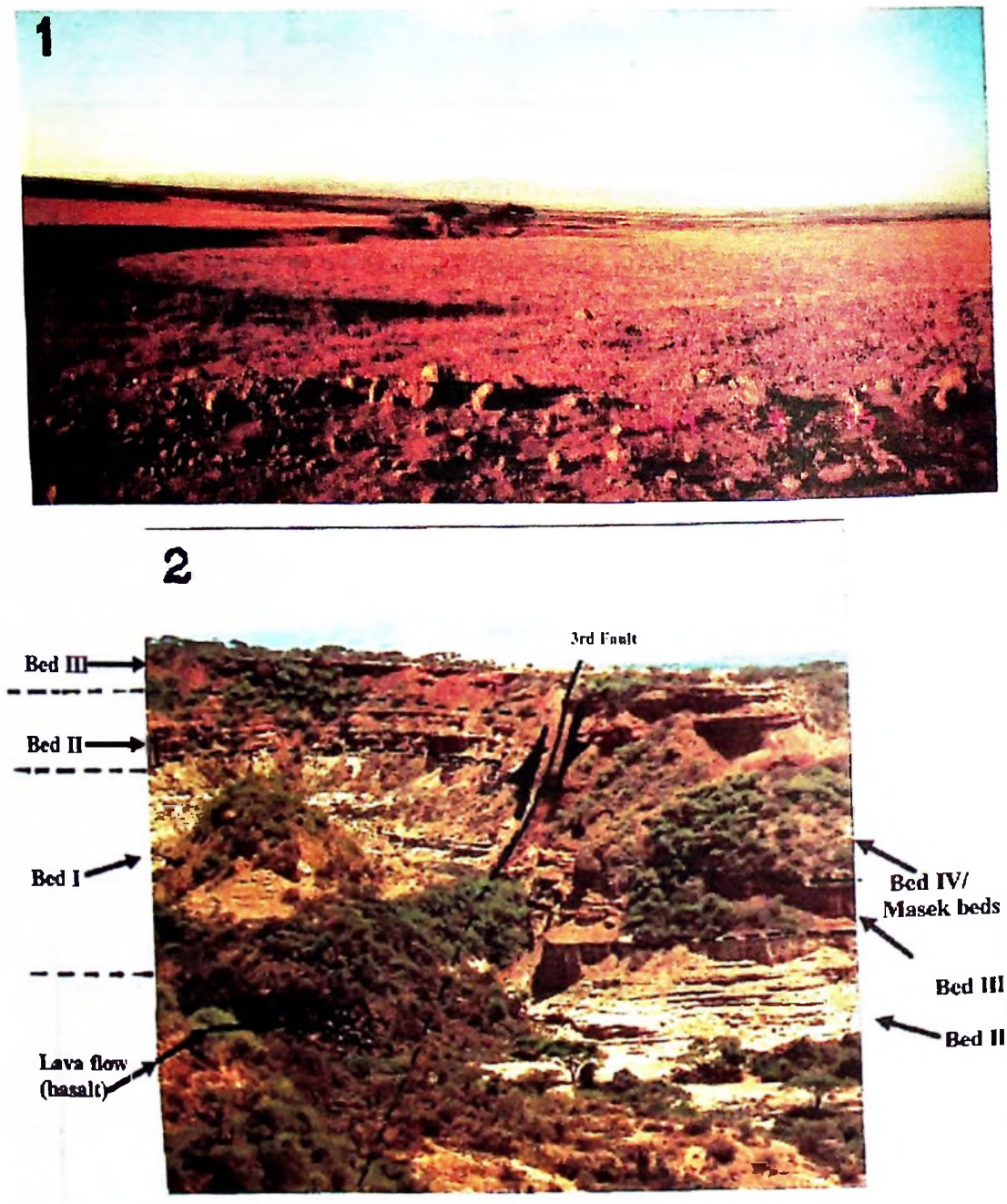

Figure 5.5a: Olduvai Gorge Geology. **1.** General view of the Olduvai Gorges. **2.** Olduvai Gorge deposits – a view at the 3rd Fault, [Stratigraphical positions of 3rd fault, lava flow, Bed I, Bed II and Bed III are indicated].

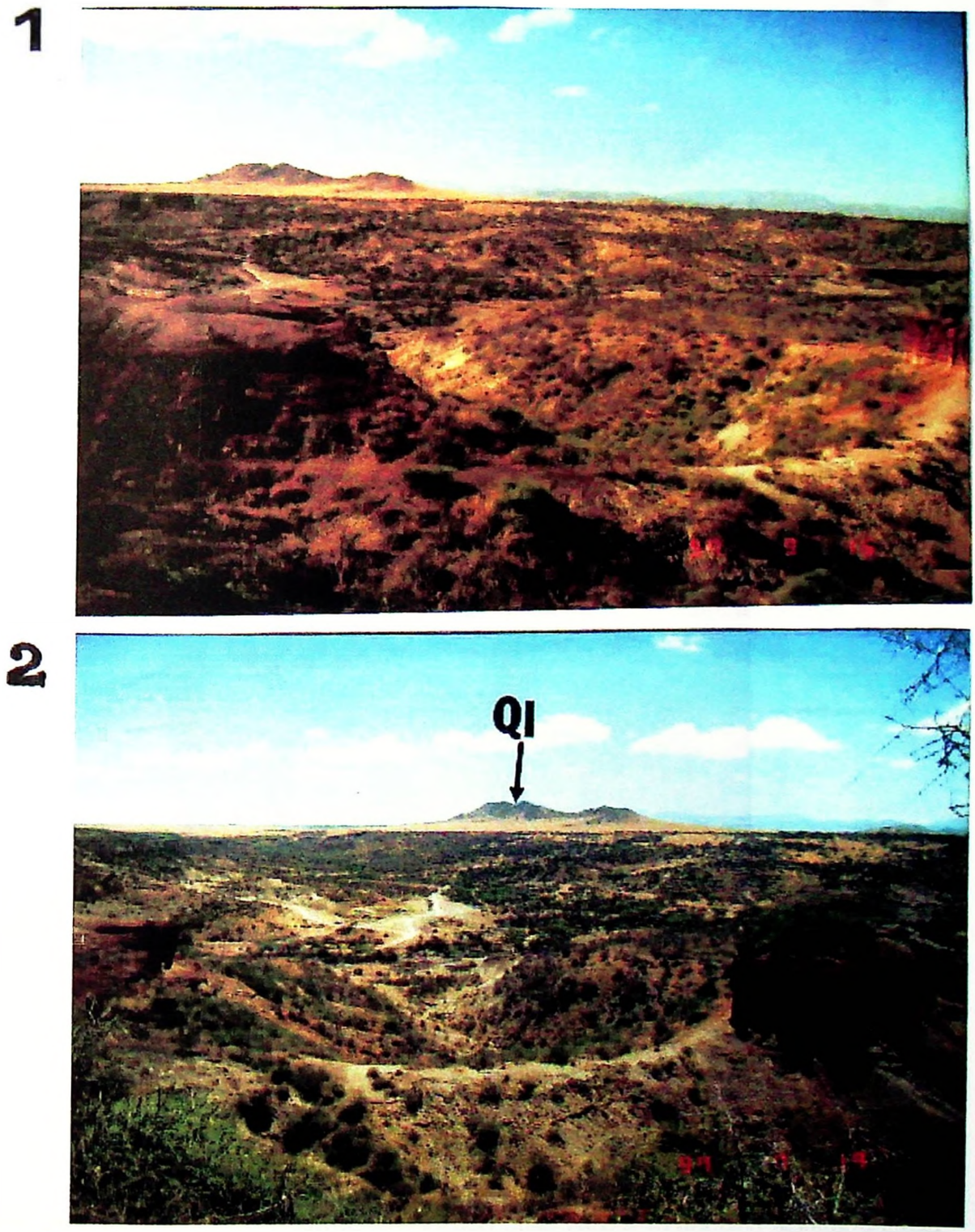

Figure 5.5b: Olduvai Gorge deposits. **1 & 2:** Views from the Olduvai Gorge Museum towards the north. Naibor Soit quartzite body (inselberg) – **(IQ)** can be seen.

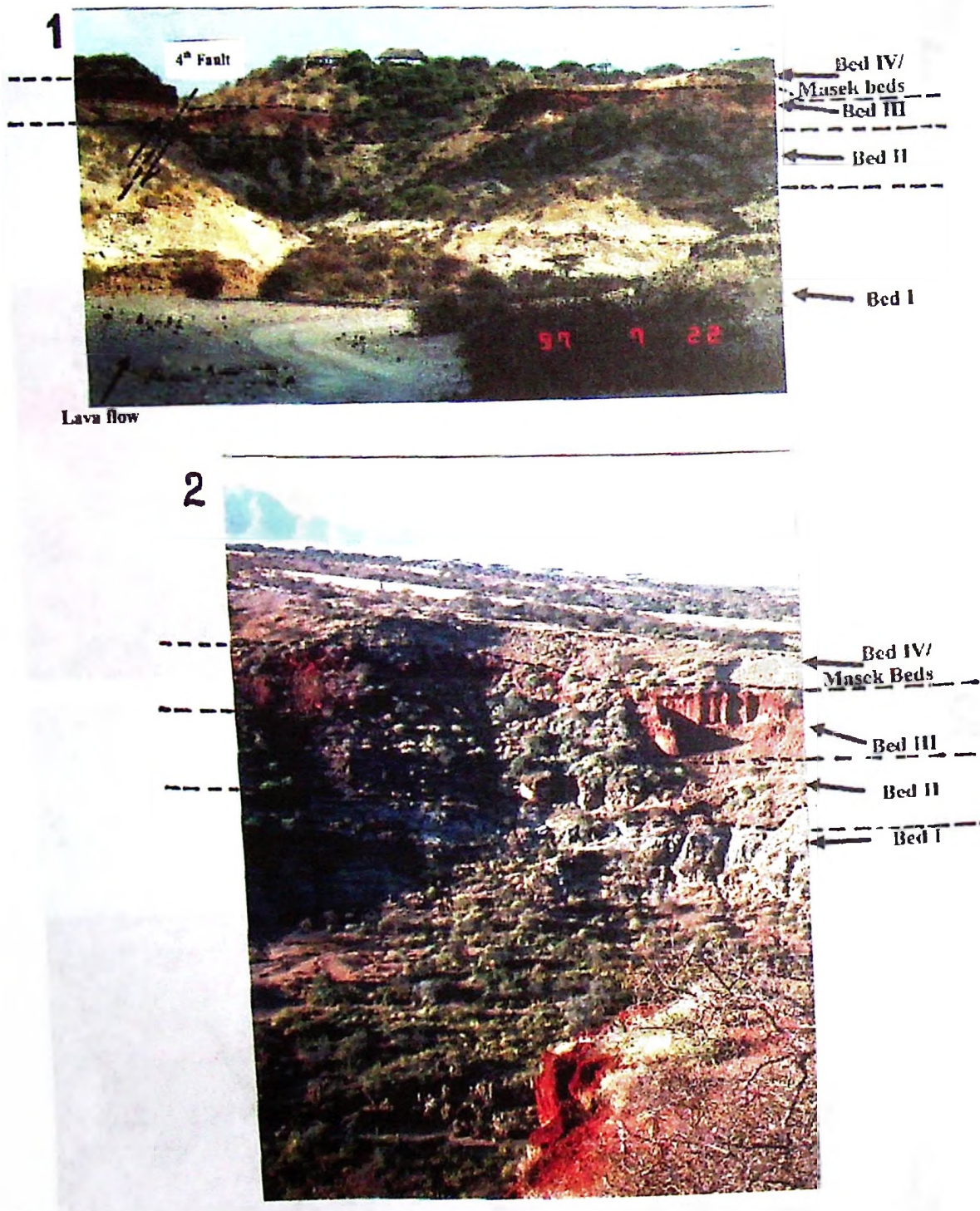

Figure 5.5c: Olduvai Gorge deposits. **1.** A view from gorge floor towards the Museum (towards the south). **2.** A view near Long Korongo site – 1km east of the Museum. [Stratigraphical position of second fault, Bed IV/Masek Beds, Bed III, Bed II and Bed I are indicated in both 1&2 sections]

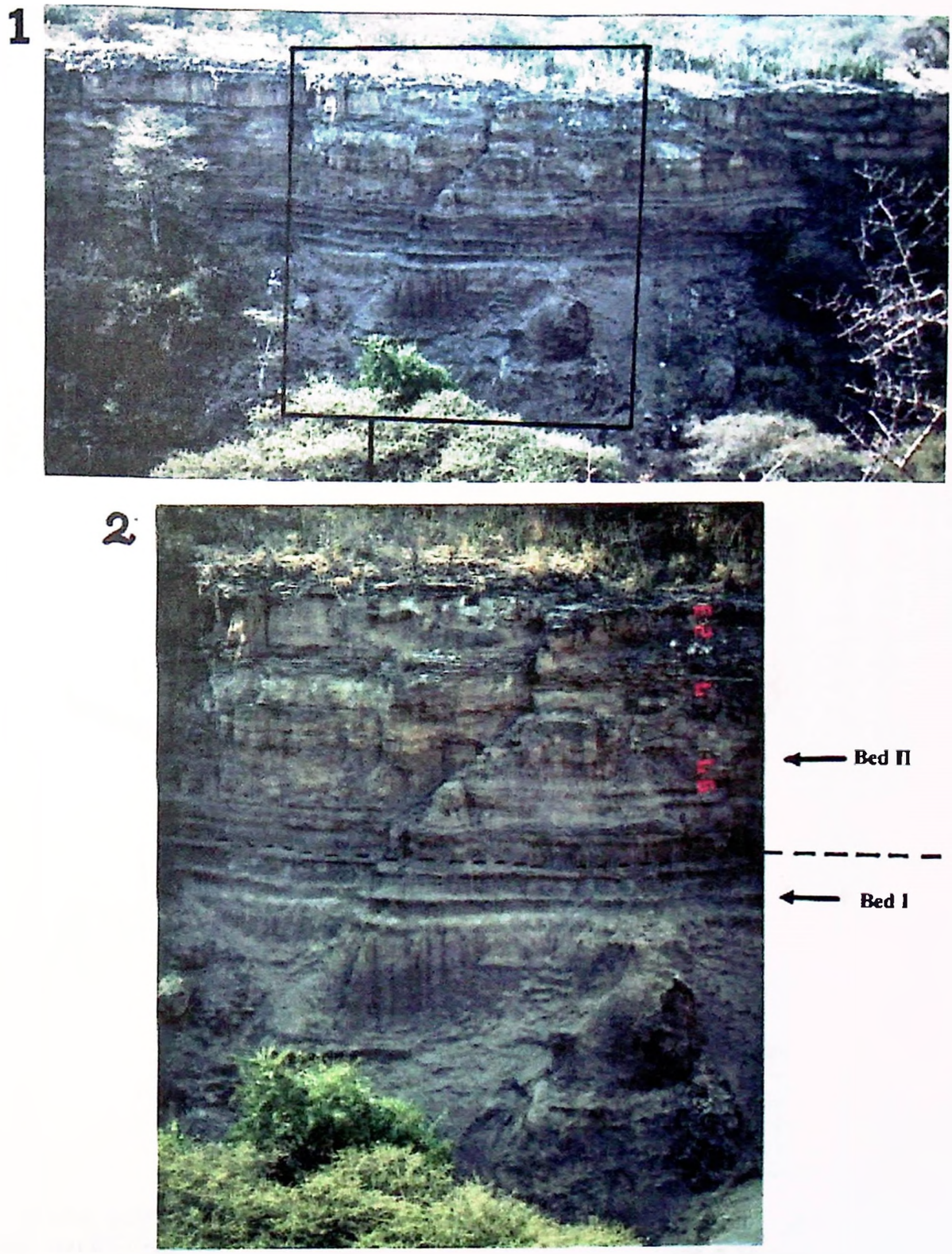

Figure 5.5d: Olduvai Gorge deposits, (2km east of the Museum). **1.** Bed I and Bed II sediments. **2.** Bed I and Bed II sediments (a close up).

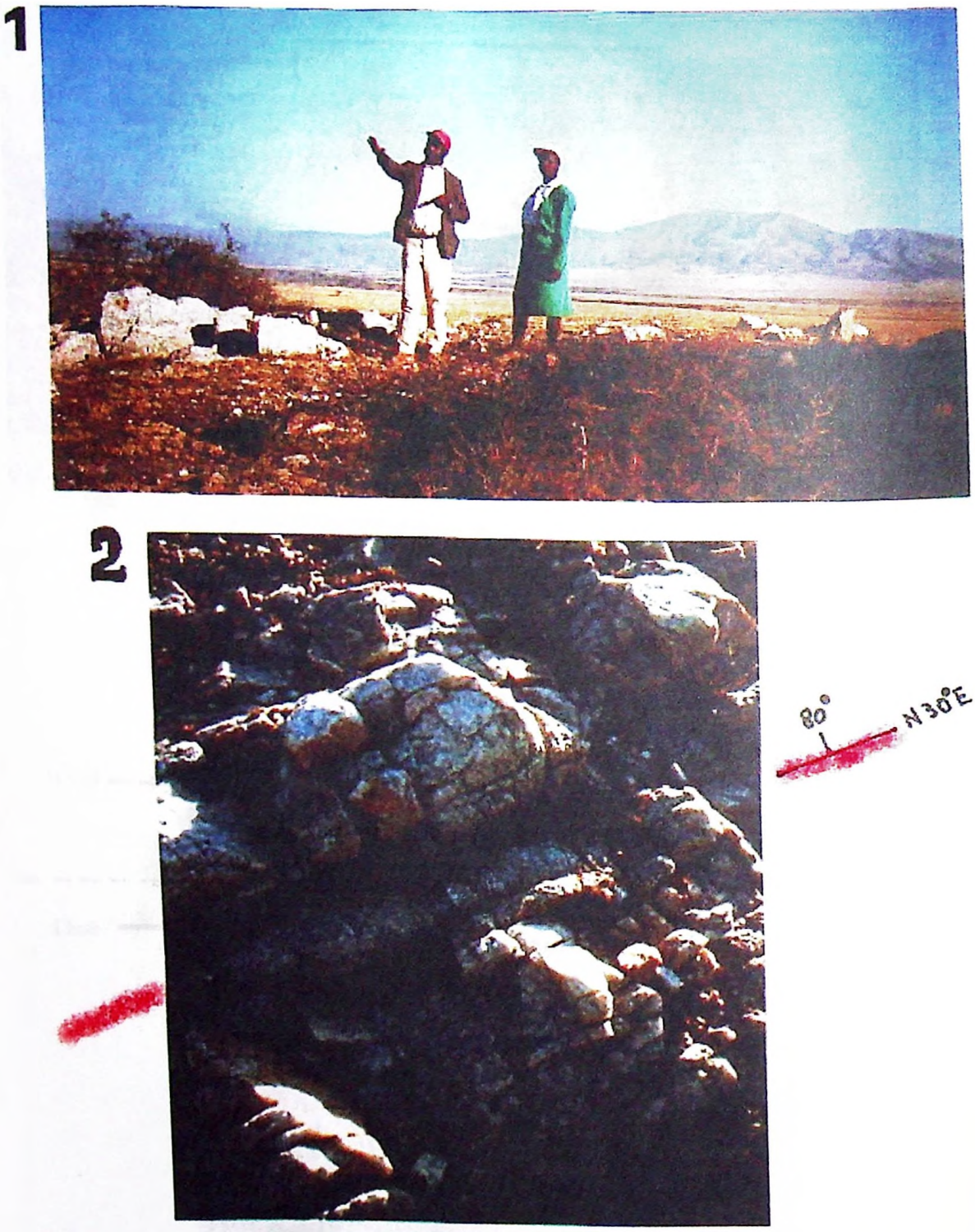

Figure 5.5e: Olduvai Gorge quartzite body (Inselberg), near the shifting sands. **1.** A general view of a small white quartzite inselberg submerged into the Olduvai Gorge lacustrine sediments. **2.** Close up of the quartzite body. The quartzite dips 80°SW and has a strike of N30°E.

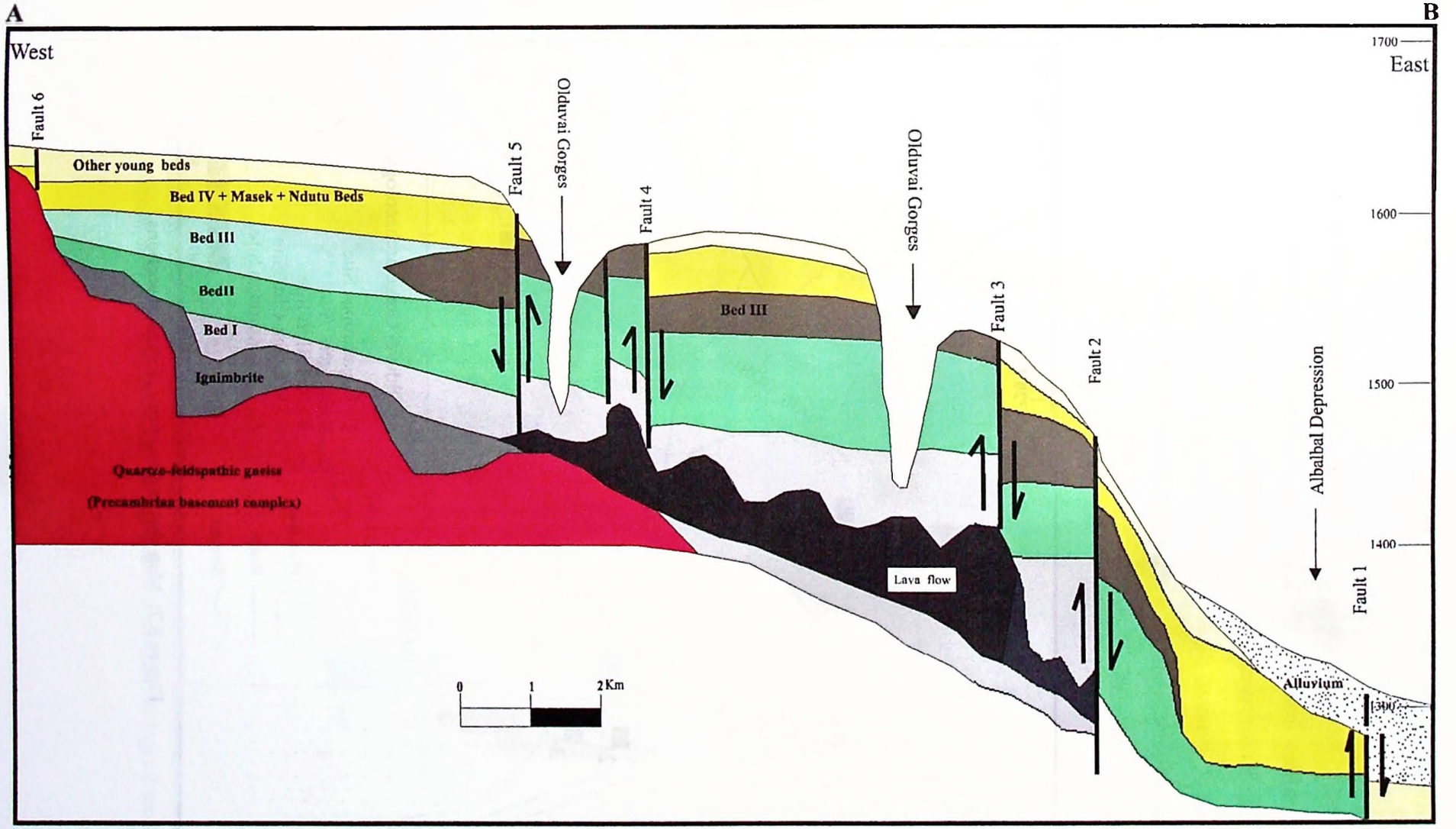

Figure 5.6: Geological cross section of Olduvai Gorge Beds [Refer figure 5]

5.4.2. Lithostratigraphical field studies

A systematic measurement (scaled drawing and photographing) and description of vertical profiles from the Olduvai Gorge section (Zinjathropus, Rutgers Section, Red Bluff, Long Korongo and Museum Cliff sites) along the gorge cliffs were made (figure 5.7). Here a general description of each studied section is offered. The detailed description of each lithological unit of the whole composite section is given in appendix 5 accompanying this text.

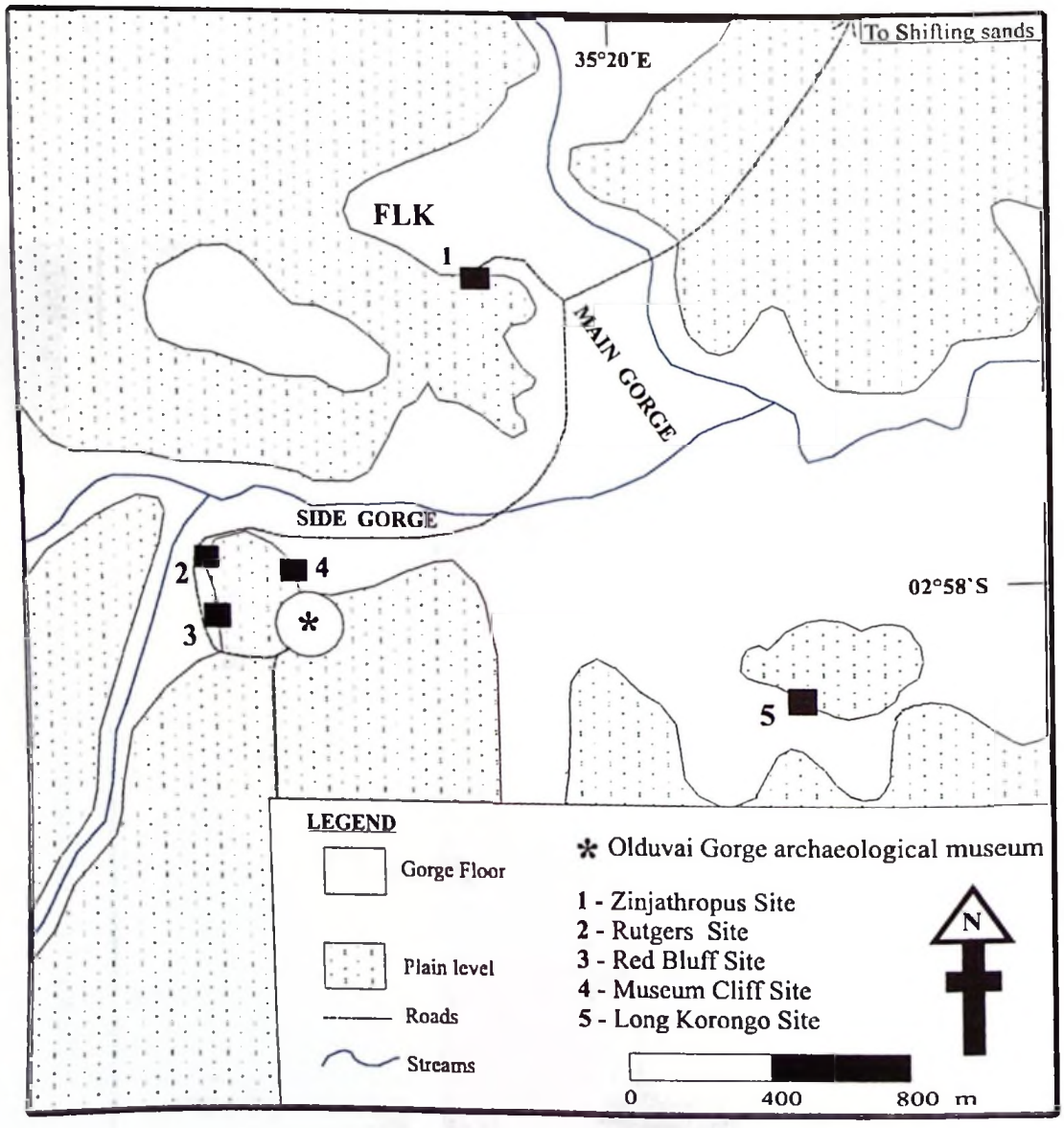

Figure 5.7: Map showing locations of studied sections

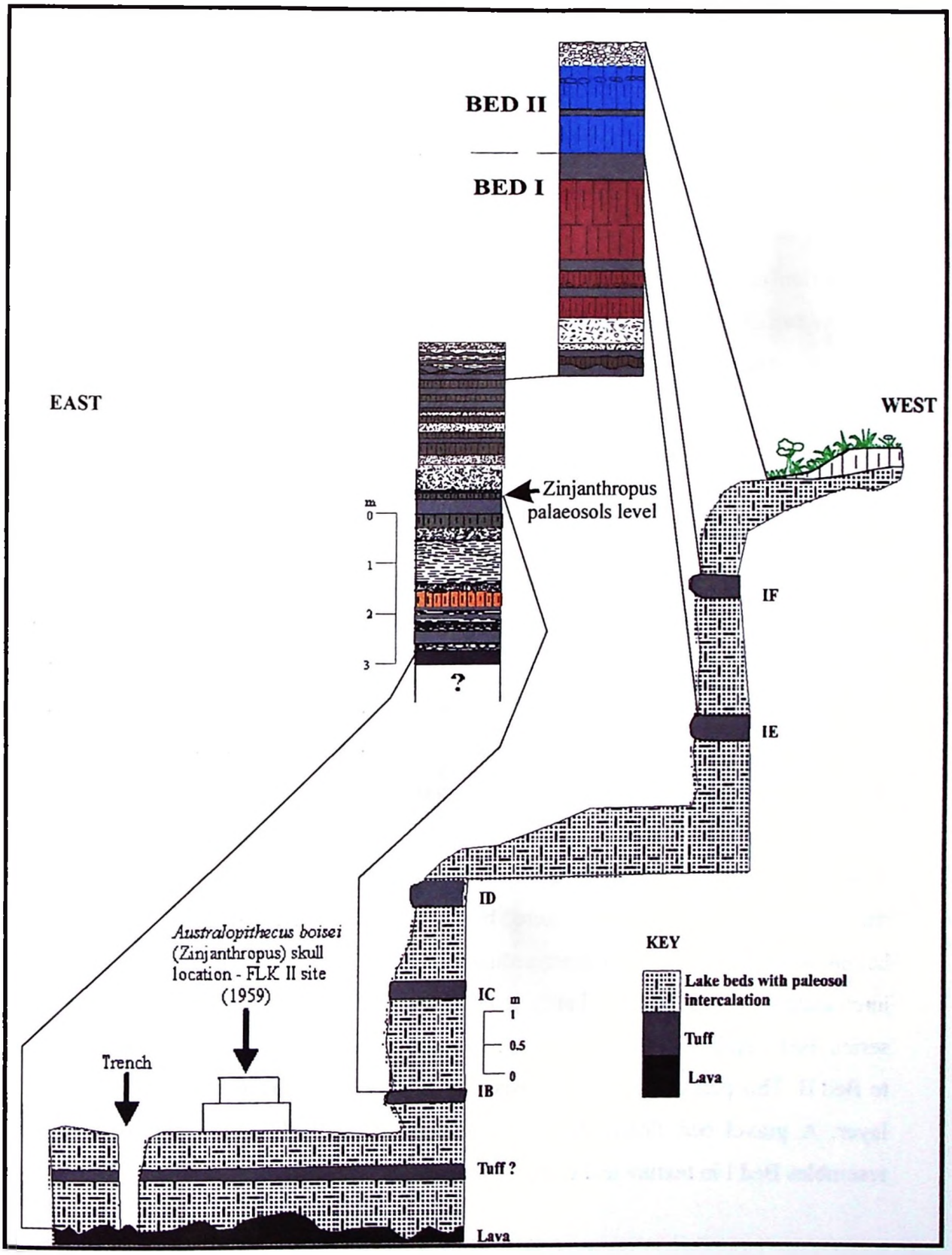

Figure 5. 8: Zinjanthropus Site Stratigraphical sections; (For legend see figure 5.14).

Zinjanthropus Site (Z) stratigraphical section

The Zinjanthropus site, (figure 5.8a) is known as FLK site where the Leakey family in 1959 (figures 5.7 and 5.8c) discovered the 'zinjanthropus' *Australopithecus boisei* skull. Figure 5.8 forms the basis of the zinj section description.

The section is a white to gray-olive lacustrine deposit mainly composed of white ash fall/flow tuffs, olive to gray clay and claystones intercalated with palaeosols. Limited sand levels and reworked pyroclasts are also present in this profile. This site covers the classical Bed I (Hay 1967 and Reck 1914) of Olduvai Gorge lakebeds.

The thickness of the profile is about 15m, beginning on basal gravel on a ragged olivine basalt lava (Kafumu 1995) surface. This profile can be divided into three main zones, the lower (Lava – tuff IB), middle (tuff IB – tuff ID) and the upper (tuff ID – tuff IF and above), (figure 5.8b). The first (approx. 3m) part is mainly alternating clay-tuff layers with three major palaeosol levels. The middle part (approx. 4m) begins with a significant reworked pyroclast layer grading into a well-sorted (eolian?) sand bed at the top. Alternating thin tuff/palaeosol levels then overlies it, which changes into tuff/clay alternations towards the end of the middle series.

A substantial sand bed then breaks it. The upper part of this profile is uniquely thick dark-gray clay palaeosols interfingered by two major tuff layers IE and IF. The sequence begins with 80cm thick pyroclast sediments followed by two thick (50cm) palaeosols intercalated by tuff layers. Finally a 1.5m thick palaeosol overlie the later palaeosol series. Bed I ends with tuff IF. The uppermost part of the profile (above tuff IF) belongs to Bed II. This part of Bed II is composed of two thick palaeosols separated by a thin tuff layer. A gravel bed finally covers the upper palaeosol. This last part of the profile resembles Bed I in texture and composition of sediments.

Rutgers site (RS) stratigraphical section

This section is located along the side gorge (figure 5.7). It is the minor Gorge cliff wall, which was an archaeological excavation site conducted by Rutgers University scientific team in 1996/97. The site represents conventional Bed II lithology. It covers about 8m in depth (figure 5.9). The profile can be categorized into two main zones. The lower part (tuff IF – tuff IIC) begins with about 60cm thick olive clay bed, (figure 5.9a). This part (6m) is essentially a clay-tuff-palaeosol alternation. Seven levels can be mapped. The upper part of the profile (from tuff IIC and above) is made up of several gray-black sand and sandstone which grade into thick gravel beds towards the end of the section. Petrographic examinations of some of the sandstone reveal that the sand particles are mainly pyroxenes with some quartz and tuff particles cemented by coarse-grained calcite. The coarse crystalline character of the cement (calcite) infers that the sandstone may have been deposited in a water rich environment. Four main tuff levels can be observed (tuff IIA – IID). Seven palaeosol levels are mapped (see palaeosol section).

Red bluff (RB) stratigraphical section

The site is a cliff along the minor gorges upstream the Rutgers site (figure 5.7). The section is about 9m thick (figure 5.10). This is the conventional red Bed III of Olduvai Gorge beds known as 'red beds' (figure 5.10a). It is mainly an alternation of sand/sandstone/gravel (figure 5.10c) to silt/siltstone, clay-marl sediments and red palaeosols, (figure 5.10b). They are fluviatile to lacustrine sandy sediments.

Figure 5.8a: The zinjanthropus site. **1.** A general view of the site (towards the east). Ngorongoro Highlands can be seen in the background as indicated by the arrow. **2.** A view towards the north. Naibor Soit inselberg is seen in the background as indicated by the arrow.

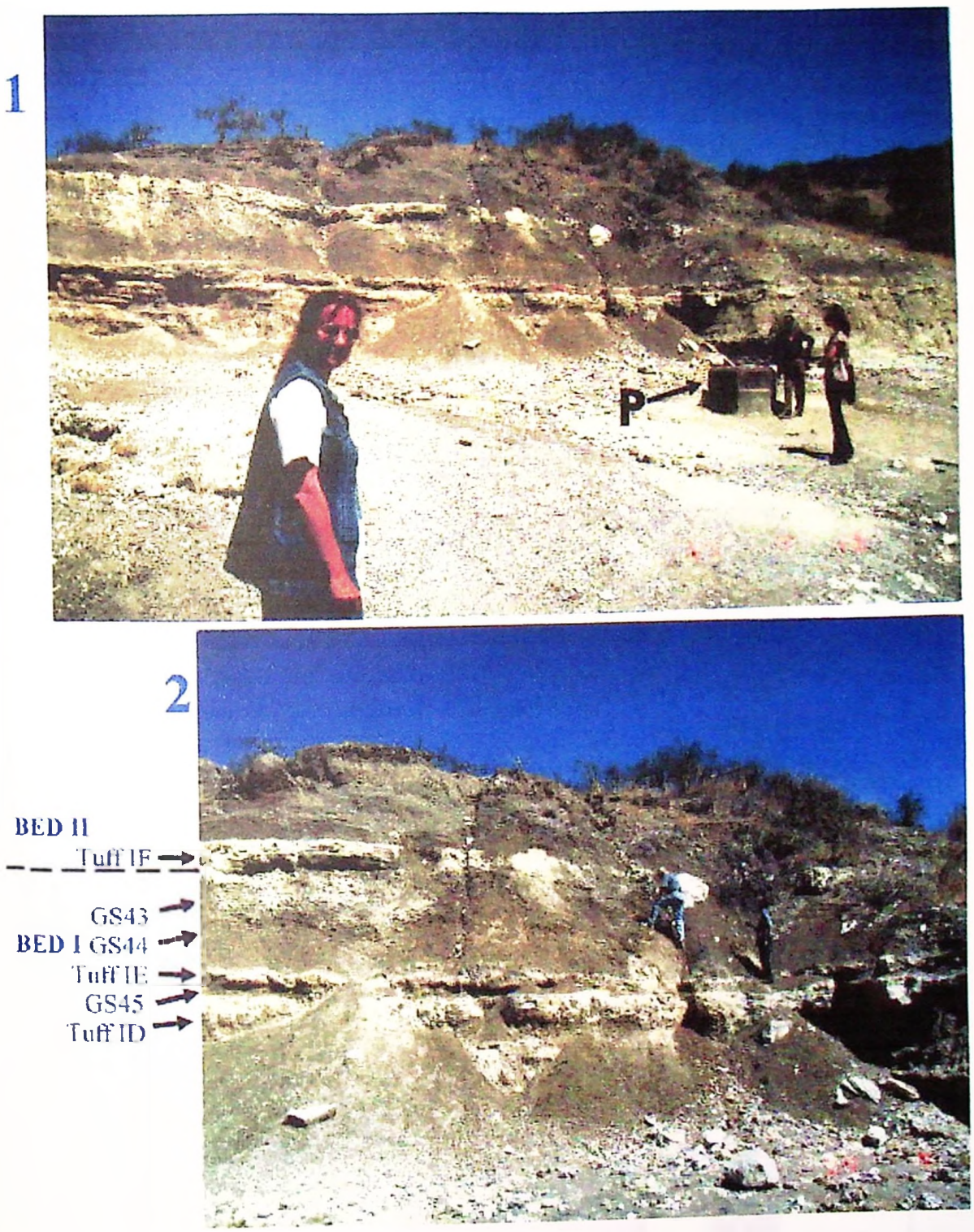

Figure 5.8b: The Zinjanthropus section. **1.** General view – the platform (p) shows where the "zinjanyhropus" *Australopithecus boisei* hominid skull was found in 1959. **2.** Stratigraphical positions of Bed I/Bed II geological boundary, palaeosol levels GS43, GS44 & GS45 and marker tuffs ID, IE & IF.

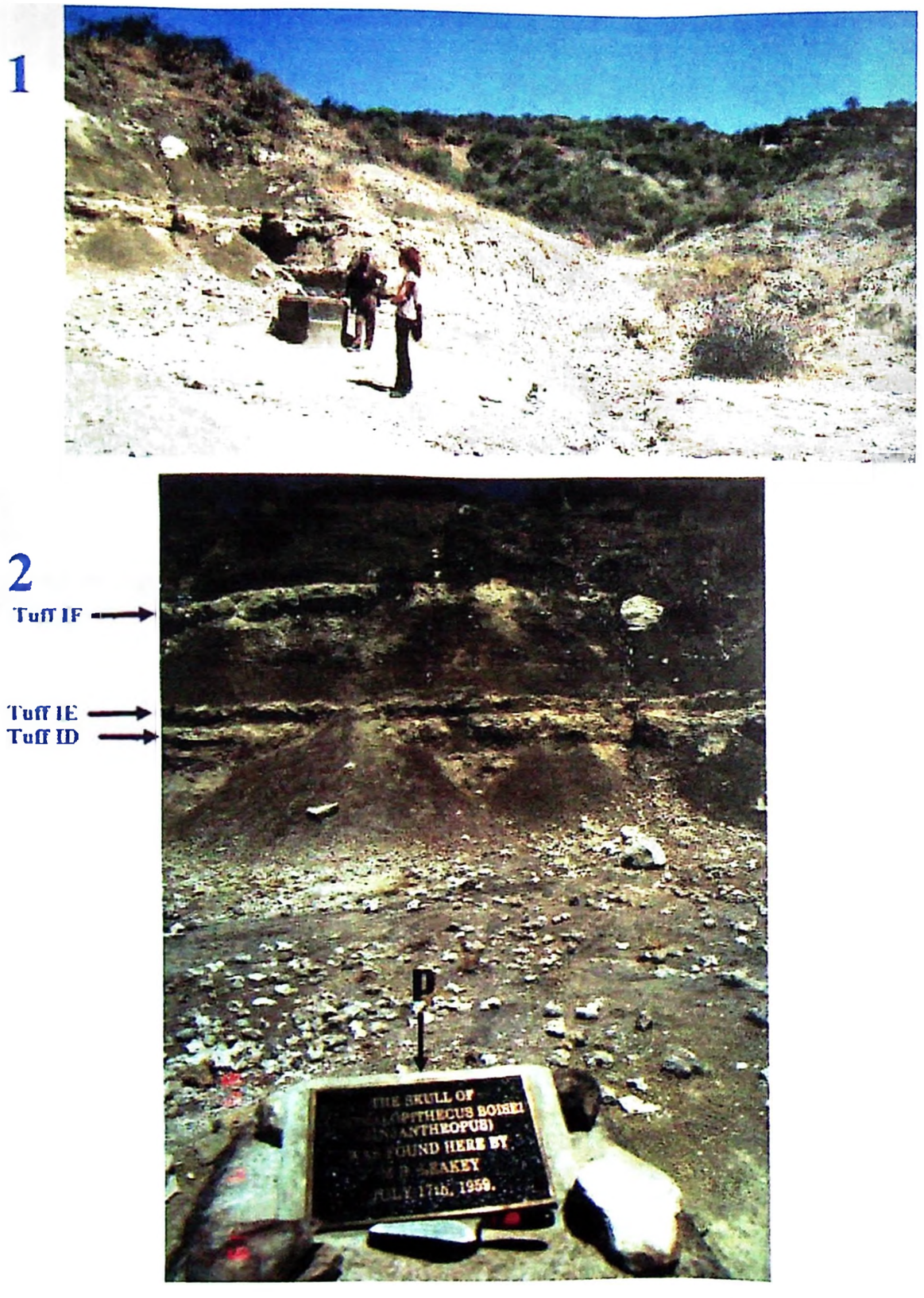

Figure 5.8c: The Zinjanthropus section. **1.** The general view of the FLK site. **2.** *Australopithecus boisei* hominid spot (p) July 17th 1959.

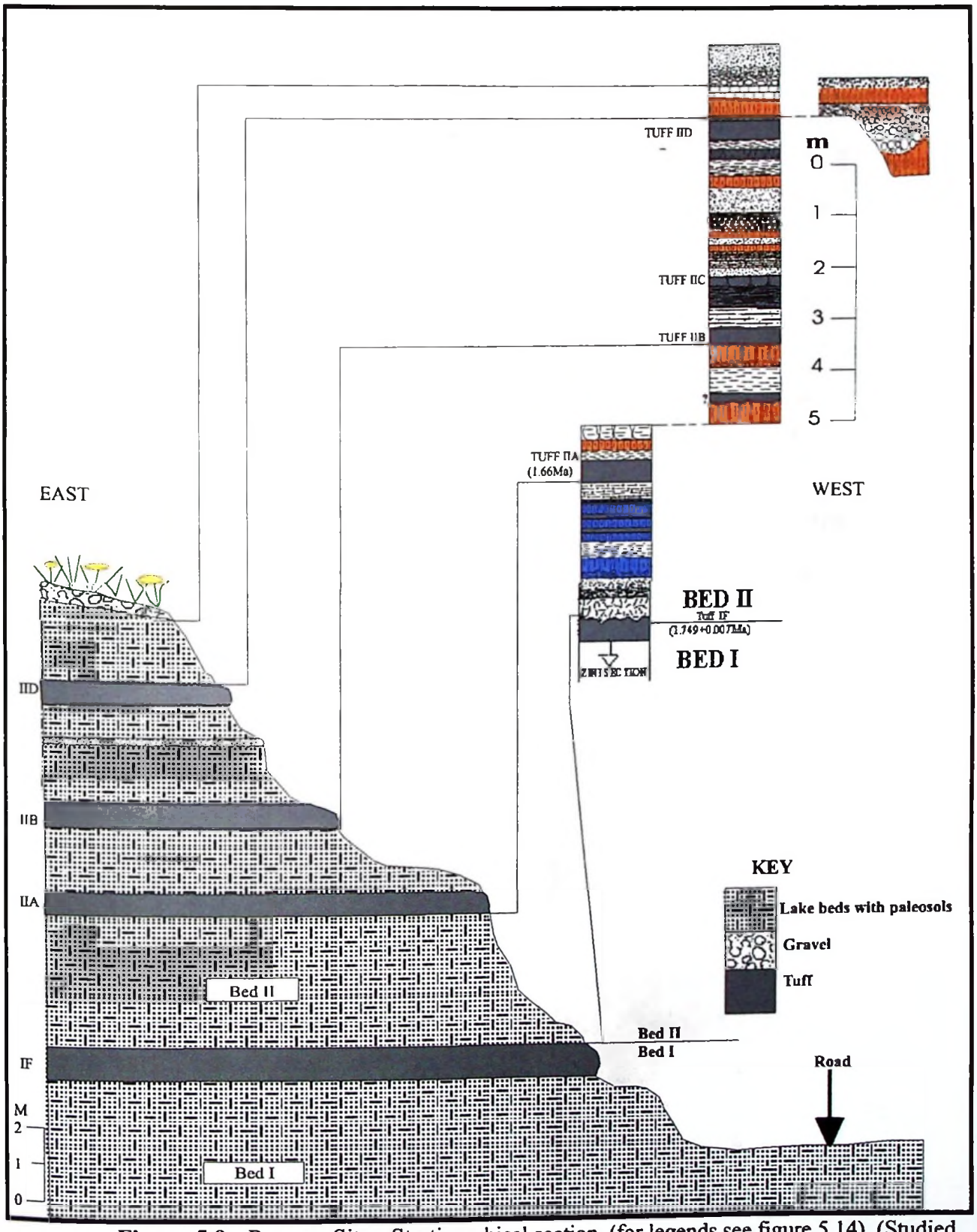

Figure 5.9: Rutgers Site - Stratigraphical section, (for legends see figure 5.14), (Studied with the permission of Rutgers University team)

1

2

Tuff IIC

Tuff IIB

Tuff IIA

Tuff IF

Figure 5.9a: Rutigers section. (Bed II site). **1.** A perspective view of the site. **2.** Palaeosol levels of the Rutigers section (Also refer figure 6.3a). [Studied with the permission of the Rutigers University scientific team].

The fluvial sediments are represented by sand-silt to gravely sediments, mainly observed in the 3m lower part. The middle part (about 2m) is mainly white marl sediments of lacustrine origin. Some of the marls are imbricated by palaeosols and are red in color. The last (4m) upper part of the profile looks like a composite red palaeosol broken here and there by thin hard banks (probably tuff?). This thick palaeosol level is overlain by thick calcarenite sediments, which grade into rounded pebbles and cobbles gravel bed.

Museum cliff (MC) stratigraphical section

The section is along the main gorge museum-cliff wall (figure 5.7 and 7.11). The profile covers about 15m depth. It begins with a 1m red palaeosol grading into gravel and calcarenite beds (approx. 2m). This major gravel bed is probably the boundary between Bed III and Bed IV/Masek Beds. Palaeosols intercalated with significant sand levels overlay the gravel beds. 1.5m of the lower part of this profile is made up of 6 palaeosols intercalated by sand levels. Tuff IV breaks the series and followed by palaeosol with a ragged surface. The palaeosol has an eroded top surface indicating a huge unconformity. 80cm thick sand layer covers the erosion surface.

The next 3m probably belongs to Ndutu Beds, is again a series of 7 clay-palaeosol levels. The rest 2m upper part of the profile was a thick level composed (from bottom to top) of lacustrine white to gray sand, mudstone and limestone. The basal sand is loose and the mudstones show a box-work of cracks and some large root casts filled with calc-materials (figures 5.11a and 5.11b_2). A hard limestone layer overlies this network of cracks.

Long Korongo (LK) stratigraphical section

This profile is part of middle Bed II and is located 1.5km east of the museum (figure 5.7). The profile is a deep gully of about 18m in thickness (figure 5.12). The lower part is mainly olive-gray palaeosol and clay. A 2m thick red palaeosol lay unconformably on tuff IIA. The upper part is again gray to olive palaeosols with carbonate concretions and a top sand layer

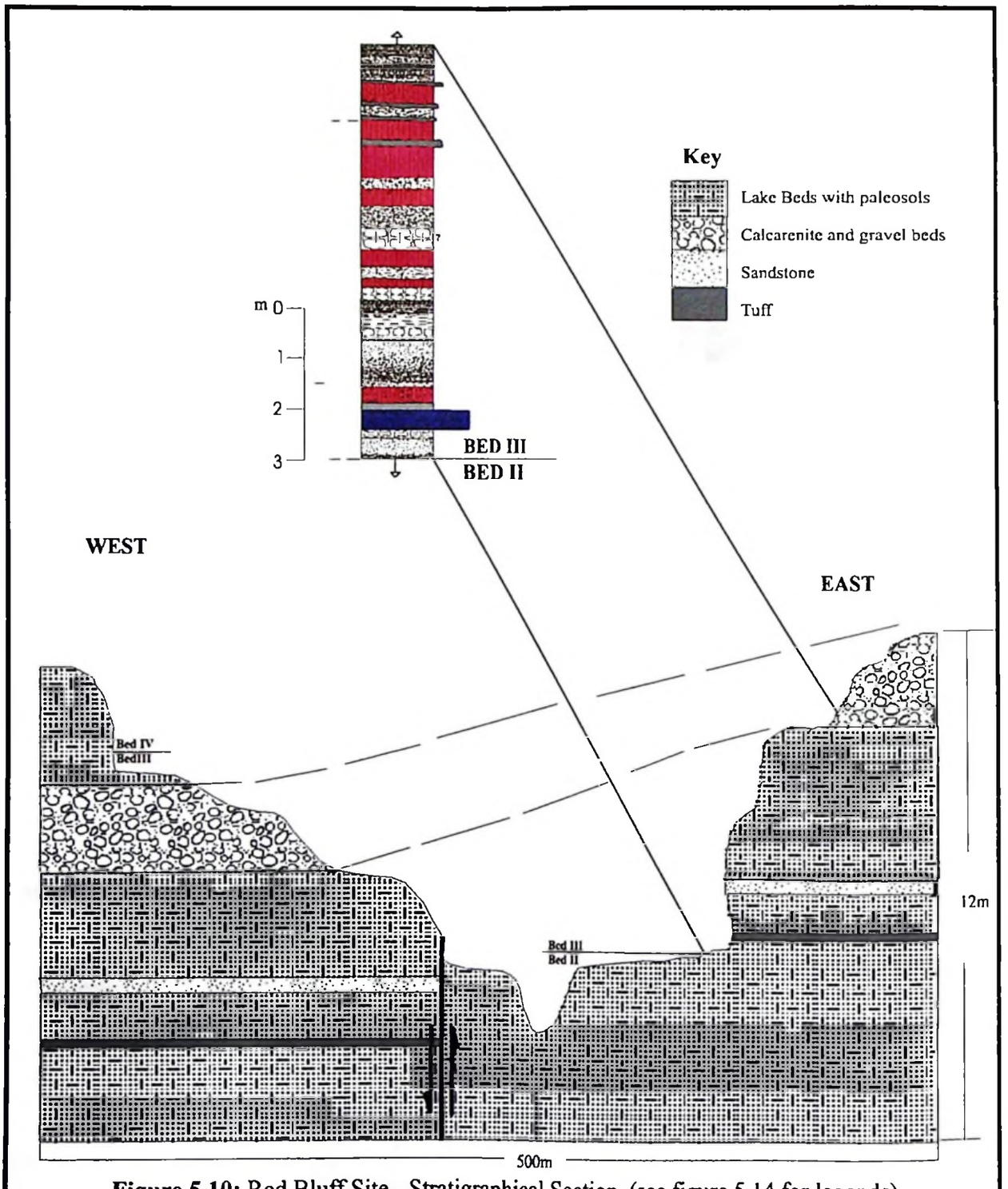

Figure 5.10: Red Bluff Site - Stratigraphical Section, (see figure 5.14 for legends)

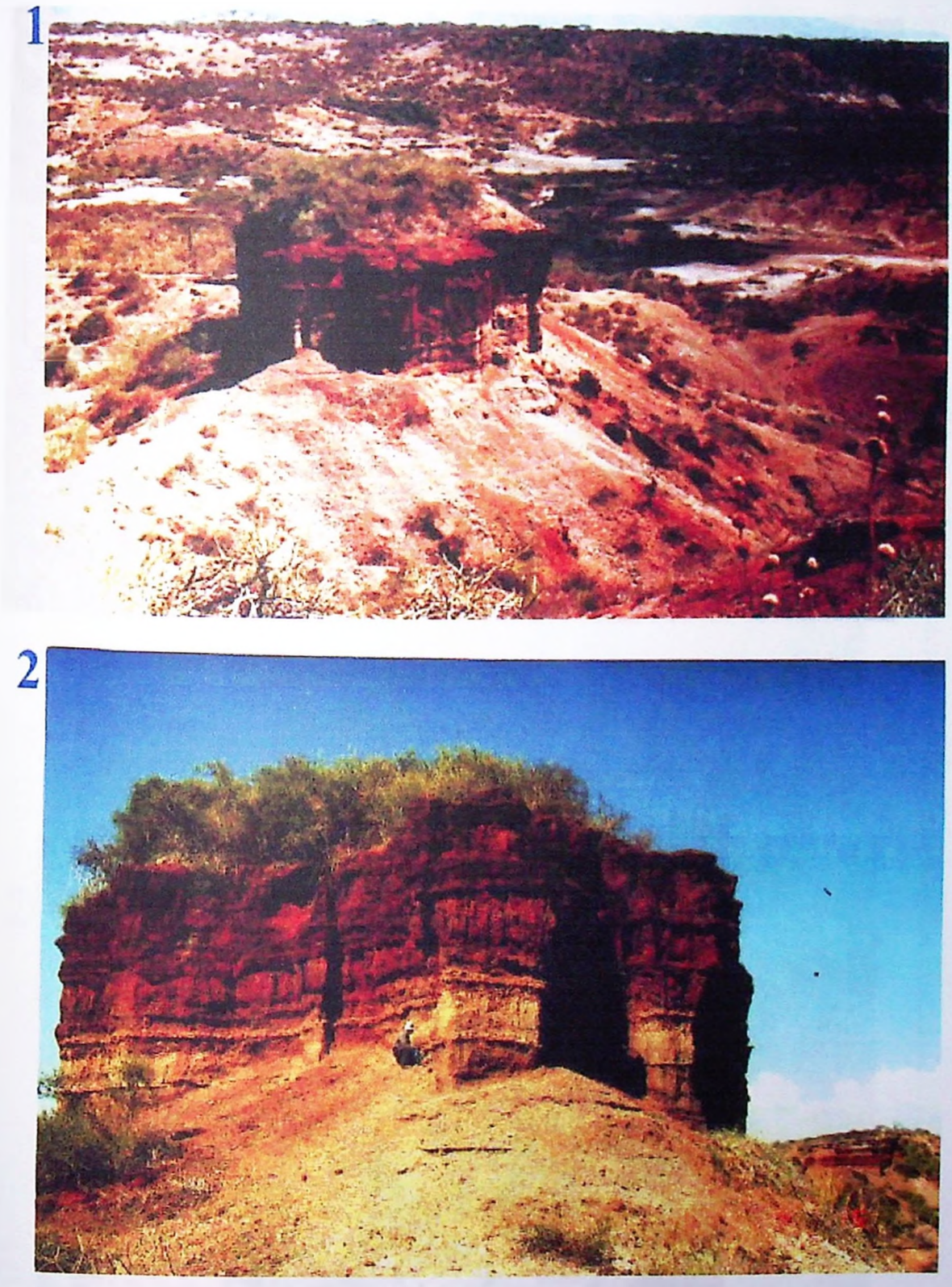

Figure 5.10a: Red Palaeosols in Bed III. **1.** General view. **2.** Closer view.

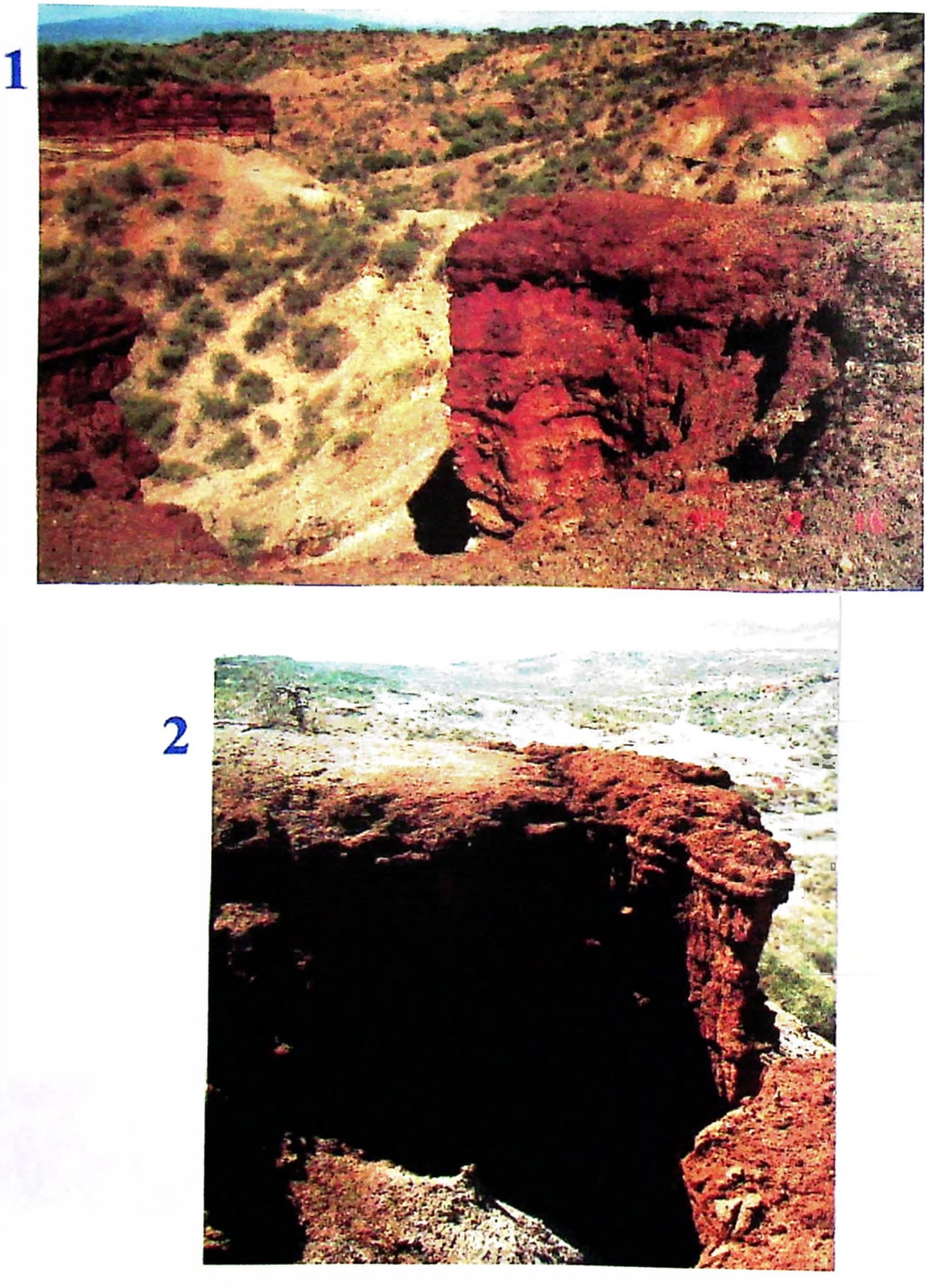

Figure 5.10b: Bed III sediments "red beds". **1.** General view. **2.** A closer view shows alternation of white clayey-marls and red paleosols.

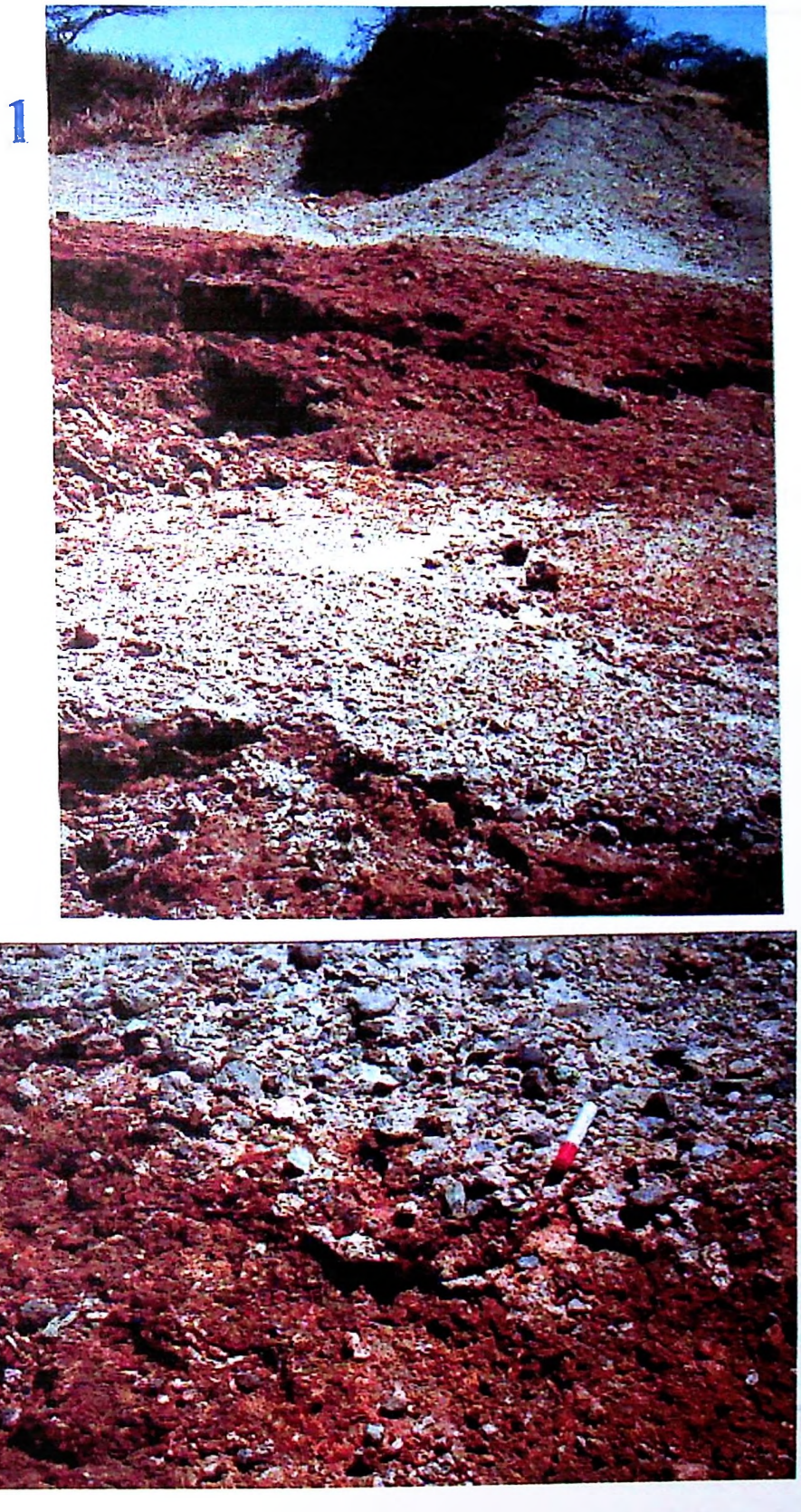

Figure 5.10c: Bed III sediments "red beds". **1.** General view. **2.** Detail view of the gravel bed in Bed III.

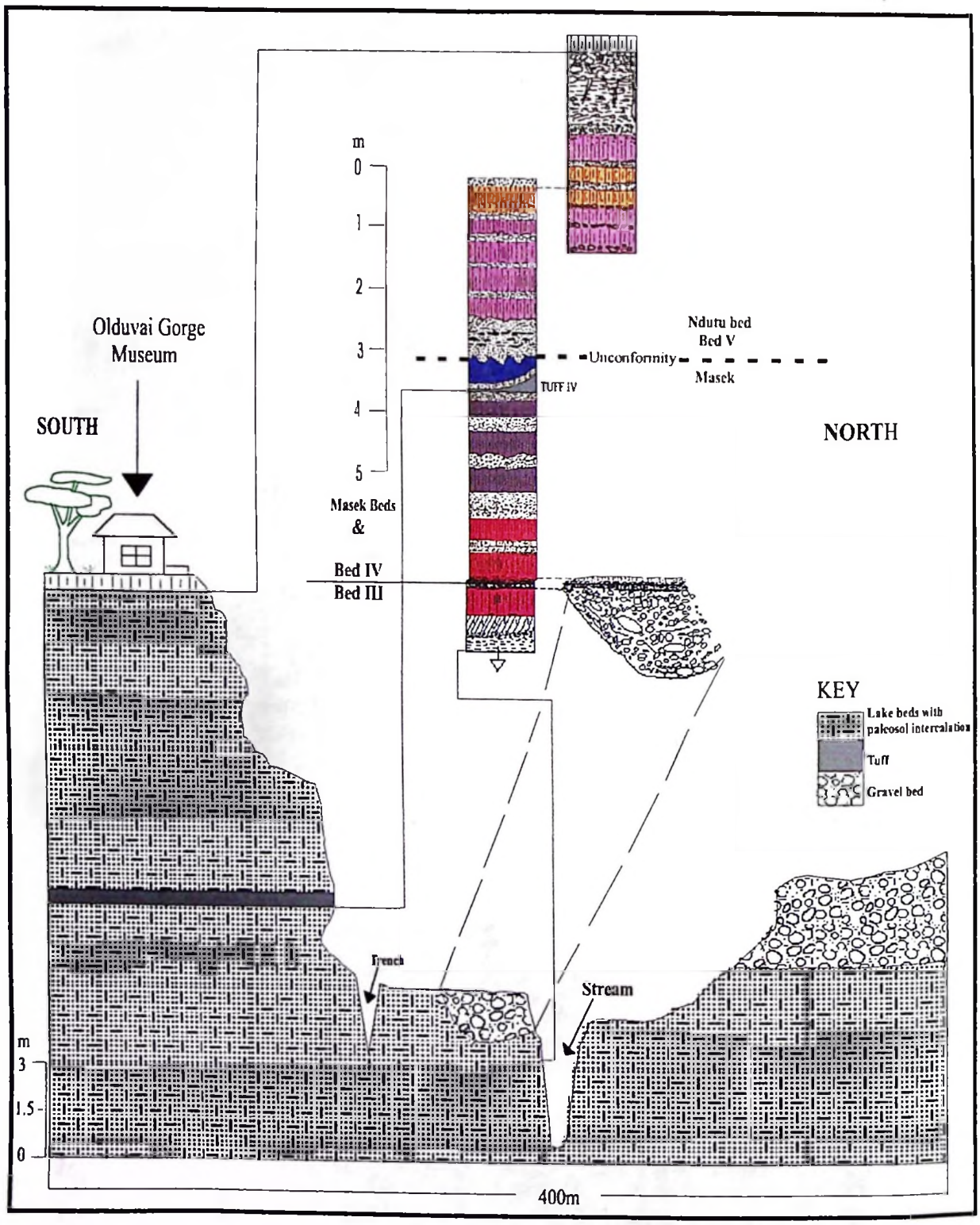

Figure 5.11: Museum cliff Site Stratigraphical Section, (see figure 5.14 for legends)

1

2

Figure 5.11a: Museum Cliff section, (Bed IV, Masek/Ndutu Beds). **1.** Cracked mudstone, (mudcracks filled with carbonate material) **2.** Close up. A boxwork of cracks filled by carbonate.

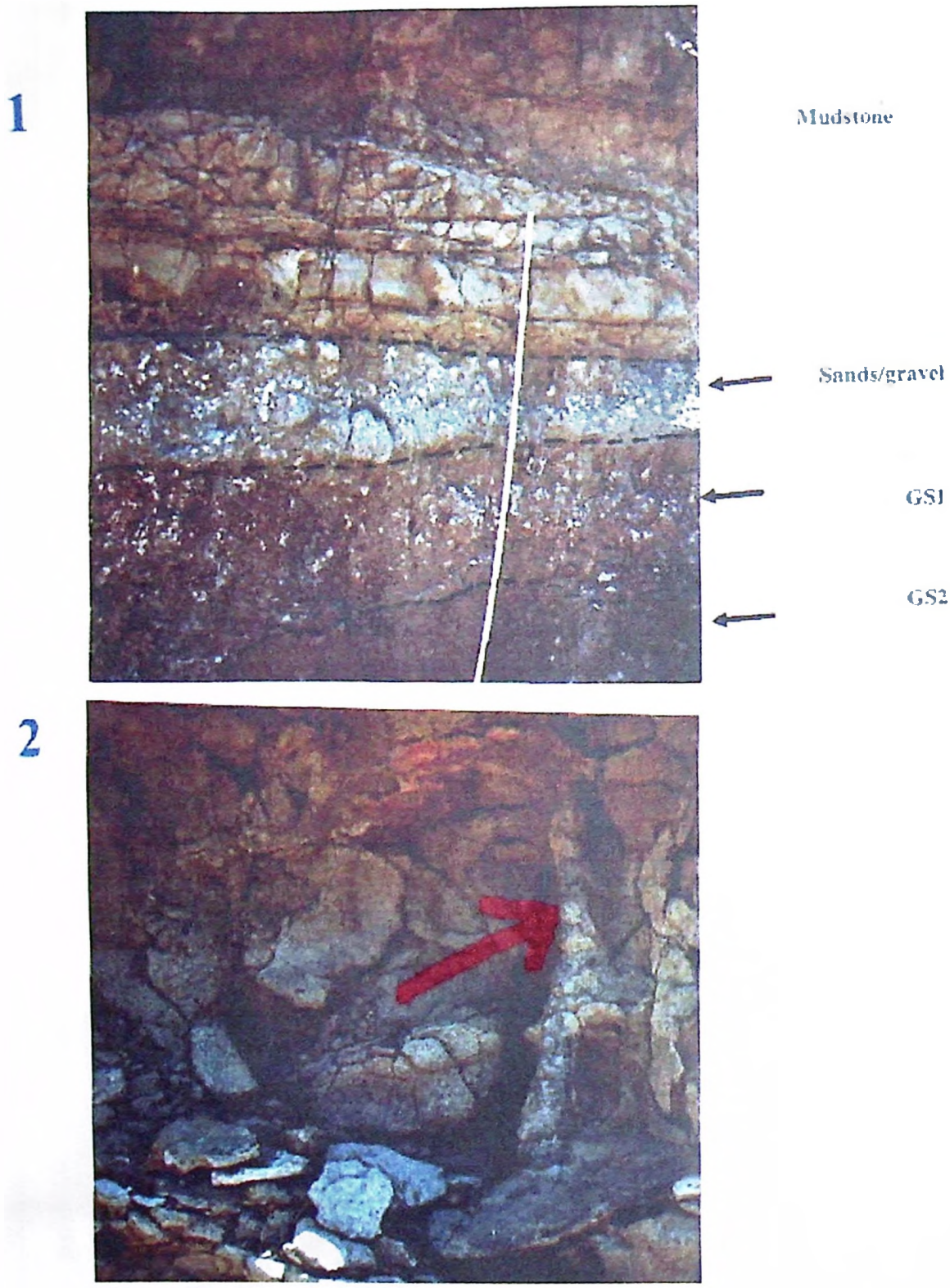

Figure 5.11b: Museum Cliff section. **1.** Stratigraphical position of mudstone, GS1 and GS2. **2.** Large root channel in mudstone infilled by carbonate.

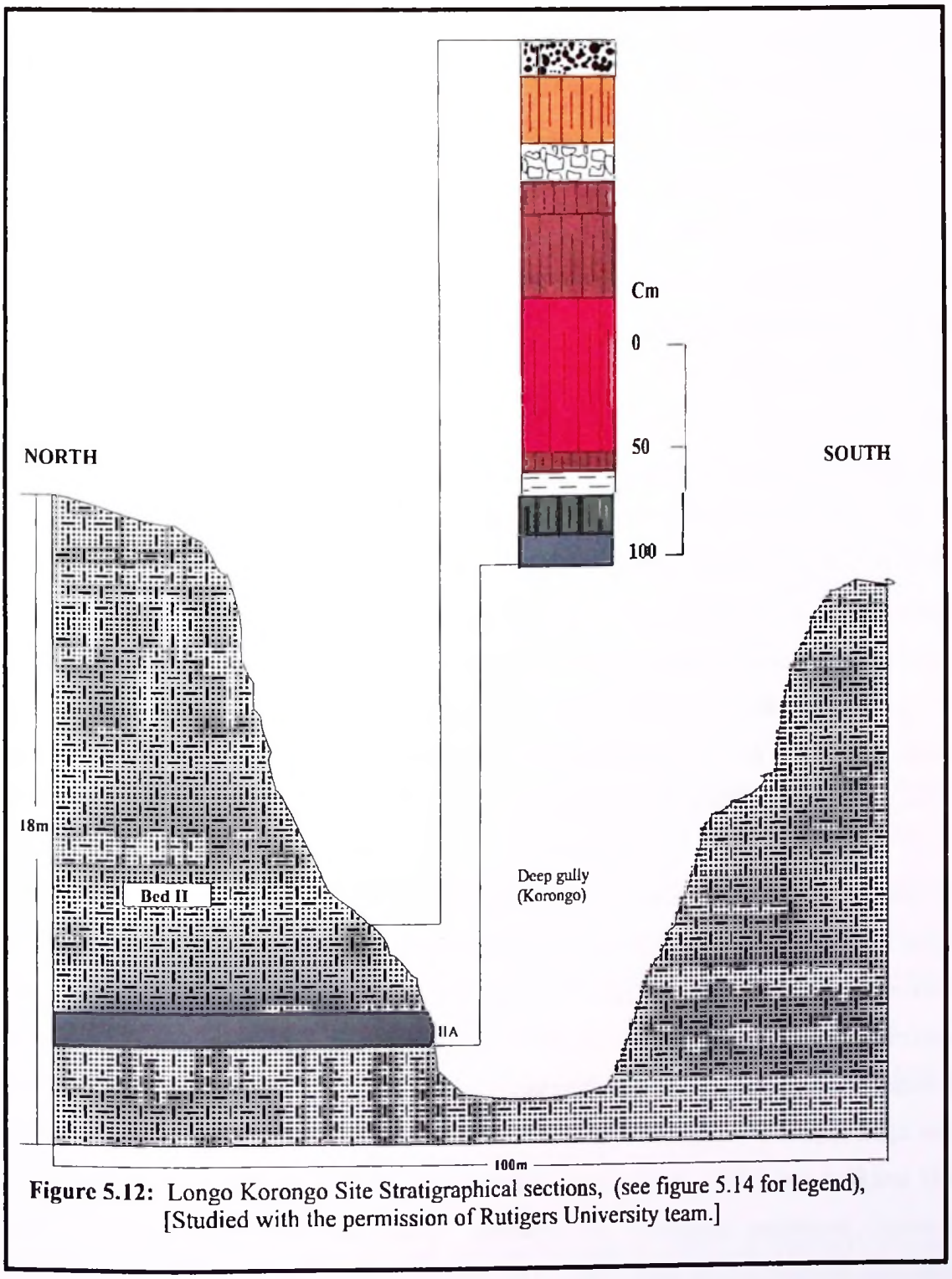

Figure 5.12: Longo Korongo Site Stratigraphical sections, (see figure 5.14 for legend), [Studied with the permission of Rutigers University team.]

5.4.3. Lithostratigraphical classification of Olduvai Gorge deposits

Although the Olduvai Gorge deposits represent a complex volcano-sedimentary-palaeosol sequence, they can still be classified into distinctive beds, Bed I to Bed V as was earlier recognised by Reck, (1914) Hay (1967, 1976). In general terms (stratigraphically) this study is consistent with these earlier studies, but it offers more detailed lithological descriptions and definitions of numerous single geological beds and layers contained in the Reck (1914) and Hay (1967, 1976) general Beds (section 5.2.2) which were not recognised before. A composite section (figure 5.13) is presented, which represents the general lithostratigraphical classification of the Olduvai Gorge deposits as briefly summarized in the following paragraphs.

Bed I

Bed I has a thickness ranging from 10m to 60m thickening to the east of the area. The bed has a basal gravel bed lying unconformably on the lava flow. The bed consists mainly of stream worked fine-grained tuffs and reworked pyloclasts intercalated with olive gray clays. 14 individual palaeosols and 14 individual tuff layers of various thicknesses were recognised during the mapping. The lower part of Bed I is composed of pyroclasts containing numerous mammal fossil bones. The *Australopithecus boisei* hominids skull was found in in palaeosol level GS54 (chapter 10) in the lower part of Bed I. Two significant sand levels are recorded in Bed I.

The term Bed I refers to olive to light-gray lithological units lying on a basaltic lava (figure 5.8) to an upper limit defined by marker horizon (tuff IF), which could easily be followed across the basin, (figure 5.8b). Bed I deposits seems to be a mixture of lacustrine (clays), fluviatile (gravel, sand and reworked tuff) and volcanic (tuff and pyroclasts) intercalated with well-developed palaeosol levels (figure 5.13). Ar/Ar and K/Ar age estimate from Bed I range from 2.22Ma (base) to 1.75Ma (top), (Walter *et al.*, 1991 and Kafumu, 1995). Bed I therefore covers the lower part of the Lower Pleistocene. However, lacustrine sediments are observed below the lava and above a welded ignimbrite dated at 2.5Ma (Hay 1986). The Pliocene/Quaternary boundary therefore lies between 2.5Ma and 2.2Ma.

Bed II

Bed II was distinguished from Bed I in the field by strong colour change from light-gray (Bed I) to dark-gray (Bed II) (figure 5.8b) and seperated by the marker tuff IF. The boundary was a clear sharp change of colour from light grey to dark gray beds. The upper boundary of Bed II is also recognised by a colour change from dark gray to red beds (Bed III).

The bed varies in thickness from a few meters to adout 30m thickening to the West. Field Observation showed that the lower part of Bed II geologically (composition and fossil content) resembles Bed I. Lower Bed II is an olive clay-palaeosol alternation sequence resembling Bed I sequences. The lower part is followed by red palaeosols of middle Bed II. The upper part of is sandy in texture with limited palaeosol levels. Significant gravel bed levels are observed in the upper parts of Bed II.

In the field 16 individual palaeosol levels were recorded in Bed II, together with clay, tuff, sand and gravel beds all totaling to more than 20 individual layers. Two thin limestone levels are recorded in the upper part of Bed II.

It can be summarised that Bed II is divided into three parts, the lower part consisting of mainly lacustrine and fluviatile deposits composed of olive-gray clays and water laid tuffs. The middle part is essentially fluviatile in nature composed of clays and some sand beds. And the upper part is again mainly fluviatile sand, gravel and some lacustrine limestone. In all the three parts palaeosols are seen interfingering the sediments. The age of Bed II is estimated by Ar/Ar and K/Ar dates to be from 1.75Ma (base) to 1.15Ma (top), (Walter *et al.*, 1991, Manega 1993 and Leakey &Roe 1995). This is the upper part of the Lower Pleistocene.

Bed III

Bed III is predominantly red coloured, refered by Leakey, (1967) as 'red bed'. The bed is about 15m thick and separated by marked sharp colour change and compositional differences from Bed II below and Bed IV on top.

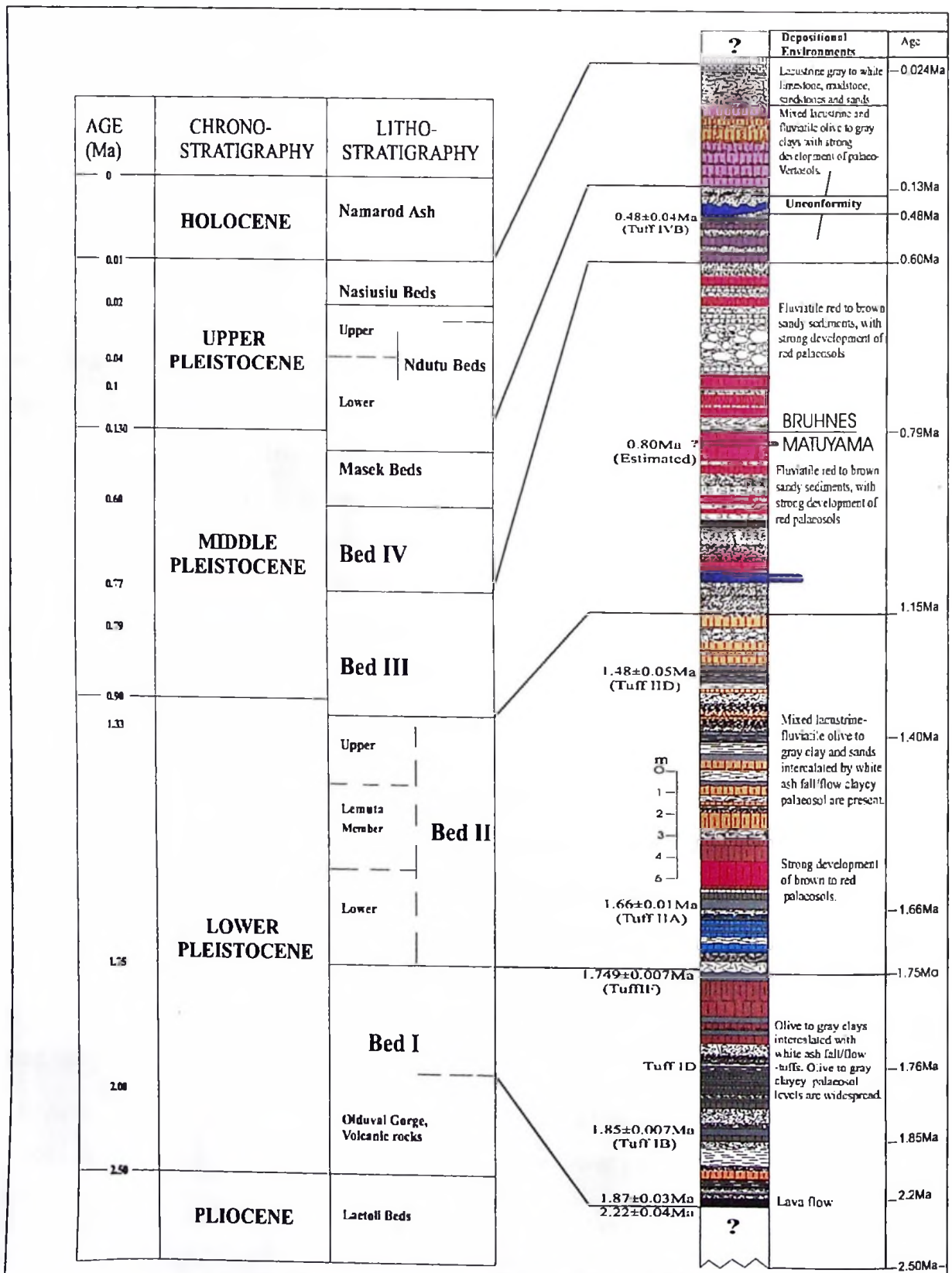

Figure5.13: Chrono-lithostratigraphical classification of Olduvai Gorge Beds [Dates are from Walter *et al.*, 1991, Manega 1993, Kafumu, 1995 and Leakey & Roe 1995] (see legends on figure 5.14)

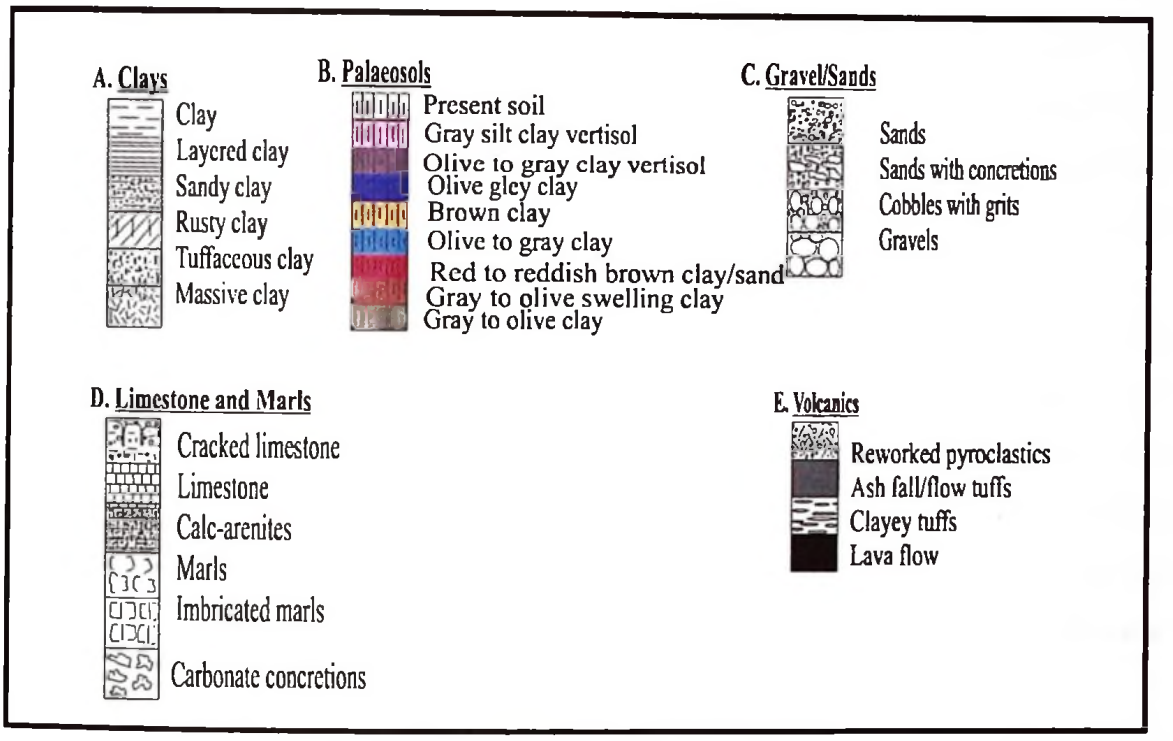

Figure 5.14: Stratigraphical legend for figures 5.8 to 5.13.

Moving from East to the West of the gorge the Bed ceases to be strongly red but it can be still recognised and traced due to its textural and compositional difference from the beds above and below. The bed is essentially composed of brownish red deposits, which are believed to be alluvial fans. Field observation revealed that the Bed III characteristic brownish red colour came from strong pedogenic processes, as sometimes indicated by root lets and traces (see chapter 6), which affected the different levels of the Bed at different geological times.

The lower part of Bed III is essentially a gravel/sand level resembling Bed II but it is red in colour. The middle part contains red palaeosols developed on sand clay sediments and the upper part is generally gravely in nature dominated by coarse-grained calcarenite sediments.

It should be emphasised here that Bed III is a complex series of deposits represented by lacustrine and partly fluviatile sediments, forming several layers of gravel, sands, clays and volcanic debris with unspecified number of unconformities (hiatuses).

The Bed is therefore a deposit of lacustrine-fluvial-alluvial-eolian assemblages, representing numerous climatic changes. The age of this bed was estimated (sedimentation rates) to be from 1.15Ma to 0.77Ma, (Leakey and Roe, 1995). These dates represent the lower part of the Middle Pleistocene (figure 5.13).

Bed IV/Masek beds.

Bed IV has light grey colour similar to that of Bed II with thickness ranging from 0m to 40m. The bed thins to the west and ultimately disappears, such that in some places Bed V is found lying unconformably on Bed III. It was observed in the field that the Bed IV begins with a series of calcarenite deposits followed by palaeosol levels all developed on sand silt deposits and terminated by a significant sand layer.

Bed IV occupies the Middle Pleistocene with K/Ar dates between 0.77Ma to 0.6Ma (Leakey and Roe 1995). Masek Beds occupy the upper part of the Middle Pleistocene. It begins at 0.6Ma and terminates at 0.4Ma (Leakey and Roe 1995). There is a huge unconformity at the marker bed tuff IV dated by Manega, (1993) to be 0.48Ma. This study considers this unconformity to be the boundary between Bed IV/Masek and Ndutu Beds.

Ndutu Beds

Ndutu beds/Bed V as observed by the author was a series of seven palaeo-vertisols each developed on top of fluviatile or lacustrine clay sediments (not distinguished in the field). A white to grey dense limestone layer of one to about one to four metres thick overlies the palaeo-vertisol sequence. The lower part of this limestone sequence is a sand level followed by sandstone that grades into mudstone and then into limestone. However, previous studies by Lekey, (1968) and Hay, (1963) mapped Bed V as divided into two main parts, the fluviatile sand and canglomerate rich lower part and the aeolian sand and ash rich upper part.

Morever, Quennell *et al.*, (1956) explains the lower part as fluviatile river teraces with

intensily rolled. Gravel beds composed of particles from the basement complex and the basal basaltic lava (quartze-feldspathic-gneisses and trachyte-basalt volcanics). The upper part as a sequence of blown fawn coloured volcanic ashes and sand, which are covered by layers of steppe limestone. The limestone layer always rests with a marked unconformity on the upper part of the Bed. Cerling, (1984) refers this Bed to us Ndutu Beds.

Ndutu Beds are estimated from sedimentation rates to cover the time span of 0.4Ma to 0.024Ma (Hay, 1967 & 1976), starting from the upper part of the Lower Pleistocene going into the Upper Pleistocene. However in this study Ndutu beds are believed to begin at about 0.13Ma and extend into the Holocene. The interval between 0.4Ma and 0.13Ma is missing.

Nasiusiu Beds or Bed VI

Nasiusiu Beds are Holocene in age covering the upper most part of the Olduvai Gorge stratigraphy. The bed represented by white calcareous present soil, which is often covered by black sand spread across the Serengeti plains. Although the bed is not well studied but Leakey (1968) mentions that it is a black layer of micaceous volcanic ash lying over Ndutu Beds. Namarod ash beds as was mapped by Hay (1968, 1976) may be considered part of Nasiusiu beds.

These are mainly wind blown volcanic tuff, which were laid down probably by eruption of the Oldoinyo Lengai volcanic centre during the Holocene. The volcanic tuffs were mainly nephelinitic, phonolitic and carbonatitic in composition, which quickly changed into pedogenic limestones (calcretes) layers (Cerling and Hay, 1984). There are however remnants of these volcanic sands which continue to roll westwards across the Serengeti plains. These rolling sands today known as *"shifting sands"*, (see chapter 7.1.5) are considered as part of the Nasiusiu/Namarod superficial Holocene cover.

CHAPTER SIX

PALAEOSOL FIELD STUDIES OF OLDUVAI GORGE BEDS

6 PALAEOSOL FIELD STUDIES

6.0 INTRODUCTION

In Olduvai Gorge substantial geological, palaeontological, palaeonthropological, archaeological, palynological and geochemical work (for the palaeoclimatic and palaeoenvironmental reconstruction) has been carried out (Hay, 1976, Hay *et al.*, 1977, Hay & Leeder, 1978, Bonnefille & Riollet 1980, Bonnefille 1984, Cerling & Hay, 1986, Manega 1993). Moreover, occurrences of palaeosols in Olduvai Gorge were long recognised four decades ago but have been less studied.

Hay (1967) refers to palaeosol levels as hominid occupation levels or living floors. He stated that such levels were numerous. Some of these levels were recognised as land laid trachyte tuffs and tuffaceous clays extensively penetrated by root channels (Leakey, 1968). A limited number of stable isotopic studies of pedogenic carbonate concretions, nodules and calcretes (from palaeosols) were carried out in Olduvai Gorge, (Cerling *et al.*, 1977, Hay & Leeder 1978, and Cerling & Hay 1986) in an attempt to establish a comprehensive palaeoclimatical stratigraphy reliable for a regional and global correlation. Nevertheless, a clearer picture of Pliocene-Pleistocene–Holocene Climatic and environmental record is still regarded as ambiguous (Manega 1993) and awaits further detailed study.

In this study a systematic lithological description and identification is performed. Several palaeosol levels with other sediments are recognised and described. Recognition and identification of palaeosol occurrence and positions and other sediment facies like sand and gravel beds in the Olduvai Gorge stratigraphy will therefore offer a good insight in

the past climate and environments in this area. How many climatical phases in Olduvai Gorge remains open debate but this paper identifies at least 57 palaeosol levels and six gravel bed levels each signifying a specific climatic condition of regional and global significance. The palaeosol levels are closely associated to the positions of fossil man.

6.1 METHODS OF INVESTIGATION

Morison, (1968) followed by Paepe (1970) and Lowe and Walker (1987) defined palaeosols as stratigraphical units possessing physical features and stratigraphical relationships that permit their recognition and mapping, termed as 'Geosoils'. Palaeosol represent stable landscapes related to a climatic (wet or dry) and environmental fluctuations and cyclicities of the past. Therefore, palaeosol stratigraphical positions and cyclicities provide sufficient information for reconstructing Quaternary paleoclimates and environments. Eolian sand levels and gravel beds that can be recognised in the field are often taken as indicating drier climates.

Lacustrine-fluviatile-volcanic sediments of Olduvai Gorge which posses numerous palaeosol levels were mapped, examined, measured and described at 5 sections along the gorge cliff walls. Fieldwork campaigns were carried out during three field seasons. The first fieldwork campaign was for two weeks, which was carried in October 1994. The second field season was a three weeks field execution in summer 1997, (July & and September 1997) and the third field campaign took place in summer 1998 (the first two weeks July).

The descriptions and measurements were according to the standard ways of describing palaeosols (Paepe, 1971 and Birkeland, 1984). Colour determinations were based on the Munsell color chart (Munsell Color, 1975). The sections were also sampled for magnetic susceptibility (bulk samples), micropedological (oriented samples) and mineralogical laboratory studies. This chapter reports the results of field lithological (sediments and palaeosols) stratigraphical vertical measurement and descriptions of Oldvai Gorge beds.

6.2 RESULTS - PALAEOSOL RECOGNITION

6.2.1 Palaeosol identification

Evidence of paleo-pedogenesis which can be observed in Olduvai Gorge beds is enormous (see figures 6.1 to 6.5, tables 6.1 & 6.2 and appendix 6.1 to 6.6). In Olduvai Gorge beds palaeosols are therefore recognised from the following features:

1. Rootlets and stems/twigs imprint usually infilled by calcareous materials or coated by red stains (probably Mn-Fe hydroxide) – mineral identification is in progress.
2. Distratification of clay. The process is intense at the top of massive or layered clay levels.
3. Animal bioturbation are infilled by carbonate material.
4. Clay macro slickensides columnar structures observed in clayey palaeosols.
5. Black to gray clay coatings on columnar surfaces and large paleo-peds.
6. Red coatings [probably Mn-Fe hydr(o)xides].
7. Carbonate nodules and concretions.
8. Imprints of gilgai macro relief structure.
9. Presence of mycelia and spicular bodies.
10. Color, especially the red and brown are characteristic soil colors. Light colors palaeosols are difficult to recognise (on the basis of color), then other criteria must be applied.

6.2.2. Field descriptions and measurements of Olduvai Gorge palaeosols

Based on field observation and the afore said criteria Olduvai Gorge palaeosols can be provisionally classified into several palaeosol types and sequence as given in figure 6.1 to 6.6 below. The field examination and mapping also made possible the recognition of 4 main types of palaeosols in Olduvai Gorge beds (see tables 6.1).

Table 6.1: Palaeosol field descriptions (Stratigraphical position is from top to bottom), (see figure 6.1 to 6.6)

Sample	Palaeosol level	Colour	Macropedofeatures
MC22 & MC21	GS1	5Y5/2 (Olive gray)	Presence of black mineral grains (clay particles?) Sandy at the top.
MC20	GS2	10YR5/3 (Brown)	White $CaCO_3$ concretions. 1-3mm size rootlets and pipestems. Fine columnar structures. Black clay coatings.
MC19	GS3	10YR5/2 (Grayish brown)	Fine columnar strctures with slickensides.
MC18	GS4	5Y5/1 (Olive black)	Black coating. rare $CaCO_3$ concretions. Columnar structures with slickensides. Categorized as palaeo-vertisol.
MC17	GS5	5Y6/2(Light olive gray)	Black coatings and mottles.
MC16	GS6	2.5Y5/2 (Grayish brown)	Columnar structures with slickensides.
MC15	GS7	5Y6/2 (Olive gray)	Black coatings Gilgai inprint lower part. 1-3cm size carbonate concretions.
MC13	GS8	5Y/8(1Light gray)	Clay distratification.Clay coating
MC11	GS9	5Y6/1(Gray)	Black mottling. Calcite infillings of root and pipes-stem. Columnar structures. Contains numerous animal fossils.
MC10	GS10	5Y6/2(Olive gray)	The same as in MC11.
MC8	GS11	5Y5/2 (Olive gray)	Black clay coatings. Irregular sand particles
MC6	GS12	10YR5/3 (Brown 5YR4/3 (red) 5YR4/2 (drank reddish gray)	Root infillings and black coating. The soil contains black pebbles.
MC3	GS14	2YR4/2 (red), 10R5/4 (Weak red)	Silty clay with red mottling. Local calcium carbonate concretions.
MC2	GS15	5YR6/4 (Light reddish brown	Red mottling.
MC1	GS16	7.5YR6/4 (light brown) 5YR6/3 (Light reddish brown)	Mottled sands.
RB24		2.5YR4/6 (Red), 2.5YR5/6 (Redish brown)	Large (3cm-size) root casts infilled by red sediments.
RB23		2.5YR5/4 (Red), 2.5YR5/6 (Reddish brown)	Numerous infillings of small rootlets.
RB22		2.5YR4/8 (Red)	Hard bank with animal bioturbation
RB21	GS17	2.5YR4/6 (Red)	Red bioturbated palaeosol with seldom fine root traces.
RB20	GS18	2.5YR6/4 (Light grayish brown)	Intense red (2.5YR4/8) mottling. The mottled zones give the palaeosol an oolitic general texture. (Field name; oolitic soil)
RB19	GS18	5YR6/4 (Light reddish brown)	Gravely sand cemented by yellowish red material. Intensely mottled. Red oolitic palaeosol.
RS18a & RS18	GS19	2.5YR5/6 (Red) & 10R4 (Red)	Mottled oolitic palaeosol with numerous small rootlets.
RB17		7.5YR6/4 (Light brown)	Root infillings with numerous carbonate concretions.
RB16		5YR7/4 (Light reddish brown)	Scarse mottling. Marls imbricated by soil
RB15	GS20	5YR5/6 (Yellowish red)	Fine root and stem infillings

RB14	GS21	10YR7/4 (Very pale brown)	Distratified (palaeosol)
LK10	GS32	5Y6/4 (pale olive)	Clay distratification and rare carbonate concretions.
LK9	GS33	5Y5/4 (olive)	Clay distratification
LK8, LK7, LK6b, LK6a, LK5, LK4 and LK3	GS34, GS35, GS35, GS35, GS35 GS36 and GS37	10R6/4 (Pale red), 2.5YR4/3 (Reddish brown), 10YR3/2 (Very dark grayish brown), 2.5YR4/6 (Red), 10YR6/4 (Light yellowish brown) and 2.5Y4/2 (Dark grayish brown).	It looks like one red zone, possibly an accretion of soils and soil sediments. Red local mottling
LK2		2.5Y7/2 (Light gray)	Clay distratification and rare carbonate concretion
RB13		10YR7/3 (Very pale brown)	Distratification and blocky ped structure.
RB12		10YR7/3 (Very pale brown)	Silty clay with marls showing distratification.
RB6a & RB6b		7.5YR6/6 (Reddish yellow)	Carbonate concretions.
RB5	GS22	5YR7/6 (Yellowish red)	Carbonate concretions
RB4 and RB3	GS23	7.5YR5/6 (Strong brown)	Carbonate concretions. Weathered tuff.
RS39	GS24	10YR6/4 (Light yellowish brown)	Sandy clay with 2 –4cm sized root traces
RS38		10YR6/4 (Yellowish brown)	Weathered tuff
RS37	GS25	10YR5/4 (Yellowish brown)	Brown layered mycelic sediments
RS35	GS26	10YR5/4 (Yellowish brown)	Silty sand with numerous small animal bioturbation)
RS31	GS27	5Y5/4 (Olive)	Clayey sand. Animal footprint on the sandstone surface).
RS29	GS28	10YR7/2 (Light gray)	Sandy sediment with root traces
RS24		5Y6/3 (Pale olive)	Clay with distratification
RS22	GS29	5Y7/1 (Light gray)	Sandy whitish sediments with concretion and root infillings
RS20		5Y7/2 (Light gray)	Clay with root traces and microbones
RS19	GS30	5Y5/4 (Olive)	Massive clay with white concretion.
RS18		5Y8/2 (White)	Pedogenized pebbly tuff, with root twigs.
RS17	GS31	5Y3/2 (Dark olive gray)	Distratified clay with root infillings
RS13	GS38	5Y3/2 (Dark olive gray)	Massive dense clay with concretions. Calcite crystalization
RS11	GS39	5Y5/3 (Olive)	As in RS9
RS9	GS40	5Y5/3 (Olive)	Clay with (3 – 5cm diameter) white carbonate concretions at the base
RS7	GS41	5Y5/4(Olive)	Carbonate concretions and root and stem infillings as in RS5.
RS6	GS41	5Y4/4 (Olive)	Massive clay with big (5 – 10cm) carbonate accretions (formed by accreation of smaller concretions) at the base, Slickenside structure observed.
RS5	GS42	5Y4/4 (Olive)	1 – 2cm root and stem infillings and carbonate concretions
RS2		5Y8/2 (White)	Accretions of salt small concretions accreted together to form a bigger particle.

5Z		5YR6/2 (Brownish gray)	Bioturbated and distratified sand
4Z		5Y5/3 (Olive)	Clay with calcareous veins and concretions
3Z	GS43	5Y4/1-2 (Dark gray to olive gray)	Distratified clay
2Z	GS44	2.5Y5/2 (Grayish brown)	Distratified clay with peds.
1Z	GS45	10YR6/2(Light brownish gray)	Distratified clayey layer showing irregular peds
ZK	GS46	5Y7/1 (Light gray)	Sandy palaeosol-numerous animal bone and root traces infilled with carbonate material.
Z21c		5Y5/2 (Olive gray)	Clay showing strong distratification and carbonate concretions
Z21a		5Y5/6 (Olive)	Distratified clay with some carbonate concretions
Z19	GS47	5Y8/2 (White)	Distratified tuff
Z17	GS48	5Y8/2 (White)	Clayey tuff – with signs of bioturbations
Z15	GS49	5Y7/2 (Light gray)	Distratified reworked pyroclast
Z13	GS50	5Y5/3 (Olive)	Clay showing distratification and numerous plant-root infillings
Z11	GS51	5Y8/2 (White)	Reworked tuff with carbonate concretions
Z9	GS52	5Y7/1 (Light gray)	Clayey sands with carbonate concretions, presence of mycelia and plant remains.
Z7	GS53	5Y7/1(light gray)	Clay sand with carbonate cocretions
Z4	GS54	5Y7/2 (Light gray)	Sands with numerous carbonate concretions
Z2	GS55	5Y5/3 (Olive)	Clay showing distratification and irregular peds.
ZI	GS56	5Y6/3 (Pale olive)	Distratified clay with root infillings
ZG		5Y6/3 (Pale olive)	Clay showing distratification
ZC		5Y6/2 (Light olive gray)	Clay with numerous carbonate concretions
ZB	GS57	5Y7/3 (Pale yellow)	Sandy clay. Contains very rare root infillings.

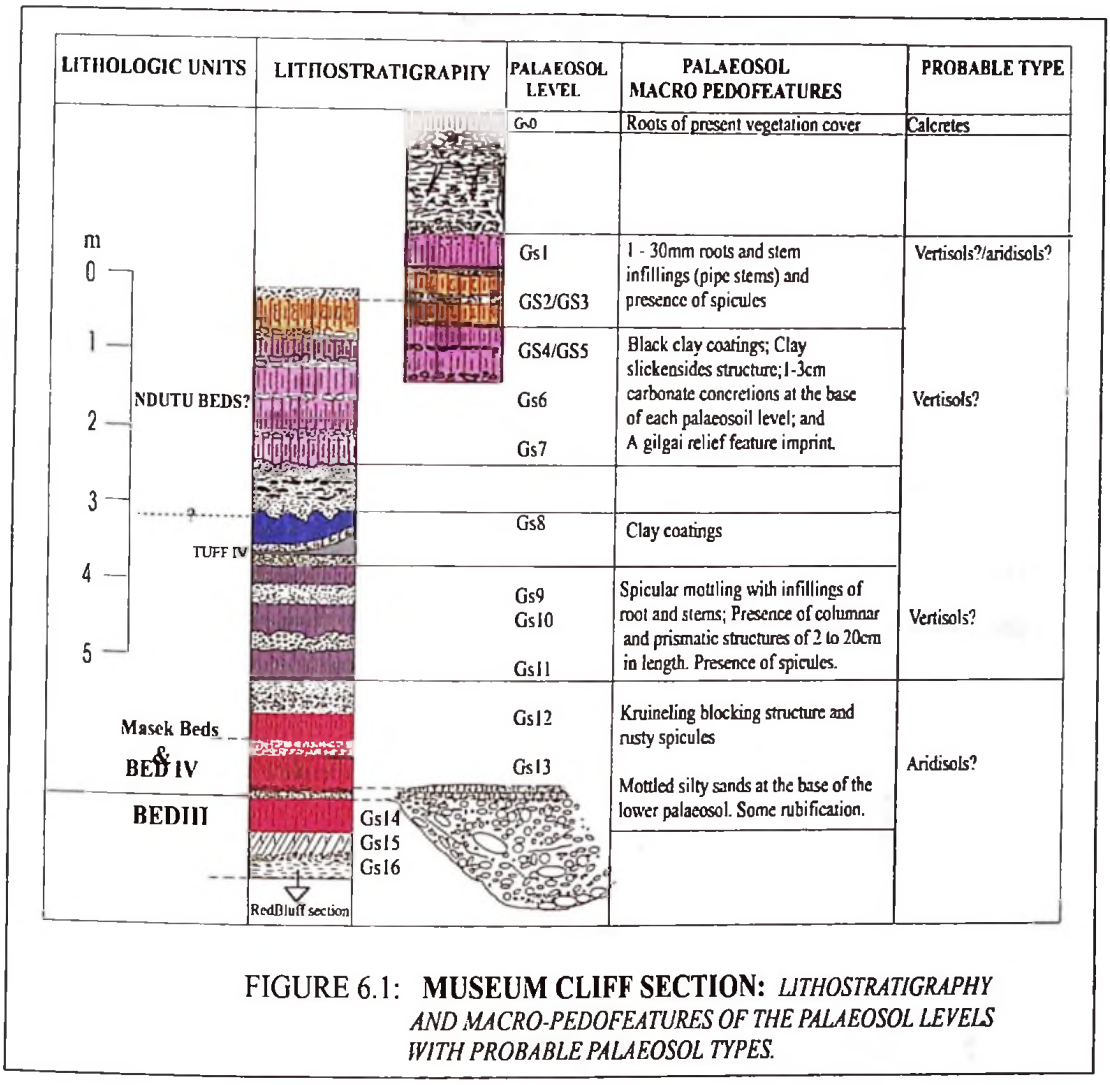

FIGURE 6.1: **MUSEUM CLIFF SECTION:** *LITHOSTRATIGRAPHY AND MACRO-PEDOFEATURES OF THE PALAEOSOL LEVELS WITH PROBABLE PALAEOSOL TYPES.*

The lower part of the Museum cliff section contains red palaeosols (GS12, GS13, GS14, GS15 and GS16) with sand and gravely texture, (figures $6.1a_{1\text{-}3}$ and $6.1b_{1\text{-}4}$). From field observation it is clear that the palaeosols developed on either sand or gravel beds. A gravel bed was observed to rest on GS14, (figure 6.1c). The palaeosol diagnostic features include red mottled silt, sand and gravel with intense rubefication, (figure $6.1b_{2\&4}$). Blocking structures and rusty spicular particles (mottled zones?) are common. GS14, GS15 and GS16 palaeosols are provisionally classified as palaeo-aridisols or palaeo-Alfisols. These former red palaeosols are considered as part of red beds of Olduvai Gorge "Bed III" and GS12 and GS13 as part of Bed IV. GS8, GS9, GS10 and GS11 are gray to olive gray palaeosol series overlying the red palaeosols, (figure 6.1d). The soils contain spicular mottling with infillings of root and stem, 2-3cm columnar and primatic structures, (figure 6.1e).

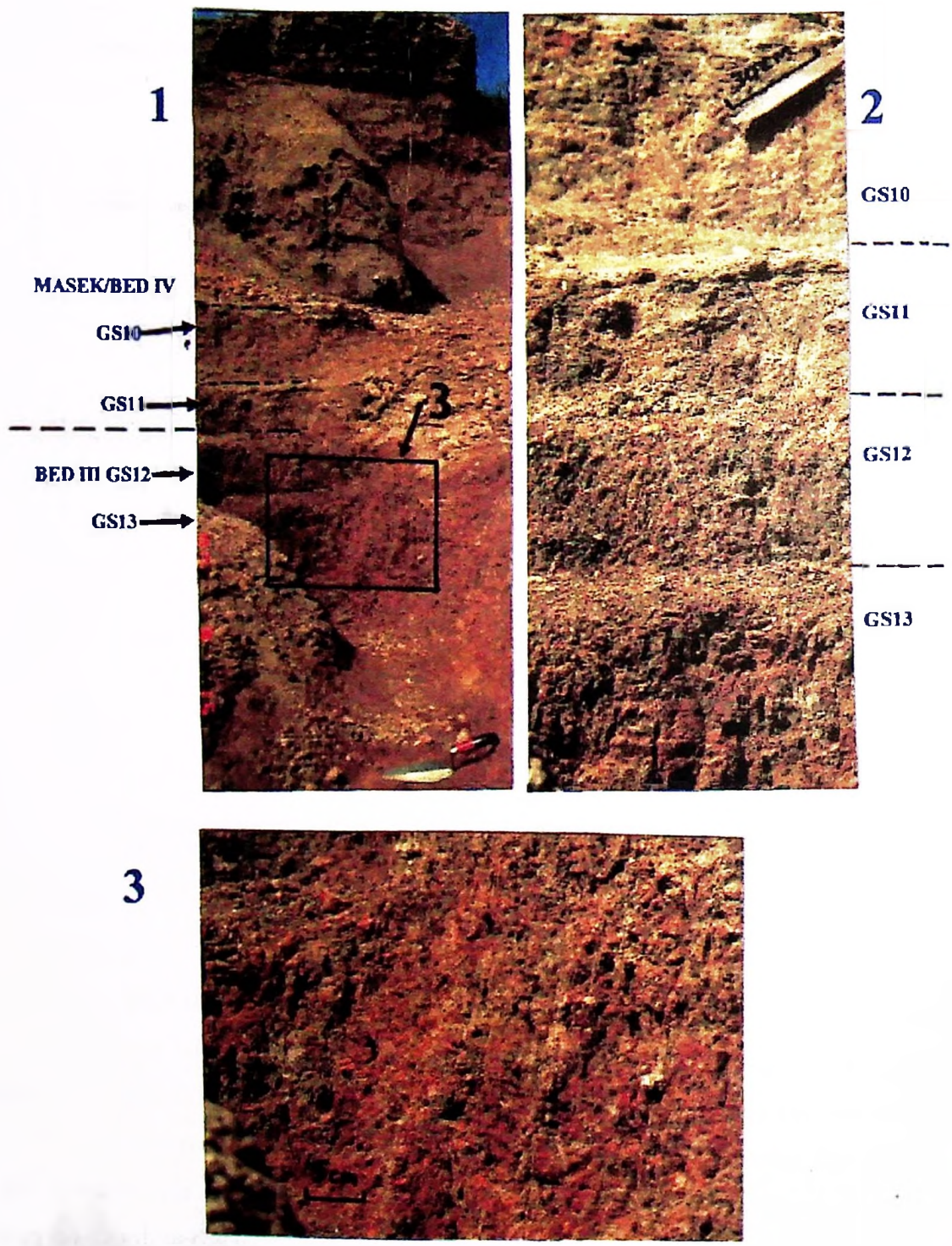

Figure 6.1a: Museum Cliff section. **1.** Stratigraphical positions of palaeosol levels GS10, GS11, GS12 and GS13. **2.** A close up of GS10, GS11, GS12 and GS13. **3.** GS13 palaeosol level showing oolitic texture (spots of red mottling).

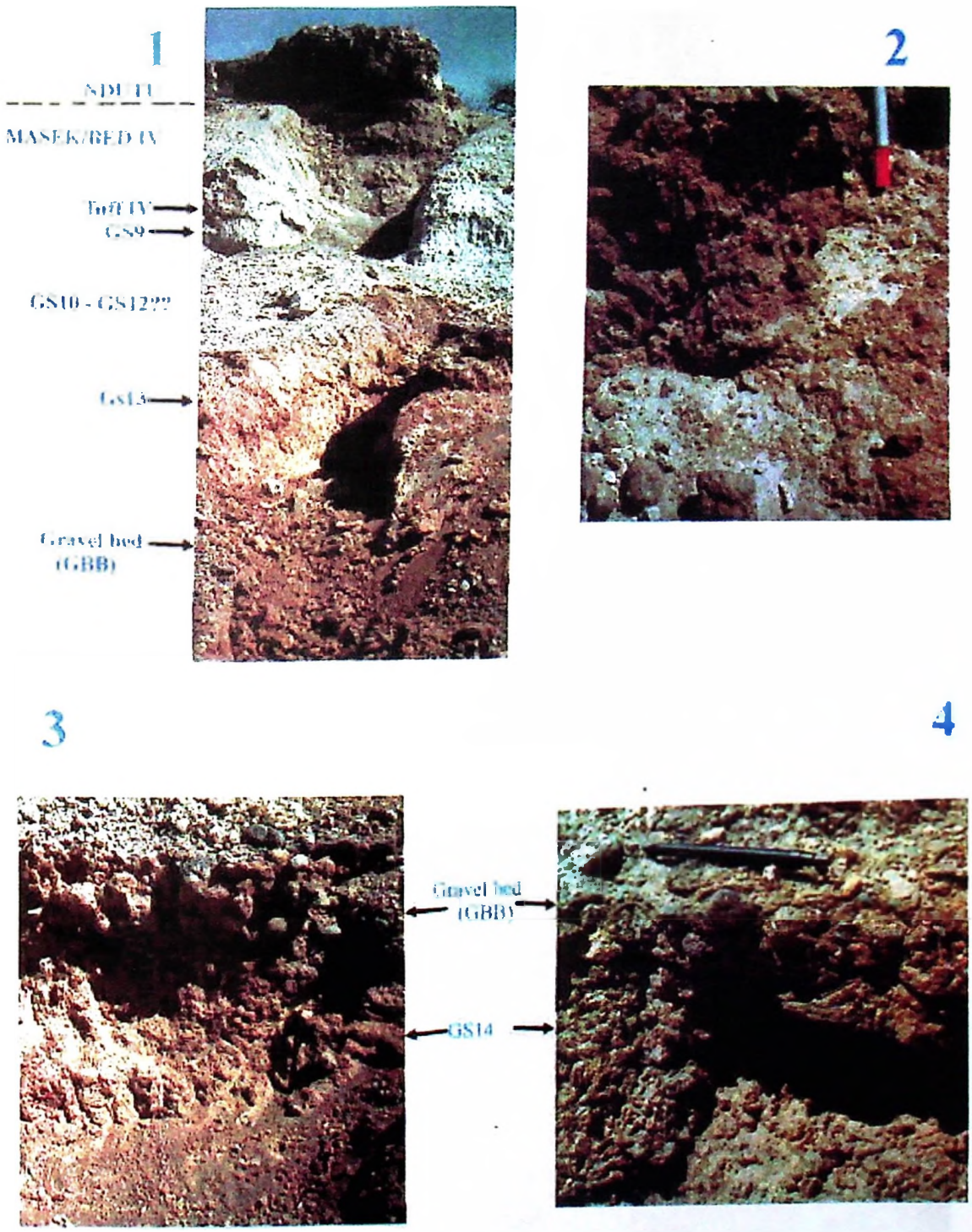

Figure 6.1b: Red palaeosols of Bed III. **1.** Stratigraphical positions of palaeosol levels GD12 and GS13. **2.** Palaeosol level GS14. **3-4.** Stratigraphical positions of Gravel Bed B and GS14, (GS14 is overlain by Gravel Bed B).

1

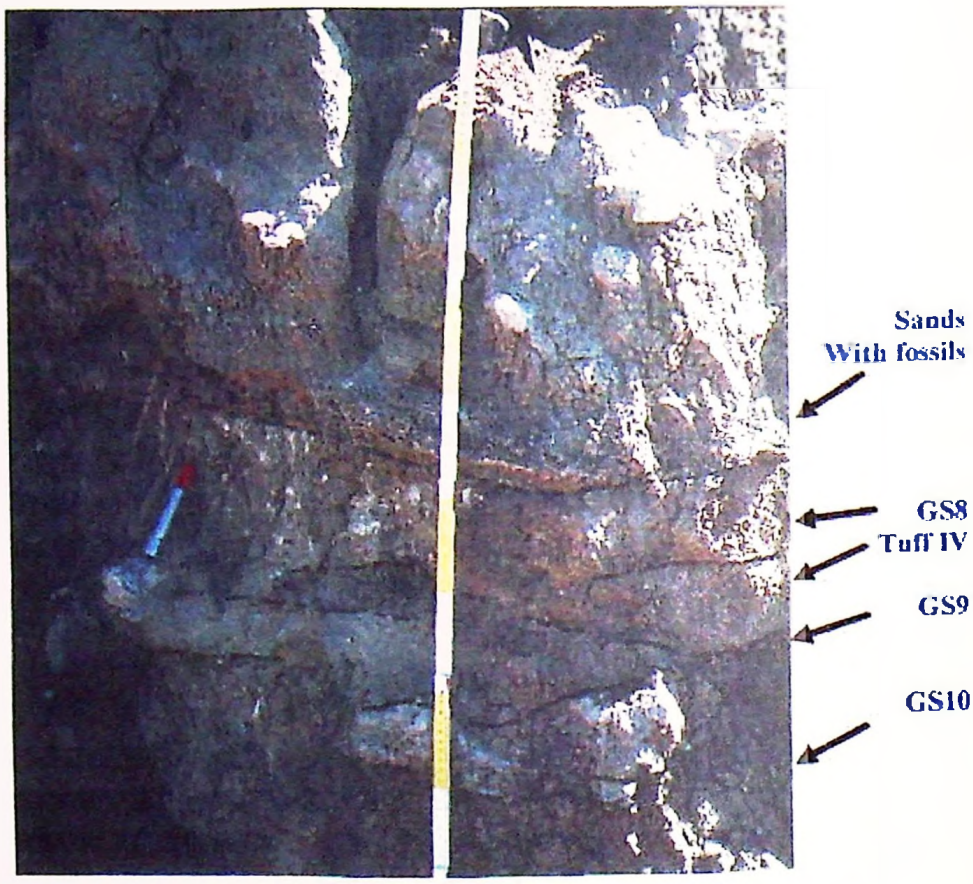

2

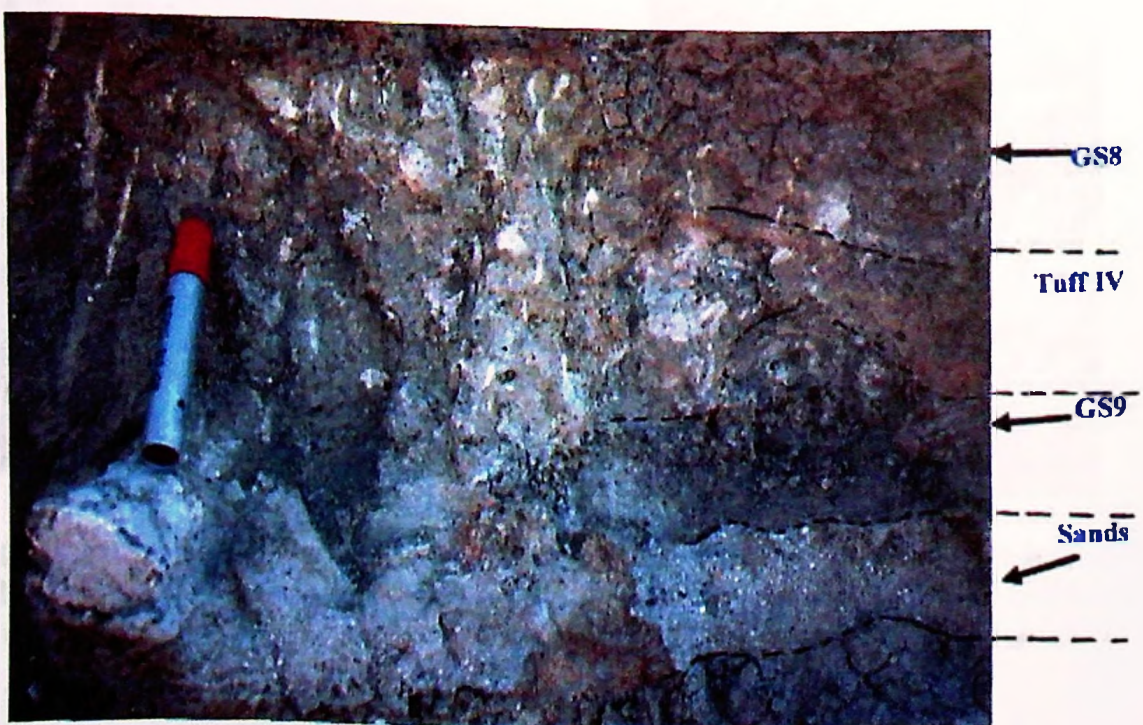

Figure 6.1c: Musem Cliff site. **1.** Stratigraphical positions of GS8, GS9 and GS10. **2.** Large fossil bone plugged between GS9 and Tuff IV.

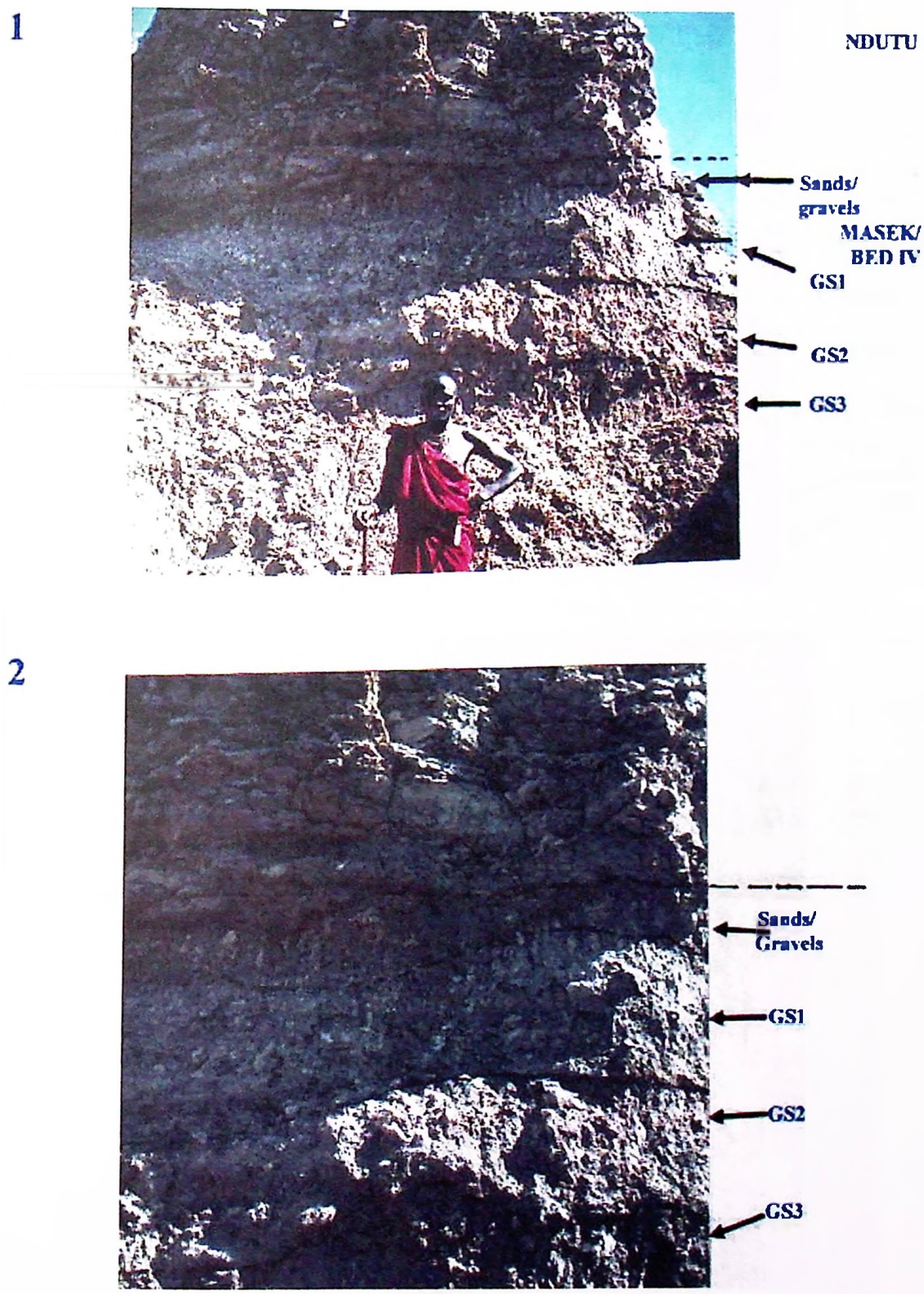

Figure 6.1d: 1. Stratigraphical positions of GS1, GS2 and GS3. **2.** A close view of GS1, GS2 and GS3.

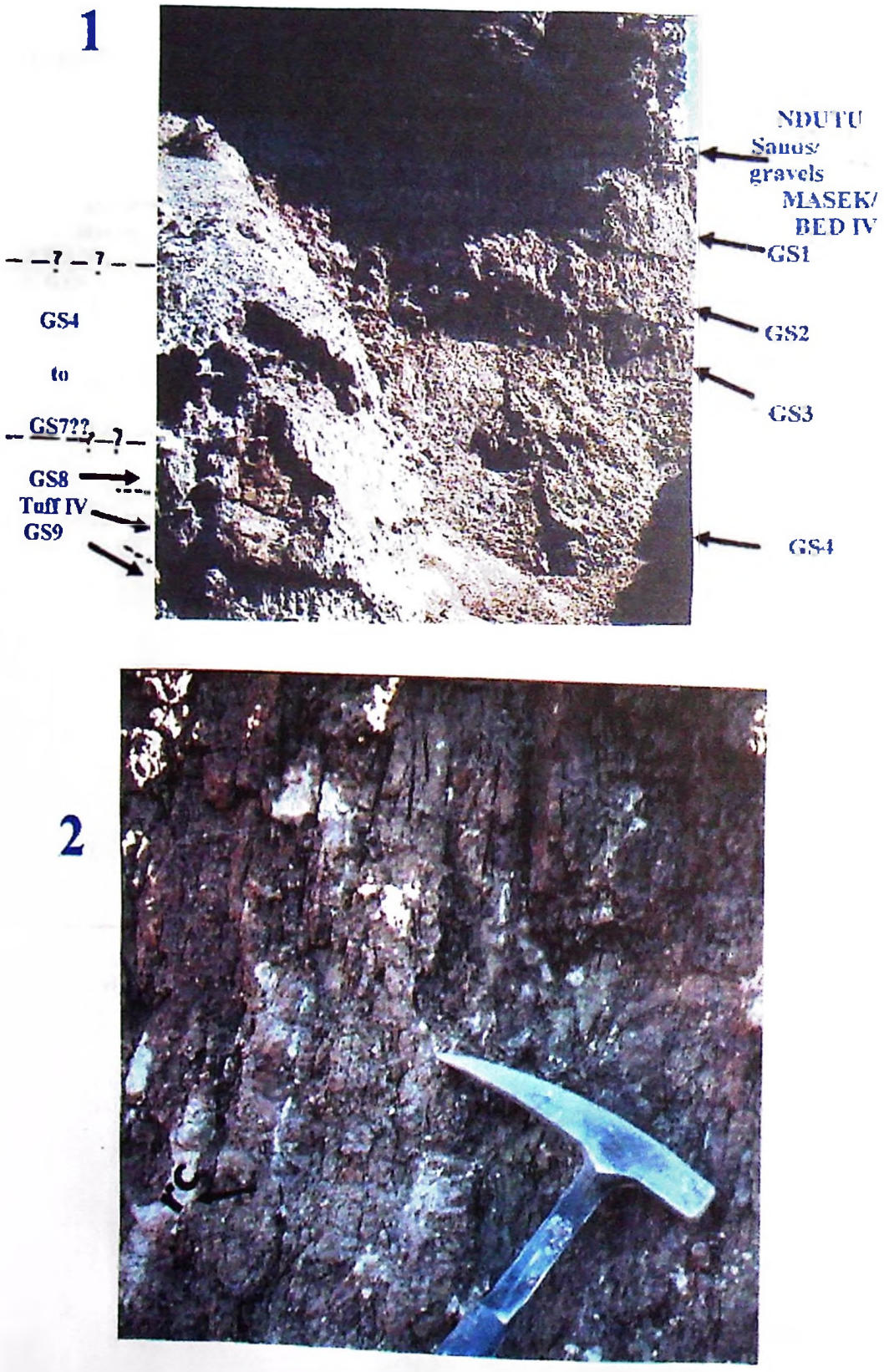

Figure 6.1e: 1. General view of the Museum Cliff section. **2.** Prismatic vertical structures in GS3 showing surfaces with slikensides and root channels (**rc**) encrusted by carbonate.

1

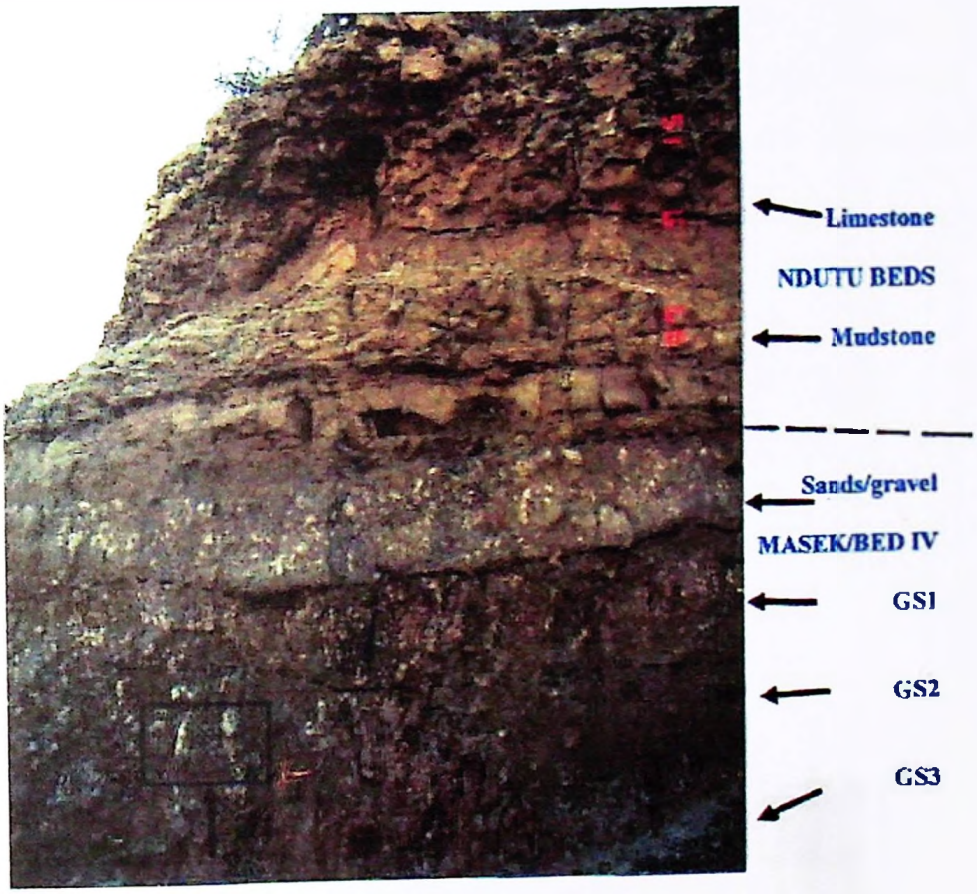

2

Figure 6.1f: 1. Stratigraphical positions of limestone, mudstone, sands and paiaeosol levels GS1 & GS2. **2.** Carbonate concretions (**c**) and root cast (**r** – rhizocretion) in GS2 as indicated by the arrow.

The upper part of the Museum cliff section is a series of palaeo-vertisols recognised by its characteristic imprints of gilgai relief macrostructures, slickensides and clay coatings. Palaeosol levels GS1 to GS11 belong to Bed IV/Masek beds and Ndutu Beds. These palaeosols are sometimes recognised by the presence of carbonate concretions and root rhizocretions (figures 6.1e and 6.1f).

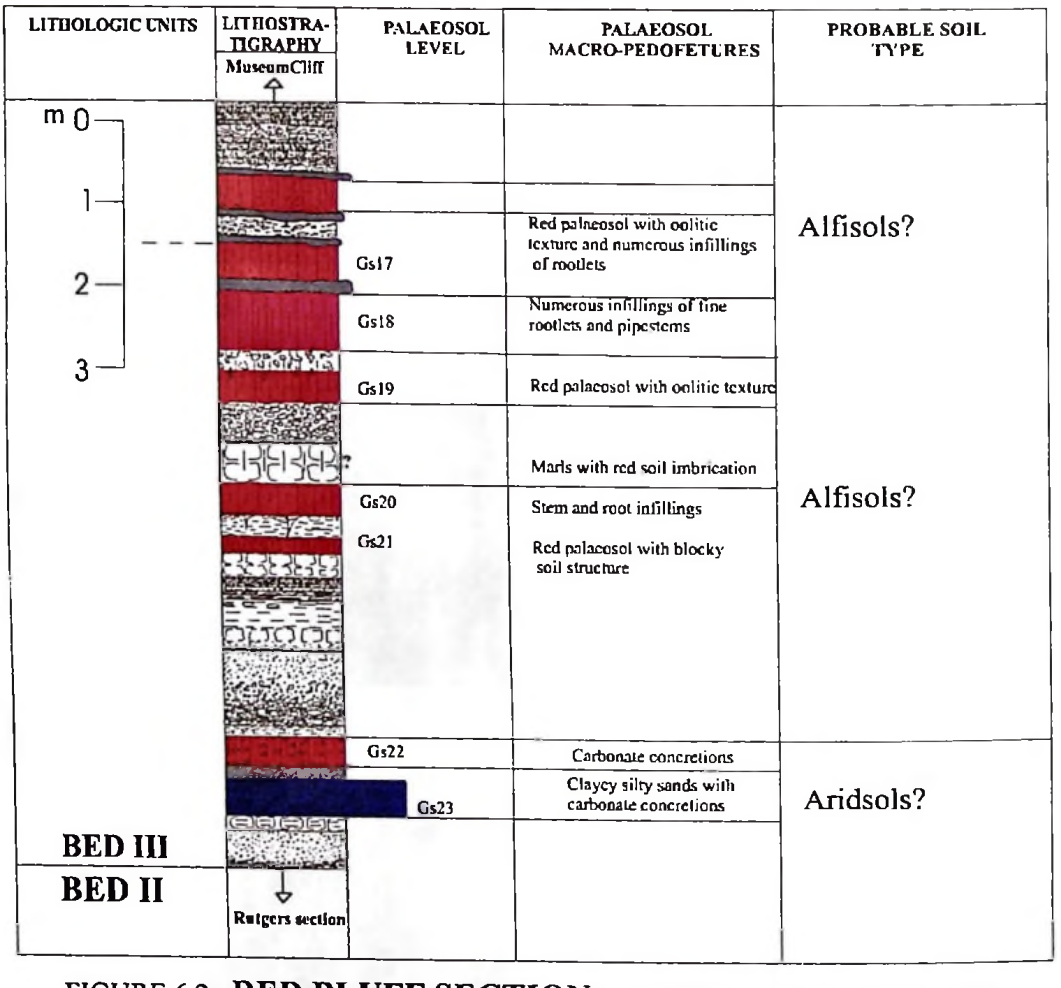

FIGURE 6.2: **RED BLUFF SECTION:** *LITHOSTRATIGRAPHY AND MACRO-PEDOFEATURES OF THE PALAEOSOL LEVELS WITH PROBABLE PALAEOSOL TYPE.*

Red bluff section is a red zone of Olduvai Gorge deposits located on the minor gorge cliff, (figure 6.2a). At a distance it looks like one massive red bed, but a closer look reveals several red palaeosol levels developed on sand or silt clay sediments. The base of the section is a brown silt sand layer with carbonate concretions. It was interpreted as palaeosol (GS23) developed on silt sand deposits. This palaeosol is classified as Aridisol or Entisol.

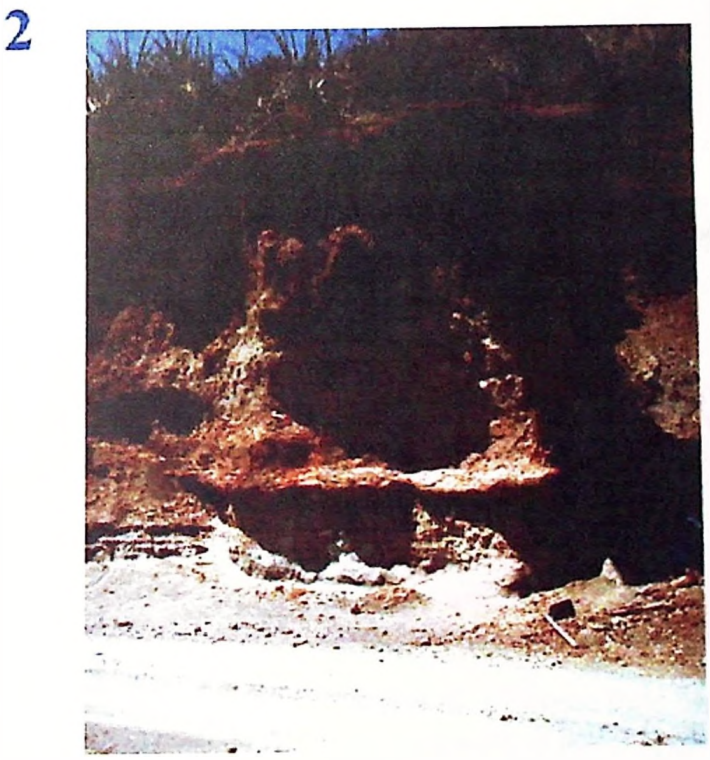

Figure 6.2a: Red bluff section (a Bed III site). **1.** General view of the Red Bluff site – the Bed II/Bed III boundary is indicated. **2.** A closer view of the Red Bluff section.

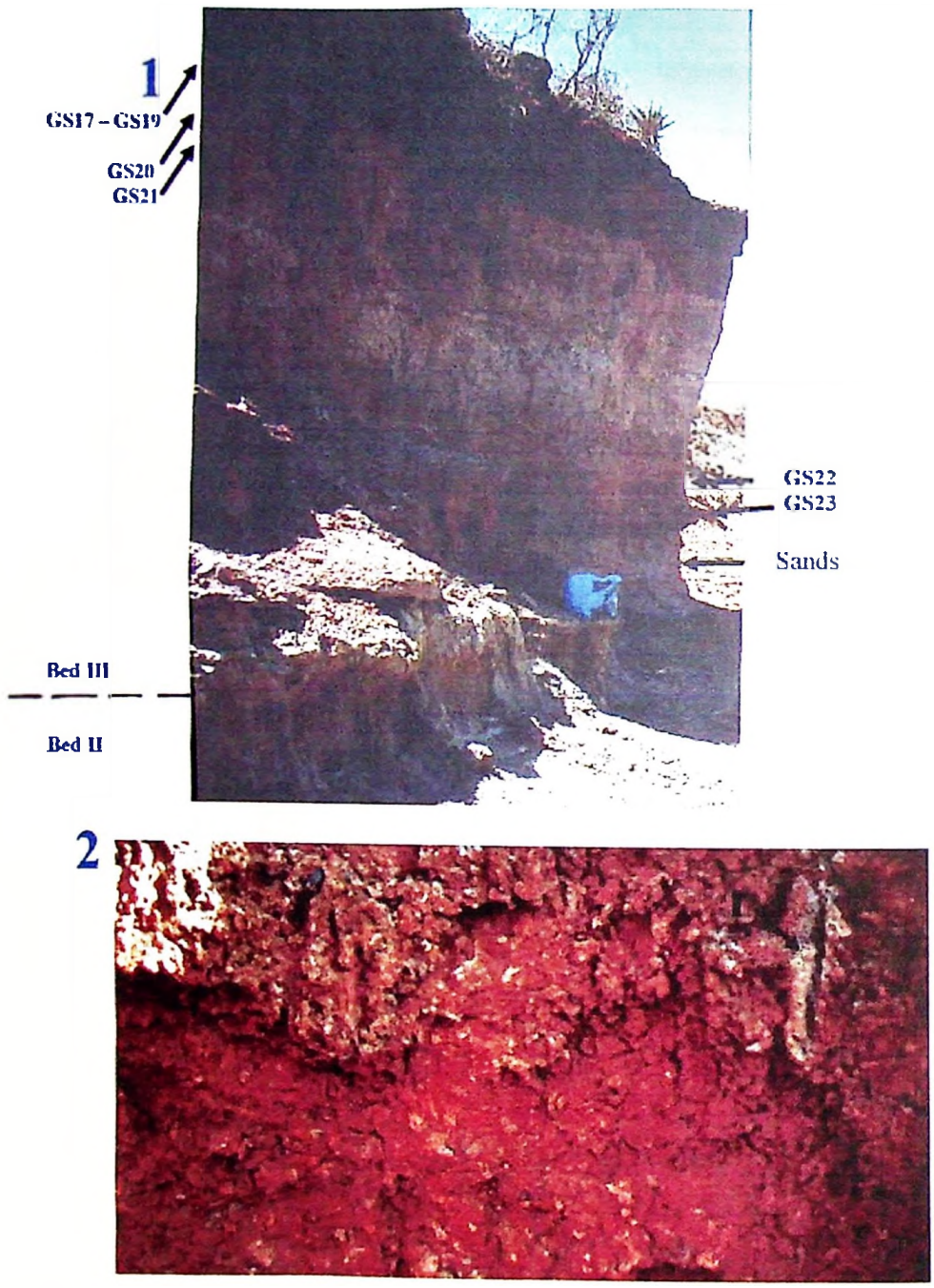

Figure 6.2b: The Red bluff section. 1. Stratigraphical position of palaeosol levels GS17 to GS23 in Bed III. Bed II – bed iii geological boundary is indicated. 2. Root cast (r) GS19 palaeosol.

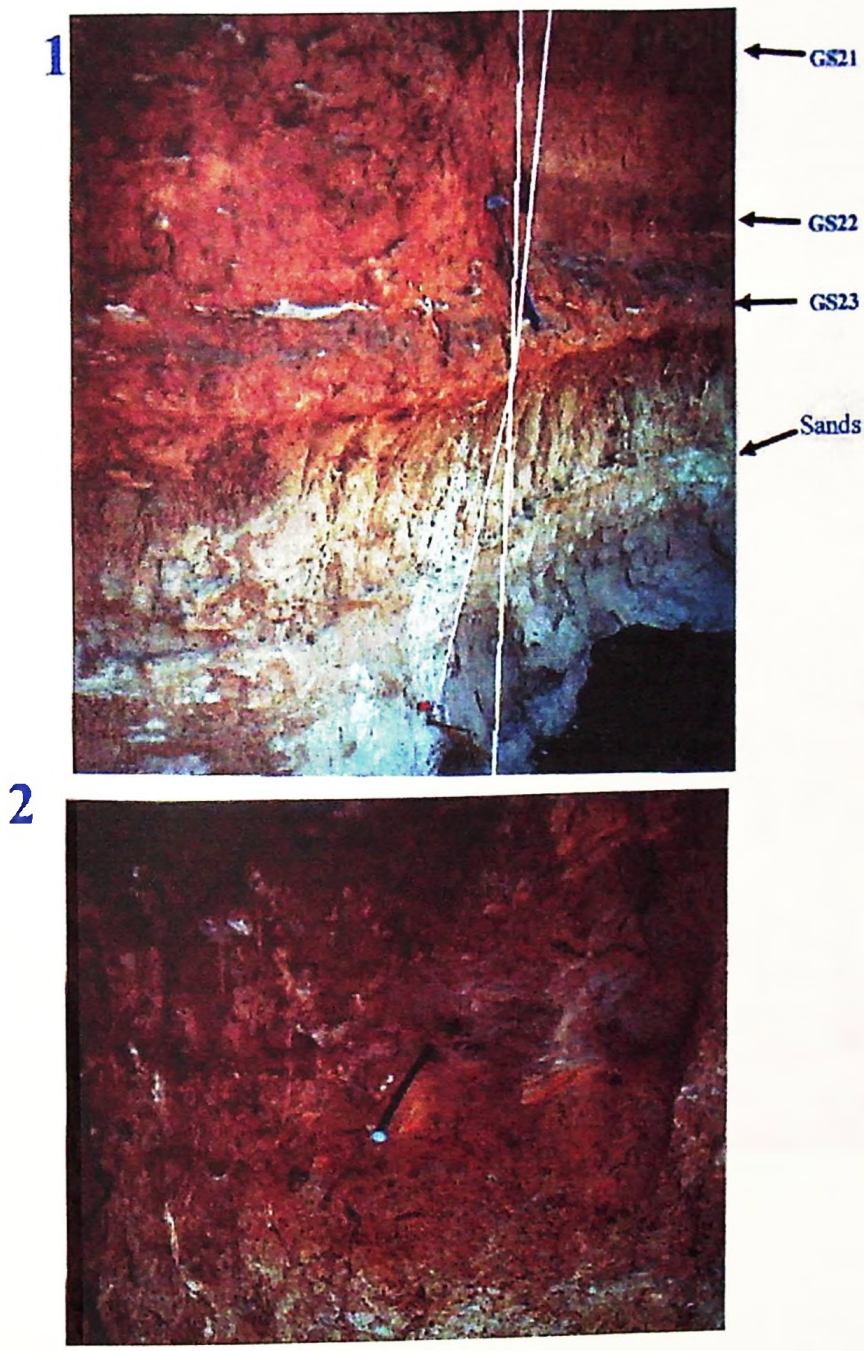

Figure 6.1c Red Bluff section **1.** Stratigraphical positions of GS21, GS22 and GS23 in Bed III. **2.** Gs21 palaeosol level.

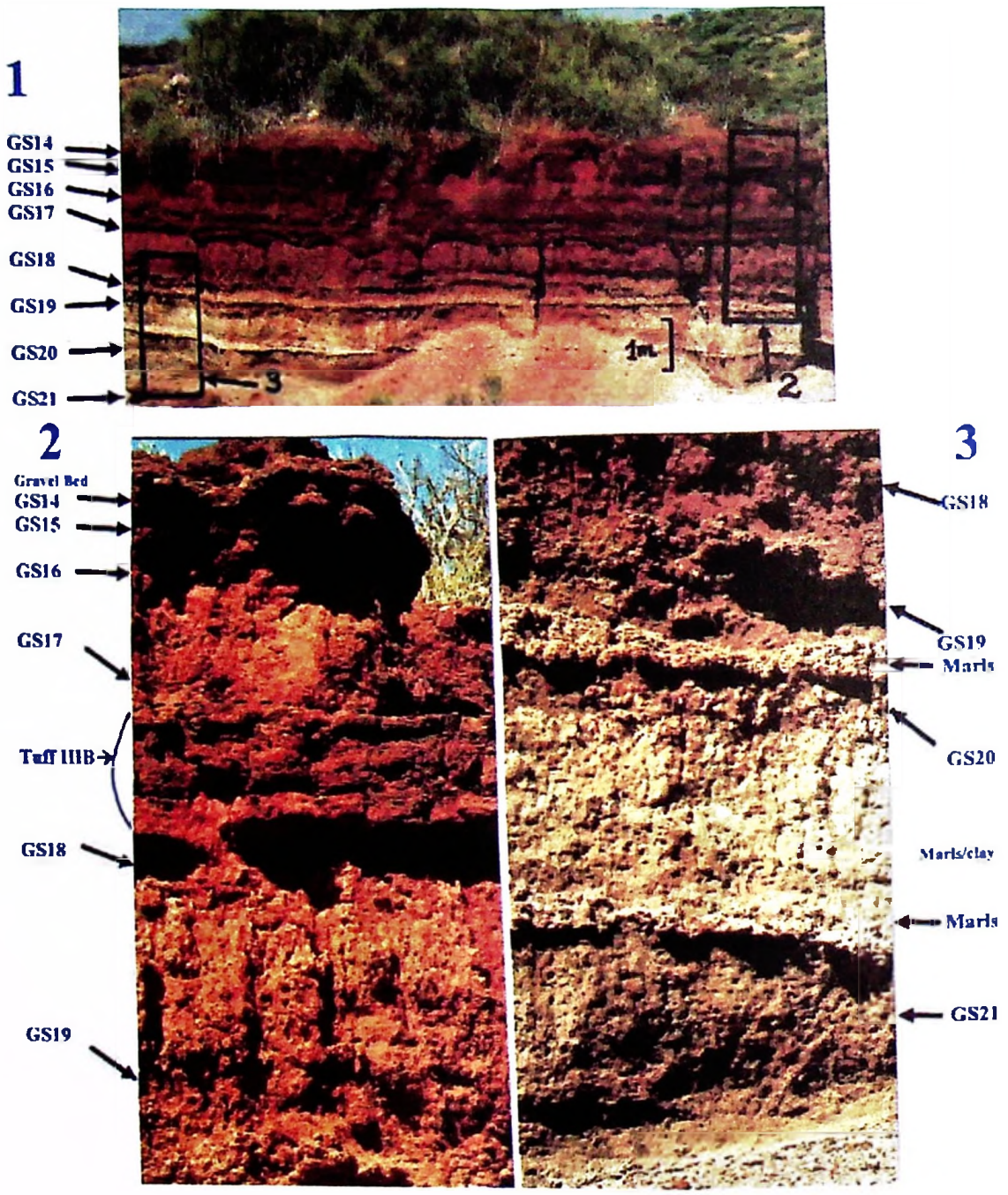

Figure 6.2d: Red palaeosol levels in Bed III. **1.** Stratigraphical positions of GS14 to GS21 palaeosol levels. **2-3.** Detail of stratigraphical positions of G14 to GS21 palaeosol levels.

Field observation revealed palaeosol levels GS19, GS20, GS21 and GS22 are red to yellowish red palaeolandscapes showing stem and root infillings and soil imbrications, (figures 6.2b and 6.2c). The palaeosols seem to develop on marls of probably lacustrine origin, (figure 6.2d). Due to their intense red colour they were provisionally (field) regarded as Alfisol? or Oxisols? (Laboratory work needed to be certain) of the past. The upper part of this section contains red palaeosols GS17 and GS18 showing distinctive red spotted texture refered to as 'oolitic texture' with intense mottling and rubification. Again due to their intense red colours these series of palaeosols were tentatively termed as alfisols or oxisols of old.

Rutgers section begins with a thick clay bed, which is covered by a well-developed olive palaeosol (GS42), (figure 6.3a). The palaeosol shows intense plant and animal activity (abundant plant and animal remains). It is difficult to classify this well-developed palaeosol based on field observation, but it will be safe to tentatively call it an alfisol based on its grade of pedogenetic activity. Palaesol levels GS38, GS39, GS40 and GS41 are olive fossil soils each developed on tuff layer they contain significant carbonate concretions. Based on their macropedofeatures (figures 6.3 and 6.3a_{1-3}) they are regarded as either andisols (ash derived soils), aridisols (presence of carbonate concetions) or vertisols (slikenside soil structures). Palaeosol levels GS38 to GS42 are stratigraphicalally regarded to be in lower Bed II.

Levels GS24 to GS31 are gray to olive fossil soils constituting the upper part of Bed II. These palaeosols were developed on sand deposits. Some of the palaeosols contain carbonate concretions. The palaeosol levels are classified as Aridisols.

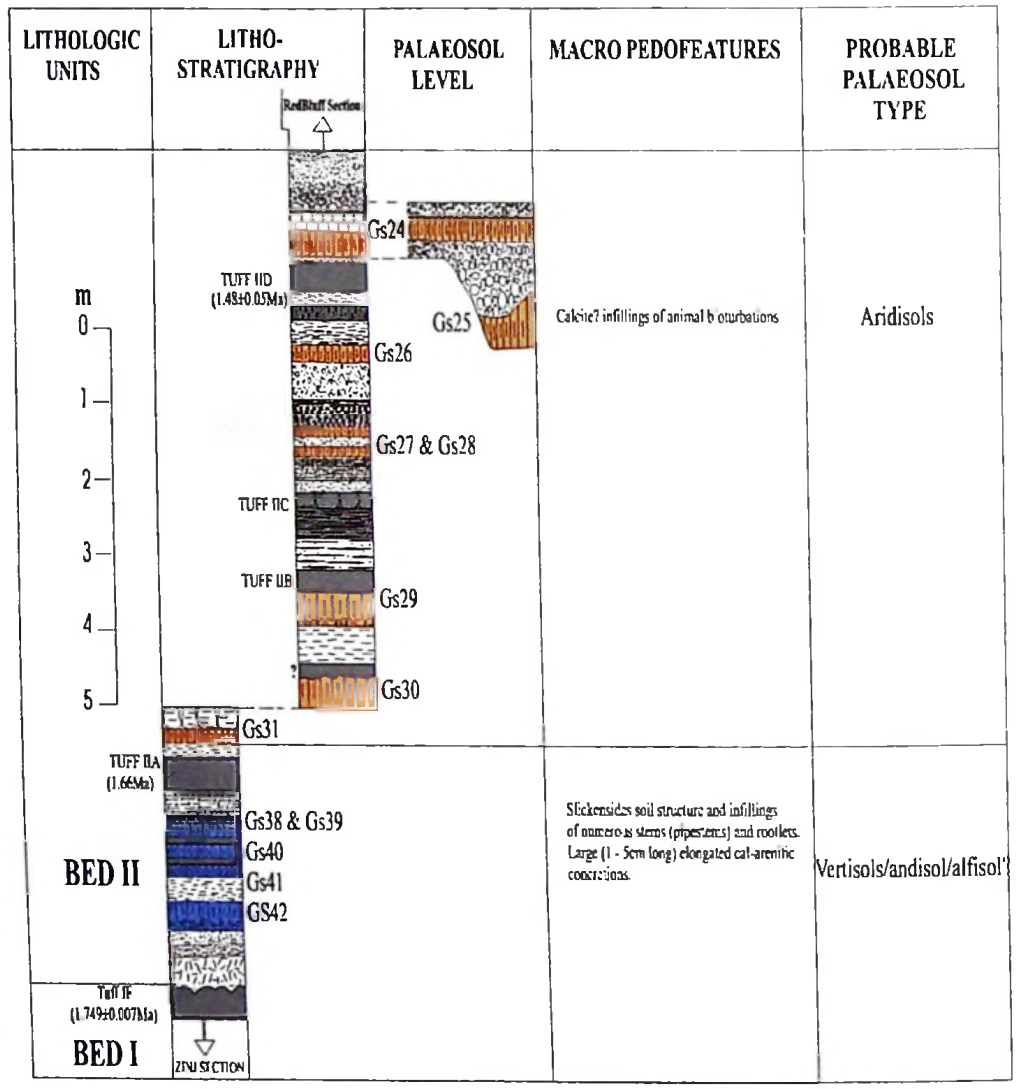

FIGURE 6.3: **RUTGERS SITE SECTION:** *LITHOSTRATIGRAPHY AND MACRO-PEDOFEATURE OF THE PALAEOSOL LEVELS WITH PROBABLE PALAEOSOL TYPE (Studied with the permission of Rutgers University)*

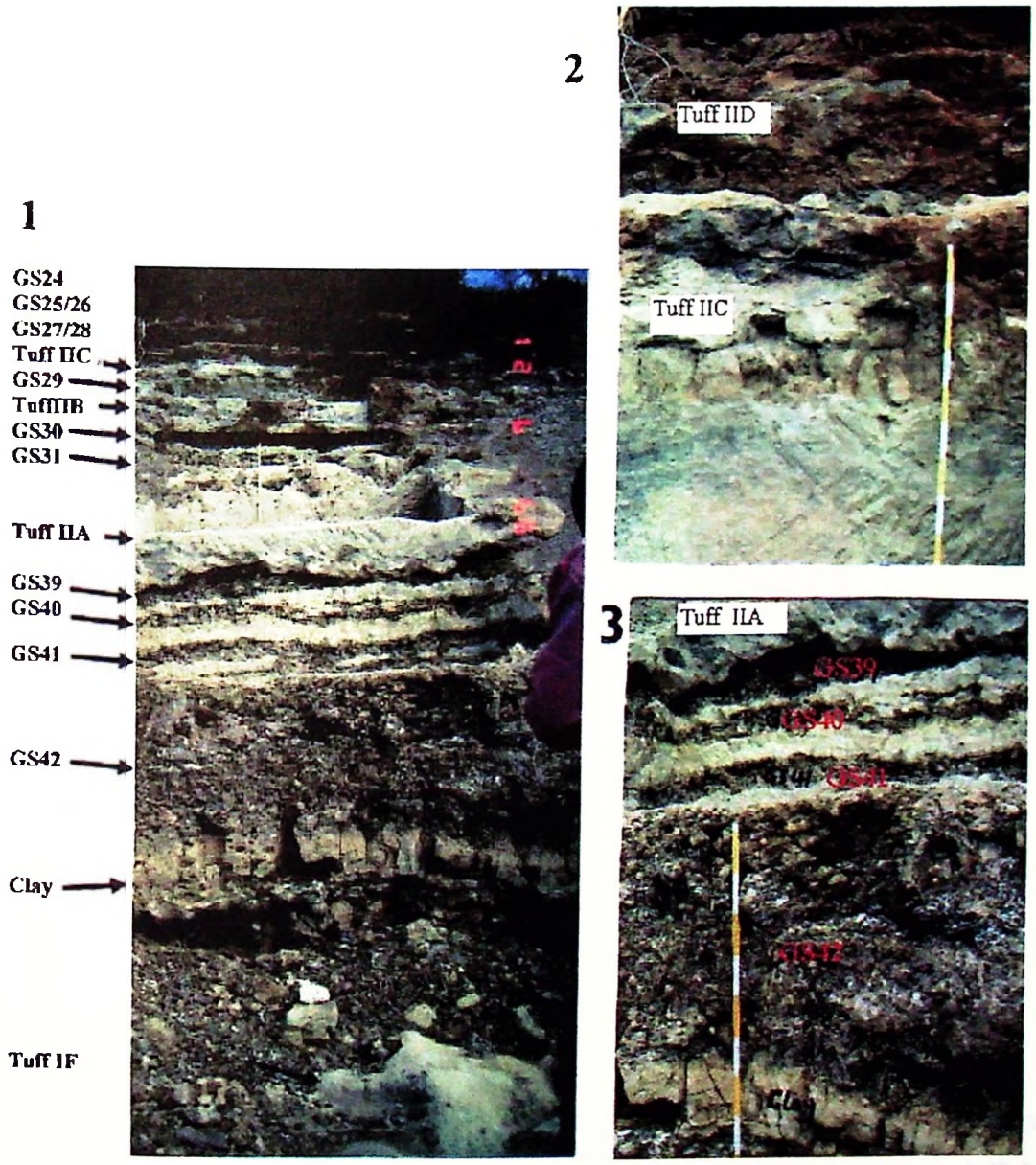

Figure 6.3a: The palaeosol levels of Rutigers section. **1.** The general view of stratigraphical positions of GS24 to GS42. **2.** Detailed view of the tuff levels. **3.** Detailed view of GS39 to GS42 palaeosol levels.

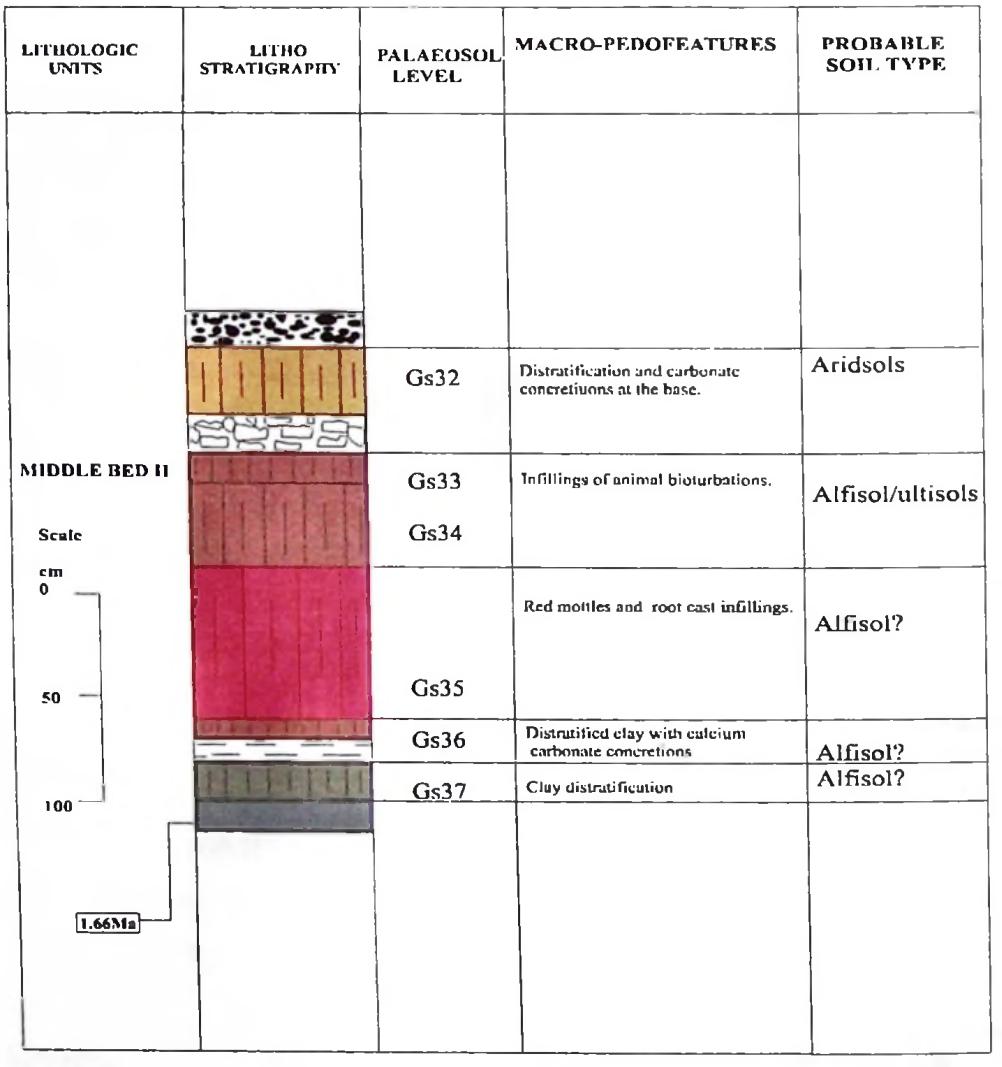

FIGURE 6.4: **LONG KORONGO SITE**: *LITHOSTRATIGRAPHY AND MACRO-PEDOFEATURES OF THE PALAEOSOL LEVELS WITH PROBABLE PALAEOSOL TYPE.*

Long Korongo site palaeosols represent palaeoenvironments of middle Bed II. Middle Bed II is a generally red zone composed of red palaeosols with red mottles and root infillings (GS32, GS33, GS34, GS35 and Gs37), (figure 6.4a_{A-B}). These palaeosols are regarded as oxisols. However, the lower part is made up of a thick dark grayish brown clay layer. The brown colour is an indication of pedogenetic activity probably forming an alfisol (GS37). The upper part is again a pedogenized clay layer. It contains significant amount of carbonate concretion at the base. This layer was recognised as a palaeo-Aridisol (GS32).

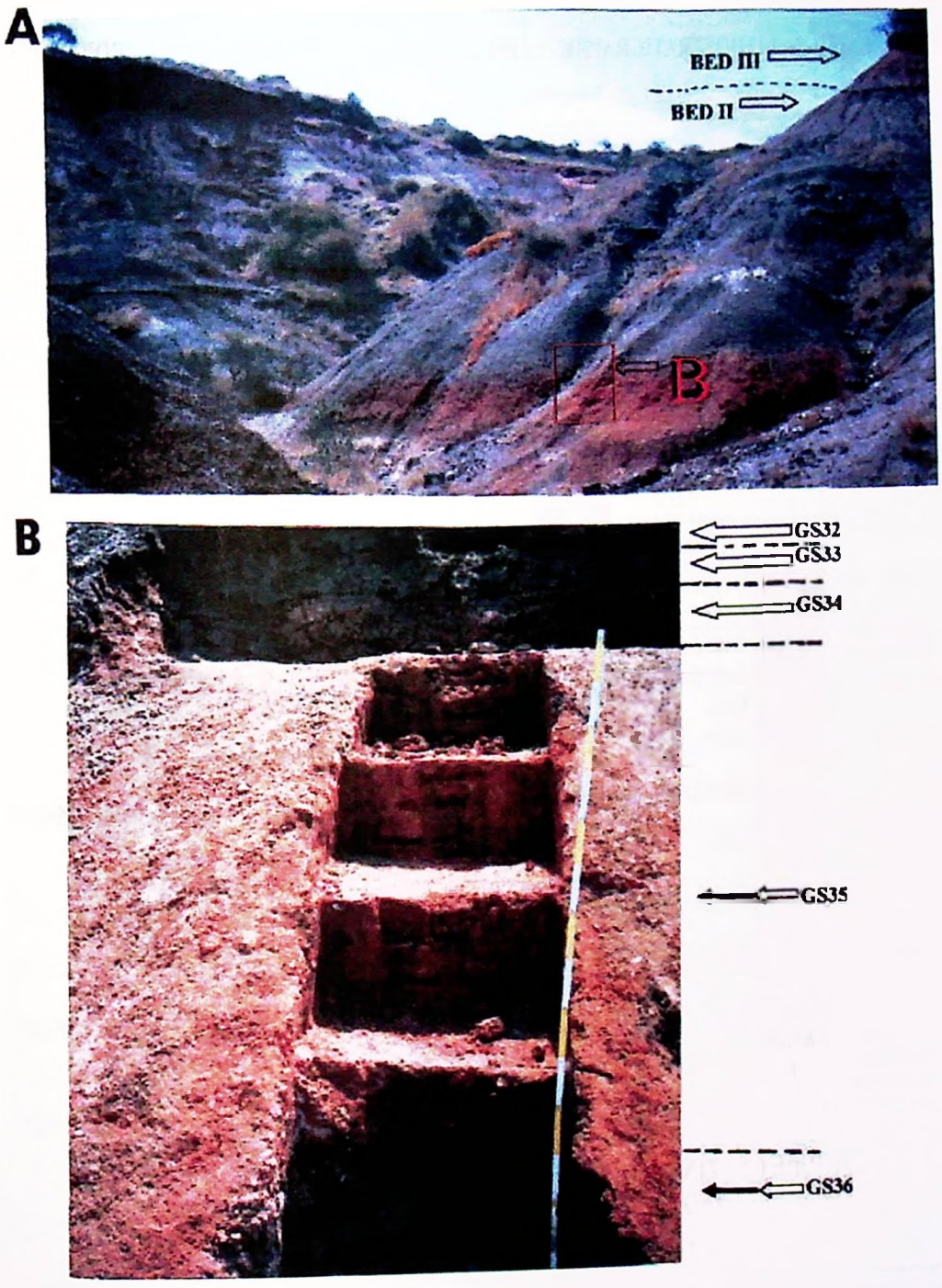

Figure 6.4a: A. Long korongo site a perspective view of the red palaeosol levels in in middle Bed II. The Bed II/Bed III boundary is observed at the upper part of the section. **B.** Close up of red palaeosol levels in middle Bed II [GS32, GS33, gs34, GS35 and GS36 levels are indicated]

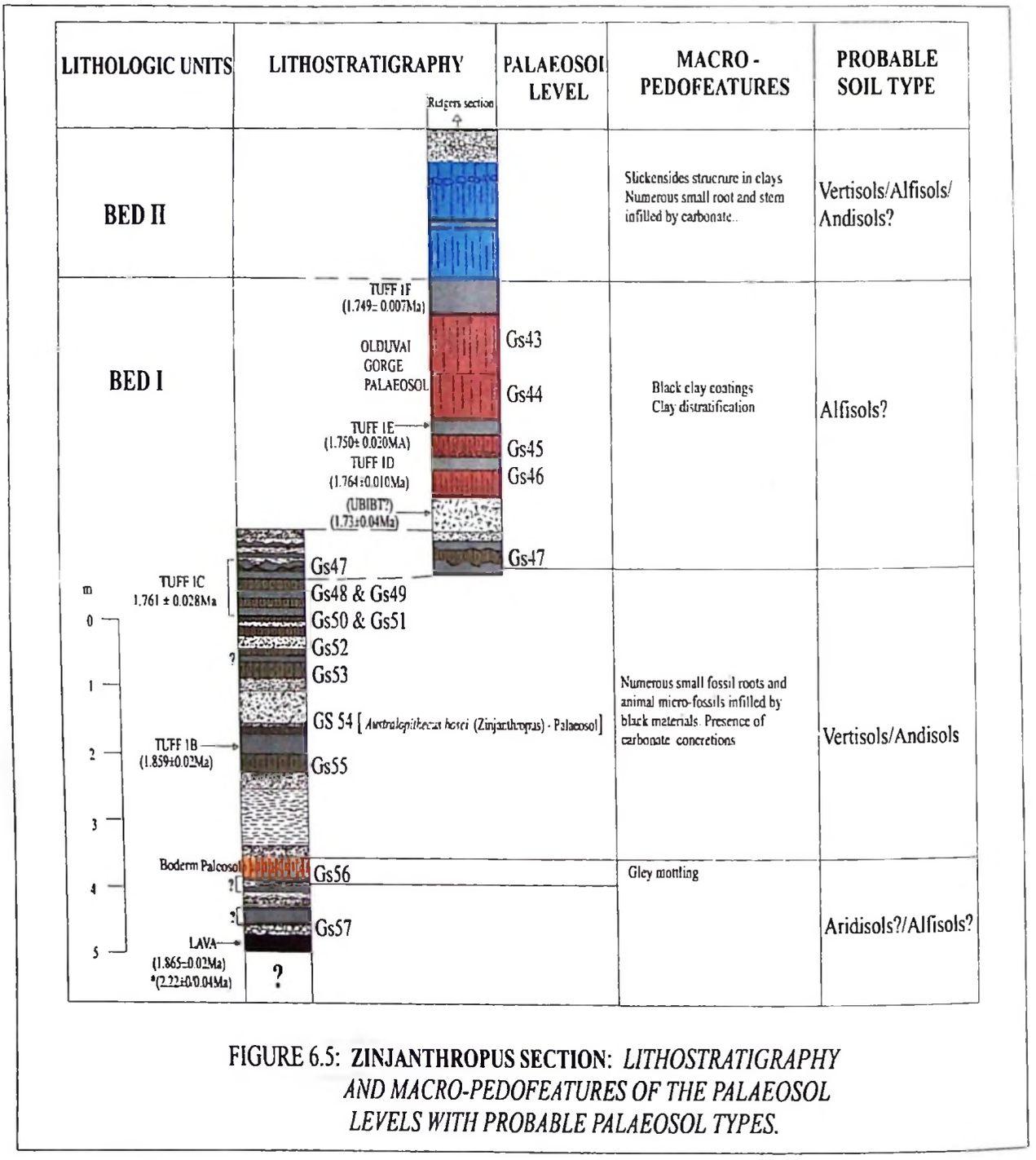

FIGURE 6.5: **ZINJANTHROPUS SECTION:** *LITHOSTRATIGRAPHY AND MACRO-PEDOFEATURES OF THE PALAEOSOL LEVELS WITH PROBABLE PALAEOSOL TYPES.*

The Zinjanthropus section is located at the site where *Australopithecus boisei* "zinjanthropus" was found (FLK archaeological site). Palaeosol levels developed on lacustrine olive to gray clay and tuff layers. GS57 and GS56 palaeosol levels which, occur at the base of the Zinj section are sandy in texture while GS43 to GS55 are more clayey and tuffaceous. Their stratigraphical positions as observed in the field occupy the middle and upper parts of the section, (figure 6.5a).

The lower part of the section was observed from a trench which was made during the mapping campaign, (photographic was not poaaible). GS56 and GS57 are regarded as andisols or degraded alfisols due to their sandy textures. GS54 is a more pyroclastic than clayey it is the level in which the skull of the zinjanthropus was found. The palaeosols of the lower part of this section (GS47 to GS55) contain numerous small rootlets and animal fossils with carbonate concretions and are grouped as andisols or vertisols. Palaeosols of the upper part of the section (GS43, GS4, GS45 and GS46) are well-developed clay soils showing clay coatings without carbonate concretions.

It is important to note that levels GS43 and GS44, are extremely thick (2m) grayish brown to brownish gray strongly developed palaeosols. In this study they are considered to represent the Olduvai Gorge geomagnetic event, (figure 6.5b). They mark a significant wet period, which favored the development of such strong palaeosols. These are termed as "Olduvai Gorge palaeosol". Palaeosol levels GS57 to GS43 represent palaeosol units of Bed I. Palaeosol levels GS43 to GS46 are regarded as alfisols due to their well developed nature and being devoid of calcium carbonate concretions.

On top of GS43 lies two thick (2m) palaeosols showing slickenside soil structured and numerous small root and stem infillings. This zone belongs to lower Bed II and these soils are stratigraphical equivalent to the palaeosols of lower part of Rutgers section (GS38, GS39, GS40, GS41 and GS42). Bed I palaeosol levels are therefore thought to be either Pleistocene aridisols or alfisols – a laboratory study is needed to ascertain this fact.

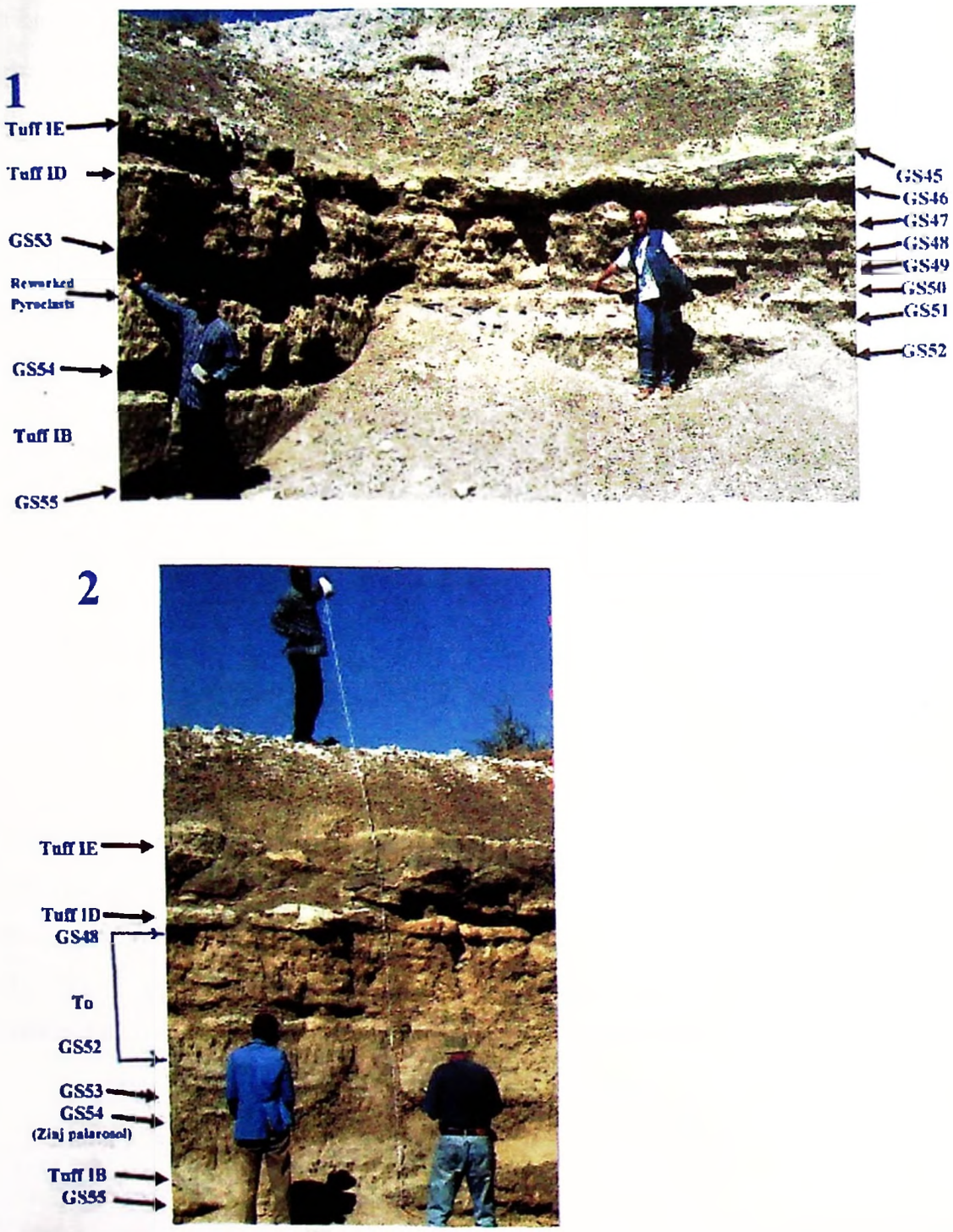

Figure 6.5a: The zinjanthropus site. **1-2.** Stratigraphical positions of GS45 to GS55 palaeosol levels, marker tuff IB tuff ID and and tuff IE.

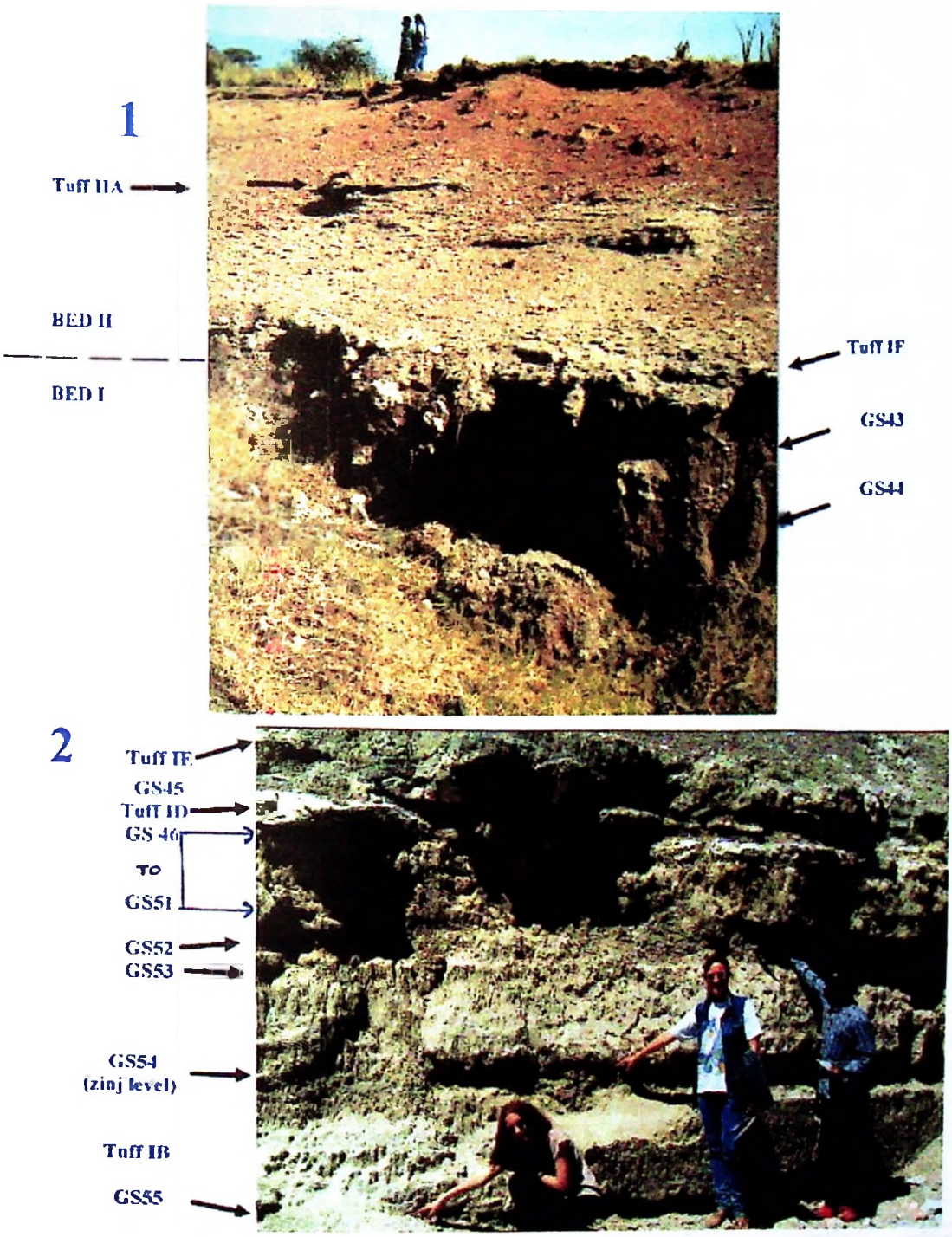

Figure 6.5b: The Zinjanthropus section palaeosols. 1. Stratigraphical positions of tuff IIA, tuff IF , GS43 and GS44. (GS44 and GS45 are named 'Olduvai Gorge palaeosols' of upper Bed I. 2. Stratigraphical positions of palaeosol levels GS46 to GS55, marker tuffs IB, ID and IE. [Australopithecus boisei was found in GS54 level]

6.2.3. Olduvai Gorge palaeosol sequence

From the above soil mapping Olduvai Gorge sediments contain four types of palaeosols, 1. Red to brown sandy palaeosols (Oxisols/latosols?) dominant in Middle-Upper Bed II and Bed III, 2. Olive to gray clayey palaeosols (Ultisol/Alfisol/Aridisol?) of Bed I, 3. Gray to brown palaeosols (Vertisol, Mollisols or Alfisols?) of Bed IV and Masek beds. 4. Occasional white tuffaceous palaeosols in Bed I and Lower Bed II are observed (table 6.2).

Table 6.2: Characteristics of 4 major palaeosol types in Olduvai Gorge Beds.

Lithology	**Tentative Palaeosol-soil taxonomy**	**Color**	**Structure**	**Macropedofeatures**	**Conventional Lithological units**
Sand, sandstone and gravel	*Sandy palaeosols* Red palaeosols (Alfisols/Ultisols) Brown Palaeosols (Alfisols)	Red to pale-red (10R6/4-10R4/8). Red to yellowish-red (2.5YR4/6-8 to 5YR5/6). Brown to reddish-yellowish-grayish brown (10YR5/3, 10YR7/4, 10YR6/4. 7.5YR6/4 10YR3/2 2.5YR5/2-6 & 5YR6/4, 2.5Y4/2).	Massive clay, sandy and gravely	Red mottles red coatings. 1-3cm root and stem encrusted by red stains or calc-materials. Some blocky ped structures pare visible. Soil imbrication in marls.	Middle Bed II and And Bed III
Fine clay and claystone	*Clayey palaeosols.* Olive palaeosols (Vertisol, aridisol or Alfisols?) Gray palaeosols (Aridisol)	Olive to pale olive (5Y5/3, 5Y5/4, 5Y4/4 & 5Y63). Olive gray to dark gray (5Y4/1-2, 5Y3/2, 5Y6/2,	Massive and layered	Clay distratification by animal bioturbation and plant actions. Slickenside soil structures. Infills of numerous small stems and rootlets. $CaCO_3$ concretions and nodules. Presence of mycelia and spicules.	Bed I and lower Bed II Upper Bed II

		5Y7/1-2 & 10YR7/2).			
Ash fall or ash flow tuffs	*Tuffaceous palaeosols* (Andisols?)	White (5Y8/1-2).	Homogeneous ash.	$CaCO_3$ concretions and nodules.	Bed I and Bed II
Fine clay to silt clay.	*Clay silt palaeosols* Gray palaeosols (Vertisols) Brown palaeosols (Vertisols or Aridisols?)	Olive gray to brownish gray (5Y5/1-2 & 2.5Y6/2). Grayish brown (2.5Y5/2).	Loose homogeneous silty and pebbly.	Black to gray clay coatings. Clay distratification. 1-3cm columnar structures. Slickenside features. Gilgai macro relief imprint. 2-5cm wide mud cracks with surfaces coated by black clays.	**Bed IV, Masek Beds and Ndutu Beds**

This preliminary field mapping indicates that Bed I and Upper bed II palaeosols were developed on fine clay and claystone as they are found on top of clay layers. The white tuffaceous palaeosols developed on ash fall or ash flow tuffs widespread in this sequence.

The red to brown palaeosols are mapped in middle Bed II and Bed III. These palaeosols show that they were formed on silt, sand and gravel sediments. Their color indicates intense oxidation process was widespread at the time of their formation suggesting alternating wet and dry conditions. The sorted sandy levels of upper Bed II show rare development of gray to brown palaeosols an indication of more dry environments during the Quaternary. The upper part of the Olduvai Gorge composite section reveals gray to brownish gray paleo-vertisols mainly clayey in nature. Again these may signify seasonal dry and wet climatic conditions in the area. Mineralogical, geochemical and micromophological studies (chapter 7) provides better understanding of their specific genesis and further sheds light to their taxonomy.

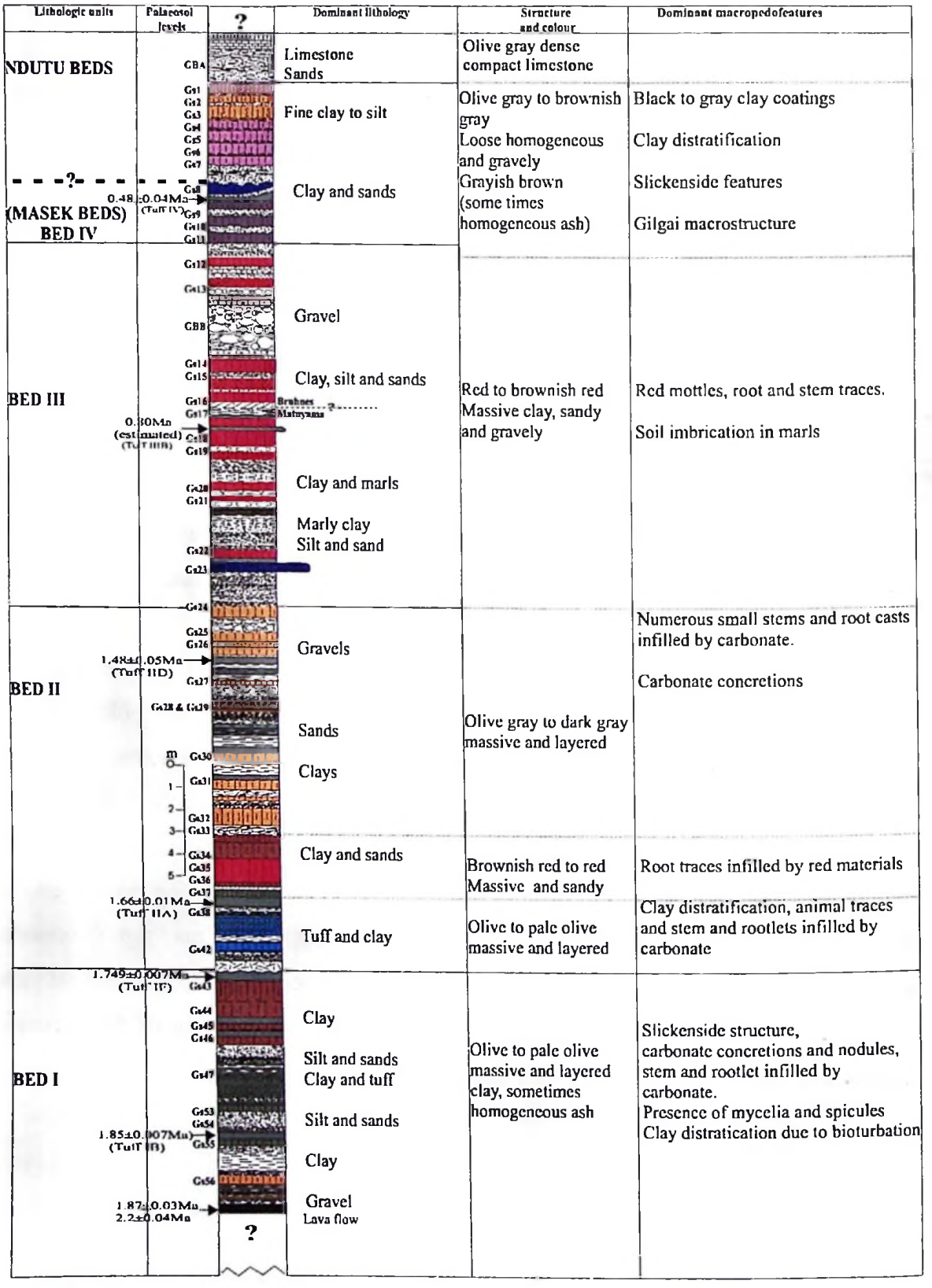

Figure 6.6: General field characteristics of Olduvai Gorge palaeosols (also see table 6.2)

CHAPTER SEVEN

OLDVAI GORGE MINERALOGICAL, GEOCHEMICAL AND MICROMORPHOLOGICAL LABORATORY STUDIES

7 MINERALOGICAL, GEOCHEMICAL AND MICROMORPHOLOGICAL ANALYSES

7.0 INTRODUCTION

This chapter gives some mineralogical, geochemical and micromorphological laboratory analyses, which were performed in this study. The analyses were carried out in order to determine the general mineralogical, geochemical composition and some micromorphologic characteristics of some palaeosols. It is well known that presence of specific types of clay minerals can indicate intensity of weathering, which in turn can suggest the type climate that existed at the time. Specific relic micromorphologic features of the palaeoasols will indicate possible palaeosol genesis and therefore suggest the palaeosol taxonomy and some specific climatic conditions in which the past soils developed. The laboratory analyses would also provide a general stratigraphical characterization of the deposits.

7.1 MINERALOGICAL ANALYSES

7.1.1 Methods of investigation

A total of 142 bulk samples were systematically sampled from the Olduvai Gorge section (Zinj, RS, RB, LK and MC sections) along the gorge cliffs for mineralogical and geochemical analyses. The sampling interval ranged from 2cm to 100cm depending on the lithological variations. Thicker lithologies had larger sapling interval and thinner ones had dense sampling intervals. The samples were analyzed by an infrared reflectance

spectrometry as explained below. Samples from sand dunes (shifting sands) were also collected and examined by a reflection microscope.

7.1.2 Mineralogical analytical procedures.

Analyses were performed using a Short Wave InfraRed (SWIR) spectrometer instrument and a reflection microscopy (Intergrated Electronics, 1993). No sample preparation was required prior to the SWIR measurement but only a flat surface was required to be exposed to the incident infra red light. Each sample was measured by exposing the sample to the infrared radiation window or optical port of the instrument. When the measure button was pressed the sample was irradiated by the infrared radiation for some seconds. The sample reflected the infrared light (radiation) back into the instrument for measurement. The radiation from the sample was then measured by the spectrometer.

A Pima View spectrometry software programme then interpreted infrared spectrum profiles of individual samples. The infrared sample profiles (appendix 7.4) were correlated to specific mineral profiles available in the software mineral libraries. The principle of the infrared spectrometry method is given in appendix 7.1.

7.1.3 Mineral identification

The minerals were identified according to their wavelength peak position (each mineral has its characteristic wavelength peak position). The intensity of the peaks is directly proportional to the concentration of the minerals. Wavelength spectrum profile of each sample was matched to library profiles of standard minerals available in the Pima View programme. The best match gave the composition of each sample. If a match was not found in the library a manual match was performed where peak positions (λnm) of sample profiles were manually compared to the standard profiles given in the manual books.

7.1.4. Short Wave Infrared Reflectance (SWIR) spectromter analyses

7.1.4.1. Results

The purpose of this study was to obtain common mineralogical assemlages in different zones of the stratigraphy and attempt to deduce palaeoclimate and palaeoenvironments. From the wavelength (peak positions) the following minerals present in the samples were identified as presented in tables 7.1 and 7.4. Detailed analytical raw data list is presented in appendes 7.4 and 7.5.

Table 7.1: Summary list of minerals identified according to their peak positions.

Peak positions - wavelength (λnm)	Mineral group and types
1900 – 1920 (Major intensity, sharp and deep). CLAY MINERALS	Kaolinites (Halloysite) Illites (Illite, Rectorite), Smectites (Montmorillonite, Natronite, and Saponite), some Zeolites (Analcime, Mordenite,)
1410 – 1470 (Major intensity fairly sharp and deep) ZEOLITES/HYDROXIDES	Zeolites (Analcime, Heulandite, Natrolite, Stilbite, Chabazite palygorskite and sepiolite), Lepidocrosite, gibbsite and limonite and clay minerals (Smectites)
2250 – 2260 (Large intensity but very shallow) SILICATES	Hornblende, Jadeite, Kyanite. Bassanite, Colemanite, Inyoite, Quartz, Micas (Lepidolite, muscovite and ephesite), Pyroxene (Jadeite), Amphibole (Lazurite), Hemimorphite,
2200 – 2250 Major intensity but very shallow.	Buddingtonite – feldspar, Lazurite, Lepidocrosite and Brucite.
2300 – 2350 (major intensity and very shallow) CARBONATES	Carbonate, Azutite, calcite, dolomite, malachite, aragonite, stronianite, smithsonite, shortite, rhodocrosite and gypsum.

Table 7.4: A summary of Infrared reflectance peak intensity variation of clay minerals (1900 – 1920 nm)λ wavelength and amorphous carbonate at (2300 – 2350nmλ) of Olduvai Gorge beds according to their stratigraphical positions (also see figure 7.1A).

No.	Sample	Peak intensity (%) Clays	Peak Intensity (%) Carbonate	Palaeosol Levels	Depth (m)
1	mc27	21.49	22.61		1.35
2	mc26	21.21	25.4		1.75
3	mc25	17.3	20.09		2.1
4	mc24	16.18	18.81		2.25
5	mc23	18.42	22.61		2.5
6	mc22	9.2	0	GS1	2.75

7	mc21	17.86	20.65	GS1	3.3
8	mc20	24.65	28.6	GS2	3.75
9	mc19	10.87	0	GS3	4.3
10	mc18	12.55	0	GS4	5.75
11	mc17	11.31	0	GS5	6.35
12	mc16	10.04	0	GS6	6.725
13	mc15	10.04	0	GS7	7.25
14	mc14	16.46	0		7.5
15	mc13a	13.95	0	GS8	7.65
16	mc13b	18.7	0	GS8	7.85
17	mc12	28.47	0		8.25
18	mc11	11.43	0	GS9	8.85
19	mc10	14.23	0		9.15
20	mc9	14.51	19.81	GS10	9.45
21	mc8	7.8	0	GS11	9.9
22	mc7	17.3	0		10.2
23	mc6	9.48	0	GS12	10.45
24	mc5	13.95	0		10.75
25	mc4	9.48	0	GS13	11.35
26	mc3	12.83	0	GS14	11.65
27	mc2	16.18	0	GS15	11.85
28	mc1	15.9	0	GS16	12
29	rb22	13.39	0		12.75
30	rb21	18.7	0	GS17	13
31	rb20	14.79	0	GS18	13.65
32	rb19	13.67	0		14.05
33	rb18	12.27	0	GS19	14.65
34	rb17	12.65	0		15.15
35	rb16	11.98	0		15.65
36	rb15	11.31	0	GS20	15.9
37	rb14	19.98	0	GS21	16.25
38	rb13	15.31	0		16.5
39	rb12	21.3	24.65		16.75
40	rb11	13.98	18.7		17.15
41	rb10	15.98	0		17.5
42	rb9	27.32	0		17.75
43	rb8	18.98	24.56		18.15
44	rb7	15.31	0		18.45
45	rb6b	17.98	0		18.65
46	rb6a	22.65	0		19.05
47	rb5	26.24	32.65	GS22	19.35
48	rb4	23.98	29.56		19.75
49	rb3	20.64	0	GS23	20.1
50	rb2	28.65	38.53		20.6
51	rb1	21.98	30.43		21.5
52	rs39	13.31	17.3	GS24	21.85
53	rs38	10.04	0		22.05
54	rs37	16.46	0	GS25	22.3
55	rs36	24.56	0		22.65
56	rs35	19.54	25.68	GS26	23
57	rs34	22.3	0		23.2
58	rs33	11.43	0		23.3

59	rs32	18.7	19.26		23.5
60	rs31	15.07	20.09	GS27	23.65
61	rs30	13.11	17.3		23.7
62	rs29	19.81	0	GS28	23.85
63	rs28	13.95	18.14		24
64	rs27	8.64	0		24.1
65	rs26	19.54	0		24.35
66	rs25	32.39	0		24.4
67	rs24	15.34	0		24.75
68	rs23	17.58	0		25.3
69	rs22	18.14	25.68	GS29	25.75
70	rs21	4.45	0		26.1
71	rs20	23.32	0		26.3
72	rs19	7.8	10.87	GS30	26.65
73	rs18	21.32	0		27.1
74	rs17	8.92	0	GS31	27.55
75	rs16	24	0		28
76	lk10	5.55	0	GS32	28.45
77	lk9	7.8	13.67	GS33	29.58
78	lk8	8.34	19.32	GS34	29.85
79	lk7	5.57	0	GS35	30.45
80	lk6b	5.85	0	GS35	30.85
81	lk6a	4.45	0	GS35	31.05
82	lk5	8.64	18.65	GS35	31.45
83	lk4	4.17	0	GS36	31.75
84	lk3	3.61	0	GS37	32.15
85	lk2	18.68	0		33.5
86	rs15	22.05	0		33.55
87	rs14	19.81	23.17		33.8
88	rs13	5.55	0	GS38	33.95
89	rs12	17.02	27.08		34.05
90	rs11	10.27	0.71	GS39	34.2
91	rs10	28.75	35.58		34.3
92	rs9	12.41	0.61	GS40	34.45
93	rs8	18.42	0		34.6
94	rs7	9.2	0	GS41	34.85
95	rs6	9.96	0		35.1
96	rs5	9.48	12.83	GS42	35.3
97	rs4	5.57	0		35.45
98	rs3	0	0		35.6
99	rs2	20.37	24.28		35.85
100	rs1	0	0		35.85
101	3z	5.01	8.08	GS43	36.45
102	2z	5.31	7.3	GS44	37.1
103	zl	17.98	31.32		37.9
104	1z	6.41	9.2	GS45	38.4
105	zk	11.17	18.7	GS46	38.6
106	z23	19.32	0		39.3
107	z22	24.65	37.98		39.9
108	z21c	19.98	31.98		40.05
109	z21b	23.98	36.65		40.1
110	z21a	9.31	15.31		40.15

111	z21	14.65	20.37		40.2
112	z20	18.98	20.2		40.25
113	z19	35.32	43.9	GS47	40.3
114	z18	32.94	45.24		40.45
115	z17	25.12	36.02	GS48	40.5
116	z16	24	35.46		40.65
117	z15	23.32	33.98	GS49	40.75
118	z14	17.58	25.98		40.9
119	z13	14.65	21.32	GS50	41.05
120	z12	25.98	38.65		41.15
121	z11	23.32	32.65	GS51	41.3
122	z10	32.65	45.32		41.5
123	z9	51.32	17.3	GS52	41.8
124	z8	19.81	27.64		42
125	z7	15.9	24.4	GS53	42.2
126	z6	24.28	33.18		42.45
127	z5	17.58	26.65		42.65
128	z4	24	33.22	GS54	42.75
129	z3	25.12	30.53		42.85
130	z2	16.18	22.33	GS55	43.05
131	z1	20.37	29.89		43.3
132	zj	14.51	23.45		43.65
133	zi	7.8	10.87	GS56	44.1
134	zh	27.08	32.39		44.9
135	zg	11.71	17.02		45.1
136	zf	22.33	27.64		45.2
137	ze	13.67	18.7		45.4
138	zd	31.27	37.97		45.55
139	zc	10.87	16.18		45.7
140	zb	15.07	23.45	GS57	46
141	za	27.32	35.9		46.25

7.1.4.2. Discussion of the climatic implication

This section therefore attempts to explain the significance of such minerals (especially clay minerals, carbonates and zeolites in soils) to the climatic and environmental changes of the Olduvai Gorge area during the Quaternary.

Basic concepts and definitions of clay minerals and zeolites

Clay minerals

Clay minerals are phyllosilicates with layered silica tetrahedral and octahedral arrangements (Deer *et al.*, 1967). There are three main groups of clay minerals, 2:1 clay

minerals [illites, smectites, and vermiculites], 1:1 clay minerals [kaolinites (kandites)] and mixed layers [usually a mixture of fore said clay minerals).

1:1 clay mineral types consists of one tetrahedral sheet and one octahedral sheet with an approximately thickness of 7A° (Weaver and Pollard, 1973). The different members of this group are characterized by the manner in which the basic 7A° are stacked together.

2:1 clay minerals consist of three sheet layer lattice of two silica tetrahedral sheets sandwitching one octahedral sheet (Deer *et al.,* 1967). These three sheets form a layer of approximately 10A° (Weaver and Pallard, 1973). The illite group of minerals belongs to this group of phyllosilicates. Smectites and vermiculite are 2:1 clay minerals that have swelling characteristics due to presence of interlayer water molecules rendering their basic sheet thickness to increase to 15A° (smectites) and 14.5A° (vermiculite).

Mixed layer clay minerals consists of a mixture of different proportions of individual clay minerals forms mixed layer clay minerals. They are attained by the way the silica octahedral and tetrahedral layers are stacked together to form the final clay mineral or sheet.

Other minerals **are palygorskite** and **sepiolites** are fibrous silicates, which lack continous octahedral sheets like other phyllosilicates. They contain inverted ribbons of 2:1 phyllosilicate structure. The thickness of the basic sheet is about 13A°.

Clay minerals occurrence in soils

2:1 clay minerals are formed in the 1st order cycle of transformation weathering processes. Usually mild weathering conditions are enough to form these types of clay minerals. The 1:1 clay minerals are formed in the 2nd cycle of transformation processes in weathering profiles. Intense wet and humid environments (warm moist regions) are needed to form 1:1 clay minerals from primary rock forming minerals through 2:1 clay minerals. As the weathering intensity increases 2:1 smectites and illites are transformed into 1:1 kaolinites and still further weathering hydroxides begin to be formed (figure 7.1).

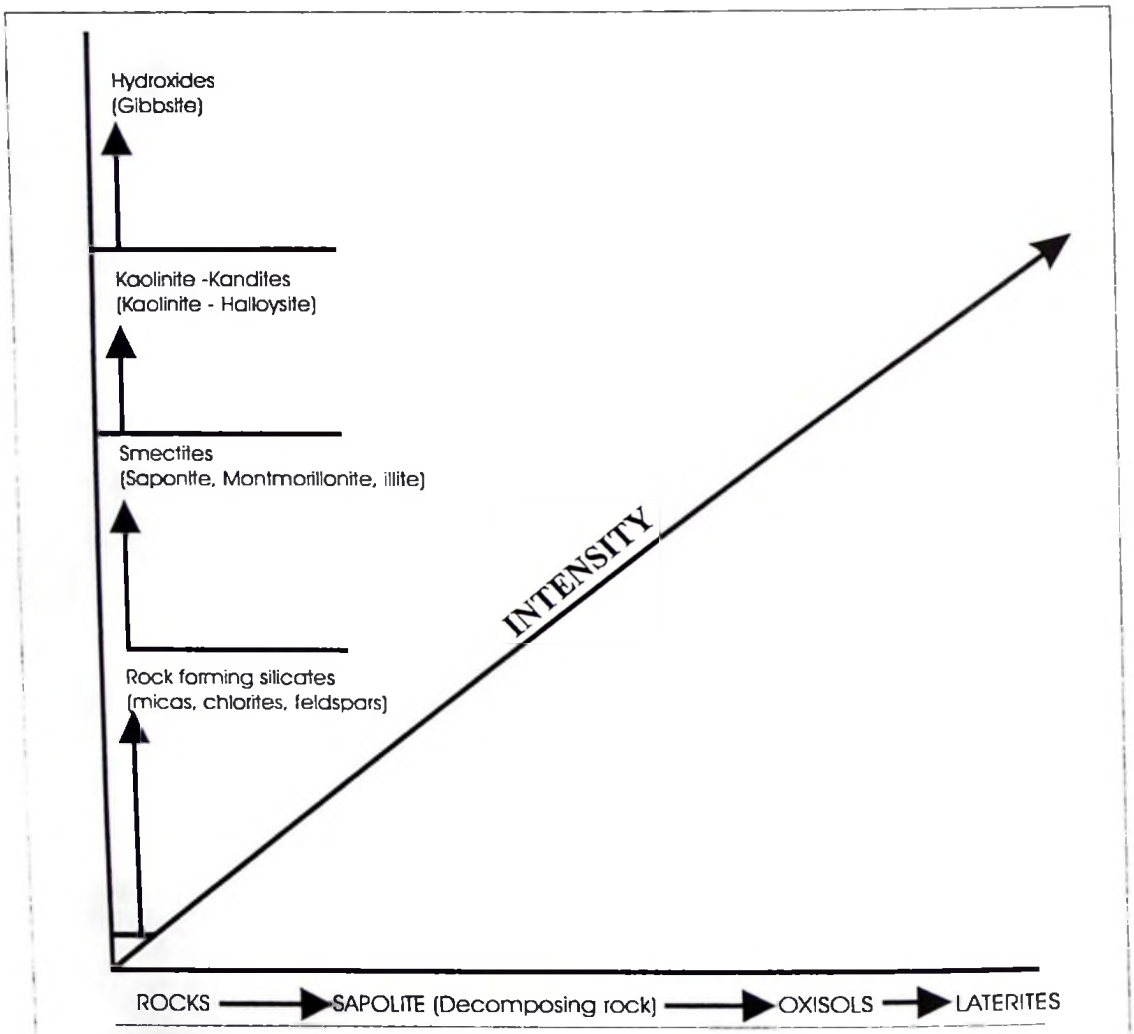

Figure 7.1: Sequence of formation of clay minerals as a function of weathering intensity in soil forming processes of tropical areas, (modified after; Velde, 1985)

However, **palygorskite** (attapugite) and **sepiolite** are formed in dry arid environments from carbonate rich sediments or rocks. Palygorskite and sepiolite are usually formed from highly concentrated solutions, (Velde 1985) and therefore are destroyed by intense weathering except in weak weathering environments. These two clay minerals are closely related to $CaCO_3$ formation. Under highly evaporite conditions palygorskite and sepiolite minerals are formed (Walker *et al.*, 1978) by subsurface water up and down movement by capillarity action. Sepiolite is formed within the $CaCO_3$ and palygorskite though related to $CaCO_3$ formation but forms outside the zone.

On the other hand smectites are known to be formed in weathering environments in temperate climates where drainage is moderately good, but they are also the common clay minerals formed in soils which produce zeolites, through the weathering processes in arid to semi arid environments (Hay 1963). In these environments smectites can be transformed to zeolites (analcime). Clay minerals therefore indicate weathering processes of varying intensity depending on the climatic condition.

Zeolites

Zeolites are tectosilicates with an infinite three-dimension crystal structure of the silica tetrahedral particles. There exist openings between the tetrahedral structures. Water molecules occupy the openings. Zeolites are therefore referred to as hydrated aluminosilicates (Deer *et al.*, 1975) which contain alikali and alikaline earth cations. Zeolites are formed by hydration of tectosilicate minerals. Their amazing ability to hydrate and dehydrate reversibly and exchange some of their cations without major change of structure has placed zeolites in a high demand category of industrial minerals in the physio-chemical industry.

Zeolites occurrence in soils

Zeolites are formed by hydration of especially eruptive rocks (Hay 1963) in arid to semi arid environments. For instance analcime is formed at the expense of 2:1 smectite clay mineral and sodium carbonates depending on the drainage pattern that exist (Velde 1985).

Zeolites are known to occur in sodic soils of arid to semi arid climates in the tropical areas. They have also been reported in cold arid soils of the Antactica (Van Ranst, 1997a). Zeolites therefore indicate mild weathering with or without cold conditions in which leaching and hydrolysis were insufficient to produce clay minerals. In hot and dry climates and with rather brief rainy seasons zeolites are formed rather than clay minerals (Hay 1963).

Other mineral species

Other minor mineral species of climatic significance found in Olduvai Gorge palaeosols includes hydroxides, carbonates and evaporites. Hydroxides indicate intense weathering during wet and humid climates. Carbonates and evaporites point to dry climatic and environmental conditions.

Olduvai Gorge minerals and their stratigraphical and palaeoclimatic implications

Palaeoclimatic reconstructions through clay minerals are not an easy task due to complex geochemical reaction pathways to form the end products. These processes can give polyminerallic clay assambleges (Thorez, 1983). Nevertheless, general palaeoclimatic inferences can be made from clay minerals occurrences in lithostratigraphical sections. An attempt is therefore made here to observe mineralogical variations across the stratigraphy and try to offer some general initial palaeoclimatic/palaeoenvironmental interpretations.

From the review (in section 7.1.4.2) the presence of several specific zeolite mineral species and pedogenic carbonate in palaeosol horizons in Olduvai Gorge is interpreted in study as being formed in arid to semi arid environments. And 2:1 clay minerals to indicate mild weathering environments indicating mild dryness to slightly wet climates. 1:1 clay minerals are taken as indicating wet climates.

Olduvai Gorge Beds show a range of mineral species across different lithological units. Mineral species found in Olduvai Gorge section are clay minerals, zeolites, evaporites, carbonates and silicates. Clay minerals and zeolites are dominant in palaeosols. Evaporites and carbonates dominate in lacustrine sediments and silicates in clastic

The clay, carbonate and zeolite mineral composition of the palaeosol levels of Olduvai Gorge and their climatic implication is therefore briefly discussed in the proceeding paragraphs. Figures 7.1a & 7.21b form the basis of this discussion.

The general mineralogical – stratigraphicalal characterization of Olduvai Gorge is summarized by figure 7.1a and briefly discussed here below. Bed I stratigraphical unit show higher concentrations of clay minerals a condition that can be associated to slightly drier environments during the Lower Pleistocene.

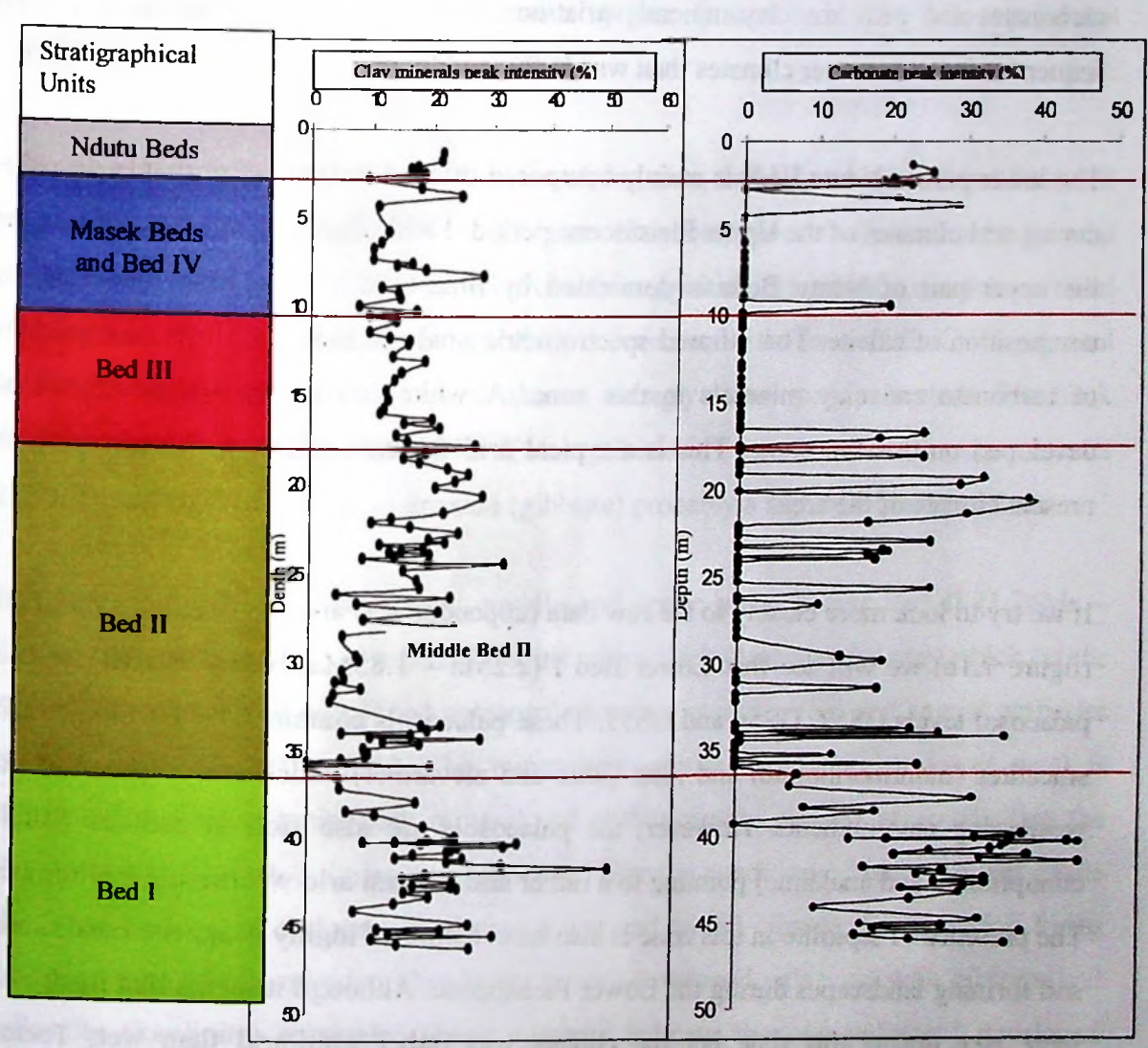

Figure 7.1a: Clay minerals and carbonates concentration variation of Olduvai Gorge Beds as derived from infrared reflectance spectometry: With a general stratigraphical characterization.

In general terms lower and middle Bed II indicates slightly low clay minerals and carbonate abundances compared to Upper Bed II, as is derived from infrared reflectance spectrometry data, (figure 7.1a). This refers probably to generally wetter climatic environments in Lower and Bed II than in Upper Bed II times.

Bed III is generally devoid of carbonates and with depressed clay mineral concentrations, (figure 7.1a) compared to Bed II. Probably there was intense weathering (wet) during this time where carbonate was leached away. The lower part of Masek/Bed IV units show higher concentrations of clay and carbonate minerals, while the middle part is devoid of carbonates and with low clay mineral variations. It is likely that the lower and upper sequences indicate wetter climates than was in the middle parts.

The lower part of Ndutu Beds is mainly composed of sand sediments probably deposited during arid climates of the Upper Pleistocene period. Field observations also indicate that the upper part of Ndutu Beds is dominated by limestone with a basic mineralogical composition of calcite. The infrared spectrometric analysis indicates high concentration of carbonate and clay minerals in this zone. A white calcareous (calcrete) soil has developed on this limestone. This is a typical arid to semi arid soil characterising the present climate of the area.

If we try to look more closely to the raw data (appendix 7.5) and the detailed stratigraphy (figure 7.1b) we will see that Lower Bed I (2.2Ma – 1.85Ma, below tuff IB) contains palaeosol levels GS57, GS56 and GS55. These palaeosols contain 2:1 clay minerals like smectites (montmorillonite) and illite (illite and alevardite) which are evidence of mild weathering environments. However, the palaeosols are also rich in zeolites (stilbite, clinoptilolite and analcime) pointing to a rather arid to semi arid weathering environment. The presence of sepiolite in this zone is also an evidence of highly evaporite conditions in soil forming landscapes during the Lower Pleistocene. Although it seems that there was a large lake during this time but the climate was rather semi-arid than wet. Tectonic activities (rather than climatic reasons), that were intense at that time might have influenced the formation of the lake. Large and deep basins were formed making it possible to collect water from the steep hills around the basin.

Middle Bed I (1.85Ma – 1.75Ma, between tuff IB and IC) the climate might have became wet as is indicated by the presence of 1:1 clay mineral kaolinites (dickite and halloysite)

in palaeosol levels GS54, GS53 and GS52. The presence of and limonite in GS53 points father to wetter environments than lower Bed I period. The 1.76Ma – 1.75Ma Bed I interval is marked by palaeosol levels GS51, GS50, GS49, GS48, and GS47 and occurrence of smectites and illites 2:1 clay minerals. Analcime and stilbite zeolite minerals also appear indicating drier climatic and environmental conditions. The climate probably became dry as is indicated further by gravely sand beds lying below palaeosol GS46.

The upper Bed I (1.75Ma – 1.74Ma interval, between tuff IC and tuff IF) indicates the presence of kaolinite together with gibbsite. However, montmorillonite, sepiolite and zeolites are reported in GS45 plaeosol probably suggesting dry climatic conditions. Field observations also revealed numerous $CaCO_3$ concretions at the base of the GS45 plaeosol level. The upper part of this zone shows strongly developed palaeosols 2m thick palaeosol complex GS44 and GS43. These palaeosol levels contain 1:1 clay minerals kaolinite (halloysite) and Al-hydroxide (gibbsite) probably a sign of a humid period.

Bed II is divided into three lower, middle and upper parts. Lower Bed II (1.74Ma – 1.66Ma, between tuff IF and tuff IIA) begins with a thick (1m) massive clay which (at the top) grades into a well developed palaeosol showing intensive root and animal activities as was observed in the field. The mineralogy of the massive (clay lower part) is dominated montmorillonite-clay mineral and stilbite-zeolite mineral indicating that the clay layer was deposited during mild (not wet) climatic conditions. The upper part of the clay layer underwent pedogenesis during a wet and humid climate. GS42, which forms the upper part of this massive clay layer, is well-developed palaeosol with gibbsite and halloysite (kaolinite) minerals. These minerals indicate that the palaeosol developed during a wet and humid (tropical?) climate of the Pleistocene Period around 1.70Ma. GS41 and GS40 palaeosols lying in succession on top of GS42 contain montmorillonite and zeolites (stilbite, natronite and analcime) probably again indicating drier conditions. GS39 is a well-developed palaeosol (field observations), which contains kaolinite and montmorillonite.

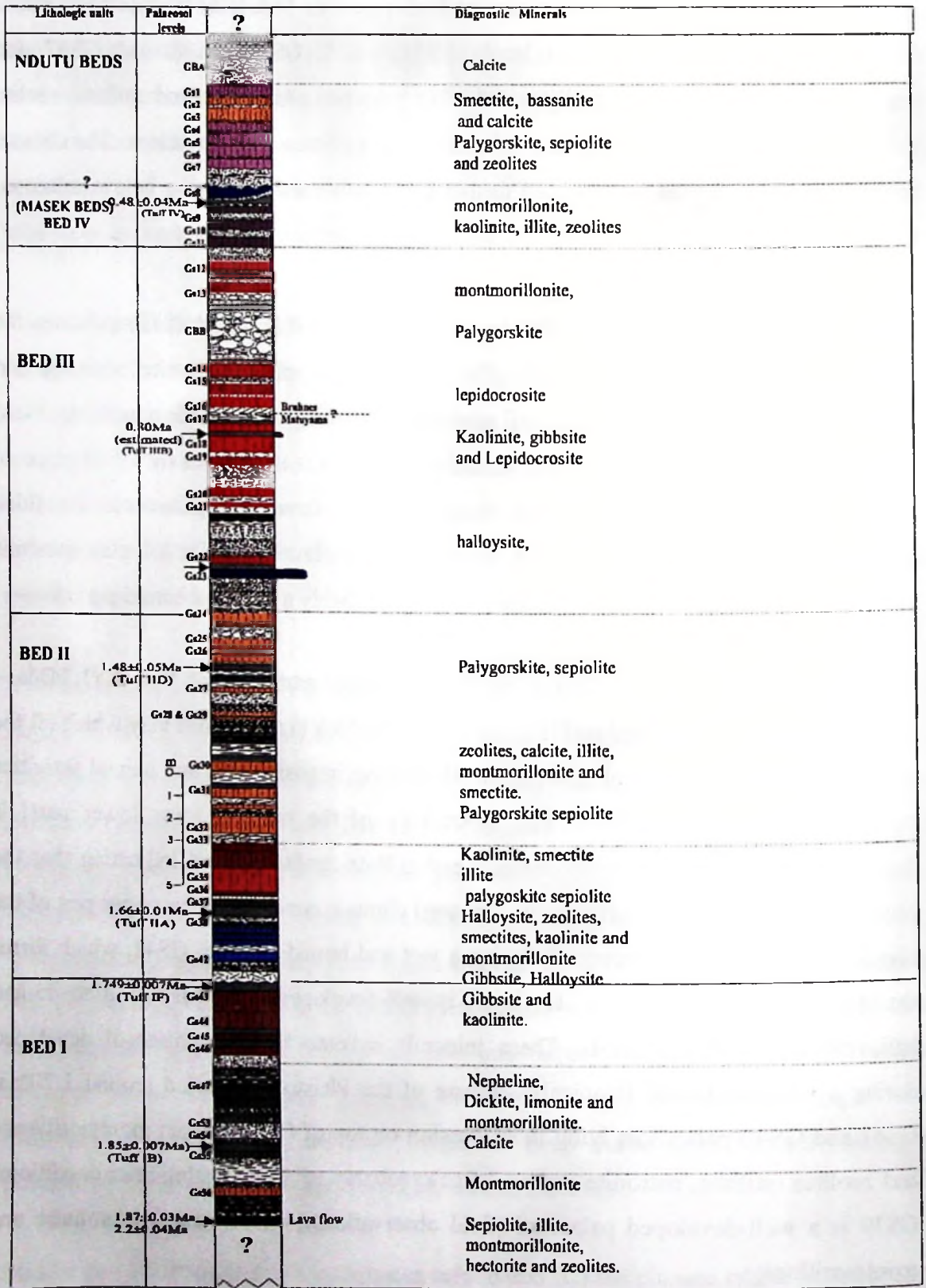

Figure 7.1b: Olduvai Gorge detailed stratigraphy with some approximate minerological sequence.

The presence of kaolinite in this (GS39) palaeosol level probably point to a slightly wet climate compared to the previous two-palaeosol levels (GS40 and GS39). GS38, which ends lower Bed II, is again dominated by sepiolite and smectite (natronite) clay minerals together with zeolilte (heulandite) mineral which are evidence of dry climatic conditions.

Middle Bed II (1.66Ma – 1.62Ma) contain two climatic episodes, the lower and the upper parts. The lower part is a very dry period indicated by the appearance of palygorskite and sepiolite in palaeosols GS37 and GS36. The upper part is slightly wet indicated by red palaeosol, GS35, GS34, GS33, GS32 and GS31. The mineralogy of GS35, GS34, GS33 and GS32 show both kaolinite (halloysite) and smectites (notronite) and illite clay minerals, while GS31 which concludes middle Bed II is a more sandy palaeosol containing zeolite (stilbite), sepiolite and smectite (montmorillonite). GS31 might have been formed in a slightly dry climatic period compared to the former palaeosols.

Upper Bed II is a sand zone (field observations) with the lower part (1.62Ma – 1.50Ma) showing minerals like sepiolite-palygorskite clay minerals, zeolites (analcime, clinoptilolite, heulandite and stilbite) with some smectites and illites pointing to drier (arid to semi arid) climates. GS31, GS30, GS29 and GS28 palaeosol levels represent this zone. The inetrval 1.50Ma – 1.15Ma of upper Bed II is represented by palaeosol levels GS27 to GS23 in which, palygorskite and sepiolite are detected probably attesting dry weathering environments.

Bed III begins at about 1.15Ma mark recognised by its distinct red colour (field observations). The zone though looks like one massive thick red palaeosol pedocomplex, it is in fact a zoned sequence of wet and dry climates. Kaolinite (halloyste) mineral is present in GS22 and GS21 palaeosols levels a sign of wet environments, while in GS20 and GS 19 palaeosols palygorskite is detected suggesting drier conditions.

Again palaeosol GS18 shows a mixture of kaolinite (halloysite) and palygorskite minerals with lepidocrosite probably indicating a seasonal wet-dry alternating conditions.

Gibbsite, limonite and kaolinite occur in GS17, GS16 and GS15 palaeosols probably a sign of wet and humid conditions. The upper part of Bed III (GS14, GS13 and GS12) shows a mixture of kaolinite (halloysite), smectite (montmorillonite) and illite clay minerals together with zeolites (analcime, chabazite, mordenite, and stilbite) and gypsic mineral like bassanite. This range of minerals probably indicates annual alternating dry and wet seasonal climatic and environmental conditions. These seasonal fluctuations of the climate is left as an inprint of a mixture of both dry and wet characteristic clay and other minerals in palaeosols.

Bed IV/Masek Beds begins around 0.6Ma and extends to about 0.4Ma, where Ndutu beds are believed to have started to be deposited. Masek/Bed IV contain a series of well-developed palaeosols of arid to semi-arid climates alternating with palaeosols of much wetter climates. In GS11 level montmorillonite and analcime minerals are present suggesting drier environments. GS10 palaeosol represent a wet to dry climate indicated by kaolinite (halloysite), zeolite (stilbite) and illite minerals. GS9 and GS8 palaeosol levels are dominated by zeolites (analcime, mordenite, aporphyllite and stilbite,) and smectite (beidelite and natronite) clay minerals which indicate drier conditions than previously (GS10). GS7, GS6, GS5, GS4, GS3 GS2 and GS1 palaeosols are strongly developed palaeosols representing Ndutu Beds. These palaeosols are dominated by palygorskite-sepiolite clay mineral group and zeolites (stilbite and shortite) evidence of semi arid climatic and environmental conditions. Note: - Radiometric dates presented in the above discussion are from Curtis and Hay (1972), Hay (1976), Drake and Curtis (1978), Walter *et. al* (1991), Manega (1993), and Kafumu (1995).

7.1.5. Stereo and scanning electron microscopic examinations

7.1.5.1 Results

Sand dunes, which can be seen across the Serengeti Plain and Agata Salei north of Olbalbal in the vicinity of the Olduvai Gorge, are identified as volcanic sands (Guest 1960). Most of the dunes have spread over the plains, but there are still several dunes of

approximately 10m high and 60m width (figure 7.2a) which continue to spread westward across the plains.

The composition of these sand dunes is largely unknown. A mineralogical study was performed using SEM and stereomicroscope to attempt to describe the basic mineralogy of these sands. The results are presented in figures 7.2b and 7.2c. Sieve grain size analysis reveals that these sands have size fraction of between 62μm and 1mm (sand fraction). Stereo microscopic, (figure 7.2a) and scanning electron microscopic examination, (figure $7.2c_{1-5}$) indicate that the sand are composed of mainly pyroxene minerals [augite = 85%, fassaite and ophacite = 10% and other minerals (5%) include quartz, garnet and feldspar].

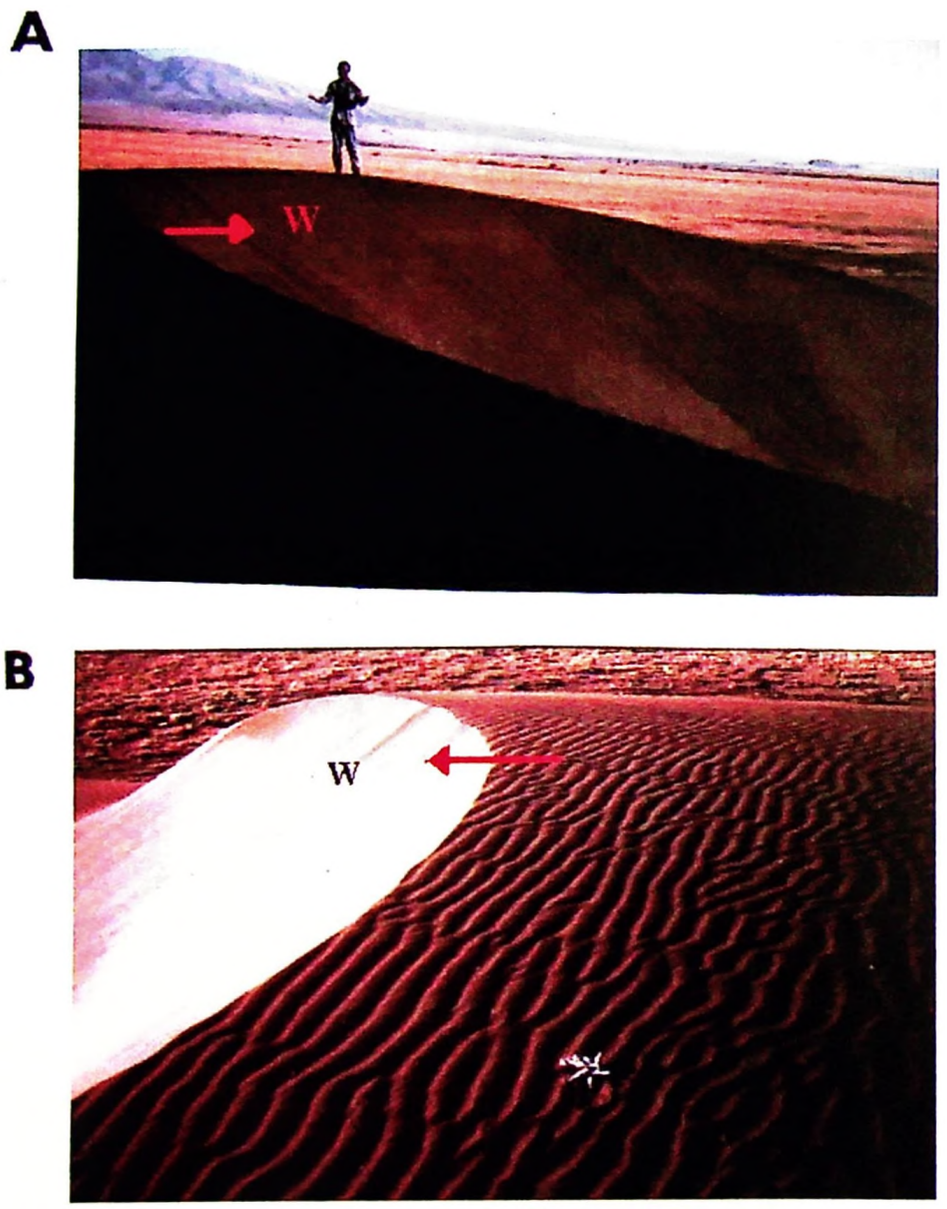

Figure 7.2a: OLDUVAI GORGE SHIFTING SANDS

A: Dunes (10m high and 60m wide) of black volcanic sands spreading across the Serengeti Plains. In the background Ngorongoro Highlands can be seen. **B:** Sand ripples created by wind that blows towards the west (steep face of the dune).

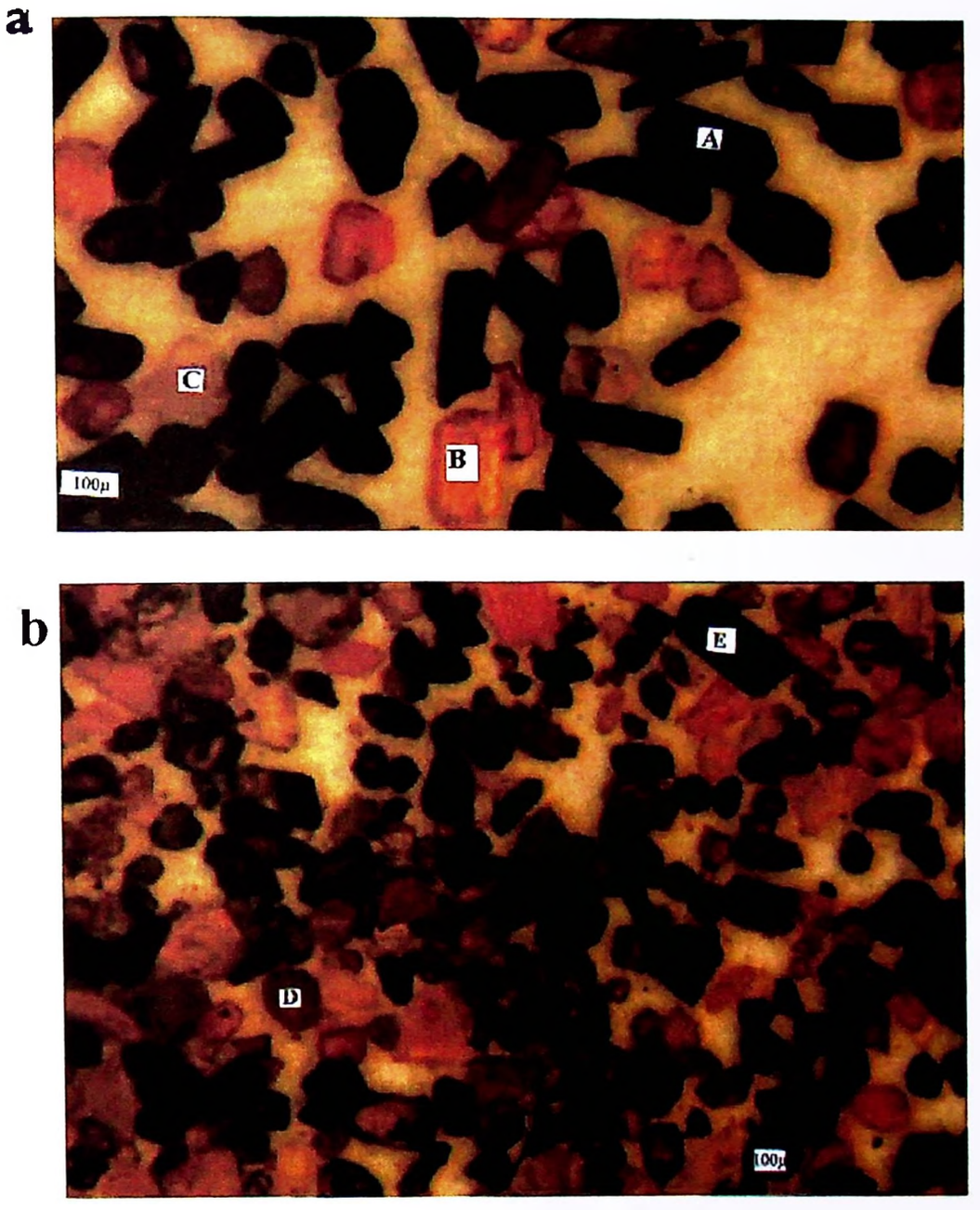

Figure 7.2b: MINERALOGICAL COMPOSITION OF THE OLDUVAI GORGE SHIFTING SANDS (Stereo-microscopic analyses).

a: [A=Augite, B=Omphacite, C=Quartz], **b:** [D=Garnet, E=Titano-augite)

Figure 7.2c: Scanning electronic microscopic analytical results; (1-4)

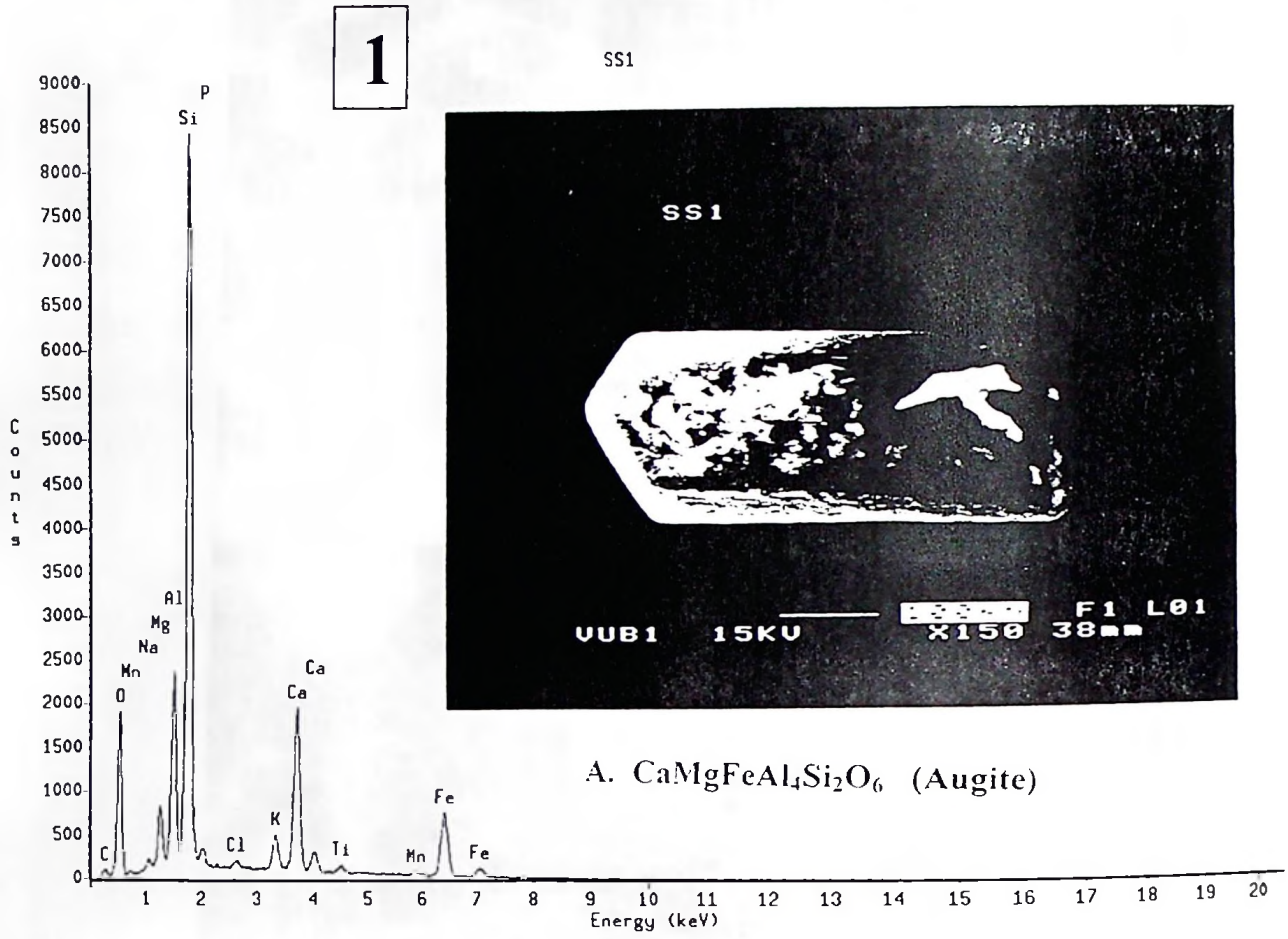

A. $CaMgFeAl_4Si_2O_6$ (Augite)

PROZA Correction Acc.Volt.= 20 kV Take-off Angle=40.00 deg
Number of Iterations = 6

Element	k-ratio (calc.)	ZAF	Atom %	Element Wt %	Wt % Err. (1-Sigma)	No. of Cations
O -K	0.0908	4.020	55.25	36.49	+/- 0.34	---
Na-K	0.0029	2.753	0.85	0.80	+/- 0.09	0.367
Mg-K	0.0139	1.930	2.68	2.69	+/- 0.05	1.166
Al-K	0.0307	1.625	4.48	4.99	+/- 0.11	1.947
Br-L	0.0411	1.533	1.91	6.31	+/- 0.43	0.830
Si-K	0.1709	1.561	23.00	26.67	+/- 0.16	9.991
P -K	0.0047	1.836	0.67	0.86	+/- 0.04	0.291
Cl-K	0.0023	1.407	0.22	0.32	+/- 0.03	0.096
K -K	0.0136	1.204	1.01	1.64	+/- 0.03	0.440
Ca-K	0.0779	1.148	5.40	8.94	+/- 0.07	2.347
Ti-K	0.0051	1.222	0.32	0.62	+/- 0.07	0.137
Mn-K	0.0038	1.208	0.20	0.46	+/- 0.06	0.087
Fe-K	0.0782	1.178	4.00	9.21	+/- 0.18	1.736
Total			100.00	100.00		19.436

The number of cation results are based upon 24 Oxygen atoms

1. ANALYSIS OF AN AUGITE MINERAL GRAIN

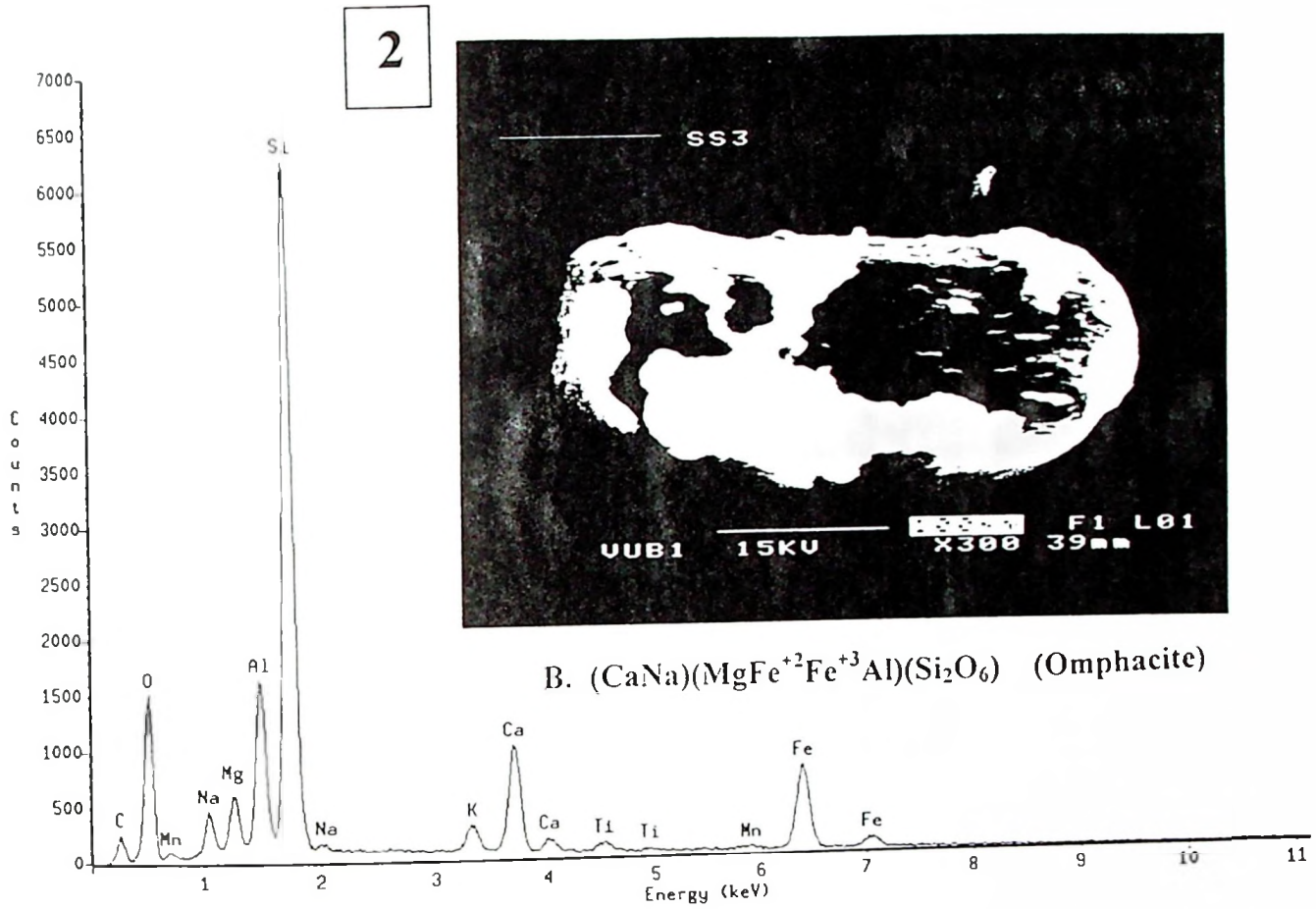

PROZA Correction Acc.Volt.= 20 kV Take-off Angle=40.00 deg
Number of Iterations = 5

Element	k-ratio (calc.)	ZAF	Atom %	Element Wt %	Wt % Err. (1-Sigma)	No. of Cations
O -K	0.1011	3.548	52.89	35.86	+/- 0.41	---
Na-K	0.0130	2.877	3.83	3.73	+/- 0.14	1.739
Mg-K	0.0139	2.096	2.83	2.92	+/- 0.08	1.284
Al-K	0.0416	1.736	6.32	7.22	+/- 0.16	2.867
Si-K	0.1779	1.540	23.02	27.40	+/- 0.17	10.448
K -K	0.0132	1.199	0.96	1.59	+/- 0.08	0.435
Ca-K	0.0580	1.143	3.90	6.63	+/- 0.07	1.770
Ti-K	0.0074	1.210	0.44	0.90	+/- 0.09	0.201
Mn-K	0.0035	1.213	0.18	0.43	+/- 0.07	0.084
Fe-K	0.1124	1.185	5.63	13.32	+/- 0.25	2.554
Total			100.00	100.00		21.381

The number of cation results are based upon 24 Oxygen atoms

2. ANALYSIS OF AN OMPHACITE MINERAL GRAIN

3

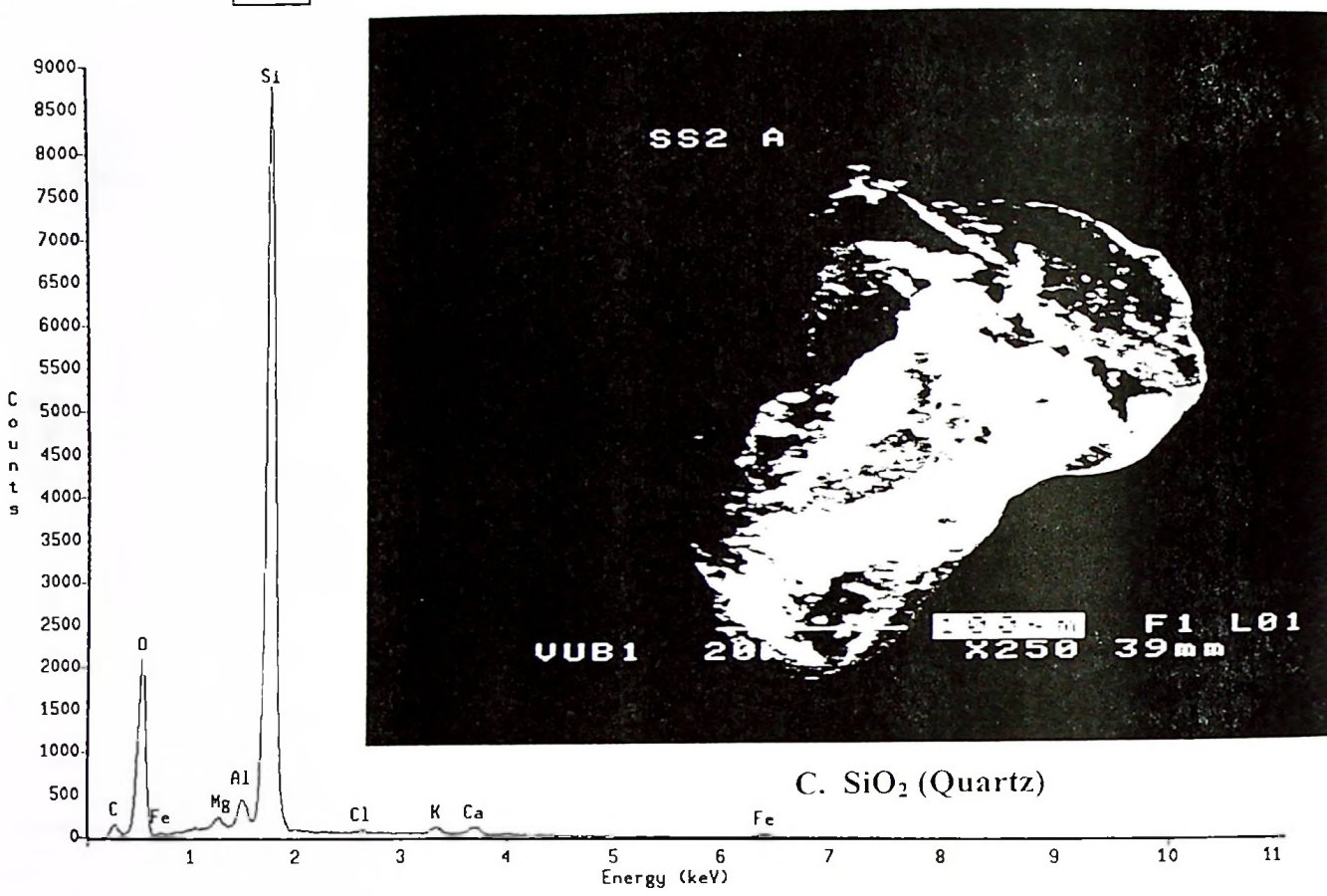

C. SiO_2 (Quartz)

PROZA Correction Acc.Volt.= 20 kV Take-off Angle=40.00 deg
Number of Iterations = 8

Element	k-ratio (calc.)	ZAF	Atom %	Element Wt %	Wt % Err. (1-Sigma)	No. of Cations
O -K	0.1890	2.862	67.74	54.10	+/- 0.51	---
Mg-K	0.0039	1.796	0.58	0.70	+/- 0.10	0.205
Si-K	0.3164	1.308	29.50	41.37	+/- 0.19	10.454
Cl-K	0.0013	1.469	0.11	0.20	+/- 0.03	0.039
K -K	0.0046	1.269	0.30	0.58	+/- 0.04	0.106
Ca-K	0.0060	1.196	0.36	0.72	+/- 0.04	0.127
Fe-K	0.0068	1.224	0.30	0.83	+/- 0.13	0.105
Al-K	0.0101	1.494	1.12	1.51	+/- 0.06	0.397
Total			100.00	100.00		11.432

The number of cation results are based upon 24 Oxygen atoms

3. ANALYSIS OF A QUARTZ MINERAL GRAIN

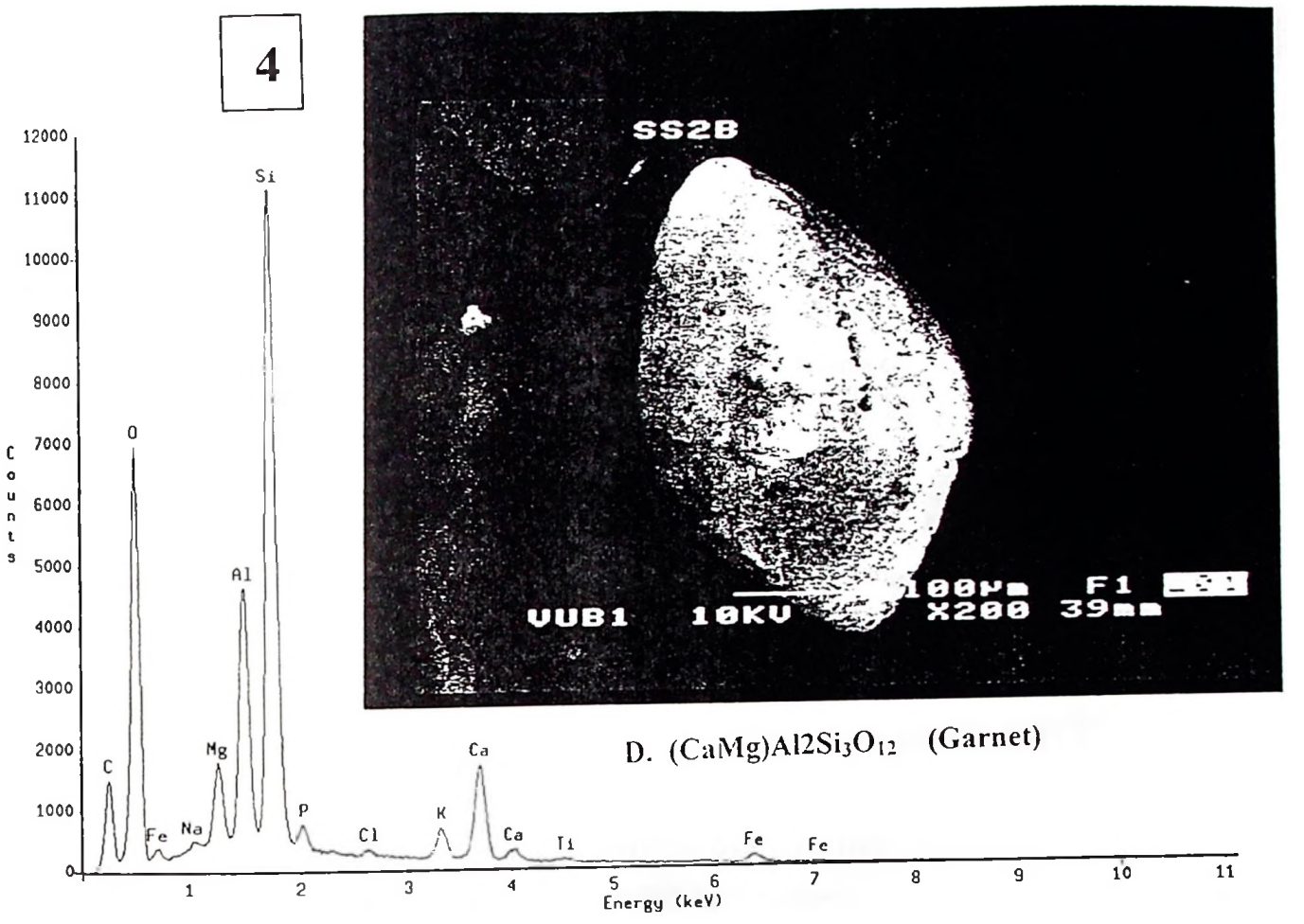

D. $(CaMg)Al2Si_3O_{12}$ (Garnet)

PROZA Correction Acc.Volt.= 20 kV Take-off Angle=40.00 deg
Number of Iterations = 10

Element	k-ratio (calc.)	ZAF	Atom %	Element Wt %	Wt % Err. (1-Sigma)	No. of Cations
O -K	0.2054	2.874	72.40	59.04	+/- 0.39	---
Na-K	0.0021	2.764	0.50	0.58	+/- 0.10	0.165
Mg-K	0.0174	1.933	2.71	3.36	+/- 0.09	0.899
Al-K	0.0512	1.657	6.17	8.49	+/- 0.11	2.046
Si-K	0.1330	1.528	14.20	20.33	+/- 0.12	4.707
P -K	0.0047	1.719	0.51	0.81	+/- 0.07	0.170
Cl-K	0.0018	1.379	0.13	0.24	+/- 0.04	0.045
K -K	0.0108	1.218	0.66	1.31	+/- 0.05	0.218
Ca-K	0.0396	1.169	2.27	4.63	+/- 0.07	0.751
Ti-K	0.0021	1.253	0.11	0.27	+/- 0.04	0.036
Fe-K	0.0076	1.225	0.33	0.94	+/- 0.07	0.109
Total			100.00	100.00		9.147

The number of cation results are based upon 24 Oxygen atoms

4. ANALYSIS OF A GARNET MINERAL GRAIN

7.1.5.2. Implication with regard to the genesis and origin of the shifting sand dunes

The sand dunes, which are distributed in an area of about 100km^2 comprise active (shifting) and inactive (fixed by grass and shrubs) dunes. Scanning electron microscopic examination indicates that the mineral grains posses elaborate crystal forms with subrounded edges. The later is a result of a long time rolling effect of the sands. The spatial distribution of the sand dunes show that their coverage widens as one moves to the east. The coverage is maximum far-east (closer to the Oldoinyo Lengai volcanic cone).

Magma melts from Oldoinyo Lengai contains a silica differentiation of clinopyroxene-garnet-nepheline assemblages (Church *et al.*, 1995) closely resembling the Olduvai Gorge shifting sand dune composition. Dawson, *et al.*, (1995) also reported magmatic plutonic rocks of clinopyroxene (dominant), titanite, garnet, tinandite and wallastonite composition in Oldoinyo Lengai volcanic rocks. Again the dominance of clinopyroxenes in the composition of the magma seems to fit well with the composition of the Olduvai Gorge sand dunes. It is then suggested that these sands originated from Oldoinyo Lengai volcanic eruption at the beginning of the Holocene. The start of the eruption was probably much more violent than today when these sands were forced out of the vent and thrown at a considerable distance from the volcanic cone.

The coarse grained (62μm - 1mm) sized nature of the sands compared to 2μm – 10μm sized grain aggregates of clinopyroxenes and garnet crystals in the Oldoinyo Lengai magma as was determined by Church *et al.*, (1995) is assumed to be related to the magma rest time before eruption. It is likely that earlier eruptions allowed the magma a considerable time to settle before eruptions, as a result crystals grew much larger. In the eruptions, which followed later the magma mix did not have enough time for the pyroxene-garnet crystals to grow. The younger magma flows of Oldoinyo Lengai contain fine-grained crystals and xenoliths and are cabornatitic in composition. The sand dunes belong to the nephelinitic tuffs and agglomerates that are on the foot slopes of the Oldoinyo Lengai volcano, (Dawson *et al.*, 1989).

7.1.6. Provisional conclusions

Clay, carbonate and zeolite initial mineralogical assemblages of Olduvai Gorge stratigraphy present a complex climatic and environmental evolution during the Pleistocene that need further detailed studies.

However, it can initially be concluded that:

1. During drier climates of the Pleistocene and the Holocene Epochs in Olduvai Gorge more zeolites might have been formed than clay minerals and probably more clay minerals were formed than zeolites during wetter periods.

2. Weathering of $CaCO_3$ rich lacustrine sediments produced palygorskite (attapugite) and sepiolite clay minerals during arid and semi arid (dry) climates. In mild wet climates and environments smectites (montmorillonite and beidellite) clay minerals might have been formed, while during wet/humid climatic conditions kaolinite (kaolinite, halloysite and dickite) were formed. Red palaeosols composed of hydroxides (lepidocrosites, limonites and gibbsite) also indicating wet climatic conditions.

3. Tuff flow/fall ash deposits, which are mainly composed, of nepheline and pyroxene silicate minerals were sometimes affected by pedogenesis during stable landscape episodes. Nepheline and pyroxenes minerals may have been transformed into zeolites during dry periods or into clay minerals during wet periods.

4. The variation of concentrations of clay minerals and carbonate infered from short wave infrared reflectance intensity roughly approximates the earlier recognised (figure 7.1a) broader Bed I to Ndutu beds.

5. Mineralogy sheds some light to the palaeosol taxonomy of Olduvai Gorge deposits. It is suggested here that the presence gypsic minerals (bassanite and gypsum), palygoskite-sepiolite and smectites minerals attest to plaeo-aridisol. These type of palaeosols (aridisol) are observed in upper Bed II and some parts of Bed I. The presence of smectite,

beidellite, calcite and gypsum seems to be associated with vertisol palaeosols of Bed IV/Masek beds. Kaolinite, lepidocrosite, gibbsite and limonite points to red-brown alfisols mainly observed in Bed III and Bed II.

6. Based on mineral comparison between the sand dunes and magma flows from Oldoinyo Lengai, the Olduvai Gorge sand dunes seems to have originated from Oldoinyo Lengai volcanism.

7.2. GEOCHEMICAL ANALYSES

7.2.5. Methods of investigation

A total of 10 representative palaeosol samples were analysed for major elements. Each sample represented a specific palaeosol sequence (a group of palaeosols) selected according to their field diagnostic characteristics and stratigraphical positions, (table 7.4).

Table 7.4: Brief descriptions and stratigraphical positions of representative palaeosol levels of Olduvai Gorge section.

Sample	Palaeosol level	Stratigraphical position & depth (m)	Descriptions	Diagnostic Mineralogy
MC19	GS3	Ndutu and Masek Beds – 3.7m	Grayish brown (10YR5/2), fine columnar structures with slickensides, gilgai relief macro structure.	Kaolinite, smectite, analcime and nepheline
MC17	GS5	Ndutu and Masek Beds – 5.75m	Light olive gray (5Y6/2). Presence of black coating and mottling, slickenside present.	Kaolinite, smectite (natronite), beidellite and aporphyllite
RB20	GS18	Bed III – 13m	Red (2.5YR4/6), large root casts filled with red sediments, red mottling.	Lepidocrosite, limonite, brucite and halloysite
RS31	GS27	Bed II – 23.5m	Olive (5Y5/4), clay sands palaeosol developed on sandstone.	Hankasite, analcime, azurite, smectite (natronite), bassanite, notrolite and beidellite.
RS19	GS30	Bed II – 26.3m	Olive (5Y5/4), massive clay	Stilbite, sepiolite, illite, smectite

				(natronite), and dolomite.
LK6A	GS35	Bed II – 31.05m	Red (2.5YR4/6), presence of brown mottling.	Lepidocrosite, halloysite and illite
RS11	GS39	Bed II – 34.05m	Olive (5Y5/2), clay with carbonate concretions.	Montmorillonite, malachite and stilbite
2Z	GS44	Bed I – 37.9m	Grayish brown (2.5Y5/2), distratified clay showing soil peds.	Montmorillonite, gibbsite, halloysite and stilbite
Z9	GS52	Bed I – 42m	Light gray (5Y7/1), clay sand with carbonate concretions and plant remains.	Montmorillonite, smectite, illite, stilbite and malachite.
ZI	GS56	Bed I – 44.9m	Olive (5Y6/3), Distratified clay with calcite root infillings.	Montmorillonite, hectorite, alevarndite (illite), natronite and modernite.

7.2.6. Analytical procedures

AAS (Atomic Absorption Spectrometer) method was employed to analyze some 10 palaesol levels of Olduvai Gorge beds for major elements. Samples were dried, crushed and powdered. The samples were then dissolved by digesting the samples according to the standard dissolution methods, (Potts, 1987 and Jenga, 1998,).

10ml of 65%HNO_3 was added to each sample and placed in CEM MD5-2000 microwave oven for 15 minutes and then washed by milli-Q water. About 0.2g of powdered sample was placed in a Teflon beaker and 4ml HNO_3 +HF added. The mixture was placed in an oven for one hour and thereafter left to cool for about 2 hours. About 50ml of 4% boric acid was added and heated in an oven for 15 minutes and then left to cool for 30 minutes. The cool solution was ready for measurement by an AAS instrument. The principle of the AAS method is given in appendix 7.2.

7.2.7. Results and discussions

7.2.3.1. Major elements analytical results

Table 7.5: Major elements AAS analyses of some palaeosol levels of Olduvai Gorge Beds

Composition (% by weight)	Palaeosol levels									
	GS3 (MC19)	GS5 (MC17)	GS18 (RB20)	GS27 (RS31)	GS30 (RS19)	GS39 (RS11)	GS35 (LK16A)	GS44 (2Z)	GS52 (Z9)	GS56 (ZI)
SiO_2	50.49	50.37	47.49	48.61	53.86	57.39	50.22	54.96	57.2	40.74
Al_2O_3	15.43	14.85	16.79	10.07	9.75	9.41	15.47	7.65	12.85	7.69
Fe_2O_3 (total)	8.62	8.25	**13.34**	11.02	7.91	8.4	9.31	6.3	7.71	4.97
MnO	0.18	0.17	**0.22**	0.15	0.08	0.07	0.07	0.13	0.12	0.11
MgO	2.56	2.45	**1.8**	5.9	6.27	7.64	2.96	14.61	5.91	8.82
CaO	4.11	4.9	3.59	7.08	1.89	0.65	0.39	1.9	1.88	15.1
Na_2O	3.83	4.23	6.77	4.88	7.17	6.2	9.21	4.45	5.94	3.83
K2O	4.7	4.37	3.9	2.8	2.35	1.34	2.17	1.71	1.96	2.15
TiO_2	1.68	1.7	**1.96**	1.61	1.83	1.78	1.45	1.38	1.01	0.94
P_2O_5	0.27	0.27	0.41	0.4	0.45	0.17	0.18	0.27	0.19	0.29
LOI	7.53	7.94	7.27	6.18	7.22	6.67	7.59	6.86	5.35	15.33
Total	99.41	99.49	99.54	99.69	98.79	99.71	99.02	100.2	100.1	99.96
Mole ratios**										
$\frac{SiO_2}{Al_2O_3}$	5.56	5.72	4.81	8.18	9.38	10.43	5.53	12.27	7.54	9.07
$\frac{SiO_2}{Fe_2O_3}$	15.85	16.27	13.62	11.74	18.37	18.46	14.48	23.59	19.8	21.94
$\frac{Al_2O_3}{Fe_2O_3}$	2.85	2.84	2.82	1.43	1.96	1.77	2.62	1.92	2.63	2.42

*Calculation procedure of derived mole ratios***

Molecular weights:
Si = 28g (28.086g), O = 16g (15.999g), Al = 27g (26.98g), Fe = 56g (55.846g)
Mole weights
1 mole of SiO_2 $\Longrightarrow$ 28 + 2(16) = 60g
1 mole of Fe_2O_3 $\Longrightarrow$ (2x56)+(3x16) = 160g
Mole ratio (example calculation)
Sample MC19 (GS3) results
SiO_2 = 50.49% (50.49g), Al_2O_3 = 15.43% (15.43g) and Fe_2O_3 = 8.62% (8.62g)
60g = 1 mole
50.49g = ? moles
$\frac{1x50.49}{60.0}$ = 0.8415moles of SiO_2, $\frac{1x15.43}{102}$ = 0.1512 moles of Al_2O_3

$\frac{1x8.62}{160}$ = 0.0538 moles of Fe_2O_3

Then $\frac{SiO_2}{Al2O_3} = \frac{0.8415}{0.1512} = 5.56$, $\frac{SiO_2}{Fe2O_3} = \frac{0.8415}{0.0538} = 15.64$, $\frac{Al_2O_3}{Fe_2O_3} = \frac{0.1512}{0.0538} = 2.81$

7.2.3.2. Discussions

Derived mole ratios of some modern tropical soils (table 7.6) forms the basis of the proceeding interpretation of the geochemical major element analyses of some palaeosol levels of Olduvai Gorge.

Table 7.6: Mole ratios (total soil analysis) of some tropical modern soils, (after; Mohr *et al.*, 1972)

Soil type	Mole ratios		
	a	b	c
Vertisols	3.7 – 5.9	11 - 30	1.4 – 6
Aridisols			
Andosols(Andisols)	1 - 4	5 - 8	1.8 – 2 (2.8 – 4.7)
Ultisols/Alfisols	2.9 - 7	3.9 – 7.8	11 - 36
a = $\frac{SiO_2}{Al_2O_3}$, b = $\frac{SiO_2}{Fe_2O_3}$, c = $\frac{Al_2O_3}{Fe2O_3}$			

The palaeosols of the upper part of the Olduvai Gorge section Bed IV and Masek beds resemble vertisols based on their derived silica/sesquioxide mole ratios. These palaesosl series are represented by GS3 with a = 5.56, b = 15.85 & c = 2.85 and GS5 with a = 5.72, b = 16.27 & c = 2.84. These values are well within the ratio range of the present day vertisols.

Vertisols are known to form on former sedimentary lowlands and denudation plains of past (as old as Pleistocene times), (Van Ranst, 1997b). Towards the end of the Middle Pleistocene and during the Upper Pleistocene (Bed IV/Masek beds times) the Olduvai Gorge climate might have became drier, lake-levels subsided and rivers became intermittent (ephemeral). Under this climatic conditions of alternating dry and wet spells

vertisols could form in alluvial deposits of former lakes and flood plains of Lower to Upper Pleistocene times.

Bed III red palaeosol geochemical signature as represented by GS18 (a = 4.81, b = 13.62 and c = 2.8) has the lowest silica-alumina ratio in the profile. The red palaeosols also contain the highest Fe_2O_3 (13.34%), MnO (0.22%) & Ti_2O (1.96%) contents and lowest MgO (1.8%) contents. These data closely compare to present-day alfisols/ultisols geochemical signatures (table 7.6). Alfisols are known to form in wet tropical regions. The data set (presence of palaeo-alfisols) therefore infers a generally wet climate during Middle Pleistocene period. Another short period is inferred in middle Bed II by GS 35 with a = 5.53, b = 14.48 and c = 2.62.

Bed II that forms the upper part of the Lower Pleistocene is dominated by palaeosols developed on sands and represented by GS27, GS30 and GS39. These palaeosols show low alumina/Fe-oxides mole ratios of 1.34, 1.96 and 1.77 respectively and are provisionally regarded as aridsols due to their typical aridisol geochemical signatures. Aridisols in Olduvai Gorge developed on residual sands. Research (Mohr *et al.,* 1972) has also shown that most present day aridisols date into the Pleistocene and have persisted through one or more glacial and interglacial periods.

Aridisols are most common on stable land surfaces of Upper Pleistocene or greater age, which suggest their diagnostic horizons require a considerable time to form. Their relic soil characteristics and geochemical and mineralogical imprints can still be recognised.

Aridisols in Bed II of Olduvai Gorge once again point to the dominance of intermittent (ephemeral) streams and braided river and sheet flood depositional regimes over lake regimes. It seems logical that eolian processes played an important role in the formation of parent sand layers.

GS44, GS52 and GS 56 in Bed I represent the lower part of the Lower Pleistocene. GS44 is probably an ultisol or alfisol based on its high silica/Fe-oxide ratio of 23.59. GS 52

represents palaeosols which, did develop on ash flow/fall tuff that can be classified as andosols (andisols) based on their parent materials.

7.3.MICROMORPHOLOGICAL STUDIES

7.3.1. Introduction

As said before palaeosols have been shown to be useful sources of palaeoenvironmental and climatic indicators in both Quaternary and Pre-Quaternary lithosequences. Although there is evidence of pedogenesis in Olduvai Gorge, (Hay 1976, Kafumu 1995) Manonga Wembere (Verniers 1997) and Holili localities (Kanza 1985) based on field studies, but laboratory (micromorphological) studies are missing.

Field observation and descriptions are often not sufficient for palaeosols recognition especially when palaeosols have undergone considerable diagenesis when buried under thick sediment. Palaeosols recognition becomes even more confusing if there exist diffuse boundaries and insignificant colour change among different lithological units (i.e. between palaeosols and other fluvial, lacustrine, or eolian sedments and rocks). Palaeosols also seem to preserve intricate records of succeding phases of pedogenesis, representing succession of cycles of soil development superimposed on top of one other. Such complex palaeosols fail to conform to the ideal A-B-C horizon model of soil profile formation as they contain evidence of polyphased evolution. This renders their field recognition even more difficult.

Under such circumstances micromorphology can provide means of ascertaining the presence or absence of a palaeosols. It also can provide genetic, temporal and spatial information on soil forming processes that are necessary to understand the past enviromental conditions. Although palaeosols can be recognised based on micromorphological features still their complex features makes palaeosol classification based on micromorphology difficult.

7.3.2 Sampling, methods and analytical procedures

60 undisturbed and some oriented samples were taken for microscopic examinations. The samples were collected as 1) hard and indurated blocks of soil and rocks, which were chipped off from the wall section and 2) samples from loose portions were collected in Kubiëna tins (7x5x4cm). 20 representative palaeosol levels were selected for micromorphologic examinations. The selection was based first on stratigraphical positions and secondly on stereo-microscopic surface examination of hand specimens (see appendix 7.6).

Marked samples from the field were air-dried and thereafter impregnated under vacuum using a polymer (resin). The samples were allowed to harden for six weeks. A small block was cut from the impregnated sample. The block was flattened on one side by a polishing machine. Then a glass was glued on the flattened surface by using a polymer and the glass was finally marked. The block was then cut into a thin section of about 1mm thickness (sample). The sample was then grinded and polished to until 30μm thickness. The appropriate thickness was determined by the interference color of quartz in XPL (yellow to gray in transmitted light). If the thin section was not uniform enough all over the surface a hand sandpaper polish was necessary. A very thin glass to protect the surface then covered the thin section. Thin sections were described at 10 – 400x magnification under a polarizing transmitted light microscope, using the terminology of Bullock *et al.*, (1985) and Stoops, (1998).

7.3.3 Results and discussions

7.3.3.1. Micromorphology – Analysis

This section presents basic micromorphological (description) features of the studied palaeosol thin sections. The descriptions and analyses will shed light on the occurrence and type of palaeosols in the study areas confirming field evidence already described in this study (see chapters 6 and 7). The typical micromorphological characteristics of some

palaeosol levels are presented in figures 7.3a, 7.4, 7.5, 7.6, 7.7, 7.8 and appendix 7.7. A summary according to stratigraphical position is give in table 7.7 and figure 7.9. Thereafter an attempt is made to present a palaeoenvironmental interpretation.

Table 7.7: Some diagnostic pedofeatures; A summary according to stratigraphical positions (Also refer micrographs – figures 7.3a&b to 7.8 and Stratigraphical section – figure 7.9).

Stratigraphical level	Micrographs of representative palaeosol levels	Some pedofeatures
Bed I and Lower Bed II	GS 56: Figure $7.3a_{1-4}$	1: common crystallitic to grano-striated b-fabric. 2: Common Fe-Mn hydroxide nodules. 3: Abundant pure calcite nodules. 4: Abundant micritic calcite nodules.
	GS54: Figure $7.3b_{5-8}$ (Zinjanthropus living floor)	5-6: Fe-Mn oxide nodules, fossil inprint?? 7-8: Animal activity imprints.
Middle Bed II	GS35: Figure 7.4_{1-4}	1: Abundant Fe-Mn hydroxide infillings. 2-4: Zeolite? mineralizations in pores.
	GS32: Figure 7.5_{1-4}	1: Common yellow clay coating in channels and then infilled by calcite. 2: Abundant Fe-Mn hydroxide coatings on pores. 3: Microfossils?? 4: Fossil (root cast?)
Upper Bed II	RS32: Figure 7.6_1	1: -
	GS31: Figure 7.6_2	2: Fossil. (Root cast?)
	GS22: Figure 7.6_{3-4}	3: Abundant yellow clay coatings. 4: Common Fe-Mn hydroxide hypo-coatings on a pore.
Bed III	GS21: Figure 7.7_{1-4}	1: Common juxtaposed yellow clay coatings and calcite infillings on channels. 2: Common calcite coatings on pores. 3: Abundant red clay coatings on pores. 4: Rare crystallitic to mono striated b-fabric.
Bed IV/Masek Beds & Ndutu Beds.	MC27 (Ndutu Beds): Figure 7.8_1	1: Juxtaposed yellow clay and calcite infillings in channels.
	GS3: Figure 7.8_{2-3}	2: Common Mono to granostriated b-fabric 3: Abundant calcite nodules
	GS6: Figure 7.8_4	4: Clay depletion hypo-coating and rare Fe-oxyhydrate nodules.

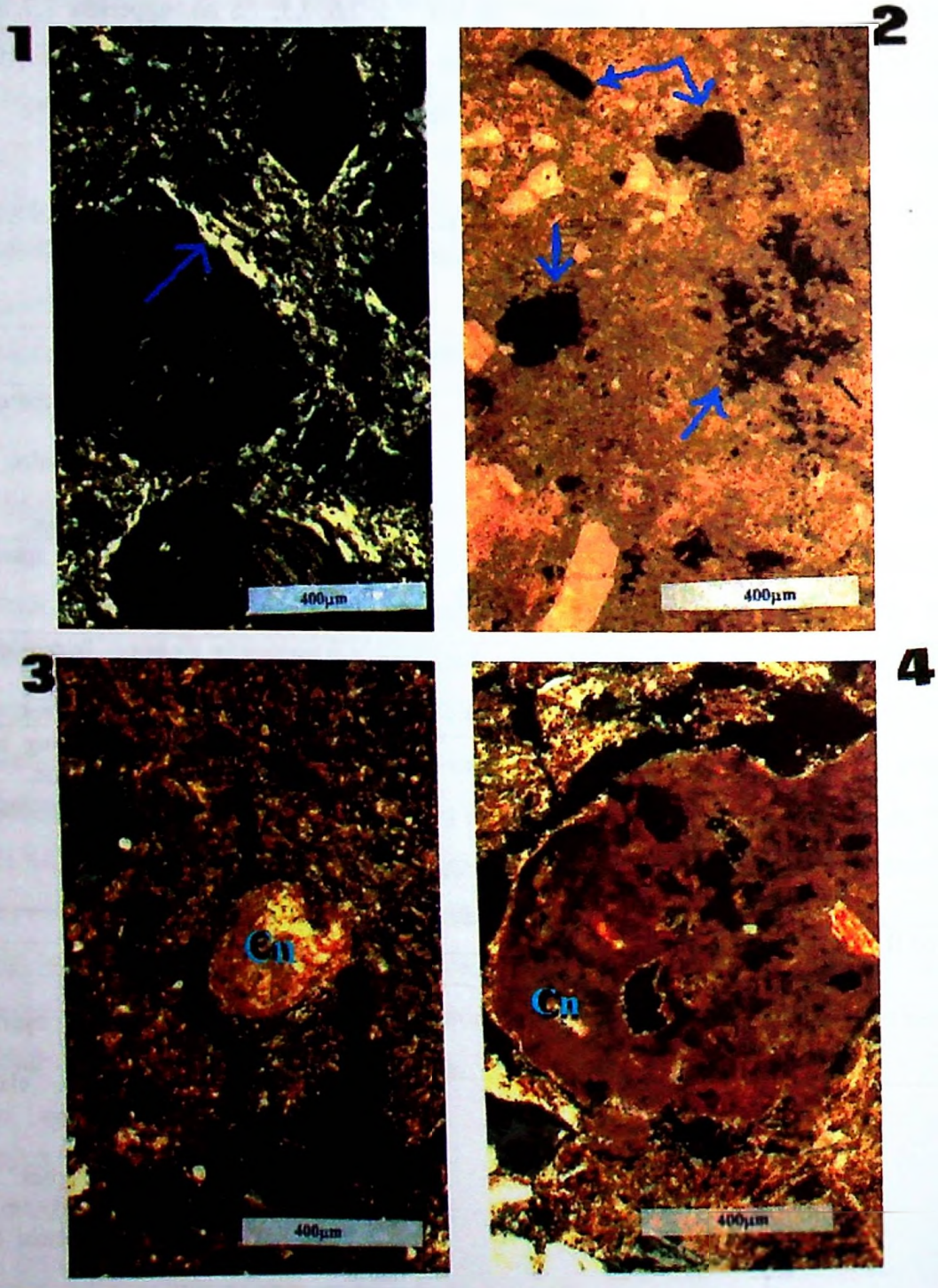

Figure 7.3a: Some micromorphological characteristics of gray to olive palaeosol levels of Bed I and Lower Bed II: GS56; **1.** Crystallitic and granostriated b-fabric (XPL). **2.** Orthic Fe-Mn hydr(o)xide nodules (PPL). **3.** A pure calcite nodule, note the crystallitic b-fabric nature of the groundmass (XPL). **4.** Micritic calcite nodule and granostriated b-fabric, (XPL).

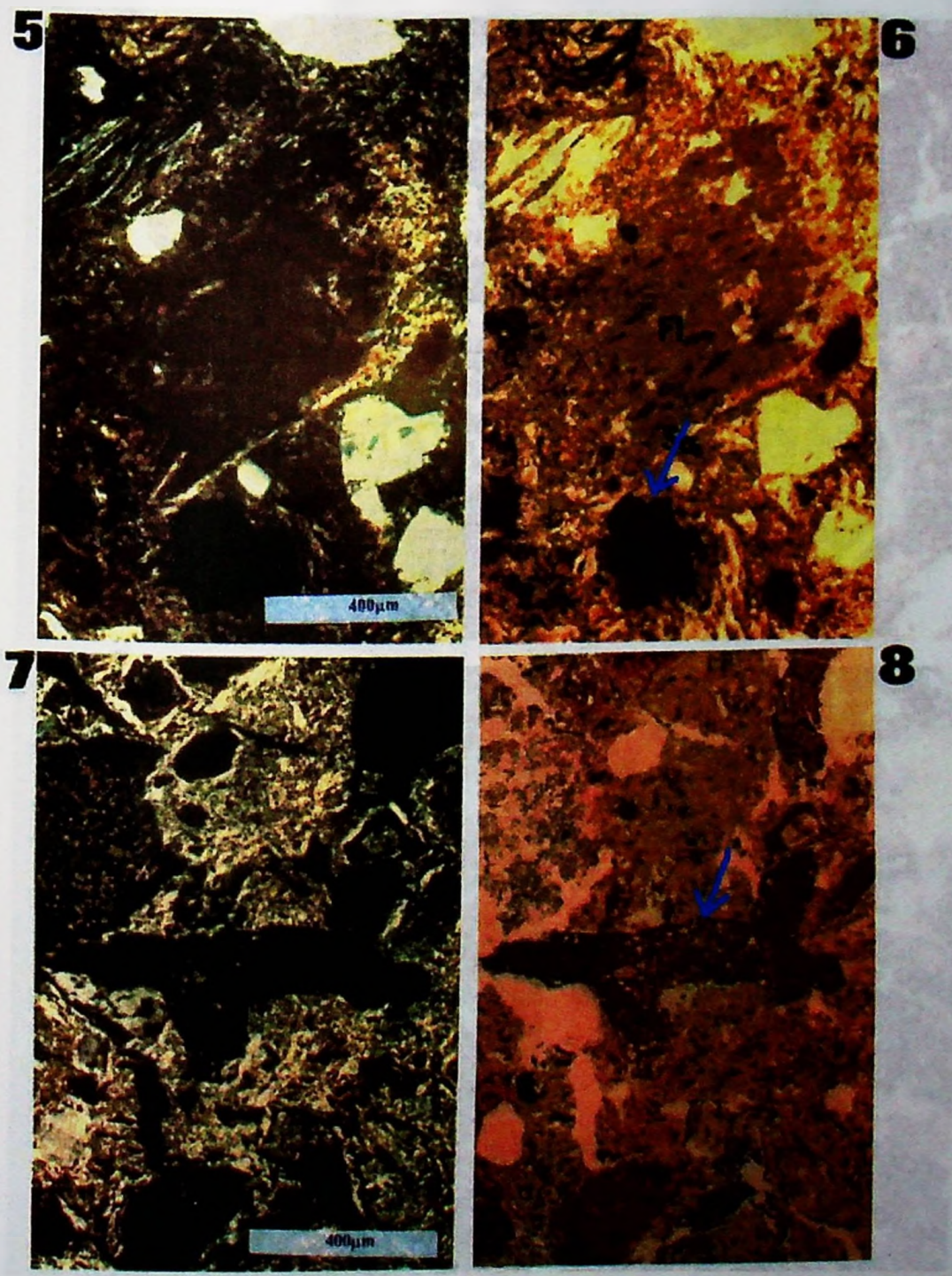

Figure 7.3b: Some micromorphological characteristics of GS54 (Zinjanthropus living floor) and GS53: **5** (XPL) and **6** (PPL); Mn-Fe nodules (So). GS53: **7** (XPL) and **8** (PPL); Animal borrows filled by dark material (opal silification?) note its inisotropism.

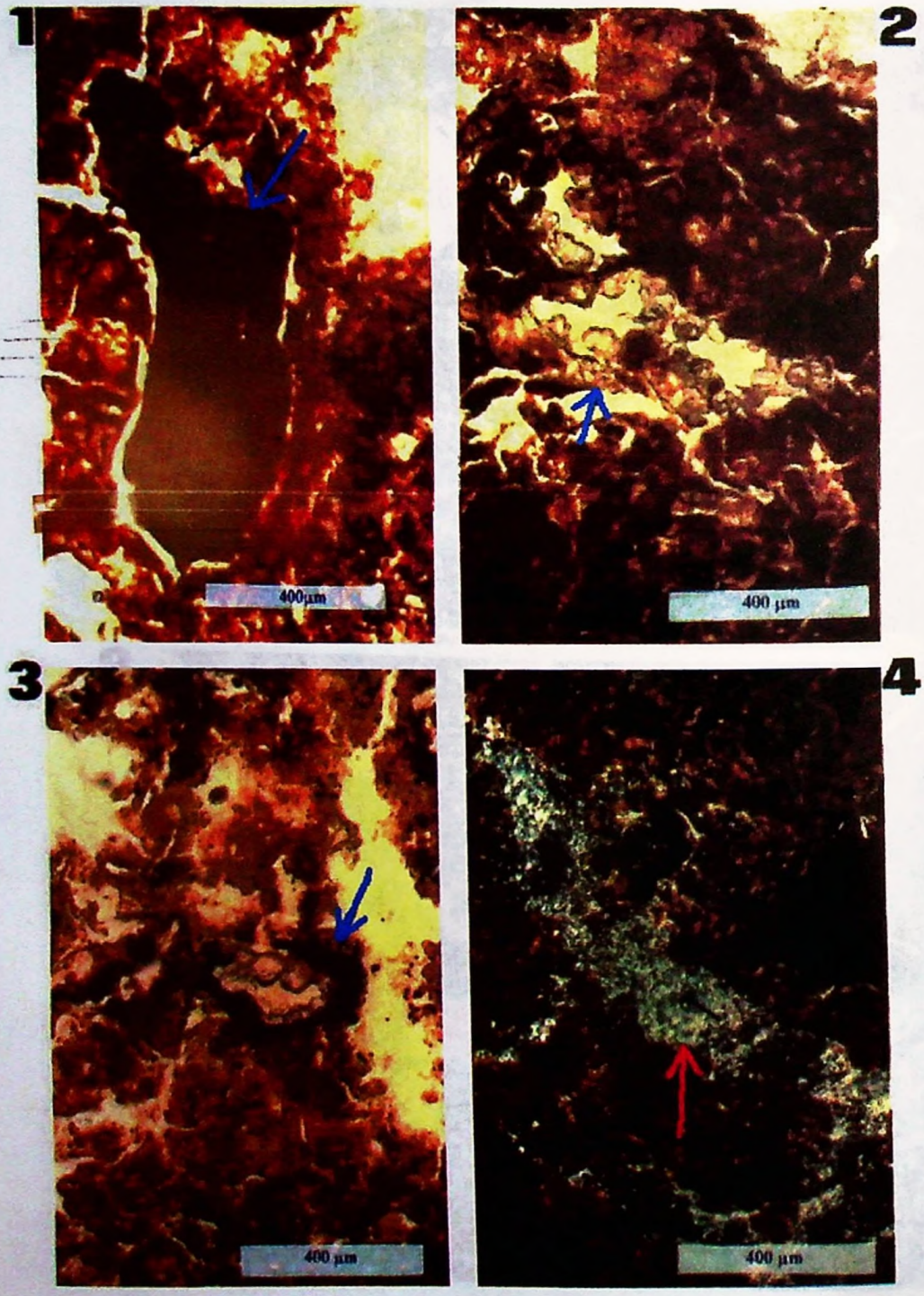

Figure 7.4: Some micromorphological characteristics of red to brown palaeosol levels of Middle Bed II. GS35; **1.** Dense continuous Fe-Mn hydr(o)xide channel infilling (PPL). **2.** Some coating or discontinuous infilling of equidimensional menerals (analcime?) in voids (PPL). **3.** Mn-Fe hydr(o)xide hypocoating on a pore with infilling of analcime? (PPL). **4.** Channel infillings of fine secondary minerals (zeolites?), note the high interference colours of the minerals and the speckled b-fabric of the groundmass (XPL).

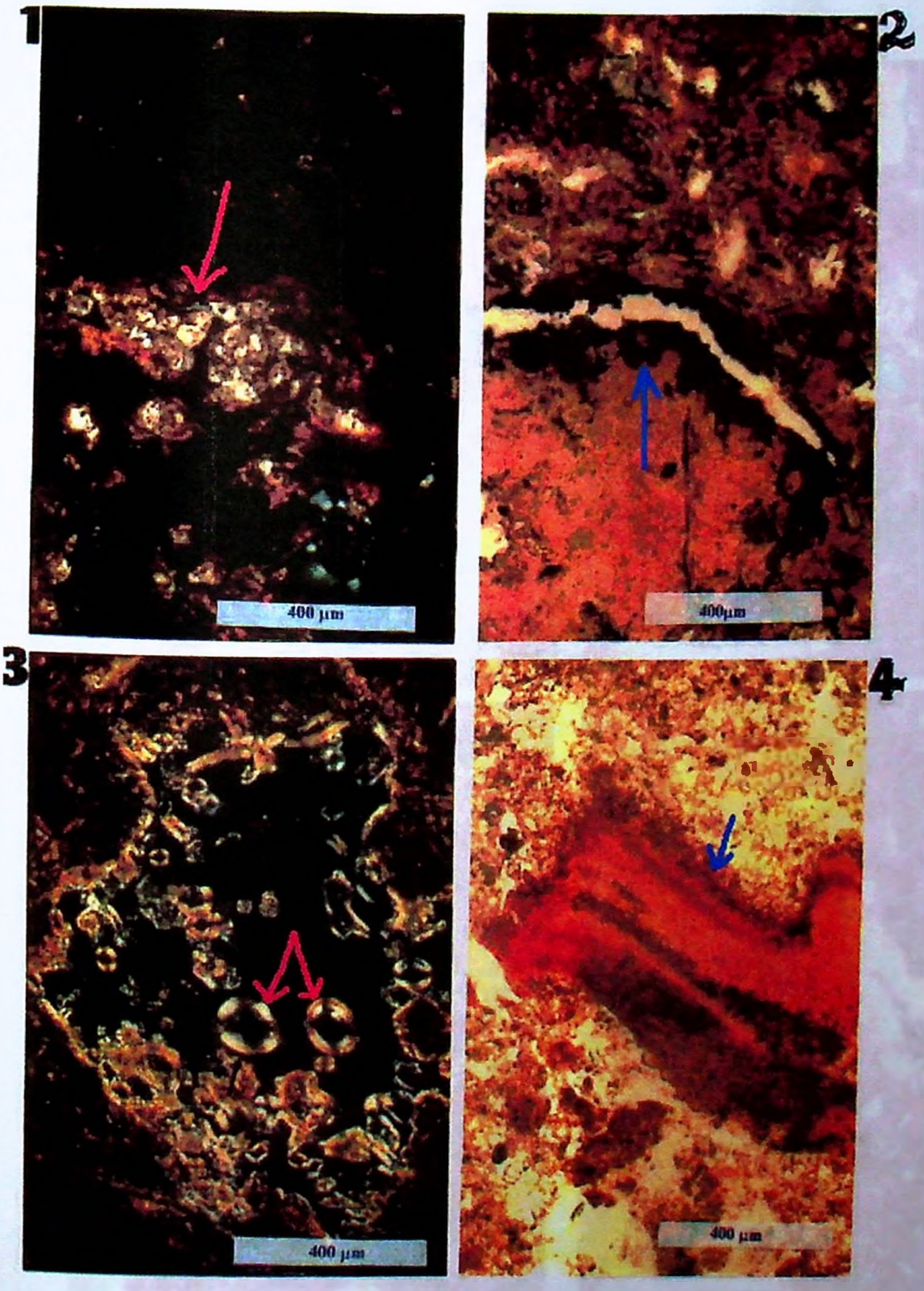

Figure 7.5: Some micromorphological characteristics of dark gray palaeosol levels of the Upper part of Middle Bed II: GS32; **1.** Yellowish red clay coating on a void and infillings of pure calcite (XPL). **2.** Mn-Fe oxide hypocoating on a channel (PPL). **3.** Microfossils? (XPL). **4.** Twigs/root? Cast infilled by partly laminated yellow clay (PPL).

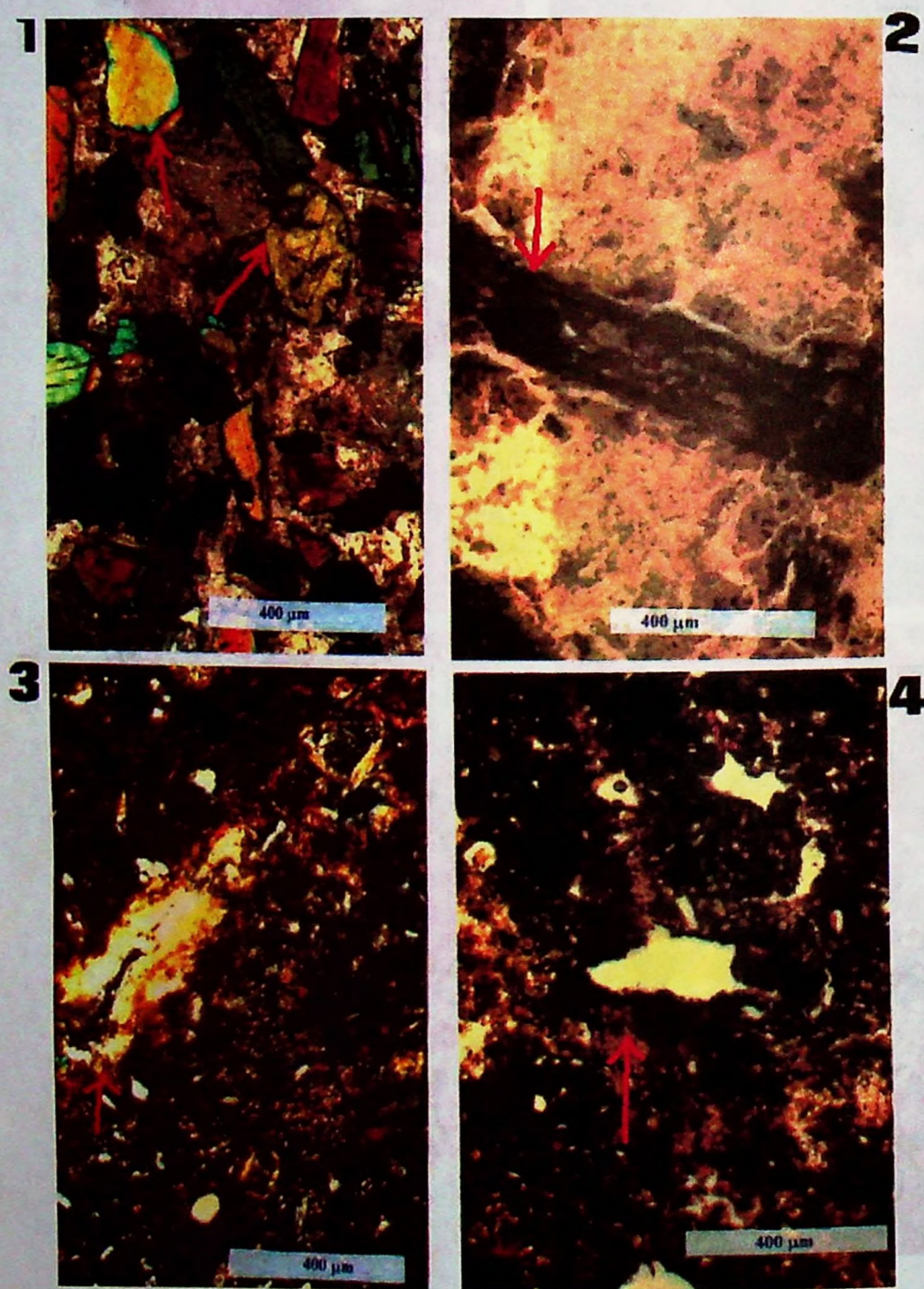

Figure 7.6: Some micromorphological characteristics of gray to olive palaeosol levels of Upper Bed II and Lower Bed III: **1.** (RS32); Mainly angular pyroxene grains cemented by calcite – calcareous sandstone (XPL). **2.** (GS31); A root/twig filled with amorphous dark material (PPL). **3.** GS22-Lower Bed III: Reddish yellow clay coating on a channel and red clay coating fragments seen in the groundmass (XPL). **4.** GS22-Lower Bed III; Mn-Fe hydr(o)xide hypocoating on a channel (PPL).

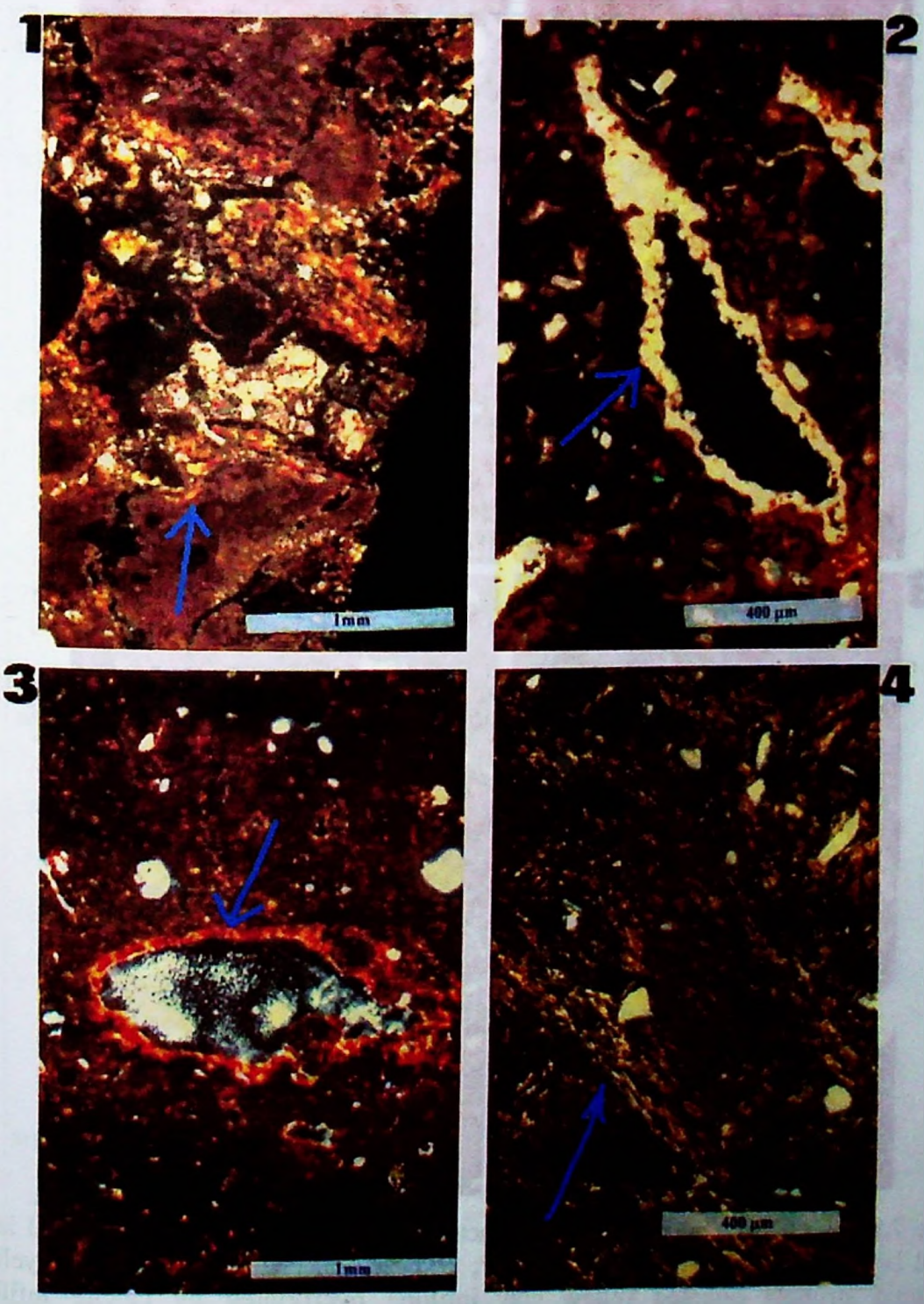

Figure 7.7: Some micromorphological characteristics of red to brown palaeosol levels of Bed III: GS21; **1.** Reddish yellow oriented clay coating in voids later infilled by calcite (XPL). **2.** Typic calcite channel coating (XPL). **3.** Typic yellowish red clay coating in a channel (XPL). **4.** Crystallitic to monostriated b-fabric (XPL).

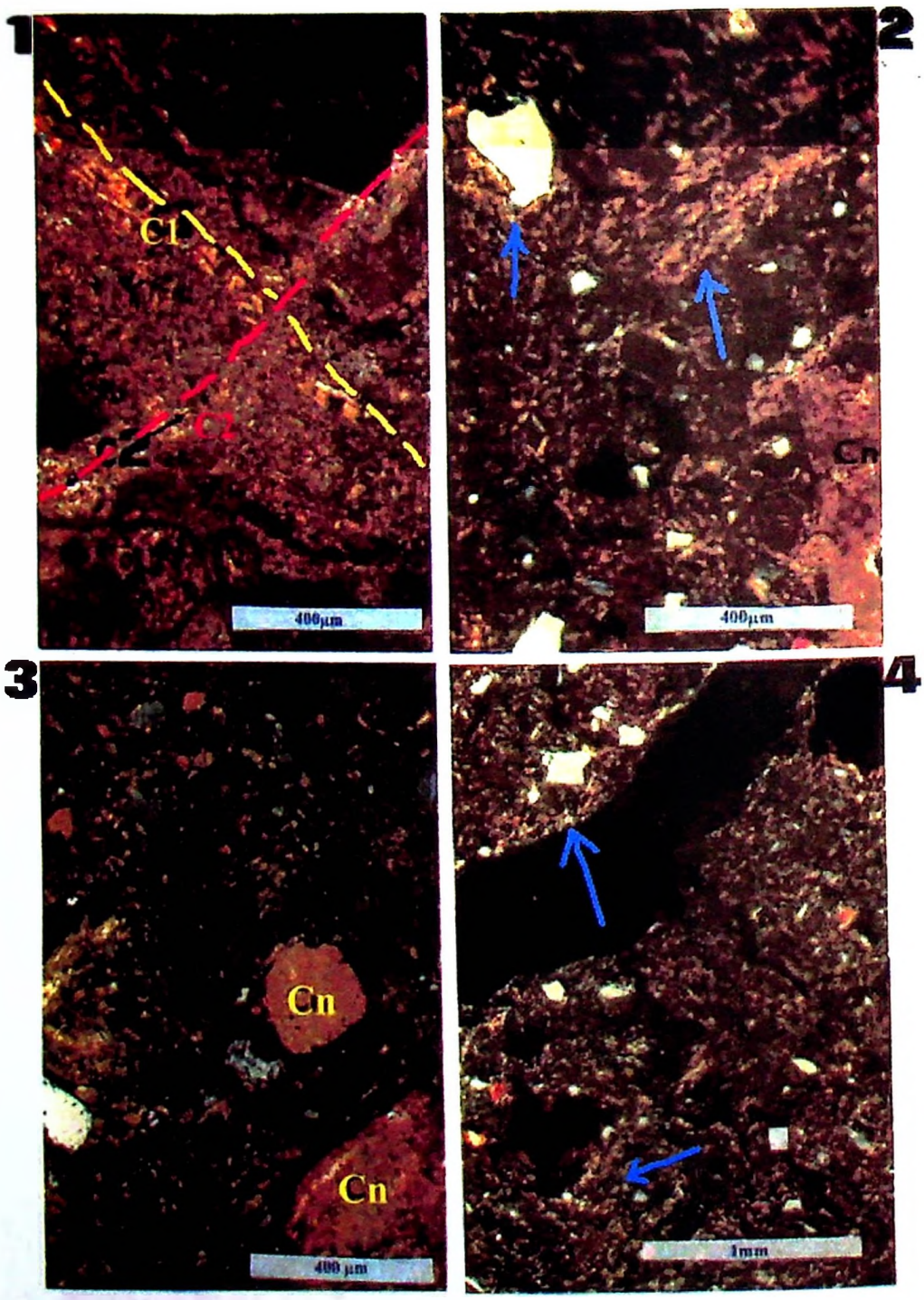

Figure 7.8: Some micromorphological characteristics of gray to olive palaeossol levels of Bed Iv/Masek and Ndutu Beds: **1.** MC27; Two sets of channels 1st set (C1-yellow) containing strongly oriented yellow clay infilling overprinted by calcite infilling, sometimes fragmenting the clay. 2rd set (C2-red) cross cut the older (C1) channel and is infilled by pure calcite (XPL). **2.** GS3; Monostriated and granostriated b-fabric. Note the micritic calcite nodule (Cn) at the lower corner of the section. **3.** GS3; Calcite nodules (Cn) in a weakely granostriated b-fabric groundmass (XPL). **4.** GS6; Weakly grano and monostriated b-fabric.

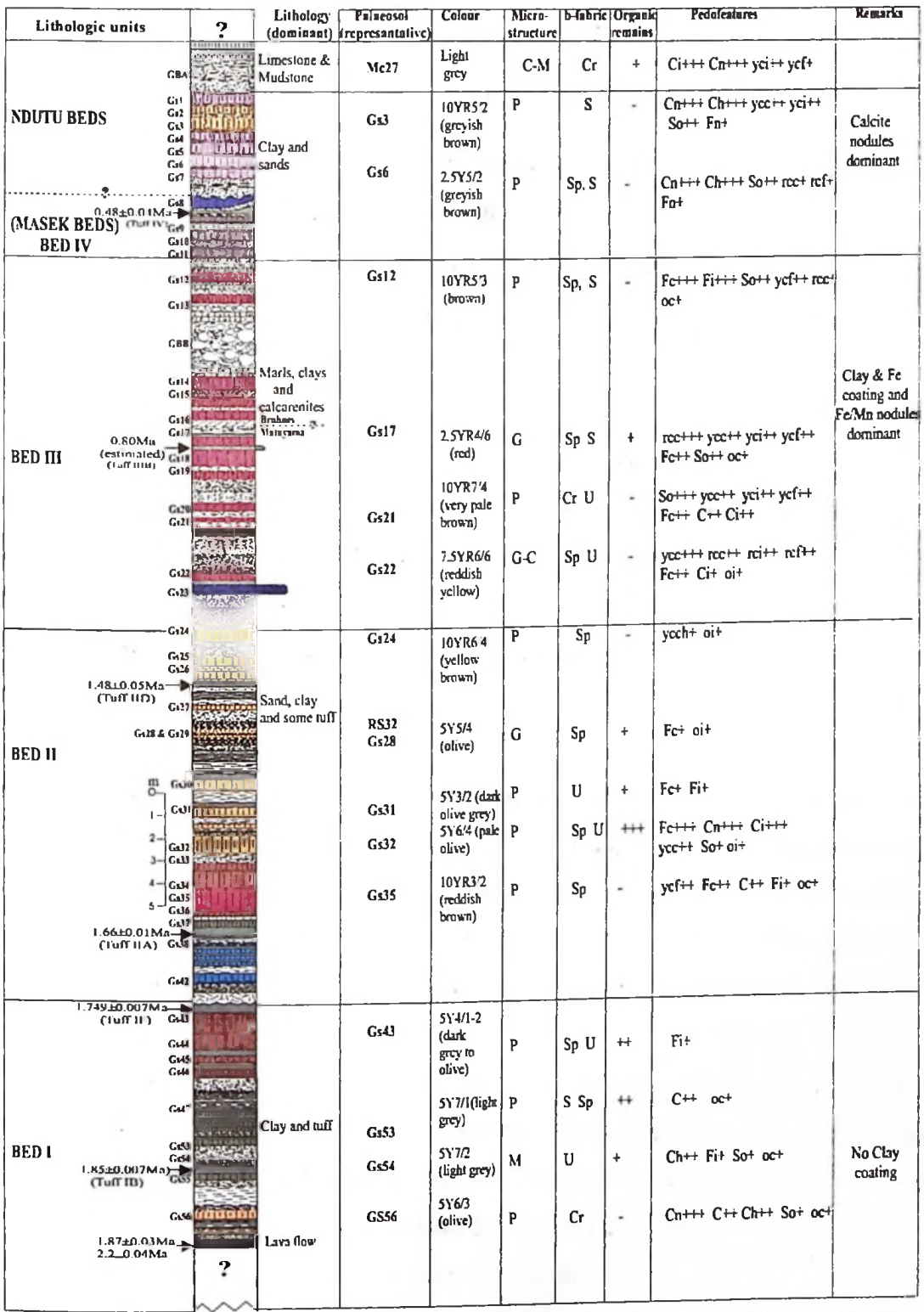

KEY COATINGS: rcc = red clay, ycc = yellow clay, rcf = red clay fragments, ycf = yellow caly fragments, rcch = red clay hypo-, ycch = yellow clay hypo-, C = calcite, Ch = calcite hypo-, oc = others, Fc = Fe-oxyhydrate: NODULES: Cn = calcite, Fn = Fe-oxyhydrate, So = Fe-Mn oxides. INFILLINGS: ycl = yellow clay, rcl = red clay, Cl = calcite, Fl = Fe oxyhydrate, oi = others. b-FABRIC: Cr = crystallitic, Sp = speckled, S = striated, U = undifferentiated. MICROSTRUCTURE: P = Peds, G = granular, M = massive, C = channel. QUANTITY: - = absent, + = rare, ++ = common, +++ = abundant

Figure 7.9: General micromorphological characteristics of some palaeosols of Olduvai Gorge deposits

7.3.3.2. Palaeoenvironmental interpretation and provisional palaeosol taxonomy of Olduvai Gorge deposits

As explained earlier that it is very difficult to classify palaeosols, because they preserve intricate records of succeeding phases of pedogenesis, representing succession of cycles of soil development superimposed on top of one other. Micromorphologic diagnostic features are difficult to disentangle for a successful classification.

Nevertheless, in recent years two approaches of palaeosol classification have emerged. First, recognition of more than one diagnostic pedogenic feature (Retallack, 1990 & 1993). The effect of burial diagenesis should be separated out and then the palaeosol may be compared to recent examples in order to interpret the ancient environmental conditions, (Retallack, 1994). In brief, this is an attempt to reconstruct the ancient soil formation features on the basis of existing taxonomies and using modern analogues as an aid in their interpretation, (Yaloon, 1995).

The second approach of palaeosol classification, which is being developed, is to separate palaeosol classification from recent or modern soil classification (Mack *et al.,* 1993 and Mack and James, 1994) and set new standards applicable to palaeosols only. In other words to develop a separate classification system for palaeosol only. Such a scheme is still being worked out by the Palaeopedology Commission (Yaloon, 1995).

In this study I therefore attempt to recognise diagnostic micromorphologic features (characteristics) and thereafter offer a palaeoenvironmental interpretation and tentative palaeosol taxonomy of the studied areas (Olduvai Gorge, Manonga-Wembere Valley and Holili localities). The interpretation is based on micromorphologic characteristics (section 7.3.3.1) as well as field observations, (chapter 6) and compared to recent soil types according to the USA Soil Taxonomy scheme.

Palaeoenvironmental interpretations

It is very difficult to make environmental interpretation by comparison with recent soil profiles, as individual palaeosols do not always posses any longer the complex A-B-C horizon sequences. In this case palaeoenvironmental interpretations will be inferred from soil processes which will be interpreted from micromorphological features (Kemp, *et al.*, 1994 and McCarthy *et al.*, 1998).

Clay coatings.

Clay coatings are mainly the result of clay illuviation, which requires water to percolate through the soil to dislocate and carry the clay. Dark red clay coatings are attributed to formation under warm humid freely drained conditions where iron and clay can move together (McCarthy, 1998). Pale yellow coatings indicate illuviation under more humid climate and possibly cooler soil conditions (Kemp, 1987 and Fedoroff, 1997). Alternating wet and dry conditions are a key factor in illuviation clay coating formation. Clay coating fragments are a result of colluvial transport or pedoturbations (mainly bioturbation), which disrupts the clay coating.

Fe-Mn oxyhydrate, Fe-Mn oxide nodules and Fe-depletion

Fe-depletion, Fe-Mn oxyhydrate and Fe-Mn oxide nodules indicate that the paleosol was at least periodically saturated by water. While Fe-Mn oxyhydrate hypo-coatings specifically indicate variations in Eh and pH conditions, ferrugeneous Fe-Mn oxide nodules indicate a wetting and drying regime (hydromorphic conditions) (Vepraskas *et al.*, 1994).

Calcite coating and nodules

Calcite coating and nodules are generally evidence of hot/arid palaeoclimates (Tandon and Gibling, 1994), they are interpreted to be formed in alternating wet and dry conditions of arid to semi arid regions.

Palaeoenvironments

This discussion is based on micromorphological results (section 7.3.3.1, figure 7.9 and appendix 7.2) coupled with field observations earlier presented in chapters 5 and 6. Field observation revealed red to brown palaeosols in middle Bed II and Bed III and gray to olive tuffaceous palaeosols dominant in Bed I and Lower Bed II. Others are olive clayey palaeosols of Bed I, Bed II and Bed IV and Olive-gray clayey to sandy palaeosols of Bed II and Masek Beds.

Bed I and Lower Bed II

Field observation revealed that pedogenesis in some clay and tuff levels in Bed I and Bed II is sometimes restricted to root activity and animal bioturbation with less illuviation evidence. Micromorphological study reveal rare or no clay coatings in such levels (figure 7.1a). Gray to olive palaeosol sequence GS38 to GS 42 of lower Bed II and GS43 to GS53 are clay/palaeosol or tuff/palaeosol alternation sequences. Pedofeatures of such soils are restricted to abundant calcite nodules and hypo-coatings. Other rare micromophological features are Fe-oxyhydrate infilings, Fe-Mn oxide nodules, which sometimes (at a macro scale) are observed as mottles. There are also rare coatings of opal and unidentified fibrous minerals in pores. A key diagnostic feature of these palaeosols is the absence of clay illuviation features (appendix 7.2).

The absence of clay coating or fragments and the presence of Fe-oxyhydrate and Fe-Mn oxide nodules may suggest a frequent wetting regime (possibly flooding), which was usually interrupted by a new phase of clay deposition forming thin layers of clay. Each clay layer is today observed to posses a thin palaeosol top zone. The zone is recognised in the field by root traces and animal bioturbation. Based on the field observations (thinly layered clays with mottling) and micromorphological characteristics the palaeosls were formed in a poorly drained environment, possibly marginal lake flood plain environments.

Flood plain hydrology in Quaternary deposits has also been indicated in some studies by the abundance and distribution of gray soil colors, organic matter, mottles, nodules and slickensides (Aslan and Autin, 1998).

Middle Bed II and Bed III

Pedogenetic illuviation seems to be more intense in red to brown palaeosols of middle Bed II (GS33 - GS36) and Bed III, (GS12 – GS22). In these palaeosol levels red to yellow clay coatings, infillings and fragments are common and sometimes abundant. Dark Fe-oxyhydrate and Fe-Mn nodules, coatings and infillings are also very common. Clay coatings are commonly seen associated with Fe-oxyhydrate typic and hypo-coatingss suggesting a highly varied hydrological condition. I think the red clay coatings were fragmented when illuviation took place together with biological activity or shrinking and swelling of the soil. These red or yellow clay-coating fragments were then incorporated in the groundmass. These multiple micromorphological characteristics suggest an alternating Eh-pH condition due to alternating wet and dry hydrological regime (Vepraskas, *et al.,* 1994 and McCarthy *et al.,* 1997b) during the Pleistocene.

Such an assemblage of red to brown palaeosols (Middle Bed II and Bed III) suggest development under relatively well drained hydrological regime, with periods of saturation alternating with long periods where sediments were close to saturation, (Ransom *et al.,* 1989). This indicates a period of increased landscape stability, which resulted in pedogenic illuviation forming more red sediments and palaeosols.

The multiple micromorphological features observed in red to brown palaeosols of Bed III and middle Bed II is linked to the climatic changes of the Quaternary. Red clay coating and fragments were formed under relatively warm and dry conditions,(McCarthy *et al.,* 1998), and pale yellow clay coating and fragments formation occurred under cooler and wetter conditions, (Fedoroff and Goldberg, 1982). Thus there was an intensive alternation of wet and dry periods during these times, which correspond to the upper Matuyama geomagnetic subcron. The type of climate changed to predominantly more dry in the Bruhnes epoch about 0.7Ma, (figure 7.1a).

Upper Bed II and Bed IV/Masek Beds and Ndutu Beds

Upper Bed II palaeosol levels are more sandy exihibiting a closed porphyric c/f related distribution. The lower part show more root activity observed as root fragments in GS 32 (figure 7.6) and dominance of calcite nodules with rare Fe-Mn hydroxide infillings and coatings in voids. The sandy palaeosols (GS31, GS28 and GS24) exhibit rare Fe-Mn hydroxide coatings, loose discontinuous infillings of fibrous (zeolite?) and some isotropic (opal?) mineral infillings in pores. Such a multiple micromorphological characterization may indicate a dry environment during soil forming processes. The sandstone layers of Bed II are composed of mainly angular pyroxene grains cemented by calcite (figure 7.6) indicating that the sandstone was formed in water rich environment.

Other gray to olive clayey palaeosols of Olduvai Gorge like GS30 to GS32 in Bed II and GS1 to GS7 in Masek/Bed IV and Ndutu Beds posses numerous calcite nodules and hypo-coatings with pale yellow clay coatings and rare ferrugenuous Fe-Mn nodules. From field observations these palaeosols also show abundant root activity. Decreasing amounts of clay coatings and increasing amounts of Fe-Mn nodules, (McCarthy 1998), can indicate poorly drained conditions. The palaeosol levels may also indicate poorly drained hydrological conditions. Field sedimentary features (fine clay layers, mud cracks etc.) indicate that the palaeosols are associated to fluvial flood plain environments. Mono-granostriated b-fabric is also a dominant micromorphological feature in Bed IV/Masek Beds palaeosol levels.

The limestone bed of Ndutu Beds is composed of mainly rounded carbonate pieces, angular feldspars and rare (1%) pyroxene grains cemented by calcite. There are also rare volcanic rock pieces and opaques. The allochtonuous limestone was probably deposited in a lake environment and then pedogenesis began creating a series of channels, clay and calcite coating superimposed on one another (figure 7.8_1) signifying an alternating wet and dry climate.

Provisional palaeosol taxonomy

USA system of modern soil classification

According to the American system of soil classification of modern soils eleven main soil groups are recognised (Miller and Donahue 1995, Dasch 1996, and US Department of Agriculture, 1996).

1. ANDISOLS AND INCEPTISOLS

Andisols (Andosols) and Inceptisols are weakely-developed soils showing some weathering of mineral grains. There is a significant accumulation of clay or carbonate, but not so much as to qualify as other soils.

Inceptisols are commonly found in mountain landscapes with steep slopes that are usually young and undeveloped. Andisols contain abundant volcanic ash remaining less affected by weathering.

2. ALFISOLS AND ULTISOLS

Alfisols are defined as soils with the presence of an argillic horizon (a subsurface zone of clay enrichment), orchric epipedon and moderate high levels of base saturation, (Bullock and Thompson, 1985). They contain substantial accumulations of clay in this subsurface horizon. Alfisols and Ultisols are distinguished on the basis of chemical tests that reflect soil fertility.

Alfisols are rich in nutrients cations like as K^+, Na^+, Mg^{2+} and Ca^{2+} and also contain commonly weathered feldspars. Alfisols are usually gray to brown soils occurring in humid-temperate climates as well as at high altitudes in tropical climates, (Mohr *et al.*, 1972).

Ultisols are soils with an argillic horizon which, have virtually no nutrients cations or easily weatherable minerals and devoid of calcite ($CaCO_3$). Ultisols soils are red to yellow soils found in warm temperate, humid tropical and subtropical temperate regions.

The micromorphological characteristics of palaeosol (Ultisols and Alfisols) include illuvial clay occuring as disrupted clay coatings (clay coating fragments). The clay coating fragments are yellow to red and sometimes with laminations, moderately oriented with a significant birefringence and abundant nodules mainly composed of Fe-Mn oxides and Fe-oxyhydrate coatings and infillings, (Bullock and Thompson, 1985 and Fedoroff and Eswaran, 1985). Several micromorphologic features in these soils are related to duration and season of water table (Bullock and Thompson, 1985).

3. OXISOLS (LATOSOLS)

Oxisols are deeply weathered clayey soils, which contain no nutrient cations nor easily weatherable minerals. 1:1 clay minerals (kaolinite), gibbsite and quartz are very common. These soils are very common in humid tropical regions reflecting semideciduous forest to savanna bush land vegetation. Oxisols can be as old as 2.0Ma, implying that Oxisol palaeosols are very common in Quaternary geological sections (Van Ranst 1997a). Oxisols are sometimes devoid of silicate clays with a SiO_2/Al_2O_3 ratio of less than 0.5% and high Fe-oxides, TiO_2 and MnO.

Micromorphological characteristics of Oxisols include abundance of silt sized sesquioxidic particles, no clay coatings, infillings or fragments, (Stoops and Buol, 1985). There are also no weatherable minerals of sand and silt size fraction. Undifferentiated, weakly developed speckled or weakly striated b-fabric, a porphyric c/f related distribution and very homogeneous material are diagnostic features, (Stoops and Buol, 1985). Inherited sesquioxidic features like lateritic fragments and well-developed granular microstructure are also among the diagnostic features (Stoops, 1989).

4. SPODOSOLS (PODZOLS)

Spodosols are infertile sandy soils without nutrient cations. They are rich in quartz and contain little clay. Spodosols frequently occur in lowlands of the tropics and are limited to extremely acid parent rocks and continually wet climates (Mohr *et al.*, 1972).

Micromorphological features of spodosols include coatings (Fe-oxyhydrate, coloids and amorphous-organic) which are isotropic. These amorphous materials upon drying form cracked coating of silt and clay size intragranular pelletes (Douglas and Mc Keague, 1985) exhibiting a chitonic c/f related distribution and a strongly developed granular microstructure. A placic (iron pan) layer caused by restricted Fe-illuviation is sometimes present.

5. VERTISOLS

Vertisols are thick clayey soils, which crack deeply in seasonally dry climates. Gilgai relief structures are common. These soils occur in seasonally dry-wet alternating climates in lowland plains, evidence of sub-humid to semi arid climates. These soils support grassland to woodland vegetation.

Micromorphological characteristics of Vertisols are briefly summarised below according to Nettleton and Sleeman (1985): 1. Because of argillipedoturbation (Buol *et al.*, 1980) which is caused by periodic swelling and cracking of the soil, clay appear stress oriented in the groundmass, with a predominantly porphyric c/f related distribution. 2. Clay coating on channels and clay coating fragments are very common in the groundmass. 3. Pseudomorphs of weatherable minerals can be seen. They appear as transformed minerals into a big mass of clay (kaolinite or verculite) but retaining the shape of the parent minerals (mica and feldspars). 4. Impregnative and calcite nodules accompanied by manganiferous nodules and coatings are common.

6. MOLLISOLS AND HISTOSOLS

Both Mollisols and Histosols are organic rich soils. Mollisol have a dark surface horizon with intimately admixed clay and organic matter (humus) with a distinctive structure of

pellets of organic clay produced by earthworm and the abundant fine roots of grasses. On the other hand Histosols are peat soils that form in bog and swamps. They contain larger pieces of organic remains. Micromorphologically Mollisols posses often a spongy fabric with a crumb-like microstructure due to soil fauna (earthworms, mites, etc.) activities producing numerous route-ways and excrements (Pauwluk and Bal, 1985). Histosols show much more floral remains in micromorphological examinations than Mollisols. Leaf and stem tissues can sometimes form part of the soil fabric, the matrix in most cases consiting of closely packed plant remains (Fox, 1985).

7. ARIDISOLS AND ENTISOLS

Aridisols are soils which form in desert and arid environments in dry climates. A long dry period and only short periods of wetness in the upper soil are the dominant soil forming processes of aridisols (Miller and Donahue 1995). These climates are too dry to leach the soil-calcite and other easily weatherable minerals. Presence of gypsic horizons is common. The diagnostic feature of aridsols is therefore the calcic and gypsic horizons reflecting accumulation and stability over a long period of time sometimes going back to Pleistocene and Tertiary geological times. Common characteristic minerals are 2:1 clay minerals (illite, montmorillonite and palygorskite) with zeolite minerals.

Entisols are weakly developed soils showing little alteration of the initial material. They may show presence of sedimentary bedding penetrated by roots. Entisols may also reflect drier climates (arid to semi arid) which lack intensive weathering environments to significantly alter the parent material. Due to less intensity of weathering, common minerals found in Entisols are 2:1 clay minerals (illites and montmorillonite) Aridisols and Entisols soils are usually covered by sparse (shrubs and grass) vegetation.

Diagnostic micromorphological features of Aridisols are the rarity or absence of clay coating and the dominance of calcite nodules and coatings (Allen, 1985). Other features are lenticular gypsum crystals and amorphous silica gels. In Entisols however, carbonate engulfed carbonate clay coating are sometimes present.

Proposed palaeosol taxonomy

Many authors have compared the types of palaeosols identified through reconstruction of genetic soil forming processes with modern analogues in order to obtain annual rainfall and temperature variations (Catt, 1991 and Tsatskin *et al.,* 1998). In this way they have tried to classify palaeosols. Here an attempt is made to propose palaeosol taxonomy based on micromorphological characteristics and field observation.

The gray to olive palaeosols of Bed I and Lower Bed II show a range of features, which include abundant calcite nodules, calcite coatings and calcite hypo-coatingss, secondary fibrous (zeolite) mineral infillings and coatings in some pores. There are also rare Fe-Mn hydr(o)xide nodules. Other micromorphological features are developed sub angular accommodating peds, crystallitic and sometimes-weakly mono or granostriated b-fabric and mainly an open porphyric c/f related distribution. Imprints of animal activity are also common (seen as borrows filled by isotropic (opal) material, (figures 7.3a and 7.3b). Based on the comparison to present soils these palaeosols are probably palaeo-Aridisols?/Vertisols?/Andisols?. In the field palaeo-Vertisols were identified by the presence of root traces, slickensides, mudcracks and carbonate concretions. Palaeosols that showed a dominance of carbonate concretions were provisionally named palaeo-Aridisols. And palaeosols developed on tuff volcanic layers were assumed to be palaeo-Andisols based on the fact that they developed on volcanic materials.

Red-brown-dark gray palaeosol levels of Upper Bed I, Middle Bed II and Bed III were recognised in the field by red mottling and root traces infilled by red materials and were tentatively termed as palaeo-Alfisols?. Micromorphological features sheds more light on their probable taxonomy. These palaeosols contain oriented red and yellow clay coatings and typic Fe-Mn hydr(o)xide coatings, nodules, infillings on channels and clay coating fragments (figures 7.4 and 7.7) suggesting wet soils probably palaeo-Alfisols.

Upper Bed II is a more sandy sequence of sediments and palaeosols. Dominance of calcite nodules with rare Fe-Mn hydr(o)xide coatings on channels and secondary

fibrous/prismatic (zeolite?) infillings in pores may also point to dry soils like palao-Aridisols. Masek/Bed IV and Ndutu Beds palaeosol levels show common monostriated to granostriated b-fabric (figures $7.8_{2,3,4}$) a sign of soil shearing stresses, mostly typical for Vertisols. There are also numerous calcite nodules, Fe-Mn hydr(o)xide nodules and less commonly pale yellow clay coatings. In the field these palaeosols show slickensides and imprints of gilgai relief macrostructure indicating that they are probably palaeo-Vertisols.

In Ndutu beds a thick (5m) dense limestone layer, which grades into mudstone towards the base was observed. Micromorphological features of this layer show some evidence of pedogenic channels (figure 7.8_1). Two sets of channels were observed, the first one (older) in-filled by oriented yellow clay then coated by calcite, which fragmented the earlier clay infillings. A new set of channels followed crosscutting the old and in-filled by pure calcite. This is limestone affected by some pedogenesis.

Global or local palaeoclimatic variability

Superimposed yellow and red clay coating reflects moisture variation in response to fluctuation in short term Milankovitch of about 20Ka (McCarthy 1995 and McCarthy et al, 1998). Also micromorphological features can be associated to local geomorphic factors and progressive pedogenesis (McCarthy, 1997a).

In this study micromorphologic variations point to specific local hydromorphic conditions and possibly indicate precipitation and temperature conditions, while the timing (cyclicities) of the palaeosol stratigraphicalal occurrence is more controlled by sedimentation regimes probably linked to the global Quaternary climatic variations. It is known today that fluvial system and lake level fluctuations respond to global climatic changes, (Blum 1994). In Olduvai Gorge the olive to gray clay layers of Olduvai Gorge deposits which often contain a thin top palaeosol layer are a result of marginal lake or fluvial flood plain developments caused by raising and falling of river and lake levels. Therefore, such fluctuations can be linked to increased or decreased precipitation most probably related to global causes. For example (figure 7.1a) the interval between 1.85Ma

and 1.66Ma (Middle Bed I to Lower Bed II) 20 palaeosol levels are recorded pointing to 10Ka cyclicity of the Milakovitch short term climatic cycle, if a constant sedimentation rate is assumed, (chapter 10).

It is important to note here that the red to brown palaeosols of Bed III and middle Bed II repesent a more stable landscape than the thinner olive to gray clay and palaeosols. In this stable landscape environment pedogenic processes had quite a long time to affect the sediments. In fact these palaeosols reveals multiple micromorphological features imprinted on top of one another. Such features point to alternating wet-dry climates probably of 10Ka or 20Ka Milankovitch cycle. Dating of such cycles using micromorphological cyclic features has not been attemped. This can be a subject of future research.

In the field the red-brown zones look like massive red palaeosols or soil sediments, which was referred to as palaeosol pedo-complexes. Other studies have also indicated that alternating wet and dry phases occurring in Pleistocene palaeosols of the tropical regions are attributed to global wet and dry periods, (Jungerius, 1976) as the Quaternary has been marked by numerous glacial-interglacial phases which resulted into rapid and extreme changes of the climate. Such local and global palaeoclimatic variability is further discussed in chapter 10 of this study.

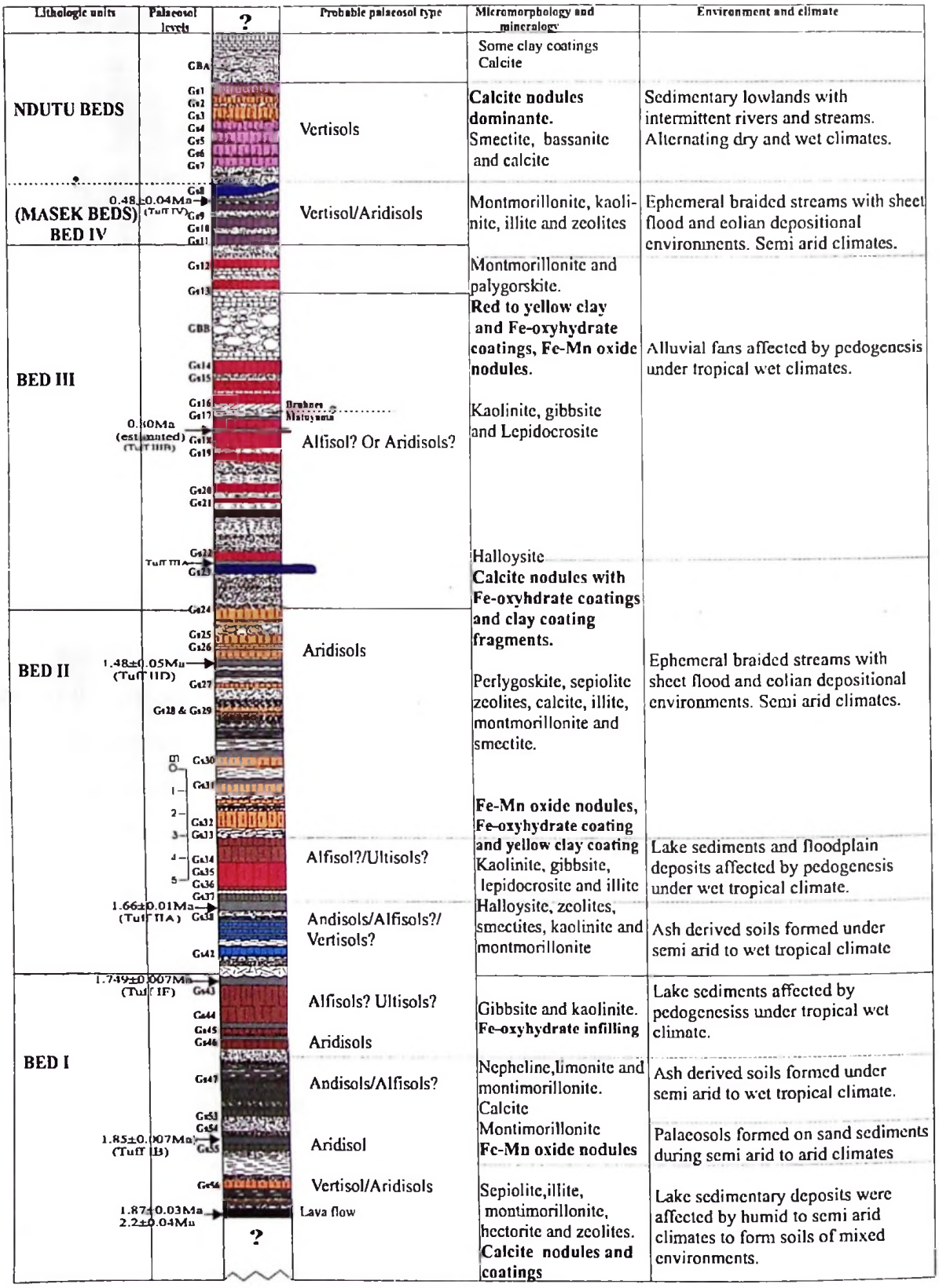

Figure 7.10: Olduvai Gorge tentative palaeoclimates and palaeoenvironments based on some micromorphological and mineralogical signatures coupled with field observations.

CHAPTER EIGHT

OLDUVAI GORGE MAGNETIC SUSCEPTIBILITY STUDIES

8 OLDUVAI GORGE MAGNETIC SUSCEPTIBILITY STUDIES

8.0. GENERAL INTRODUCTION

This chapter presents the bulk magnetic susceptibility studies conducted in Olduvai Gorge deposits. Magnetic susceptibility measurements of bulk samples were measured and a mgnetic susceptibility curve was produced. Then an attempt to observe the salient features in relation to the stratigraphy was made.

8.1. GENERAL CONSIDERATIONS

8.1.1. Magnetic susceptibility and magnetic minerals

Low field magnetic susceptibility (χ) is defined as the ratio of the induced magnetic moment (induced magnetization) to the intensity of the magnetizing field (magnetizing force).

$$\chi = \frac{M}{F}$$

where, M = Induced magnetic moment,
F = $\mu_o H$, (H = Magnetic field strength)
(μ_o = Mgnetic susceptibility in free space)

This ratio depends on the nature, concentration, effective grain size and shape of magnetic minerals in a particular material (in this case in soils). Studies of magnetic materials (rocks, minerals and soils) have shown that there are two large groups of minerals, namely diamagnetic minerals and paramagnetic minerals (see table 8.1). Common diamagnetic minerals (especially in soils) are poor in iron and include quartz,

carbonate, feldspars and water. Paramagnetic minerals are rich in iron and they mainly include Fe-oxides, Fe-hydroxides, Fe-sulfides and Fe-rich silicates.

All diamagnetic minerals have a negative magnetic susceptibility ($\chi_{dia} < 0$). The atoms of such minerals have no magnetic moments. They contain even number of outer electrons and the spin of the unpaired electrons is disordered in the external magnetic field thus being repelled by the field. On the other hand paramagnetic minerals have a positive susceptibility ($\chi_{para} > 0$). They contain atoms with odd number of electrons with electron spin of the unpaired electron in the direction of the applied external field, thus enhancing the induced field from the tiny magnetic moments of the electrons.

Table 8.1: A list of magnetic minerals (Compiled from; Tarling, 1971 and Tucker, 1991)

Some diamagnetic minerals	**Paramagnetic minerals**
Quartz - SiO_2 Carbonate - $CaCO_3$ Feldspar - $R_xAlSi_3O_8.O_x.XH_2O$ Water - H_2O	**Iron oxides** Magnetite – Fe_3O_4 Maghaemite – γFe_2O_3 Haematite – αFe_2O_3 Ilmenite – $FeTiO_3$
	Iron hydroxides Goethite – $\alpha FeOOH$ Lepidocrosite - $\gamma FeOOH$ Akagenite - $\beta FeOOH$ (Unstable in nature) Ferroxyhyte - $\delta FeOOH$ Ferrihydrite – $5Fe_2O_3.9H_2O$ Limonite – $FeOOH.n\ H_2O$
	Sulphides Pyrhotite – FeS Pyrite – FeS_2
	Iron rich silicates (very weak magnetic minerals) Amphiboles Pyroxenes Biotite

However, there are two types of paramagnetic minerals, those with a weak positive susceptibility and those with a strong susceptibility. The paramagnetic minerals with a strong positive susceptibility are called ferromagnetic minerals. They remain magnetized even after the magnetizing force is removed (they remain permanent magnets). The paramgnetic minerals are further subdivided into paramagnetic (par se), ferromagnetic, ferrimagnetic and antiferromagnetic minerals according to their different magnetic properties as summarized in table 8.2 below.

Table 8.2: Magnetic characteristics of magnetic minerals, (After; Tarling, 1971)

Type of magnetization	**Orientation and type of moments**	**Example minerals**
Paramagnetism (par se)	Electron spin magnetization is randomly oriented producing a very weak magnetism	Lepidocrosite Fe-rich silicates
Ferromagnetism	Electron spin magnetization is parallel to each other producing a strong magnetization	Pyrhotite Pure iron
Ferrimagnetism (canted)	Electron spin magnetisation is antiparallel to each other producing a Weak magnetization.	Magnetite Titanomagnetite Maghaemite
Antiferromagnetism (canted)	Electron spin magnetisation is randomly orientd but produce a net magnetization effect even in the absence of external field	Haematite Goethite Ilmenite

The most common magnetic minerals are the iron oxides and titano-iron oxides as irepresented in the diagram in the next page, as was taken from Tarling, (1977).

Figure 8.1: Ternary diagram showing most common iron oxide magnetic minerals, (After; Tarling, 1971)

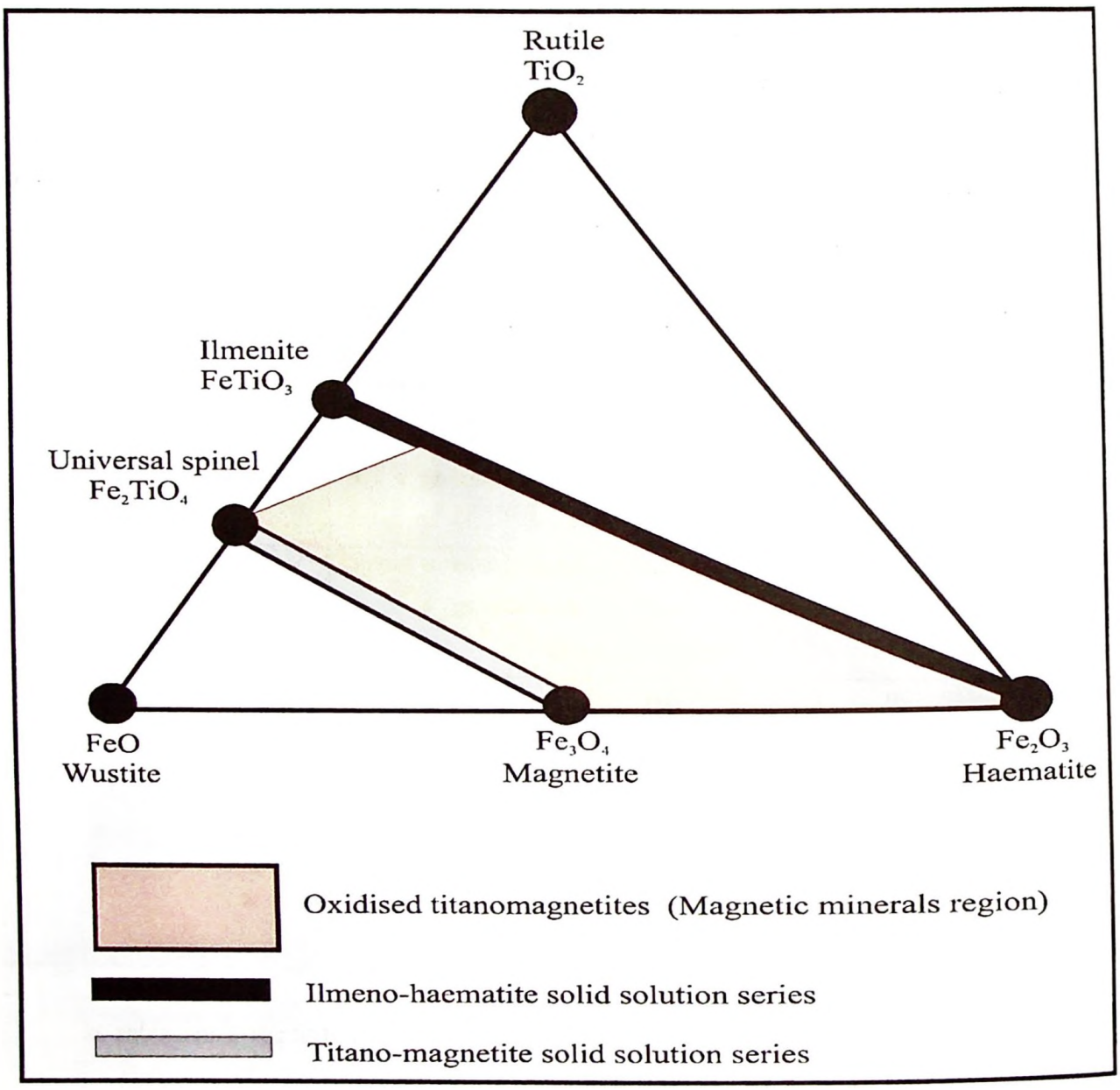

8.1.2. Magnetic minerals in soils

Studies of magnetic minerals present in soils have shown that the most dominant diamagnetic minerals are quartz, calcite, feldspars and water. These minerals are regarded as dilutant of bulk magnetic susceptibility in soils. Organic Matter though not minerals are also regarded as a dilutant.

Paramagnetic minerals (including ferromagnetic, ferrimagnetic and antiferrimagnetic) which occur as both primary and secondary minerals in soils are the main contributors to the total magnetic susceptibility measurements in soils.

The distribution of such minerals varies a great deal according to climate and environment in which the soils are formed. Hematite occurs in relatively drier and oxidized conditions in tropical and semi tropical climates, while goethite is predominant in well-drained soils of temperate climates. Lepidocrosite is more restricted to poorly drained gleyed soils and occurs mostly as mottles (concretions), coatings and infillings in pores and root channels. Magnetite occurs as a primary mineral in soils normally derived from basic igneous and volcanic rocks. Sometimes it can be formed as a secondary mineral in soils mainly from soil firing (Alam, 1994).

Maghaemite occurs as concretions in highly weathered soils of tropical and subtropical climates. Goethite is generally the least restricted iron oxide in terms of climate, in other words it can be found in a variety of soils across a varied range of climates (Schwertmann and Taylor 1977). Therefore, most soils contain goethite. Table 8.3 summarizes some of the soil environments in which Fe-oxides and Fe-hydroxide dominate.

Table 8.3: Occurrence of Fe-oxides and Fe-hydroxide in soils (After; Schwertmann and Taylor 1977)

Type of mineral	Chemical formula	Magnetism	Environmental association
Haematite	αFe_2O_3	Canted antiferromagnetic	Relatively dry, highly oxidized soils and in hot areas
Goethite	$\alpha FeOOH$	Canted antiferromagnetic	Moist soils and well drained temperate climates
Magnetite	Fe_3O_4	Ferrimagnetic	Restricted occurrence of the mineral, it is mainly primary in origin and also in areas were soil firing can occur
Maghaemite	γFe_2O_3	Ferrimagnetic	Found abundantly in highly weathered tropical and sub tropical soils
Lepidocrosite	$\gamma FeOOH$	Paramagnetic	Found in poorly drained soils
Ferrihydrite	$5Fe_2O_3.9H_2O$	Paramagnetic	Occurs mainly in spodsols and poorly drained environments

8.1.3. Enhancement or dilution of magnetic minerals in soils

There is evidence of an association between magnetic mineral variations with types of soil forming environments (Maher 1986), thus magnetic minerals in soils reflects soil-forming processes. In this respect magnetic mineral variations in soils have extensively been used in environmental studies like assessment of erosion processes (Mruma, 1990) and in palaeoclimatic studies (Hus and Han, 1992).

Pedogenic processes and soil environments in which concentration or dilution of magnetic minerals as discussed by Fine *et al.*, (1972), Taylor and Schwertmann ($1974_{a\&b}$) Tarling, (1977), Longworth *et al.*, (1979), Fassbinder *et al.*, (1989), Nahon, (1986), Hus and Han (1992) and Alam (1994) are briefly reviewed here below. A higher bulk magnetic susceptibility in soils is attributed to higher concentrations of magnetic minerals in the soils. Soil forming processes can enhance or dilute magnetic minerals inherited from parent materials. The enhancement can be due to insitu conversion of antiferromagnetic Fe-oxides or hydroxide into ferrimagnetic oxides or hydroxides by oxidation-reduction processes in soils during pedogenic processes.

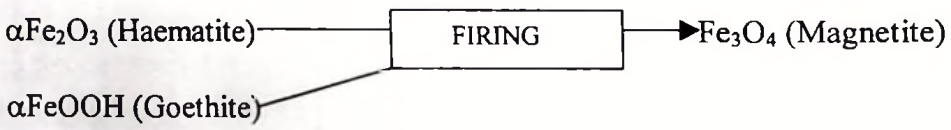

In some soils derived from acid igneous or volcanic rocks, magnetic mineral concentration can be attained by the formation of Fe-hydroxides that are formed from Fe-rich silicates. In this case magnetic susceptibility enhancement occurs at the base of most soil profiles under humid tropical and well drained conditions where parent minerals may weather to amorphous or crstallized ferruginous oxyhydroxides. This can happen also as a direct reprecipitation in the form of periferal pseudomorphs after the original mineral or can also be formed together with clay minerals as diffuse segregations, patches and micronodules. For example an iron rich pyroxene (titano-augite) can react with water during pedogenesis to form lepidocrosite or goethite together with clays, as shown below.

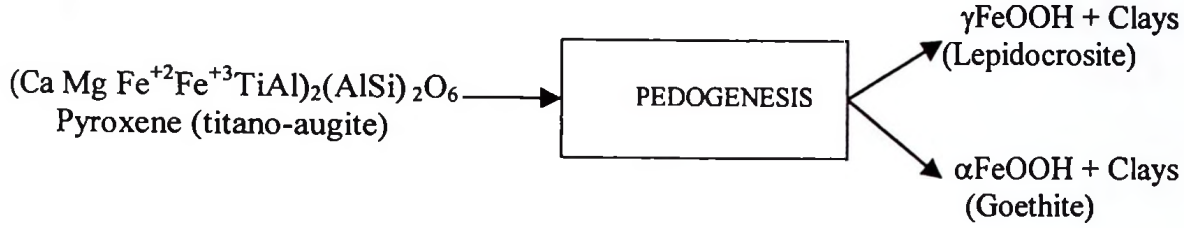

A dilution can take place by conversion of say magnetite minerals to ferrihydrate minerals by hydrolysis during pedogenesis.

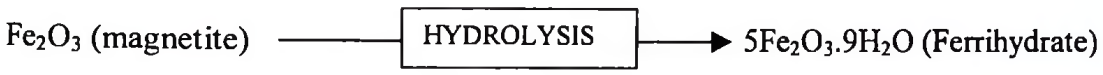

Dilution can also take place by a strong magnetic primary or secondary strong magnetic (ferrimagnetic or antiferromagnetic) oxide mineral reacting with water to form weak manetic (paramagnetic) hydroxide minerals as shown below.

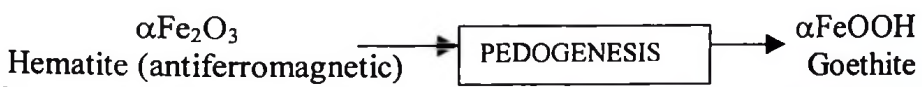

In summary therefore, enhancement or dilution of magnetic minerals in soils can either be due to a reduction or oxidation chemical process of Fe-oxides or hydroxides in already existing soils. Or it can be a transformation of Fe-rich silicates by complex chemical reactions into Fe-oxides or hydroxides from parent materials (sediments and rocks). In thin layers of soil profiles firing in presence of organic matter can occur under high tropical temperatures. Other mechanisms discussed in the literature include organic matter decay caused by microorganisms under aerobic conditions. All these processes can be directly linked to the environment and climate in which different soil form.

8.2. MAGNETIC SUSCEPTIBILITY STUDIES

8.2.1. The importance of magnetic susceptibility in palaeoclimatical and stratigraphical studies

Magnetic susceptibility patterns are strong tools for regional stratigraphical and paleoclimatical correlations. Pedogenic processes have been suggested to influence magnetic susceptibility variations. Soil forming processes (pedogenesis) of the past is said to have contributed to the enhancement of magnetic particles in the palaeosols (Heller & Liu 1984, Hus & Han 1992). Studies have also shown that magnetic susceptibility variations are influenced by lithogenic factors like sedimentation processes and origin of sediments (Grimley *et al.*, 1998). These factors (pedogenic and lithogenic) have made possible the isolation of palaeosol (for climatic changes) and stratigraphical formation/member classification.

Magnetic susceptibility measurements have been used to scan paleoclimatic variation in the loess-palaeosol sequences (Sun & Din, 1998) The concept behind these studies lies in the fact that loess deposit is assumed to have been deposited during cold and dry conditions. They are usually intercalated by palaeosol levels, which were formed during wet and warmer past climates. Palaeosol levels show higher susceptibility values in comparison to the loess sediments because during formation magnetic minerals tend to be concentrated (An *et al.*, 1997).

Moreover, stratigraphical classification has been aided by magnetic susceptibility variation in Lake Sediments. Sedimentation processes like sorting or syngenetic recrystalization (Feng *et al.*, 1994) can concentrate or dilute magnetic minerals. Also sediments show different values of magnetic susceptibility due to origin of sediments (parent material). The MS strength or weakness will depend on whether the material were rich or depleted in magnetic minerals. For instance, low magnetic susceptibility in clay are due to absence of primary magnetic minerals, which occur in the silt fraction and not in the clay fraction and also carbonate concretions are dilutants in palaeosols (Grimley *et al.*, 1998).

8.2.2. **Methods of investigation**

A total of 142 bulk samples were systematically sampled from the Olduvai Gorge section (Zinj, RS, RB, LK and MC sections) along the gorge cliffs (figure 3 and 5). The sampling interval ranged from 2cm to 100cm depending on the lithological variations. The samples were dried and sieved using a bronze 1000μm sieve. Weights of dry sample ranging from 0.62grams to 6grams were placed in a Kappa-Bridge-KLY2 meter to measure the susceptibility of each individual sample.

The results were converted into weight susceptibility quantities of the order of $10^{-7}m^3kg^{-1}$ (SI units) (table 8.4). A plot of depth (m) versus susceptibility ($m^3 kg^{-1}$) was produced and correlated to the general lithology of the section (figure 8.6 & 8.7). Magnetic susceptibility of bulk samples from stratigraphicalally positioned sediments and palaeosols are measured (in the laboratory) with the purpose of trying to observe their response. Tentative results and discussions are presented in the next proceeding paragraphs.

8.2.3. **Results**

The magnetic susceptibility record of Olduvai Gorge section shows a clear six major parted zonation as shown in figures 8.1 – 8.7, table 8.4 and appendix 8) and described below.

Table 8.4: Magnetic susceptibility results presented according to their stratigraphical positions [Refer figures 8.6 and 8.7]

S.No	Sample	MS (SI units) (x 10^{-7})	ZONE	S.No	Sample	MS(SI units) (x 10^{-7})	ZONE	S.No	Sample	MS(SI units) (x 10^{-7})	ZONE
1	Mc27	No data		51	Rb4	34.69		101	Rs3	1.45	
2	Mc26	30.12	Six	52	Rb3	6.30		102	Rs2	1.30	
3	Mc25	64.62	47.05	53	Rb2	191.30		103	Rs1	1.07	
4	Mc24	53.83		54	Rb1	18.29		104	Z25	16.00	
5	Mc23	39.61		55	Rs39	84.84		105	Z24	12.27	
6	Mc22	16.29		56	Rs38	75.48		106	3z	5.68	
7	Mc21	20.64		57	Rs37	46.33		107	2z	10.18	
8	Mc20	12.41		58	Rs36	58.85		108	Zl	6.20	
9	Mc19	14.42		59	Rs35	73.29		109	1z	12.10	
10	Mc18	10.38		60	Rs34	126.42		110	Zk	14.97	
11	Mc17	11.98		61	Rs33	57.27		111	Z23	32.53	
12	Mc16	17.48		62	Rs32	125.85		112	Z22	5.32	
13	Mc15	10.61	Five	63	Rs31	169.57		113	Z21c	8.41	
14	Mc14	92.66	14.32	64	Rs30	26.84		114	Z21b	2.68	
15	Mc13b	9.45		65	Rs29	133.05		115	Z21a	5.74	
16	Mc13b	16.87		66	Rs28	223.48	Three	116	Z21	3.47	
17	Mc12	15.752		67	Rs27	242.44	65.67	117	Z20	6.11	
18	Mc11	8.85		68	Rs26	135.55		118	Z19	7.39	One
19	Mc10	18.81		69	Rs25	30.36		119	Z18	5.10	8.89
20	Mc9	21.50		70	Rs24	84.62		120	Z17	5.33	
21	Mc8	9.29		71	Rs23	244.85		121	Z16	5.69	
22	Mc7	38.11		72	Rs22	81.34		122	Z15	9.32	
23	Mc6	21.28		73	Rs21	8.12		123	Z14	12.98	
24	Mc5	21.94		74	Rs20	4.95		124	Z13	8.20	
25	Mc4	25.90		75	Rs19	16.29		125	Z12	9.27	
26	McHB	100.14		76	Rs18	14.32		126	Z11	15.93	
27	Mc3	81.19		77	Rs17	84.90		127	Z10	10.41	
28	Mc2	35.31		78	Rs16	23.25		128	Z9	14.10	
29	Mc1	53.75		79	Rs15	28.50		129	Z8	28.12	
30	Rb24	54.65		80	Rs14	25.69		130	Z7	14.85	
31	Rb23	53.72		81	Lk10	50.32		131	Z6	12.02	
32	Rb22	37.11		82	Lk9	17.87		132	Z5	14.41	
33	Rb21	51.67		83	Lk8	16.43		133	Z4	11.83	
34	Rb20	49.25		84	Lk7	31.24		134	Z3	19.11	
35	Rb19	40.93		85	Lk6b	33.25	Two	135	Z2	33.36	
Cont.	Cont....	Cont....	Cont....	Cont..	Cont....	Cont....	Cont....	Cont..	Cont....	Cont....	Cont....
36	Rb18	61.14	Four	86	Lk6a	27.87	25.62	136	Z1	13.79	
37	Rb17	63.52	45.32	87	Lk5	28.28		137	Zj	3.40	
38	Rb16	46.64		88	Lk4	12.75		138	Zi	91.15	
39	Rb15	60.48		89	Lk3	5.12		139	Zh	10.61	
40	Rb14	51.85		90	Lk2	32.99		140	Zg	50.22	
41	Rb13	85.39		91	Rs13	3.00		141	Zf	2.27	
42	Rb12	60.31		92	Rs12	6.22		142	Ze	23.14	
43	Rb11	44.00		93	Rs11	4.67		143	Zd	6.86	
44	Rb10	49.59		94	Rs10	4.00	One	144	zc	No data	
45	Rb9	20.76		95	Rs9	3.42		145	Zb	7.17	
46	Rb8	48.69		96	Rs8	5.25		146	Za	7.72	
47	Rb7	66.13		97	Rs7	6.46					
48	Rb6b	40.91		98	Rs6	3.83					
49	Rb6a	43.05		99	RS5	4.55					
50	Rb5	44.83		100	Rs4	1.69					

Zone 1. The lower part of the section (Bed I and Lower Bed II) show low susceptibility values (Usually below 10 x10^{-7} m^3kg^{-1}). Palaeosols and sands show enhanced MS values [9 x10^{-7} m^3kg^{-1} - 99 x10^{-7} m^3kg^{-1}]. Clays and ash falls/flows have MS values in the range [2 x10^{-7} m^3kg^{-1} - 19 x10^{-7} m^3kg^{-1}] (figures 8.1, 8.3, 8.6 and 8.7 and table 8.4).

Zone 2. This is Middle Bed II stratigraphical unit which posses average susceptibility values approximately equal to 40 x10^{-7} m^3kg^{-1}. It is a red palaeosol zone which show less

local MS variation (figures 8.2, 8.6 and 8.7). This zone might be an agradation or accretion of several palaeosols.

Zone 3. (Upper Bed II). Average magnetic susceptibility values are higher than 60 $x10^{-7}$ m^3kg^{-1}, (figures 8.3, 8.6 and 8.7). This is the zone with highest values in the profile due to dominant sand layers [greater than 100 $x10^{-7}$ m^3kg^{-1}]. Other sediments have MS [less than 100 $x10^{-7}$ m^3kg^{-1}] with very few palaeosols levels showing higher values than the clays and tuffs. Whenever a palaeosol is developed on a sand layer its MS values is usually less than the parent sand lithology.

Zone 4. This coincides with Bed III of the stratigraphical unit of Olduvai Gorge. The zone shows average MS values of about equal to 40 $x10^{-7}$ m^3kg^{-1}, (figures 8.4, 8.6 and 8.7) ressembling that of middle Bed II. In the field this zone was mapped as a red palaeosol zone. From afar it looks like a massive single bed, but a closer mapping revealed that it is composed of several palaeosols. It is probably a thick aggradational pedocomplex within fluviatile-lacustrine lithological sequences of Olduvai Gorge.

Zone 5. The upper part of the section again shows two divisions, the lower (Masek beds/Bed IV and Ndutu Beds) with average susceptibility values below 15 $x10^{-7}$ m^3kg^{-1} and the upper division is described as zone 6 (upper Ndutu beds) in the next paragraph, (figures 8.5, 8.6 and 8.7). The Masek beds/Bed IV and lower Ndutu Beds zone is mainly composed of gray palaeosols developed on silt clay lithologies. There is less fluctuation of MS values in this zone.

Zone 6. Zone 6 is the upper part of the section (Ndutu Beds/Bed V) that shows higher average values greater than 40 $x10^{-7}$ m^3kg^{-1} (figures 8.5, 8.6 and 8.7). This zone is sandy in texture and composed of gray to dark gray clay sands.

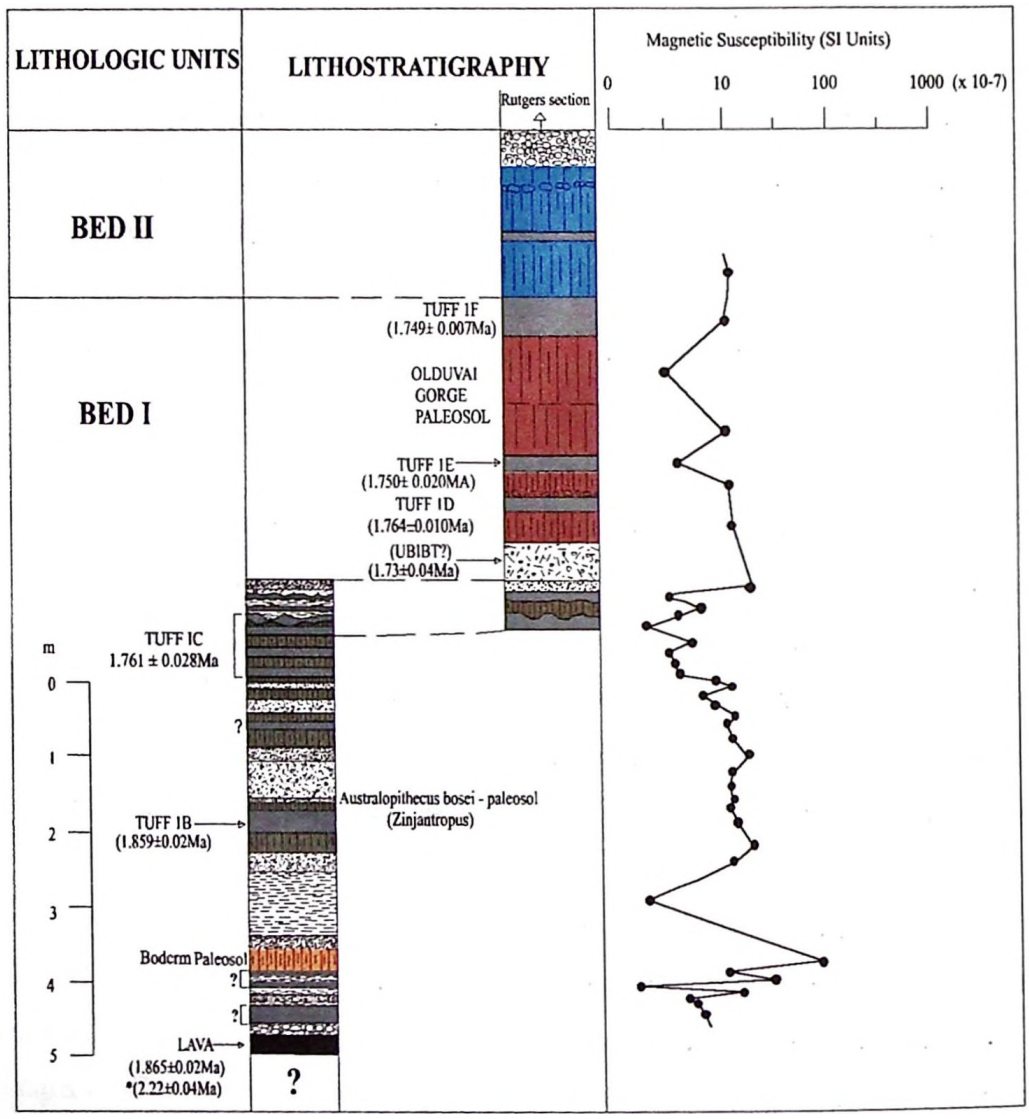

FIGURE 8.1: **ZINJANTHROPUS SECTION**: *MAGNETIC SUSCEPTIBILITY RECORD* [Palaeosol levels show higher MS values compared to clay layers.Ssands have always highest values]

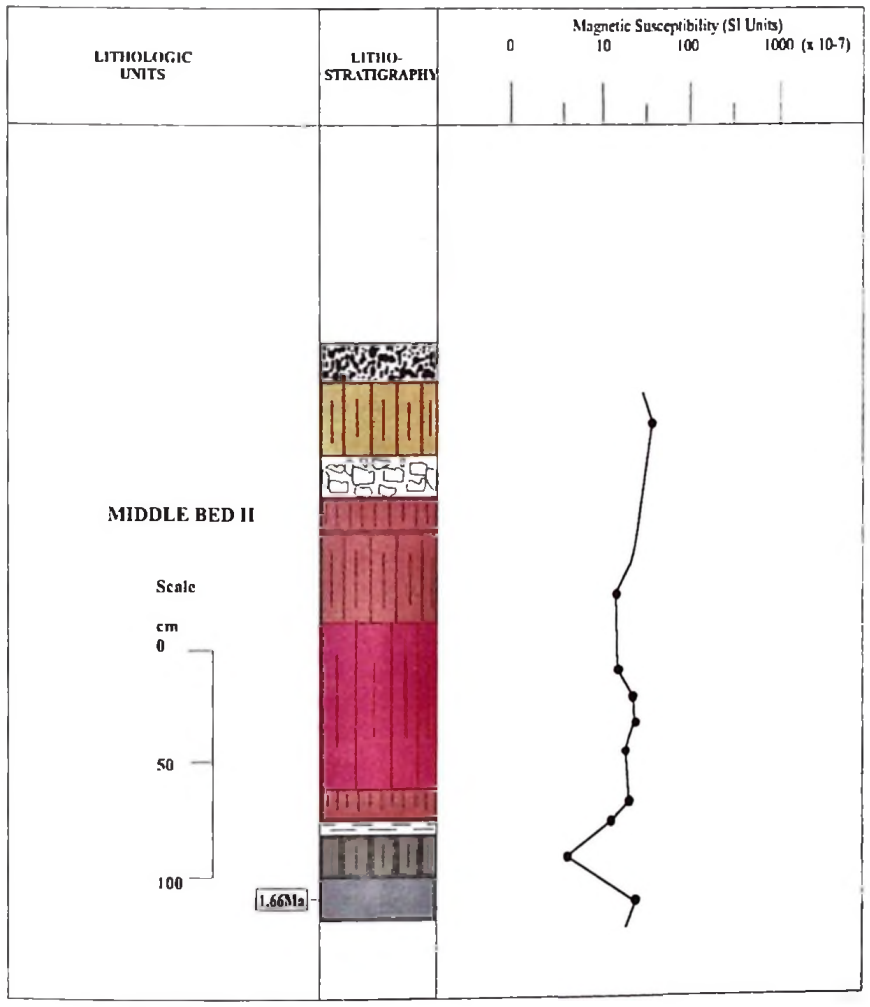

FIGURE 8.2: **LONG KORONGO SITE**: *MAGNETIC SUSCEPTIBILITY RECORD*, [Red units show high MS values without much variation across the section], (Studied with the permission of Rutgers University)

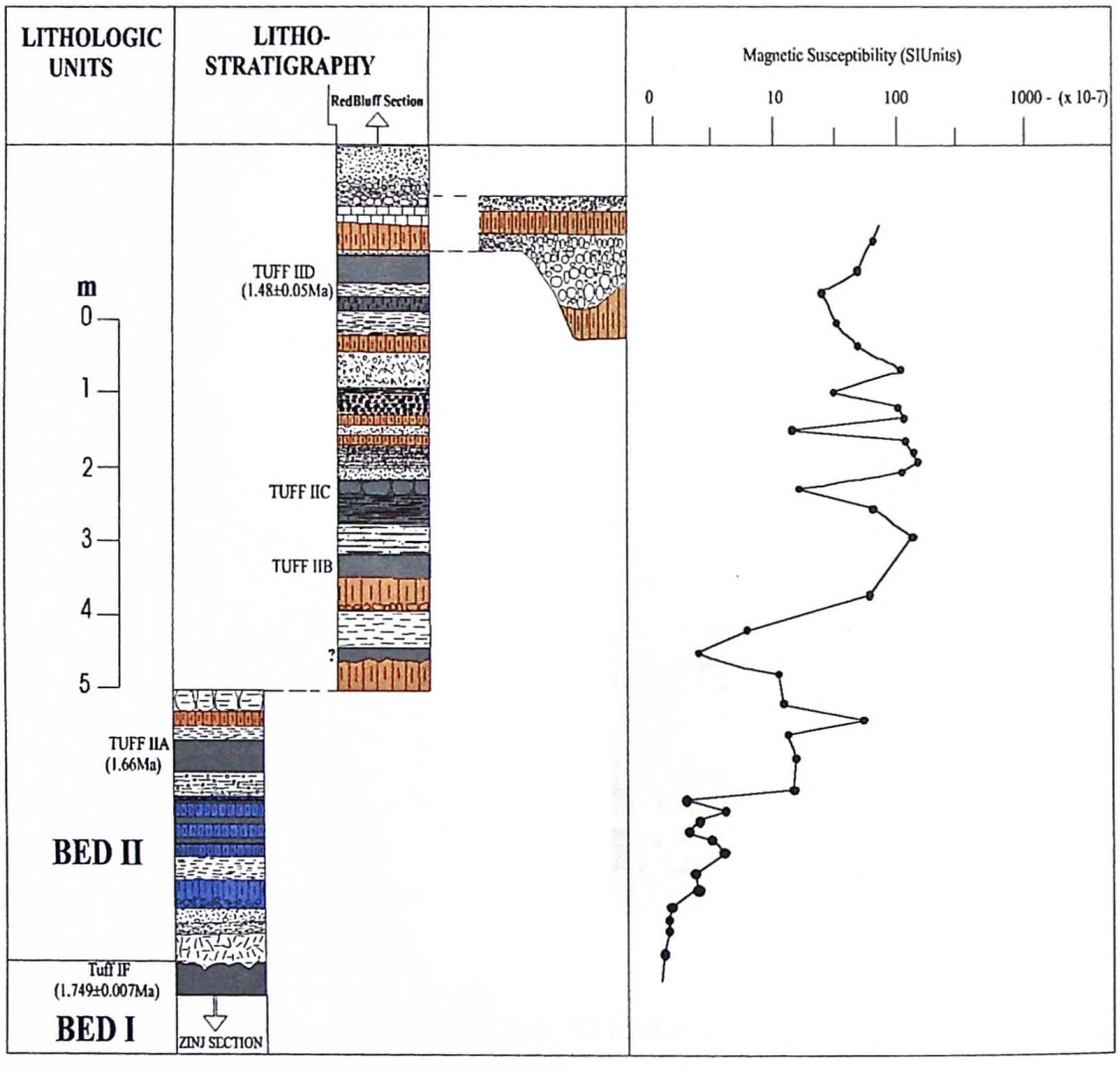

FIGURE 8.3: **RUTGERS SITE SECTION:** *MAGNETIC SUSCEPTIBILITY RECORD*
[Lower Bed II palaeosol levels show eleveted MS compared to other units; the upper Bed II show low MS values for palaeosol levels compared to sand layers]
(Studied with the permission of Rutgers University).

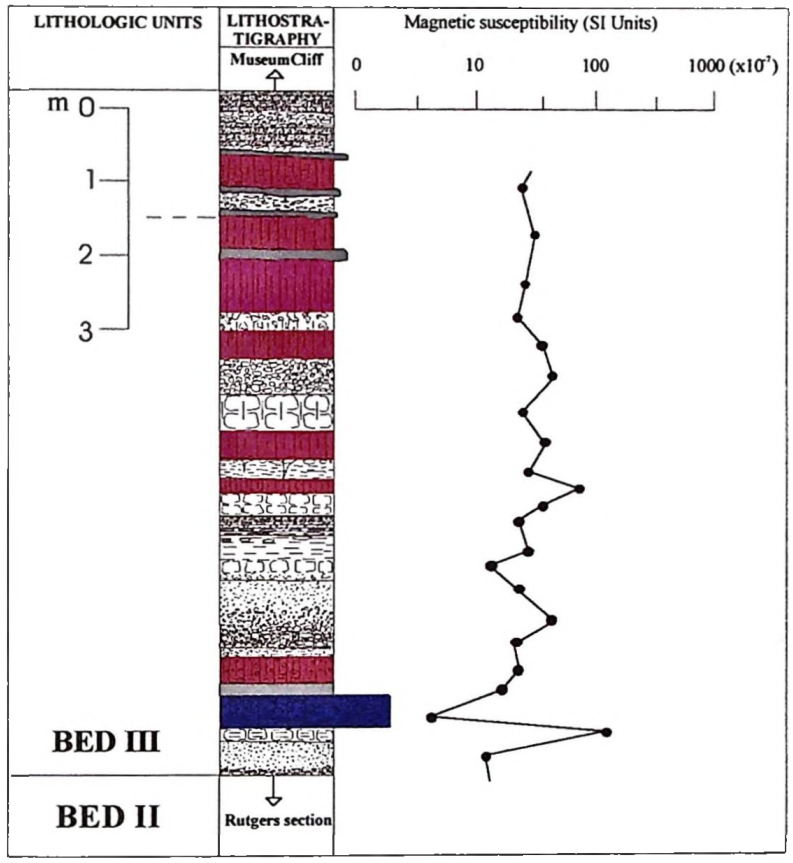

FIGURE 8.4: **RED BLUFF SECTION:** *MAGNETIC SUSCEPTIBILITY RECORD* [Sand and palaeosol levels indicates higher MS values compared to other sediments].

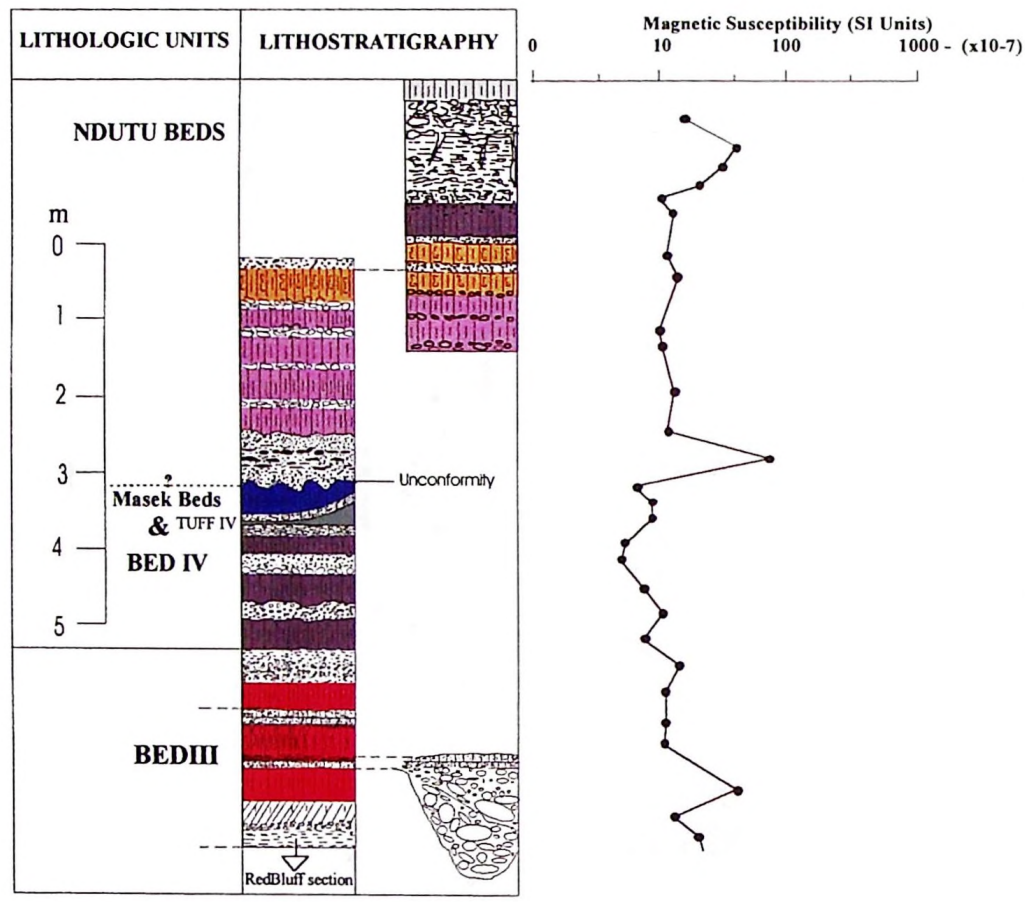

FIGURE 8.5: **MUSEUM CLIFF SECTION:** *MAGNETIC SUSCEPTIBILITY RECORD,* [Sand levels have higher MS values compared to palaeosol levels]

8.3. DISCUSSION, INTERPRETATION AND IMPLICATION

8.3.1. Discussion and interpretation

The MS pattern of Olduvai Gorge as described above is related to the general stratigraphy. In each zone either paleo-pedogenetic activity or facies changes influence the MS record variation. Apart from this zonation the MS record shows an increasing trend from older to younger formations, (figure 8.6 & 8.7). The trend is discussed below.

Zone 1, the Lower part of the section, (Bed I and Lower Bed II) is composed of lacustrine and marginal lake sediments mixed with volcanic ashes. They are mainly olive to gray clays and white ash fall and flow tuffs. These sediments usually have very low magnetic susceptibility. The low magnetic susceptibility in clay is probably due to depletion of primary magnetic minerals in the clay fraction (Grimley *et al.*, 1998).

The sources of the clay and volcanic ash-tuff might have been depleted in magnetic minerals or was a result of sorted sedimentation in the paleolake. Heavy minerals depositing earlier along rivers and lakeshore line and the lighter (suspension material) ones (non-magnetic) deeper in the lake. The lakeshore is represented by sands, which also show higher susceptibility values.

More strikingly is the slightly enhances magnetic susceptibility values of palaeosol compared to the clays and ash-tuffs in this zone (figure 8.1 and figure 8.2). It is clear that the magnetic particles were concentrated during soil forming processes.

Zone 2 (Middle Bed II) is mainly mixed fluviatile-lacustrine deposits, which might have received sediments of higher magnetic affinities. From field observations it is clear that this part is composed of silt and silt sands sediments showing a strong development of red palaeosols. The palaeosol levels show limited local variation of MS record. I believe that this zone is probably a pedocomplex as research has shown elsewhere that paleo-pedocoplexes show less MS variations (McCarthy *et al.*, 1998). The pedogenetic processes seemed to concentrate the magnetic particles in this part but with minimum local variation.

Zone 3 (Upper Bed II) (figures 8.6 and 8.7) is mainly composed of fluviatile deposits intercalated with some ash falls/flows. The lower part of this zone shows the highest values in the profile. It is a more sandy part with dominant gravel, sand and sandstone layers showing susceptibility values of the order $100x10^{-7}$ to $250x10^{-7}$ m^3kg^{-1}. Again these high values are related to the sediment sources and sedimentation processes. The black sands, which dominate the zone, might be responsible for the higher susceptibility

values. One of the interesting results of this study is that palaeosols in this area show reduced susceptibility values compared to sand layers. The reason behind this reduction lies in soil-forming processes, which might have diluted the strong magnetic minerals by organic activity and hydrolysis. Other sediments (clays and tuffs) also show low susceptibility values compared to palaeosols and sands, (figure 8.6).

Zone 4, (Bed III) is a red zone consisted of red palaeosol levels and probably enriched in Fe-hydroxides due to high oxidation processes during pedogenesis. The zone seems to have undergone intense rubification. In the field, from a distance this zone looks like one massive red zone usually known as a "red bed" of Olduvai Gorge. A closer field examination revealed 9 red palaeosols in alternation with other sediments, (figure 8.4). This zone ressemle middle Bed II (zone 2) in background MS record and colour tone.

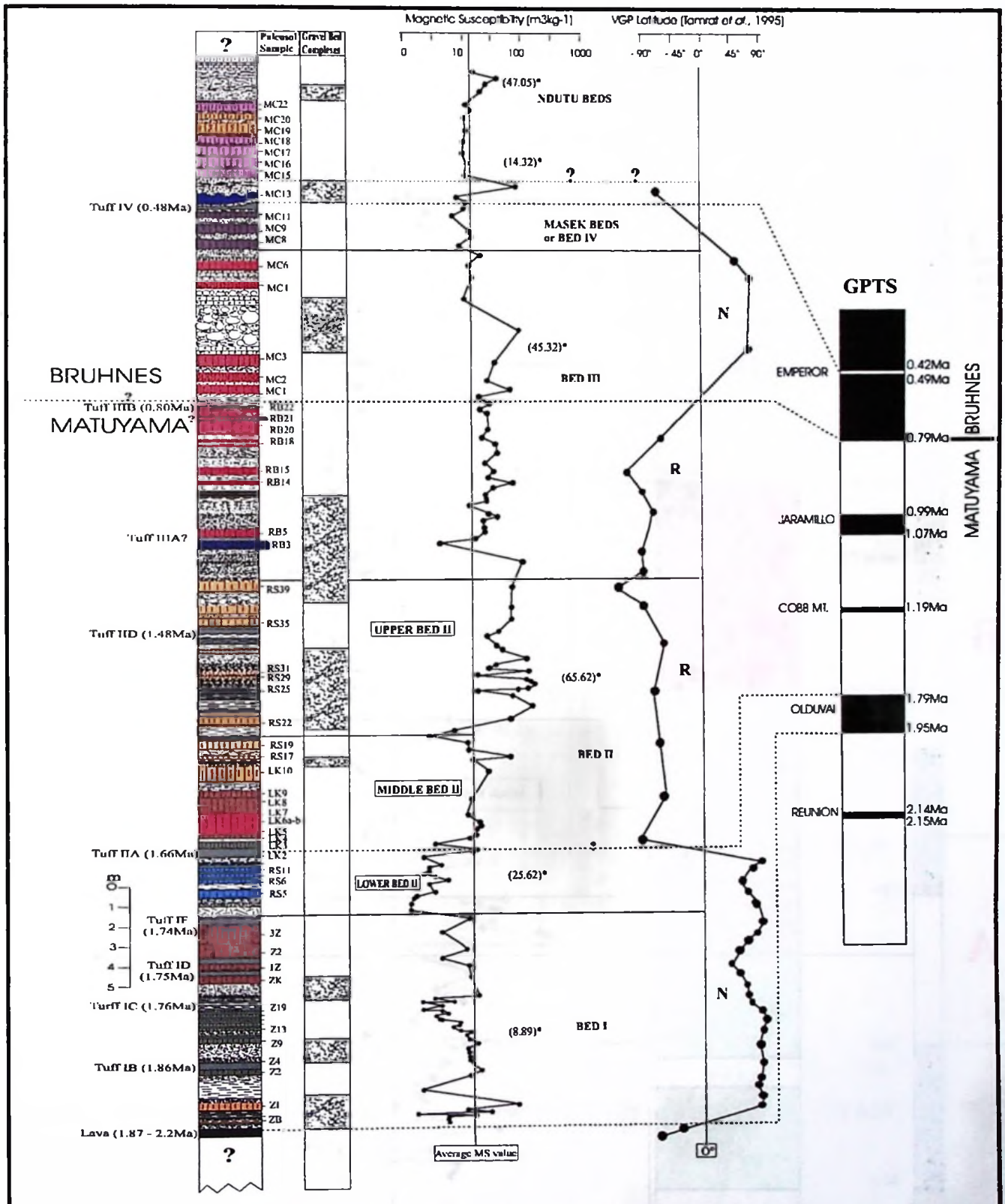

Figure 8.6: Magnetic susceptibility patterns of Olduvai Gorge beds, (The stratigraphy and the geomagnetic record - Magnetic susceptibility and VGP-latitude). [It is evident that the low magnetic susceptibility signature zone of Bed I and lower Bed II is a normal mgnetozone and the rest of Bed II and Bed III with slightly higher MS values show reversed porality. Upper Bed III and Masek beds again show a normal polarity. Sand and gravel beds are more prominent MS zones. *Average MS value in a zone].

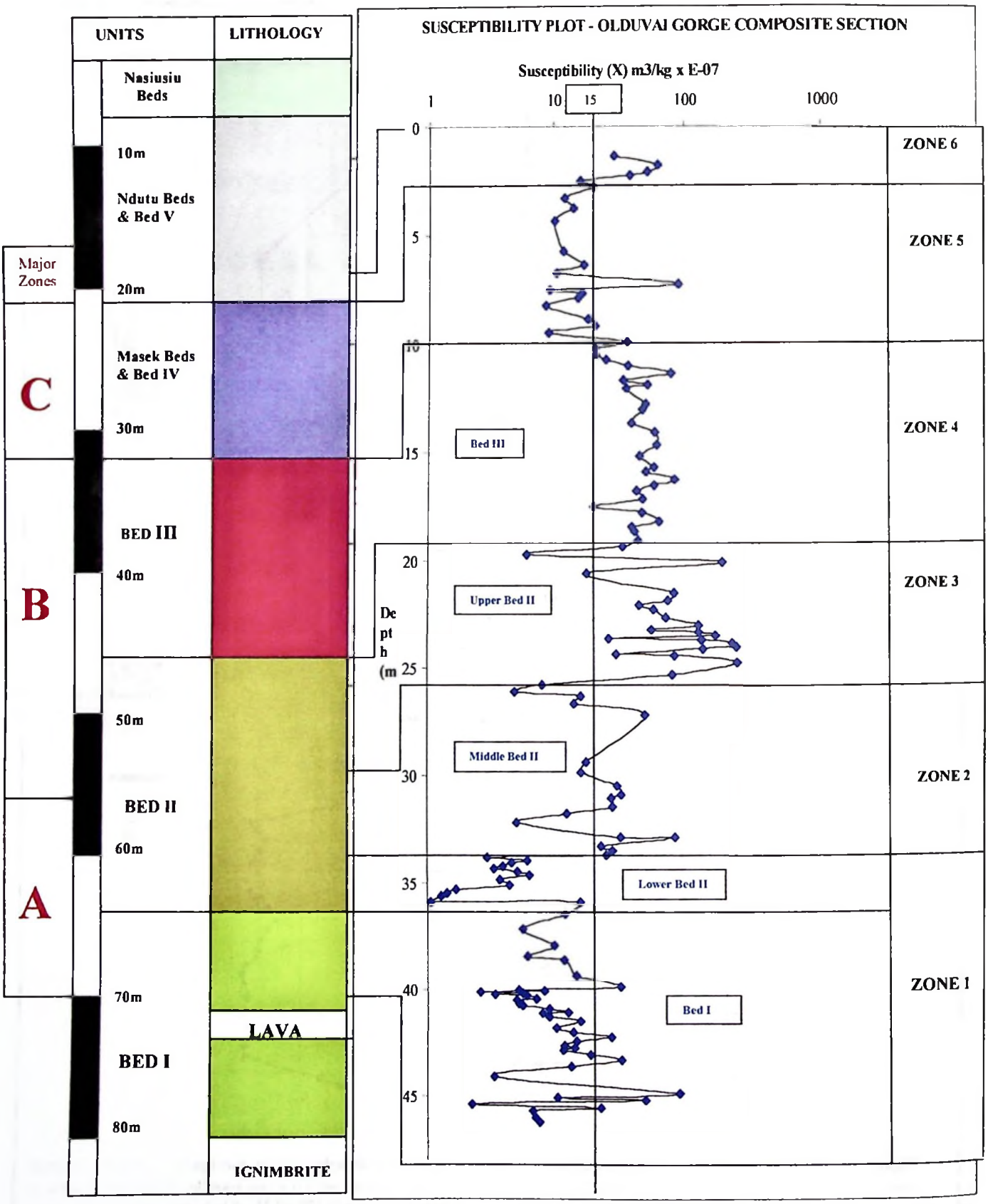

Figure 8.7: Magnetic Susceptibility Plot of Olduvai Gorge composite section: Simplified stratigraphical correlation. [Note the major stratigraphical zonation A, B & C].

Lacustrine sediments mainly composed of clay deposits and clayey palaeosols again dominate zone 5 (Masek beds/Bed IV and lower Ndutu Beds). The deposits generally show low susceptibility values, (figure 8.5). The sediment source was low in magnetic materials. However, in the lower part pedogenesis has slightly decreased the susceptibility values of palaeosols against the sand layers. In the upper part it was not possible to distinguish the clays and the palaeosols in the field, so the whole part was mapped as a series of clayey palaeosols. Micromorphological work is expected to reveal more on this section.

Zone 6 (upper Ndutu Beds) is loose clayey sand level of lacustrine to fluviatile origin (figure 8.5) showing higher MS values that the upper part of zone 5. This is probably a result of differential sedimentation of sand and clay layers. The sand layers having a concentration of heavy minerals including magnetic particles.

8.3.2. General conclusions

The general magnetic susceptibility (MS) record of Olduvai Gorge section shows a clear general pattern of increasing magnetic susceptibility values from the base of the section towards the upper part.

In general terms three main magnetic suscepto-stratigraphical zonations can be detected; (a) Zone A [Bed I until Middle Bed II – sub-zones 1 and 2] that shows low MS values (b) Zone B [Upper Bed II until Bed III – sub-zones 3 and 4] showing higher MS values and (c) Zone C [Masek/Bed IV – sub-zone 5] with again low MS values.

The dark sandy layers have the highest MS. In the sandy part (Upper Bed II - with extremely high MS values) palaeosols show reduced MS values compared to sand MS background values.

Another significant association is that the red zones of middle Bed II and Bed III, which have higher MS values compared to other sediments in that particular zone. This is

probably due to intense palaeo-pedogenic processes (probably rubification) which did affect the zones (micromorphological studies may ascertain this fact). There is no much MS fluctuation in this zone.

It is generally proposed that this trend of magnetic enhancement and dilution in the Olduvai Gorge section is due to two main reasons.

1. Depositional origin [stratigraphical]. A flux of magnetic materials is brought from various remote sources by volcanic activity, stream/river action and probably eolian activity.
2. Pedogenic origin [palaeoclimatical]. There is either an in situ concentration or dilution of magnetic minerals during soil forming processes.

CHAPTER NINE

MANONGA-WEMBERE AND HOLILI LOCALITIES QUATERNARY STUDIES

9 QUATERNARY STUDIES OF MANONGA-WEMBERE VALLEY AND HOLILI LOCALITIES

9.0 INTRODUCTION

This chapter presents study results and interpretations of the Quaternary geology and environments of Manonga-Wembere and Holili areas. The study undertaken includes; the geology and stratigraphy, the magnetic susceptibility, mineralogy and micromorphology record of some palaeosol levels. It is in possible completion of of the Olduvai gorge section.

9.1 MANONGA-WEMBERE LOCALITY

9.1.1 Geological setting

The geology (figure 9.1) and stratigraphy (figure 9.2) of the Manonga-Wembere valley begins with the Nyanzian rock system of Upper Archaean age (2.7Ga), (Borg 1992, and Walraven *et al.,* 1994). The rocks are composed of weakely metamorphosed acidic and basic volcanic rocks, schistace meta-sediments and banded iron formations (BIF), (Stockely 1947, Borg 1992 and Harris & Mbago 1997). The BIF meta-sediments are composed of chert bands laminated with magnetite rich bands. These rocks are mainly observed in the middle part of the area – Igunga-Igurubi stretch and the Iramba Plateau to the east of the area, (figure 9.1). They are the main host rocks for gold and basemetals minaralization. Several exploration ventures have been initiated in the area since the 1980's, for instance the UNDP prospected for gold in Igogo-Belenya hills 10km west of

Igunga and Mwamapuli area 12km south of Igunga and Canuck near Igusule in 1983 - 1987. Several copanies have recently taken the trail to find gold in the area, these include, Skeat Mining which, explored gold in Matinje area near Nzega in 1993 to 1994). Stilton Mining (T) Ltd is exploring gold in Igunga District since 1993, (United Republic of Tanzania, 1998).

Granites which, are believed to be a result of numerous granitization episodes during the Archean also extensively intrude the Nyanzian rocks. The composition of the ganatoids range from granites – gneisses – gneissose granites to migmatites, (stockely 1948). The granitization processes were so extensive such that most of the Nyanzian metasediments (BIF and volcanic) have been replaced by granites. The remaining patches of the Nyanzian BIF and meta-volcanics are now observed as roof pendants in a sea of granites. These granites are dominant along the Itumba-Mngazi western elevated block of the Wembere depression, SW corner of the area-Nzega area and North of Mwadui, figure (chapter 6 and figures 9.1 and 9.1b). A significant number of dykes and kimberlite pipes are recorded in the area. These rocks represent an extensive intrusive episode.

The Shinyanga (Mwadui and Kizumbi), Nzega (Ussongo) and Itumba (Ikoka) kimberlite pipes represents these intrusive bodies, (figure 9.1). The Shinyanga kimberlite pipes are diamondiferous and are mined for diamonds.

These old Nyanzian rocks were subjected to peneplanation during the End Tertiary Period, followed by downwarping of the Central Plateau (Manonga Vallley). The process created shallow basins resulting in the deposition of extensive terrestrial deposits during the Eocene Period. In the field it was observed that the conglomerates and gravels found in the Sekenke ridge and Mwansarara represent a basal gravel deposit lying unconformably on the Precambrian Nyanzian rocks marking the beginning of the Tertiary-Quaternary Manonga-Wembere deposits. The conglomerates and gravels are poorly sorted granitic and metamorphic detritus materials cemented together by calc-silicic-ferrugeneous material.

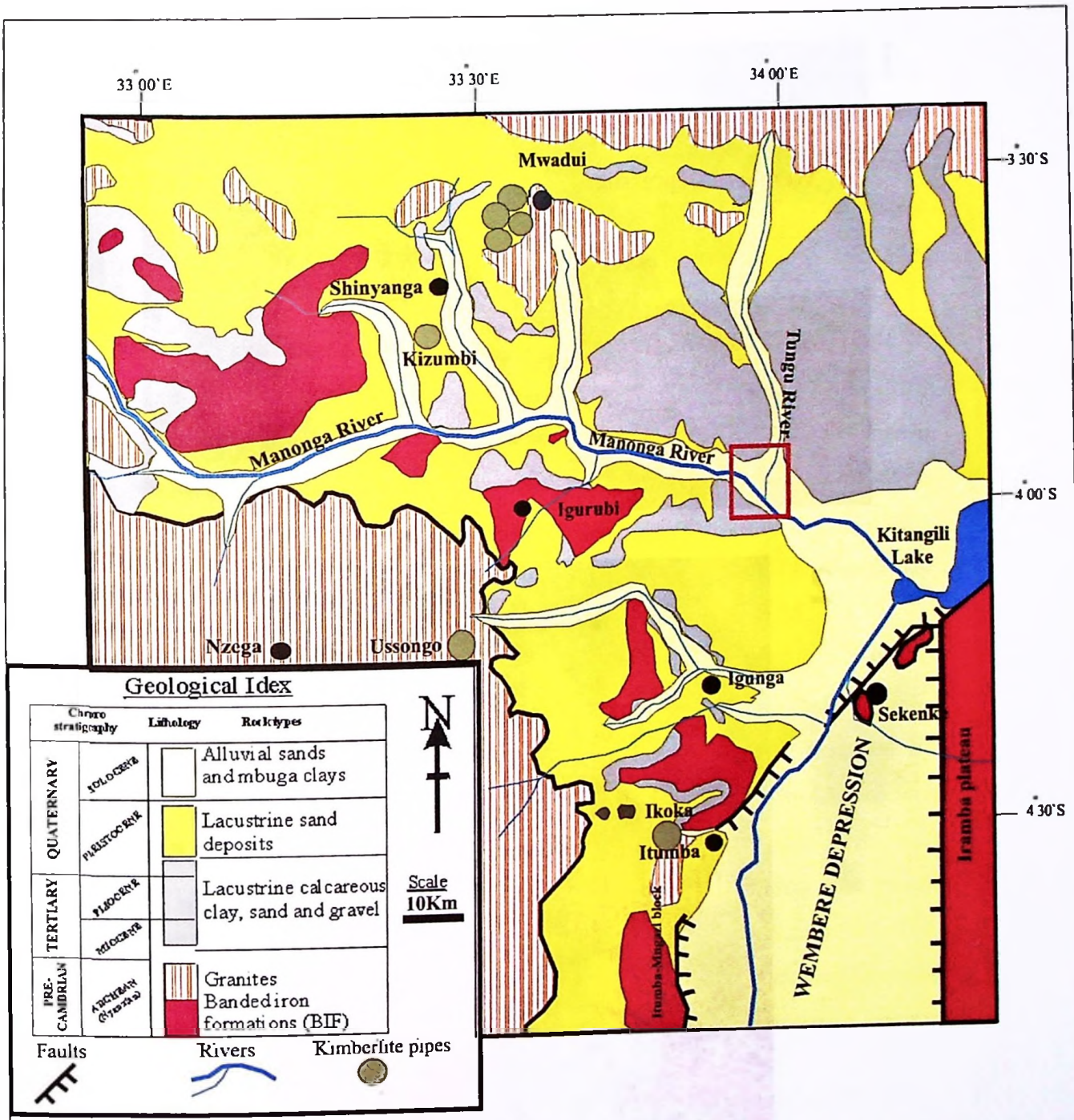

Figure 9.1: The geology of Manonga-Wembere Valley [The red rectangle indicates the study area - Kininginila section]

The beginning of the Pliocene was dominated by complex rifting regime patterns producing a shallow lake basin (Stockely, 1930) which initiated once again a new depositional regime in and around the shoreline of the Manonga-Wembere palaeolake.

1

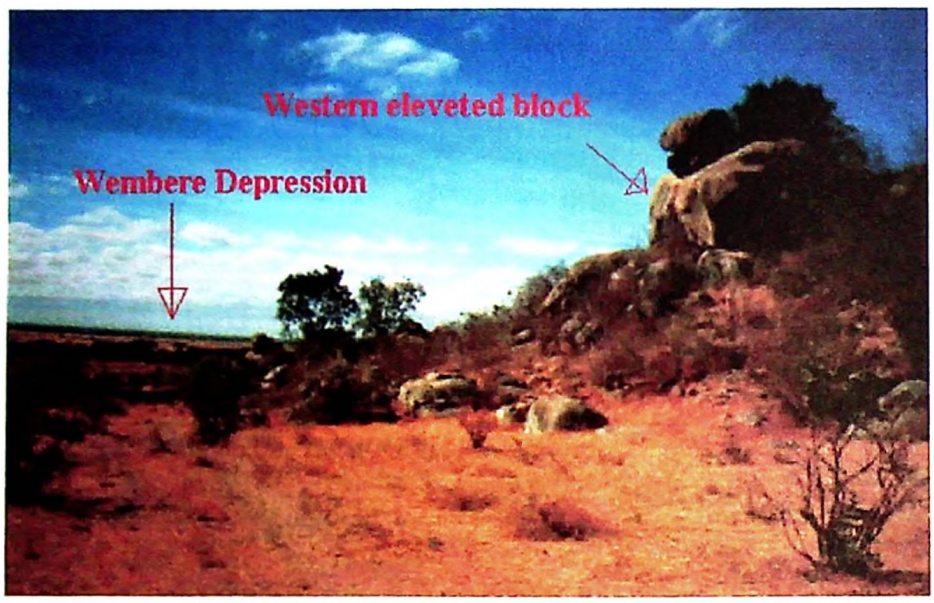

2

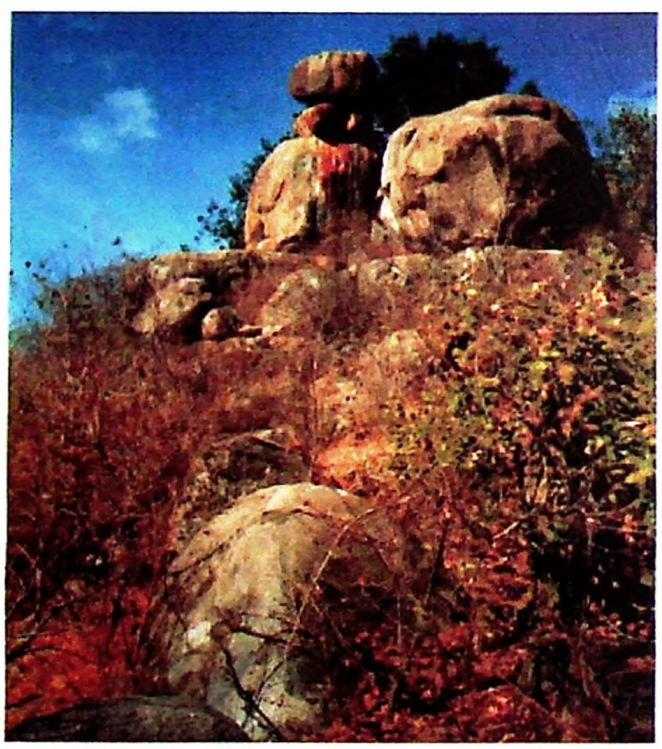

Figure 9.1b: Itumba granite of the western eleveted block and the Wembere depression. 1. Wembere depression as seen from the western eleveted block. 2. Granite kopjes in Itumba village.

From Pliocene to the Quaternary clay sediments filled the Central basin and calcareous clays, pebbly gravel and sand sediments filled the periphery (shoreline). The calcareous clay sediments are composed of grey sand marls, clays and limestones, occuppying the Central part of the Manonga-Wembere basin. These facies were described in detail by Verniers (1997) as formations consisting of Lake Deposit with deep marl facies composed mainly of swelling clays in the lower and middle parts and silt and non-swelling clays in the upper part of the section.

The limestone facies of Manonga-Wembere deposits grades from poor calcareous clays into pure layered (>90% carbonate) limestone. An outcrop of relatively pure limestone was observed 5km south of Igunga. Extensive palaeosol levels which, were developed on top of the lake sediments during periods of Lake Regression and transgression also intercalate these sediments. Coarse deposits observed interfingering the calcareous clay and sand deposits has been interpreted as shoreline accumulations.

Field observation revealed that the composition of the gravely sediments includes well-rounded gravel of granite, limestone and BIF rock fragments loosely cemented by calcareous clay material. The Late Quaternary (Upper Pleistocene and Holocene) was dominated by the shaping of the present topography where the Manonga River was curved eroding the sediments creating a huge (10km wide) Manonga valley. The valley was later filled with mbuga and alluvial sands during the Holocene (figure 9.3). The upper terrace (cliff faces) of the valley now expose the old (Miocene-Pliocene-Pleistocene) sediments of the Manonga-Wembere sediments while the lower terrace represent the Holocene mbuga clays and sands (figure 9.3a).

Manonga-Wembere deposits are poorly dated due to lack of datable volcanic materials. The only dates available are based on stratigraphical methods placing the deposits within early Pliocene through Pliocene-Pleistocene to Holocene – 3.0Ma to 2.0Ma interval (William and Eades 1939, Quennel *et al.*, 1956, Pickering 1958 and Barth 1990). However, Harris and Mbago (1997) based on palaeontological evidence estimated that the calcareous lacustrine sediments have an age range of between 5.5Ma and 4.0Ma (Late

Miocene to Early Pliocene). They further estimate that the upper mbuga clays and alluvial sands are either Late Pleistocene or Holocene in age.

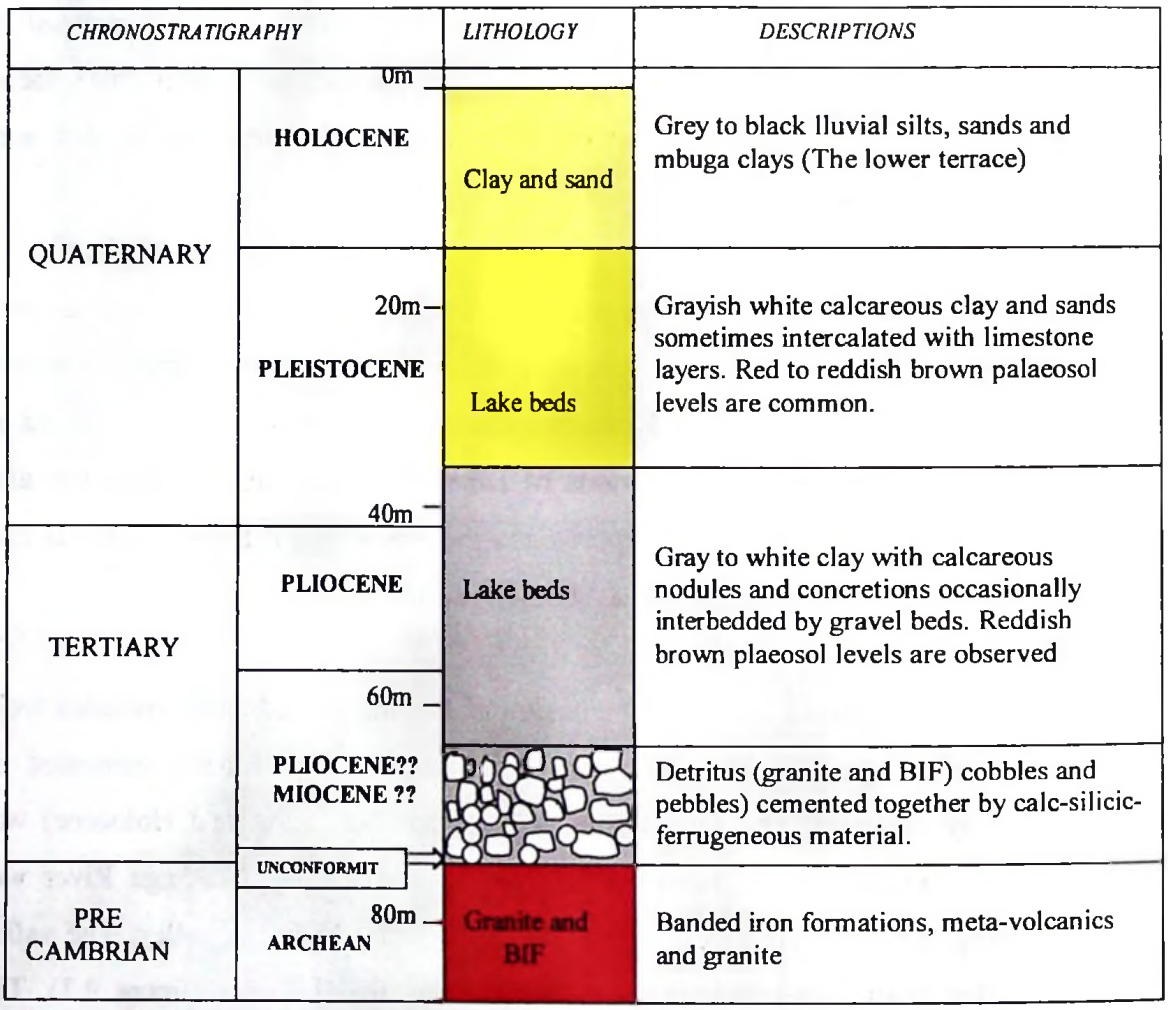

Figure 9.2: General stratigraphy of Manonga-Wembere deposits.

However, this study favors an age of Pliocene-Pleistocene for the Manonga-Wembere sediments as supported by stratigraphical evidence. The author believes that these deposits based on compositional (Mutakyawa 1997) and stratigraphical position (William and Eades 1939, Quennel *et al.*, 1956, Pickering 1958 and Barth 1990) equivalency are age equivalent to the Laetoli volcano-sedimentary deposits dating from 3.5Ma and younger. Nevertheless, an Ar/Ar dating of the Manonga-Wembere volcanic ashes and pyroclasts will remain to be of vital importance in ascertaining the absolute age of the deposits.

The economic importance of the Manonga-Wembere deposits lies in the conglomerates (Senkenke and Mwansarara) as sources of placer gold and diamond deposits. Efforts have been going on in the area to discover more gold reserves. So far gold is being recovered by artisan (small-scale) miners in Sekenke conglomerates and some gravely sediments in Kinungu near Igurubi. A gold mine is due to open soon in Lusu (Western part of the Manonga Valley) near Nzega town. Placer diamonds has been locally mined in garvels in Mdalagwigwe (near Susujanda) in the extream south of the area (figure 6.1 – chapter 6).

9.1.2 Geological, stratigraphical and palaeosol studies

9.1.2.1. Kininginila geology and stratigraphy

The Kininginila section is located in the central part of the Manonga-Wembere Valley. The geology comprises of the calcareous lacustrine deposits occupying the upper terrace, remnant of the filled Manonga-Wembere Pliocene palaeolake. The central part (around Manonga and Tungu River) forms the lower terrace which is covered by Holocene mbuga clays and alluvial sand, (figure 9.3). The stratigraphy is recorded on the Ing'ongholyambiti cliff near Kininginila settlement (figures 9.4A_{a-b}).

Figure 9.4 forms the basis of the following discussion. The stratigraphy begins with about 6m white to gray clay with two gravel bed levels (figure 9.4E_{a-c}). A reddish-brown (1m thick) palaeosol overlies the upper gravel bed. A 5m thick white to gray clay bed containing numerous calcareous nodules and concretions lies on top of the palaeosol. This bed grade into a white sandy siltstone at the top of the clay bed thereafter followed by a (3m thick) layered reddish-brown clay showing numerous distratification features.

Red to reddish brown palaeosol overlie the layered clay bed separated by a thin band of dark gray clay layer. Another thick (3m) reddish-brown palaeosol level is observed lying on a grayish white clayey siltstone layer separating it from the previous palaeosol (figure 9.4A_b). The upper part of the section is a series of grayish white silty mudstone, pale yellow clay and layered dark clay lying in succession on the reddish brown palaeosol.

The sequence is finally covered by a white calcareous (present) soil, which in places becomes a black (cotton) soil. At the middle of the valley lies the present Manonga river coarse cutting deep the alluvial and mbuga clays of the lower (Holocene) terrace (figure 9.3). These sediments are mainly black mbuga clays mixed with alluvial sands deposited by the present Manonga River and Tungu tributary mainly in the eastern edge of the valley.

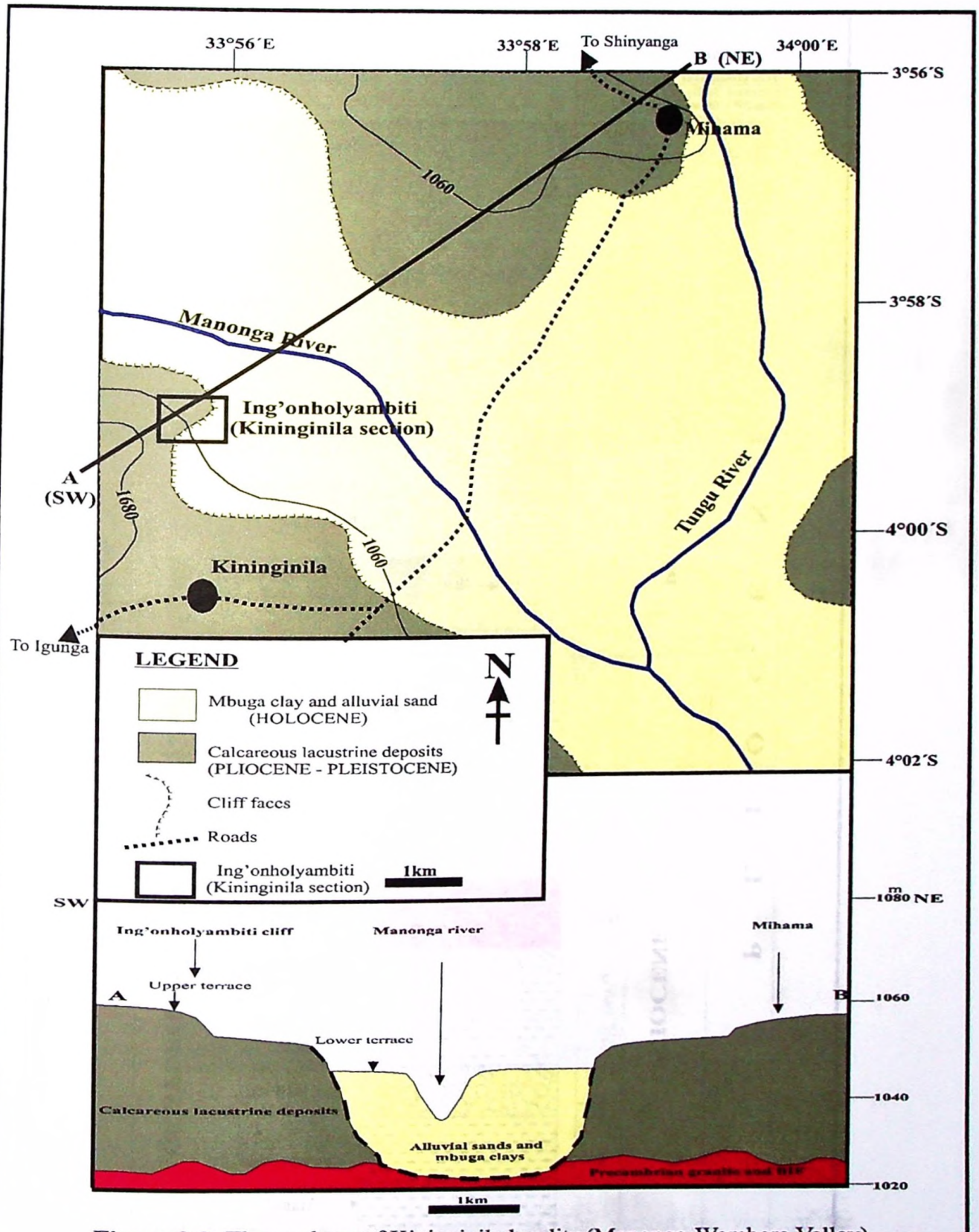

Figure 9.3: The geology of Kininginila locality.(Manonga-Wembere Valley). [The cross-section AB indicates the stratigraphical positions of Manonga-Wembere Valley deposits at the Kininginila locality]

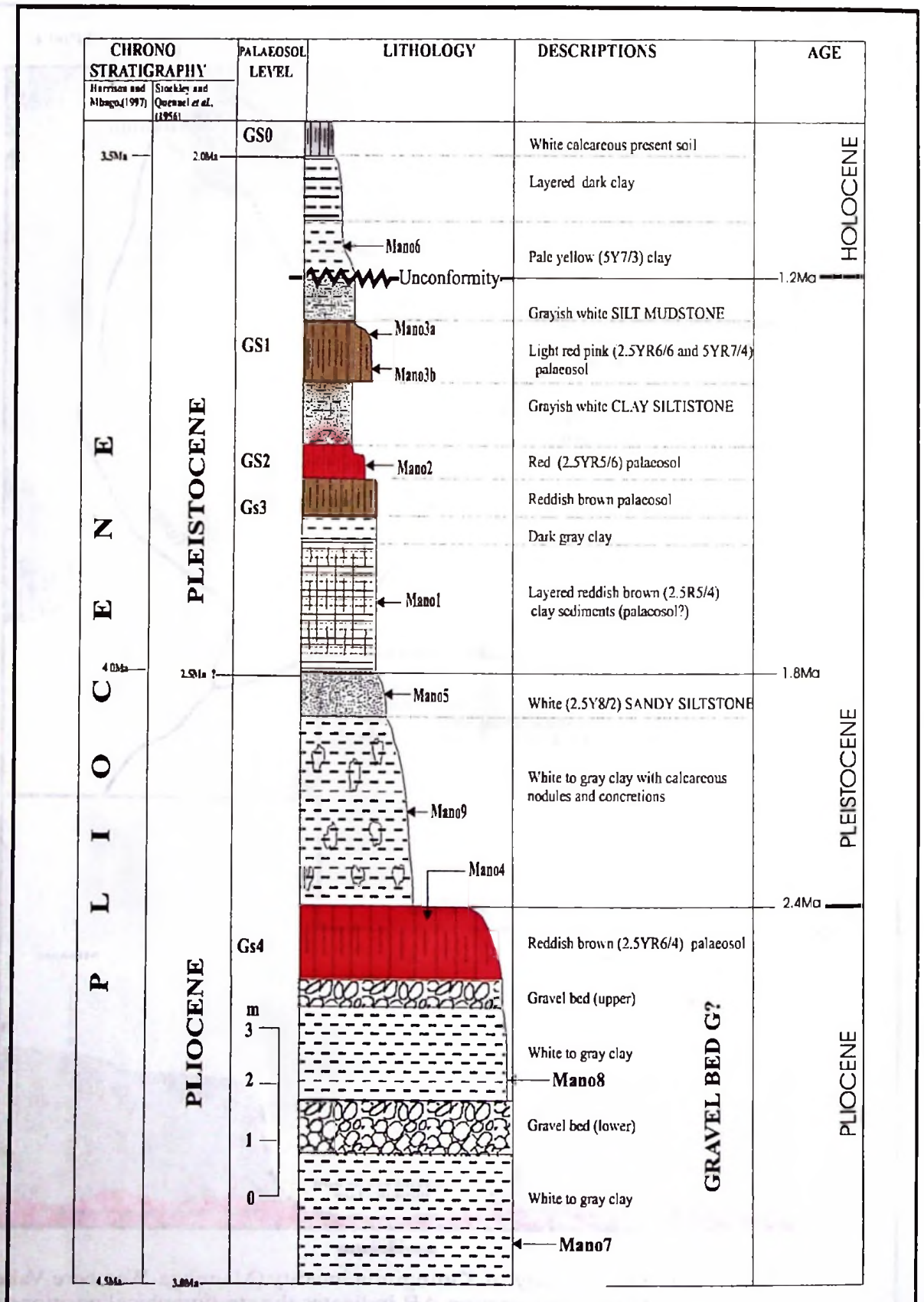

Figure 9.4: The chronostratigraphical column of Kininginila section in Manonga-Wembere Valley.

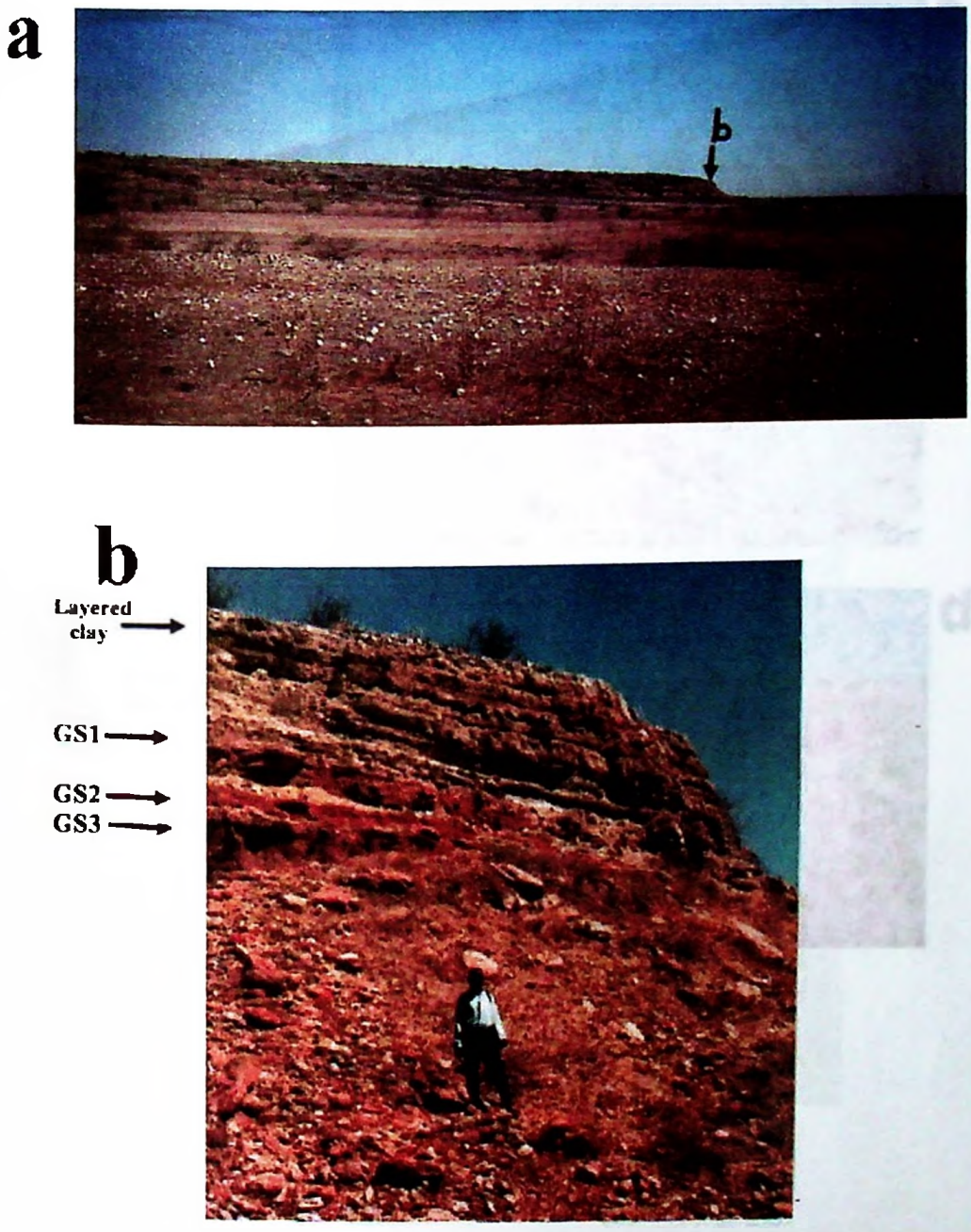

Figure 9.4A: Manonga-Wember Valley locality, **a:** The perspective view of the Kininginila area, **b:** The upper terrace cliff exposing the layered dark clay and the reddish brown palaeosol levels GS1, GS2 and GS3.

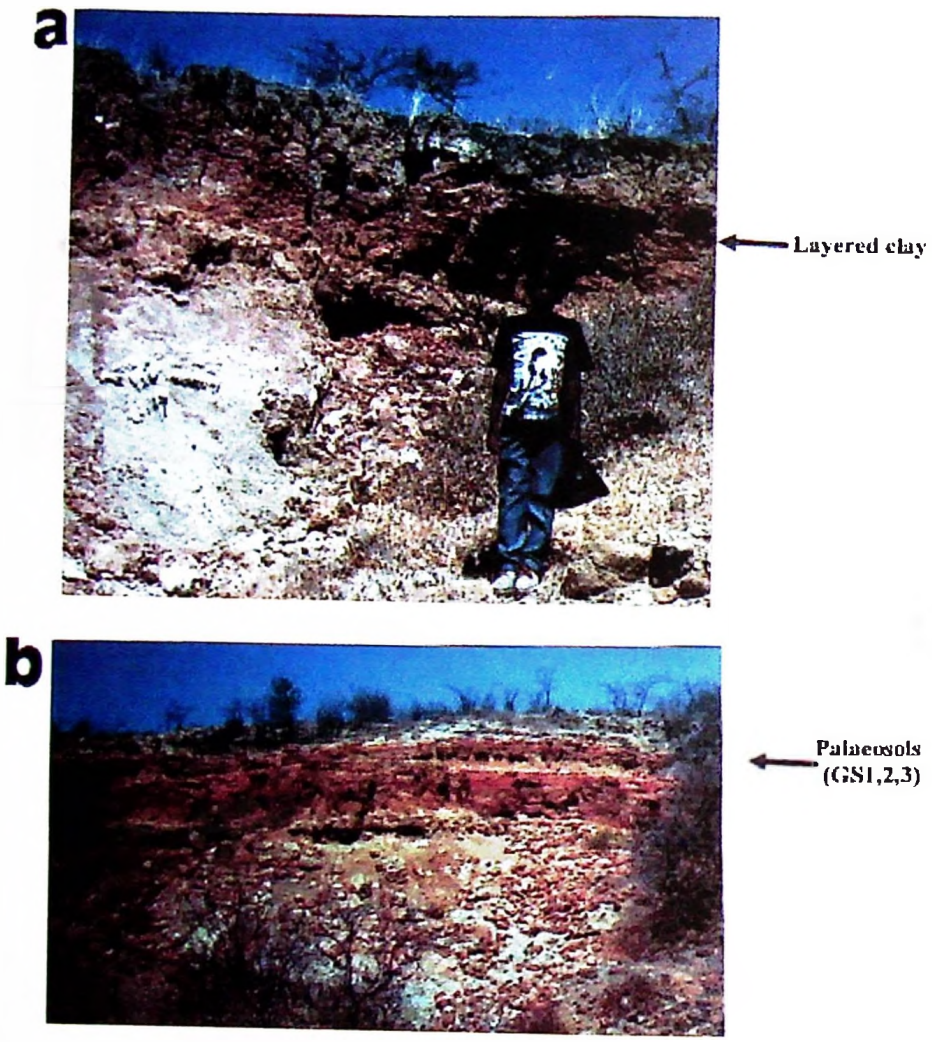

Figure 9.4B: The Kininginila section (Manonga-Wembere deposits), **a:** Detail of a layered dark clay, **b:** Detail of the red to reddish brown palaeosol levels GS1, GS2 and GS3,

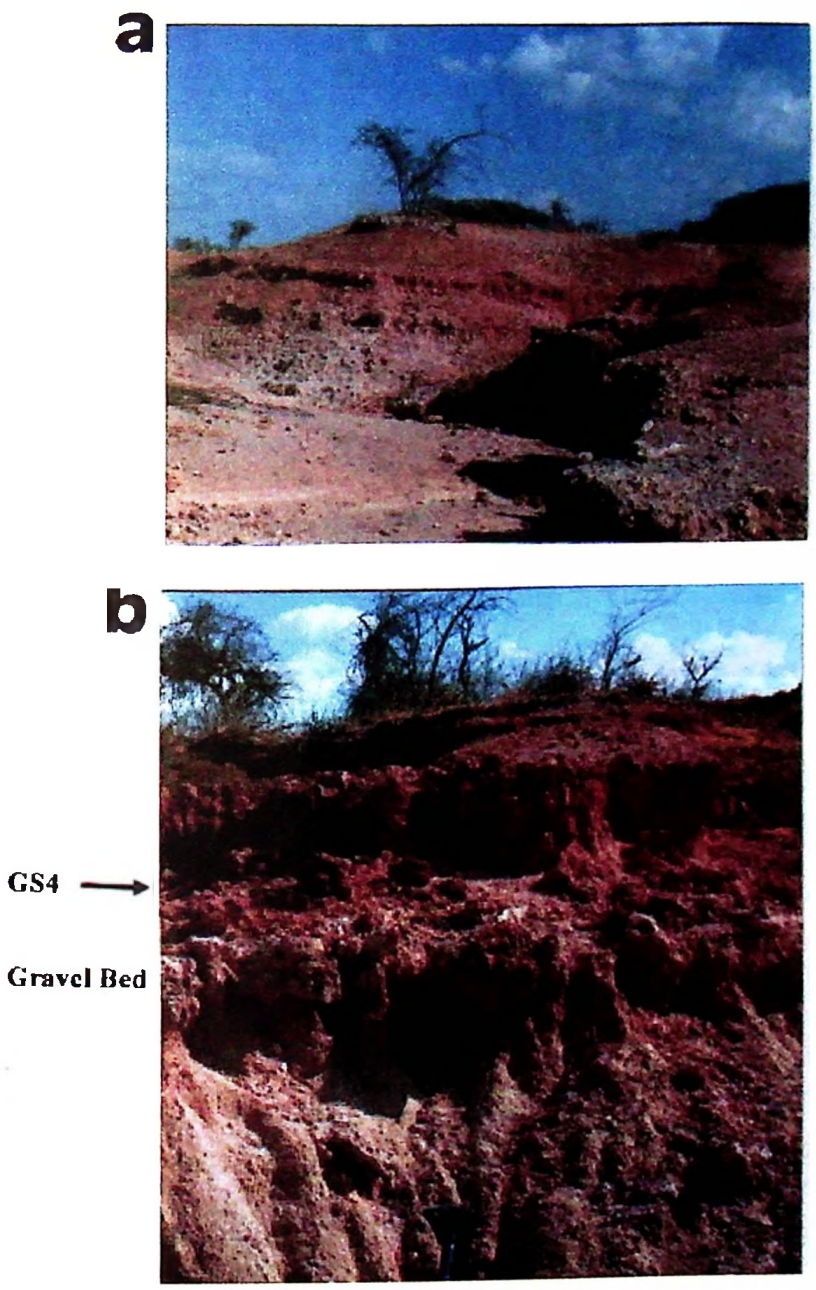

Figure 9.4C: GS4 palaeosol level of Manonga-Wembere deposits, **a:** A perspective view of the red to reddish GS4 palaeosol level, **b:** Close up of GS4 indicating the gravel bed lying below the palaeosol.

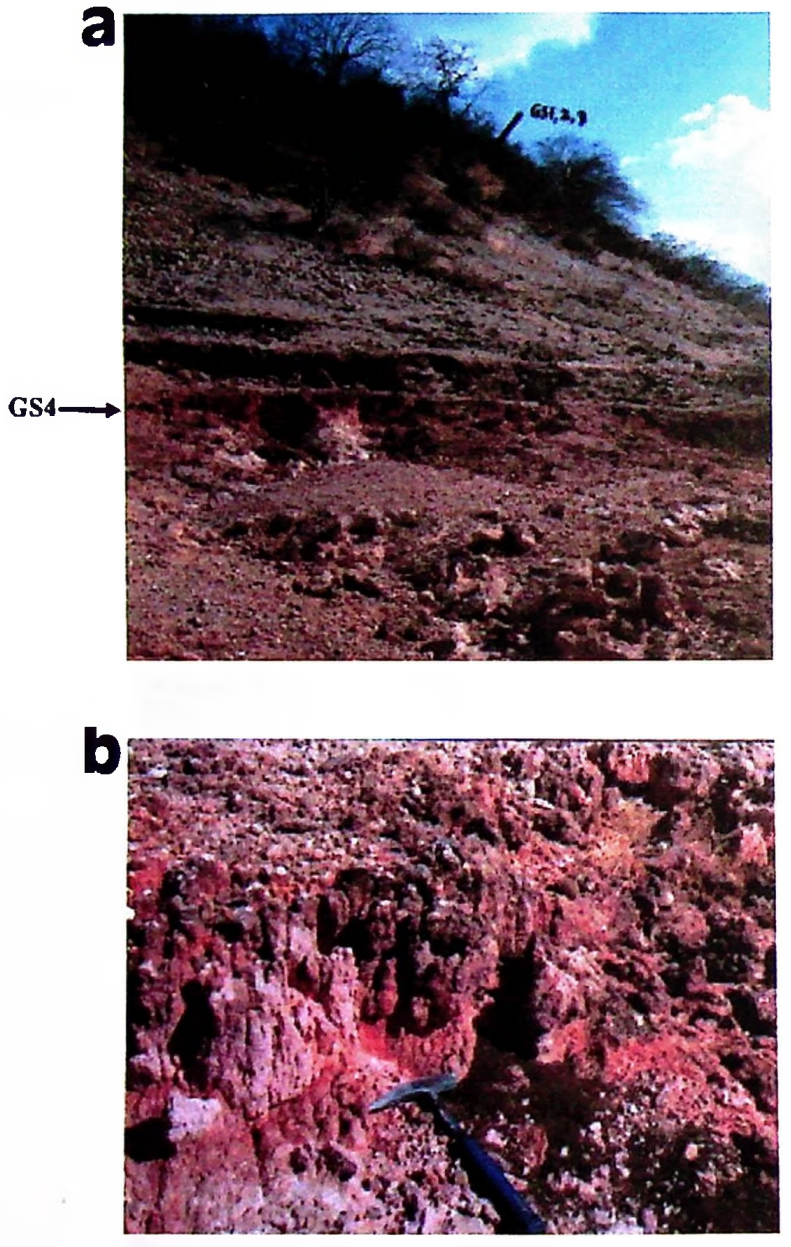

Figure 9.4D: GS4 palaeosol level, **a:** The position of GS1, GS2 and GS3 is indicated by arrow relative to GS4, **b:** Close up of GS4.

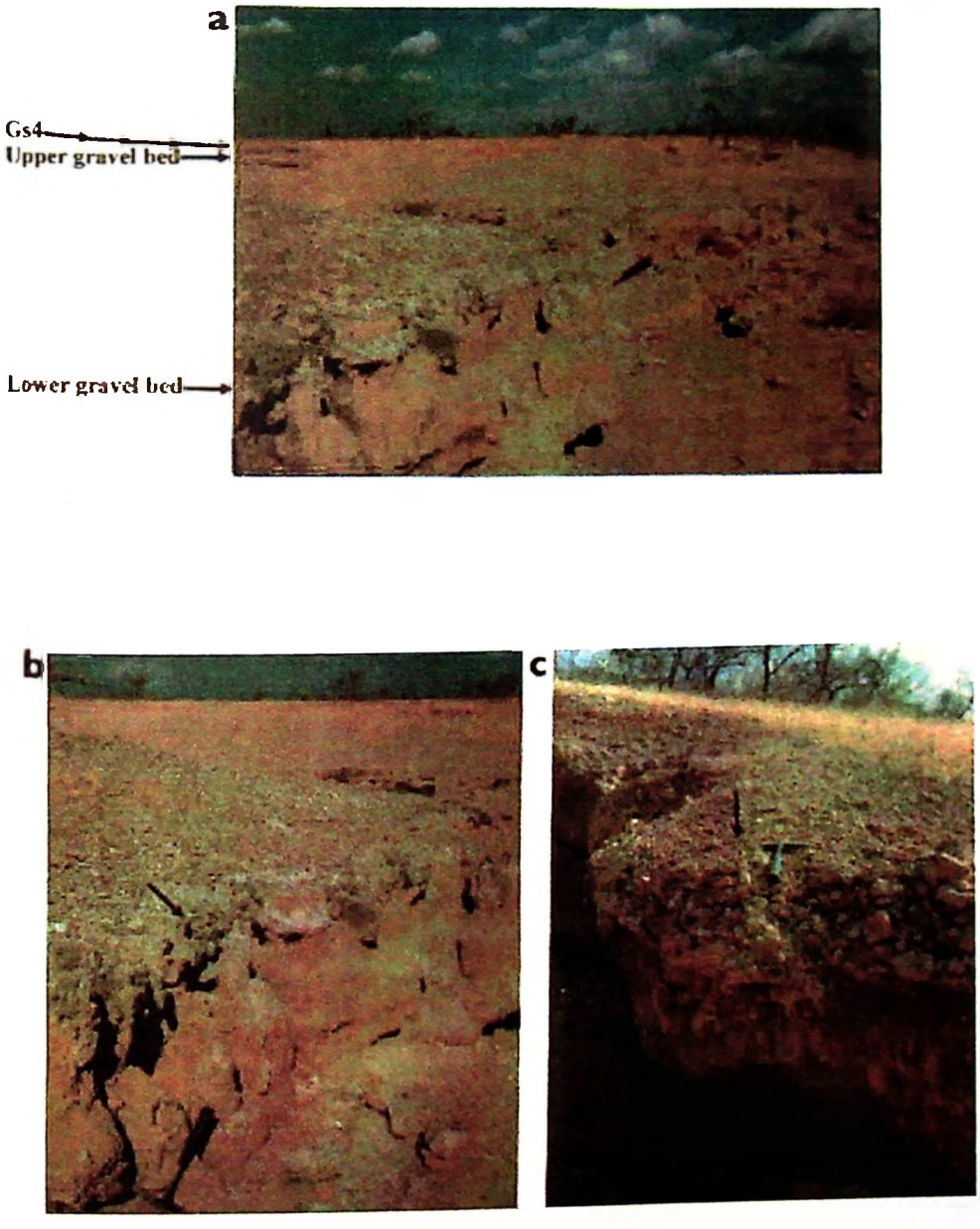

Figure 9.4E: The gravel bed of Kininginila section (Manonga-Wembere Valley): **a:** Stratigraphic positions of GS4, upper and lower gravel beds as observed in the middle terrace of the valley; **b:** Close up of the the lower gravel bed and **c:** close up of the upper gravel bed.

9.1.2.2. Magnetic susceptibility and Short Wave Infrared Reflectance (SWIR) spectrometry record of palaeosols of Kininginila section

Although the Manonga-Wembere palaeosols levels characterize the occurrence of animal fossil beds, their stratigraphical and pedogenic aspects are still under study (Harris & Mbago 1997, and Verniers 1997). This part presents magnetic susceptibility and (SWIR) spectrometry mineralogy (clay and carbonate) studies (table 9.2) of some palaeosol levels of the Kininginila section.

In the Kininginila section four red to reddish brown palaeosols (GS1, GS2, GS3 and GS4) are observed, (figure 9.4A-D). The present soils (GS0), (figure 9.4B) is a white soil developed on the calcareous lakebeds. The summary of the important characteristics of the palaeosols is given in table 9.1.

Table 9.1: Clay mineral composition and description of the palaeosol levels of the Kininginila section.

Palaeosol	Depth/thickness (m)	Lithology	Description	Characteristic minerals
GS0	0 – 0.55	Calcareous sediments	Present soil with present root activity	
GS1	4.5 – 7	Clay	Light red (2.5YR6/6) showing red mottling.	Palygorskite, sepiolite, analcime, stilbite.
GS2	8 – 8.5	Massive clay	Red (2.5YR5/6) showing gray mottling	Illite, Kaolinite, Halloysite, gibbsite.
GS3	8.5 – 9	Layered clay	Reddish brown (2.5R5/4) with gray mottling	Palygorskite, stilbite, Analcime
GS4	18.4 – 19.6	Clay	Reddish brown (2.5YR6/4) with carbonate concretions.	Kaolinite, halloysite Stilbite, gibbsite

Table 9.2: Clay minerals, Carbonate and magnetic susceptibility variation of some palaeosol levels of manonga-Wembere deposit (Kininginila section)–Refer figure 9.5.

No	Sample	X(m3/kg) x 10^{-8} (SI units)	Carbonate IR(%)intensity	Clay minerals IR(%)intensity	Depth(m)	Plaeosol level
1	mano6	19.2994	17.32	15.31	1.5	
2	mano3b	36.3903	15.98	8.65	3.5	GS1
3	mano3a	18.8619	20.65	11.31	3.9	GS1
4	mano2	16,685.30	15.1	5.2	5.3	GS2 &GS3
5	mano1	19.6459	29.9	20.04	7.2	
6	mano5	12,276.10	25.98	17.32	9.5	
7	mano9	20.2226	No data	No data	11	
8	mano4	14,541.10	33.97	21.98	13.8	GS4
9	mano8	23.384	No data	No data	15	
10	mano7	38.706	No data	No data	16.4	

Palaleosol levels GS1 and GS3, (figure 9.4A_b) are dominated by palygorskite and sepiolite clay minerals together with zeolites (analcime and stilbite) indicating that pedogenesis took place during a dry climate where precipitation was not sufficient to leach out the zeolite minerals. Palaeosol levels GS2 and GS4 are dominated by kaolinite and halloysite 1:1 clay minerals and gibbsite a sign of wet environments during the formation of the palaeosols. Low concentration of clay minerals and carbonate also suggest that most of the 2:1 clay minerals may have been converted to 1:1 clay mineral or into gibbsite. And the carbonate completely leached out during intense weathering conditions. Magnetic susceptibility, carbonate and clay minerals quantity (concentration) variations (table 9.2 and and figure 10.2) indicate a considerable climatic fluctuation in the Manonga-Wembere Vallley during the Upper Pliocene and Lower Pleistocene. Red to reddish brown palaeosol (GS2 and GS4) show very high magnetic susceptibility values suggesting that magnetic minerals might have been concentrated during soil forming processes, in which clay rich lake beds were affected by pedogenesis during wet climates.

During these wet climates most of the carbonate minerals were leached away and clay mineral varieties reduced in number as earlier explained in the preceeding paragraphs. Palaeosol GS1 and GS3 on the other hand show low magnetic susceptibility values with more concentration of carbonates, indicating that soil-forming processes did not leach out the carbonates and that no magnetic minerals were concentrated during pedogenesis. This suggests a drier climatic condition.

9.1.2.3. Palaeosol micromorphology and palaeoenvironments of Manonga-Wembere Valley.

The Manonga-Wembere Valley deposits are mainly calcareous clay deposits. They have a high calcium carbonate content (5% - 95%) indicating that they were formed in a predominantly saline lake environment thus refered to as lacustrine lakebeds, (Quennell, *et al.*, 1956 and Veniers, 1997). The Manonga-Wembere Valley red to brown palaeosols contain enomous evidence of clay illuviation as is indicated in figure 9.5. The micromorphological characteristics show yellow to red illuviation clays (red to yellow clay coating and coating fragments) and the presence of Fe-Mn hydr(o)xide coatings and nodules. Micrographs show a red argillic fabric generally consisting of an accumulation of oriented reddish yellow clay coating fragments indicating an intense illuviation. Such illuviation fronts are common in calcareous sediments in warm and humid (mediteranean type) climates, (Stoops, 1999 – personal communications and Kafumu *et al.*, 1999).

Palaeosol levels of manonga-Wembere Valley deposits therefore attets to the presence of a warm humid climate during the Upper Pilocene and Lower Pleistocene. The presence of Fe-Mn hydr(o)xide coating indicate a substantial hydromorphic regime during this time. Field observation show that these palaeosols levels posses a strong red to brown color. The yellow to red illuviation clays (red and yellow clay coatings and fragments) accompanied by the absence of calcite and reddening of groundmass in a predomintly gray calcareous clayey sediments points to weathering during a wet/humid climate. The above micromorphologic features and field evidence may provisionally suggest that the palaeosols were probably alfisols.

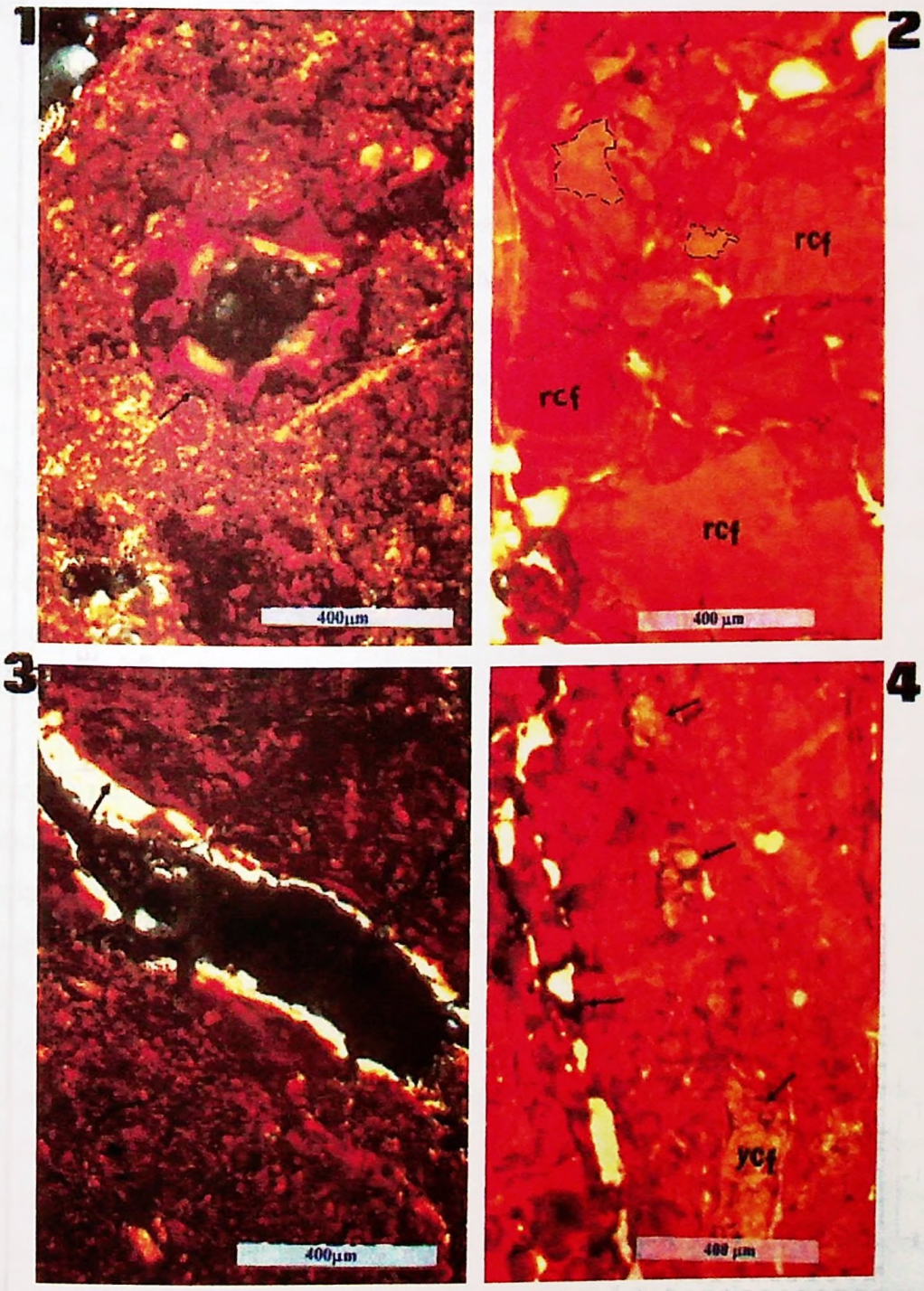

Figure 9.5: Some micromorphological characteristics of red to brown palaeosol levels of Manonga-Wembere Valley deposits (Kininginila section): **GS1; 1.** Strongly oriented homogeneous red clay coating on channels. The groundmass consists of a yellow mass of clay (PPL). **2.** A groundmass composed of microlaminated yellowish red clay coating fragments (rcf) (PPL). **GS4; 3.** Typic yellowish red clay coating on a void. **GS2; 4.** Yellowish clay coating fragments (ycf) in a turbated yellowish red groundmass. Fe-Mn (hydr)oxide hypocoating on a chain of parallel channels infilled by yellow clay. Note the parallel orientation of the clay coating fragments and the channels.

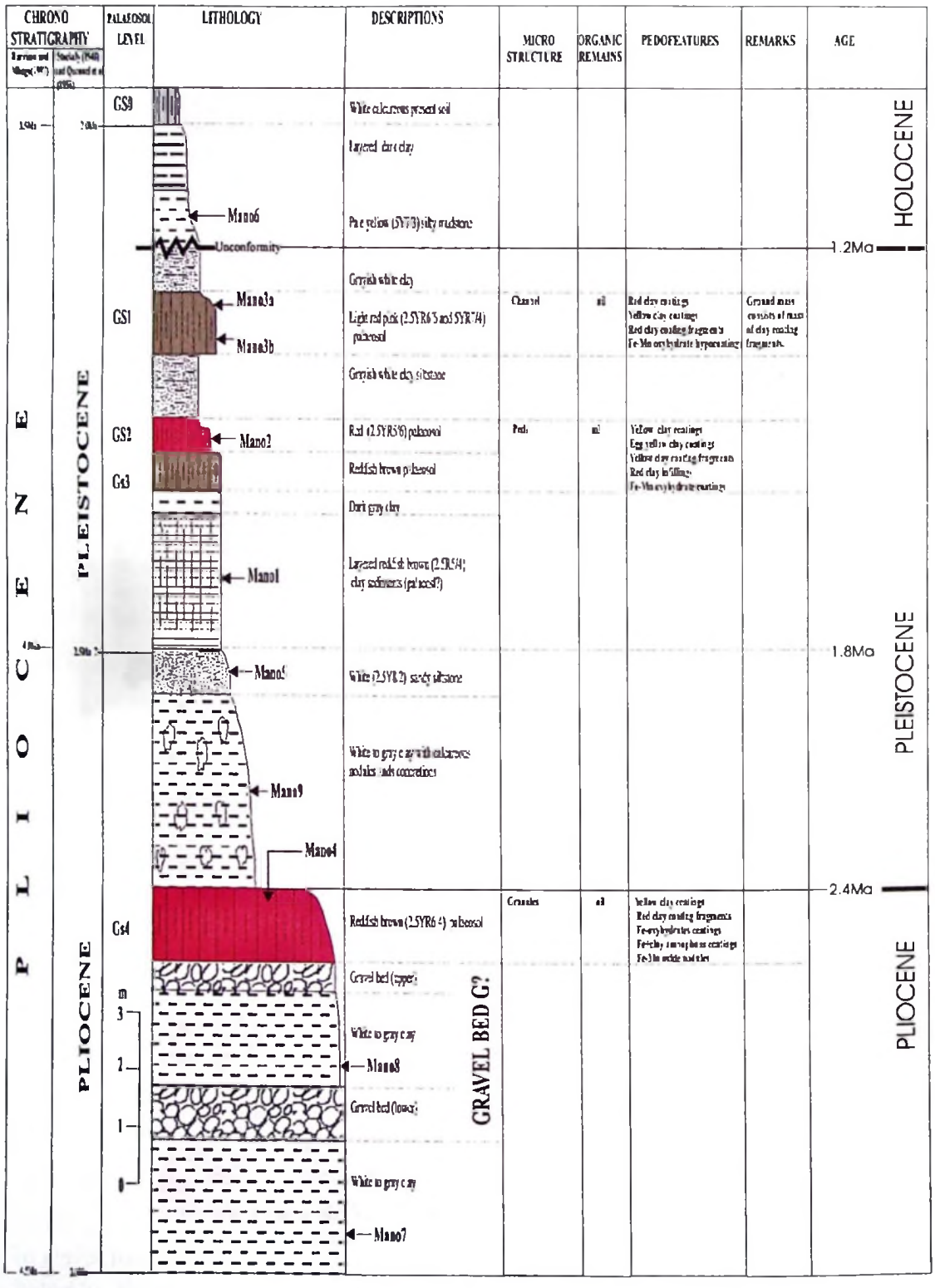

Figure 7.1b: Manonga-Wembere Valley stratigraphy showing some red to brown palaeosol levels with their micromorphological pedofeatures

9.2 HOLILI LOCALITY

9.2.1 Geological setting

Holili locality is located in northern Tanzania (figure 9.6) in the Kilimanjaro volcanic field. The Kilimanjaro volcanic field is a mountaneous massif rising abruptly from the plateau country at about 1,700m a.s.l and ends up on the Kibo Uhuru peak at 5,896m a.s.l, the highest point on the African Continent, (figure 9.6A_{a-b})

The summary of the geology consists of a pile of Pleistocene-Holocene volcanic rocks frequently interbedded with sedimentary units. These rock deposits accumulated on eroded surface of Precambrian metamorphic rocks. The volcanic products are a result of three major volcanic centers, which now correspond to the three main topographic summits of Shira, Kibo and Mawenzi (Figure 9.6).

Shira is the oldest eruption center and is composed of mainly basalt-trachyte-andesite volcanic rock assemblages, (Downie *et al.,* 1964). The volcanics of the Shira outcrop mainly to the north, south and west. The eastern part has been covered by younger eruptions (figure 9.6). Kibo volcanic rocks occupy the central and northern part of the Kilimanjaro geology. These rocks show a strong alkaline differentiation and range from trachyandesite-nepheline to phonolite. The Mawenzi volcanics are composed of ankaramite, trachytes, andesites and basalt series. The former lava flows extend far to the south (Downie *et al.,* 1964) up the Holili area where they have been classified into Rombo series. In this area the lava series consists of dense vesicular olivine basalt. These lavas are covered by extensive calcareous tuffaceous grit identified as a pyroclastic unit. The lava flows are exposed in highly incised stream walls and the walls of Lake Chala.

In brief the geology of the Kilimanjaro volcanic field therefore consists of volcanic rocks from Shira, Kibo and Mawenzi volcanic centers covering the field. Shira volcanic episode is the oldest (about 0.75Ma) followed by Kibo. Mawenzi is the youngest (0.35Ma) volcanic eruption.

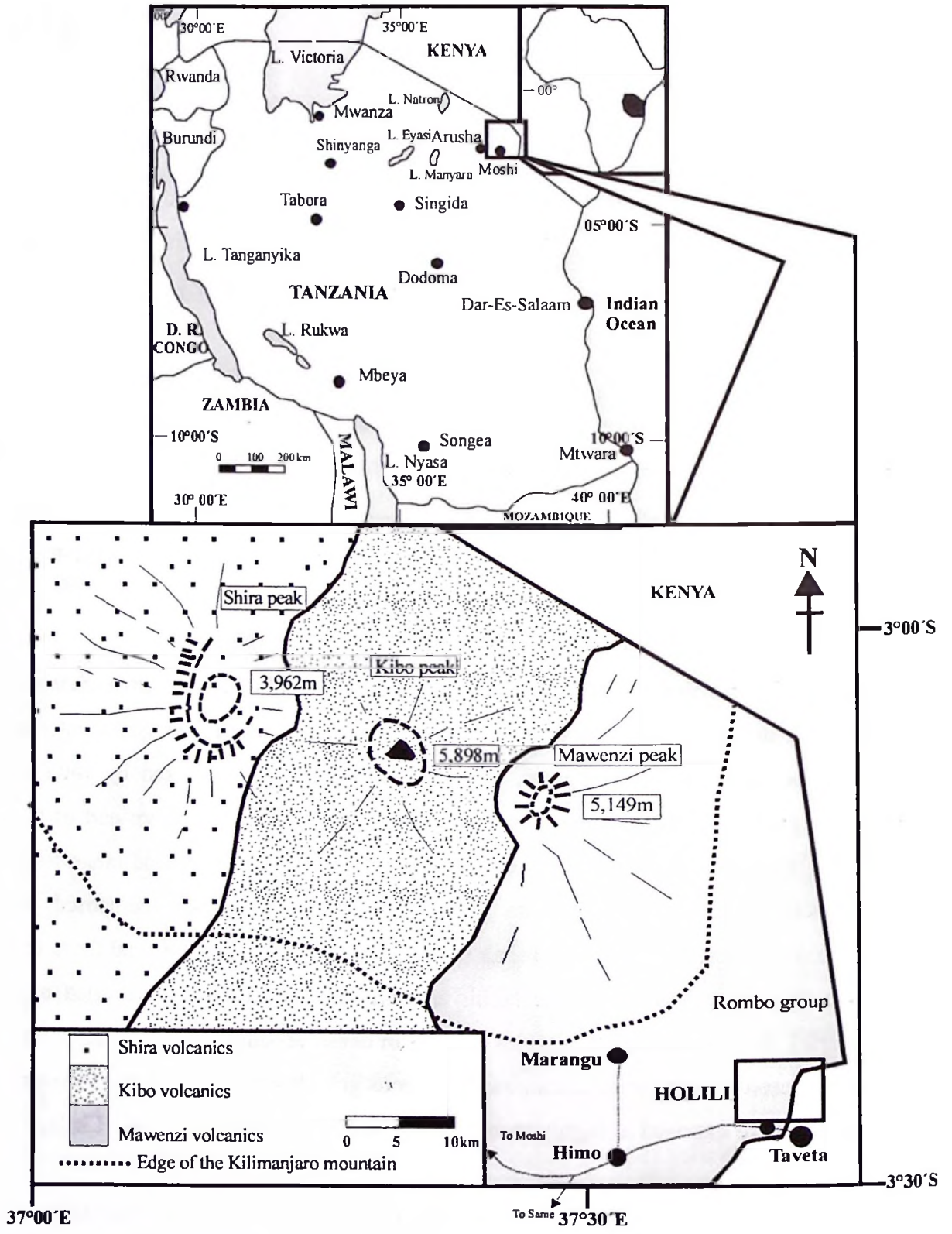

Figure 9.6: Geology and location of the Kilimanjaro volcanic field [Holili locality (SE edge of the field) is covered by Mawenzi volcanic rocks referred to as Rombo group.

a

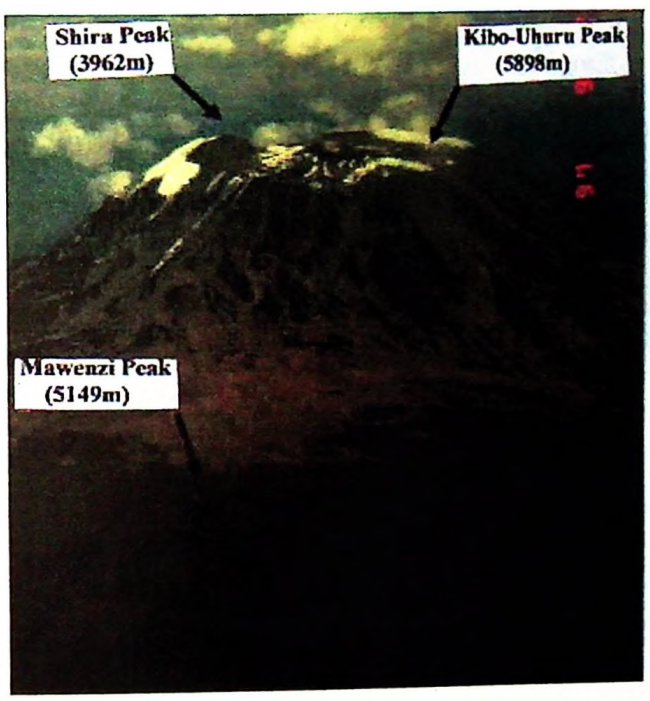

b

Figure 9.6A: The Kilimanjaro Mountain. **a:** View of the Mawenzi (fore ground), Kibo (middle) and Shira (in background) peaks. **b:** The Kibo-Uhuru (5896m above sea level) peak, the highest point on the African Continent.

Mawenzi volcanic rock referred to as Rombo group covers Holili locality (SE edge of the field). The Holili area contains thinner volcanic cover above the paleolandscape making it possible for archaeological research.

9.2.2 Geological, stratigraphical and palaeosol studies

9.2.2.1. Geology and stratigraphy

Holili area has a gently undulating topography (between 1200m and 1700m above sea level) dissected by streams. The streams form steep gorges (20m deep). The area is covered by basalt lava flows laid on a Precambrian surface of Usagaran metamorphic rock system. This basement complex appears as relic inselbergs of an old peneplanation. The Kilimanjaro volcano grew from a gently undulating plain (1600m a.s.l) to a huge mountain of over 6000m-a.s.l elevation during the Middle Pleistocene – 0.75Ma to 0.25Ma (Hanby, 1987). The Holili age range of the basalt is estimated between 0.25Ma and 0.35Ma (Wilkinson *et al.,* 1986). The Middle Pleistocene corresponds to a time of reduced volcanic activity in which the basalt formed a stable landscape and pedogenesis took place forming a blanket of red soils on the basalt. Field observations indicate that root casts channels and rootlets, penetrate the 0.5cm to 3m thick palaeosol. This landscape was an animal living floor that could probably including hominids. Another period of volcanic activity occurred during the Upper Pleistocene (Kanza, 1985). A carbonate rich tuff erupted from the present day Crater Lake Chala about 5km to the north (figure 9.7a) which covered the area with thick tuffaceous grit deposits (Figures 9.7b and $9.8a_{1\text{-}2}$).

The base of the gritstone grades into a tuffaceous mudstone. This mudstone lies unconformably on the red palaeosol (Figure 9.7b and 9.8A). The grit is composed of sand-sized basalt, quartzite, and gneiss fragments cemented by calcareous material of amorphous carbonate or crystalline (calcite) carbonate. Under the influence of water the carbonatite tuff cemented rock fragments to form a light hard grit. The upper part of the gritstone is loose probably because of continuous exposure to weathering. On top of the loose gritstone present (Holocene) red soil continues to form (figure 9.8_{a1})

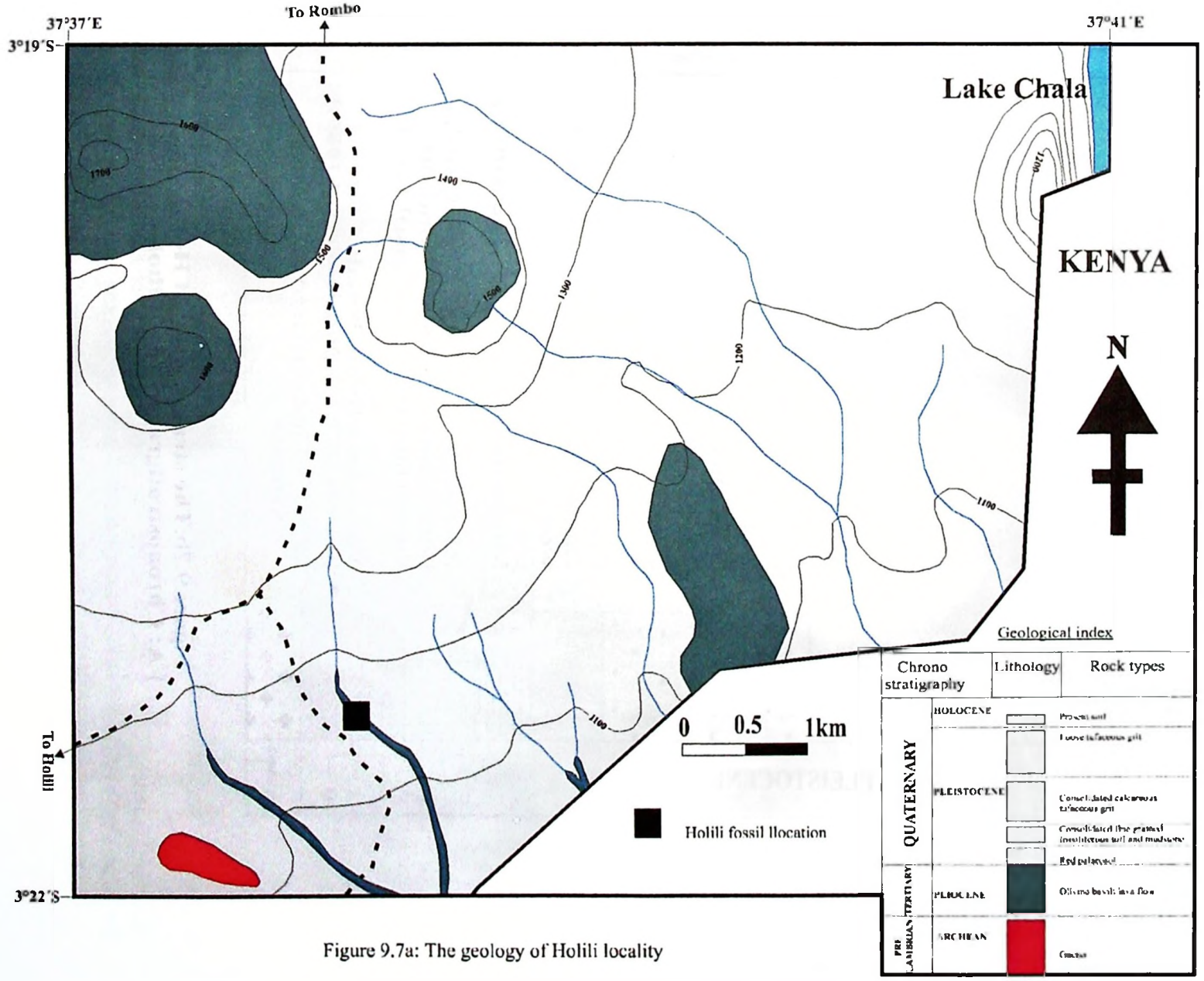

Figure 9.7a: The geology of Holili locality

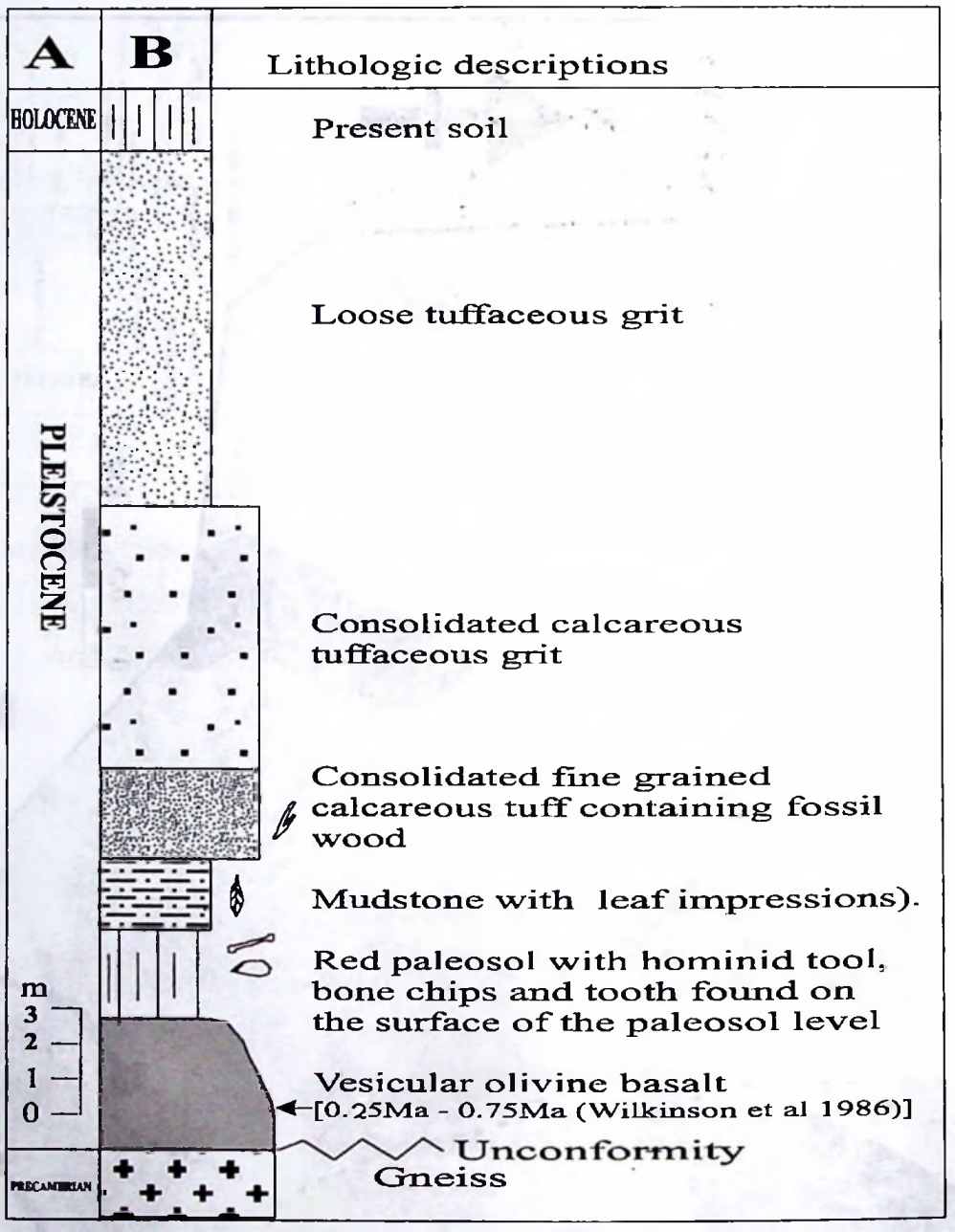

Figure 9.7b:**The stratigraphy of Holili**
[A: Chronostratigraphy; B: Lithologic units]

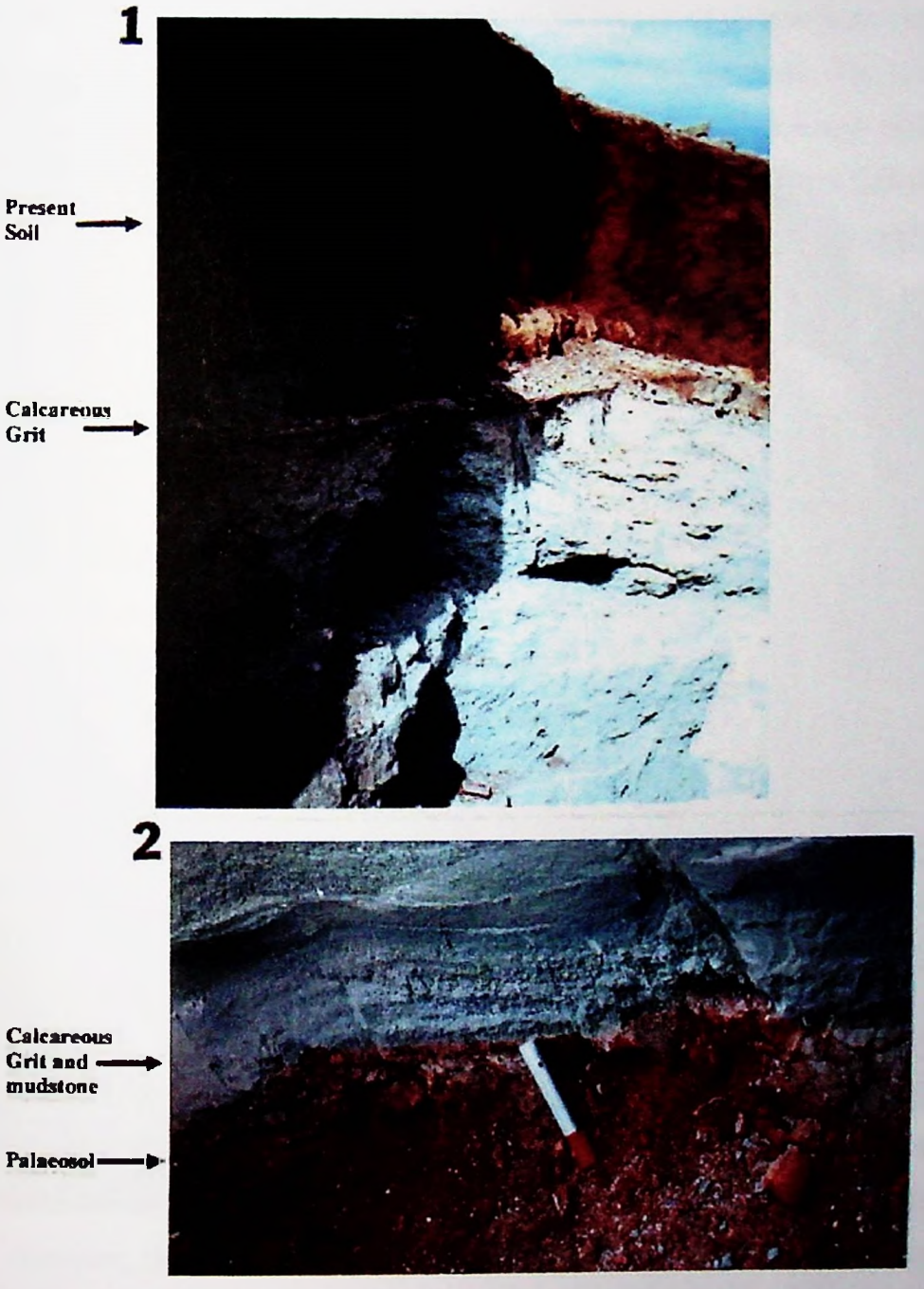

Figure 9.8a: Soil and palaeosol levels of Holili locality. **1:** Holocene (red soil) developing on a loose calcareous grits. **2:** Consolidated calcareous grits overlying a red Pleistocene palaeosol.

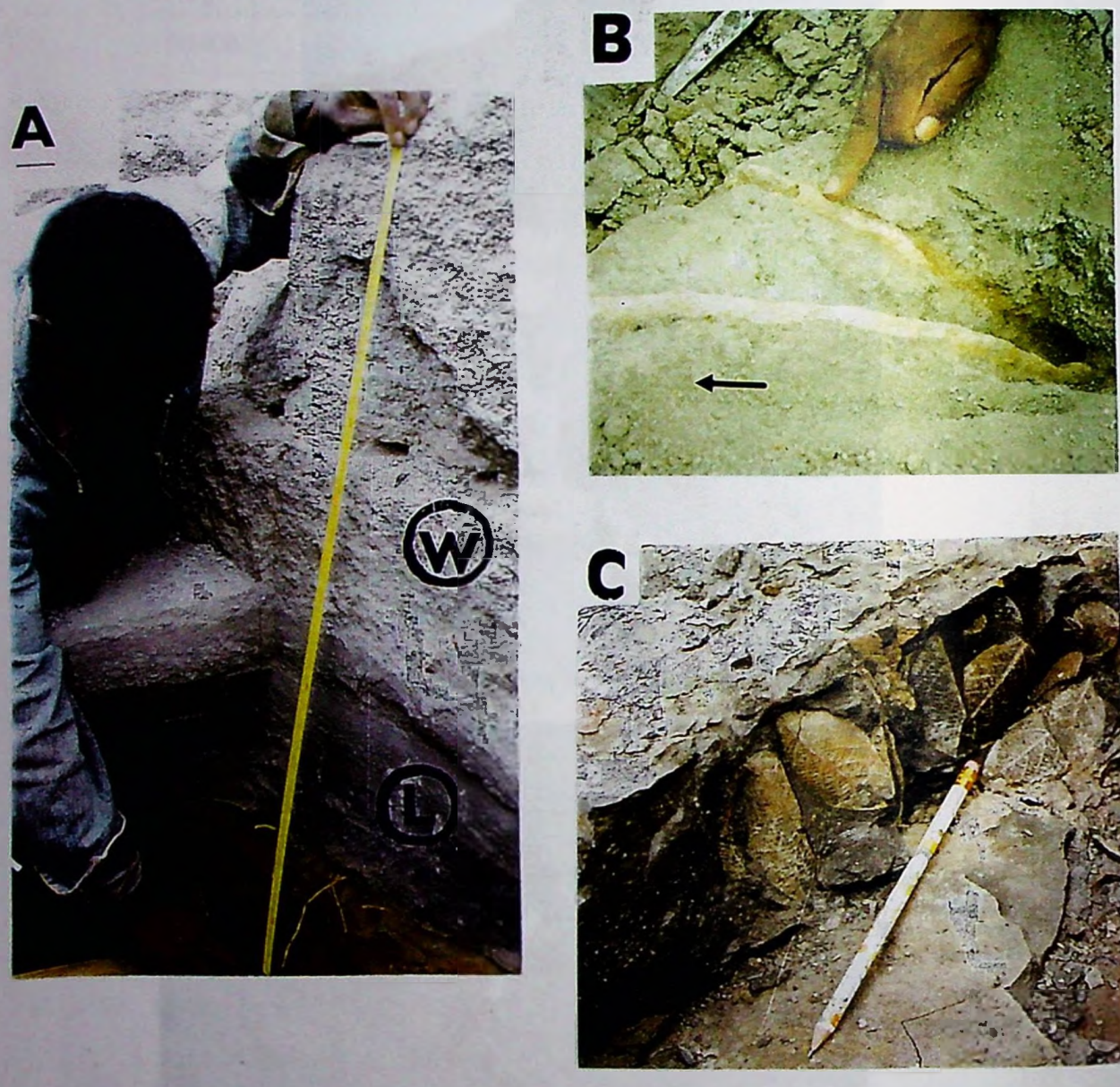

Figure 9.8b: A: Red palaeosol/grit geological boundary (palaeolandscape). Animal fossil remains and a *hominid* tool were found on this boundary. **B:** Insitu fossil wood in the tuffaceous grits – position W in A. The arrow in B indicates the direction of tuff flow. **C:** Insitu leaf impression of an *angiosperm-dicotyledon* plant in mudstone position L in A.

The detailed geology and stratigraphy of Holili area can thus be summarized as follows (figure 9.7a-b). The Precambrian basement rocks is covered by lava flows (basalt) of the Kilimanjaro volcanic episode. Then a soil developed on the basalt. The landscape was finally covered in succession by tuffaceous mudstone and calcareous tuffaceous grit erupted from Lake Chala 5km NE of the area. The palaeosol (red)/grit (gray) geological boundary (figure 9.8a) is a palaeolandscape with a big potential of recovering palaeosol mammal fossils including hominids. The hominid stone tool was found together with animal fossil remains on this boundary.

9.2.2.2. Palaeosol and the fossil record

Fossil record and the palaeoenvironment

Some animal and plant remains were recovered from the Holili Quaternary deposits as described in this section. Tooth (figure $9.9A_1$), fragments of a fossil bone (articulation of a canon bone of a large animal - figure $9.9A_2$) crushed by mining activity, 2 horn cores (figure $9.9A_3$), and bone chips, (figure $9.9A_4$). These represent the fauna of Middle to Upper Pleistocene times in Holili area. Due to the nature of the fragments it is not possible to tell what kind of animals the bones represent. Nevertheless, the tooth shows a *selenodont* dentition indicating a herbivorous animal (probably a *bovid*). The bone horn core points to an antelope-like animal.

Hominids might have lived in the area as indicated by the presence of a primitive stone tool (figure $9.9A_{5-7}$). The hominid tool was found together with the bone chips, tooth and horn bone cores. This might indicate that the fossils were found on a hominid-butchering site. However, the sub-rounded texture of the tool disputes the former assumption as the tool and the fossils might have been transported before being re-deposited in the final site. If the former view is adapted it then should be assumed that the sub-roundness of the tool might be due to ware and tare because it was long used. There were also leaf impressions, which were found in a mudstone layer overlying a palaeosol level. The mudstone shows leaf impressions (figure 9.8b and $9.9B_{1-2}$) sometimes with twigs and small branches (figure $9.9B_{3\&4}$) of an *angiosperm dicotyledon* flowering plant. The plants

and mudstone indicate presence of water bodies in the landscape where plant and animal life might have flourished during the Middle Pleistocene.

The calcareous tuffaceous grit overlying the mudstone contains wood (branches?), (figure 9.8b) fossils as indicated by position W in figure 9.8b. The trees were rapidly covered by the invading calcareous tuff causing them to slant in the direction of the tuff flow as is indicated by the arrow in figure 9.8B. It was observed that the upper part of the plant (branches) is found in the calcareous grit and mudstone, while the lower part (roots) rest in the palaeosol. This indicates that the tuff flow covered the landscape quite rapidly and preserved it.

Holili occupation level (paleolandscape) would be a pontetial research locality for human origin, as it is covered by tuff material of carbonatite rock composition. The carbonate acted as cement when it was wet to seal off the taphonomical sites.

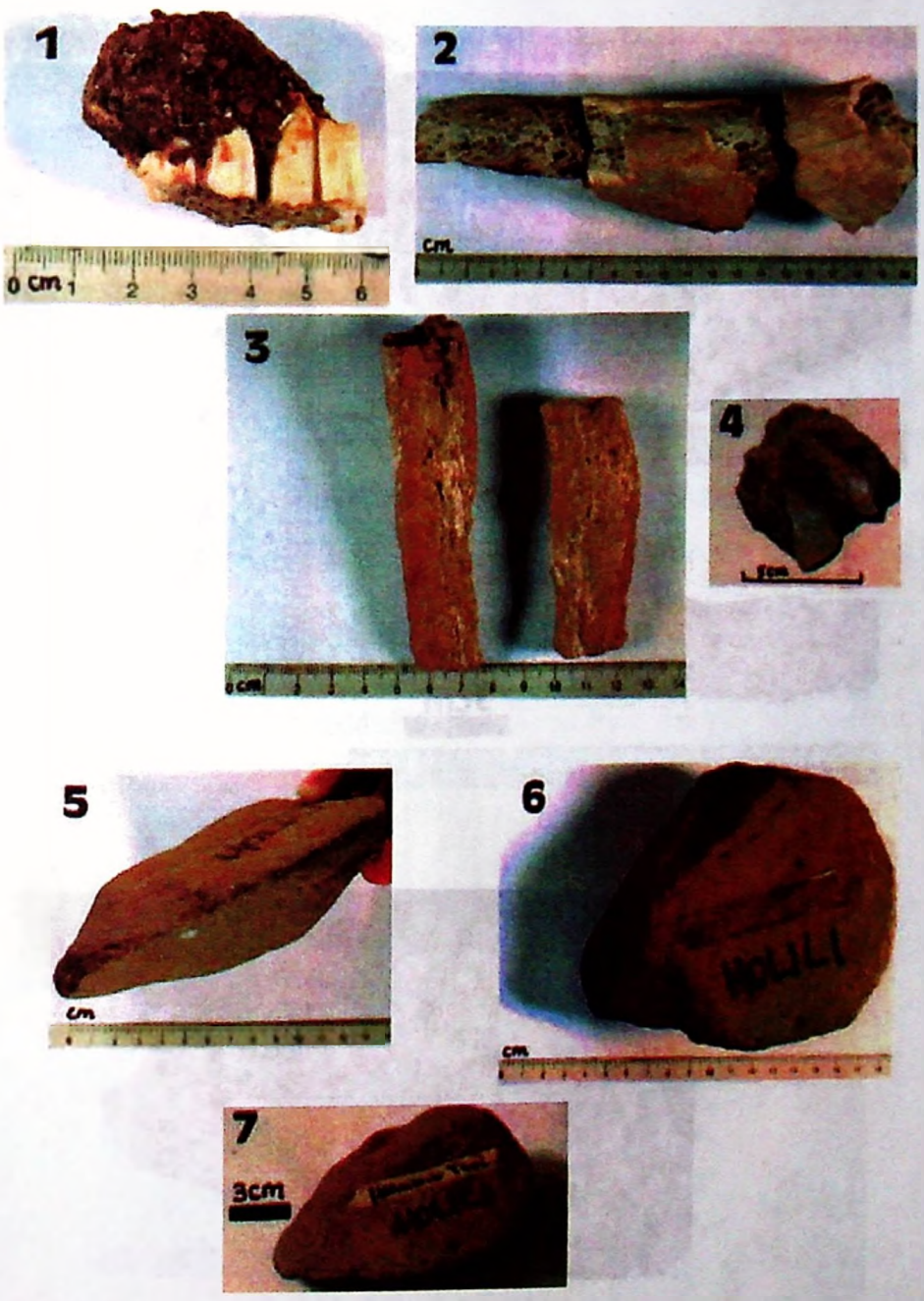

Figure 9.9A: Fauna fossil remains of Holili. 1: Tooth (*selencdont* dentition – bovid?). 2: Canon bone fragment. 3: Horn cores (bovid?). 4: Bone chips. 5=adge view, 6=plan view, 7=side view of a *hominid* tool. [The presence of a primitive tool indicates the possibility of discovering hominid remains in the area]

Figure 9.9B: Floral fossil remains of Holili: **1:** Specimens of leaf imptressions of an *angiosperm dicotyledon* flowering plant. **2:** Dark gray mudstone containing leaf impressions. **3:** Specimen of fossil wood. **4:** Mudstone containing impressions of leaves, twigs and small brances.

Palaeosol micromorphological characteristics

The red color (Munsell color – 10R4/6 light red) palaeosol level present in the Holili stratigraphy rests on a basalt lava flow and thereafter covered by thick sediments of calcareous grits. Micromorphological features of the palaeosol level are described below and some diagnostic features given in figure 9.8b.

In general the palaeosol contain microagregate microstructure. The coarse components consist of silt sized angular quartz grains (2%). Very rare pseudomorphs of primary minerals sometimes completely leached away. The palaeosol have a very open porphyric coarse-fine related distribution and an undifferentiated striated b-fabric. No organic remains are observed (appendix 7.2). The pedofeatures include numerous (>50%) Fe-Mn oxides nodules. Common Fe-oxyhydrate coatings in relict pores and some (2%) fragments of reddish yellow clay coating fragments are seen in the groundmass. An increasing color trend from light reddish brown to red from one side to the other side of the thin section is observed.

Figure 9.10: Micrograph of Holili palaeosol showing typic Mn-Fe oxide coating on Relict pores in a yellowish red microaggregated groundmass.

Some palaeoenvironmental interpretations

The Pleistocene palaeosol level (living floor) is presently observed along deep cut streams in the area. Newly excavated areas also provide a good exposure of the palaeosol level. Some micromorphological features of the palaeosol level as described above contain include common Fe-Mn hydr(o)xide coatings in relict pores (figure 9.10) and some (2%) fragments of reddish yellow clay coating fragments seen in the groundmass. The increasing color trend from light reddish brown to red from one side to the other side of the thin section probably infers to an iron hydroxide illuviation (accumulation) zone in the vicinity.

The presence of mineral clay pseudomorphs and Fe-Mn hydr(o)xide coatings indicates a wet (probably humid-warm) climate during the Lower Pleistocene. The red colour, absence of weatherable minerals and microaggregate microstructure may indicate that the palaeosol was probably an Alfisol?. Deep red ancient Alfisols signify wet-humid deep wethering tropical climates, which existed during the Middle Pleistocene.

CHAPTER TEN

QUATERNARY CLIMATIC, ENVIRONMENTAL AND STRATIGRAPHICAL IMPLICATIONS OF THIS STUDY

10 PALAEOCLIMATIC, PALAEOENVIRONMENTAL AND STRATIGRAPHICAL IMPLICATIONS

10.0 INTRODUCTION

This chapter presents in brief personal reflections and interpretations on the local and global implication of this study findings to the Pliocene – Quaternary climatic changes. The implication to distribution of fossil man is also reviewed on the basis of the recorded climatic fluctuations in Olduvai Gorge, Manonga-Wembere and Holili localities. The synchroneous global climatic change is irrevocably demonstrated by attempting to correlate this study with the global palaeosol geo-traverse as was developed by Paepe (1990) and Van Overloop and Paepe (1994 & 1998).

10.1 LOCAL IMPLICATIONS

10.1.1 Implication to climatic changes

10.1.1.1. Olduvai Gorge locality

The palaeoclimatic and environmental changes of Olduvai Gorge are deduced from palaeosol stratigraphical positions, type and cyclicities as well as facies changes of the sediments (field studies) coupled with laboratory studies (Meneralogy, magnetic susceptibility and micromorphology of palaeosols levels (table 10.1 and figure 10.1). The implications of these studies to the local climatic changes and variations of the Quaternary are reflected here below.

Bed I and Lower Bed II

Bed I and Lower Bed II deposits covers the time span of 2.2Ma till 1.66Ma. These are lacustrine and marginal deposits which, are mapped by low MS values indicate great extension of fresh

water conditions. This paleoenvironment is indicated by the presence of fine-grained clays and silts with some rare occurrences of coarser sediments. The sediments can be followed over long distances in the Olduvai Gorge basin and beyond. The slightly enhanced MS values of palaeosols indicate pedogenesis (Heller & Liu, (1986) on either lacustrine clays or ash fall/flow-tuffs. Mineralogical studies indicate that palaeosol which formed during drier climates are rich in 2:1 clay minerals and zeolites while palaeosol formed during wet climates have 1:1 clay minerals and gibbsite mineralogy.

Micromorphological characteristics of palaeosol levels of Bed I and lower Bed II generally reflect more calcite coating and nodules, with little if any clay coatings together with the abundance of Fe-Mn oxyhydrate coating and nodules. These characteristics suggest a significant wet environment. Actually these palaeosols were formed in the Lake Margin and flood plains during periodical retreats of the lake. The clay developed in flood plains or in the lake was subject to pedogenesis during the period of reduced precipitation.

Twenty palaeosols (figure10.1) were observed (in the field) in the time span 2.0Ma till 1.65Ma of the Lower Pleistocene Epoch. Seventy percent of these palaeosols show a high MS signal compared to the clay layers. Micromorphological characteristics and field observations suggest that these palaeosols were probably Vertisols, Andisols or Aridisols.

Accordingly there were more than 20 climatic occurrences in Bed I and lower Bed II as depicted by the palaeosol levels. This is quite consistent to the animal fossil levels of Kappelman, (1984). Kappelman conducted a paleoenvironmental analysis of Bed I and Lower Bed II based on mammal habitat indicators and found 17 fossil levels all assumed to be located on palaeosols.

In the time period of 1.81Ma till 1.76Ma in between Tuff IB and tuff ID fossil soils are composed of essentially clay palaeosols with more plant remains than the other considered interval. However, two major sand levels are noted in this sequence. This indicates that spells of dry climates existed within the generally wet period of this interval. Indeed the 2 sand levels which, before were considered as probably of eolian origin may indicate dry conditions in Olduvai Gorge. The MS signature of these sand layers was higher than that of the palaeosol and clay levels. This is consistent to several other researches in lake sediments that indicated that higher magnetic susceptibility records from coarse detrital sediments correspond to cold and drier climates (Thouveny *et al.*, 1994)

In the time period of 1.75Ma till 1.749Ma in between tuff ID and tuff IF it was likely generally to be more wet than in the former as no sand beds are noted in this part. This interval show also well developed clay palaeosols with numerous plant remains but the absence of sand layers may point to wetter conditions than the former interval.

In the time period of 1.749Ma till 1.66Ma in between tuff IF till tuff IIA well developed palaeosols (probably palaeovertisols) with abundant features of plant activity than in the former period indicate much better conditions for animals and plants to survive. Some other authors refer to this period as of mudflats or marshland (Blumenschine & Masao, 1991) surrounded by grassy woodland.

In general the interval of Bed I till Lower Bed II shows very low MS in a normal magnetozone (Tamrat *et al.*, 1995) which is often correlated to the Olduvai subcron [1.95Ma - 1.79Ma]. I consider these well-developed palaeosols to belong to the Olduvai Event (1.97Ma – 1.79Ma) although dates by Walter *et al.*, (1991) and Manega (1993) are lower than this event. As the 20 palaeosols are recorded in precisely the period of 1.85Ma till 1.66Ma it infers at every 10,000 years a soil developed indicating as well that the aggradation rate of the whole interval remained constant.

Middle Bed II – Bed III

Middle Bed II (1.66Ma – 1.62Ma) and Bed III (1.15Ma – 0.6Ma) red palaeosol levels are very distinct and similar in the micromorphological, MS and mineralogical records. These zones show strong red colour and multiple micromorphological characteristics. Field observations and micromorphological studies indicate that they are probably palaeo-alfisols. They show slightly higher MS values compared to the previous lower intervals. In the field they show localized segregation of bright red to reddish brown stains which are known to be formed when sediments are subjected to alternating periods of dryness and humidity associated with high temperatures (Stoops, 1998). These stained were recorded (in the field) as red mottled or oolitic palaeosols.

Their micromorphological features include phases of red-yellow clay coating and fragments with Fe-Mn hydr(o)xide coating and nodules overprinted on top of the other. These multiple micromorphological characteristics suggest an alternating Eh-pH condition due to alternating wet

and dry hydromorphic regime during the Pleistocene. These levels are associated with wet alternating with dry periods in Olduvai Gorge area.

Middle Bed II red palaeosols occupy an approximately time interval of between 1.66Ma and 1.62Ma. This time was a brief drier period in Olduvai Gorge compared to Bed I and lower Bed II. δO^{18} data indicate similar drier interval between 1.62Ma – 1.67Ma called Lemuta member of Bed II (Cerling and Hay 1986). Statigraphically middle Bed II is well developed in the eastern part of the Olduvai Gorge paleo-basin. Moving to the west this palaeosol marker horizon grade into a more clayey palaeosol with numerous macro nodules and calcrete deposits.

Bed III palaeosol occupy an approximately time interval of 1.15Ma to 0.6Ma (Manega 1993 and Somi 1993). This is a period of increased landscape stability where thick sediments were deposited and thereafter affected by pedogenesis for a relatively long interval of time forming thick red palaeosols. The multiple micromorphological features red to pale yellow clay coating and clay caoting fragmants) indicate warm and dry conditions alternating with cool and wet conditions during thia time. There are about 10 observable palaeosol levels in this zone showing that they were formed at every 57Ka interval. This is probably related to the 60Ka astronomical cyclicity. Bed III also laterally thins out towards the west and become more calcretic and calcareous with nodules and concretions.

Table 10.1: Infrared intensity variation of clay minerals (1900-1920nm peak) and carbonates (2300-2350nm peak) with magnetic susceptibility variation in palaeosol levels of Olduvai Gorge beds.

No	Sample	Palaeosol Levels	Peak intensity (%) clay minerals	Peak intensity (%) [CO_3]	MS (SI units)	Depth (m)	Approx. Age (Ma)
1	mc22	GS1	9.2	0	16.29	2.75	0.268
2	mc21	GS1	17.86	20.65	20.64	3.3	0.285
3	mc20	GS2	24.65	28.6	12.42	3.75	0.302
4	mc19	GS3	10.87	0	14.42	4.3	0.319
5	mc18	GS4	12.55	0	10.38	5.75	0.336
6	mc17	GS5	11.31	0	11.99	6.35	0.353
7	mc16	GS6	10.04	0	17.48	6.725	0.37
8	mc15	GS7	10.04	0	10.62	7.25	0.387
9	mc13b	GS8	13.95	0	9.46	7.65	0.421
10	mc13a	GS8	18.7	0	16.88	7.85	0.438
11	mc11	GS9	11.43	0	8.85	8.85	0.477
12	mc9	GS10	14.51	19.81	21.5	9.45	0.531
13	mc8	GS11	7.8	0	9.29	9.9	0.558
14	mc6	GS12	9.48	0	21.28	10.45	0.612
15	mc4	GS13	9.48	0	25.9	11.35	0.666

continues No	continues Sample	continues Palaeosol Levels	continues Peak intensity (%) clay minerals	continues Peak intensity (%) [CO_3]	continues MS (SI units)	continues Depth (m)	continues Age (Ma)
16	mc3	GS14	12.83	0	81.19	11.65	0.72
17	mc2	GS15	16.18	0	35.31	11.85	0.747
18	mc1	GS16	15.9	0	53.76	12	0.774
19	rb21	GS17	18.7	0	51.67	13	0.828
20	rb20	GS18	14.79	0	49.25	13.65	0.855
21	rb18	GS19	12.27	0	61.15	14.65	0.909
22	rb15	GS20	11.31	0	60.49	15.9	0.99
23	rb14	GS21	19.98	0	51.85	16.25	1.017
24	rb5	GS22	26.24	32.65	44.84	19.35	1.287
25	rb3	GS23	20.64	0	6.3	20.1	1.348
26	rs39	GS24	13.31	17.3	84.84	21.85	1.402
27	rs37	GS25	16.46	0	46.34	22.3	1.438
28	rs35	GS26	19.54	25.68	73.3	23	1.474
29	rs31	GS27	15.07	20.09	169.58	23.65	1.5007
30	rs29	GS28	19.81	0	133.06	23.85	1.5145
31	rs22	GS29	18.14	25.68	81.34	25.75	1.5628
32	rs19	GS30	7.8	10.87	16.29	26.65	1.5835
33	rs17	GS31	8.92	0	84.91	26.78	1.59178
34	lk10	GS32	5.55	0	50.32	27	1.59454
35	lk9	GS33	7.8	13.67	17.87	27.15	1.59592
36	lk8	GS34	8.34	19.32	16.43	29.35	1.5973
37	lk7	GS35	5.57	0	31.24	29.85	1.6042
38	lk6b	GS35	5.85	0	33.25	30.45	1.6111
39	lk6a	GS35	4.45	0	27.88	30.85	1.618
40	lk5	GS35	8.64	18.65	28.29	31.05	1.6249
41	lk4	GS36	4.17	0	12.75	31.45	1.6318
42	lk3	GS37	3.61	0	5.12	31.75	1.6387
43	rs13	GS38	5.55	0	3	33.95	1.666
44	rs11	GS39	10.27	0.71	4.67	34.2	1.678
45	rs9	GS40	12.41	0.61	3.42	34.45	1.69
46	rs7	GS41	9.2	0	6.47	34.85	1.702
47	rs5	GS42	9.48	12.83	4.56	35.3	1.714
48	3z	GS43	5.01	8.08	5.69	36.45	1.744
49	2z	GS44	5.31	7.3	10.18	37.1	1.749998
50	1z	GS45	6.41	9.2	12.1	38.4	1.756042
51	zk	GS46	11.17	18.7	14.97	38.6	1.77
52	z19	GS47	35.32	43.9	7.4	40.3	1.783
53	z17	GS48	25.12	36.02	5.34	40.5	1.7845
54	z15	GS49	23.32	33.98	9.33	40.75	1.786
55	z13	GS50	14.65	21.32	8.2	41.05	1.7875
56	z11	GS51	23.32	32.65	15.94	41.3	1.79075
57	z9	GS52	51.32	17.3	14.1	41.8	1.79383
58	z7	GS53	15.9	25.4	14.85	42.2	1.79849
59	z4	GS54	24	33.22	11.83	42.75	1.80548
60	z2	GS55	16.18	22.33	33.37	43.05	1.81014
61	zi	GS56	7.8	10.87	91.16	44.1	1.81713
62	zb	GS57	15.07	23.45	7.18	46	1.86

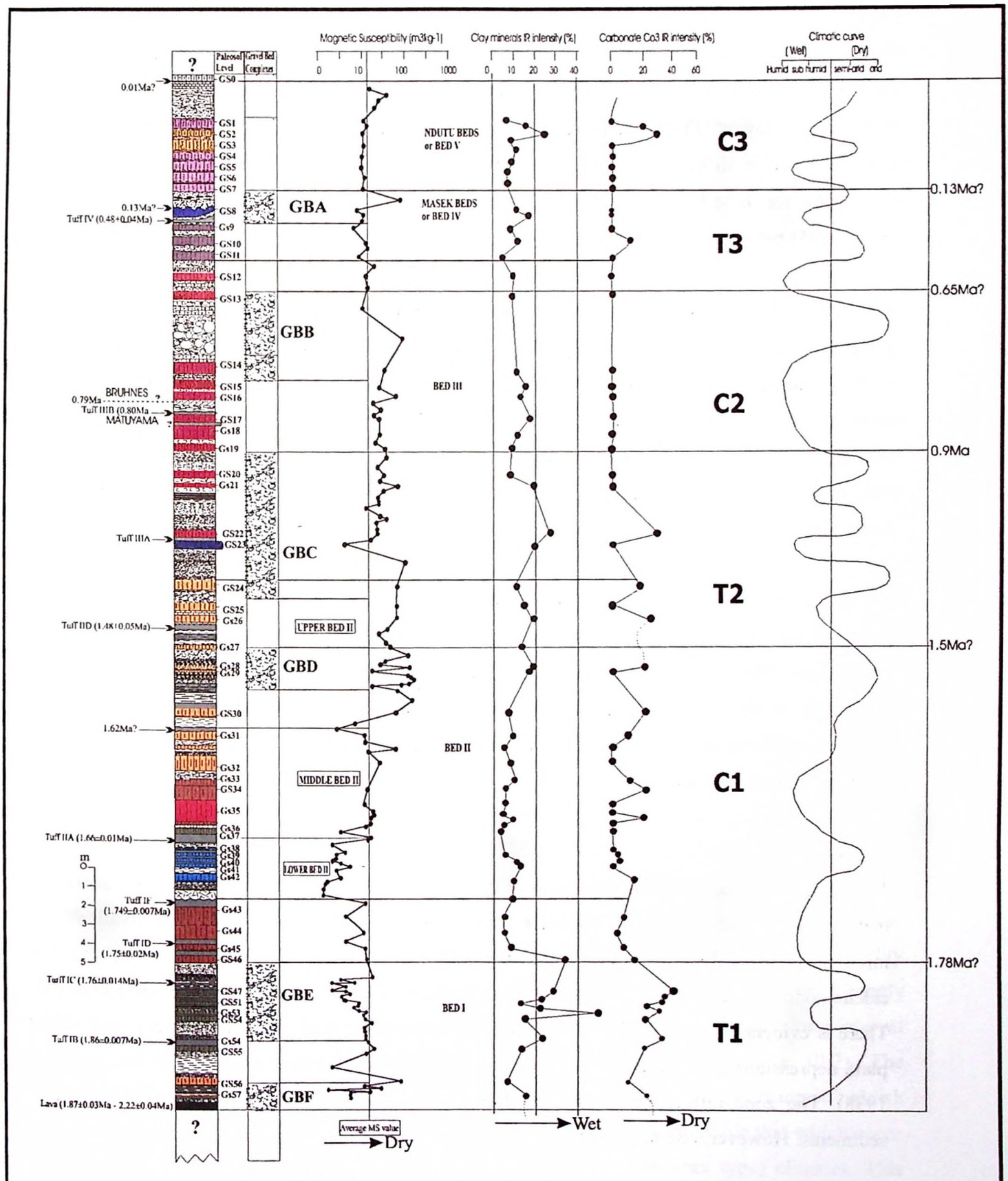

Figure 10.1: Climatic variability of Olduvai Gorge area based on magnetic susceptibility , clay minerals and carbonate variation of the palaeosol levels

Upper Bed II

Upper Bed II covers the time span of 1.62Ma till 1.15Ma (figure 10.1). As discussed in chapter 8 the MS record of this zone is the highest in the whole profile. This is due to the presence of gray to black sand layers. This zone therefore is regarded as probably a dry period due to change of facies from fine to coarse and the presence of aridisols. The black minerals are probably responsible for these high MS values. The zone (Middle Bed II) show reversed polarity (Tamrat *et al.*, 1995) belonging to the Matuyama geomagnetic epoch.

The palaeosols present in this zone show lower MS values compared to the sand layers. The palaeosols show multiple micromorphological characteristics (like calcite nodules, infillings of zeolite? and opal? minerals in pores and very rare Fe-Mn hydroxide coatings) indicating dry environments. These are probably palaeoaridsols. These palaeosols represent cycles of slightly wetter periods where rainfall necessitated the development of soils on the sand layers. Five major sand layers and 7 palaeosol levels were observed in the field and consequently picked out by MS measurements in the laboratory

It is important to note here that, the process of dilution of magnetic minerals in the sands to form paleosols with low MS signature is inversely anologous to loess-palaeosol sequences of China, where loess shows lower MS values and palaeosols showing enhanced MS values. This is significant to the future palaeoclimatic studies in highly magnetic sandy palaeosols in volcanic areas nevertheless; this concept need to be developed further to be able ascertained as a proxy in studying similar profiles.

Masek Beds/Bed IV

The Masek and Bed IV is the time span of 0.6Ma till 0.4Ma. The interval posses fine sediments mainly composed of clay together with clayey palaeosol. Field observation and micromorphological studies revealed that the palaeosol were mainly vertisols showing abundant calcite nodules and coatings, slickensides, and imprints of deep cracks and gilgai relief structures. There is evident from research that such soils are usually formed in seasonal backswamps-flood plain depressions away from active lake shores and abandoned river channels (Aslan and Autin 1998). The zone reflects generally low MS values mainly due to the presence of fine clay sediments. However, one major sand level show higher MS values.

Paleo-vertisols indicate short-term alternating dry and wet conditions. Generally this sequence represents increased aridity evident from the presence of paleo-vertisols. The appearance of the land snail *limicolaria* in the sediments (Hay 1976) also points to the drier climate. 12 palaeosol can be observed in the field with a major sand bed lie unconformably on a hiatus at about 0.4Ma. The approximately time interval of these palaeosols is between 0.6Ma to 0.4Ma indicating an interval of about 20Ka between each palaeosol development.

Ndutu Beds

The upper part of the Olduvai Gorge profile (Ndutu Beds) occupy an approximate time interval of between 0.13Ma and younger. Again this interval show low MS values in the lower parts and higher MS results towards the top of the bed. It was observed in the field that a series of palaeo-Vertisols lie on the sand level right after the unconformity. Seven palaeosol levels were observed to cover the time interval of between 0.13Ma and 0.02Ma, indicating a palaeosol development at every 10Ka interval. The upper part of the Ndutu beds is composed of loose sands at the base followed by a dense mudstone/siltstone grading into limestone towards the surface.

Micromorphological features of the limestone lithology show a series of channels within the limestone. The channels are infilled by clay and calcite superimposed on one another. Field observation of the mudstone indicates a box-work of cracks infilled with carbonate. These field and laboratory characteristics may infer a dry climate that changed into a wet lake environment towards the upper part where limestone could precipitate along the paleolake shorelines.

10.1.1.2. Manonga-Wembere Valley and Holili localities

Kininginila section in Manonga-Wembere Valley represents the Upper Pliocene and Lower Pleistocene (3.0Ma to 1.2Ma). The presence of palygorskite and sepiolite clay minerals (chapter 9.1.2.2) characterizes generally dry weathering environments. Preliminary magnetic susceptibility and clay and carbonate (SWIR) record point to a 250Ka-variation cycle. Moreover, Strongly developed palaeosols (probably infering wet periods) are observed to occur after a long interval (2.4Ma – 1.6Ma) of time (about 800Ka) and last for a short time (figure 10.2). The micromorphological characteristics of the palaeosols include accummulation of oriented reddish yellow clay coating fragments indicating an intense illuviation front comparable that which occur in present day calcareous sediments of warm and humid (Meditteranean type) climates. This

atudy therefore considers palaeosol levels as an indication of spells of warm humid climate in the 3.0Ma – 1.2Ma time interval during the Upper Pliocene-Lower Pleistocene.

Animal fossils found in Manonga area are bound to the top of palaeosol levels attesting to suitable climatic environments where animals could survive during the palaeosol development. The other long intervals of time between the palaeosol levels was probably a harsh (drought like) environment where animals could not survive. The climatic variability impact is further discussed in chapter 10.1.2 of this study.

Based on age equivalency Holili palaeosol level is correlated to the upper part of the Bed III red palaeosols of Olduvai Gorge stratigraphy. Based on the micromorphological characteristics of the palaeosol level (chapter 9.2.2.2) this period (development of the palaeosol level) indicates a generally wet climate in Holili in which animals and plant life survived as is demonstrated by fossil plants and animal remains found in this area.

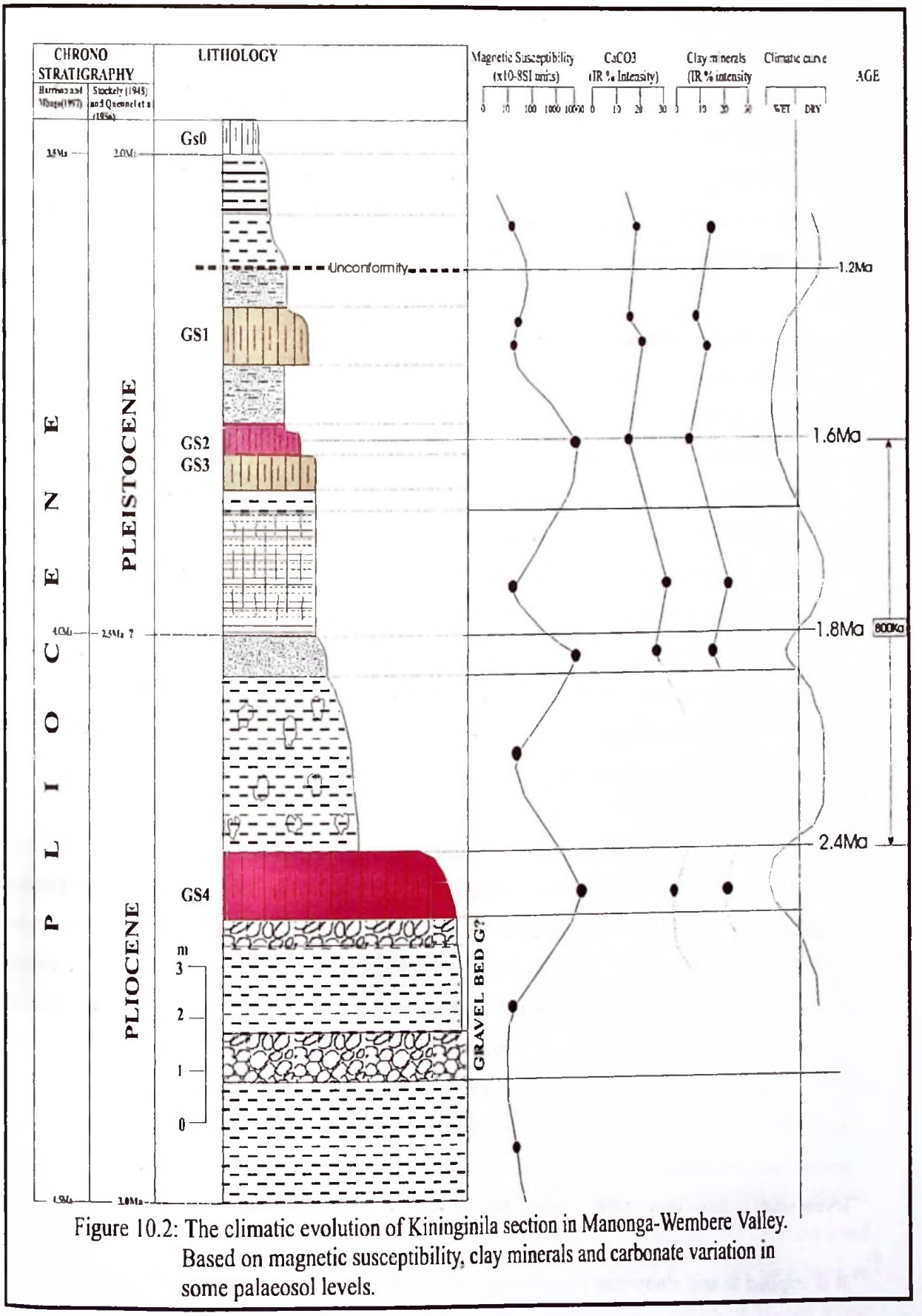

Figure 10.2: The climatic evolution of Kininginila section in Manonga-Wembere Valley. Based on magnetic susceptibility, clay minerals and carbonate variation in some palaeosol levels.

10.1.2. Implication to hominid occurrence

For five decades geo-scientists have been searching for hominid remains and their cultures in the Olduvai Gorge and Laetoli archaeological sites, Tanzania. The most common environments to find hominid remains are lacustrine sediments and volcanic ash deposits. Rapid sedimentation and burial under volcanic ashes accompanied by a rapid cementation have enabled effective preservation of fossils in such depositional environments.

In Olduvai Gorge an enormous amount of hominid remains has been found in lakebeds mostly associated to palaeosol levels and often covered by tuff flow/fall ashes. These palaeosol levels, referred to as hominid living floors or occupation levels (Leakey 1967, Kappelman 1984, Tobias 1991 and Fernandez-Jalvo *et al.*, 1998) have always provided suitable fossil preservation sites especially when tuff, $CaCO_3$ and water are involved during the sedimentation, burial and diagenesis of these units. In Laetoli locality the preservation of the *Australopithecus aferensis* footprints is related to the active phases of the nearby (Sadimani) volcano and the composition of the ejected volcanic materials. Agnew & Demas (1998) propose that the cementation of the footprints was favored because the ashes emitted by Sadimani volcano were cabornatites rich in calcite [$CaCO_3$] or dolomite [$MgCa(CO_3)_2$] which acted as a cement when wet. Denys (1985) also indicated that in Laetoli, fossil rodents were trapped in their borrows in palaeosol levels covered by accumulated ash falls during volcanic eruptions.

Besides these two major archaeological sites attempts have been made to find hominid remains and their associated cultures in the extensive Manonga-Wembere lakebeds in central Tanzania. Although these efforts have not yet yielded results but significant amount of mammal fossils have been discovered. As in the former sites the presence of $CaCO_3$ and palaeosols are the essential parameters for fossil preservation. Animal fossil bearing levels formed in situ are restricted to a light gray calcareous clay layer impregnated with a honey comb-like calcareous matrix (Verniers, 1997). Just below these fossil horizon lies a distinctive bright red clayey palaeosol layer. It seems likely that the diagenetic procesess involved in the formation of the calcareous clay layer were responsible for conditions suitable for the preservation of the animal fossil remains. The palaeosol levels seem to have been suitable platforms for animal remains fossilization.

It is implied in this study that palaeosols presence seems to be the main indicator parameter for animal (sometimes including hominids) fossil occurrences. This study shows that hominid

occurrence and evolution in Olduvai Gorge stratigraphy is bound to palaeosol levels and gravel layers. In Manonga-Wembere Valley and Holili localities the fauna and flora fossil levels are also closely associated to palaeosol levels (figure 10.2a). In all the three localities animal fossils were probably laid down on palaeosol surfaces and then covered, cemented and preserved by crystallization of carbonaceous sediments or tuff which hardened fast enough to preserve the fossils.

10.1.2.1. Olduvai Gorge locality

This discussion is based on figures 10.3 and table 10.1. The oldest (2.22Ma – 1.85Ma) fossil discoveries in Olduvai Gorge area are those of *Homo habilis* OH4 and OH24 specimens found in DK1 and DK2 archaeological sites (Tobias 1991) on palaeosol levels GS56 and GS55 respectively (figure 10.3). This period is regarded as the FAD of the *Homo habilis* species as no fossil finds are recorded below 2.0Ma. *Homo habilis* hominids were probably extinct in gravel bed D complex. GS56 and GS55 are weakely developed sand-clay palaeosol levels in which the homonid remains were found. The palaeosols show rare root casts and infillings indicating a dry climatic condition. Although a lake existed in Olduvai Gorge at this time it was at a lower level.

The time period of between 1.85Ma and 1.75 (tuff IB and tuff IF) 11 palaeosols were recorded. This time interval has recorded numerous *Homo habilis* fossil remains and each hominid fossil level at least corresponds to one palaeosol level. This is a time of *Homo habilis* activity. The *Australopithecus boisei* (zinjanthropus) OH5 specimen was found in palaeosol level GS54 dated between 1.85Ma - 1.79Ma. The zinjanthropus fossil thus occurs at approximately OIS 68. GS54 is approximately 25cm thick, it is very sandy and with numerous carbonate concretions indicating dry conditions. Palaeosol GS52, GS51, GS50, GS49, GS48, GS47 and GS46 all represent archaeological levels FLK-FLKI-FLKNN (figure 10.3) where numerous *Homo habilis* fossil remains were recovered in palaeosol occupation levels e.g. OH7, OH8, OH17, OH21, OH33, OH45 and OH 46 specimens (Leakey 1967, Tobias 1991 and Fernandez-Jalvo *et al.*, 1998). OH10 hominid was found on palaeosol GS45 or GS44 on archaeological levels/site FLK-N5.

Lower Bed II (1.66Ma –1.75Ma) represents a marshland environment (Blumenschine and Masao, 1991) where hominds continued to enjoy life. FLKII and HWKE archaeological sites did yield *Homo habilis* hominid remains OH16 and OH41 respectively. These levels are correlated to palaeosol levels GS42, GS41, GS40, GS39 and GS38 of lower Bed II, (figure 10.3). The levels

are also very rich in other large mammal fauna. Middle Bed II strata, which is in the interval 1.66Ma – 1.62Ma shows red palaeosols indicating a marked change of climate from relatively permanent wet to seasonal alternating dry and wet. No hominid has been recovered in this zone.

Upper Bed II (1.62Ma –1.15Ma) sands and gravel sediments dominate the profile. *Homo habilis* OH13 was recovered in MNKII site (GS32 or GS31? Palaeosols) in the lower part of the series. In the upper parts of the profile *Homo erectus* was for the first time discovered at an approximate position level of GS29 and GS28 palaeosols. Olduvai Gorge *Homo erectus* hominid specimens include, OH9 and OH59. This part is made up of sand-clay palaeosols, sand and gravel sediments, again indicating an increased dryness. The gravel bed D complex is regarded as the (Last Appearance Datum) LAD for *Homo habilis* and *Australopithecus boisei* and the (First Appearance Datum) FAD for the *Homo erectus*. At about 1.4Ma *Homo habilis* might have disappeared and *Homo erectus* appeared. Increased dryness might necessitate the extinction of *Homo habilis* and the appearance of *Homo erectus*. The later was probably more adapted to the climate with much more technology to survive in this new harsh environment.

In Bed III (1.15Ma – 0.4Ma), (figure 10.3) red palaeosols, with alternating seasonal dry and wet climates no *Homo habilis* were recorded except Homo erectus which still thrived. OH59 *Homo erectus* hominid was discovered in middle Bed III at approximately GS18 – GS20 palaeosol levels. In the upper Beds (Bed IV, Masek and Ndutu) *Homo erectus* OH9, OH12, OH28 and OH51 fossil remains are recorded in the lower parts, (Leakey and Roe, 1995) at about 0.7Ma corresponding to palaeosol levels GS11, GS10, GS9 and GS8. A major gravel bed is recorded at about 0.5Ma in Bed IV and beyond this mark OH11 and OH 23 *Homo erectus* specimen is still recorded. The species became rare and probably became extinct around 0.4Ma.

Table 10.1: Some Olduvai hominids (OH) fossil levels and localities as correlated to palaeosol levels of this study. (Compiled from Leakey 1959, Leakey 1967, Leakey 1971, Leakey and Hay 1983, Tobias 1991 and Leakey & Roe 1995) – Also se figure 10.3.

Name of specimen	Description	Level and site	Probable palaeosol level (this study)
OH11	Palate and maxillary arch *of Homo erectus*	Ndutu Beds or Masek Beds	GS7 – GS5??
OH28	Left femoral shaft and left OS coxae discovered in 1969, *Homo erectus.*	Bed IV, Site PDK I-III	GS8
OH12	Calvaria and maxilar of *Homo erectus*	Bed IV, Site TK fish gully	GS9

Continued	Continued	Continued	Continued
OH51	Left mandibular corpus with teeth. *Homo erectus*	Bed IV, Site PDK IV	**GS11**
OH9	*Homo erectus* skeleton remains discovered in 1963	Bed IV? Discovered in sand layer between	**GS8 and GS9.**
OH29	Molar fragments of *Homo erectus*	Bed III, Site JK	**GS14, GS12 or GS11?**
OH34	Femur and tibia discovered in 1964. *Homo erectus*	Bed III, Site JK	**GS12 or GS11**
OH23	Left mandibular corpus with molars and premolars. *Homo erectus.*	Masek Beds, Site FLK.	**GS57 – GS55**
OH59	*Homo erectus* skeleton remains discovered in 1963	Upper Bed II to Middle Bed III?	**GS19 or GS18**
OH13	*Homo habilis* - Many parts of the skull	Bed II 7.5m above tuff IF Site MNKII	**GS32 or GS31? OR GS30?**
OH16	*Homo habilis* cranial vault and teeth, discovered in 1963	Bed II, 1m above tuff IF. Site FLKII	**GS42**
OH24	*Homo habilis* heavily crushed cranium discovered in 1968	Bed I, between lava and tuff IB. Site DK1-2	**GS56 or GS55**
OH4	*Homo habilis* teeth and cranium. Discovered in 1959.	Between lava and tuff IB. Site MK and DK1	**GS57 or GS56?**
OH5	*Australopithecus boisei* skull. Discovered in 1959.	Bed I btween tuff IB and IC. Site FLK22	**GS54**
OH7 & OH8	*Homo habilis* teeth, bones and parts of skull discovered in 1960	Bd I (between tuff IB and tuff IC). Site FLKNN - FLKNNI	**GS53 to GS47**
OH45 and OH46	*Homo habilis* premolar teeth. Discovered in 1960	As above	**As above**
OH33	*Homo habilis* occipical bones. Discovered in 1969	As above	**As above**
OH17, OH21 & OH40	*Homo habilis* premolar and molar teeth	Bed II (between tuff IF and tuff IIA. Sites FLK, FLKN and FLKS	**As above**
OH41	*Homo habilis* premolar teeth	Bed II (above tuff IF). Site HWKEE	**As above**
OH14, OH15 & OH 32	*Homo habilis* tooth and worn out cheeks	Bed II (between IIA & IID). Site MNKII	**GS29 and GS28**
OH10	Distal phalanx and right hallux. *Homo habilis*	Bed I between tuff IE and tuff IF. Site FLK N5	**GS44**

To summarise, the occurrence of fossil man (hominid) in Olduvai Gorge is closely related to the long-term climatic cycles of 400Ka which are bound to specific gravel boundaries. Palaeosol levels of Olduvai Gorge present a very good study parameter of the past climatic variations and cyclicities not only because they indicate a stable landscape but also because locate and position much of the animal fossil levels including hominids.

Palaeosols of Bed I and lower Bed II (developed on clay or tuff layer) indicate more wet and humid climates with brief dry spells. These well-developed palaeosols are associated with the thriving of *Australopithecus boisei* and *Homo habilis* hominids. The FAD for *Homo habilis* coincides with sand level (gravel bed E complex) at about 1.78Ma. The upper Bed II sandy and sometimes calcrete palaeosols represent semi-arid to arid savanna where *Australopithecus boisei* and *Homo habilis* may have been affected by the climate and extinct paving way to the emergence of *Homo erectus* more adapted to the new conditions. Again sand bed (gravel bed D complex) in upper Bed II marks the *Australopithecus boisei* and *Homo habilis* LAD and *Homo erectus* FAD. Drier climate (marked by a sand bed) of Masek Beds might have caused the *Homo erectus* hominids to probably perish around 0.4Ma.

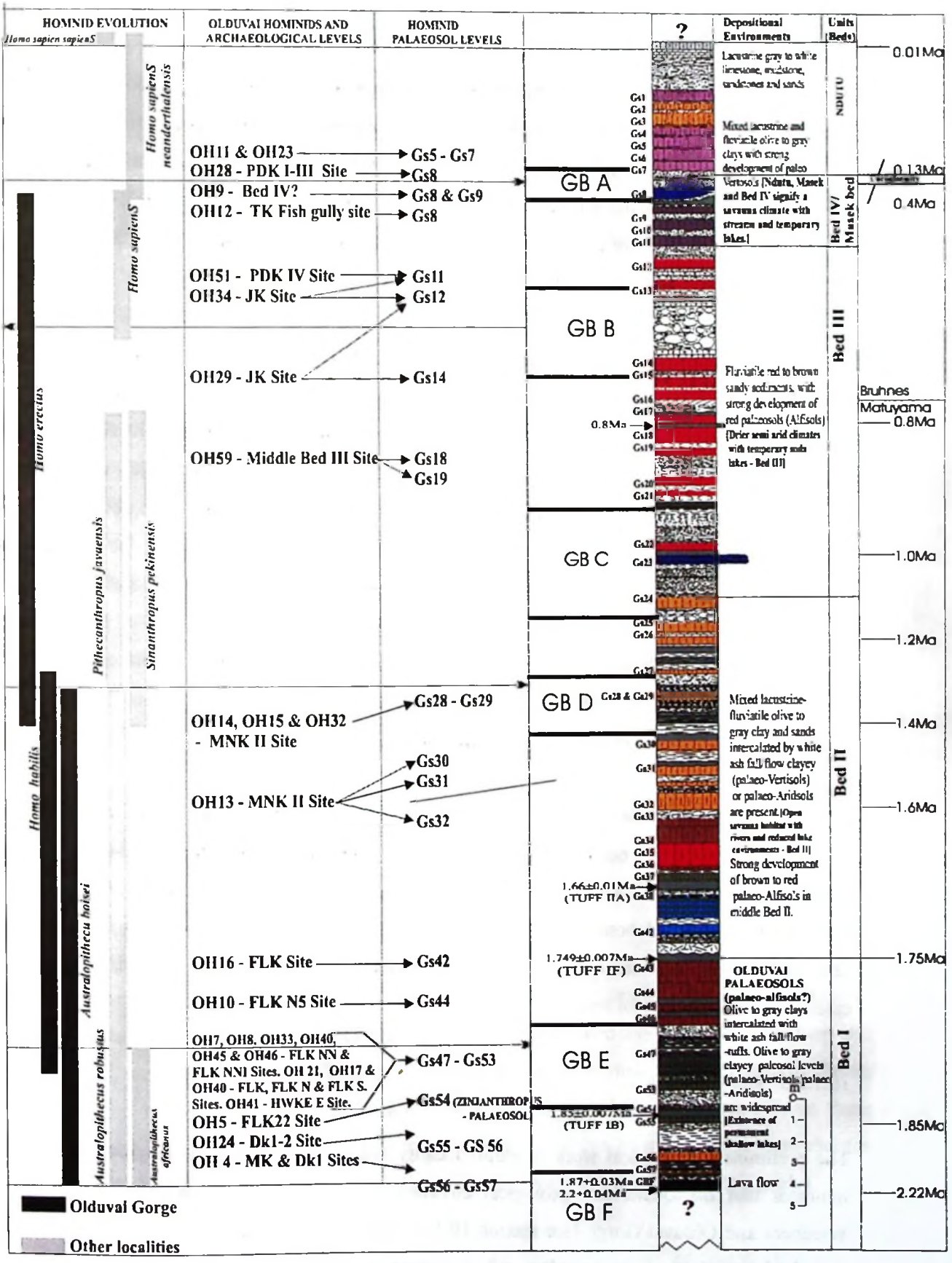

Figure 10.3: Olduvai Gorge palaeosol levels and hominid occurrence. [The correlation between palaeosol levels and archaeological levels (hominid occupation levels)].

10.1.2.2. Manonga-Wembere locality

The question why there are no hominid finds in Manonga-Wembere Valley (although substantial amounts of fossil mammals have been found) sounds enigmatic. Popular speculations are either; hominids might have been geographically restricted to rift valley areas during the Late Miocene and Pliocene (not extending far enough south to encompass the Manonga valley). Or hominids are very rare components of the East African fauna during the Late Miocene and Early Pliocene. But the question remains why such a distribution?

Based on climatic cyclicities (this study) observed in the Kininginila site. It likely to me that the long-term dry climatic (800Ka) cycles that are marked by brief palaeosol wet periods in the Manonga Valley) (figure 10.2) might have caused the hominids to be restricted in small pockets of suitable climates within the valley. Or migrated to relatively wetter localities with slightly shorter cycles of dry periods like Laetoli and Afar in Ethiopia in the north. With such a climatic restriction fossilisation of hominids becomes a matter of chance, as it would also be restricted to certain (rare) places of the valley. However, there is still a greater chance that hominids lived in Manonga-Wembere Valley during brief periods of slightly wetter climates – indicated by palaeosols. One is likely to find fossil hominid remains on palaeosol levels as the case has been for other animal fossils found in close association with palaeosols. It is possible that palaeontologists and archaeologists have been searching in the wrong places.

In this regard it is therefore suggested that a detailed stratigraphical vertical and lateral mapping be systematically carried out in the area to accurately map the palaeosol levels. It is thereafter a systematic excavation of such palaeosol levels sites could be carried out and probably might yield better results. As the Manonga-Wembere Vallley is extensive and wide it will remain a waste of time and money to execute excavations in a random way rather than following the lateral extensions of the palaeosol levels.

10.1.2.3. Holili locality

The preliminary geological work in Holili locality not only reveals new fossil finds but also indicates that the Quaternary geological environments of Holili resemble that of Manonga Wembere and Olduvai Gorge (see section 10.1.2). Therefore, it would be interesting to further map the lava-palaeosol-grit boundary, which represents volcanic tuff covering large areas of the

landscape probably trapping the fauna and flora of old. These calcareous grit deposit represent a perfect preservation condition of animal and plant remains contained in or on the covered paleo-landscape (palaeosol).

Presence of favorable depositional environments in Holili that include a palaeosol level (living floor) covered by a 'preserving' calcareous tuff deposit qualify the area as a possible future potential palaeontological/archaeological site. The advancing calcareous ash flow tuff during a volcanic eruption is likely to have preserved large quantities of the fauna and flora on the living floor (palaeosol) in Holili locality. The task is now to find this archaeological gold mine in this area by initiating intensive archaeological and paleontological searches.

Fossil fauna (canon bone, tooth and horn) that has already been found during this preliminary geological mapping qualifies the Holili locality as a potential archaeological and paleontological detailed research area. It is quite hard to find in situ fossil flora (plant remains) in Tanzania and elsewhere, Holili therefore stands as one of these rare places containing fossil flora worthy investigating. Furthermore, the presence of an in situ hominid tool in the palaeosol indicates that the area was once roamed by hominids hunting and scavenging on animals in the area. There is a great possibility of finding their remains in this area.

10.2 GLOBAL IMPLICATIONS

10.2.1 The global palaeosol traverse and the synchronous nature of global Quaternary climates

10.2.1.1. Olduvai Gorge locality

The global palaeosol traverse known as geo-soil stratigraphical sequential investigation (Paepe *et al.*, 1990b, Paepe and Van Overloop 1990a, Paepe and van Overloop 1994 and Van Overloop and Paepe 1998,) have led to the identification of regional stratotype sections (Loess Plateau of China, Plateau region of Greece and the Great Lakes region of East and central Africa). From these stratotype sections correlations of geo-soil traverse land record can be made. These land records can also easily be compared to OIS and Ice Core Isotopic records, (chapter 1.1.2 this study).

It is intended here to correlate the Olduvai Gorge palaeosol stratigraphy of this study with the standard Sparta-Peloponnesos (Greece) stratotype section of Paepe *et al.*, (1996) and Van Overloop and Paepe (1998), in order to observe the salient features attesting to the global synchroneous climatic changes and cyclicities.

The standard regional stratotype section of Greece (Peloponnesos and Sparta) was described by Paepe *et al.*, (1996) in a steep (160m) high red bluff composed of gravel eolian/fluvial deposits along the edge of the city of Sparta, (Van Overloop and Paepe 1998). This section is selected because it is located at the climatic transition (Meditteranean climate) between tropical and temperate climates and serves as a good link between the tropical and temperate climates. The Sparta continental section is also much more complete in terms of continual sedimentation from the Pliocene to the Holocene. And thirdly the section has been found to be consistently correlatable to the continous Loess Plateau sections of China.

The section (figure 10.4 and descriptions according to Van Overloop and Paepe, 1998) contains 72 palaeosols with 1 oxisol (latosol) of Miocene age. Which correlates to OIS 113. GS 71 to GS61 are Pliocene in age followed by Pleistocene palaeosol levels GS60 – GS1 and finally covered by Holocene palaeosols (HS8 – HS1). The most important features of the section is the occurrence of gravel beds A, B, C, D, E, F and G at a consistent cycle of about 400Ka and each two adjacent gravel beds bounding (bracketing) about 8 – 10 palaeosol levels indicating that the palaeosol have a 40Ka cycle. Gravel bed D (below oxisol GS72) is Miocene in age. There are red and yellow silt palaeosols, which are encompassed between gravel bed G, and F covering the Pliocene Period. The Matuyama-Gauss boundary, which corresponds to OIS103-105, occurs at the base of gravel bed F. Gravel bed F till gravel bed C represents the Lower Pleistocene (2.27Ma – 0.91Ma). This period contains 38 palaeosol levels (GS60 – GS23) with the palaeosol cyclicity of about 40Ka comparable to OIS of ODP 677 site (Shackleton, 1973). The interval between gravel bed C and gravel bed A represent the Upper Pleistocene (0.91Ma – 0.11Ma time interval). This period contains 21 palaeosol levels within a 800Ka time interval. Again this infers to 40Ka cyclicity comparable to OIS23-5. The Holocene is represented by 8 palaeosol levels (HS1 – HS8) pointing to a millennial (1Ka) cyclicity.

Olduvai Gorge palaeosol stratigraphy is very similar to that of Greece with some minor age discripancies. Olduvai Gorge section (figure 10.4) begins at about 2.2Ma – the Lower Pleistocene. It has 6 notable gravel bed complexes very correlatable to A, B, C, D, E and F gravel

beds of Greece standard stratotype section. The gravel beds are recorded at approximate intervals of (0.1Ma – 0.20M: A), (0.6Ma – 0.70Ma: B), (0.95Ma – 1.15Ma: C), (1.3Ma – 1.5Ma: D), (1.76Ma – 1.85Ma: E) and (2.2 and older: F).

However, it is observed that the bottom of Gravel Bed E in Olduvai Gorge stratigraphy is dated by Ar-Ar at about 1.8Ma while in the Greece section is located at about 2Ma. It is known that gravel beds are not always stratigraphically time stable and also the correlation between the palaeosols and deep sea stages in the Greece section might have been confused because some Marine Isotopic Stages covers sometimes one soil and some other times more soils. I therefore suggest that instead of having 1.8Ma at the top of gravel bed E it may as well occur at the bottom of the gravel bed E.

Gravel bed F to gravel bed E interval – Bed E inclusive (2.2Ma – 1.76Ma) contain 11 palaeosol levels (GS57 – GS47). This is an interval of 440Ka infering to a palaeosol cyclicity of 40Ka. The gravel bed E to gravel bed D (1.76Ma – 1.4Ma) is a 360Ka interval with 11-14 (GS46 – GS30) palaeosols, which points to a soil cyclicity of about 30Ka. Gravel bed D and gravel bed C interval (1.4Ma – 1.0Ma) is 400Ka cycle with 10 palaeosols (GS29 –GS 22) pointing to an approximate 40Ka palaeosol cycles. The gravel bed C to gravel bed B covers the approximate time interval of 0.95Ma to 0.6Ma – 350Ka. These gravel beds brackets 8 – 10 palaeosols (GS21 – GS12) pointing to a palaeosol cyclicity of 35Ka.

And finally Gravel Bed B to Gravel Bed A interval covers the Upper Pleistocene between 0.6Ma and 0.2Ma (400Ka) encompassing 13 (GS1 – GS11) palaeosol indicating a 31Ka cycle of palaeosol development.

The above observations indicates a Gravel Bed cyclicity in Olduvai Gorge of between 350Ka and 400Ka [i.e. F-E (440Ka), E-D (360Ka), D-C (400Ka), C-B (350Ka) and B-A (600Ka)], averaging into long-term 400Ka – cyclotherms (thermomers and cryomers). This seems consistent to the Greece section (figure 9.7). The deviation of about +/-50Ka observed is probably due to difficulties in age estimates encountered all along in dating continental sediments (this study employs radiometric dates of Manega, 1993 and Kafumu 1995).

As said before these gravel bed complexes observed in Olduvai Gorge represent severe droughts of which in most cases affected the fossil man causing one species to extinct and another to

appear (see chapter 10.1.2 – this study). For instance *Homo habilis* FAD coincides with Gravel Bed E and Gravel Bed D is the LAD for *Australopithecus boisei* and *Homo habilis*. Gravel Bed D is also the FAD for *Homo erectus* hominids.

The palaeosol cyclicities bounded in two specific adjacent gravel beds range from 22Ka to 31Ka [i.e. F-E (40Ka), E-D (30Ka), D-C (40Ka), C-B (35Ka) and B-A (31Ka)] disregarding deviations this would average into a 40Ka palaeosol cycicity (i.e. obliquity) if the datings were perfect. Again this is in agreement with the Greece standard section.

Palaeosol field studies (chapter 6) and laboratory studies (chapters 7 and 8) data of this study indicate that the interval between gravel bed F and gravel bed E was more wet than interval between gravel bed E and D. Again gravel bed D-C interval was wetter than gravel bed interval C-B which was much dry. And finally gravel beds B-A interval was relatively wet compared to the previous interval C-B. The data set further attest that within a generally wet or gravel bed intervals there were alternating dry and humid climates (figure 10.1). Palaeosol and clay levels pointing to wet climates and sand layers to dry climates with a reccurrence of about 40Ka. This attests further the synchroneous nature of the climate all over the globe during the Quaternary.

Moreover, previous studies (Hay 1976, Bonnefille and Riollet 1980, Kappelman 1984 & 1986, Cerling and Hay 1986 and Manega 1993) in Olduvai Gorge earlier pointed to long-term climatic variability of 2.03 – 1.73Ma (300Ka) as a wet and probably cool period. 1.73 – 1.33Ma (400Ka) was a dry and probably a hot period. And in the 1.33 – 0.85Ma (400Ka) interval conditions became generally wet and warm again. Data between 0.85 and 0Ma is lacking. A comparison between long-term climatic cycles deduced from previous studies with the findings of this study in Olduvai Gorge reveals just extraordinarily similar patterns, (table10.2). This is another confirmation of the global nature of the climatic variation during the Quaternary in Olduvai Gorge.

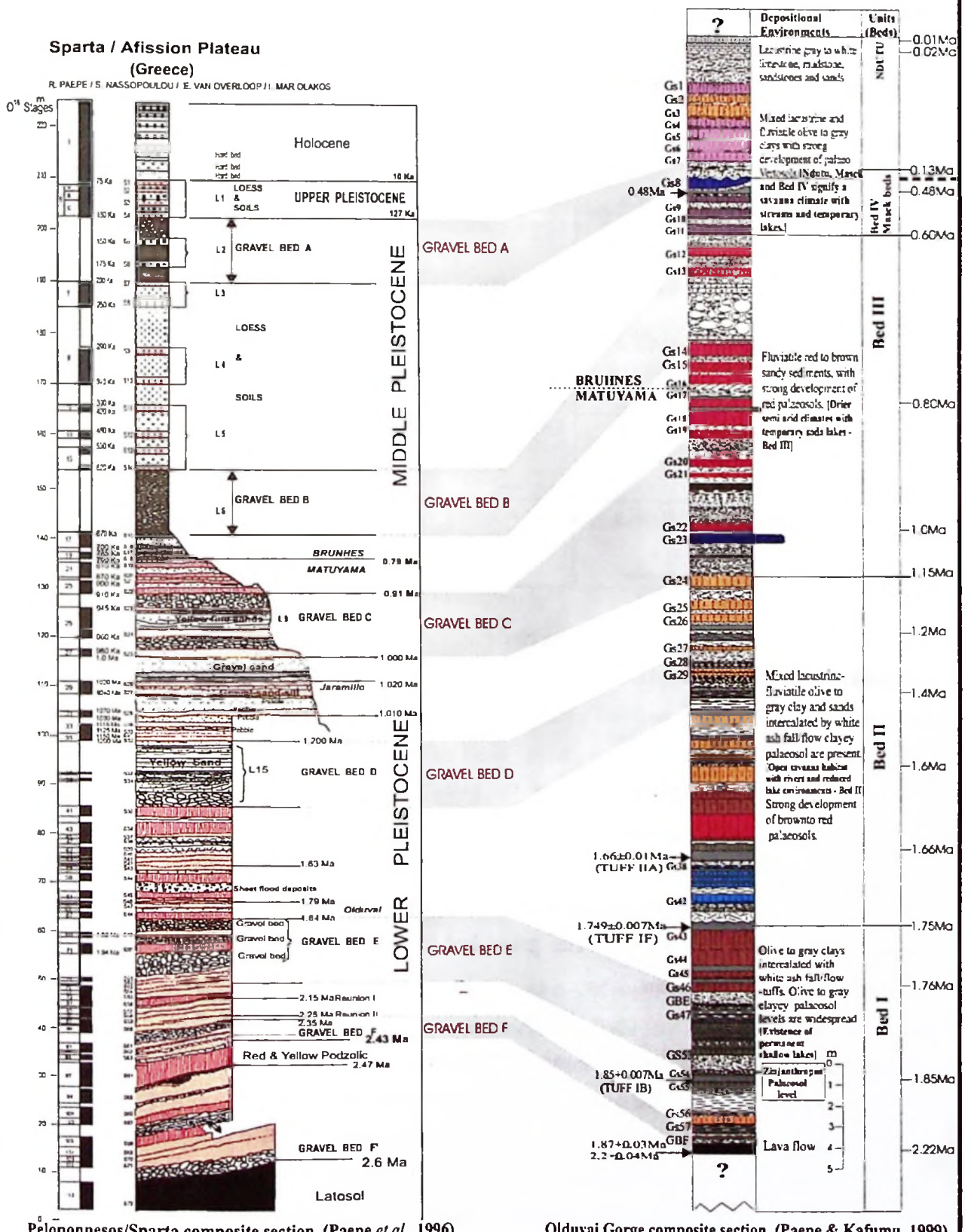

Figure 10.4: A correlation of the Pleistocene palaeosol sequences of Olduvai Gorge - Tanzania with the plaeosol sequences of Peloponnesos/Sparta Plateau stratotype section of Greece

Table 10.2: A comparison of interpretation results of long-term Quaternary climatic variability of Olduvai Gorge. [This Study (Kafumu 1999) = **TS**: Previous Studies (Hay 1976, Bonnefille and Riollet 1980, Kappelman 1984 & 1986, Cerling and Hay 1986 and Manega 1993) = **PS**]

Time interval	Cycle	Climate (Interpretation)	Cyclotherms	Lithlogic units
TS ⇨ 2.20 – 1.76Ma	440Ka	Wet – warm	Thermomer	Lower Bed I
PS ⇨ 2.03 – 1.73Ma	300Ka	Wet – cool		
TS ⇨ 1.76 – 1.40Ma	360Ka	Dry – cool	Cryomer	Upper Bed I lower Bed II and middle Bed II
PS ⇨ 1.73 – 1.33Ma	400Ka	Dry – hot		
TS ⇨ 1.40 – 1.00Ma	400Ka	Wet – warm	Thermomer	Upper Bed II
PS ⇨ 1.33 – 0.85Ma	400Ka	Wet – warm		
TS ⇨ 0.95 – 0.60Ma	350Ka	Dry – cool	Cryomer	Bed III
PS ⇨ ----	----	----		
TS ⇨ 0.60 – 0.2Ma	400Ka	Wet – warm	Thermomer	Bed IV and Masek Beds
PS ⇨ ----	----	----		

10.2.1.2. Manonga-Wembere Valley and Holili localities

Manonga-Wembere Valley

Based on the stratigraphical positions of the palaeosols, magnetic susceptibility, clay and carbonate mineral records of sediments as presented in chapter 9.1.2 and summarized in figure 10.2 the climatic and environmental fluctuation of the Manonga-Wembere area varied considerably. The Upper Pliocene and Lower Pleistocene (3.0Ma – 1.2Ma) began with a dry period marked by two gravel beds. This gravel bed level probably indicates a severe drought towards the end of the Pliocene.

Gravel beds at the base of the section can probably be correlated to gravel bed G of the Greece section (chapter 10.2.1.1). The correlation is based on age equivalence according to Stockely (1948) and Quennel *et al.*, (1956). Three distinct red palaeosol levels that were observed in the field, (GS1 & GS2, GS3 and GS4) in the time period of between 3.0Ma and 1.2Ma, points to a palaeosol cyclicity of 800Ka. This observation suggests that during the Pliocene-Pleisrocene strong red soils may have developed at every 800Ka periodicity in Manonga-Wembere Valley.

GS4 palaeosol level overlying the upper gravel bed marks a significant wet period. Clay bed with numerous carbonate concretions that overlies GS4 is probably the final phase of a dry period towards the end of the Pliocene. GS3, GS2 and mark several series of significant wet periods in the Lower Pleistocene occuring at every 400Ka cycle. There are also 7 long term alternating dry and wet climatic cycles (figure 10.2) in the time interval 2.4Ma –1.2Ma (Upper Pliocene – Lower Pleistocene) pointing to climatic cycles of about 250Ka deduced from magnetic susceptibility and mineralogical studies.

Holili

The lone strong red palaeosol level in Holili points to a very wet period during the Middle Pleistocene at about 750Ka. During this time the areas of East Africa experienced a strong wet/humid climate which is recorded as an interglacial in Europe and correlated to OIS 19.

10.3. THE GEO-SOIL STRATIGRAPHY OF OLDUVAI GORGE

10.3.1. The Importance of the Olduvai Stratigraphy

The stratigraphy of the Olduvai Section of the southeastern Serengeti Plains owns its importance to the discovery of number of fossil animal bones and early Man remains from Olduvai Gorge in East and Central Africa, during expeditions organised by the German Kattwinkel in 1911 and Reck in 1914 (Leakey *et al.*, 1976). The latter investigator introduced the first stratigraphic subdivision of Olduvai composed of Beds I till V. This stratigraphy would become famous and be consequently used by all later investigators including Leakey senior, since his first expedition in 1927 after the British had taken over the Tanganyika Territory (now Tanzania) after World War I.

Soon it became clear that the hominid remains found in Olduvai were old and so the beds. The British geologist Hay (1976) furthermore subdivided the Beds into a series of different layers mainly according to the presence of several volcanic tuff layers. That enabled investigators as Leakey to date not only the beds but the hominid finds as well, However, a detailed geological stratigraphical record failed to exist to date.

Despite the presence of numerous well identifiable clay, sand, tephra and soil layers, none of the previous investigators were successful in setting up a combined detailed litho-, tephra- and soil-

stratigraphic record in order to better date the layers in which the hominid remains occurred as well as the soil levels on which these hominids were living.

Therefore, the numerous Olduvai Hominid (OH) levels which happen to occur in several of these Beds were henceforth, originally badly located in the section. It furthermore remains absolutely impossible to correlate such unprecise stratigraphy with better recorded land, marine and ice sections as known today.

Taking the importance of the Olduvai hominid site into account it is aimed here at the establishment of a reference stratigraphic section for both geological and prehistoric events.

10.3.2. The Pedolithostratigraphical Methodology: Geo-Soil and Geo-Soil-Traverse

The recording of Geo-Soil sequences was taken as a preliminary basic methodology. Actually, a detailed soil stratigraphic record leads to the reconstruction of the sequence of wooded landscapes in which early Man was dwelling around. Then, the interfering clay and gravel layers may correspond to respectively wet lake and arid desertic environments as will be commented hereafter. The tephra layers serve as benchmarks for the time series of the combined soil and sediment layers.

Paepe developed the Geo-Soil Stratigraphical methodology systematically since 1967 (Paepe & Vanhoorne 1967; Paepe 1968, Zagwijn & Paepe 1968, Paepe and Sommé 1970, Sommé, Paepe & Lautridou 1980, Paepe 1971, Paepe & Vanhoorne, 1976, Paepe *et al.*, 1984, Paepe & Van Overloop, 1990, Paepe *et al.*, 1990, Paepe *et al.*, 1993, Paepe *et al.*, 1995, Van Overloop *et al.*, 1995, Paepe *et al.*, 1996, Paepe *et al.*, 1997, Van Overloop & Paepe 1998). In his first publications he dealt with the Upper Pleistocene fossil soils only and subsequently the fossil soil series was broadened to the entire Pleistocene sequence. In doing so he introduced first the concept of GEO-SOIL and later the GEO-SOIL TRAVERSE. Indeed, the connotation Geo-Soil was borrowed by Paepe from Morrison (1967) by which it was stated that in using this connotation, it was clearly emphasised that the fossil soil was being considered as a litho-stratigraphical unit. This was done so in order to avoid discussions at the pure pedological level for which palaeosoils are not quite suitable.

Following Hedberg's "INTERNATIONAL STRATIGRAPHIC GUIDE" (Hedberg, 1975) as proposed to the IUGS - Commission on Stratigraphy in 1975, Sommé, Paepe & Lautridou

furthermore introduced in 1980 the connotation Geo-Soil at the level of Member (Assise) in litho-stratigraphy. This was mainly because in its status of Member, a fossil soil can adhere to more than one Formation and hence serve as an important key horizon. Thus geo-soil correlation became possible between Formations of different lithological composition and of different geomorphological position such as loess-plateau, river terraces and subsidence basins, as well.

This ultimately has led to the GEO-SOIL TRAVERSE concept along a North-South traverse in Europe, starting from the Dutch-Belgian boundary till the Mediterranean in Crete (Greece), and was first introduced by Paepe *et al.* in 1990 for the Last Interglacial - Last Glacial Cycle and furtheron by Paepe *et al.* in 1996 for the entire Pleistocene and for the Holocene.

Van Overloop & Paepe (1998) applied this Geo-Soil-Traverse Methodology also on the Pleistocene Soil Stratigraphic Record in Central Africa from the investigations they have conducted with IFAQ research fellows in Central Africa: in the Ruzizi Valley by Ilunga (1982), in the Lake George - Edward Basin by Musisi (1991), in the Olduvai Gorge by Kafumu (1995) and in the Lower Congo Basin by Kaseba (1996), The work carried out in the Rutshuru Valley by Yamba (1993) was not taken up in this Central and East Africa Geo-Soil-Traverse because stratigraphically was considered as unsound (Paepe, 2000). Anyhow, the Geo-Soil-Traverse methodology proved also here quite excellent through its correlation with the Sparta/Afission section in the Peloponnesos, Greece (Paepe *et al.*, 1996) and with the Huangling/Jiacun section on the Loess Plateau in China (Paepe *et al.*, 1993).

10.3.3. The Geo-Soil Section of Olduvai

There have been in total 57 geo-soils recorded at the section of Olduvai. The nature of the soils was described in another section of this thesis. Here it will essentially be dealt with how they split up over the five Beds and how they can possibly be dated.

In the time span of the upper part of section of Bed I above the lava bed of 2.22Ma, **15** fossil soil layers from GS 57 till GS 43 are counted. The last mentioned palaeosoil is covered by Tuff layer IF of 1.75Ma. The lower part of Bed I under the lava bed and resting on the ignimbrite dated at 2.5Ma as generally reported for the Plio-Pleistocene boundary (Hay 1976, Curtis and Hay 1972 and Drake and Curtis 1978), has not been observed in this section of Olduvai. Gravel Bed F rests directly on the lava bed. Between GS55 and GS46 occurs the next Gravel Bed E in between Tuff

IB and Tuff IC respectively of 1.86 and 1.76Ma and which position will be discussed furthermore hereafter.

In the time span of Bed II starting above Tuff IF, **19** fossil soil layers from GS42 till GS24 are counted. GS31 although doubled was confused as one single soil because of the separating layer being unclear. Age estimates are provided by Tuff IIA 1.66Ma at the base, between GS38 and GS37 and Tuff IID 1.48Ma at the top, between GS27 and GS26. Gravel Bed D in Upper Bed II occurs in the range of GS29 and GS27.

In the time span of Bed III starting at the hard ground GS23, **12** fossil soils occur till GS12. Tuff IIIB above GS17 dates at 0.80Ma the Brunhes/Matuyama boundary in the middle of Bed III. In the lower part below GS19 till the base, a thick gravel body occurs indicates Gravel Bed C while in the upper part between GS14 and GS13 occur Gravel Bed B.

In the time span of Bed IV and Masek Beds, **4** fossil soils from GS11 till GS8 occur and are covered entirely by Gravel Bed A. The age of Tuff IV between GS9 and GS8 is estimated at 0.48Ma.

Finally 7 fossil soils GS7 through GS1 encompass the Ndutu Beds which are covered by coarsely broken clastic materials in which dry cracks occur. The latter may totally correspond to the Nasiusiu Beds.

The topsoil GS0 is the Holocene (Brown) Soil, which generally occurs at the surface in the landscape surrounding Olduvai Gorge.

10.3.4. Dating of Geo-Soils and Boundaries

The series of 57 fossil soils with interfering Gravel Beds can lithostratigraphically perfectly be correlated with the type section of Sparta/Afission section of Greece in which Geo-Soil horizons and Gravel Beds were first described (Paepe *et al.* 1996).

10.3.4.1. Dating of the base of the Geo-Soil Sequence

In the Greek section, fossil soil labelled S57, occurs slightly above Gravel Bed F. This soil horizon encompasses OIS (OXYGEN ISOTOPE STAGE) 83 which on basis of the alternative

astronomical calibration of the Lower Pleistocene Timescale based on ODP Site 677 (Shackleton *et al.* 1990) was dated at 2.06Ma. This date may closely correspond to the one of GS 57 in Olduvai as this fossil soil is almost immediately lying on the lava bed dated about 2.22 Ma and separated from it by a thin gravel bed. Its lithostratigraphical position and close occurrence to the lava bed points at a similar position as Gravel Bed F in Greece.

10.3.4.2. Dating the Lower Pleistocene Boundary in Olduvai

The base of the Greek fossil soil series and the base of Olduvai fossil soil series correlate well in both lithostratigraphical and pedostratigraphical means. Gravel Bed F and GS 57 in both places are key beds for dating the base of the Pleistocene in both sections.

As stated before Gravel Bed F and GS 57 form the base of the upper part of Bed I resting on the lava bed dividing Bed I in two parts. The lower part of Bed I occurs under the lava bed and is resting on the ignimbrite which is dated at about 2.5Ma. The ignimbrite is considered to bear the Plio-Pleistocene boundary and thus to consist of a Pleistocene upper part and a Pliocene lower part. This infers that the lower Bed I section is sandwiched in time between 2.5 and 2.2Ma. An estimate of time of the base of Bed I may then be estimated at 2.4 or 2.3Ma years.

Both latter estimates are close to the Pleistocene lower boundary revealed from other places as in the loess sections of Belgium and China. Indeed, Van Overloop (1998) computed on basis of spectral analysis of the combined Milankovitch cycles, Planetary cycles and Sunspot cycles that the Pleistocene lower boundary of the geo-soil series is located between 2.4 and 2.2Ma.

In comparing again the position of GS57 of Olduvai/Tanzania with S57of Sparta/Greece and the common position of Gravel Bed F, it is clear that in Greece another series of fossil soils (S61, S62 and S63) occur between this gravel and the Red (and Yellow Podzolic) Silt Soil (S64) below. The latter soil corresponds to OIS Stage 97, which is dated at 2.47Ma (Shackleton *et al.* 1990). This date is also obtained for the Red Silt Soil at the base of the Pleistocene Loess fossil soil series in China occurring slightly above the well dated level of the Matuyama/Gauss boundary of 2.6Ma years. As the soil is an environmental key horizon because of a stronger tropical development than all hitherto described overlying soil series of the common Pleistocene record, the Red Silt Soil is generally assumed as being of Pliocene Age. This assumption is also in agreement with all Red Silt Soils dated in other mentioned places of occurrence.

The 2.6Ma boundary occurs in another gravel bed under the Red Silt Soil which also occurs in Greece and which was referred to as Gravel Bed E. The afore discussion reveals that the position of Plio-Pleistocene boundary is certainly above the 2.6Ma and most probably above the Red Silt Soil in the first weaker soil horizon of Pleistocene nature which in Greece complies with S63 corresponding to OIS Stage 95 dated at 2.43Ma. This stratigraphic situation of the Plio-Pleistocene boundary complies in time with the interval of the Lower Bed I of Olduvai between the lava bed of 2.2Ma and the ignimbrite of 2.5Ma as described by Hay, (1976).

10.3.4.3. Dating of the Bed Boundaries in the Olduvai section

The Lower Pleistocene

For Bed I the lower boundary of Bed I (upper part) in Olduvai has been dated at 2.2Ma. While the upper boundary of Bed I is fixed by the age of Tuff IF, 1.749Ma or 1.75Ma. But for the upper soil levels (GS46-43) and the lowermost soils (GS56-57), Bed I entirely falls within the range of the Olduvai event 1.95-1.77Ma. It is complying with the range of OIS 71-63 (Shackleton *et al.* 1990) covering the soil sequence of GS/S55 through 48 in Olduvai.

For Bed II the range extends from lower boundary 1.75Ma till the top of GS24 which coincides with base of Bed III dated by Hay at 1.15Ma. This is suitable with the Tuff IIA and Tuff IID datings of respectively 1.66 and 1.48Ma. Bed I and Bed II were correctly incorporated with the Lower Pleistocene by Hay, (1976).

The Middle Pleistocene

4.3.2.1. Bed III occurs between the boundaries of 1.15Ma and 0.60Ma as stated by Hay. Tuff IIIB (0.80Ma) perfectly separates at the level of the Brunhes/Matuyama boundary in the middle of the strong soil sequence of GS19 till GS14, in two parts: below GS19 Bed III coincides with Gravel Bed C and above GS14, with Gravel Bed B. Gravel Bed C extending from 1.15Ma till almost 0.80Ma covers part of the upper Lower Pleistocene. Actually as of 1.15Ma a serious climatic break is known to exist in the Loess of China and of Belgium as well which was lasting as a period of intensive drought till about 0.8/0.9Ma. After 0.9Ma period of strong soil development followed lasting till about 0.70Ma as the Middle Pleistocene is reached. Hereafter drought returned with Gravel Bed B lasting till almost 0.60Ma.

4.3.2.2. Bed IV and Masek Beds cover the upper half of the Middle Pleistocene. First Bed IV with the soils GS11-GS9 is extending from 0.60Ma till 0.48Ma as dated by Tuff IV and then in the second half lasting till 0.127Ma it is becoming gradually dryer.

The Upper Pleistocene

Starting with the Last Interglacial at 0.127Ma, the Upper Pleistocene very likely is subdivided by the Ndutu Beds with fossil soils GS7 till GS1. It is probably extending till 0.027Ma before the extreme dry cooler phase encompassing the Last Glacial Maximum and the Late Glacial of Europe and elsewhere, starts and which is complying with the Nasiusiu Beds.

The Holocene

The sole evidence of the Holocene is a thin modern soil layer together with the Namarod Ash covering the landscape in the surroundings of the Olduvai section. As the Holocene is generally defined to start at 10.000 BP it is quite possible that this started slightly earlier in the tropical regions. In this respect the dating of the Namarod Ash may be important.

CHAPTER ELEVEN

CONCLUSIONS

11.0 CONCLUSIONS

The stratigraphy and climatic evolution of an area can be better-understood if and only if the a) sedimentological stratigraphy, b) the geomorphological evolution of the landscape and c) the edaphic position and development of the palaeosols are understood. One can not neglect any of these three points for the understanding of the stratigraphy and the climatic variations. This study examined some of the litho-stratigraphical variations (sediments and palaeosols) of Olduvai Gorge and annex areas with a clear mind on the forementioned points and therefore provides the general conclusions that are drawn from this study as follows:

Stratigraphy

The study is a high-resolution stratigraphical identification of numerous beds of Quaternary deposits. Composition of the sediments in all the areas of study are generally sedimentary (clay, mudstone, marls, limestone, sand and gravel) of either fluviatile of lacustrine origin. The sediments are often intercalated with numerous palaeosol levels and volcanic (lava flows and ash flow/fall tuffs) sediments sometimes with calcareous (carbonatites) compositions.

In all the three areas of study these (Pliocene-Pleistocene) sediments are laid down unconformably on a Precambrian basement complex. As expected a huge unconformity prevails between the Precambrian rocks and the Pliocene-Pleistocene sediments. The Precambrian basement is a remnant planation surface. Isolated granite kopjes, quartzite and gneiss inselbergs and hills sticking out from the present plain level, often represent the planation that probably took place at the beginning of the Tertiary (Shackleton, 1978).

Palaeoclimatical and environmental changes

The climatic and environmental changes in Olduvai Gorge, Manonga-Wembere and Holili localities seems to be linked to the global causes of climatic changes. 400ka Gravel beds cyclicity and 40Ka palaeosol are observed in Olduvai Gorge and 800Ka-palaeosol occurrence intervals are observed in Manonga-Wembere valley. This suggests a global synchroneous climatic change known elsewhere in the world.

Hominids

Hominid and fossils (other animals) are closely associated to the palaeosol levels. The palaeosol levels represent landscapes of the past, it is then logical to find fauna and flora in close association with the palaeosol levels. Olduvai Gorge Pleistocene long periods (400Ka) of generally wet periods marked by gravel beds favoured the survival of homonids. The first appearance datum (FAD) and last appearance datum (LAD) of hominid species in Olduvai Gorge area is bound to gravel beds.

In the Manonga-Wembere valley Pliocene long (800Ka) periods of generally dry climates marked by red palaeosols most likely did not favour the survival of hominids it affected their distribution during this time, may be that is why hominids are so rare in Miocene-Pliocene sites. The discovery of a hominid tool in Holili opens new search ground for hominid occurrences in Tanzania.

11.1 OLDUVAI GORGE LOCALITY

11.1.1 Geology and stratigraphy

Olduvai Gorge Quaternary deposits lies unconformably on Archean gneiss and granites of the Usagaran System. The Archean rocks are observed as inselbergs in the Serengeti plains. There was a significant volcanic activity, which produced lava flows and ignimbrites that covered the Archean (Precambrian) peneplained granites and gneisses at about the end of the Pliocene. Then the Olduvai Gorge Quaternary volcano-sedimentary sediments began to be laid down at the beginning of the Quaternary (about 2.5ma).

The Olduvai Gorge stratigraphy covers about 120m thick sediments. It is classified into seven distinct lithostratigraphical members, Bed I – Bed IV, Masek Beds, Ndutu Beds and Nasiusiu Beds (from top to bottom). This present geological work confirms the same units, which were earlier recognised by Reck (1914a) and Hay, (1976) with better a resolution of the single beds and layers within the Bed I – Bed IV which were earlier unmapped. Of specific interest are the numerous palaeosol levels (chapter 6) and gravel beds (chapter 10) which were not recognised by earlier workers. The Old naming nomenclature is maintained in this study. The units are recognised based on their strong natural colour differences, texture and magnetic susceptibility characteristics (see later) as briefly described below:

Bed I is light gray coloured 10m – 60m unit lower member of the Olduvai Gorge beds. It is essentially lacustrine clays interfingering with pyroclasts and ash fall or flow tuffs, some sand beds and palaeosols. Age (Ar-Ar and K-Ar dating) range estimate of Bed I is between 2.30Ma and 1.75Ma (Hay 1976, Walter *et. al.* 1991, Manega 1993 and Kafumu 1995 and references therein)

Bed II is about 30m thick and generally dark gray coloured unit composed of mixed lacustrine-fluviatile olive to gray clay and sand intercalated with white ash fall/flow tuff and clay palaeosols. The middle of this unit contains strongly developed brown to red palaeosols which, are observed to the east of the valley. The upper part of this unit (Bed II) is very sandy in texture. Bed II has an average age range estimate of between 1.75Ma and 1.15Ma (Curtis and Hay, 1972).

Bed III is predominantly a red coloured unit. It is about 16m in thicness marked by sharp colour boundaries. This zone is a mixture of lacustrine and fluviatile sediments mostly affected by pedogenesis. These deposits are composed of essentially fluvial alluvial fans (sands) and gravel with intercalation of lacustrine olive to grey clay and white marls. Numerous red palaeosol levels are observed within this bed. The estimated the age of Bed III is between 1.15Ma and 0.6Ma (Curtis and Hay 1972, Hay 1976 and Manega 1993).

Bed IV and Masek Beds are generally light grey coloured similar to Bed II. Their thickness range from 5m to 40m. The beds thins out to the west and somertimes Ndutu (overlying units) can be found lying unconformably on Bed III. These units are mixed lacustrine and fluviatile olive to grey sediments (mainly clay and silt clay) showing strong development of palaeo-vertisols. Bed IV and Masek beds are grouped together in this study in the age range of 0.6Ma to 0.2Ma.

Ndutu beds as observed by the author of this study are lacustrine and fluviatile gray to white deposits composed of sand-sandstone-mudstone and limestone (from bottom to top). The limestone shows a boxwork of cracks filled by mudstone. 0.2Ma and younger are termed as Ndutu Beds and Nasiusiu Beds (Hay, 1976).

11.1.2. Magnetic susceptibility

Bulk magnetic susceptibility (MS) pattern of Olduvai Gorge is related to the general stratigraphical division and palaeoclimatic fluctuation. Palaeopedogenetic process or to

sedimentation processes are the main factors, which have influenced the MS record of Olduvai Gorge.

Bed I, lower Bed II and Bed IV/Masek bed are grouped as MS zones 1 and 5. The zones posses palaeosols developed on clays, claystone and ash fall/flow tuffs. These palaeosols show enhanced MS values (>$10x10^{-7}$SI units) compared to the parent (clay and tuffs) materials which has MS values less than $10x10^{-7}$SI units. Pedogenesis of the past seems to have enhanced the MS values in the palaeosols.

Upper Bed II and Ndutu beds – zone 3 and zone 6 show highest MS values (>$100x10^{-7}$SI units) in the profile. However, the MS values of the palaeosols in these zones are mostly lower than the background values (<$100x10^{-7}$SI units) of the sand units. Soil forming processes of the past might have diluted the strong magnetic minerals in the sands probably by hydrolysis and organic activity.

Middle Bed II and Bed III (zone 2 and zone 4) posses slightly high MS values (=40 $x10^{-7}$ SI units) which are mainly associated with red palaeosol complexes, sand and silt clay sediments. There is minimum MS fluctuation in these two zones. Gravel and sand beds across the profile always have the highest (>$100x10^{-7}$SI units) magnetic susceptibility values compared to clay or tuff lithologies. This MS enhancement according to lithological type is likely to be related to the sediment origin, where a flux of sediments rich or depleted in magnetic minerals was brought from various source areas by volcanic, river/stream or eolean activity.

The general MS pattern of Olduvai Gorge shows an increasing trend from older to younger units. The Olduvai Gorge MS profile generally indicates that fine grained (clay and tuff facies) sediments have low MS values than the coarse grained (sand and gravel facies) sediments. The reason behind this is that magnetic minerals tend to be concentrated in the sand fraction than in the clay faction (Grimley *et al.*, 1998).

11.1.3. Mineralogy and geochemistry

Short Wave Infrared Reflactance (SWIR) spectrometer analyses revealed that characteristic minerals of Olduvai Gorge palaeosols and clay layers are mainly 1:1, 2:1 clay minerals and zeolites. The relatively fresh tuff layers contain nepheline minerals. Other minerals include carbonates and hydroxides.

The specific 2:1 clay minerals found include, illite (alevardite – rectorite), smectite (beidellite, hectorite, montmorillonite, natronite and saponite). Other 2:1 clay minerals are palygorskite (attarpugite) and sepiolite. 1:1 clay minerals dominating the Olduvai Gorge stratigraphy include kaolinites (halloysite and dickite). Zeolite minerals detected are analcime, natrolite, chabazite, heulandite, clinoptilolite, mordenite and stilbite. The hydroxides are hydroxide (gibbsite, brucite, lepidocrosite and limonite), carbonates (calcite, dolomite, malachite, stronianite and aragonite) and evaporites (gypsum, bassanite, alum, alunite and hankasite).

Sand dunes that are seen covering and spreading on the Serengeti plains were examined by scanning electron microscope and found that they are composed of mainly clinopyroxenes (augite, omphasite and titanoaugite), quartz and garnet.

The Short Wave Infra Red Spectrometry analytical data (especially clay minerals) presented in this study offers little palaeoclimatic signature. It is very difficult to decipher palaeoclimatic trends using SWIR clay minerals variations, as the minerals are depicted as a group of minerals. The formation of some of the clay minerals do not come as a direct consequence of the climate (Thorez, 2000 and Van Overloop 2000 – personal communications) and also weathering processes may give polyminerallic assemblages, (Thorez, 1983).

Nevertheless, the variation trend of carbonate shows that Bed I palaeosols and sediments (2.2Ma – 1.75Ma) indicated higher presence of carbonate minerals. Bed II until lower Bed III (about 0.9Ma) significant fluctuation of carbonate content is depicted in the profile. Upper Bed III until Lower Ndutu Beds indicates the absence of carbonates in palaeosols except at about 0.5Ma. Upper Ndutu and Nasiusiu Beds show presence of carbonates in palaeosols probably referring to dry climates of the late glacial in Europe and elsewhere.

Again it seems likely that during drier climates more zeolites were formed that clay minerals and during wet climates clay minerals were formed more than zeolite minerals. The occurrence of palygorskite (attarpugite) and sepiolite clay minerals in Olduvai Gorge may also point to drier (arid to semi arid) climates, while gibbsite, brucite and limonite may indicate wet/humid climates during the Quaternary. Therefore the mineralogical signatures of Olduvai Gorge beds reflect the general strutigraphical characterization of the beds. This data set is consistent to the earlier recognised broad beds (Bed I, II, III, IV, Masek and Ndutu).

AAS geochemical analyses of major elements in palaeosol levels revealed that red to brown palaeosols (Alfisols) are slightly richer in FeO-Fe_2O_3 and MnO values than other palaeosol levels. Silica/sesquioxide mole ratios of both palaeo-Alfisols and palaeo-Vertisol resemble modern alfisols and Vertisols.

11.1.4. Micromorphology

Pedofeatures of olive-gray palaeosols from Bed I and Lower Bed II are restricted to abundant calcite nodules and hypo-coatings and rare Fe-oxyhydrate infilings, Fe-Mn oxide nodules. There are also rare coatings of opal and unidentified fibrous minerals in pores. A key diagnostic feature of these palaeosols is the absence of clay illuviation features. The absence of clay coating or fragments and the presence of Fe-oxyhydrate and Fe-Mn oxide nodules suggest a frequent flooding hydrological regime. These Geo-soils may probably be palaeo-Aridisols or palaeo-Vertisols.

Upper Bed II, Masek and Bed IV Olive to gray palaeosol levels posses numerous calcite nodules and hypo-coatings with pale yellow clay coatings and rare ferrugenuous Fe-Mn nodules. From field observations these palaeosols also show abundant root activity. Decreasing amounts of clay coatings and increasing amounts of Fe-Mn nodules can indicate poorly drained conditions. Again these Geosoil Levels may be palaeo-Aridisols or palaeo-vertisols.

Pedogenetic illuviation seems to be more intense in red to brown palaeosols of middle Bed II and Bed III. In these palaeosol levels red-yellow clay coating, infillings and fragments are common and sometimes abundant. Dark Fe-oxyhydrate and Fe-Mn nodules, coatings and infillings are also very common. Clay coatings are commonly seen associated with Fe-oxyhydrate typic and hypo-coatings suggesting a highly varied hydromorphic condition associated with alternating wet and dry climates. The multiple micromorphological features that are observed in Bed III and middle Bed II red to brown palaeosols is linked to the climatic changes of the Quaternary. These palaeosols may probably be palaeo-Alfisols (see further explanations in section 11.1.5).

11.1.5. Palaeosol levels

Olduvai Gorge palaeosol stratigraphy contains about 57 palaeosol levels (not studied by previous workers). Based on their origin (parent materials), colour, geochemistry, mineralogy and

micromorphology a tentative taxonomy is proposed. Four-five types of palaeosols are recognised, namely alfisols, aridsols, andisols and vertisols, as briefly described below.

1. Alfisols

Alfisols are classified as red and brown palaeosols with dominant colour range of red (10R6/4), reddish brown (10YR3/2) and yellowish red (5YR5/6). These palaeosols probably developed on sand, sandstone or gravel lithologies. The palaeosols are clayey to massive sandy and gravely in texture. Their macro-pedofeatures include red mottling and red clay-Fe-hydroxide coatings and plant root and twig fossils encrusted with red materials. Alfisol dominant mineralogy includes kaolinite clay minerals, and hydroxides like lepidocrosite, gibbsite and limonite. The geochemistry shows that the palaeosol levels show high values of FeO/Fe_2O_3 and silica/alumina mole ratios resembling modern Alfisols. Red to yellow clay coating and fragments, Fe-Mn hydroxide coating and nodules are the dominant micromorphological features. Alfisols are mapped in middle Bed II and Bed III. These palaeosols infer a wet/humid cilamate during the Quaternary.

2. Alfisols/Vertisols?

These are olive (5Y5/3-4) to pale-olive, (5Y4/4 and 5Y6/3) which are seen to develop on fine clay and claystones. Their pedofeatures include clay distratification by animal and plant activity. Slickenside soil structures are common. Root and stem fossil infills are sometimes observed. Their mineralogy includes kaolinite and gibbsite without $CaCO_3$. These palaeoslols occur in Bed I and Bed II. These are again wet to humid palaeosols. Calcite nodules and coatings are dominant with rare clay coatings and Fe-Mn hydroxide nodules.

3. Aridisols

These are olive grey (5Y4/1-2, 5Y3/2, and 5Y6/2) to dark grey (5Y7/1-2 and 10YR7/2) palaeosol levels which were observed developed on some fine clay and claystones of Bed I and Bed II. Their diagonostic features include presence of $CaCO_3$ concretions and nodules with rare fossil plants. They contain 1:2 clay minerals (smectites and Illites) with zeolite (analcime, chabazite, clinoptilolite and stilbite) minerals and sometimes gypsum and bassanite an indication of arid and semi arid environments of the past. Micromorphological feratures include calcite nodules and coatings.

4. Andisols? (Tuffaceous palaeosols).

These are weakely developed palaeosol levels, usually white (5Y8/1-2) in colour. Such palaeosols are observed to develop on top of ash falls/flow tuff layers. They contain abuntant volcanic ash remainings unaffected by palaeo-pedogenesis. Sometimes $CaCO_3$ concretions are observed. These palaeosols are common on tuff layers of Bed I and BedII.

5. Vertisols

These palaeosols are olive gray to brownish gray (5Y5/1-2 and 2.5Y6/2) and grayish brown (2.5Y5/2) in colour. The common lithology on which the palaeosols developed is on fine clay and silt. Their diagnostic features include clay distratification, slickenside soil structure, gilgai macrostructures and mudcracks. Also mineralogical and geochemical signatures point to palaeo-vertisols. Root traces are sometimes present. These palaeosols dominate in Bed IV and masek Beds in the upper part of the Olduvai Gorge section. Mono-granostriated b-fabric is a common micromorphologic feature of these types of palaeosols. These palaeosols are associated with the seasonally alternating dry and wet climatic conditions in Olduvai Gorge during the Quaternary.

11.1.6 Palaeoclimatic/palaeoenvironmental variability and position of fossil man

The palaeoclimate/palaeoenvironment of Olduvai Gorge as infered by sediment lithological variation, mineralogical, geochemical, micromorphological and magnetic susceptibility data set presented earlier indicate an alternating long-term wet and dry (350Ka - 400Ka cycle) periods consistent to 400Ka cycles of Van Overloop and Paepe (1998).

A gravel bed complex bound each long-term cycle. Five cycles are recognised as mentioned below;

1. Lower Bed I (2.2Ma – 1.76Ma), a relatively humid/wet and probably warm.
2. Middle Bed I and lower Bed II (1.76Ma – 1.4Ma), which was generally, dry and probably cool, compared to lower Bed I.
3. Upper Bed II (1.4Ma – 1.15Ma), probably a generally dry and hot period.
4. Bed III (1.55Ma – 0.60Ma) was an alternating dry/wet period with a generally dry and cool climate.
5. And finally Masek Beds/Bed IV and younger (0.6Ma – 0.20Ma) was a generally wet and warm period.

Palaeosol levels within these long-term cycles indicate short spells of generally wet climates. The palaeosol cycles point to cyclicities of between 35Ka and 40Ka consistent to the Milankovitch (obliquity 40Ka cycle). These long and short term climatic variability attest to the global synchronous of the climatic fluctuations. In some intervals of time there also exist 10Ka palaeosol cycles consistent to Glacial-Interglacial climatic cyles of the Quaternary Epoch of which Holocene is the current Interglacial which is coming to an end.

The paleoclimate of the Olduvai Gorge therefore indicates an alternating wet and dry periods with a general upward drying up trend. Dry environments are indicated by coarse facies (sand and Gravel) and showing high MS values. Palaeosols formed during dry climates contain mainly 2:1 clay and zeolite minerals. On the other hand wet environments are infered by the presence of fine facies and palaeosols containing 1:1 clay and Fe-Al-hydroxide minerals. Quaternary climatic cyclicities in Olduvai gorge points to a global variation of 40Ka and 400Ka consistent to the known astronomically enforced cycles.

The position of hominids (fossil man) in Olduvai Gorge is bound to palaeosol levels (palaeolandscape surfaces of the Quaternary). Most hominid fossil remains (*Australopithecus boisei, Homo habilis and Homo erectus*) in the Olduvai Gorge profile was found in palaeosol levels. It is also interesting to note that the beginning or termination of these specific hominid species coincides with gravel bed complex locations. For instance Gravel Bed E (in Bed I) is the 'last appearance datum' LAD for *Australopithecus boisei* and it is a 'first appearance datum' FAD for *Homo habilis*. Gravel Bed D in upper Bed II is LAD for *Homo habilis* and FAD for *Homo erectus*. A stance is assumed here that the gravel bed complexes mark significant periods of drought in which primitive hominids were forced to disappear and new species well adapted to the new environment were to appear.

Future hominid search would be more successful if palaeosol levels are mapped and followed over long distances. Magnetic susceptibility and palaeosol study can pick more palaeosol levels for palaeoclimatic reconstructions in Olduvai Gorge if a more systematic high resolution (sampling interval of less than 3cm) sampling will be undertaken. I propose more research in this direction to set up a tool for recovering palaeoclimatic information in sand-clay-palaeosol sediment sequences in the world.

11.2 MANONGA -WEMBERE VALLEY LOCALITY

11.2.1 Geology and stratigraphy

The general geology of the Manonga-Wembere valley locality entails mainly lacustrine sediments (clay, sands, gravel, mudstone and limestone) of Pliocene to Pleistocene in age intercalated with palaeosol levels. The palaeosol levels are closely related to the occurrence of animal fossil remains that have been found in the area. Manonga-Wembere sediments were laid down on palaeolake basin (grabens and valleys) which had developed on peneplained Precambrian granites and banded iron formations (BIF) metasediments during the Tertiary.

The studied section (Kininginila) in Manonga-Wembere valley is about 20km thick and is believed to span from 3.0Ma to 1.2Ma in age (Upper Pliocene to Lower Pleistocene). The lower part of the section is essentially gray clay containing gravel beds. This lower unit is overlain by a red palaeosol. Then a nodular or concretion (carbonate) clay level which grades into a white mudstone lie unconformably on the clay levels. The mudstone is followed by layered reddish brown clay sediment which inturn is overlaid by two red and reddish brown palaeosols. Another reddish brown palaeosol layer is observed lying on a grayish whiet clay bed which seperates this palaeosol to the previous ones. The upper part of the section is a series of grayish white, pale yellow and layered dark clay levels laid in succession on top of one another and finally all covered by the present soil level.

11.2.2 Magnetic susceptibility, mineralogy and micromorphology of palaeosol levels

The mineralogy of the red palaeosol levels of the Manonga-Wembere deposits contains halloysite (kaolinite), kaolinite and illite clay minerals together with gibbsite (Al hydroxide) mineral. The reddish brown palaeosol dominant mineralogy is 1:2 clay minerals palygorskite and sepiolite, zeolites (analcime and stilbite) and calcium carbonate. This indicates that the former (red palaeosols) was developed during wet/humid climates where as the later (reddish brown palaeosol) developed during semi-arid climates.

During pedogenic processes in wet/humid climates 1:1 clay minerals could be concentrated probably by conversion of 1:2 clay minerals, while carbonates were leached away. During arid and semi-arid climates no enough water was present to leach out the carbonates and zeolites were formed in place of clay minerals.

The magnetic susceptibility records of these palaeosols indicate that the red palaeosols have higher values compared to the reddish brown ones. This suggests that magnetic minerals were concentrated during the soil forming processes of the red palaeosols. The reddish brown palaeosols Low MS values is attributed to low intensity of weathering during the formation of these palaeosols.

Micromorphological features of Manonga-Wembere Valley palaeosols indicate a dominance of red to yellow clay coating and fragments together with Fe-Mn hydroxide coatings on channels. The groundmass is an accumulation of strongly oriented clay coating fragments. This strong illuviation indicate that pedogenesis took place during a wet climate, probably resembling the present day Meditterranean climates.

11.2.3 Quaternary climatic variability and hominid evolution

Magnetic susceptibility, micromorphology and mineralogy records points to long-term (250Ka) alternating dry and wet climatic cycles. The red palaeosol levels occur at about 800Ka cyclicity. It is concluded here that at every 800Ka cycle a very humid/wet climate may have prevailed. The prevalence of generally dry periods in most parts of the world during the Pliocene probably affected the distribution of hominids as a whole and in Manonga-Wembere Valley in particular.

For future research it is recommended here that an intensive dense sampling campaign coupled with careful lateral and vertical mapping can be undertaken to identify short-term palaeosol cycles, (for stable oxygen isotope, magnetic susceptibility, mineralogical and micromophological studies). As animal fossil occurrences in Manonga-Wembere deposits is associated to palaeosol levels, it is therefore important to accurately map the palaeosol levels and systematically follow their lateral extensions during archaeological excavations rather that execute excavations at randomly selected sites. This may lead into discovering hominid remains in this area.

11.3 HOLILI LOCALITY

11.3.1 Geology and stratigraphy

The stratigraphical sequence of Holili locality is about 30m thick and begins with Precambrian rocks (gneisses). After a long period of peneplaination and pediplanation during Tertiary the rocks were covered by lava flows belonging to the Kilimanjaro volcanic eruption episodes. Then the basalts formed a stable landscape for some time (Pliocene-Pleistocene) where pedogenesis

took place forming a blanket of red soils, which is now observed as a red palaeosol (palaeo-Alfisol). Finally during the Middle Pleistocene the landscape was covered in succession by tuffaceous mudstone, calcareous tuff and grit that erupted from Lake Chala NE of the area.

11.3.2 Palaeoclimatic and palaeoenviromental implications

This study (preliminary geological work) in Holili locality revealed new fossil finds (not reported before) of animal remains (canon bone, tooth and horn cores) of probably a bovid mammal and fossil plants (stem – branches, and leaf impressions) of *angiosperm dicotyledon* plants. These fossils occur on or just above the palaeolandscape (palaeosol level).

The preservation of the fossils was made possible on the palaeolandscape by the carbonate rich tuff flow (carbonatite) which erupted from Lake Chala volcanic centre and covered the Holili landscape of the time. The calcareous tuff quickly harderned and sealed off the landscape to preserve its climatic and life evidence.

The presence of animal fossils, plant remains and a red (alfisol?) palaeosol levels attests to a wet/humid climate during the Lower Pleistocene beginning at about 0.8Ma. This wet period can be correlated to OIS 19, which was a strong interglacial period in Europe.

The lone hominid tool discovered on the palaeo-landscape (palaeosol) in Holili locality is an indication that hominid might have lived in the area during the Pleistocene. So there is a great possibility of finding hominid remains in these deposits. In other words Holili locality stands a chance of joining the 'hominid sites family' of Tanzania.

A detailed geological, palaeontological and archaeological work is worth in the area. Such work should emphasize the mapping of the palaeosol levels, which are often associated with fossil preservations. The potentiality of using $CaCO_3$ from the extensive (>20m thick) calcareous grit deposits to scan the palaeoclimatic (high-resolution) variation using stable oxygen isotope parameter should be explored. New Ar-Ar dating of the basalt and tuff would provide better age estimates of the deposits. It is quite hard to find in situ fossil flora in Tanzania and elsewhere, Holili therefore stands as one of these rare places containing fossil flora worthy investigating.

REFERENCES

Agnew, N. and Demas, M., (1998). Preserving the Laetoli footprints. *Scientific American 279 (3),* 26-37.

Alam, S. MD., (1994). *Stratigraphicalal and palaeoclimatic studies of the Quaternary deposits in North-Western Bangladesh*, pp. 295 (unpublished). Ph.D thesis at the Free University of Brussels (VUB).

Allen, J.R. & Wright, V.P., (1989). *Palaeosol in siliciclastic sequences. A short course book prepared for British Sedimentological Research Group Workshop*, pp6. Oxford, 6th, May 1989.

Allen, B. L., (1985). Micromorphology of Aridsols. In L. A. Douglas and M. L. Thompson (eds). *Soil micromorphology and classification*, (pp 197-216). SSSA special publication number 15. Soil Science Society of America, Madison.

An, Z. S. & Porter, S. C., (1997). Millennial-scale climatic oscillations during the last interglaciation in Central China. *Geology 25,* 603-606.

Arnold R.W., Szaboles I., & Targuilian V.O., (1990). *Global soil Change. Report of an IIASA-ISSS- UNEP task force on the role of soil in global change.* International Institute for Applied System analysis, Luxembourg, Austria.

Aslan, A. and Austin, W., (1998). Holocene flood plain soil formation in Northern lower Mississipi Valley; Implications for interpreting alluvial palaeosols. *Geological Society of America Bulletin 110(4),* 433-449.

Bai Bater, (1993). *Palaeosol cycles in and magnetic properties of the Jiacun Loess section in Northern China*, pp196. Ph.D. thesis at the Free University of Brussels, Belgium.

Barth, H., (1989). *The Lake Victoria gold fields, Tanzania; Provisional Geological Map, 1:500,000,* Hanover/Dodoma, Text and colored map.

Barth, H., (1989). *The Lake Victoria gold fields, Tanzania; Provisional Geological Map, 1:500,000,* Hanover/Dodoma, Text and colored map.

Beck, J. W., Recy, J., Taylor, F., Edwards, R. L. & Cabioch, G. (1997) Abrupt changes in early Holocene tropical sea surface temperatures derived from coral records, *Nature 385,* 705-707.

Behrensmeyer, A. K. & Boaz, D. D., (1980). The recent bones of Amboseli National Park, Kenya in relation to East African paleoecology. In A. K. Behrensmeyer & A.P. Hill, (eds). *Fossils in the making,* (pp. 72-93), Chicago University Press.

Berggren, W. A., Kent, D. V. & Couvering, J. A., (1985). The Neogene, Part II; Neogene geochemistry and chronostratigraphy. In Snelling (ed). *The chronology of the geological record, Memoir 10*, (pp. 211-259). Geological Society (London), Blackwell Scientific Publishers, London.

Bergonzini, L., Chalie, F. & Gasse, F., (1997). Paleoevaporation and paleoprecipitation in the Lake Tanganyika Basin at 18,000 years BP. Infered from hydrologic and vegetation proxies. *Quaternary Research 47*, 295-305.

Betzler, C. and Ring, U., (1995). Sedimentology of theMalawi Rift: Facies and stratigraphy of Chiwondo Beds, Northern Malawi. *Journal of Human Evolution 28*, 23-35.

Birkeland, P. W., (1984). *Soil and geomorphology*; pp 372, Oxford University Press, London.

Bird, I. M. & Cali, J. A., (1998). A million year record of fire in Sub-Saharan Africa. *Nature 394*, 767-769.

Blum, M. D., (1994). Genesis architecture of incised valley fill sequences: A late Quaternary example from the Colorado river, Gulf coastal plain of Texas. In P. Wemer and S. Posamentier, (eds), Silisclastic sequence stratigraphy: Recent developments and applications. *Memoir of the American Association of Petrology and Geology 58*, 259-288.

Bullock, P. and Thompson, M. L., (1985). Micromophology of alfisols. In L. A. Douglas and M. L. Thompson (eds). *Soil micromorphology and classification*, (pp 16-46). SSSA special publication number 15. In L. A. Douglas and M. L. Thompson (eds). *Soil micromorphology and classification*, (pp 121-142). SSSA special publication number 15. Soil Science Society of America, Madison.

Blum, M. D., (1994). Genesis architecture of incised valley fill sequences: A late Quaternary example from the Colorado river, Gulf coastal plain of Texas. In P. Wemer and S. Posamentier, (eds), Silisclastic sequence stratigraphy: Recent developments and applications. *Memoir of the American Association of Petrology and Geology 58*, 259-288.

Blumenschine, R. and Masao, F. T., (1991). Living sites at Olduvai Gorge, Tanzania? Preliminary landscape archaeology results in the basal Bed II lake margin zone. *Journal of human evolution 21, 451-462.*

Blunier, T., Chappelar, J., Schwander, J., Dallembach, A., Stauffer, B., Stocker, T. F., Raynand, D., Jonzel, J., Clausen, H. B., Hamme, C. U. & Johnsen, S. J., (1998). Asynchrony of Antarctic and Greenland climate change during the last glacial period. *Nature 394*, 739-743.

Bullock, P., Fedoff, N., Jongerius, A., Stoops, G., Tursina, T. and Babel, U., (1985). *Handbook for soil thin section description*, pp152. Waine Research Publications. Wolverhampton, UK.

Bullock, P. and Thompson, M. L., (1985). Micromophology of Alfisols. In L. A. Douglas and M. L. Thompson (eds). *Soil micromorphology and classification*, (pp 16-46). SSSA special publication number 15. In L. A. Douglas and M. L. Thompson (eds). *Soil micromorphology and classification*, (pp 121-142). SSSA special publication number 15. Soil Science Society of America, Madison.

Bongole, Z., (1994). *Development of low energy construction materials from Tanzania geological resources, technical, technological and academic aspects*, pp68. M.Sc. thesis at the Free University of Brussels.

Bonnefille, R. & Riollet, G., (1980). Palynologic vegetetion et climats de Bed II `a Olduvai Gorge , Tanzanie. *Proceedings of the 8th Pan African Congress of pre-history and Quiaternary studies,* 123-127. TILLLI MIAP, Nairobi

Bonnefille, R. & Riollet, G., Buchet, G., Icole, M., Lanfort, R., Arnold, M. & Jolly, D., (1995). Glacial/Interglacial record from intertropical Africa, high resolution pollen and carbon dates at Rusaka, Burundi. *Quaternary Science Review 14,* 917-936.

Bonnefille, R., (1984). Palynologyical research at the Olduvai Gorge. *National Geographic Society Research report 17,* 227-243.

Bonnefille, R., Chalie, F., Guiot, J. & Vincens, A., (1992). Quantitative estimates of full glacial temperatures in Equatorial Africa from palynological data. *Climate dynamics 6,* 251-257.

Bonnefille, R., Roeland, J. C. & Guiot, J., (1990). Temperature and rainfall estimates for the past 40,000 years in Equatorial Africa. *Nature 346,* 347-349.

Bornhardt, W., (1900). *Zur Oberrflachengestaltung und geologie Deutsch-Ostafrikas. Deutsch-Ost-Africa, Bd. VII,* pp 247. Dietrich, Reimer, Berlin.

Botha, G. A. & Fedoroff, N., (1995). Palaeosols in Late Quaternary colluvial, Northern Kwa Zulu-Natal, South Africa. Journal of African Earth Scieces 21 (2), 291-311).

Botha, G. A., Scott, L., Vogel, J. C. & von Brunn, V., (1992). Palaeosols and palaeoenvironments during Late Pleistocene hypothermal in Northern Natal. *South African Journal of science 88/89,* 508-512.

Bullock, P., Fedoff, N., Jongerius, A., Stoops, G., Tursina, T. and Babel, U., (1985). *Handbook for soil thin section description,* pp152. Waine Research Publications. Wolverhampton, UK.

Casanova, J. & Hillaire-Micel, C., (1992). Late Holocene hydrological history of Lake Tanganyika, East Africa, from isotopic data and fossil stromatolites. *Paleogeography, paleoclimatology, paleecology 91,* 35-48.

Catt, J. A., (1991). Soils as indicators of Quaternary climatic change in mid-latitude regions. *Geoderma 51,* 167-187.

Cerling, T. E. & Hay, R. L., (1986). An isotopic study of palesol carbonates from Olduvai Gorge. *Quaternary research 25,* 63-78.

Cerling, T. E., Hay, R. L. & O'Neil, J. R. (1977). Isotopic evidence for dramatic climatic changes in East Africa during the Pleistocene. *Nature 267,* 137-138.

Church, A. A. and Jones, A. P., (1995). Silicate-carbonate immiscibility at Oldoinyo Lengai. *Journal of petrology 36 (4),* 869-889.

Clack, J. D. & Cole, S., (1957). Subdivision of the African Quaternary. *Proceedings of the third Pan African Congress on pre-history of Northern Rhodesia,* Rhodesia, 1957.

Clack, J. D., (1965). The later Pleistocene cultures of Africa. *Science 150,* 833-847.

Clack, J. D., (1988). The middle stone age of East Africa and the beginnings of regional identity. *Journal of world prehistory 2*, 235-304.

Clinton, H. R., (1997). *Talking it over:* First lady Hillary Rodham Clinton trip to Africa. *http://www.whitehouse.gov/WH/EOP/First-Lady/html/Africa/040297.html*

CLIPMAP, (1981). *Project members technical report map & chart, serial MC-36, Geological Society of America*, Boulder, Colorado, 1981.

Correns, C. W., (1969). *Introduction to mineralogy*, pp484. Springer – Verlang, Berlin.

Croll, N., (1864). On the physical cause of climate during geological Epochs. *Phil. Mag. 28*, 121 – 137.

Crowley, T. J. & Kim, K. Y., (1996). Comparison of proxy records of climate change and solar forcing. *Geophysics Research Letters 23*, 359-362.

Curry, W. B. & Oppo, D. W., (1997). Synchronous high-frequecy oscillations in Tropical sea surface temperatures and North Atlantic deep-sea water production during the last glacial cycles. *Paleoceonography 12*, 1-14.

Curtis, G.H. and Hay, R. L., (1972). Further geological studies and potassium-argon dating at Olduvai Gorge and Ngorongoro Crater. In W.W. Bishop and J. A., Miller, (eds). *Calibration of human evolution.* (pp287-301). Scottish Academic Press.

Dansgaard, W., Johnsen, S. J., Clausen, H. B. & Langway, C. C., (1971). Climatic record revealed by the Camp Century ice core. In K.K. Terekien, (ed). *The Late Cenozoic glacial ages,* (pp. 37-56). Yale University Press, New Haven.

Dansgaard, W., Johnsen, S. J., Moller, J. & Langway, C. C., (1969). One thousand centuries of climatic record from Camp century on the Greenland ice sheet. *Science 166*, 377-381.

Dasch, E. J., (1996). *Macmillan encyclopedia of earth sciences*, pp1273. Simon & Schuster Macmillan, New York.

Dawson, J. B., (1989). Late Tertiary and Quaternary development of the Northern Tanzania sector of the Gregory rift valley. *Symposium on Afro-Arabian rift system*, Karlusruhe F. R. G., Abstracts.

Dawson, J. B., Smith, J. V. and Steele, I. M. (1995). Petrology and mineral chemistry of plutonic igneous xenoliths from the carbonatite volcano, Oldoinyo Lengai, Tanzania. *Journal of petrology 36*, 797-826.

Dawson, J. B., Smith, J. V. and Steele, I. M. (1989). $(Na_{2.33}Ca_{1.74}others_{0.12})Si_3O_9$ combeite from Oldoinyo Lengai, Tanzania. *Journal of geology 97*, 365-372.

De Conick, F. and Mc Keague, J. A. (1985). Micromorphology of Spodosols. In L. A. Douglas and M. L. Thompson (eds). *Soil micromorphology and classification*, (pp 121-142). SSSA special publication number 15.

Deer, W. A., Howie, R. A. and Sussman, J. (1967). *Rock forming minerals; sheet silicates,*

Volume 3, pp270. Longmans, London.

Deer, W. A., Howie, R. A. and Sussman, J. (1973). *Rock forming minerals; Framework silicates, Volume 4,* pp435. Longmans, London.

DeMenocal, P. B., (1995). Plio-pleistocene African climate. *Science 270,* 53-59.

Downie, C. & Wilkinson, P., (1972). *Geology of Kilimanjaro,* pp 269, University of Shefield, UK.

Downie, C., Humphries, D. W., Moore, L. R., Neves, R., Wilcockson, W. H. & Wilkinson, P., (1953-1957*). Geological map of Kilimanjaro-Moshi (QDS 42, 52 & 57, 1:125,000).* Geological Survey Division, Dodoma, 1963-1964.

Drake R. and Curtis, G. H., (1978). Geochronology of the Laetoli fossil localities in M. D. Leakey and J. M. Hariss (eds). *Laetoli a Pliocene site in Northern Tanzania,* (pp48-52). Claredon Press, London.

Eames, F. E. and Kent, P. E., (1955). Miocene beds of Eastern African coast. *Geological magazine XCII.*

Ebinger, C. J., Deino, A. L., Drake, A. and Tesha, A. L., (1989). Chronology of Volcanism and rift propagation: Rungwe volcanic Province, Africa. *Journal of geophysics research 94,* 15783-15803.

Ebinger, C. J., Deino, A. L., Drake, A. and Tesha, A. L., (1993). Tectonic control on rift morphology: Evolution of the Northern Malawi (Nyasa) rift. *Journal of geophysics research 98,* 17821-17836.

Evans A. L., Fairhead, J. D. and Mitchell, J. G. (1971). Potassium argon ages from the volcanic province of Northern Tanzania. *Nature 229,* 19-22.

Fassbinder, J. W., Stanjek, H. and Vali, H., (1989). Occurrence of magnetic bacteria in soils. *Nature 343,* 161-163.

Fedoroff, N. and Eswaran, H., (1985). Micromorphology of Ultisols. In L. A. Douglas and M. L. Thompson (eds). *Soil micromorphology and classification,* (pp 145-164). SSSA special publication number 15. Soil Science Society of America, Madison.

Fedoroff, N. and Goldberg, P., (1982). Comparative micromorphology of two Late Pleistocene palaeosols (in Paris basin). *Catena 9,* 227-232.

Fedoroff, N., (1997). Clay illuviation in red Mediterranean soils. *Catena 28,* 171-189.

Feng, D. D., (1996). Climatic implication of magnetic susceptibility and 10Ba flux in Chinese loess. *Catena 27,* 143-147.

Feng, Z. D., Johnson, W. C. and Diffendal, Jr., R. F., (1994). Environments of eolian deposition in South Central Nebraska during the last glacial maximum. *Physical geography 15,* 249-261.

Fernandez-Jalvo, Y., Denys, C., Andrews, P., William, T., Dauphin, Y. and Humphrey, L. (1998). Taphonomy and paleoecology Olduvai Gorge Bed I (Pleistocene, Tanzania). *Journal of human evolution 34, 137-172.*

Fine, P., Singer, M. J., La Ven, R., Verosub, K. and Southard, R. J., (1989). Role of pedogenesis in distribution of magnetic susceptibility in two California chronosequences. *Geoderma 44,* 287-306.

Fitzpatrick, M., (1999). *Tanzania, Zanzibar and Pemba*, pp 344. Lonely Planet Publicatons, London, UK.

Flint, R. F., (1959). Pleistocene climates in Eastern and Southern Africa. *Bulletin of the Geological Society of America 70*, 343-374.

Fox, C. A., (1985). Micromorphological characterization of Histosols. In L. A. Douglas and M. L. Thompson (eds). *Soil micromorphology and classification*, (pp 85-104). SSSA special publication number 15. Soil Science Society of America, Madison.

Frake, L. A., (1979). *Climate throught geologic time*, pp261, Elseviers, Amsterdam.

Ganopolski, A., Rahmstorf, S., Petoukhov, V. & Claussen, M., (1998). Simulation of modern and glacial climate with a coupled global model of intermediate complexity. *Nature 391*, 351-356.

Grace, C. & stockley, G. M., (1931). Geology of part of Ussongo area, Tabora Province, Tanganyika Territory. *Journal of East Africa National History Society 37,* 185-192.

Grantham, D. R., (1953). Preliminary note on beds of possible Tertiary age in Southern Province. *Tanganyika Colony Geological mineral resources 3(3),* Dodoma, Tanzania.

Grantham, D. R., (1955b). *The Tunduru-Ruvuma area of Southern Province. Report of Geological Survey of Tanganyika 1,* 1955. Dodoma, Tanzania.

Gratham, D. R., Temperly, B. N. & McConnell, R. B., (1945). Explanation of the Degree Sheet 18, (Kahama). *Bulletin of the Geological Survey of Tanganyika 15,* 1-35.

Grimley, D. A., Follmer, L. R. & McKay, E. D., (1998). Magnetic susceptibility and mineral zonation controlled by provenance in loess along the Illinois and Central Mississippi River Valleys. *Quaternary Research 49*, 24-36.

Grove, A. T. & Goudie, A. S., (1971). Secrets of Lake Stephanie's past. *Geographical Magazine 43,* 542-547.

Guiderson, T. P., Fairbanks, R. G. & Rubenstone, J. L., (1994). Tropical temperature variations since 20,000 years ago; Modulating interhemispheric climatic change. *Science 263,* 663-665.

Haligan, R., (1956). Geology of Tanga area. *Records of the Geological Survey of Tanganyika VI,* 1956.

Handely, J. F. R., (1955). *Raw materials for cement manufacture on Wazo hill, Kisarawe District.* Report JRFH/42 pp26, (unpub.) Geological Survey of Tanzania, 1955, Dodoma.

Handley, J. R. F., (1956). *Quarter Degree Sheet 28, (Nzega), Geological map, 1:125,000. Mwambiti South B 36/D1*, Geological Survey, Dodoma, 1956.

Harris, J. F., (1981). *Summary of the geology of Tanganyika, Part IV, Economic geology, Memoir no. 1*, pp 143. Reprint, Government Printer, Dar-Es-Salaam.

Harrisson, T. & Mbago, M. L., (1997). Introduction: Paleontological and geological research in the Manonga valley, Tanzania. In T. Harisson, (ed), *Neogene paleontology of Manonga Valley, Tanzania; A window into the evolutinary history of East Africa,* (pp. 2-32). Plenum Press, New York, 1997.

Harrisson, T., (1997). Paleoecology and taphonomy of the fossil localities in Manonga Valley – Tanzania. In T. Harisson, (ed), *Neogene paleontology of Manonga Valley, Tanzania; A window into the evolutinary history of East Africa,* (pp. 79-105). Plenum Press, New York, 1997.

Harrison, T. & Baker, E., (1997). Paleontology and biochronology of fossil localities in Manonga Valley, Tanzania. In T. Harisson, (ed), *Neogene paleontology of Manonga Valley, Tanzania; A window into the evolutinary history of East Africa,* (pp. 361-393). Plenum Press, New York, 1997.

Hay, R. L. & Leeder, R. J., (1978). Calcretes of Olduvai Gorge and Ndolanya Beds, Northern Tanzania. *Journal of Sedimentology 25*, 649-673.

Hay, R. L., (1963). Zeolitic weathering in Olduvai Gorge, Tanganyika. *Geological Society of America Bulletin 74*, 1281-1286.

Hay, R. L., (1967). Revised stratigraphy of Olduvai Gorge. In W. W. Bishop and J. D. Clark (eds). *Background to evolution in Africa.* University of Chicago Press, Chicago, 1968.

Hay, R. L., (1976). *Geology of Olduvai Gorge. A study of sedimentation in a semi-arid basin,* pp. 203. University of Califonia Press, Berkley, Chicago.

Hay, R. L., (1986). Geology of the Laetoli area. In M. D. Leakey & J. M. Harris, (eds), *Laetoli; A Pliocene site in Northern Tanzania,* (pp23-47). Clarendon Press, Oxford.

Hays J. D., Imbrie, J. & Shackleton, N. J. (1976). Variation in the earth's orbit; Pacemakers of the ice ages. *Science 194*, 1121-1132.

Hedberg, H.D., (1975). *International Stratigraphic Guide.* IUGS Commission on Stratigraphy, John Wiley and Sons, 200pp.

Hecky, R. E., (1971). *The paleolimnolgy of the alkaline, saline lakes on the Mount Meru lahar,* (unpublished). Ph.D. Thesis at the Duke University UK.

Heller, F. & Liu, T. S., (1982). Magnetostratigraphical dating of loess deposits in China. *Nature 300,* 431-433.

Heller, F. & Liu, T. S., (1984). Magnetism of Chinese loess deposits. *Geophysical journal of the Royal Astronomical society 77*, 125-141.

Heller, F. & Liu, T. S., (1986). Palaeoclimatic and sedimentary history from magnetic susceptibility of Loess of China. *Geophysics Research Letters 13*, 1169 – 1172.

Hopwood, A. T., (1931). Pleistocene mammalia from Nyasaland and Tanganyika Territory. *Geological Magazine 68*, 133-135.

Hopwood, A. T., (1931). Pleistocene mammalia from Nyasaland and Tanganyika Territory. *Geological Magazine 68*, 133-135.

Howard, W. R., (1997). A warm future in the past. *Nature 388*, 418-419.

Howell, F. C., Haesaerts, P. & De Heinzelin, J., (1987). Depositional environments, archaeological occurrences and hominids from members E & F of Shungura Formation (Omo Valley, Ethiopia). *Journal of human evolution 16*, (665-700).

Hus, J. J. & Han, J., (1992). The contribution of loess magnetism in China to the retrieval of past global changes; some problems. *Physical Earth Planet International 70*, 154-168.

Ilunga, L. K. P., (1982). *Le Quaternaire de la Pleine de la Ruzizi*, (unpublished). Ph.D. Thesis at the Free University of Brussels (VUB).

IMAGES (1998). *IMAGE scientific purpose and objectives*: Web-site: http://www.images.cnrs-gif.fr.

Imbrie, J.Z., Hays, J. D., Martinson, D. G., McIntyre, A., Morley, J. J., Pisias, N. G., Prell, W. & Shackleton, N. J., (1984), In A. Berger, J. Z. Imbrie, J. D. Hays, G. Kukla & B. Salzman, (eds), *Orbital theory of Pleistocene climate; Support from a reversal chronology of marine $\delta^{18}O$ record.* (pp 269-303), Reidel Publishing Company, Boston.

Imbrie, T. & Imbrie, J. Z., (1980). Modeling the climatic response to orbital variations. *Science 207*, 947-953.

Intergrated Electronics, (1993). *Pima view (SWIR) software user manual, version 4*. Pty, Ltd. USA.

Ivanov, A. V., Rasskazov, S. V., Boven, A., Andre, L. Maslovskaya, M. N. and Temu. E. B., (1998). Late Cenozoic alkaline-ultrabasic and alkaline basaltic magmatism of Rungwe Provinve – Tanzania. *Petrology 6(3)*, 208-229.

Jenga, S. N., (1998). *Tertiary-Quaternary gold bearing lateritic profiles in the Kahama and Rwamagaza belts, NW Tanzania: A stratigraphicalal geochemical and environmental study,* (unpublished). Ph.D. Thesis at the Free University of Brussels, Belgium.

Johnson, T. C., Scholz, C. A., Talbot, M. R., Kelts, K. Ngobi, G., Beuning, K., Ssemmanda, I. & McGill, J. A., (1996). Late Pleistocene desiccation of late Victoria and rapid evolution of cichlid fishes. *Science 273*, 1091-1093.

Johnson, W. H., (1988). The Pleistocene. In S. Parker (ed), *Mc Graw Hill Encyclopedia of Geological Sciences*, pp722. Mc Graw Hill.

Jungerius, P. D., (1976). Quaternary landscape development of the Rio Magdalena basin between

Neiva and Bogota (Colombia). *Palaeogeography, palaeoclimatology, palaeoecology 19,* 89-137.

Kaaya, Z. Ch. (1985). *The Quaternary stratigraphy, tectonics and sea level fluctuations in Northern Dar-Es-Salaam area: Tanzania,* (unpublished). MSc. Thesis at the University of Dar-Es-Salaam, Tanzania.

Kafumu, P. D., (1995). *The palaeosols in the lithosequences of the Olduvai Gorge Beds Tanzania,* pp82, (unpublished). M.Sc. thesis at the Free University of Brussels, Belgium.

Kafumu, P. D., Stoops, G. and Paepe, R, (1999). *Application of micromorphology to pedostratigraphy; Examples from Olduvai Gorge and Manonga-Wembere Valley, Tanzania.* A paper presented at the Soils and palaeoenvironment reconstruction, application in geo-pedology and archaeo-pedology workshop, 10th November 1999. Belgian Soil Science Society – Thematic Day. Earth Science Institute, University of Gent, Belgium.

Kanza, E. G., (1985). *Holili building stone, 1982 IDRC project report EGK/2,* pp 10 (unpublished), Ministry of Energy and Minerals, Dodoma, Tanzania.

Kappelman, J., (1984). Plio-Pleistocene environments of Olduvai Gorge, Tanzania. *Paleogeography, paleoclimatology, paleoeclogy 48,* 171-196.

Kappelman, J., (1986). Plio-Pleistocene marine-continental correlation using habitat indicators from Olduvai Gorge, Tanzania. *Quaternary research 25,* 141-149.

Kaseba, M.K., (1996). *Formations bauxitiques lateritique de Base-Zaïre: Distribution verticale des facies, evolution and modele, genese et transformation,* pp297. Ph.D. Thesis at the Free University of Brussels, (VUB), Brussels.

Kemp, R. A., Derbyshire, E. & Xingmin, M., (1997). Micromorphological variation of the SI palaeosol across northwest China. *Catena 31,* (77-90).

Kemp, R. A., (1987). Genesis and environmental significance of a burried Middle Pleistocene soil in Eastern England. *Geoderma 41,* 49-77.

Kemp, R. A., Grottenthaler, W. and Preece, R. C., (1994). Pedosedimentary fabrics of soils within loess and colluvial in Southern England and Southern Germany. In A. J. Ringrose-Voase and G.S. Humphreys, (eds), *Soil micromorphology:Studies in management and genesis,* (pp. 207-220). Elseviers, Amsterdam.

Kendall, R. L., (1969). Ecological history of the Lake Victoria basin. *Ecological monographs 39,* 121-176.

Kennedy, M., (1998). *The stratigraphy, sedimentology and thermoluminescence dating of the Upper Kalahari Beds of Weatern Zimbabwe,* pp. 254, (unpublished). Ph.D. Thesis at the Free University of Brussels, (VUB).

Kent, P. E., Hurt, J. A. and Johnstone, D. W., (1971). *The geology and geophysics of coastal Tanzania. Geophysics paper number 6,* pp101. Institute of geological Science, London.

Kukla, G. J., (1987). Loess stratigraphy in Central China. *Quaternary Science Reviews 6,* 191-219.

Heller, F. & Liu, T. S., (1986). Palaeoclimatic and sedimentary history from magnetic susceptibility of Loess of China. *Geophysics Research Letters 13*, 1169 – 1172.

Hopwood, A. T., (1931). Pleistocene mammalia from Nyasaland and Tanganyika Territory. *Geological Magazine 68*, 133-135.

Hopwood, A. T., (1931). Pleistocene mammalia from Nyasaland and Tanganyika Territory. *Geological Magazine 68*, 133-135.

Howard, W. R., (1997). A warm future in the past. *Nature 388*, 418-419.

Howell, F. C., Haesaerts, P. & De Heinzelin, J., (1987). Depositional environments, archaeological occurrences and hominids from members E & F of Shungura Formation (Omo Valley, Ethiopia). *Journal of human evolution 16*, (665-700).

Hus, J. J. & Han, J., (1992). The contribution of loess magnetism in China to the retrieval of past global changes; some problems. *Physical Earth Planet International 70*, 154-168.

Ilunga, L. K. P., (1982). *Le Quaternaire de la Pleine de la Ruzizi*, (unpublished). Ph.D. Thesis at the Free University of Brussels (VUB).

IMAGES (1998). *IMAGE scientific purpose and objectives*: Web-site: http://www.images.cnrs-gif.fr.

Imbrie, J.Z., Hays, J. D., Martinson, D. G., McIntyre, A., Morley, J. J., Pisias, N. G., Prell, W. & Shackleton, N. J., (1984), In A. Berger, J. Z. Imbrie, J. D. Hays, G. Kukla & B. Salzman, (eds), *Orbital theory of Pleistocene climate; Support from a reversal chronology of marine* $\delta^{18}O$ *record.* (pp 269-303), Reidel Publishing Company, Boston.

Imbrie, T. & Imbrie, J. Z., (1980). Modeling the climatic response to orbital variations. *Science 207*, 947-953.

Intergrated Electronics, (1993). *Pima view (SWIR) software user manual, version 4.* Pty, Ltd. USA.

Ivanov, A. V., Rasskazov, S. V., Boven, A., Andre, L. Maslovskaya, M. N. and Temu. E. B., (1998). Late Cenozoic alkaline-ultrabasic and alkaline basaltic magmatism of Rungwe Provinve – Tanzania. *Petrology 6(3)*, 208-229.

Jenga, S. N., (1998). *Tertiary-Quaternary gold bearing lateritic profiles in the Kahama and Rwamagaza belts, NW Tanzania: A stratigraphicalal geochemical and environmental study,* (unpublished). Ph.D. Thesis at the Free University of Brussels, Belgium.

Johnson, T. C., Scholz, C. A., Talbot, M. R., Kelts, K. Ngobi, G., Beuning, K., Ssemmanda, I. & McGill, J. A., (1996). Late Pleistocene desiccation of late Victoria and rapid evolution of cichlid fishes. *Science 273*, 1091-1093.

Johnson, W. H., (1988). The Pleistocene. In S. Parker (ed), *Mc Graw Hill Encyclopedia of Geological Sciences*, pp722. Mc Graw Hill.

Jungerius, P. D., (1976). Quaternary landscape development of the Rio Magdalena basin between

Neiva and Bogota (Colombia). *Palaeogeography, palaeoclimatology, palaeoecology 19*, 89-137.

Kaaya, Z. Ch. (1985). *The Quaternary stratigraphy, tectonics and sea level fluctuations in Northern Dar-Es-Salaam area: Tanzania,* (unpublished). MSc. Thesis at the University of Dar-Es-Salaam, Tanzania.

Kafumu, P. D., (1995). *The palaeosols in the lithosequences of the Olduvai Gorge Beds Tanzania,* pp82, (unpublished). M.Sc. thesis at the Free University of Brussels, Belgium.

Kafumu, P. D., Stoops, G. and Paepe, R, (1999). *Application of micromorphology to pedostratigraphy; Examples from Olduvai Gorge and Manonga-Wembere Valley, Tanzania.* A paper presented at the Soils and palaeoenvironment reconstruction, application in geo-pedology and archaeo-pedology workshop, 10th November 1999. Belgian Soil Science Society – Thematic Day. Earth Science Institute, University of Gent, Belgium.

Kanza, E. G., (1985). *Holili building stone, 1982 IDRC project report EGK/2,* pp 10 (unpublished), Ministry of Energy and Minerals, Dodoma, Tanzania.

Kappelman, J., (1984). Plio-Pleistocene environments of Olduvai Gorge, Tanzania. *Paleogeography, paleoclimatology, paleoeclogy 48*, 171-196.

Kappelman, J., (1986). Plio-Pleistocene marine-continental correlation using habitat indicators from Olduvai Gorge, Tanzania. *Quaternary research 25,* 141-149.

Kaseba, M.K., (1996). *Formations bauxitiques lateritique de Base-Zaïre: Distribution verticale des facies, evolution and modele, genese et transformation,* pp297. Ph.D. Thesis at the Free University of Brussels, (VUB), Brussels.

Kemp, R. A., Derbyshire, E. & Xingmin, M., (1997). Micromorphological variation of the SI palaeosol across northwest China. *Catena 31*, (77-90).

Kemp, R. A., (1987). Genesis and environmental significance of a burried Middle Pleistocene soil in Eastern England. *Geoderma 41*, 49-77.

Kemp, R. A., Grottenthaler, W. and Preece, R. C., (1994). Pedosedimentary fabrics of soils within loess and colluvial in Southern England and Southern Germany. In A. J. Ringrose-Voase and G.S. Humphreys, (eds), *Soil micromorphology:Studies in management and genesis,* (pp. 207-220). Elseviers, Amsterdam.

Kendall, R. L., (1969). Ecological history of the Lake Victoria basin. *Ecological monographs 39*, 121-176.

Kennedy, M., (1998). *The stratigraphy, sedimentology and thermoluminescence dating of the Upper Kalahari Beds of Weatern Zimbabwe*, pp. 254, (unpublished). Ph.D. Thesis at the Free University of Brussels, (VUB).

Kent, P. E., Hurt, J. A. and Johnstone, D. W., (1971). *The geology and geophysics of coastal Tanzania. Geophysics paper number 6,* pp101. Institute of geological Science, London.

Kukla, G. J., (1987). Loess stratigraphy in Central China. *Quaternary Science Reviews 6*, 191-219.

Kukla, G. J., Heller, F., Liu, X. M., Ku, T. C., Liu, T. S. & An, Z., (1988). Pleistocene climates in China dated by magnetic susceptibility. *Geology 16*, 811-814.

Lafferty, P. & Rowe, J., (1997). *Dictionary of science*, Pp 678. Brockhampton Press, London.

Leakey, D. and Roe, D. (1995). *Olduvai Gorge, Volume 5; Excavations in Bed III, IV and the Masek Beds, 1968 – 1971*, pp 327. Cambridge University Press, Cambridge.

Leakey, M. D., Hay, R. L., Curtis, G. H., Drake, R. E., Jackes, M. K. & White, T. D., (1976). Fossil hominid from Laetoli Beds, Tanzania. *Nature 262,* 460-465.

Leakey, L. S. B, (1967*). Introduction.* In L. S. B. Leakey (1967). Olduvai Gorge, 1951 – 61, Volume 1. A preliminary report on the geology and fauna. (pp XI-XIV). Cambridge University Press. Cambridge.

Leakey, M. D., Hay, R. L., Curtis, G. H., Drake, R. E., Jackes, M. K. & White, T. D., (1976). Fossil hominid from Laetoli Beds, Tanzania. *Nature 262,* 460-465.

Longworth, G. Becker, L. W., Thomson, R., Oldfield, F., Dearing, J. A. and Rummery, T. A., (1979). Mossbauer effect and magnetic studies of secondary iron oxides in soils. *Journal of Soil Science 30*, 93-110.

Lowe, J. J. & Walker, M. J. C., (1987). *Reconstructing Quaternary environments.,* pp 389, Longman Scientific Technical, New York, 1987.

Lyell, C., (1839). *Principles of geology*. Pp. 398, Murray, London.

Macinntyre, R. M. Mitchell, J. G. and Dawson, J. B., (1974). Age of fault movements in Tanzanian sector of East African Rift System. *Nature 247,* 354-356.

Mack, G. H. and James, W. C., (1994). Palaeoclimate and the global distribution of palaeosols. *Journal of geology 102*, 360-366.

Mack, G. H., James, W. C. and Monger H.C., (1993). Classification of palaeosols. *Bulletin of the Geological Society of America 105,* 129-136.

Maher, B. A., (1986). Characterization of soils by mineral magnetic measurements. *Phsics of the earth and planetary interions 42*, 76-92.

Mahaney, W.C., (1980). Palaeoclimate reconstructions from palaeosols; Evidence from Rocky Mountains and East Africa, In W.C. Mahaney (ed), *Quaternary palaeoclimates*, (pp227-247). Geo Abstruct Ltd, Norwich, 1980.

Manega, P., C., (1993). *Geochronology, geochemistry and isotopic study of the Pliocene-Pleistocene hominid sites and the Ngorongoro volcanic highlands in Northern Tanzania*, pp. 382, (unpublished). Ph.D. Thesis at the University of Colorado, USA.

Mann, M. E., Bradley, R. S. and Hughes, M. K., (1998). Global scale temperature patterns and climate forcing over the past six centuries. *Nature 392*, 779-787.

Massola, S. M. B., (1997). (*Personal communications on the ongoing drilling research in Rukwa Lake Sediments*).

Mbawala, F. (1995). *Monthly Field Report File.* Geological Survey of Tanzania, Dodoma.

Mbede, E. I., (1991). The sedimentary basins of Tanzania – Reviewed. *Journal of African Earth Sciences 13 (3-4)*, 291-297.

McCabe, A. M. & Clark, P. U., (1998). Ice sheet variability around the North Atlantic Ocean during the last deglaciation. *Nature 392*, 373-377.

McCall, G. J. H., Baker, B. H. & Walsh, J., (1967). Late tertiary and Quaternary Sediments of the Kenya Rift Valley. In W.W. Bishop and J. D. Clark (eds), *Background to evolution in Africa*, (pp191–220). University of Chicago Press.

McCarthy, P. J., (1995). *Anatomy and evolution of a Lower Cretaceous alluvial plain: Continental sedimentation and pedogenesis, Mill Creek Formation, Alberta.*, (unpublished). Ph.D. Thesis at the University of Guelph, Canada.

McCarthy, P. J., Martin, I. P. and Leckie, D. A., (1997a). Anatomy and evolution of a Lower Cretaceous alluvial plain: Sedimentology and palaeosols in the Upper Blairmore Group, Southwestern Alberta, Canada. *Sedimentology 44*, 197-220.

McCarthy, P. J., Martin, I. P. and Leckie, D. A., (1997b). Pedosedimentary history and floodplai dynamics in the Lower Cretaceous upper Blairmore Group, Southwestern Alberta, Canada. *Canadian Journal of Earth Sciences 34*, 598-617.

McCarthy, P. J., Martini, I. P. and Leckie, D. A., (1998). Use of micromorphology for paleoenvironmental interpretation of complex alluvial palaeosols: an example from the Mill Creek Formation (Albian), southwest Alberta, Canada. *Paleogeography, paleoclimatology, paleoecology 143*, 87-110.

Mckinlay, A. C. M., (1954). The geology of Kateweka-Mchuchuma coal fields, Njombe District. *Bulletin of the geological Survey of Tanganyika 21.*

Milankovitch, M., (1941). *Kanon der Erdbestrahlung und Seine an wendung auf da Eiszeiten problem.* Royal Serb Academy, Special publication 133, 1-1633.

Miller, R. W. and Donahue, R. L., (1995). *Soil in our environment*, 7th eddition, pp649, Prentice Hall Inc. Englewood Cliffs, USA.

Mohr, E. C. J., Van Baren, F. A. and Schuylenborgh, J. (1972). *Tropical soils; A comprehensive study of their genesis*, pp481. Mouton – Ichtiar Baru – Van Hoeve, The Hague.

Morrison, R. B., (1967). Principles of Quaternary soil stratigraphy in means of correlation of Quaternary succession. In Morrison, M. B. and Wright, M. E. (eds), *INQUA proceedings VII – Congress 9*, (pp1-69).

Mruma, H. H. H. (1990). *Tracing movements of topsoils by magnetic measurements in Maarke-Kerkem (Belgium)* pp60, (unpublished). M.Sc. thesis at the Free University of Brussels, Belgium.

Muller, R. A. & Macdonald, G. J., (1995). Glacial cycles and orbital inclination. *Nature 377,* 107-108.

Munsell Color Macbeth - Kollmorgen Corporation (1975). *Munsell soil color charts,* 1975 edition. Baltimore, Maryland.

Museum of Science, Boston, (1996). Scanning electron microscope; How the SEM works. Web-site: *http://www.mos.org/sln/sem/seminfo.html.*

Mushi, A. G. (1979). *Final project report – Pugu kaolin drilling* (unpublished) – ASTAMICO, Dodoma, Tanzania.

Musisi, J. H., (1991). *The Neogene-Quaternary geology of the Lake Edward basin, Uganda.*, Pp. 299, (unpublished). Ph.D. Thesis at the Free University of Brussels, VUB.

Mutakyawa, M., (1997). Minerology of Wembere-Manonga Valley, Tanzania and possible provinence of the sediments. In T. Harisson, (ed), *Neogene paleontology of Manonga Valley, Tanzania; A window into the evolutinary history of East Africa,* (pp. 67-78). Plenum Press, New York, 1997.

Nahon, D. B., (1986). Evolution of Tropical iron crust in Tropical landscapes. In S. M. Colman and D. P. Dethier, (eds), *Rates of chemical weathering of rocks and minerals*, (pp 169-189). Academic Press Inc. UK.

Nettleton, W. D. and Sleeman, J. R., (1985). Micromorphology of Vertisols. In L. A. Douglas and M. L. Thompson (eds). *Soil micromorphology and classification*, (pp 165-195). SSSA special publication number 15. Soil Science Society of America, Madison.

Nikiforova, K. V., (1978). Status of the boundary between Pliocene and Pleistocene. *American Association of Petroleum Geologists,* 171-178.

Nilsson, T., (1983). *The Pleistocene geology and life in the Quaternary Ice Age,* Pp 651. Reidel Publishing Company, Dordrecht, Boston, London

Paepe, R. (1966). Comparative stratigraphy of Wurm loess depositsin Belgium and Austria. *Bull. Soc. Belge Geol 75 (2)*, 203-216.

Paepe, R. & Vanhoorne, R., (1967). The stratigraphy and paleobotany of the Late Pleistocene in Belgium. *Memoir 8,* pp. 96, (Geological map of Belgium).

Paepe, R., (1968). Les sols fossiles plèistocëne de la Belgique. *Pedologie, 18 (2),* 176-188.

Paepe, R. (1970). *Dating and naming of fossil soils in Belgium Pleistocene stratigraphy. Soil science palaeopedology symposium papers,* pp. 261-269. Jerusalem, 1971.

Paepe, R., & Sommé, J., (1970). Les Loess et la Stratigraphie du PlÈistocËne rÈcent dans le Nord de la France et en Belgique. *Ann. Soc. GÈol. du Nord, 90,* 4: 191-201.

Paepe, R., (1971). Dating and Position of Fossil Soils in the Belgian Pleistocene Stratigraphy. In: D. Yaalon (ed.) *Palaeopedology, Origin, Nature and Dating of Palaeosols.* Israel Universities Press, Jerusalem: 261-269.

Paepe, R., (1974). Correlation of Middle Pleistocene deposits with aid of paleosoils in Belgium. *Quaternary glaciation in the Northern Hemisphere, report 1*, pp. 69-77, Brussels, 1974.

Paepe, R., & Vanhoorne, R., (1976). *The Quaternary of Belgium (in its relationship to the stratigraphical legend of the Geological Map).* Memoir of the Geological Survey of Belgium, 18: 38pp.

Paepe, R. Van Overloop, E. & Thorez, J. (1984). Desertification cycles in historical Greece. *Progress in biometeorology 3*, 55-64.

Paepe, R., Mariolakos, I., Van Overloop, E., & Keppens, E., (1990). Last Interglacial-Glacial north-south geosoil traverse. *Quaternary International 5*, 57-70.

Paepe, R. & Ilunga, L., (1990). Climatic oscillations as registered through Ruzizi plain deposits (North Lake Tanganyika), In R. Paepe, Farbridge, R. W. & Jelgersma, S. (eds), *Greenhouse Effect, Sea Level and Drought, NATO ASI Series C,* (pp. 297-300), Kluwer Academic Publishers.

Paepe, R., & Van Overloop, E., (1990). River and soil cyclicities interfering with sea level changes, In : Paepe, R., R.W. Fairbridge and S. Jelgersma, (eds), *Greenhouse Effect. Sea Level and Mitigation of Drought, Kluwer Academic Publishers*, Boston: 253-280.

Paepe, R., Zhang H.P., Haesaerts, P., Hus, J., Shi J.S. & Zhang Z.G., (1993). The Huangling Loess Section. In: *Report on the Joint Quaternary Loess Project in China of the Geological Survey of Belgium and the Institute of Hydrology and Engineering Geology of China* 1992-1993: 110pp.

Paepe, R. & Van Overloop, E., (1994). Mitigation of drought from global geological evidence. *World resource review 6 (4)*, (545-558).

Paepe, R. (1995). *Geologie, geomorphologie et stratigraphie du Quaternaire: Seminaire de geologie du Quaternaire Universite du Burundi,* pp90. International postgraduate course for fundamental applied Quaternary geology; IFAQ-UNESCO, VUB, Brussels.

Paepe, R., Hadziotis, M.E. & Van Overloop, E., (1995). Twenty Cyclic Pulses of Drought and Humidity during the Holocene. In: Charles, W. Finkl (ed.), Holocene Cycles: Climate, Sea Levels and Sedimentation. *Journal of Coastal Research Special 17,* 55-61.

Paepe, R., Mariolakos, I., Nassopoulou, S. S., Van Overloop, E. & Vouloumanos, N. J., (1996). Quaternary periodicities of drought in Greece. In A. N. Angelakis and A. S. Issar (eds), *Diachronic climatic impacts on water resources, NATO ASI series 136* (pp77-110), Springer – Verlag, Berlin, Heidelberg.

Paepe, R., Van Overloop, E. & Fairbridge, R.W., (1997). Klimaatveranderingen en astronomische chronologie van de laatste 10.000 jaren (Holoceen Tijdvak). *Medededelingen der Zittingen van de Koninklijke Academie der Overzeese Wetenschappen, Brussel, 43 (3).* 393-419.

Paepe, R. and Kafumu, P. D. (1999). Palaeosol sequences as evidence of long and short-term climatic cycles in Olduvai Gorge Pleistocene sedimentary deposits – Tanzania. *(In Press).*

Paepe, R., (2000). Personal communications.

PAGES (1998a). *News of the International paleoscience community; A core project of International Geosphere-biosphere program (IGBP) 6(1),* pp 19. PAGES International Project office, Bern, Switzerland.

PAGES (1998b). Global palaeoclimate and environmental variability: Web site; *http://www.pages.unibe.ch.*

Paillard, D. (1998). The timing of Pleistocene glaciation from a simple multiple-state climate model. *Nature 391*, 378-381.

Pawluk, S. and Bal, L., (1985). Micromorphology of selected mollic epipedons. In L. A. Douglas and M. L. Thompson (eds). *Soil micromorphology and classification*, (pp 121-142). SSSA special publication number 15. Soil Science Society of America, Madison.

Petit-Marie, N., (1990). Natural aridification or man-made desertification?. In R. Paepe, Farbridge, R. W. & Jelgersma, S. (eds), *Greenhouse Effect, Sea Level and Drought.*

Petro, F. N. S, and Hakika, S. (1994). *Brief explanation of the geology of QDS120.* Geological Survey of Tanzania, Dodoma.

Petro, F. N. S, and Mafwimbo, W. Z. (1994). *Brief explanation of the geology of QDS100.* Geological Survey of Tanzania, Dodoma.

Pickering, R. (1956 – 1957). *A brief explaination of the geology of Oldoinyo Ogol (Serengeti Plain East) QDS 38, Scale, 1:125,000.* The Geological Survey of Tanzania, 1958, Dodoma.

Pickering, R., (1958). A Pleriminary note on the Quaternary geology of Tanganyika. *Joint meeting East-Central, West-Central and Southern Regional Committee for geology. Leopoldsville 1958*, 77-89.

Pickering, R. (1958 – 1961). *A brief explaination of the geology of Enduleni, QDS 52, Scale, 1:125,000.* The Geological Survey of Tanzania, 1964, Dodoma.

Pickering, R., (1960). *Brief explaination of the geology of the areas in QDS 38, QDS 39, QDS 52 and QDS 53.* Geological Survery of Tanzania. 1964, Dodoma, Tanzania.

Pickering, R., (1993). *Ngorongoro's geological history*, pp46. NCAA, Arusha, Tanzania.

Pokras, E. M. & Mix, A. C. (1985). Eolian evidence for spatial variability of Late Quaternary climates in Tropical Africa. *Quaternary Research 24*, 137-149.

Potts, P., J. (1987). *A hand book of silicate rock analysis.* Blackie, London.

Prasad, G. I., Dixit, P. C. and Nanyaro, J. T., (1981). A study of limestone around Wazo hill, Dar-Es-Salaam. *Dar-es-salaam University Science Journal 7(1&2),* 117-131.

QRA (1998). *The Quaternary.* Web site: http://qra.org.uk/what.html.

Quennell, A. M., Mckinlay, A. C. M. & Aitken, W. G., (1956). *Summary of the geology of Tanganyika; Part I: Introduction and Stratigraphy, Memoir 1,* pp 264. Reprint, Government Printer, 1986, Dar-Es-Salaam, Tanzania.

Rake, A., (1990). *Traveller's guide to East Africa,* pp360. IC Publications Ltd, London.

Reck, H., (1914b). Zweste volaufige mitteilung uber fossile, tier-und menschenfunde ans Oloway in Zentralafrika. *Sond. Sitz. Ges. Naturf. Freunde, Berlin 7,* 305-318.

Retallack, G.J., (1990). *Soils of the past; An introduction to palaeopedology,* pp520. Unwin Hyman, London.

Retallack, G.J., (1994). The environmental factor approach to the interpretaion of palaeosols. In R. Amundson, J. Harden and M. Singer, (Eds); *Factors of soil formation.* A 50th anniversary retrospective. SSSA Special publication, 33. Madison Wl pp 31-64.

Retallack, G.J., (1993). Classification of palaeosols; Discussion. *Geological Soceity of America Bulletin, 105,* 1635-1637.

Retallack, G.J., (1994). The environmental factor approach to the interpretaion of palaeosols. In R. Amundson, J. Harden and M. Singer, (Eds); *Factors of soil formation.* A 50th anniversary retrospective. SSSA Special publication, 33. Madison Wl pp 31-64.

Roberts, N., Taieb, M., Barker, P., Damnati, B., Icole, M. N. & Williamson, D., (1994). Timing of Younger Dryas event in East Africa from Lake level changes. *Nature 366,* 146-148.

Ruddiman, W. F., McIntyre, A. & Yaymo, M., (1986). Matuyama 41,000-year cycles: Norht Atlantic Ocean and Northern Hemisphere ice sheets. *Earth planetary science letters 80,* 117-129

Ruddiman, W. F., Mcntyre, A. & Raymo, M., (1986). Matuyama 41,000-year cycles; North Antlantic ocean and Northern Hemisphere ice sheet. *Earth planetary science letters 80,* 117-129.

Rutgens, F. K. & Tabuck, E. J., (1989). *Essentials of geology,* pp. 378, Third edition, Merrill Publishing Company, Columbus, Ohio.

Sampson, D. N., (1953). *Contribution to the Sheffield University geological expedition to Kilimanjaro 1953. "Detailed field notes of Lower Rhombo zone – Merti to Lake Chala". Report No DNS/48,* pp 4 (unpublished). Geological Survey of Tanganyika, April 1955, Dodoma.

Schulz, H., Von Rad, U. & Erlenkense, H., (1998). Correlation between Arabian Sea and Greenland climatic oscillations of the past 110,000 years. *Nature 393,* 54-57.

Schwertmann, U. and Taylor, R. M., (1977). Iron oxides in J. B (ed), *Minerals in soil environments,* (pp 145-180). Soil Science Society of America.

Shackleton, N.J. & Opdyke, N.D., (1977). Oxygen isotope and paleoclimatic evidence for early Northern Hemisphere glaciation. *Nature 270,* 216-217.

Shackleton, R. M., (1978). Structural development of Eastern African Rift system. In W.W. Bishop, (ed) *Geological background to fossil man: recent researches in the Gregory Rift valley of east africa.* (pp 7-15) Scotish Academic Press. 1978, London.

Shackleton, N.J., Berger, A. & Peltier, W. R., (1990). An alternative astronomical calibration of the Lower Pleistocene time scale based on ODP Site 677. Transactions of the Royal society of Edinburgh. *Earth Sciences, 81,* 251-261.

Simpson, G. G., (1963). Foreword. In L. S. B. Leakey (1967). *Olduvai Gorge, 1951 – 61, Volume 1. A preliminary report on the geology and fauna.* (pp IX-X). Cambridge University Press. Cambridge.

Somi, E. J., (1993). *Palaeoenvironmental changes in Central and Coastal Tanzania during the Upper Cenozoic,* Pp 100, (unpublished). Ph.D. thesis at the Stockholm University, Sweden.

Sommé, J., Paepe, R. & Lautridou, J.-P., (1980). Pricipes, méthodes et système de la Stratigraphie du Quaternaire dans la Nord-Ouest de la France et la Belgique. *Supplément au Bull. AFEQ N.S. 1,* 148-162.

Spence, J., (1957). The geology of part of the Eastern Province Of Tanganyika. *Bulletin of the Geological Survey of Tanganyika 28.*

Spurr, A. M. M., (1954). The Songwe guano caves, Mbeya District. *Records of the Geological Survey of Tanganyika 1,* 1951.

Stager, J. C., Cumming, B. & Meeker, L., (1997). A high resolution 11,400-yr diatom record from Lake Victoria, East Africa. *Quaternary Research 47,* 81-89.

Stewart, K. M., (1997). Fossil fish from Manonga Valley – Tanzania, Description, paleoecology & biogeographic relations. In T. Harisson, (ed), *Neogene paleontology of Manonga Valley, Tanzania; A window into the evolutinary history of East Africa,* (pp. 334-349). Plenum Press, New York, 1997.

Stockely, G. M., (1928). *The geology of Zanzibar protectorate.* H.M.S.O., London.

Stockely, G. M., (1932b). The geology of Ruhuhu coal fields. Tanganyika Territory. *Quaterly Journal of the Geological Society of London 88,* 610-622.

Stockely, G. M., (1937). Geological notes on the coastal region of Tanganyika. *Tanganyika notes 3,* 82-86.

Stockely, G. M., (1943). The geology of Rufiji District including a small portion of the Northern Kilwa District (Matumbi hill). *Tanganyika notes 16.*

Stockely, G. M., (1947). The geology of the country around Mwanza Gulf. *Short paper, Geological Survey of Tanganyika 29, 1- 25.*

Stockely, G. M., (1948). The geology and mineral resources of Tanganyika Territory. *Bulletin of the Geological Survey of Tanganyika 20,* 1948. Dodoma, Tanzania.

Stockley, G. M., (1930). *Tinde bone Beds and further notes on the Ussongo Beds. Annual report, Geological Survey of Tanganyika 1929*, 21-23, Dodoma.

Stoops, G. (1998). *Guidelines for thin section description of regolith material; Based on the "Handbook for soil thin sections description". By Bullock, P., Fedoff, N., Jongerius, A., Stoops, G., Tursina, T. and Babel, U.* Course notes for International Training Center for postgraduate soil scientists, (unpublished). University of Gent.

Stoops, G. J. and Buol, S. W., (1985). Micromorphology of Oxisols. In L. A. Douglas and M. L. Thompson (eds). *Soil micromorphology and classification*, (pp 105-118). SSSA special publication number 15. In L. A. Douglas and M. L. Thompson (eds). *Soil micromorphology and classification*, (pp 121-142). SSSA special publication number 15. Soil Science Society of America, Madison.

Stoops, G., (1989). Relict properties in soils of humid tropical regions with special reference to Central Africa. In A, Bronger and A Catt, (eds). *Palaeopedology: Nature and application of palaeosols*, (pp. 95-106). Catena Supplement 16, Cremligen.

Sun, J. & Din, Z. (1998). Deposits and soils of the last 130,000 years at desert – loess transition in Northern China. *Quaternary Research 50*, 148-156.

Tamrat, E., Thoveny, N., Taeib, M. and Opdyke, N. D., (1995). Revised magnetostratigraphy of the Plio-Pleistocene sedimentary sequence of the Olduvai Gorge Formation (Tanzania). *Paleogeography, paleoclimatology, paleoecology 114*, 273-283.

Tandon, S. K. and Gibling, M.R., (1994). Calcrete and coal in Late Carboniferous cyclotherms of Nova Scotia, Canada: Climate and sea level changes linked. *Geology 22*, 755-758.

Tarling, D. H., (1971). *Principles and applications of palaeomagnetism*, pp164. Chapman and Hall, New Fetter Lan, London.

Teale, E. O and Oates, F., (1935). The limestone caves and hotsprings of Songwe River. (Mbeya) area, with notes on the associated guano deposits. *Journal of East African Uganda national history society 12.*

Taylor, R. M. and Schwertmann, U. (1974a). Maghaemite in soils and its origin; I Proper ties and observations on soil maghaemites. *Clay mineralogy 10*, 289-298.

Taylor, R. M. and Schwertmann, U. (1974b). Maghaemite in soils and its origin; II Synthesis at ambient temperatures and pH 7. *Clay mineralogy 10*, 299-310.

Teale, E. O., (1931). Shinyanga diamond fields. *Short paper, Geological Survey of Tanganyika 9*, 5-6.

Teale, E. O., (1932a). Kimberlite. *Annual report of the Geological Survey of Tanganyika 1931.*

Teale, E. O., (1932b). The kimberlite and associated occurences of the Iramba Plateau. *Short paper of the Geological Survey of Tanganyika 10.*

Teale, E. O., (1936). Provisional geological map of Tanganyika with explanatory notes. *Bulletin of the Geological Survey of Tanganyika 6*, 5-6.

Temu, E. B., Kafumu, P. D., Marwa, E. E. and Abraham, A., (1992). *Preliminary report on the assessment of the reported fault in the Lakes Manyara-Natron area.* Special report No. 3887 (unpublished). Geological Survey of Tanzania, Dodoma.

Thorez, J., (1983). Palaeoclimatic reconstruction through clay minerals; A problem of parameterization. In R. Paepe and C. Baeteman, (eds), *Contribution of the joint meeting held on 18-20, April 1983*, (pp 15-18). Center for Quaternary stratigraphy and palaeoclimatology, Brusels.

Thorez, J., (2000). Personal communications

Thouveny, N. J., de Beaulieu, J., Bonifay, E., Creer, K. M., Gulot, J., Icole, M. Johnsen, S., Jozel, J., Reille, M., Williams, T. and Wlliamson, D., (1994). Climatic variations in Europe over the past 140Kyr deduced from rock magnetism. *Nature 371,* 503-506.

Tobias, P.V., (1991). *Olduvai Gorge. The skulls endocasts and teeth of Homo habilis, Volume 4,* Pp921. Cambridge University Press, New York.

Tsatskin, A., Heller, F., Hailwood, E. A., Gendler, T. S., Hus, J., Montgomery, P. Sartori, M. and Virina, E. I., (1998). Pedosedimentary division, rock magnetism and chronology of the loess/palaeosol sequence at Roxolany (Ukraine). *Palaeogeography, palaeoclimatology, palaeoecology 143,* 111-133.

Tucker, M. E., (1991). *Sedimentary petrology,* pp Blackwell Scientific Publications, UK.

UNDP (1998). *Tanzania-Opportunities for mineral resources development,* pp108. LK- Printing, Denver, Colorado.

United Republic of Tanzania, (1965). *Aerial photographs: Sheet numbers 38/3 (Olduvai-FIN/3 Photo No 023 to 029), 52/1 (Naigataati-FIN/1 photo No 061 to 082) and 38/4 (Engitati-FIN/2 photo No 108 to155), 39/3.* Survey and Mapping Division, Ministry of Housing and Urban Development, Tanzania, Dar-Es-Salaam, 1975.

United Republic of Tanzania, (1975). *Topographic maps: Sheets numbers 38/3 (Olduvai), 38/4 (Engitati), 39/3 (Angata Salei) and 52/1 (Naigataati), scale, 1:50,000.* Survey and Mapping Division, Ministry of Housing and Urban Development, Tanzania, Dar-Es-Salaam, 1975.

US State Department of Agriculture (1996) *Keys to soil taxonomy.* Web site: http://www.statlab.iastate.edu/soils/keytax/, 1998.

Van Damme, D. & Gautier, A., (1997). Late Cenozoic fresh-water mollusks of Wembere Manonga Valley, Tanzania. In T. Harisson, (ed), *Neogene paleontology of Manonga Valley, Tanzania; A window into the evolutinary history of East Africa,* (pp. 351-360). Plenum Press, New York, 1997.

Van Overloop, E., 1986: Comparison of climatic evolution during post-glacial times in Greece, tropical and subtropical regions in relation to desertification, *Proceedings of Inf. Symp. CEE progr. Climat,* Reidel: 49-59.

Van Overloop, E., Paepe, R., Peirlinckx L. & Van Biesen, L.P., (1995). The 60 Kyr Periodicity in the Pleistocene, *Workshop on "Geological Aspects of Global Change in Continental Environments,* VUB, Brussels, Belgium.

Van Overloop, E., (1998). *Geological Continental Cyclicities based on Geo-Soils in the Quaternary System.* 145pp + Annex Text and Tables. PhD Thesis at Uppsala University, Sweden.

Van Overloop, E. & Paepe, R., in colaborations with Ilunga, L. P., Kaseba, M. K., Kafumu, P. D. and Musisi, J. (1998). The Quaternary geology around the Great Lakes in Central Africa. Pluvials and Interpluvials are not the equivalent of Glacials and Interglacials. In G. Demaree, J. Alexandre and M. De Dapper (eds). *Tropical climatology, meteorology and hydrology in memoriam Franz Bultol,* (1924 – 1995), (pp 142 – 175). Royal Meteorological Institute of Belgium and Royal Academy of Overseas Sciences, Brussels.

Van Overloop, E., (2000). Personal communications.

Van Ranst, E. (1997a). *Soil mineralogy,* pp198, (unpublished). Course notes for Master of Science in Physical Land Resources, University of Gent, Belgium.

Van Ranst, E. (1997b). *Tropical soils; Geography, classification, properties and management,* pp310, (unpublished). Course notes for Master of Science in Physical Land Resources, University of Gent, Belgium.

Velde, B. (1985) *Clay minerals; A physico-chemical explanation of their occurrence, Developments in sedimentology 40,* pp427. Elsevier, Amsterdam.

Vepraskas, M. J., Wilding, L. P. and Drees, L. A., (1994). Aquic conditions for soil taxonomy: Concepts, soil morphology and micromorphology. In A. J. Ringrose-Voase and G.S. Humphreys, (eds), *Soil micromorphology:Studies in management and genesis,* (pp. 117-132). Elseviers, Amsterdam.

Verniers, J., (1997). Detailed stratigraphy of the Neogene sediments at Tinde and other localities in Central Manonga Basin. In T. Harisson, (ed), *Neogene paleontology of Manonga Valley, Tanzania; A window into the evolutinary history of East Africa,* (pp. 33-64). Plenum Press, New York, 1997.

Wade, F. B., (1937). A stratigraphicalal classification and table of Tanganyika Territory. *Bulletin of the Geological Survey of Tanganyika 9,* 1-62.

Walker, T. R., Waugh, B. and Grone, A. J. (1978). Diagenesis in first cycle desert alluviaon of Cenozoic age, Southwestern United States and Northern Mexico. *Bulletin of the Geological Society of America 89, 19-32.*

Walter, R.C., Manega, P. C., Hay, R. L. and Curtis, G. H. (1991). Laser fusion 40Ar/39Ar dating of Bed I, Olduvai Gorge – Tanzania. *Nature 354,* 145-149.

Walter, M. & Trotman, F., (1995). *Dictionary of earth sciences; Mini illustrated science dictionary,* pp160. Godfrey Cave Associates, London.

Watson, A., Prince-Williams, D. & Goudie, A. S., (1984). The Palaeoenvironmental interpretation of colluvial sediments and palaeosols of the Late Pleistocene hypothermal in Southern africa. *Paleogeography, paleoclimatology, paleoecology 45*, 225-249.

WCMC (1998a). *The Kilimanjaro National Park – World heritage site.* http://www.wcmc.org.uk/protected_areas/data/wh/kilimanj.html

WCMC (1998b). *The Ngorongoro conservation area – World heritage site.* http://www.wcmc.org.uk/protected_areas/data/wh/ngorongoro.html

Weaver, A. J., Eby, M., Fanning, A. F. & Wiebe, E. C., (1998). Simulated influences of carbon dioxide, orbital forcing and ice sheets on the climate of the the Last Glacial Maximum. *Nature 394*, 847-853.

Weaver, C. E. and Pollard, L. D., (1973). *The chemistry of clay minerals; Developments in sedimentology 15*; pp213. Elsevier, Amsterdam.

Webb, R. S., Rind, D. H., Lehman, S. J., Healy, R. J. & Sigman, D. (1997) Influence of ocean heat transport on the climate of the last Glacial maximum. *Nature 385*, (695-699)

Werth, E. A., (1915). *Das Deutsch-Ostafrikanische Kustenland und die vorgelageten Inseln.* Dietrich Reimer, Berlin

West, R. G. (1980). Pleistocene forest history in East Anglia. *New phytologist 85*, 571-622.

Weyland, E. J., (1934). *Pleistocene history and the Lake Victoria Region*. Annual report, Geological Survey of Uganda, 1933. Kampala.

Wilkinson, P., Mitchell, J. G., Cattermole, P. J. and Downie, C. (1986). Volcanic chronology of Meru-Kilimanjaro region; Northern Tanzania. *Journal of the geological Survey London 143*, 601-605.

William, G. J. & Eades, N. W., (1939). Explanation of the geology of Degree Sheet 18, (Shinyanga). *Bulletin of the Geological Survey of Tanganyika 13*, 5-20.

Williams, M. A. J., (1975). Late Pleistocene Tropical aridity synchronous in both hemispheres. *Nature 253*, 617-618.

Yaloon, D.H., (1995). The soils we classify; Essay review of recent publications on soil taxonomy. *Catena 24*, 233-141.

Yamba, T. K. & Boven, A., (1998). Evolution Pliocene et Quaternaire du remplisage sedimentaire dans le sud du basin du Lac Edouard, branche accidentale du Rift Est-Africain. In D. Delvaux & M.A. Khan, (eds), Tectonics, sedimantation and volcanism in the Eastern African Rift system. *Journal of African earth Sciences 26*, 423-439.

Yamba, T., K., (1993). *Etude lithostratigraphique des dépôts Quaternaires de la Plaine de Rutshuru*, pp174. Ph. D. Thesis at the Free University of Brussels, (VUB), Brussels.

Zagwijn, W. H. & Paepe, R., (1968). Die stratigraphie der Weichselzeitlichen Ablagerungen der Niederlande und Belgiens. *Eiszeitalter und Gegenwart 19*, 126-146.

Zagwijn, W. H., (1974). The Pliocene-Pleistocene boundary in Western and Southern Europe. *Boreas 3*, 75-97.

Zagwijn, W. H., (1985). An outline of the Quaternary stratigraphy of the Netherlands. *Geologie en mijnbouw 64*, 17-34.

APPENDICES

APPENDIX 5:

SUMMARY OF FIELD DESCRIPTIONS OF SAMPLES FROM OLDUVAI GORGE COMPOSITE SECTIONS

APPENDIX 5: SUMMARY OF FIELD DESCRIPTIONS OF SAMPLES FROM OLDUVAI GORGE COMPOSITE SECTIONS

A: MUSEUM CLIFF SECTION (MC Site)

Sample No.	Thickness (cm)	Colour name/code	Description	Remarks
MC27	50	Light gray (2.5Y7/2)	Hard dense limestone showing cracks.	Limestone
MC26	21	Light yellowish brown (2.5Y6/4)	Hard mudstone to siltstone	Mudstone/siltstone.
MC25	25	Pale olive (5Y6/3)	Loose sediments showing flat carbonate concretions	Silt sediments
MC24	23	Light brownish gray (2.5Y6/2)	Loose sediments showing layering and containing rounded clay pebbles	Massive clay
MC23	25	Olive (5Y5/4)	Loose sand clay sediments containing rock pebbles and concretions	Sandy clay
MC22	35	Olive gray (5Y5/2)	Clay Layer with columnar clay structures and numerous pipestems.	Paleosol
MC21	34	Olive gray (5Y5/2)	Clay Layer with columnar clay structures and numerous pipestems.	Paleosol
MC20	36	Brown (10YR5/3)	Brown soil with fine columnar structures and some white calc-concretions	Paleosol
MC19	50	Grayish brown (10YR5/2)	Brown clay soil with fine columnar structures, black clay coatings and slickensides	Paleosol
MC18	50	Grayish brown (2.5Y5/2)	Clay sediments with root traces	Paleosol (vertisol?)
MC17	50	Olive to dark gray (5Y6/2 to 5Y4/2)	Distratified silt clay with grit and concretions.	Paleo-vertisol
MC16	50	Olive (5Y4/3)	Silt clay soil with columnar clay structures, clay lickensides and clay black coatings	Paleo-vertisol
MC15	42	Dark to olive gray (5Y4/1 to 5Y6/2)	Clay with fine sand containing clay slickenside structure, clay coatings and gilgai macro structure	Paleo-vertisol
MC 14	40	Light yellowish brown (10YR6/4)	Layered silt sand with flat concretions. Contains large animal fossil bones	Gravely sandstone
MC13a	17	Gray to light gray (5Y6/1 to 5Y7/1)	Clay sediments with root infillings and rootlets	Gley paleosol
MC13b	18	Gray (5Y6/1)	Fine sand sediments, grit and concretions	Fine gravely sands
MC12	35	Light gray (5Y7/2)	Sandy tuff containing large animal fossil bones.	Tuff
MC11b	18	Light gray (5Y6/1)	Black and silt soil with spicular mottling	Paleosol

MC11a	18	Pale brown (10YR6/3)	Clay sand silt containing pipestems	Sanstone/paleosol?
MC10	50	Olive gray (5Y6/2)	Clayey sands with spicular columnar structures and black clay coatings	Paleosol
MC9	20	Olive gray (5Y5/2)	Clayey sediments containing white carbonate grit and cobbles	Grit Calc-arenites
MC8	43	Olive gray (5Y5/2)	Gray black irregular sand with pebbles and columnar calc-structure	Paleosol
MC7	21	Olive gray (5Y5/2)	Grit and cobbles	Araneceous gravel bed
MC6	43	Reddish brown (5YR4/3)	Red brown sediments with kruineling blocking structure, root infilings and clay coatings	Paleosol
MC5	10	Brown (10YR5/3)	Araneceous gravel bed with pedogenic alterations	Calc-arenites
MC4	36	Red (5YR4/6)	Gravely soil with strong development of clay slickensides and large (2 – 3cm) vertical calcareous structures	Gravely red paleosol
MC3	43	Red (2.5YR4/6)	Sandy paleosol	Strongly developed paleosol (wet land?)
MCHB	10	Light brownish gray (2.5Y6/2)	Rounded gravels cemented by red calc-sediments.	Cal-araneceous gravel bed
MC2	42	Light reddish brown (5YR6/4)	Silt sand with rusty spicules	Silt sand paleosol?
MC1	20	Light reddish brown(5YR6/3)	Mottled silt sand	Sand?/paleosol?

B: RED BLUFF SECTION (RB Site)

Sample No.	**Thickness (cm)**	**Colour name/code**	**Description**	**Remarks**
RB24	50	Red to reddish brown (2.5YR4/6 – 2.5YR5/6)	Red calcarenite sediments	Weakely developed paleosol.
RB23	57	Reddish brown to red (2.5YR5/4-6)	Clay sand olitic paleosol with spicules	Strongly developed red paleosol
RB22	14	Red (2.5YR4/8)	Red soft tuffaceous layer	Tuff
RB21	70	Red (2.5YR4/6)	Red oolitic paleosol	Paleosol
RB20	86	Light grayish brown to red (5YR6/4 - 7.5YR6/4) brown (5YR6/4)	Sand silt sediments with numerous rootlets and traces. Red mottling is common.	Strongly developed red paleosol
RB19	8	Light reddish brown (5YR6/4) and Yellowish red (5YR5/8)	Cemented gravely sand with red mottling	Strongly developed red paleosol
RB18b	31	Red (10R4/8)	Red oolitic paleosol (mottling)	Strongly developed red paleosol
RB18a	33	Red (2.5YR5/6)	Red mottled oolitic paleosol with numerous pipestems	Strongly developed red paleosol

RB17	40	Light brown (7.5YR6/4)	Distratified layer showing root infillings and sand/$CaCO_3$ concretions (Breccia textured).	Strongly developed red paleosol
RB16	35	Light reddish brown (5YR7/4)	Reddish brown oolitic paleosol with red mottling and imbricated marls.	Strongly developed red paleosol
RB15	43	Yellowish red (5YR5/6)	Red paleosol showing oolitic structure.	Strongly developed red paleosol
RB14	36	Very pale brown (10YR7/4)	Distratified clay or reworked pyroclatic?	Paleosol
RB13	43	Very pale brown (10YR7/3)	Distratified clay layer with blocky soil structure	Paleosol
RB12	45	White (2.5Y8/2)	Clay with marls showing distratification	Clay marls
RB11	36	Olive brown to dark brown (2.5Y4/4 – 10YR4/3)	Layered clay sands	Sand
RB10	40	Pale olive (5Y6/3)	Olive clay with marl concretions	Clay
RB9	35	White (2.5Y8/2)	Marls	Marl sediments
RB8	20	Light gray (10YR7/2)	Reworked silt sands	Reworked pyroclasts?
RB7	46	Grayish brown (2.5Y5/2)	Grit silt sands	Sand sediments
RB6b	15	Reddish yellow (7.5YR6/6)	Massive sandy	Strongly developed paleosol
RB6a	15	Reddish yellow (7.5YR6/6)	Massive sandy	Strongly developed paleosol
RB5	35	Yellowish red (5YR5/6)	Paleosol with $CaCO_3$ concretions	Well developed paleosol
RB4	21	Strong brown (7.5YR5/2)	Yellowish brown tuffaceous paleossol.	Well developed paleosol.
RB3	43	Pale yellow (5Y7/3)	Homogeneous silt sands	Fluviatile or lacustrine sediments?
RB2	25	White (2.5Y8/0)	Stratified marls	Lacustrine sediments
RB1	60	Light orange (10YR7/2)	Clay silt or fine sand	Fluvial sediments

C: RUTGERS SECTION (RS Site)

Sample No.	**Thickness (cm)**	**Colour name/code**	**Description**	**Remarks**
RS39	21	Light yellowish brown (10YR6/4)	Sandy clay with 2 – 4cm sized root traces	Paleosol
RS38	35	Yellowish brown (10YR5/4)	Weathered tuff	Paleosol?
RS 37	36	Yellowish brown (10YR5/4)	Brown layered mycolin sediments	Paleosol
RS 36	20	Pale brown (10YR6/3)	Clay sediments	
RS35	14	Yellowish brown (10YR5/4)	Silty sand with numerous small animal bioturbation	Paleosol
RS34	45	Light olive gray	Silty sand, (reworked	

		(5Y6/2)	pyroclasts?)	
RS33	10	Very dark gray to Balck (5Y3/1 5Y2.5/1)	Sand	
RS32	30	Light olive gray (5Y6/2)	Sandstone	
RS 31	29	Olive (5Y5/4)	Clayey sand. Animal footprint on the sandstone surface.	Paleosol
RS30	25	Olive gray (5Y4/2)	Sands	
RS29	15	Light gray (10YR7/2)	Sandy sediment with root traces	Paleosol
RS 28	25	Olive gray (5Y4/2)	Sandstone	
RS27	10	Black (5Y2.5/1)	Sands	
RS26	15	Light olive gray (5Y6/2)	Sands	
RS25	15	White (5Y8/2)	Cracked limestone or mudstone	
RS 24	15	Pale olive (5Y6/3)	Clay with distratification	Paleosol?
RS 23	35	Light olive gray (5Y6/2)	Stratified tuffaceous silt sand. Formation of neddlelike minerals	
RS 22	70	Light gray (5Y7/1)	Sandy whitish sdiments with concretion and root infillings	Paleosol
RS21	43	Olive gray (5Y4/2)	Massive clay with large concretions at the base	Clay
RS 20	15	Light gray (5Y7/2)	Clay with root traces and micro bones	Paleosol?
RS19	36	Olive (5Y5/4)	Massive clay with white concreation.	Paleosol?
RS18	30	White (5Y8/2)	Pedogenized pebbly tuff, with root twigs.	Paleosol
RS17	36	Dark olive gray (5Y3/2)	Distratified clay with root infillings	Paleosol
RS16	55	White (5Y8/2)	Fossiliferous tuff	
RS15	20	White (5Y8/2)	Tuff	
RS14	10	White (5Y8/2)	Pebbly clayey tuff	
RS13	28	Dark olive gray (5Y3/2)	Massive dense clay with concretions. Calcite crystalization	Paleosol?
RS12	5	White (5Y8/1)	Tuff	
RS11	30	Olive (5Y5/3)	As in RS9	Paleosol
RS10	10	White (5Y8/2)	Tuff	
RS9	30	Olive (5Y5/3)	Clay with big white carbonate concretions at the base	Paleosol
RS8	10	White (5Y8/2)	Tuff	
RS 7	24	Olive (5Y5/4)	Carbonate concretions and root and stem infillings as in RS5.	Paleosol

RS6	26	Olive (5Y4/4)	Massive clay with big (>5cm) carbonate accretions at the base, Slickenside structure observed..	Paleosol
RS 5	36	Olive (5Y4/4)	1 – 2cm root and stem infillings and carbonate concretions	Paleosol
RS4	15	Olive gray (5Y4/3)	Massive clay	Clay
RS3	15	Light olive gray (5Y6/2)	Massive clay	Clay
RS2	15	White (5Y8/2)	Accretions of salt	Natro-carbonate? Carbonate? Gysum?
RS 1	45	Olive to Olive gray (5Y4/2-4)	Compact and massive clay	Claystone

D: LONG KORONGO SECTION (LK Site)

Sample No.	Thickness (cm)	Colour name/code	Description	Remarks
LK10	90	Light gray (5Y6/4)	Sands with numerous carbonate concretions	Paleosol
LK9	100	Olive (5Y5/4)	Distratified clay layer	Paleosol
LK8	36	Pale red (10R6/4)	Sandy sediments with root channel infilings	Red paleosol
LK7	36	Reddish brown (2.5YR4/3)	Sandy sediments with root channel infilings	Brown paleosol
LK6b	30	Very dark brown (10YR3/2)	Sandy sediments with root channel infilings	Dark brown paleosol
LK6a	20	Red (2.5YR4/6)	Sandy sediments with root channel infilings	Red paleosol
LK5	17	Light yellowish brown (10YR6/4)	Sand sediments with carbonate concretions	Paleosol
LK4	20	Dark grayish brown (2.5Y4/2)	Massive dark distratified clay layer	Dark paleosol?
LK3	60	Olive gray (5Y5/2)	Distratified clay layer	Paleosol?
LK2	60	Light gray (2.5Y7/2)	Sandy tuff	Tuff

E: ZINJATROPUS SECTION (Zinj Site)

Sample No.	Thickness (cm)	Colour name/code	Description	Remarks
5Z	86	Brownish gray (5YR6/2)	Bioturbated and distratified sand	Sandy paleosol
4Z	80	Olive (5Y5/3)	Clay with calcareous veins and concretions	Paleosol
Z24	55	Sandy tuff (5Y7/2)	Semi consolidated layered tuff. Animal footprints on the surface of the tuff.	Ash flow - **TUFF IF**
3Z	107	Dark gray to Olive gray (5Y4/1-2)	Distratified clay	Paleosol
2Z	71	Grayish brown (2.5Y5/2)	Distratified clay with peds.	Paleosol
ZL	20	White (5Y8/2)	Sandy tuff	**Ash flow – TUFF IE**

1Z	21	Light brownish gray (10YR6/2)	Distratified clayey layer showing irregular peds,	Paleosol
ZK	20	Light gray (5Y7/1)	Sandy paleosol – numerous animal bone and root traces infilled with carbonate material.	Paleosol
Z23	15	Pale yellow (5Y7/2)	A layer of homogeneous sand	
Z22	10	Pale yellow (5Y8/3)	Tuffaceous clay	
Z21c	6	Olive gray (5Y5/2)	Clay showing strong distratification and carbonate concretions	Paleosol
Z21b	5	Pale yellow (5Y8/3)	Tuff	Ash fall
Z21a	7	Olive (5Y5/6)	Distratified clay with some carbonate concretions	Paleosol
Z21	5	Olive (5Y4/3)	Massive clay	
Z20	15	White (5Y8/2)	Consolidated clayey tuff	**Ash fall - TUFF I**
Z19	14	White (5Y8/2)	Distratified tuff	Weak paleosol
Z18	10	White (5Y8/1)	Fossiliferous tuff	Ash fall/flow?
Z17	14	White (5Y8/2)	Clayey tuff – with signs of bioturbations	Very weak paleosol
Z16	10	White (5Y8/2)	Tuff	Ash fall – **TUFF IC**
Z15	14	Light gray (5Y7/2)	Distratified reworked pyroclast	Paleosol
Z14	10	White (5Y8/2)	Sandy tuff	Ash flow
Z13	14	Olive (5Y5/3)	Caly showing distratification and numerous plant-root infillings	Paleosol
Z12	5	White (5Y8/2)	Tuff	Ash fall
Z11	29	White (5Y8/2)	Reworked tuff with carbonate concretions	Weak paleosol
Z10	18	White (5Y8/2)	Tuff	Ash fall
Z9	10	Light gray (5Y7/1)	Clayey sands with carbonate concretions, presence of mycelia and plant remains.	Paleosol
Z8	15	Pale olive (5Y6/3)	Coarse to medium grained sands	
Z7	45	Light olive gray (5Y6/2)	Gravely sands cemented by white tuff	Probably a reworked sandy tuff
Z6	10	White (5Y8/2)	Sands with white concretions	Probably a reworked sandy tuff
Z5	10	Light gray (5Y7/2)	Sandy sediments (Sands)	
Z4	21	Light gray (5Y7/2)	Sands with numerous carbonate concretions	Paleosol
Z3	30	White (5Y8/2)	Clayey sand tuff	
Z2	29	Olive (5Y5/3)	Clay showing distratification and irregular peds.	Paleosol
Z1	50	White (5Y8/1)	Sandy clay tuff	Ash flow **TUFF IB**
ZJ	70	Pale olive (5Y6/4)	Massive clay	
ZI	36	Pale olive (5Y6/3)	Distratified clay with root infillings	Paleosol (pedoderm)
ZH	15	White (5Y8/2)	Consolidated clayey tuff	Ash flow
ZG	5	Pale olive (5Y6/3)	Clay showing distratification	A very weak clayey paleosol?
ZF	5	White (10YR8/1)	Consolidated clayey tuff	Ash flow

ZE	5	Pale yellow (5Y7/3)	Clay	
ZD	5	White (5Y8/2)	Consolidated clayey tuff	Ash flow
ZC	15	Light olive gray (5Y6/2)	Clay with numerous carbonate concretions	Paleosol?
ZB	10	Pale yellow (5Y7/3)	Sandy clay. Contains very rare root infillings.	Very weak paleosol at the upper part of the clay layer
ZA	35	Pale yellow (5Y7/3)	Tuffaceous silty clay	Reworked Tuff

APPENDIX 7

INFRA RED SPECTROMETRY RESULTS, STEREO MICROSCOPIC EXAMINATION AND MICROMORPHOLOGICAL DESCRIPTIONS OF SAMPLES FROM OLDUVAI GORGE GEOLOGICAL SECTION

APPENDIX 7.1. PRINCIPLE OF THE INFRARED SPECTROMETER

APPENDIX 7.2: THE PRINCIPLE OF AAS (ATOMIC ABSORPTION SPECTROMETRY)

APPENDIX 7.3: PRINCIPLE OF A SCANNING ELECTRON MICROSCOPE (SEM)

APPENDIX 7.4: SOME INFRARED SPECTROMETER SPECTRA (PROFILES) OF SAMPLE S FROM OLDUVAI GORGE BEDS.

APPENDIX 7.5: INFRARED SPECTROMETER MEASUREMET RESULTS OF OLDUVAI GORGE BEDS.

APPENDIX 7.5A: A SYNTHESIZED LIST OF MINERAL SPECIES OF OLDUVAI GORGE COMPOSITE SECTION.

APPENDIX 7.6: STEREO MICROSCOPIC EXAMINATION OF PALAEOSOLS OF OLDUVAI GORGE (SURFACE OBSERVATIONS OF HAND SPECIMENS)

APPENDIX 7.7: MICROMORPHOLOGIC CHARACTERISTICS OF SOME PALAEOSOL LEVELS OF OLDUVAI GORGE STRATIGRAPHY

APPENDIX 7.1: PRINCIPLE OF THE INFRARED SPECTROMETER

Infrared spectrometry is quite a new method of mineral analysis (usually used by geologists in the field to assess mineral deposits). This is an optical method designed to obtain infrared light quality spectra of minerals by observing their reflectance characteristics and use these characteristics to identify the minerals. The infrared spectrometer (PIMA) consists of an optical port where the samples can be placed (one at a time) for measurement. Infrared radiation passes through the port and onto the sample where it is then reflected back into the instrument for measurement.

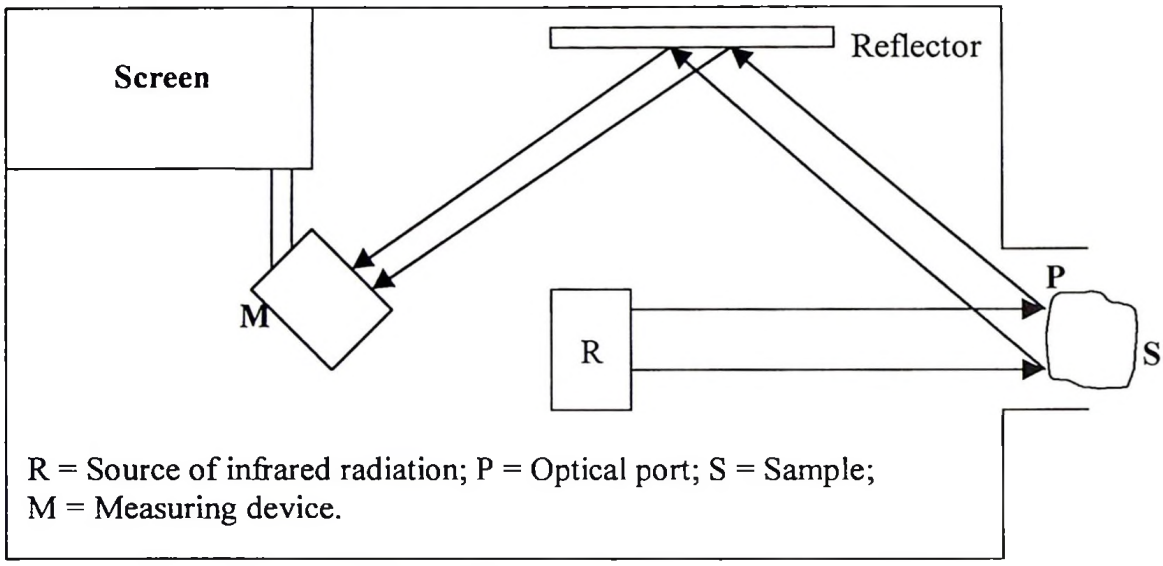

Figure 7.1: Simple illustration of the PIMA instrument

APPENDIX 7.2: THE PRINCIPLE OF AAS (ATOMIC ABSORPTION SPECTROMETRY)

The atomic absorption spectrometer (AAS) consists of a hollow cathode lamp or an electrode-less discharge lamp (the atomic line), a flame burner head, monochromator, a detector (photomultiplier) and a recording system. The hollow cathode lamp is designed to emit intense atomic line spectrum of a specific element. The sample is atomized by means of a flame. The solution is atomized into an atomic vapor for absorption measurements. The atomization process is enabled by means of a nebulizer, which converts the sample solution into an aerosol mist. The mist is mixed with oxidant and fuel gases suitable for burning as a flame. A radiation from the cathode lamp is passed through the sample flame during measurements. The degree of atomic absorption is detected by a monochromator tuned to the wavelength of the atomic emission line. A simplified instrumental plan is given in figure 7.2.

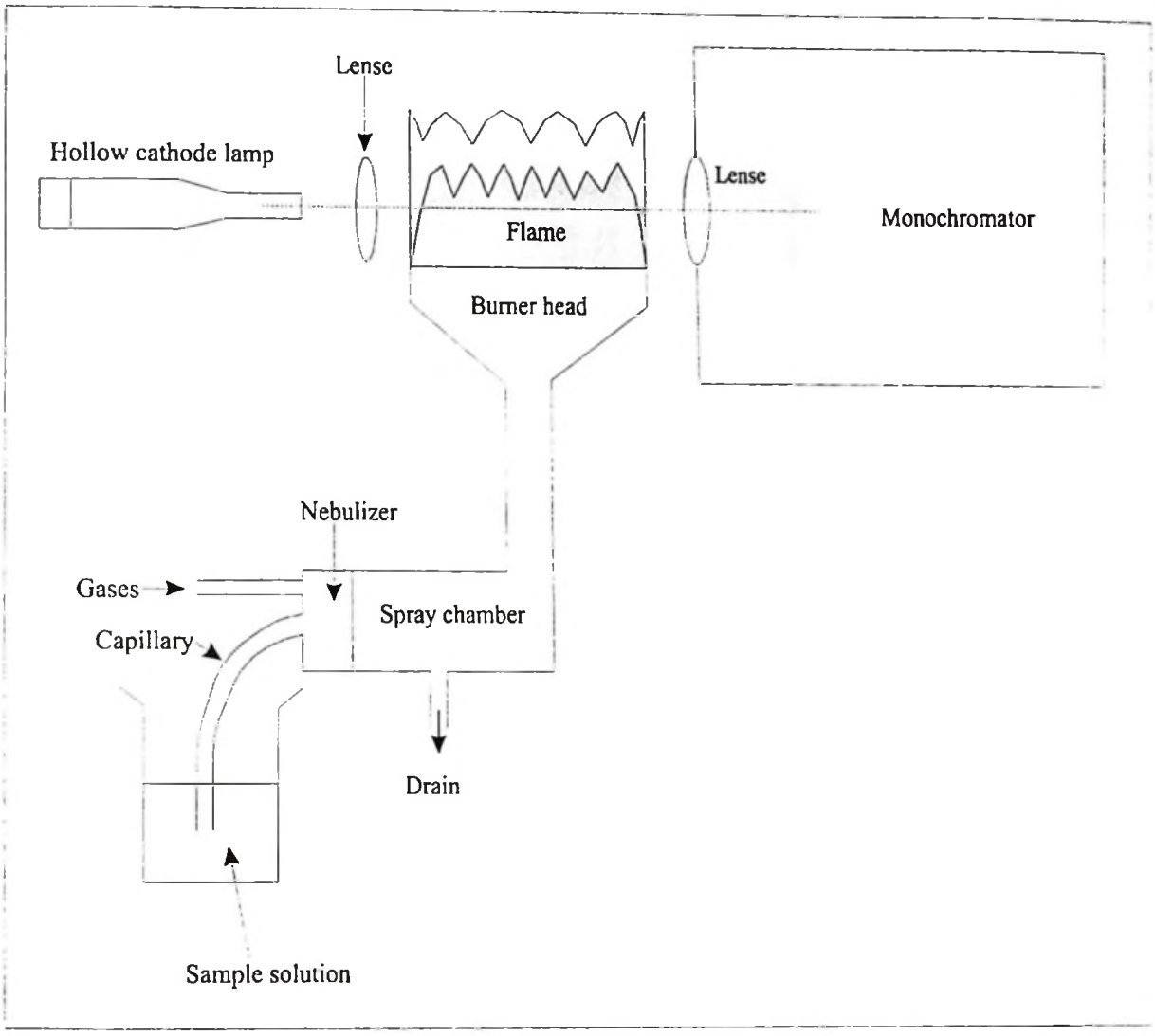

Figure 7.2: Conventional atomic absorption spectrometer (AAS) configuration (after Pott, 1987)

APPENDIX 7.3: PRINCIPLE OF A SCANNING ELECTRON MICROSCOPE (SEM)

The scanning electron microscope uses electron beam instead of normal light beam. In order the sample to be examined it should be conductive (to conduct electricity). If the sample is not conductive a conductive material must coat it (usually a thin layer of gold is coated on a sample by a sputter coater).

The sample is placed inside the microscope's vacuum column through an airtight door. The air is pumped out and an electron gun emits a beam of high-energy electrons. The beam travels down through a series of magnetic lenses designed to focus the beam to a very fine spot. A set of scanning coils moves the focuses beam back and forth across the sample row by row. As the electron hits the sample each spot on the sample secondary

electrons are knocked loose from the surface. A detector counts these electrons and sends the signal to an amplifier. The final image is built up from the number of electrons emitted from each spot on the sample. Scanning electron microscope can reveal new levels of detail and complexity in the amazing world of micro-miniature structures. The basic SEM build up is shown in figure 7.3 below.

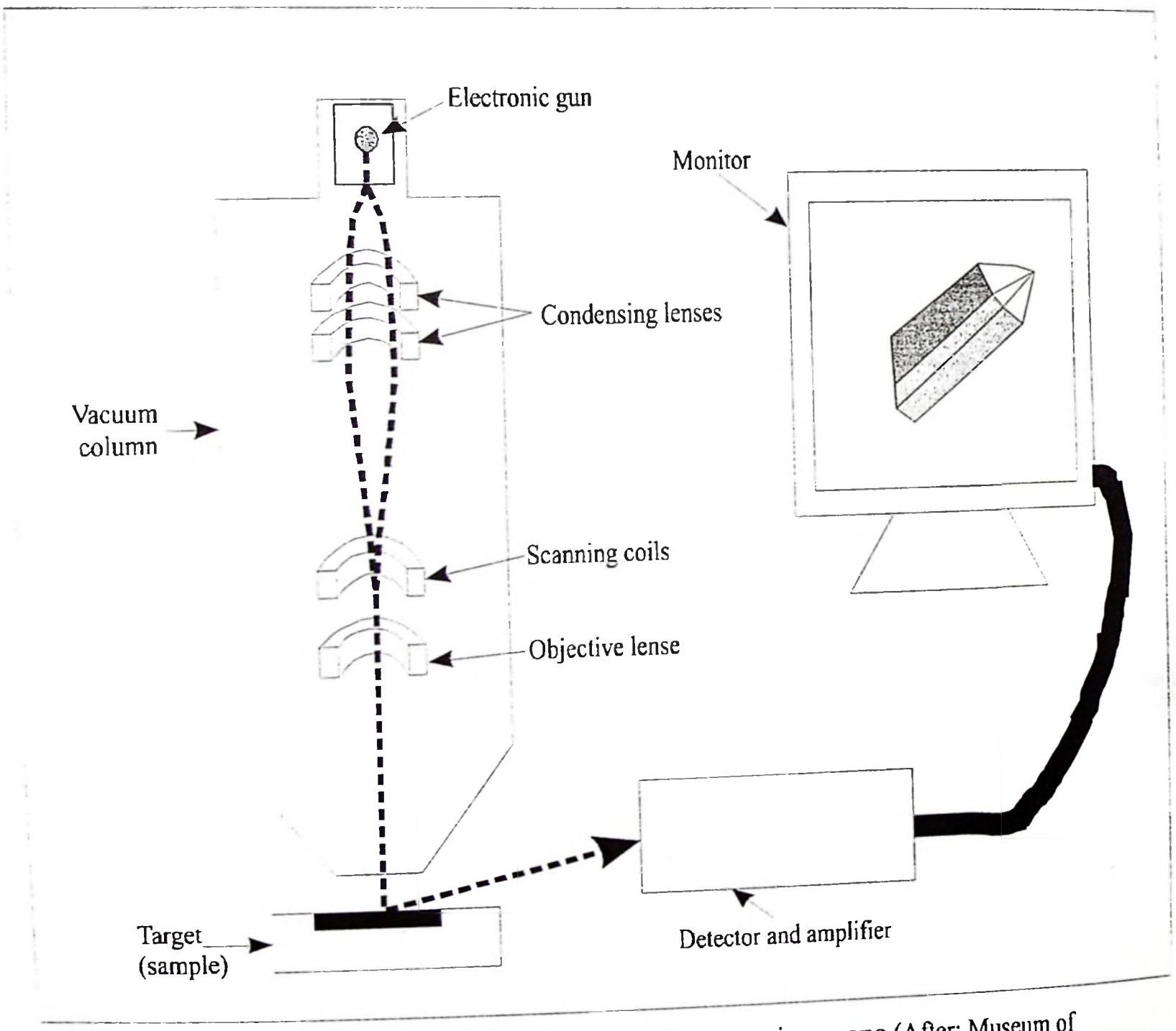

Figure 7.3: The principle of the scanning electron microscope (After; Museum of Science, Boston, 1996).

APPENDIX 7.4: SOME INFRARED SPECTROMETER SPECTRA (PROFILES) OF SAMPLES FROM OLDUVAI GORGE

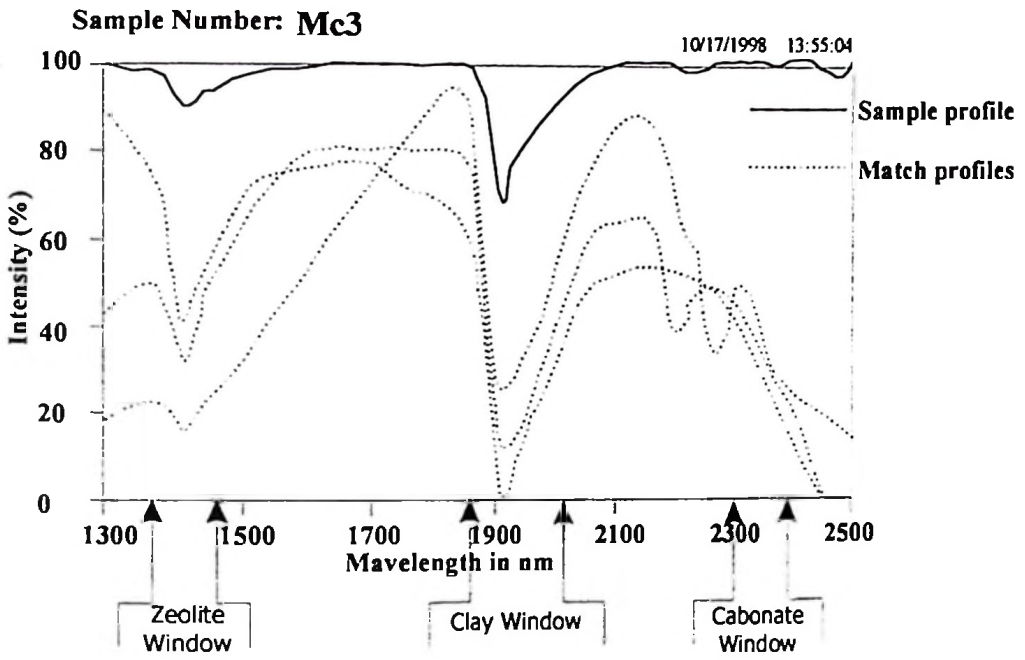

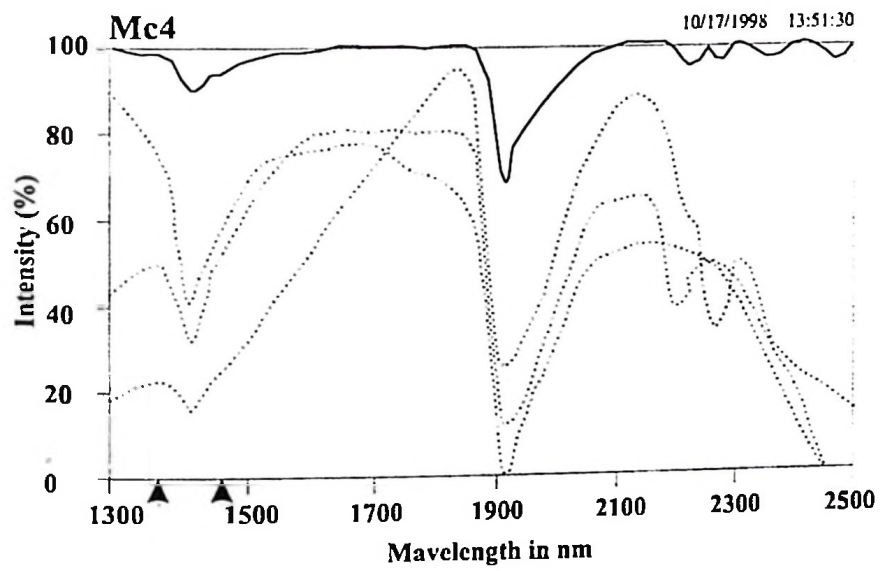

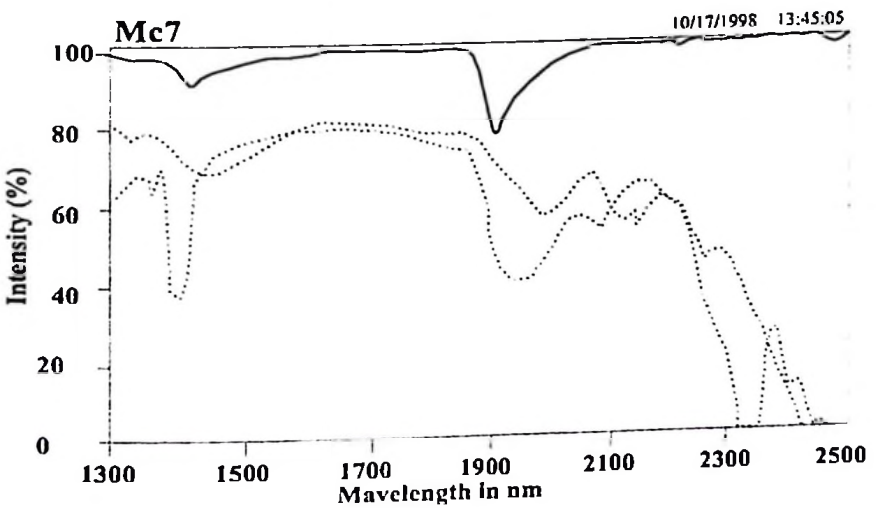

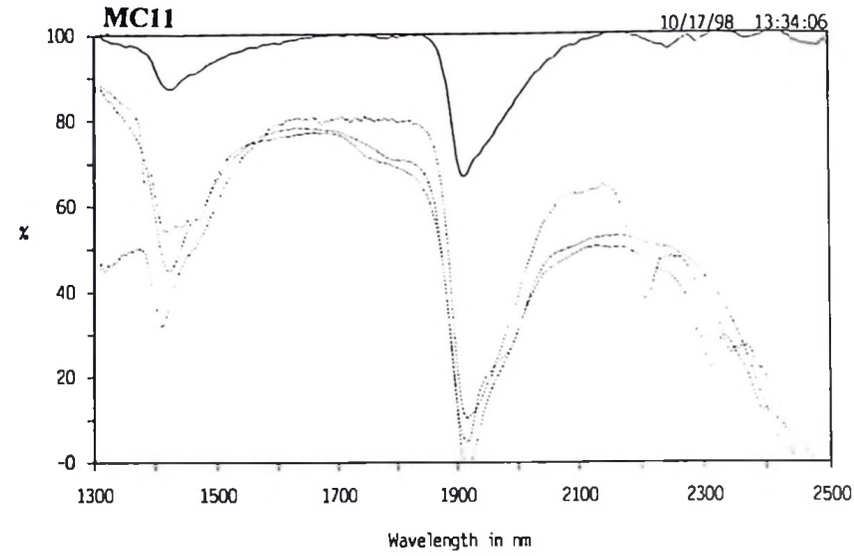
MC11
10/17/98 13:34:06
100
80
60
40
20
-0
%
1300
1500
1700
1900
2100
2300
2500
Wavelength in nm

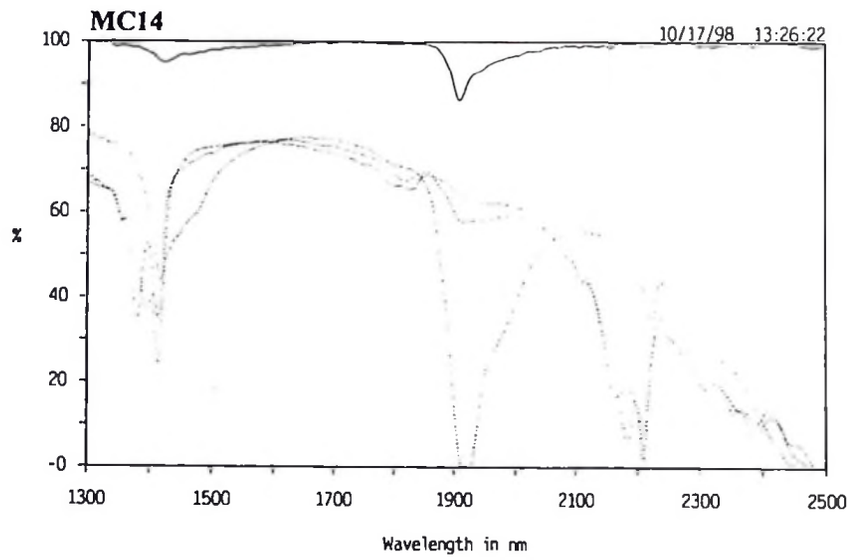
MC14
10/17/98 13:26:22
100
80
60
40
20
-0
%
1300
1500
1700
1900
2100
2300
2500
Wavelength in nm

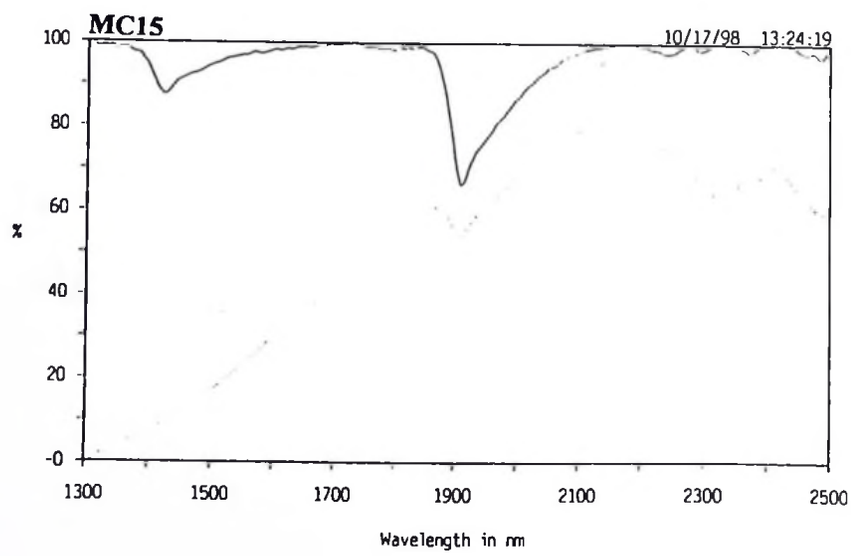
MC15
10/17/98 13:24:19
100
80
60
40
20
-0
%
1300
1500
1700
1900
2100
2300
2500
Wavelength in nm

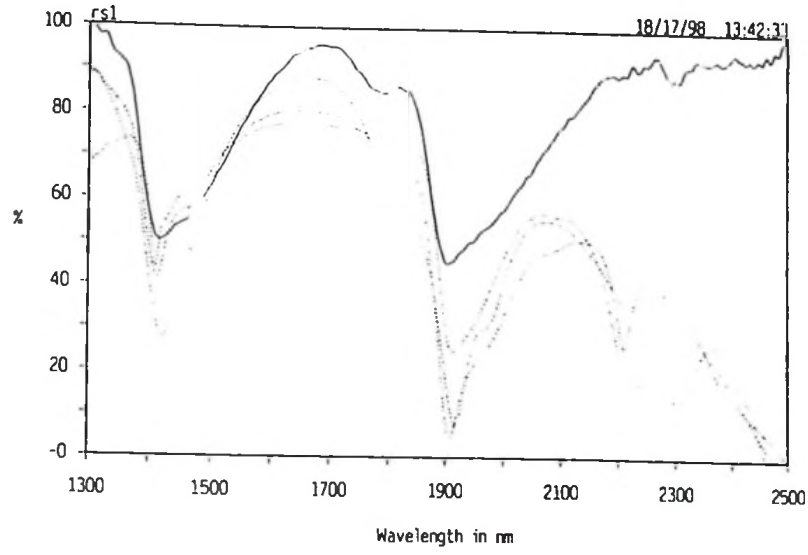
rs1
18/17/98 13:42:3
100
80
60
40
20
-0
%
1300
1500
1700
1900
2100
2300
2500
Wavelength in nm

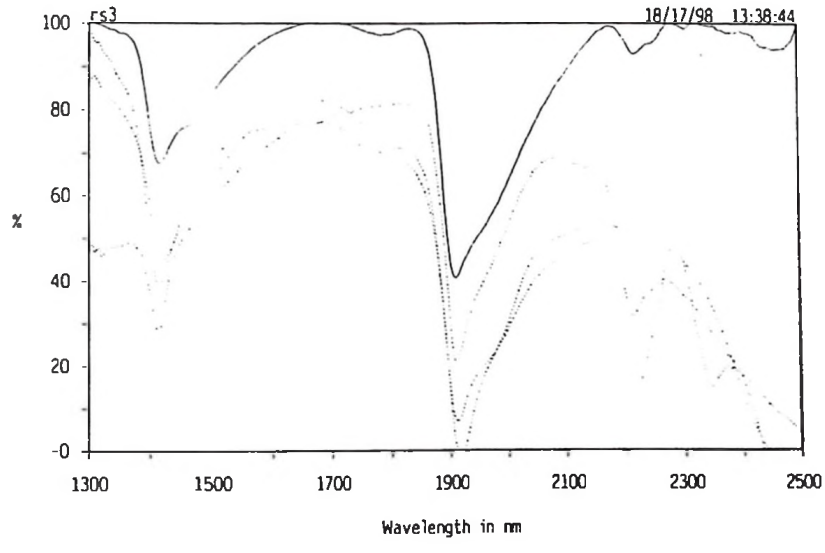
rs3
18/17/98 13:38:44
100
80
60
40
20
-0
%
1300
1500
1700
1900
2100
2300
2500
Wavelength in nm

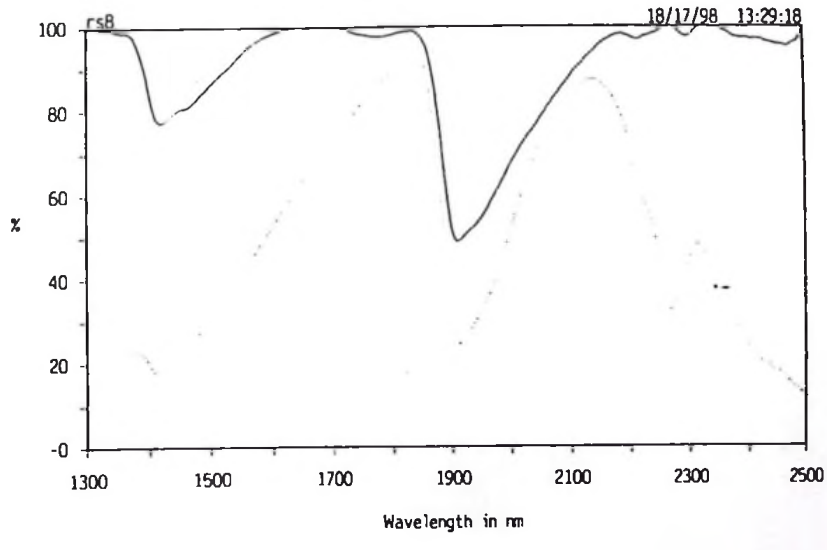
rs8
18/17/98 13:29:18
100
80
60
40
20
-0
%
1300
1500
1700
1900
2100
2300
2500
Wavelength in nm

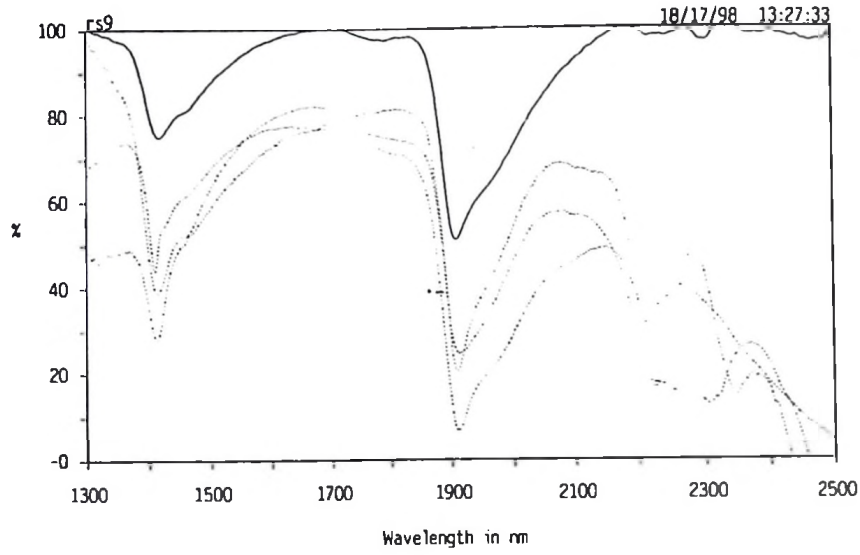
rs9
18/17/98 13:27:33
100
80
60
40
20
-0
%
1300
1500
1700
1900
2100
2300
2500
Wavelength in nm

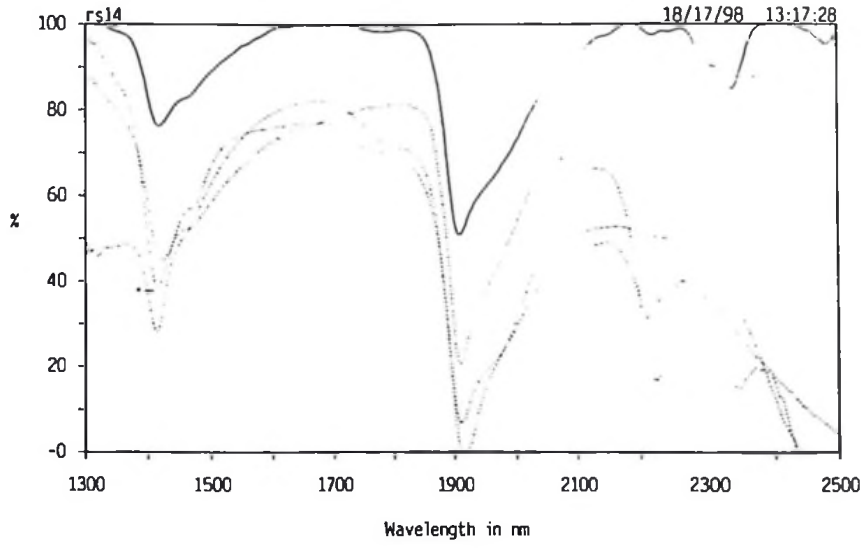
rs14
18/17/98 13:17:28
100
80
60
40
20
-0
%
1300
1500
1700
1900
2100
2300
2500
Wavelength in nm

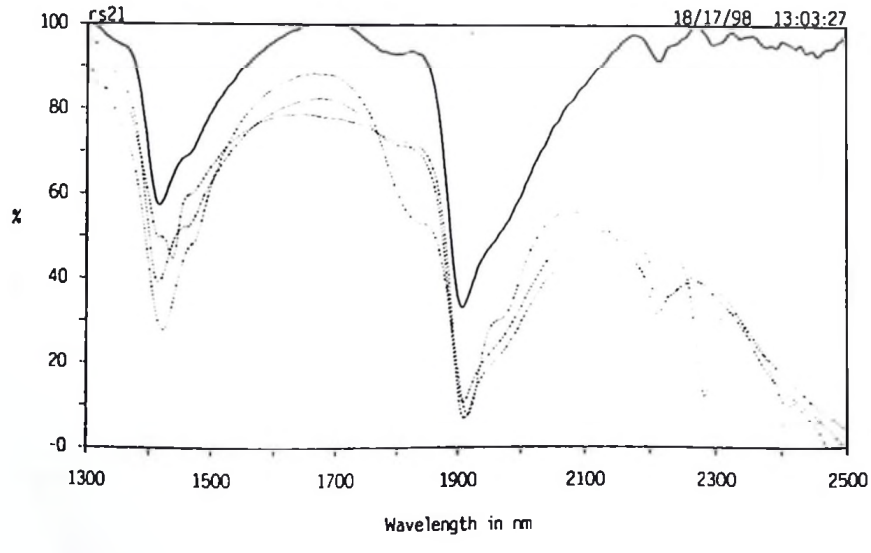
rs21
18/17/98 13:03:27
100
80
60
40
20
-0
%
1300
1500
1700
1900
2100
2300
2500
Wavelength in nm

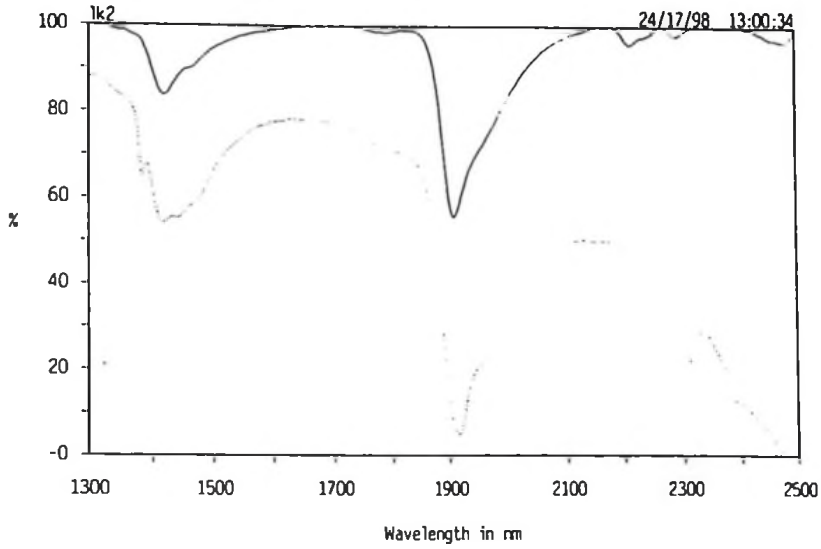
1k2
24/17/98 13:00:34
100
80
60
40
20
-0
%
1300
1500
1700
1900
2100
2300
2500
Wavelength in nm

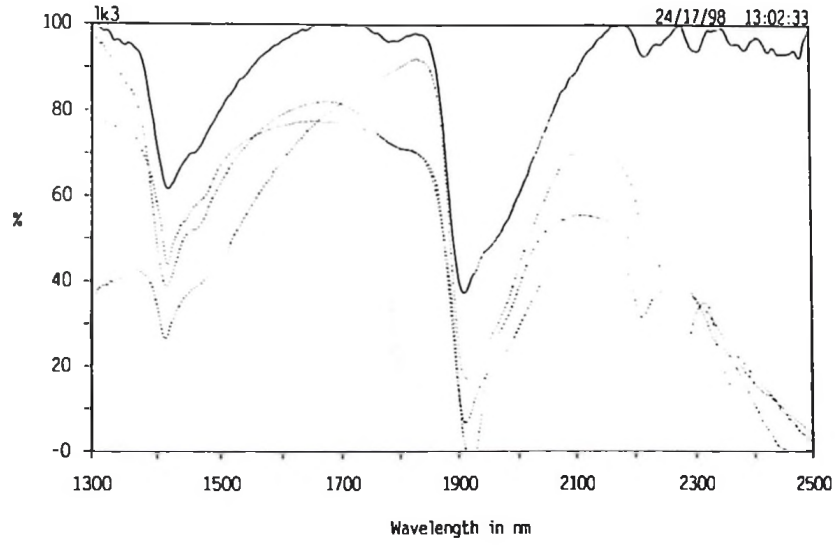
1k3
24/17/98 13:02:33
100
80
60
40
20
-0
%
1300
1500
1700
1900
2100
2300
2500
Wavelength in nm

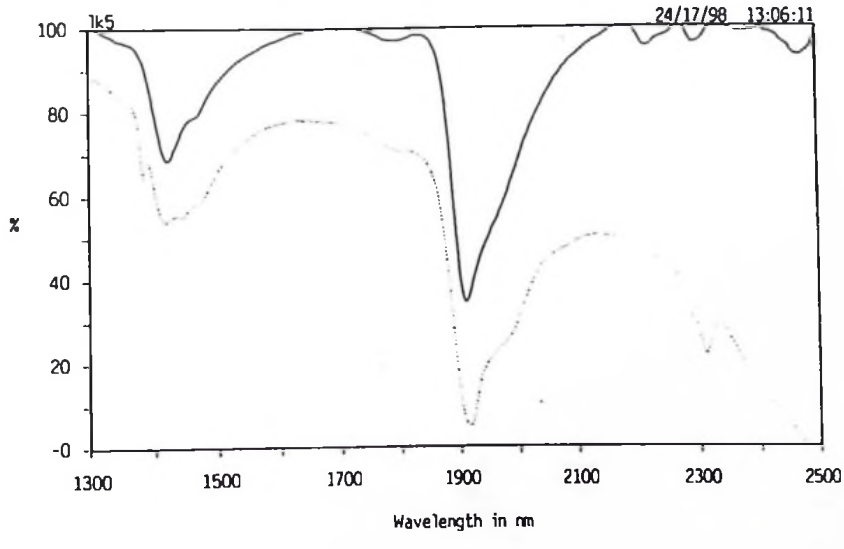
1k5
24/17/98 13:06:11
100
80
60
40
20
-0
%
1300
1500
1700
1900
2100
2300
2500
Wavelength in nm

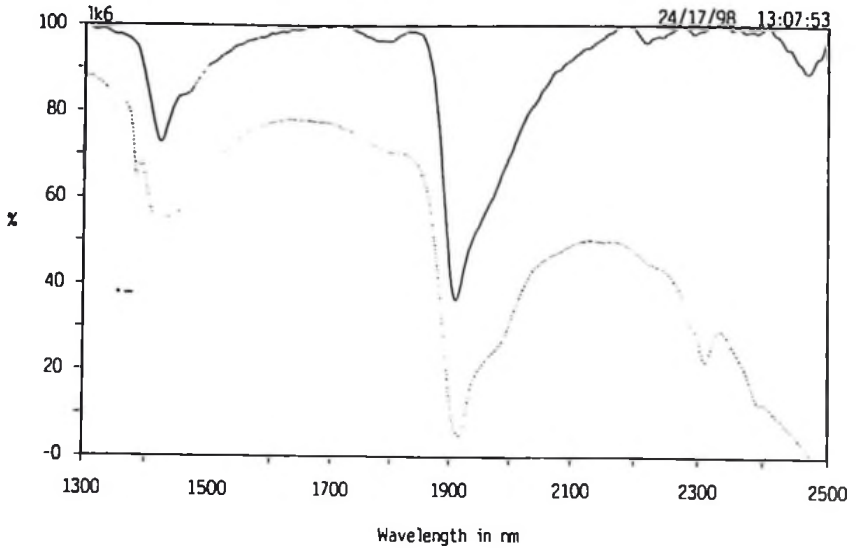
1k6
24/17/98 13:07:53
100
80
60
%
40
20
-0
1300
1500
1700
1900
2100
2300
2500
Wavelength in nm

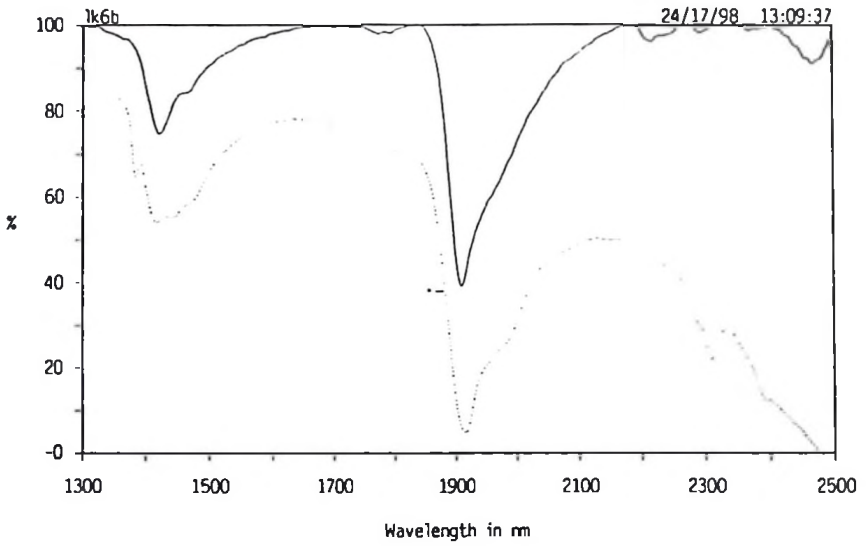
1k6b
24/17/98 13:09:37
100
80
60
%
40
20
-0
1300
1500
1700
1900
2100
2300
2500
Wavelength in nm

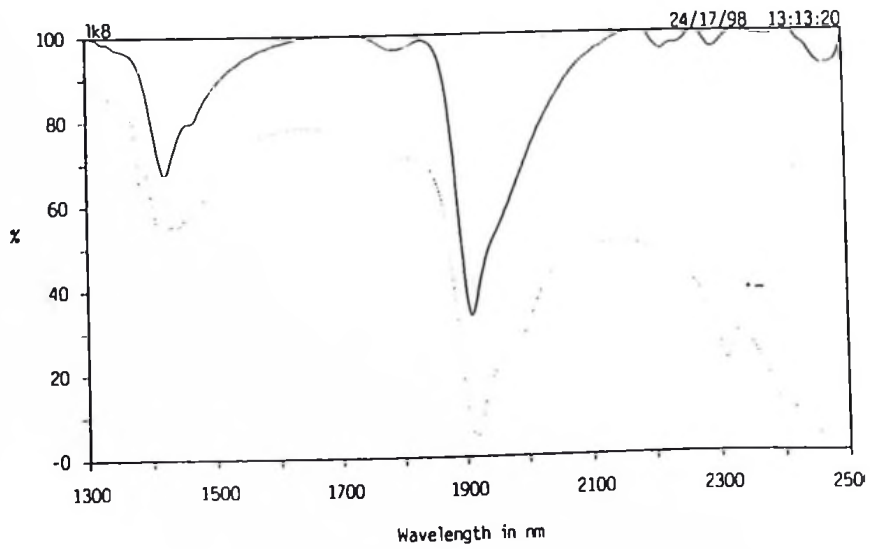
1k8
24/17/98 13:13:20
100
80
60
%
40
20
-0
1300
1500
1700
1900
2100
2300
Wavelength in nm

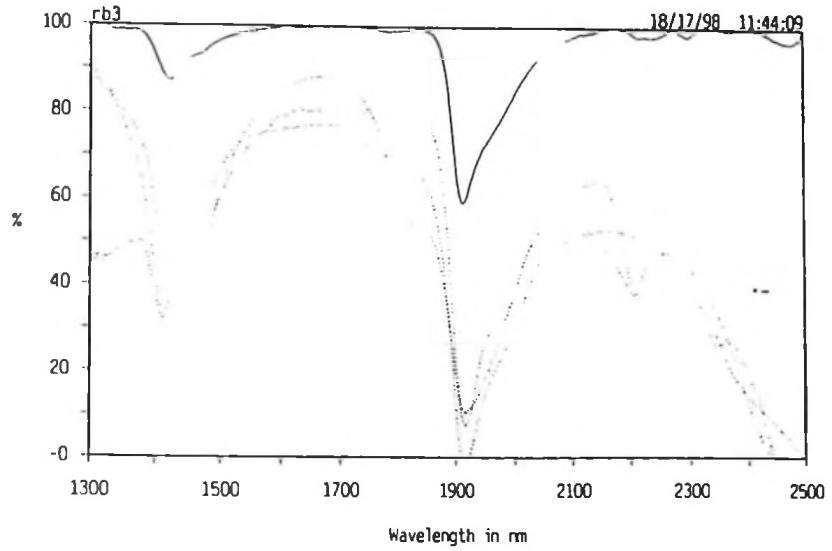
rb3
18/17/98 11:44:09
100
80
60
40
20
-0
%
1300
1500
1700
1900
2100
2300
2500
Wavelength in nm

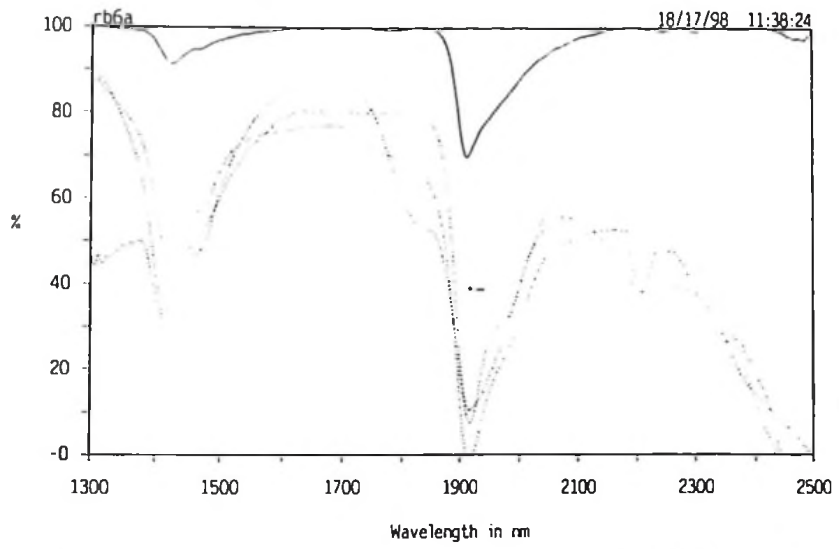
rb6a
18/17/98 11:38:24
100
80
60
40
20
-0
%
1300
1500
1700
1900
2100
2300
2500
Wavelength in nm

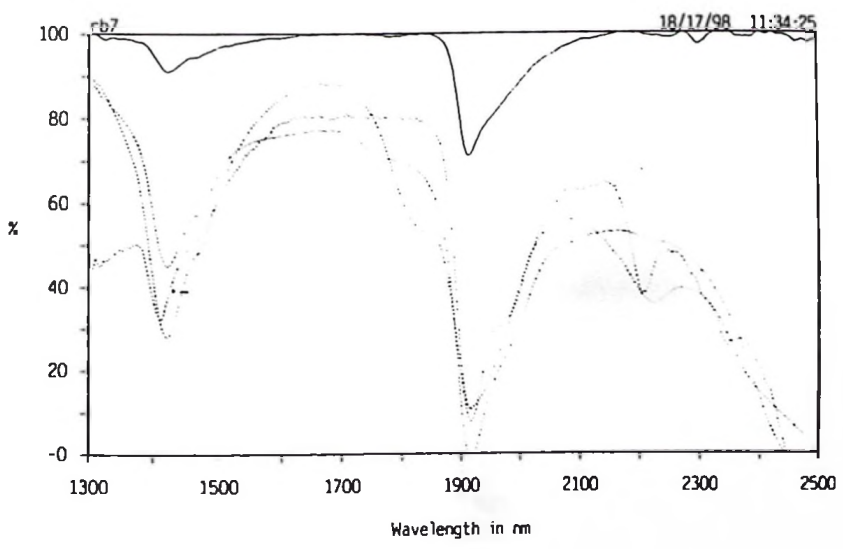
rb7
18/17/98 11:34:25
100
80
60
40
20
-0
%
1300
1500
1700
1900
2100
2300
2500
Wavelength in nm

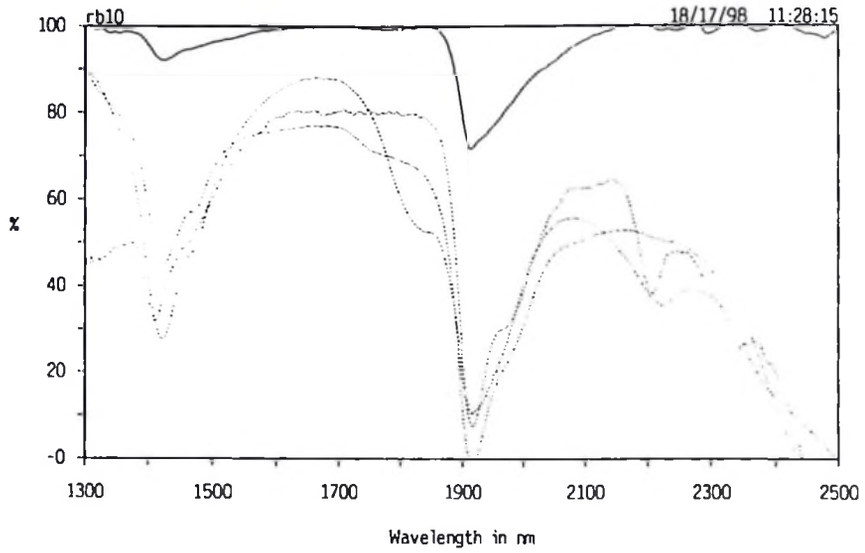
rb10
18/17/98 11:28:15
100
80
60
40
20
-0
%
1300
1500
1700
1900
2100
2300
2500
Wavelength in nm

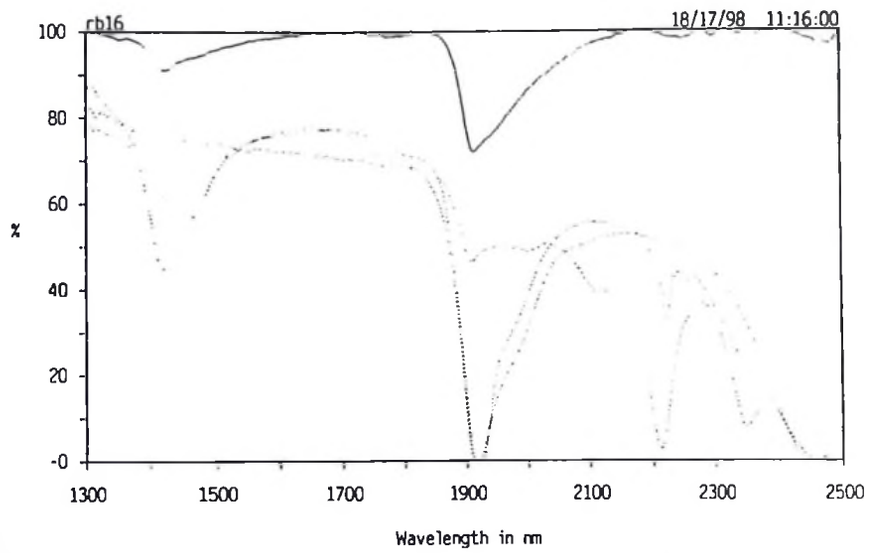
rb16
18/17/98 11:16:00
100
80
60
40
20
-0
%
1300
1500
1700
1900
2100
2300
2500
Wavelength in nm

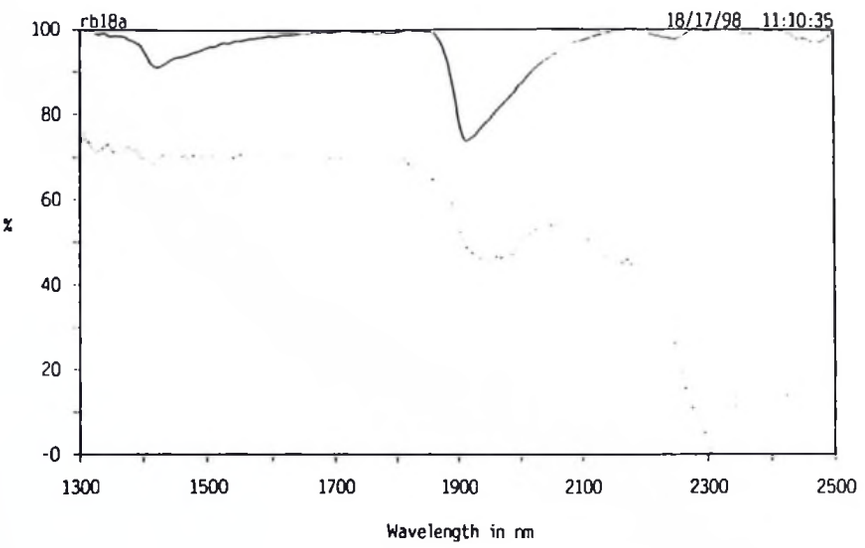
rb18a
18/17/98 11:10:35
100
80
60
40
20
-0
%
1300
1500
1700
1900
2100
2300
2500
Wavelength in nm

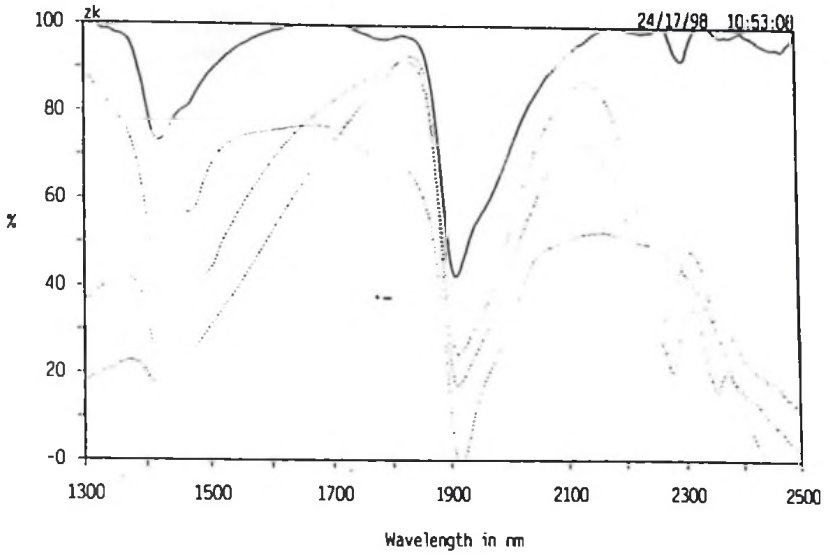
zk
24/17/98 10:53:08
100
80
60
40
20
-0
%
1300
1500
1700
1900
2100
2300
2500
Wavelength in nm

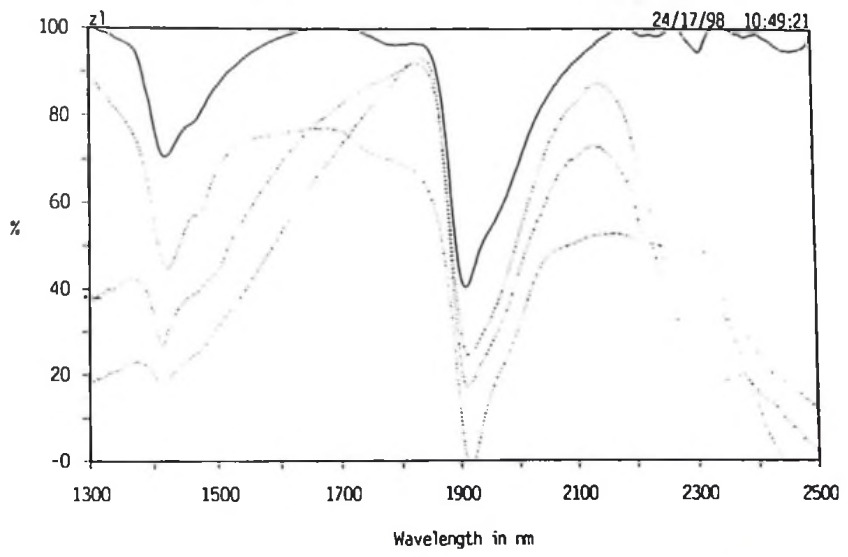
z1
24/17/98 10:49:21
100
80
60
40
20
-0
%
1300
1500
1700
1900
2100
2300
2500
Wavelength in nm

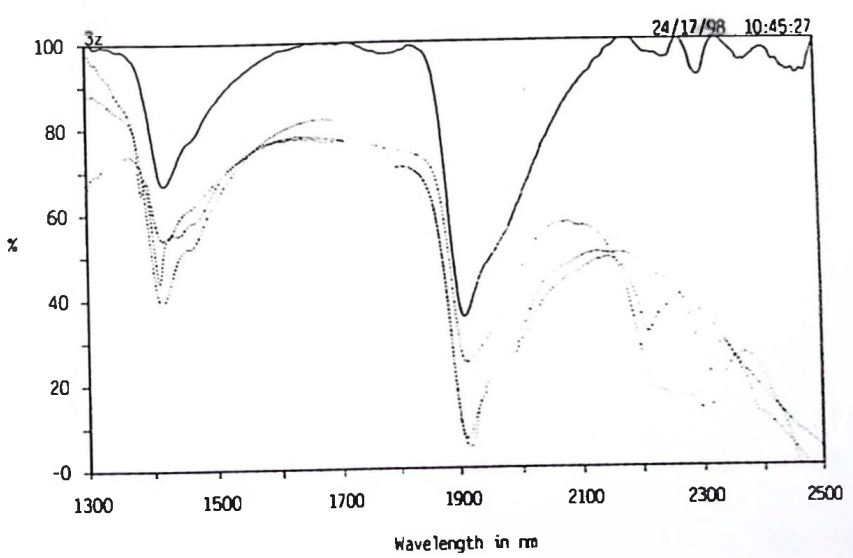
3z
24/17/98 10:45:27
100
80
60
40
20
-0
%
1300
1500
1700
1900
2100
2300
2500
Wavelength in nm

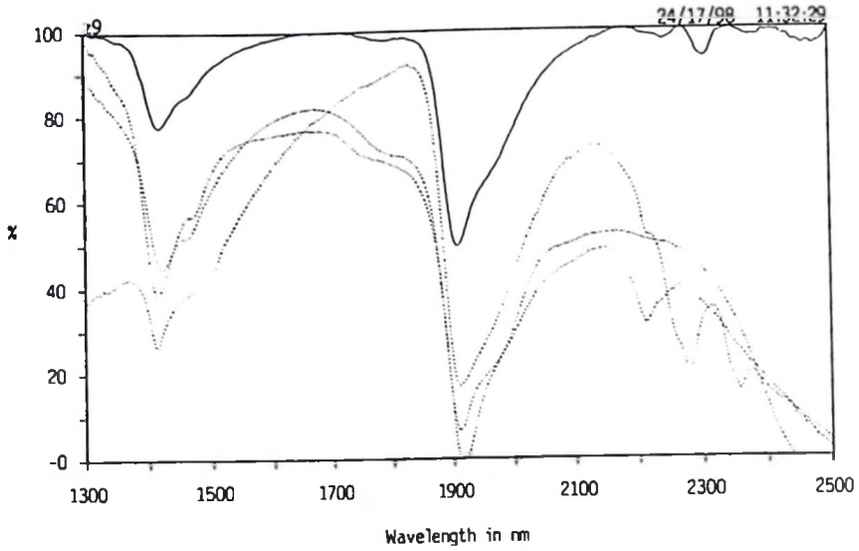
z9
24/17/98 11:32:29
100
80
60
40
20
-0
%
1300
1500
1700
1900
2100
2300
2500
Wavelength in nm

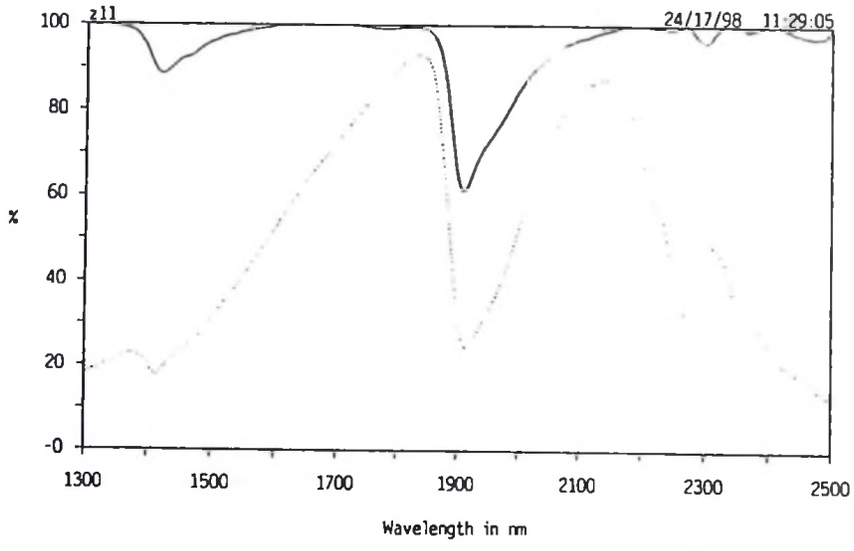
z11
24/17/98 11:29:05
100
80
60
40
20
-0
%
1300
1500
1700
1900
2100
2300
2500
Wavelength in nm

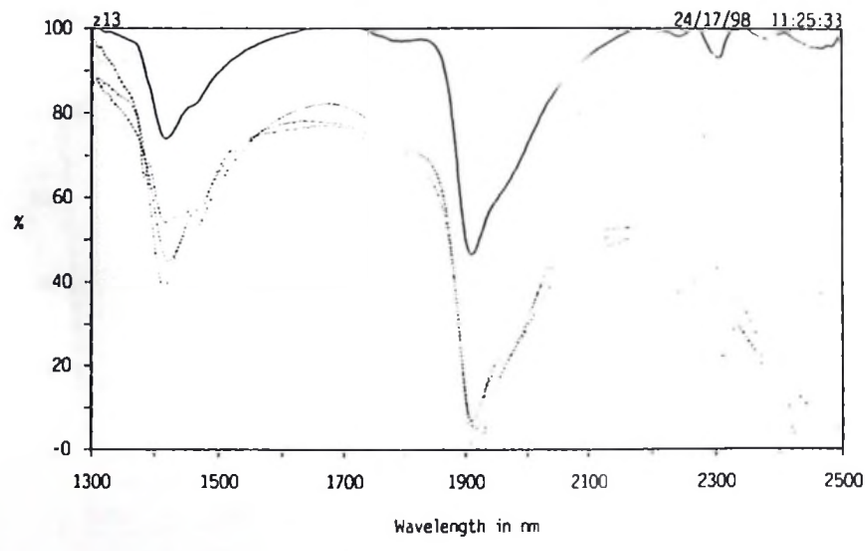
z13
24/17/98 11:25:33
100
80
60
40
20
-0
%
1300
1500
1700
1900
2100
2300
2500
Wavelength in nm

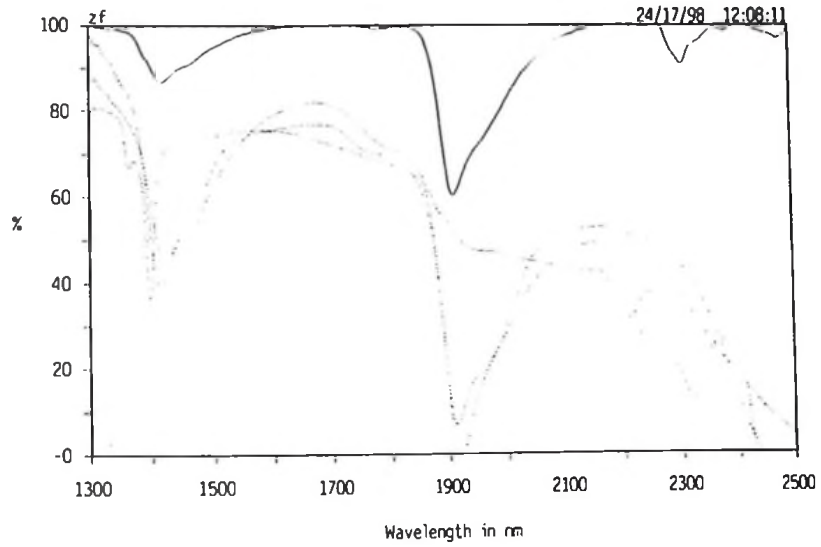
zf
24/17/98 12:08:11
100
80
60
40
20
-0
%
1300
1500
1700
1900
2100
2300
2500
Wavelength in nm

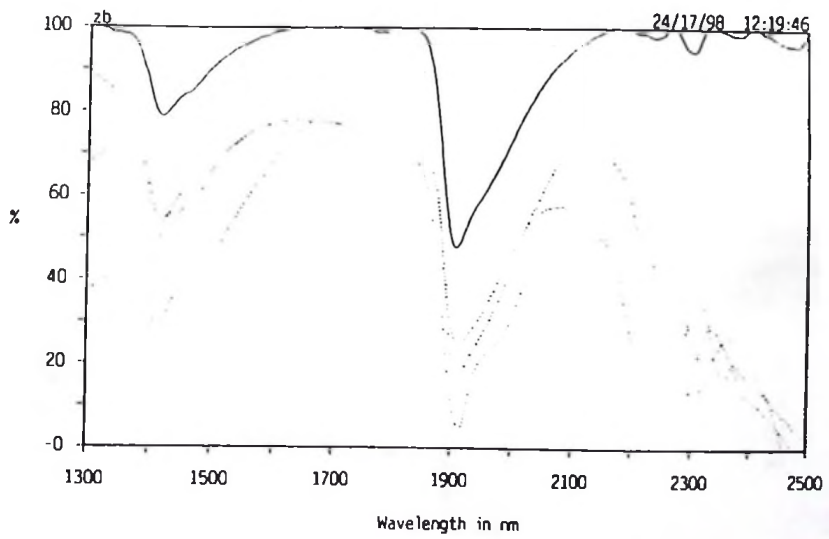
zb
24/17/98 12:19:46
100
80
60
40
20
-0
%
1300
1500
1700
1900
2100
2300
2500
Wavelength in nm

APPENDIX 7.5: INFRARED SPECTROMETER MEASUREMET RESULTS OF OLDUVAI GORGE BEDS.

MC section

Sample	Peak position λ(nm)	Peak intensity (%)	Peak depth	Peak width	Mineral matches	
					Automatic	Manual
MC27	1919.0 2306.8 2093.4	21.49 22.61 27.08	8.53 1.09 0.72	51.0 27.2 418.6	-	Calcite, Hectorite
MC26	1916.7 1427.2 2305.5	21.21 31.27 25.40	14.23 5.17 2.82	55.3 54.8 32.5	Palygorskite	Calcite, Dickite, Heulandite,
MC25	1916.0 1423.4 2305.3	17.30 22.05 20.09	6.34 2.29 1.01	48.0 48.6 32.7	Topaz, pyrophyllite, palygorskite	Calcite, Dickite, Muscovite
MC24	1915.1 1426.7 2259.6 2303.2	16.18 22.17 21.77 19.81	10.58 4.06 0.72 1.70	50.9 59.3 26.4 22.8	Palygorskite,	Analcime, Palygorskite, Sepiolite, Calcite
MC23	1915.6 2305.2	18.42 22.61	9.81 1.31	46.4 28.8	-	Brucite, Hermimophite, Calcite
MC22 (GS1)	1912.6 1423.0 1347.8	9.2 13.11 11.7	5.76 2.64 0.47	47.4 45.0 32.2	Stilbite, palygorskite	Sepiolite, Bassanite , calcite
MC21 (GS1)	1913.1 1423.1 2254.3 2345.5	17.86 23.17 22.61 20.65	7.66 2.81 0.83 0.86	46.9 46.9 33.7 22.5	Palygorskite, stilbite	Sepiolite, Stronianite, **Illite**, Smithsonite, Antigorite, Margarite, Shortite
MC20 (GS2)	1912.5 1424.7 2254.7 3250.1	24.65 33.32 30.65 28.60	11.21 4.79 1.01 0.72	43.5 51.3 35.3 37.9	-	**Kaolinite**, Sepiolite, **Smectite,** Analcime, Antigorite, Nepheline, Jaedite, Kyanite
MC19 (GS3)	1912.6 1423.7 2252.9	10.87 15.07 15.07	6.85 2.75 0.69	47.4 56.3 39.1	-	Kaolinite, Sepiolite, Notronite, Aporphylite
MC18 (GS4)	1912.6 1423.6 2249.4	12.55 18.98 18.98	9.23 3.74 1.01	47.4 56.4 46.6	-	**Kaolinite**, Sepiolite, Notronite, Aporphylite
MC17 (GS5)	1912.6 1423.9 2253.8	11.31 17.32 16.74	8.87 3.84 0.93	43.4 52.1 43.0	-	**Kaolinite,** Sepiolite, Notronite, Aporphylite, Horneblende
MC16 (GS6)	19122.2 1425.7 1459.3	10.04 14.23 14.79	5.32 2.06 1.40	47.8 50.3 130.7	Stilbite	Analcime, Beidellite, Aporphylite, Mordenite, Notronite, Sepiolite, Smectite
MC15 (GS7)	1911.8 1424.7 1344.0 2056.0	10.04 14.23 16.18 14.23	5.30 2.31 0.90 0.58	44.2 51.3 68.0 96.0	Glauconite	Analcime, Beidellite, Aporphylite, Mordenite, Notronite, Sepiolite, Smectite, Colemanite, Hermimorphite, Nepheline, Smithsonite

MC14?	1911.1 1422.1 1462.3 1520.0	16.46 18.42 18.98 18.98	2.73 1.34 0.97 0.65	30.9 73.9 213.7 368.0	Dickite, kaolinite palygorskite,	Illite, Montmorillonite.
MC13b (GS8)	1912.3 1422.5 1529.0 1352.3	18.70 23.45 22.84 25.12	6.57 2.29 0.74 0.55	43.7 47.5 63.0 105.7	-	Analcime, Beidellite, Aporphylite, Mordenite, Notronite, Smectite, Colemanite, Hermimorphite, Nepheline, Smithsonite, Ambligonite, Hydromagnesite, **Vermiculite**
MC13a (GS8)	1911.3 1424.5 1464.3	13.95 19.54 20.37	6.66 2.59 1.64	38.7 57.5 147.7	-	**Kaolinite, Dickite, Halloysite**, Illite, Sauconite, Beryl, Smithsonite
MC12	1912.2 1422.8 2250.2	28.47 34.34 33.78	7.64 2.69 0.63	43.8 53.2 45.8	-	Analcime, Beidellite, Aporphylite, Mordenite, Notronite, Antlerite
MC11b (GS9)	1912.2 1424.2 2297.3	14.23 19.26 18.98	8.06 3.74 0.81	47.8 59.8 18.7	Stilbite	Analcime, Beidellite, Aporphylite, Mordenite, Notronite, **Smectite**, Smithsonite
MC11a	1913.2 1425.7 1462.3 1532.2 2094.2	11.43 15.35 16.46 17.00 16.18	5.76 2.49 1.83 0.92 0.71	42.8 64.3 137.7 305.8 80.2	Stilbite, Scheelite, sepiolite	Lepidorite, Borax?
MC10	1911.7 1422.0 1356.9 2251.8	14.23 19.81 22.33 19.81	8.05 3.41 0.96 0.73	38.3 56.0 69.1 48.2	Stilbite	Montmorillonite, Analcime, Sauconite, Bassanite, Siderite
MC9 (GS10)	1911.4 1422.8 2251.5 2302.2	14.51 20.37 20.65 19.81	10.09 4.23 0.85 0.61	46.6 61.2 30.5 105.9	Stilbite	**Halloysite, Illite, Montmorillonite,** Analcime
MC8 (GS11)	1912.2 1419.4 1460.0	7.80 9.20 9.70	3.43 1.42 1.01	41.8 68.6 134.0	Stilbite, scheelite	**Halloysite, Illite, Montmorillonite,** Sauconite, Epidote
MC7	1910.9 1423.6 1542.5	17.30 21.20 22.33	5.37 2.02 0.49	35.1 52.4 107.5	Antigorite, cerussite	Sepiolite
MC6 (GS12)	1911.7 1420.8	9.48 13.67	6.20 2.87	46.3 51.2	-	Analcime, Chabazite, Mordenite, Bassanite, Beidellite, **Illite, Kaolinite**, Smectite, Uralite, Colemanite, Montmorillonite, Azurite, Clinochlore, Notronite, Sepiolite, Chysocolla, Hemimorphite, Nepheline.

MC5	1911.5 1421.71 1335.7 2249.0	13.95 17.58 18.70 18.42	5.79 2.00 0.64 0.49	38.5 46.3 48.3 49.0	-	Cerrucite, , Sauconite, Phlogopite,
MC4 (GS13)	1911.9 1420.5 1537.1	9.48 13.95 14.79	5.32 2.60 0.91	48.1 55.5 312.9	Malachite, Stilbite, Scheelite, sepiolite	Bassanite, Beidellite, **Kaolinite, Illite**
MCHB	-	-	-	-	No data	Not analysed
MC3 (GS14)	1912.7 1423.2 1319.6 1554.6	12.83 18.14 20.65 20.09	7.09 2.73 0.52 0.54	39.3 52.8 28.4 385.4	-	**Kaolinite,** Pyrophyllite, Colemanite, Gibbsite
MC2 (GS15)	1911.7 1422.1	16.18 20.93	7.25 2.69	40.3 51.9	-	**Kaolinite**, Bassanite, Beidellite,
MC1 (GS16)	1912.0 1422.4 2243.0	15.90 21.77 22.61	8.82 3.21 0.65	40.0 47.6 41.0	-	Analcime, Chabazite, Mordenite, Bassanite, Beidellite, **Illite, Kaolinite, Smectite,** Uralite, Colemanite, Azurite, Clinochlore, Notronite,

RB section

RB24	1912.3 1425.0 1464.5 1360.9	12.27 16.74 17.86 18.42	6.05 2.34 1.06 0.56	35.7 39.0 115.5 31.1	Calcite, scheelite	kaolinite, Brucite
RB23	1912.8 1424.2 1467.9 1784.3 1808.3	14.51 18.70 19.81 20.09 19.98	5.97 2.35 1.27 0.52 0.51	35.2 43.8 164.1 71.7 93.7	-	Nepheline, kaolinite, sepiolite bassanite
RB22	1913.5 1425.5 1462.0	13.39 17.58 18.14	5.84 2.36 1.39	34.5 46.5 148.0	-	Nepheline, smithsonite
RB21 (GS17)	1914.5 1424.4 2251.5	18.70 25.40 24.84	8.79 3.06 0.82	43.5 47.6 38.5	-	**Gibbste, kaolinite,** hankasite
RB20 (GS18)	1915.9 1425.1 1347.4	14.79 20.65 22.89	7.52 2.91 0.78	42.1 54.9 52.6	Palygorskite	**Limonite,** hemimorphite **Halloysite**
RB19	1917.2 1423.5 1456.6	13.67 19.54 20.65	6.71 2.77 1.98	52.8 46.5 139.4	Palygorskite	Heulandite, Natrolite
RB18b (GS19)	1916.6 1425.5 1457.6 1351.6	12.27 17.02 17.32 18.60	5.13 1.94 1.36 0.53	43.4 52.5 112.4 40.4	Stilbite, **palygorskite,** hemimorphite	Heulandite, lazurite, cerussite, amblygonite
RB18a (GS19)	1913.9 1423.6	14.65 18.65	5.22 2.17	47.1 62.0	Dolomite	Jadeite, **palygorskite**
RB17	1913.9 1423.6 1463.0 1536.6 1356.0	12.65 15.98 16.65 16.74 17.30			Scheelite	Scheelite
RB16	1913.8	11.98	4.59	38.2	Stilbite, palygorskite,	Analcime, colemanite,

	1422.2 1356.0	15.98 17.32	1.68 0.49	41.8 48.0	illite, hemimorphite. Scheelite	notronite, inyoite, Heulandite.
RB15 (GS20)	1919.1 1426.1	11.31 16.65	5.88 2.24	54.9 55.9	-	Lazurite
RB14 (GS21)	1914.4 1424.8 1465.5	19.98 27.32 27.98	6.88 2.64 1.72	43.6 47.2 140.5	-	Scheelite, **Halloysite,** stilbite
RB13	1913.7 1424.0	15.31 21.32	7.26 2.72	38.3 52.0	Palygorskite, stilbite	Halloysite, alum,
RB12	1913.0 1423.1 2088.0 2304.0	21.30 29.32 26.65 24.65	8.20 2.91 0.89 0.64	39.0 40.9 416.0 27.8	Sepiolite, Stilbite	Dolomite, dickite,
RB11	1913.1 1424.0 2253.2 2304.7	13.98 20.65 18.70	8.27 3.22 19.98 19.32	42.9 46.0 0.51 0.48	Palygorskite, stilbite	sepiolite, hornblende
RB10	1914.1 1425.0 2120.4	15.98 21.32 20.65	6.22 2.16 0.46	37.9 59.0 473.6	Hemimorphite, scheelite, stilbite, palygorskite, sepiolite	Hanksite, jadeite, alum, mordenite
RB9	1913.3 1424.0	27.32 35.98	9.78 3.37	42.7 57.0	Sepiolite, stilbite, scheelite	Lepidolite
RB8	1912.6 1421.9 2302.3	18.98 26.52 24.56	9.03 3.08 0.56	43.4 55.1 33.7	Stilbite, sepiolite	Aragonite, hanksite
RB7	1912.5 1423.7 2299.8 1460.3	15.31 20.65 19.32 21.32	6.29 2.25 0.60 1.46	43.5 56.3 14.2 135.7	-	Hydromagnesite, natrolite
RB6b	1912.0 1423.7 1356.4 1553.2	17.98 23.98 26.24 25.96	8.15 2.99 0.73 0.57	40.0 46.3 77.6 361.7	-	Analcime, smectites, Mordenite, nepheline
RB6a	1912.5 1423.5 1460.0	22.65 29.03 30.15	9.43 2.85 1.78	39.5 42.5 104.0	-	Lepidolite, analcime, borax, nepheline, montmorillonite-Fe, Natrolite, alunite
RB5 (GS22)	1912.6 1425.7 2303.9	26.24 33.22 32.65	8.55 2.36 0.55	39.4 52.3 20.1	Stilbite	Lepidolite, **kaolinite,** analcime, borax.
RB4	1912.6 1423.9 2301.3	23.98 29.32 29.59	6.92 1.85 0.50	39.4 48.1 24.7	-	Analcime, borax. Carbonate.
RB3 (GS23)	1912.0 1422.0 2120.0 2244.2 12298. 6	20.65 29.97 32.66 31.27 30.43	13.87 4.60 0.54 0.71 0.70	44.0 52.0 60.0 53.8 9.4	-	Analcime, bassanite, mordenite, lepidolite, **illite, smectite,** **kaolinite**
RB2	1912.7 1421.8 2307.3	28.63 36.65 38.53	12.75 3.07 0.55	39.3 52.2 24.7	-	montmorillonite-Fe, Natrolite, alunite
RB1	1913.5 1423.6 2305.4	21.98 30.65 30.43	11.47 3.37 0.54	38.5 46.8 32.6	Stilbite, palygorskite	Mordenite, okenite

RS Section

RS39 (GS24)	1912.7 1424.8 1314.1 2301.4	13.31 18.14 19.81 17.30	6.25 2.41 0.69 0.49	43.3 63.2 45.9 18.6	-	**Kaolinite,** lepidolite, sepiolite, hanksite
RS38	1912.5 1424.6 1348.0	10.04 13.67 14.51	5.12 1.64 0.56	39.5 61.4 88.4	-	lepidolite, sepiolite, hanksite, natrolite
RS 37 (GS25)	1912.4 1423.8	16.46 22.61	8.20 2.46	39.6 42.2	-	Analcime, azurite, beidellite, bassanite, smectite, notronite, **Kaolinite**
RS 36	1913.1 1426.0	24.56 33.22	10.31 3.05	38.9 52.0	-	lepidolite, sepiolite, hanksite
RS35 (GS26)	1912.1 1424.6 2301.8	19.54 25.68 25.68	8.25 2.46 0.45	3939 47.4 22.2	-	Analcime, azurite, beidellite, bassanite, **smectite,** notronite, **Kaolinite**
RS34	1914.0 1424.8 2152.0	22.3 31.83 29.03	9.30 2.29 0.66	38.0 47.2 536.0	Hemimorphite, palygorskite	Hemimorphite, palygorskite, hanksite, calcite
RS33	1910.6 1413.8 1394.0 1454.0	11.43 10.32 10.04 10.60	1.86 0.71 0.61 10.62	41.4 92.2 130.0 72.0	Cordierite	smectite, brucite, natrolite, dolomite, cordierite
RS32	1911.5 1416.3 2338.1	18.70 19.81 19.26	2.39 0.58 1.31	34.5 53.7 3939	Calcite, scheelite, stilbite	Calcite, stilbite, scheelite, chysocolla,
RS 31 (GS27)	1912.4 1421.3 2300.8	15.07 19.29 20.09	7.27 1.93 0.65	43.6 50.7 19.2	-	Hanksite, Analcime, azurite, beidellite, bassanite, **smectite,** notronite **kaolinite**
RS30	1911.0 1420.0 2304.6	13.11 15.62 17.30	5.81 1.60 0.72	39.0 56.0 33.4	-	Rhodocrosite, Cordierite, illite, brucite, natrolite, dolomite
RS29 (GS28)	1911.8 1422.3	19.81 29.59	12.17 3.79	42.2 51.7	Stilbite, sepiolite, palygorskite	Analcime, azurite, beidellite, bassanite, smectite, notronite, stilbite, Heulandite, inyoite, stellerite, ephesite
RS28b	1911.7 1417.9 2305.5	13.94 17.02 18.14	5.58 1.45 0.51	44.3 54.1 16.5	-	Azurite, beidellite, bassanite, notronite, epidote, paragonite, quartz
RS28a	1911.5 2339.0 1419.0	17.58 19.24 19.54	4.42 1.39 1.22	38.5 45.0 103.0	-	Stilbite, sepiolite, scheelite, alunite, Calcite, chysocolla
RS27	1911.1 1416.1 1454.0 1484.0	8.64 8.36 8.64 8.64	1.40 0.69 0.57 0.48	48.9 149.9 116.0 100.0	Scheelite, sepiolite, stilbite	Palygorskite, stilbite, hemimorphite, muscovite, azurite, bassanite, smectite, notronite, stilbite, Heulandite, inyoite,

						stellerite, ephesite
RS26	1915.9 1422.3 2120.0 2156.0	19.54 28.75 25.12 25.12	8.90 2.52 1.25 0.61	52.1 47.7 472.0 554.0	Stilbite, hemimorphite	Gypsum, hemimorphite, glauconite, jarosite.
RS25	1940.9 1504.0 1424.2 1491.0	32.39 44.68 44.40 44.68	9.04 1.12 1.72 1.20	91.1 120.3 53.8 145.0	-	Sepiolite, Hanksite, Analcime, azurite, beidellite, bassanite, smectite, notronite
RS 24	1913.2 1420.8	15.34 25.12	10.87 3.82	46.8 47.2	-	Malachite, azurite, bassanite, notronite, stilbite, Heulandite, inyoite, stellerite, ephesite
RS 23	1911.4 1421.9	17.58 24.00	7.49 2.21	38.6 56.1	Malachite, sepiolite	Malachite, tyremolite, epidote, notronite, feldspar(buddingtonite), Hanksite, smectite, Analcime, azurite, beidellite, bassanite,
RS 22 (GS29)	1910.9 1420.6 2309.4 1556.0	18.14 30.71 25.68 33.50	13.45 5.31 0.56 1.05	43.1 51.4 408.2 348.0	Malachite	Sepiolite, palygorskite, hemimorphite, notronite, clinoptilolite
RS21	1908.9 1416.9 2218.2	4.45 10.32 8.36	8.88 1416.9 0.83	55.1 7.87 25.8	notronite, hemimorphite	Stilbite, malachite, Analcime, azurite, beidellite, bassanite, notronite, Heulandite, inyoite, stellerite, ephesite
RS 20	1912.2 1422.3	23.32 35.98	14.02 3.95	47.8 47.7	Stilbite, malachite, palygorskite	Stilbite, sepiolite, chrysoprase(silica), Rhodocrosite, Cordierite, illite, brucite, natrolite, dolomite,
RS19 (GS30)	1909.7 1420.3 2166.0 2306.2	7.80 13.67 12.50 10.87	8.49 7.03 0.54 0.50	54.3 55.7 580.0 25.8	Stilbite, sepiolite, chrysoprase	Sepiolite, lepidolite, stilbite, analcime, **palygorskite**
RS18	1912.7 1423.1	21.32 37.96	17.10 7.54	51.3 50.9	Sepiolite	stilbite, scheelite, malachite, epidote, Rhodocrosite, Cordierite, halloysite, brucite,
RS17 (GS31)	1910.4 1418.9	8.92 17.56	11.79 6.52	51.6 51.1	Scheelite, stilbite, sepiolite, malachite, epidote	Alunite, cerussite, haulandite, **palygorskite,** hydrobiotite, apatite
RS16	1917.7 1931.5 1424.8	24.00 24.28 40.77	13.85 13.51 5.42	54.3 85.5 51.2	-	Analcime, azurite, beidellite, bassanite, smectite, notronite,
RS15	1915.7 1423.6 1458.0	22.05 37.41 37.97	13.42 5.61 4.64	50.3 56.4 112.0	-	stilbite, sepiolite,

RS14	1909.8 1418.2 2328.3	19.81 34.90 23.17	19.09 10.92 4.08	52.2 51.8 43.7	stilbite, sepiolite.	Sepiolite, notronite, Alunite, cerussite, haulandite, hydrobiotite, apatite
RS13 (GS38)	1909.2 1418.0	5.57 10.32	7.57 6.67	64.8 56.8	Sepiolite, notronite	Sepiolite, analcime, mordenite, okenite, bassanite, **smectite**
RS12	1910.4 1419.6 2308.0	17.02 35.43 27.08	20.87 11.23 0.98	51.6 46.1 24.0	Sepiolite,	Chrysoprase, stilbite, hemimorphite, dickite, notronite, clinoptilolite.
RS11 (GS39)	1909.1 1419.3 2304.0	10.27 8.83 0.71	0.689 0.624 0.017	54.9 60.7 22.0	**Montmorillonite,** chrysoprase, stilbite, hemimorphite	**Kaolinite,** lepidolite, sepiolite, hanksite
RS10	1913.4 1421.0 2032.9	28.75 52.22 35.58	19.48 10.46 9.50	50.6 47.0 297.1	-	Chrysoprase, malachite, stilbite.
RS9 (GS40)	1919.8 1419.4 2306.2	12.41 7.96 0.61	0.750 0.490 0.015	52.2 50.6 23.8	**Illite, montmorillonite,** chrysoprase, malachite, stilbite.	Hanksite, Analcime, azurite, beidellite, bassanite, smectite, notronite
RS8	1913.1 1421.6 1455.0	18.42 36.86 37.97	19.00 10.84 9.04	54.9 50.4 131.2	Malachite	Stibite, sepiolite, hemimorphite, notronite, clinoptilolite
RS 7 (GS41)	1909.4 1418.6 2129.0 2250.3	9.20 18.14 17.58 16.46	12.88 8.78 1.19 0.51	56.6 57.4 519.2 35.7	**Montmorillonite,** stilbite, sepiolite	Stilbite, chrysoprase, **montmorillonite,** hemimorphite, notronite, clinoptilolite,
RS6	1908.8 1418.6 2152.0	6.96 12.83 11.15	8.10 6.92 0.60	59.2 55.4 552.0	Stilbite, chrysoprase.	Stilbite, chrysoprase(silica), Rhodocrosite, Cordierite, halloysite, illite, brucite, calcite.
RS 5 (GS42)	1909.6 1418.4 2341.8	9.48 17.86 12.83	11.36 6.30 5.58	52.4 51.6 536.4	Stilbite, Analcime, Montmorillonite.	Cordierite, **illite, smectite,** dolomite
RS4	1911.0 1418.9 2247.3	5.57 10.60 8.36	7.56 6.83 0.50	69.0 61.1 56.7	-	Stilbite, hemimorphite, Organic matter?.
RS3	1909.4 1416.9 2217.4 2246.5		18.42 12.58 1.77 1.08	56.6 47.1 30.6 83.5	illite, stilbite, hemimorphite	Stilbite, calcite,
RS2	1909.2 1416.7 2340.0	20.37 38.25 24.28	23.10 13.58 4.33	46.8 47.3 44.3	Stilbite, illite.	Hemimorphite, chrysoprase,
RS 1	1907.6 1422.4 1948.1 2126.3 2148.0 2168.0	 5.31 6.68 	5.73 7.71 4.97 1.72 1.42 1.08	74.4 79.6 165.9 511.7 556.0 590.0	Hemimorphite, chrysoprase,	Hemimorphite, chrysoprase,
LK section						
LK10 (GS32)	1910.2 1420.0 2221.8	5.57 10.60 11.31	7.66 4.08 0.52	51.8 56.0 32.2	Stilbite, sepiolite, **montmorillonite,** chrysoprase, malachite	Stilbite, sepiolite, **montmorillonite (smectite), illite,**

						kaolinite
LK9 (GS33)	1910.3 1421.1 2302.7	7.80 13.93 13.67	8.68 4.25 0.62	47.7 50.9	-	Hanksite, **kaolinite,** saponite, **montmorillonite**
LK8 (GS34)	1910.9 1422.7 2222.5 2305.2	8.36 18.70 21.21 19.32	17.16 9.42 0.92 0.71	47.1 51.3 57.0 22.8	-	**Halloysite (kaolinite) Lepidocrosite,** notronite
LK7 (GS35)	1911.1 1422.6	5.57 10.32	7.30 3.24	42.9 51.4	-	Sepiolite, analcime, notronite, **illite, kaolinite**
LK6b (GS35)	1910.8 1422.6 2218.8	5.85 11.99 13.11	9.17 4.41 0.52	43.2 51.4 33.2	-	**Illite,** sepiolite, inyoite, notronite, **kaolinite**
LK6a (GS35)	1911.0 1422.8 2219.7	4.45 9.48 10.32	7.71 3.87 0.46	47.0 47.2 18.3	-	**Lepidocrosite, Halloysite, illite**
LK5 (GS35)	1911.3 1421.4 2220.5 2307.8	8.64 18.42 19.54 18.65	15.98 8.57 0.96 6.58	46.7 56.6 68.6 32.2	Sepiolite	Sepiolite, **lepidocrosite,** hectorite, **kaolinite.**
LK4 (GS36)	1910.9 1419.9 2219.0	4.17 7.80 6.96	5.91 4.52 0.57	59.1 60.1 19.0	Sepiolite, chrysoprase, stilbite, hemimorphite	**Palygorskite, sepiolite,** stilbite, azurite, hemimorphite,
LK3 (GS37)	1910.0 1418.5 2221.4	3.61 6.68 7.57	6.50 4.52 0.59	66.0 59.5 32.6	**Palygorskite, sepiolite,** azurite, montmorillonite-Fe, malachite, hemimorphite, chrysoprase.	**Palygorskite,** azurite, Malachite, chrysoprase, hemimorphite,
LK2	1910.3 1420.2 2218.9	18.68 30.65 30.71	15.46 6.12 1.38	43.7 51.8 23.1	Sepiolite	Sepiolite, Beidellite, clinoptilolite, quartz, hemimorphite, notronite.
ZINJ section						
5Z	1916.4 1935.0 1423.7 1461.0	14.23 15.07 19.81 20.09	4.73 4.37 1.49 0.95	43.6 91.0 42.3 125.0	-	Brucite,
4Z	1911.2 1419.4 2311.0	8.65 21.32 14.65	18.51 12.26 1.37	60.8 56.6 33.2	Chrysoprase, sepiolite, Stilbite	Chrysoprase, sepiolite,
Z24	1915.2 1425.8 2305.1 2180.7	16.74 31.83 27.84 31.55	54.8 56.2 26.9 601.3	54.8 56.2 26.9 601.3	Stilbite	Chrysoprase, sepiolite, Malachite
3Z (GS43)	1910.9 1420.0 2306.0 2140.0	5.01 11.71 8.08 11.15	9.32 5.98 0.79 0.53	51.1 52.0 27.5 533.6	Sepiolite, **montmorillonite,** chrysoprase, stilbite, malahite	**Montmorillonite, gibbsite, halloysite,** illite, stilbite
2Z (GS44)	1910.5 1421.8 2310.6	5.31 9.31 7.30	7.41 5.58 1.14	59.5 76.2 39.4	Sepiolite, montmorillonite	**Montmorillonite,** sepilite, **halloysite,** analcime, **illite, Gibbsite**
ZL	1912.4	17.98	26.06	55.6	Malachite, stilbite,	Malachite, azurite,

	1420.2 2311.6	34.65 31.32	14.44 1.66	59.8 24.4	azurite, sepiolite, chrysoprase	sepiolite, chrysoprase,
1Z (GS45)	1911.4 1420.8 2310.9 2124.5	6.41 12.83 9.20 12.27	9.14 5.50 1.15 0.86	60.6 63.2 27.1 499.5	Sepiolite, **montimorillonie,** malachite, chrysoprase, stilbite	Sepiolite, **Kaolinite, Gibbsite, Montmorillonite,** malachite, stilbite, chrysoprase,
ZK (GS46)	1912.0 1421.4 2307.2 2132.8	11.17 22.05 18.70 23.17	15.46 8.13 1.53 0.92	56.0 54.6 26.8 531.2	Malachite, azurite, stilbite	**Illite,** stilbite, analcime, **smectite, kaolinite,** lepidolite , **montmorillonite**
Z23	1913.4 1425.9	19.32 25.98	7.19 2.09	42.6 60.1	Stilbite	Stilbite, lepidolite
Z22	1915.2 1426.6 2305.5	24.65 46.65 37.98	24.82 11.72 1.89	54.8 59.4 22.5	Hemimorphite, sepiolite	Sepiolite, hemimorphite, jadeite, nepheline.
Z21c	1911.9 1420.6 2303.1	19.98 34.65 31.98	22.82 11.07 1.73	56.1 51.4 26.9	Malachite, sepiolite	Malachite, sepiolite, smectite, illite, mordenite.
Z21b	1914.9 1424.9 2306.4	23.98 43.98 36.65	25.40 13.13 1.42	55.1 55.1 33.6	Hemimorphite	Hemimorphite, jadeite, nepheline
Z21a	1910.2 1418.2 2305.8	9.31 19.32 15.31	15.69 10.49 1.43	55.8 51.8 33.0	Stilbite, hemimorphite, sepiolite, chrysoprase	Stilbite, hemimorphite, Sepiolite, malachite, chrysoprase, smectite, illite, mordenite.
Z21	1912.7 1420.2 22254. 2 2303.2	14.65 26.65 22.65 20.37	14.90 8.63 0.46 1.31	51.3 51.8 27.8 32.8	Sepiolite, malachite, chrysoprase	Sepiolite, malachite, chrysoprase
Z20	1914.0 1424.6 2168.3 2304.4	18.98 36.02 33.32 28.20	20.04 9.54 0.67 1.86	56.0 55.4 577.7 27.6	Sepiolite,	Sepiolite, hanksite, Alunite
Z19 (GS47)	1912.2 1421.8 2304.0	35.32 48.65 43.90	16.29 4.67 2.24	47.8 46.2 32.0	Stilbite.	Stilbite, Haulandite, inyoite, notronite, **Illite, Smectite (montmorillonite)**
Z18	1912.3 1421.9 2124.0 2306.1	32.94 51.66 50.82 45.24	22.29 7.83 1.36 2.00	51.5 52.1 500.0 25.9	Azurite, malachite	Azurite, malachite, sepiolite, mordenite.
Z17 (GS48)	1911.4 1420.9 2309.4	25.12 42.44 36.02	20.38 8.38 1.39	46.6 51.1 32.6	Malachite, stilbite, **Illite**	Malachite, stibite, **smectites (montmorillonite?)** analcime, mordenite
Z16	1911.0 1420.0 2249.7 2309.1	24.00 40.21 39.09 35.46	21.58 8.74 0.66 1.61	47.0 52.0 26.3 28.9	-	Notronite.
Z15 (GS49)	1911.7 1421.2 2305.5	23.32 38.65 33.98	20.05 7.60 2.00	52.3 46.8 32.5	Sepiolite, malachite, stilbite	Sepiolite, malachite, stilbite, **smectite, illite**
Z14	1912.4	17.58	15.06	51.6	Azurite, malachite	Azurite, malachite,

	1421.2 2306.5	30.15 25.98	5.94 1.44	46.8 27.5		analcime, beidellite, lepidolite,
Z13 (GS50)	1910.7 1418.8 2308.1	14.65 23.65 21.32	16.69 9.42 1.61	55.3 55.2 27.9	Stilbite, sepiolite, montmorillonite, malachite	Stilbite, sepiolite, **montmorillonite,** malachite, **illite,** hectorire,
Z12	1912.0 1421.4 2305.0	25.98 46.64 38.65	25.85 12.07 2.54	52.0 50.6 32.9	Malachite, sepiolite stilbite	Malachite, sepiolite, stilbite, analcime
Z11 (GS51)	1912.8 1422.0 2306.0	23.32 36.64 32.65	15.10 4.89 1.32	47.2 58.0 27.8	Malachite, **illite**	Malachite, **montmorillonite** sepiolite, notronite, stellerite, lepidolite,
Z10	1912.8 1423.1 2307.3	32.65 51.32 45.32	23.13 8.56 1.67	47.2 50.9 32.7	Stilbite	Stilbite, malachite, kaolinite, sepiolite, notronite, stellerite, lepidolite,
Z9 (GS52)	1909.7 1418.6 2308.0	51.32 20.09 17.30	11.82 5.96 1.18	46.3 55.4 32.0	Stilbite, azurite, **Montmorillonite, Dickite, halloysite**	**Montmorillonite, kaolinite**, stilbite, hemimorphite, Sepiolite, malachite, chrysoprase, smectite, illite, mordenite.
Z8	1913.4 1423.8 2306.5	19.81 30.21 27.64	13.60 4.38 1.42	46.6 50.2 37.5	Stilbite	Stilbite, Malachite, sepiolite, notronite, stellerite, lepidolite,
Z7 (GS53)	1916.1 1425.6 2304.5	15.90 29.87 25.40	16.44 7.36 1.20	55.9 54.4 27.5	Stilbite,	Stilbite, **halloysite, limonite, Dickite.**
Z6	1914.5 1424.5 2306.6	24.28 42.16 33.18	21.84 9.03 2.14	55.5 55.5 25.4	Scheelite, stilbite	Scheelite, stilbite, jadeite,
Z5	1912.0 1423.3 1800.5 2306.9	17.58 30.43 35.74 26.65	17.33 7.69 0.63 1.84	52.0 54.70 43.5 37.1	Sepiolite, stilbite	Sepiolite, stilbite, analcime, malachite, smectite, illite, mordenite.
Z4 (GS54)	1913.0 1423.3 2126.0 2306.8	24.00 34.34 35.74 33.22	13.48 3.89 0.60 1.00	47.00 50.7 104.0 33.2	-	Malachite, kaolinite, sepiolite, notronite, stellerite, lepidolite, **Kaolinite, dickite**
Z3	1914.4 1424.7 2304.2	25.12 45.52 30.53	23.07 12.08 2.11	55.6 55.3 21.8	Stilbite	Stilbite, diopside, borax, hanksite, dickite, halloysite, dolomite
Z2 (GS55)	1911.3 1420.1 2310.0	16.18 25.12 22.33	11.41 4.35 1.24	52.7 59.9 32.0	Sepiolite, **Montmorillonite,**	Sepiolite, **illite, Montmorillonite,**
Z1	1908.9 1417.5 1804.0 2307.8	20.37 34.62 41.32 29.89	20.33 8.26 0.72 2.34	47.1 46.5 44.3 28.2	sepiolite	Sepiolite, quartz, notronite, calcite, analcime.
ZJ	1913.3 1420.9 2312.9	14.51 23.17 23.45	14.19 5.21 0.47	50.7 59.1 25.1	Malachite	Malachite, lepidolite, kaolinite, sepiolite.
ZI (GS56)	1909.0 1417.6	7.80 15.07	9.76 5.27	51.0 62.4	Sepiolite, **Montmorillonite**	**Montmorillonite, sepiolite, palygorskite,**

	2310.7	10.87	1.32	25.3		**Alevardite (illite),** notronite, mordenite.
ZH	1908.3 1416.7 2340.1 2311.7	27.08 41.60 33.32 32.39	19.44 7.75 2.19 4.35	47.7 63.3 91.9 40.3	Sepiolite, malachite	Malachite, tremolite, clinoptilolite, stilbite.
ZG	1908.6 1417.3 2310.6	11.71 22.89 17.02	15.90 7.67 2.71	51.4 68.7 27.4	Malachite	Sepiolite, malachite, Saponite.
ZF	1908.8 1418.7 2343.8 2310.8	22.33 33.22 28.20 27.64	14.66 5.30 0.88 2.78	43.2 73.3 102.2 35.2	Stilbite	Brucite, stilbite, hectorite.
ZE	1910.0 1419.1 3210.2	13.67 22.89 18.70	12.65 5.06 1.88	52.0 64.9 27.8	Azurite, sepiolite,	Azurite, sepiolite, Clinoptilolite, notronite, quartz, glaucophane, antlerite.
ZD	1908.5 1417.4 2336.0 2311.6	31.27 44.96 37.41 37.97	19.37 7.13 2.57 4.21	43.5 64.6 89.8 40.4	Stilbite	Stilbite, **alevardite (illite),** notronite, clinoptilolite.
ZC	1909.7 1419.1 2310.1	10.87 20.65 16.18	14.70 7.65 1.49	50.3 64.9 27.9	Scheelite, sepiolite, azurite, montmorillonite, stilbite, malachite	Scheelite, sepiolite, azurite, montmorillonite, stilbite, malachite.
ZB (GS57)	1910.9 1419.8 2310.1	15.07 25.96 23.45	16.53 7.25 1.32	51.1 60.2 22.9	Sepiolite, azurite, crhysoprase	Sepiolite, azurite, chysoprase, **halloysite,** rhodocrosite
ZA	1910.2 1419.1 2307.8 2131.6	27.32 39.33 40.77 35.90	16.53 5.30 1.78 0.56	47.8 50.9 524.4 32.2	-	Clinoptilolite, notronite, saponite, stilbite, dolomite, hectorite.

APPENDIX 7.5A: A synthesized list of mineral species of Olduvai Gorge composite Section.

Mineral group and name	**Chemical formula**
1. Clay Minerals	
Illites	
- Alevardite-Rectorite	
- Illite	$(Na, Ca)Al_4(SiAL)_8O_{20}(OH)_4.2H_2O$
- Glauconite?	$KAl_4(Si7Al_{20})(OH)_4$
	$(K,Na)(Fe^{+3}Al,Mg)_2(Si,Al)_4O_{10}(OH)_2$
Kaolinites	
- Dickite	$Al_2Si2O_5(OH)_4$
- Halloysite	$Al_2Si2O_5(OH).2H_2O$
- Kaolinite	$Al_2Si2O_5(OH)_4$
- Palygorskite (Attapulgite)	$(Al,Fe)Si_2O_5(OH)_4$
- Sepiolite	$(Al,Mg)_2Si_4O_{10}(OH)_2(Al,Si)_4$
	$Mg_4Si_6O_{15}(OH)_2.6H_2O$
Smectites	

- Beidellite $(Na,Ca)Al_2(OH)_2(Al,Si)_4O_{10}.4H_2O$
- Hectorite $Na(Li,Mg)_3Si_4O_{10}(F,OH)_2$
- Montmorillonite $(Na,Ca)(Al,Mg)_2Si_4O_{10}(OH)_2$
- Notronite $NaFe_2^{+3}(SiAl)_4O_{10}(OH)_2.H_2O$
- Saponite $(Ca_2Na)(MgFe^{+2})_3(Si,Al)_4O_{10}(OH)_2.4H_2O$

2. Zeolites

Na-Zeolites

- Analcime $NaAlSi_2O_6.H_2O$
- Natrolite $Na_2Al_2Si_3O_{10}.2H_2O$

Ca-Zeolites

- Chabazite $Ca_2Al_2Si_4O_{12}.6H_2O$
- Heulandite $CaAl_2Si_7O_{18}.6H_2O$

Na/Ca/K-Zeolites

- Aporphyllite $KCa_2(Si_4O_{10})_2F.8H_2O$
- Clinoptilolite $(Na,K,Ca)_2Al_3(Si_4O_{12}).6H_2O$
- Mordenite $K_2(Ca,Na)Al_2Si_{10}O_{24}.7H_2O$
- Stilbite $Na_2Ca_2Al_5Si_{13}O_{36}.16H_2O$

3. Hydroxides

- Brucite $Mg(OH)_2$
- Gibbsite $AL(OH)_3$
- Lepidocrosite $FeO.OH$
- Limonite $FeO.OH.nH_2O$

4. Carbonates

- Amorphous $[CO_3^{-2}]$
- Aragonite $CaCO_3$
- Azurite $Cu_3(OH)_2(CO_3)_2$
- Calcite $CaCO_3$
- Cerrucite $PbCO_3$
- Dolomite $CaMg(CO_3)_2$
- Malachite $Cu_2(OH)_2CO_3$
- Stronianite $SrCO_3$
- Shortite $Na_2Ca_2(CO_3)$
- Smithsonite $ZnCO_3$
- Scheelite
- Rhodochrosite $MnCO_3$

5. Evaporites

Sulphate

- Alum $KAl(SO_4).12H_2O$
- Alunite $KAl_3(SO_4)_2(OH)_6$
- Antlerite $Cu_2^{+3}(SO_4)_2(OH)_6$
- Bassanite $2CaSO_4.H_2O$
- Gypsum $CaSO_4.2H_2O$
- Hankasite $Na_2K(CO_3)_2Cl(SO_4)_9$

Borates

- Borax $Na_2B_4O_5(OH)_4 8H_2O$
- Colemanite $Ca_2B_3O_4(OH)_3.H_2O$
- Inyoite $CaB_3O_3(OH)_5.4H_2O$

6. Silicate minerals

Amhpiboles

- Glaucophane $Na_2(Mg,Fe^{2+})_3Al_2Si_8O_{22}(OH)_2$
- Lazurite $(Mg,Fe)A_{12}(PO_4)_2(OH)_2$
  $Ca_2(Mg,Fe)_5Si_8O_{22}(OH)_2$

Micas

- Ephesite $NaLiAl_2(Al_2Si_2)O_{10}(OH)_2$
- Lepidolite $K(Li,Al)_3(Si,Al)_4O_{10}(FOH)_2$
- Muscovite $K,Al_2(Si_3Al)O_{10}(F,OH)_2$

Other silicates

- Clinozoisite	$Be_2Al_2Si_5O_{18}$
- Epidote	$Ca_2(Al,Fe)Al_{2O}(SiO_4)(Si_2O_7)(OH)$
- Feldspars (Buddingtonite)	$NH_4AlSi_3O_8.0.5H_2O)$
- Horneblende	$(Na,Al)Ca_2Mg_4Fe_2(Al,Fe)(OH)_2Si_2Al_2O_{22}$
- Nepheline	$NaAlSiO_4$
- Pyroxene (Jaedite)	$NaAlSi1_2O_6$
- Quartz	SiO_2
- Hemimorphite	

APPENDIX 7.6: STEREO MICROSCOPIC EXAMINATION OF PALAEOSOLS OF OLDUVAI GORGE (SURFACE OBSERVATIONS OF HAND SPECIMENS)

RS Site

Sample no. RS7 – GS41

Microstructure: Layered clay without peds but showing distratification of discontinuous oval shaped patches (<1mm) of white material, occupying about 2% of the palaeosol volume.

Groundmass:

- Basic components: (> 600μm) rare grains of quartz (<2%)
- Fine material: (<600μm) greenish gray clay ground mass.

Organic remains:

No organic remains were observed.

Pedofeatures:

The white patches might be gypsum minerals, (does not react with 2N HCl).

Illustration

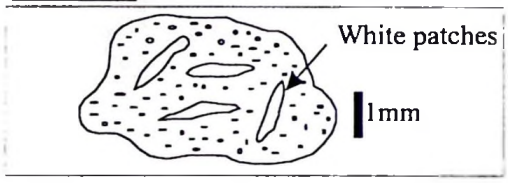

Sample RS9 – GS40

Microstructure: Massive clay without peds but showing distratification of discontinuous patches of white material, occupying about 2% of the palaeosol volume.

Groundmass:

- Basic components: (>600μm) rare grains of quartz (<2%)
- Fine material: (<600μm) greenish gray clay ground mass and calcite.

Organic remains:

No organic remains were observed

Pedofeatures:

1 –3cm in diameter large carbonate concretions usually present at the base of the level (field observation). The white patches (as in RS7) might be gypsum minerals.

Sample RS 11- GS39

Microstructure: Massive clay without peds but showing distratification of discontinous patches of white material, occupying about 10% of the palaeosol volume.

Groundmass:

- Basic components: (>600μm) rare grains of quartz (<2%)
- Fine material: (<600μm) greenish gray clay ground mass with calcite.

Organic remains:
No organic remains were observed
Pedofeatures:
1 – 3cm well rounded carbonate concretions. The concretions consist of accretion of smaller concretions. White patches might be gypsum (as in RS 9).
Illustration

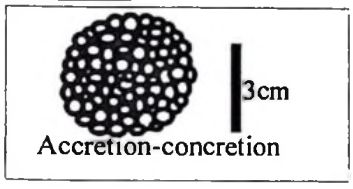

Sample RS15
Microstructure: Sandy homogeneous white ash, no peds observed.
Groundmass:

- Basic components: (>600μm) quartz (50%), pyroxene/hornblende (30%) newly formed fragile fibrous minerals (<10%).
- Fine material: (<600μm) White ash like material.

Organic remains:
Snail shell microfossil (<1mm). 1 – 5cm carbonized rootlets/twigs filled with carbonate sediments.
Illustration

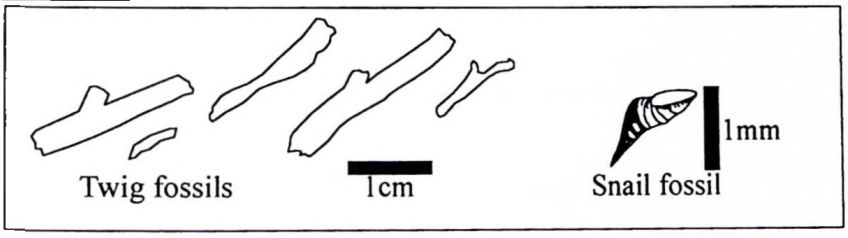

Pedofeatures:
Root channels and rootlets infilled by carbonate.

Sample RS 17 – GS31
Microstructure: Vertical channels (>1mm long) which are filled by carbonate materials.
Illustration

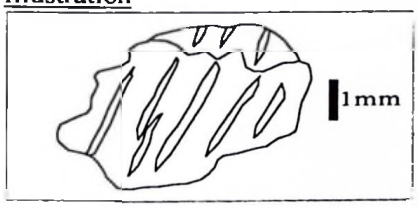

Groundmass:

- Basic components: (>600μm) not observed.
- Fine material: (<600μm), yellowish dark gray clay groundmass.

Organic residue: not observed
Pedofeatures: Channels infilled by Carbonate

Sample RS 19 – GS30
Microstructure: Massive clay.
Groundmass:

- Basic components: (>600μm), newly formed fibrous white minerals
- Fine material: (<600μm), olive gray clay.

Illustration

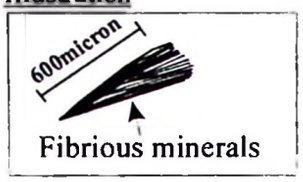

No organic remains nor pedofeatures observed at this scale.

Sample RS 29 – GS28
Microstructure: Well developed accomadating peds cross cut by recently formed cracking planes.
Groundmass:
- Basic components: (>600μm) quartz (40%), pyroxenes (20%), red garnet (<2%), other very rare minerals include beryl and tourmaline.
- Fine material: (<600μm), yellowish gray clay.

Fabric: C/f related 1/3. Silt-sand.
Organic residue; root casts observed.
Pedofeatures
Clay coated surfaces. 0.5mm animal trace routes occupying about 1% by volume. Rare (<1%) of red to dark brown mottled zones (Fe or Mn concretions?).

Sample RS 31 – GS27
Microstructure: Well developed peds.
Groundmass:
- Basic components: (>600μm) quartz (50%), pyroxenes (20%) other coloured minerals (<5%).
- Fine material: (<600μm), gray clay.

Fabric: C/f = 5/1
Neither obvious pedofeatures nor organic residues were observed.

Sample RS32 (Sandstone rock sample)

Sample RS 34
Microstructure: Homogeneous sands
Groundmass:
- Basic components: (>600μm) quartz (>90%).
- Fine material: (<600μm), yellowish clay (<2%).

Fabric: C/f 10/1
Organic Remains: Bivalve shell microfossil.
Pedofeatures: Animal bioturbations coated by black minerals.

Sample RS 35 – GS26
Microstructure: Well-developed sub-angular blocky structure filled by red crusts.
Groundmass:
- Basic components: (>600μm) quartz (40%), dark minerals (60%)
- Fine material: (<600μm), yellowish clay (<1%).

Fabric: C/f 10/1
Organic residues: Numerous root traces.
Pedofeatures
The root traces and animal routes (2%) are all filled (encrusted) by red material (FeOOH??)

Sample RS 36
Microstructure: Homogeneous sands
Groundmass:
- Basic components: (>600μm) quartz (>90%).
- Fine material: (<600μm), grayish broun clay (<1%).

Fabric: C/f 10/1

Organic residues: Only root traces observed.
Pedofeatures
The root traces and animal routes (2%) are all filled (encrusted) by red material (FeOOH??)

Sample RS 39 – GS24
Microstructure: Homogeneous sands, relic peds filled with calc-materials.
Groundmass:
- Basic components: (>600μm); feldspar (20%), quartz (>10%), black minerals <2%) and rock fragments (<2%).
- Fine material: (<600μm), greenish yellowish olive clay.

Fabric: C/f- related 1/5.
Organic residues: some root traces observed
Pedofeatures: Carbonate concretions.

LK Site
Sample LK2 (A rock sample composed of sandy tuff with qurtz and volcanic glass minerals all cemented by fine calcite crystals).

Sample LK3 – GS37 (A massive yellowish clay mass with few (<2%) quartz grains. No microstructure or pedofeatures observed at this scale).

Sample LK5 – GS35
Microstructure: Weakly developed sub-angular blocky structure with ped borders filled by carbonate material. Recently formed places cross-cut the relic ped and channel structures. There is a presence of intrapedal yellow mottles.
Illustration

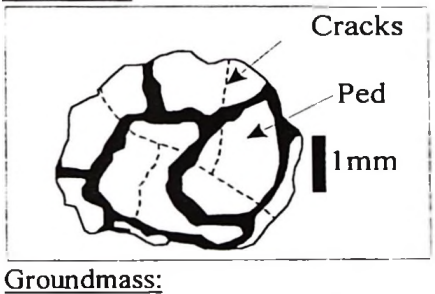

Groundmass:
- Basic components: (>600μm); quartz (<2%).
- Fine material: (<600μm), yellowish gray clay.

Fabric: C/f- related 1/10.
Organic residues: Not observed
Pedofeatures: Channels filled with carbonate materials.

Sample LK 7 – GS35
Microstructure: Vertical channels
Groundmass:
- Basic components: (>600μm); quartz (<2%), recently formed fibrous white minerals (5%) on exposed surfaces.
- Fine material: (<600μm), greenish yellowish olive clay.

Organic residues: Not observed
Pedofeatures:
1 – 3cm root casts filled by calcite and the vertical channels are all infilled by calcite.

Sample LK8 – GS34
Microstructure: Relic peds partly damaged by cracks developed during drying up of the sample. The relic peds have partly accomodative features.

Groundmass:
- Basic components: (>600μm); not observed.
- Fine material: (<600μm), brown to red clay.

Organic residues: Not observed
Pedofeatures: Clay coatings.

Sample LK9 – GS33
Microstructure: Massive clay with limited channels.
Groundmass:
- Basic components: (>600μm); not observed.
- Fine material: (<600μm), light brownish gray clay.

Organic residues: Not observed
Pedofeatures: Channels filled with white calcite. Black concretions (Fe?, Mn?) and rare root traces.

Sample LK10 – GS32
Microstructure: Well-developed channels filled with white carbonate material. Recent cracks present.
Illustration

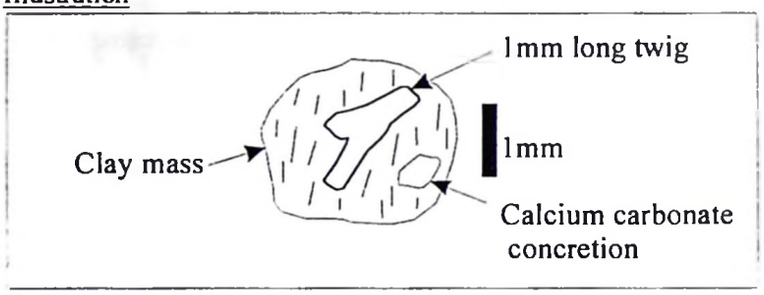

Groundmass:
- Basic components: (>600μm); not observed.
- Fine material: (<600μm), light brown gray clay.

Organic residues: Not observed
Pedofeatures: 1mm size root casts and animal tunnels infilled with carbonate.

ZINJ Site

Sample 4Z: (Massive grayish olive clay without peds and no organic remains).

Sample 3Z –GS43
Microstructure: Massive clay with weakly developed peds. Ped boundaries field with calcareous white materials.
Groundmass:
- Basic components: (>600μm); quartz (>2%), black minerals (volcanic glass and pyroxenes (<2%).
- Fine material: (<600μm), olive gray clay.

Fabric: C/f- related 1/10.
Organic residues: Not observed
Pedofeatures: Ped boundries filled by carbonate materials.

Sample 2Z – GS44
Microstructure: Cracked massive clay

Groundmass:
- Basic components: (>300μm); Coloured minerals (<1%).
- Fine material: (<300μm), yellowish clay.

Organic residues: Not observed
Pedofeatures: Very rare channels filled by carbonate materials.

Sample 1Z – GS45
Microstructure: Well-developed sub-angular blocky structure.
Groundmass:
- Basic components: (>600μm); black minerals (hornblende? and pyroxenes? - 10%).
- Fine material: (<600μm), yellowish clay.

Fabric: C/f- related 1/10.
Organic residues: Not observed
Pedofeatures: Carbonate concretions (<2%), and relic channels filled by red material.

Sample Z4 – GS54
Microstructure: Homogeneous white sediment
Groundmass:
- Basic components: (>600μm); very rare black minerals (volcanic glass and pyroxenes (<1%).
- Fine material: (<600μm), white crystalline calcite.

Organic residues: 1-3mm sized imprints of small branches completely replaced by calcite. Other large (2-5cm) plant imprints observed.
Illustration

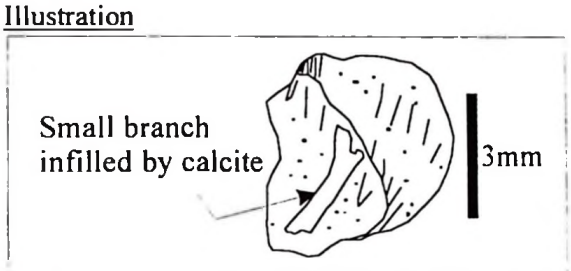

Pedofeatures: 1-3mm, calcite infills of root traces and twigs.

Sample Z9 – GS52
Microstructure: Homogeneous massive sediment
Groundmass:
- Basic components: (>600μm); feldspars (>20%), quartz (10%), black minerals (volcanic glass and pyroxenes (<2%) and rock fragments (2%).
- Fine material: (<600μm), greenish yellowish clay.

Organic residues: 1-3mm sized imprints of small branches completely replaced by calcite. Other large (2-5cm) plant imprints observed.
Pedofeatures: 1-3mm, calcite infills of root traces and twigs.

Sample Z7 – GS53
Microstructure: Massive and homogeneous.
Groundmass:
- Basic components: (>1.5mm); feldspars (>30%), quartz (30%), black minerals (volcanic glass and pyroxenes (<10%) others (10%). The grains are well rounded.
- Fine material: (<600μm), light brown to white calcite.

Fabric: c/f; 10/1 – monic distribution
Illustration

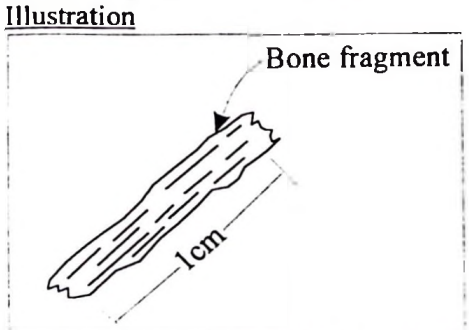

Organic residues: Burned bone pieces (1cm sized)

Pedofeatures: Grains are coated by calcite.

Sample Z11 – GS51
Microstructure: Massive homogeneous sediments
Groundmass:
- Basic components: (>300μm); feldspars (>20%), quartz (50%), black minerals (pyroxenes - 20%) others (30%).
- Fine material: (<300μm), white calcite (90%) and clay (10%).

Fabric: c/f; 1/5
Organic residues: Carbonized bone pieces.
Pedofeatures: 1-3cm animal bioturbation route ways with face walls coated by calcite or red brown crystalline material some filled completely. Calcite concretions (size 1mm diameter) are present.

Sample Z13 – GS50
Microstructure: Massive
Groundmass:
- Basic components: (>600μm); None
- Fine material: (<600μm), yellowish clay material (90%) and white material (gypsum? 10%).

Organic residues: 2-5cm bone remains.
Pedofeatures: Nodules of white material (gypsum?, bassanite?, zeolite? evaporite?) – Not reactive to 2N HCl.

Sample Z15 –GS49
Microstructure: Highly bioturbated clay, with few planes and channels. Weakly developed peds.
Groundmass:
- Basic components: (>600μm); feldspars (>20%), quartz (30%), black minerals (pyroxenes (5%) and rock fragments (<2%).
- Fine material: (<600μm), white calcite.

Fabric: c/f; 5/1
Organic residues: Very rare root traces and channels.
Pedofeatures: 1-3mm route ways with face walls coated by brown to black minerals (Fe-hydroxides?). Calcite concretions are present.

Sample Z17 – GS48
Microstructure: Well-developed sub-angular blocky structure. Partly accomodated peds.
Groundmass:
- Basic components: (>300μm); feldspars (>20%), quartz (20%), black minerals (pyroxenes (5%).
- Fine material: (<300μm), yellowish clay.

Fabric: c/f; 1/5
Organic residues: Microfossil bones (<1mm).
Pedofeatures: Ped boundaries filled by calcite.

Sample Z19 – GS47
Microstructure: Layered clay showing horizontal planes.
Groundmass:
- Basic components: (>600μm); feldspars (>10%), quartz (50%), mica (2%) and others (10%)
- Fine material: (<300μm), mixed yellowish clay (70%) and white calcite (30%).

Fabric: c/f; 1/5
Organic residues: Microfossils of bone remains.
Pedofeatures: Animal route ways and planes are coated by clay.

Sample ZJ
Microstructure: Massive.
Groundmass:
- Basic components: (>300μm); not observed.

- Fine material: (<300μm), Yellow clay (30%) and white calcite (70%).

Organic residues: Not observed.
Pedofeatures: (<1mm diameter) route ways filled with calcite and sometimed black minerals (Fe/Mn hydroxides?).

Sample ZI – GS56
Microstructure: Well-developed sub-angular blocky structure with partly accomodating peds.
Groundmass:
- Basic components: (>600μm); quartz (60%), pyroxenes (20%), garnet (1%), feldspar (<1%) and other minerals (<20%).
- Fine material: (<600μm), Yellowish green clay.

Organic residues: Not observed.
Pedofeatures: (<1mm diameter) carbonate concretions and some animal routeways filled by calcite.

Sample ZG
Microstructure: Well-developed accomdating blocky structure of peds? Or drying crack?.
Groundmass:
- Basic components: (>600μm); Coloured minerals (pyroxenes, volcanic glass etc – 20%), red garnet (1%) and quartz (<2%).
- Fine material: (<300μm), greenish yellow clay.

Fabric: c/f ratio; 1/5.
Organic remains: Not observed.
Pedofeatures: Carbonate concretions (about 1%).

Sample ZC
Microstructure: Weakly developed peds with numerous drying cracks.
Groundmass:
- Basic components: (>300μm); red to black grains (<1%).
- Fine material: (<300μm), Bright yellowish white (mixture of clay and calcite)

Organic residues: Not observed.
Pedofeatures: 1-2mm in diameter carbonate concretions (30%).

RB SITE

Sample RB5 – GS22
Microstructure: Channels and animal bioturbations.
Groundmass:
- Basic components: (>300μm); Very rare grains of quartz (<1%).
- Fine material: (<300μm), A mixture of yellow clay (30%) and white calcite (>60%).

Organic residues: Not observed.
Pedofeatures: 1-5mm, size animal route ways walls coated with white-reddish calcite/dolomite crystals.

Sample RB6B

Structure: >3cm thick layers (L1, L2 and L3) of red and brown sediments. Presence of (1cm diameter) cobbles.

Illustration

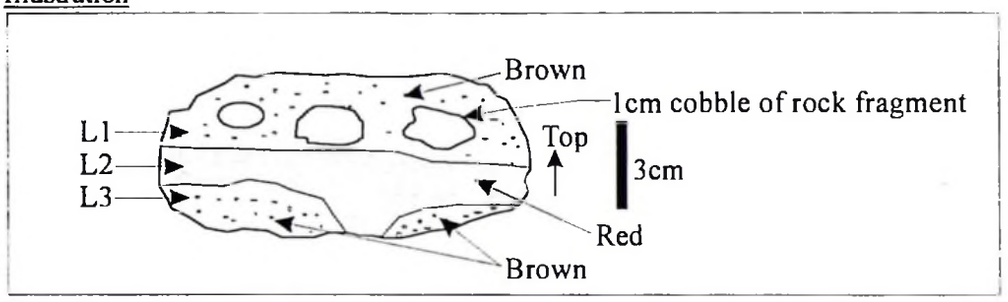

Groundmass:

- Basic components: (>300μm); quartz (20%) feldspars (2%) and pyroxenes (2%).
- Fine material: (<300μm), calcite crystals.

Organic residues: Not observed.

Pedofeatures: Animal bioturbation cavities filled by calcite crystals.

Sample RB21 – GS17 (as RB20)

Microstructure: Massive homogeneous with red and brown snake-like skin (oolitic appearance).

Groundmass:

- Basic components: (>300μm); Not observed.
- Fine material: (<300μm), A mixture of yellow clay and white calcite.

Organic residues: Not observed.

Pedofeatures: Mottling and animal bioturbation.

Sample RB14 – GS21

Microstructure: Very weakly developed peds.

Groundmass:

- Basic components: (>300μm); not observed.
- Fine material: (<300μm), A mixture of yellow clay and white calcite.

Organic residues: Not observed.

Pedofeatures: Animal bioturbation tunnels filled with calcite cystals.

Sample RB15 – GS20 (Same as RB21)

Sample RB18 – GS19

Microstructure: Relic well developed peds and planes filled by calcite.

Groundmass:

- Basic components: (>300μm); not observed.
- Fine material: (<300μm), yellow to red calcite and clay mixture.

Organic residues: Not observed.

Pedofeatures:

Some localized carbonate concretions. Animal activity route ways coated by calcite crystals and black minerals.

Sample RB20 – GS18

Microstructure: Gravely sand without peds but showing red spots. The red portions might be relic crumbs or granule ped structures.

Groundmass:

- Basic components: (>300μm); quartz (>70%).
- Fine material: (<300μm), A mixture of yellow clay and white calcite.

Fabric: c/f = 1/3

Illustration

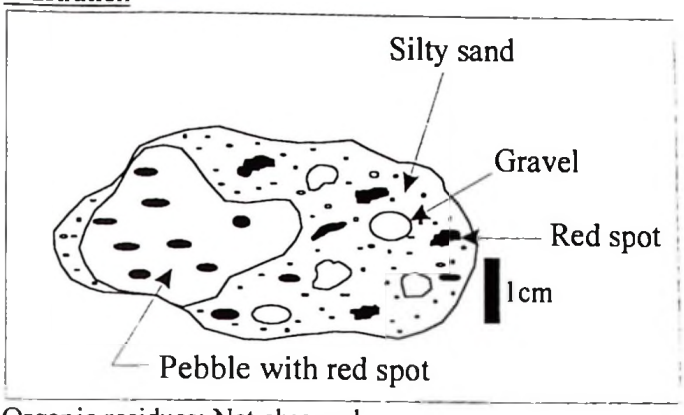

Organic residues: Not observed.
Pedofeatures: Few animal channels coated by Fe-Mn rich hydroxides. Red mottling.

Sample RB22 (Same as RB20)

MC SITE

Sample MC27 (Limestone/sandstone rock sample)

Sample MC20 – GS2
Microstructure: Reworked carbonate sediments showing cracks closely resembling peds.
Groundmass:
- Basic components: (>300μm); not observed.
- Fine material: (<300μm), white calcite.

Organic residues: Not observed.
Pedofeatures:
Not recognized

Sample MC19 – GS3
Microstructure: Weakly developed peds.
Groundmass:
- Basic components: (>300μm); very rare black rounded particles (<1%).
- Fine material: (<300μm), yellowish clay.

Organic residues: Not observed.
Pedofeatures:
Calcite concretion (1-2mm) and ped surfaces coated by black materials.

Sample MC17 – GS5 (as MC16)
Microstructure: Large (>5cm) columnar planes and peds
Illustration

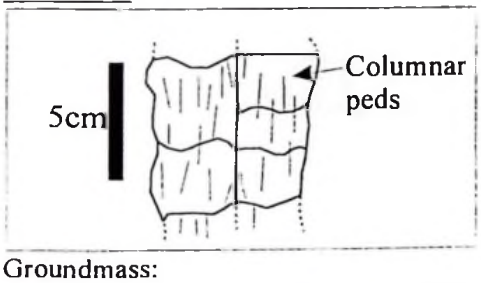

Groundmass:
- Basic components: (>300μm); Black rounded particles (<1%).
- Fine material: (<300μm), yellow fine clay.

Organic residues: Not observed.
Pedofeatures:
Planes and ped faces coated by clay. Clay slickenside structure present.
Calcite concretion observed.

Sample MC15 – GS7
Microstructure: Weakly developed peds.
Groundmass:
- Basic components: (>300μm); quartz (2%).
- Fine material: (<300μm), yellowish clay.

Organic residues: Not observed.
Pedofeatures:
Calcite concretionS (2%) and some dark brown nodules (Fe-nodules?).

Sample MC5
Microstructure: Weakly developed peds.
Groundmass:
- Basic components: (>300μm); quartz (>10%).
- Fine material: (<300μm), brown clay.

Organic residues: Root casts observed.
Pedofeatures:
Root cast encrusted by black materials, black-red nodules (Fe or Mn?)

Sample MC4 – GS13
Microstructure: Well developed peds with a sub-angular blocky structure
Illustration

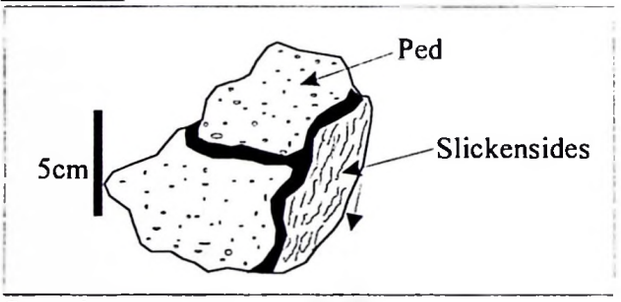

Groundmass:
- Basic components: (>300μm); quartz (2%) and black minerals-pyroxenes? (1%).
- Fine material: (<300μm), Brown clay with yellow patches.

Organic residues: Not observed.
Pedofeatures:
Calcite crystals coat some of the ped faces. Other large vertical ped boundaries are coated by brown clay, which show slickenside features.

Sample MC3 – GS14
Microstructure: Homogeneous gravely sands.
Groundmass:
- Basic components: (>300μm); quartz (2%), Rounded black minerals (15%) and rock particles with diameter 2mm (10%).
- Fine material: (<300μm), brown clay.

Fabric: c/f ratio 1/5
Organic residues: Not observed.
Pedofeatures:
Red patches – Fe-concretion? And organism activity routes coated by calcite.

Sample MC1 – GS16 and sample MC2 – GS15 (Same as MC3)

APPENDIX 7.7: MICROMORPHOLOGIC CHARACTERISTICS OF SOME PALAEOSOL LEVELS OF OLDUVAI GORGE STRATIGRAPHY.

1. OLDUVAI GORGE

BED I

Thin section No: ZI (GS56)

MICROSTRUCTURE
Well-developed partially accommodating (1 - 2mm size) peds and some channels (2%).

GROUNGMASS
Fabric:
C/F ratio at 10μm limit is 1/3 with porphyric c/f related distribution. There are zones which have a higher concentration of coarse materials (2/1 c/f ratio).

Basic component:
Coarse material (>10μm) consists of mainly angular to sub-angular feldspar grains (30%), pyroxenes (20%), basalt fragments (10%), quartz (5%) and volcanic rock fragments (2%). Other coarse materials are opaques (magnetites?, pyrite? or hematite? about 2%). Some green minerals (1%) which remain green in XPL probably tourmaline or zircon? Silt texture.

Fine material, (<10μm): Consists of yellowish gray mass (the gray colour indicate the absence of Fe-rich materials and organic matter. The material has a speckled limpidity and a crystallitic and granostriated b-fabric.

ORGANIC MATERIAL
Not observed

PEDOFEATURES
Pure calcite and micritic (fine-grained) nodules. Thin calcite coating around basalt fragments. There are also calcite hypocoating on channels and ped surfaces. Rare needle-like crystals (zeolite?) in pores.

Fe-Mn hydroxide nodules are very common.

SUGGESTED PALAEOENVIRONMENTS:
Calcite redistrution and shearing indicate a varied climate probably alternating between wet and dry.

Thin section No: Z4 (GS54) – Zinjatropus palaeosol

MICROSTRUCTURE
The section is more or less massive with rare (1%) voids consisting of 2mm sized chambers and channels.

GROUNGMASS
Fabric:
C/F distribution at 10μm limit is 1/2 with closed to open porphyric c/f related distribution.

Basic component:
Coarse material (>10μm) consists of mainly angular to sub-angular feldspar grains (30%), quartz (20%), pyroxenes (20%) and volcanic rock (basalt) fragments (20%), opaques (2%) and rutile (1%). Some of the basalt fragments are Fe-rich. Sand size.

Fine material, (<10μm): Colour: yellowish gray. The material has a speckled limpidity. The b-fabric consists of zones of mainly undifferentiated and rarely speckled and rarely granostriated.

ORGANIC MATERIAL
Not observed

PEDOFEATURES
Some rare voids are filled by organic or Fe-hydroxide? Fe-Mn/hydroxide? dendritic nodules

Calcite hypocoating on voids (vughs and chambers). Secondary fibrous (calcite/zeolite?) coating and loose continuous in-fillings in some channels. Some mineral grain boundaries are observed to undergo a calcification process (calcite attack).

SUGGESTED PALAEOENVIRONMENTS:
The palaepedogenic processes include weak hydromorphism and some newly weathered materials indicating some young soil forming processes. The iron hydroxides indicate a wet climate, which was followed by a dry (savanna?) climate. Palaeo-aridisol/alfisol,vertisol.

Thin section No: Z9 (GS53)

MICROSTRUCTURE
Moderately developed accommodating (3mm size) peds.

GROUNGMASS
Fabric:
C/F distribution at 10μm limit is 1/3 with porphyric c/f related distribution.
Basic component:
Coarse material (>10μm) consists of mainly angular to sub-angular feldspar mineral grains (20%), pyroxenes (5%) and rounded slightly transformed basalt fragments (10%), tuff pieces and pumice (10%). Others are opaque grains (about 10%). Medium sand texture.

Fine material, (<10μm): Consists of light brownish yellow clay groundmass. The material has a cloudy limpidity with a speckled to granostriated b-fabric.

ORGANIC MATERIAL
Imprint of small root pieces. Animal borrows filled by dark material. Microfossil with septaric cellular structures. Brown fragment (0.2mm) with round cellular structures.

PEDOFEATURES
Very thin calcite coating around mineral grains and rock fragments. Remnant (relic) animal workings (borrows) or microfossils filled with dark materials (opal? – silicification). Some of the volcanic rocks are altered (weathered) to calcite.

Dark portions being weathered (attacked) away (replaced by elongated mineral zeolite? crystals). Fe-Mn oxide nodules. Coatung and infillings of isotropic colourless substance sometimes pseudomorphs of often rock fragments

SUGGESTED PALAEOENVIRONMENTS:
Evidence of argilliturbation and crystalization of minerals suggests dry palaeoenvironments and climates. Palaeo-aridisol/alfisol?:

Thin section No: 3Z (GS43)

MICROSTRUCTURE
Moderately developed peds of 1mm – 5mm size. Some intrapedal channels present (<2%).

GROUNGMASS
Fabric:
C/F distribution at 10μm limit is 1/20 with open porphyric c/f related distribution.

Basic component:
Coarse material (>10μm) consists of angular quartz grains (2%), angular pyroxenes (1%) and opaques (1%). Very fine sand size.
Fine material, (<10μm): Consists of light brownish yellow material. Limpidity: Dotted. And b-fabric: Speckled to granostriated in some places.

ORGANIC MATERIAL
Silicified root piece?.

PEDOFEATURES
Very rare Fe-hydroxide nodules and abundant Fe-Mn oxide nodules? Crystalization or deposition of isotropic colourless minerals (analcime?) in pores

SUGGESTED PALAEOENVIRONMENTS:
Evidence of argilliturbation and crystalization of minerals suggests dry palaeoenvironments and climates. Palaeo-aridisol/alfisol?:

MIDDLE BED II

Thin section No: LK7 (GS35)

MICROSTRUCTURE
Moderately developed accommodating. Some places show microgranule ped structure. Voids include vurghs and channel (>40% porosity). Compound packing voids.

GROUNGMASS
Fabric:
C/F distribution at 10μm limit is 1/20 with very open porphyric c/f related distribution.
Basic component:
Coarse material (>10μm) consists of mainly rounded volcanic rock fragments (10%), angular pyroxene minerals (5%), angular quartz grains (5%), feldspars (2%) and muscovite (2%). Sand size.

Fine material, (<10μm): Consists of yellowish brown to reddish brown material. Limpidity: specked. And b-fabric: Speckled.

ORGANIC MATERIAL
No observed.

PEDOFEATURES
Typic Fe-oxyhydrate coating around old channels and rare dense continous Fe-hydroxide channel inffilings. Some feldspar grains are coated by Fe-oxyhydrates.

Very rare oriented reddish yellow clay coating in channels later filled by opel?. Secondary loose continuous fine and some coarse calcite in-fillings in channels. Some zeolite coatings or infillings in voids (seen with crystal faces).

Suggested palaeoenvironments:
Clay coating imprinted by Fe-hydroxide coating and later new channels formed that are being filled by calcite. Alteration processes followed by bioturbations may indicating moderately wet to wet alternating environments, which became drier. Alfisol/aridisol???.

Thin section No: LK10 (GS32)

MICROSTRUCTURE
Moderately developed peds of 0.5cm - 1cm size. Some places show microgranule ped structure. Voids include intergranular vurghs, channel and some planes (20% porosity).

GROUNGMASS
Fabric:
C/F distribution at 10μm limit is 1/5 with a open porphyric c/f related distribution.

Basic component:
Coarse material (>10μm) consists of mainly angular pyroxene mineral particles (30%), opaques (20%), angular quartz grains (20%), tourmaline and some volcanic rock fragments (5%). Sand size.
Fine material, (<10μm): Consists of yellowish brown material. Limpidity: specked. And b-fabric: Speckled with some granostriated zones.

ORGANIC MATERIAL
One plant (twig/root) fragment replaced (in-filled) by yellow clay. Root/stem cast filled by speckled massive clay. Other unidentified organic tissue remains. Globular microfossil activity (micro-animals??).

PEDOFEATURES
Rare Fe-oxyhydrate coating and in-filling on channels. Homogeneous oriented yellowish red clay coating on channels in spaces left by animal or plant remains. Calcite nodules (sand to 3mm sized) sometimes coated by a thin rim redish yellow clay. Reddish yellow clay coating and Fe-oxyhydrate coating juxtaposed on a void and the void filled by pure calcite. Some opal? infillings in voids. Fe-Mn oxide nodules and numerous Mn-Fe hydroxide coating on voids.

Suggested palaeoenvironments:
Clay hypocoating and animal/plant remains/activities are older events than calcite in-fillings and Fe-oxyhydrate coating in-fillings. Imprints of soils indicating moderately wet to wet alternating environments. The palaeopedogenic event of process show weathering with restricted clay illuviation, formation of calcite nodules and weak hydromorphism

UPPER BED II

Thin section No: RS17 (GS31)

MICROSTRUCTURE
Well-developed (3mm-5mm size) accommodating peds. Plane and channel microstructure.

GROUNGMASS
Fabric:
C/F distribution at 10μm limit is 1/100 with a very open porphyric c/f related distribution.
Basic component:
Coarse material (>10μm) consists of rare pyroxene mineral particles (<1%) and opaques (2%). Medium to fine sand size.

Fine material, (<10μm): Consists of Dark yellow to yellowish black material. Limpidity: Dotted/cloudy. Some garnostriated b-fabric.

ORGANIC MATERIAL
Rootlets/twigs?? remain filled with dark-gray material (silicified?).

PEDOFEATURES
Very rare (<2%) in-fillings and coating of Fe-hydroxide in some voids (channels). Common (zeolite?) loose continuous infillings or coatings voids. Some rare opel coating in voids.

Suggested palaeoenvironments:
Dry probably cold environment.

Thin section No: RS31 (GS28)

MICROSTRUCTURE
Granular microstructure, packing voids (20%) with channels and large (>1cm long) planar voids.

GROUNGMASS
Fabric:
C/F distribution at 10μm limit is 10/1 with enaulic to gefuric c/f related distribution.

Basic component:
Coarse material (>10μm) consists of mainly angular pyroxene mineral particles (>50%), opaques (30%) and some angular quartz grains (2%). And presence of isotropic grains (probaby opel). Coarse sand size.
Fine material, (<10μm): Consists of yellow material. Limpidity: Dotted. And b-fabric: Speckled.

ORGANIC MATERIAL
Not seen.

PEDOFEATURES
Very rare (one) Fe-oxyhydrate coating on channel. Some discontinuous loose channel and vughs in-fillings of elongated minerals (zeolites?).

Suggested palaeoenvironments:
Soil developed on sand. Probably developed in a dry environment.

Thin section No: RS32

MICROSTRUCTURE
No peds observed. Voids consist of very rare, 1-%) spaces left by ejected minerals. Massive microstructure.

GROUNGMASS
Fabric:
C/F distribution at 10μm limit is 10/1 with a close porphyric c/f related distribution.

Basic component:
Coarse material (>10μm) consists of mainly angular pyroxene mineral particles (>50%). Large crystals (50μm –100μm) of calcite with defuse boundaries with the matrix. Opaques (20%). Some angular quartz grains (2%) with sharp boundaries between grains and cement. Other mineral grains are; rounded feldspars (2%), amphibole (2%) and rutile (1%). Some (1%) volcanic rock fragments are also seen. Medium to fine sand size.

Fine material, (<10μm): Consists of cream to translucent crystalline calcite material.

ORGANIC MATERIAL
Not observed.

PEDOFEATURES
Not observed

Suggested palaeoenvironments:
This is calcareous sandstone (calc-arenite sandstone). The coarse nature of the calcite cementing material indicates that the sandstone was formed in a water rich environment.

Thin section No: RS39 (GS24)

MICROSTRUCTURE
Weakely developed accomodating peds. Voids are mainly intrapedal channels, about 10% porosity.

GROUNGMASS
Fabric:
C/F distribution at 10μm limit is 1/2 with a closed porphyric related distribution.

Basic component:
Coarse material (>10μm) consists of mainly angular feldspar mineral particles (>20%), Opaques (20%), some angular pyroxene grains (2%) and volcanic rock fragments (10%). Medium to fine sand size.
Fine material, (<10μm): Consists of brownish yellow material. Limpidity: specked. b-fabric: speckled.

ORGANIC MATERIAL
Not observed

PEDOFEATURES
Common newly crystallizing loose to dense discontinuous infillings of elongated fine (zeolite?) minerals. in ped faces and channels. Some very rare Fe-hydroxide hypocoating on channels. Numerous Fe-Mn oxyhydrate nodules and opel coatings and infillings in channels.

Suggested palaeoenvironments:
Very weak hydromorphism, abundant biological activity and mineral crystalization. This is probably a weakely developed palaeosol on a sandstone.

BED III

Thin section No: RB6B (GS22)

MICROSTRUCTURE
It is a heterogeneous material. Compacted granular to channel microstructure. The microstructure consists of irregular compound packing voids (40%). There are also rare (<2%) planes and channels.

GROUNGMASS
Fabric:
C/F distribution limit at 10μm and a 1/3 c/f ratio with porphyric c/f related distribution.

Basic component:
Coarse component (>10μm) consists of mainly angular feldspar grains (>20%) with opaques (magnetite? or pyrite?) of up to 10% and volcanic rock pieces (basalt? – 5%). Other mineral grains are pyroxenes, fresh quartz particles all about 6% in total volume. Silt to fine sand size.

Fine component, (<10μm): Dark brown to yellowish brown with a speckled limpidity and undifferentiated b-fabric.

ORGANIC MATERIAL
Not observed

PEDOFEATURES
Channels with typic, homogeneous oriented yellow and sometimes, red clay coatings and infillings. Some brownish-yellow to reddish-yellow strongly oriented distinct clay coatings appear as fragments or infilling remnants in the ground mass. There are also Fe-oxyhydrate coatings around channels and pores (50%). Depletion nodules – Fe-staining depletion and clay dominate (2%). Large (2mm – 5mm) channels with typic Fe-hydroxide coating. Some channels show secondary loose continuous fine calcite or infillings. Some well crystallized (zeolites?) minerals are seen inside channel coatings. Mn-Fe oxide nodules are common.

Suggested palaeoenvironments:
There is evidence of weathering and intense clay illuviation. Indicate wet palaeoclimates and environments during the Pleistocene. The secondary calcite in-fillings infer that the climate deteriorated during the later part of the Pleistocene

Thin section No: RB14 (GS21)

MICROSTRUCTURE
Well-developed blocky (1cm – 3cm) relic peds, with intrapedal channels.

GROUNGMASS
Fabric:
C/F distribution at 10μm limit is 1/5 with an open porphyric fabric.

Basic component:
Coarse component (>10μm) consists of mainly rounded to subrounded feldspar grains (>40%) and sub-angular to angular pyroxenes (<10%). Other mineral grains are; Sub-angular to angular quartz (2%), euhedral olivine (2%), biotite (2%), weathered basalt fragments (2%). There are also numerous opaque grains. Fine sand size.

Fine component, (<10μm): Consists of yellowish brown mass with dark patches. The material has a speckled limpidity and a crystallitic b-fabric with locally undifferentiated b-fabric.

ORGANIC MATERIAL
Not seen

PEDOFEATURES
Reddish yellow strongly oriented clay coatings and some in-fillings on channels. Remnants of fragmented yellow clay in-filled channels are common in the groundmass. The clay coating and in-filling fragments are floating in the calcite ground mass. Some of the reddish yellow oriented clay coated channels are infilled by calcite.

Typic pure calcite coatings and hypocoatings on channels. Dense continuous channel in-fillings of coarse (0.1mm – 0.2mm) grained calcite. Some voids with clay coatings are in-filled by coarse-grained calcite. Some calcite coatings around mineral grains are observed.

Typic coating of Fe-oxyhydrate/hydroxide on pores. (1-2mm) Fe-Mn hydroxide nodules/concretions (20%) cementing pyroxene and quartz grains. Basalt, gneiss, pyroxene and some feldspars are observed to be attacked by some black spots – this is probably a weathering effect where Fe-hydroxides replace Fe-rich minerals.

Suggested palaeoenvironments:
The clay and Fe-hydroxide coating indicate wet palaeoclimates and environments during the Pleistocene. The wet climate and environment was followed by a dry period, which introduced the calcite coating, in-

fillings and calcification in some places. A calcareous parent material wethered giving clay coatings and later again a calcification took place. The last phase of calcite formation show relatively coarse calcite grains.

Thin section No: RB21 (GS17)

MICROSTRUCTURE
Compacted granular to vughy microstructure consisting of irregular vughs (10%) with isolated channels.

GROUNGMASS
Fabric:
C/F distribution limit at 10μm and a 1/20 c/f ratio with very open porphyric c/f related distribution.

Basic component:
Coarse materials (>10μm) consists of mainly feldspars (20%), fresh volcanic rock fragments, [laths of feldspars are seen submarged in dark materials – basalt? – 5%]. Feldspar grains (<2%) are also seen.

Fine materials, (<10μm): Consists of yellowish to dark brown coloured mass with a a cloudy to speckled limpidity and a speckled b-fabric.

ORGANIC MATERIAL
One piece of root seen

PEDOFEATURES
Strongly oriented homogeneous yellow clay coatings (10%) in channels. Strongly oriented homogeneous red clay coatings in channels. Remnant (cracked) channels reddish yellow clay in-fillings can be seen. Some oriented yellow clay coating fragments in the groundmass.

Juxtaposed coating of Fe-oxyhydrate and red clay coating on channels. Round Fe-Mn (hydroxide?) nodules. Some rare Fe-oxyhydrate hypocoating on vughs. Some zeolite? Mineralisation in pores.

Suggested palaeoenvironments:
Indicate wet palaeoclimates and environments during the Pleistocene. Presence of Fe-oxyhydrate indicate that the palaeosol underwent significant hydromorphic processes.

Thin section No: MC6 (GS12)

MICROSTRUCTURE
Well-developed accommodating blocky (<0.01mm) peds, Voids consists of channels and transpedal planes with about 30% porosity and compound packing microstructure.

GROUNGMASS
Fabric:
C/F distribution at 10μm limit is 1/2 with an closed porphyric c/f related distribution.
Basic component:
Coarse component (>10μm) consists of mainly rounded to sub-rounded quartz grains (40%), feldspar grains (<20%) and sub-angular to angular pyroxenes (<10%). Other coarse components are fine-grained volcanic rock pieces (1%), zircon (<1%) and opaques (>2%).

Fine component, (<10μm): Consists of yellowish brown to brownish yellow mass. The material has a speckled limpidity and a speckled and weakly granostriated b-fabric.

ORGANIC MATERIAL
Not seen

PEDOFEATURES
Abundant typic coating and in-fillings of Mn-Fe-(hydr)oxide on pores. Fe-Mn nodules (0.1mm to 1mm size).

Very rare (<1%) oriented yellow to red clay coatings fragments in the groundmass. Weathered basalt fragments.

Some gray (remains dark in X-polars) opal? coatings in channels.

Suggested palaeoenvironments:
The clay and Fe-hydroxide coating with some illuviation and hydromorphism indicate wet palaeoclimates and environments during the Pleistocene. Vertisol?

BED IV/MASEK BEDS and NDUTU BEDS

Thin section No: MC16 (GS6)

MICROSTRUCTURE
Partially developed accommodating peds with compound packing voids and some channels.

GROUNGMASS
Fabric:
C/F distribution at 10μm limit is 1/3 with porphyric c/f related distribution.

Basic component:
Coarse component (>10μm) consists of mainly angular to sub-angular feldspar (with inclusive microcline) grains (40%), sub-angular to angular quartz (2%) and sub-angular to angular pyroxenes (<1%). Fine sand size.

Fine component, (<10μm): Consists of yellowish brown. The material has a speckled limpidity and a speckled and striated b-fabric.

ORGANIC MATERIAL
Not seen

PEDOFEATURES
Rare (2%) yellowish red homogeneous fragments of clay coatings are seen overprinted by the groundmass. Very thin homogeneous red clay coating around some particles. Some feldspar mineral grains have been altered into clay mass (kaolinization?).

Fe-Mn nodules (aggregates). Some rare Fe-hydroxide iron nodules.

Pure calcite nodules and impregnative (<5mm size) calcite nodules, this is rather a calcification zone of about 5mm diameter size. Some calcite nodules have their centers filled by coarse-grained crystals of pure calcite. Calcite, hypo-coating on ped boundaries.

Suggested palaeoenvironments:
Alternating dry and wet climate and environment as indicated by calcite coating and in-fillings, pure nodules and impregnative (calcification) in some places. The clay and Fe-hydroxide coatings and Fe-Mn nodules indicate short spells of wet palaeoclimates and environments during the Pleistocene. Vertisol?.

Thin section No: MC19 (GS3)

MICROSTRUCTURE
Well-developed (3mm size) angular blocky peds.

GROUNGMASS
Fabric:
C/F distribution at 10μm limit is 1/2 with porphyric c/f related distribution.

Basic component:
Coarse material (>10μm) consists of mainly angular to sub-angular quartz grains (40%), pyroxenes (10%) and some feldspars (2%). Basalt and tuff fragments (2%). Coarse to medium sand size.

Fine material, (<10μm): Consists of brownish yellow groundmass. The material has a speckled limpidity and a granostriated, concentric and some monostriated b-fabric.

ORGANIC MATERIAL
Not seen.

PEDOFEATURES
Fragments of oriented and homogeneous reddish yellow clay coatings and relict channel clay in-fillings in the groundmass. The clay shows strong interference colours..

Common Mn-Fe-oxide nodules and diffuse Fe nodules and some amorphous material (organic or Fe-hydroxide?) hypocoating around some pores.

Calcite coating on channels and planes. Numerous calcite nodules about 20%, some of which are geodetic.

Impregnative (<5mm size) calcite nodule, this is rather a calcification (micritic calcite) zone of about 5mm diameter size. Some calcite nodules have their centers filled by coarse-grained crystals of pure calcite. Calcite, hypo-coating on ped boundaries.

There is a congruent disolution of horneblende and weathering after vertric movements.

Suggested palaeoenvironments:
Palaeo-vertisol: Calcite nodules and coating are an evidence of a dry climate. The clay coating fragments and relict in-fillings indicate wet palaeoclimates and environments, which existed before the climate became dry. Hydromorphic conditions are infered by Fe-oxyhydrates and Fe-Mn nodules.

Thin section No: MC27

MICROSTRUCTURE
No pedality observed. Relic voids consisting of large (5cm – 10cm) sized channels and planes (10%).
(There are two layers in the thin section.)

GROUNGMASS
Fabric:
C/F distribution at 10μm limit is 10/1 with close porphyric c/f related distribution.

Basic component:
Coarse material (>10μm) consists of mainly of very rounded carbonate pieces (50%), the carbonate particles are sometimes leached away. Angular feldspars - plagioclase (10%). Opaques (2%) and Pyroxenes (1%). Rounded volcanic rock fragments (<1%). A tourmaline grain with internal ateration to calcite. Medium to fine sand size.

Fine material, (<10μm): Brownish gray colour fine calcite groundmass. The material has a speckled limpidity and a crystallitic b-fabric. A thin rim of calcite around some grains (granostriated??).

ORGANIC MATERIAL
Not seen

PEDOFEATURES
Strongly oriented homogeneous to micro-laminated yellow clay coating fragments (>10%) are seen in the calcite in-fillings, it seems that the calcite in-fillings were superimposed on the clay coating or in-fillings and fragmented the clay. Few reddish yellow microlaminated oriented clay coatingfragments can be seen.

There are two series of channels, the oldest containing calcite in-fillings with clay coating fragments floating in the calcite and the youngest series of channels which is observed cutting the old ones is in-filled with pure calcite materials. The third type of channels shows juxtaposed coatings of fine calcite, coarse calcite and clay. The clay coatings filling the center of the channel.

Depletion (calcite) and carbonate nodules are common (10%). The carbonate nodules are sometimes surrounded by brown material

Some feldspar pieces have been transformed into clay mass (kaolinization?) and others show calcite alteration rims.

Suggested palaeoenvironments:
Aulloctonous carbonate (limestone) materials were first deposited (probably a lake environment dominated) and pedogenesis began. Palaeo-pedogenic features indicating an alternating wet – dry climates. Clay coatings indicate a wet environment, which was followed by a dry environment (calcite coating and infillings). This is a complex pedogenic and sedimentation history where a calcareous crust is deposited and a clayey soil on top, then illuviation of clay in the crust takes place followed by calcite precipitation.

APPENDIX 8:

MAGNETIC SUSCEPTEBILITY MEASUREMENT RESULTS FROM OLDUVAI GORGE COMPOSITE SECTION

APPENDIX 8: MAGNETIC SUSCEPTEBILITY MEASUREMENTS FROM OLDUVAI GORGE COMPOSITE SECTION

No.	Sample	Wgt-tot (gms)	Wgt (gms)	χ (tot) x 10^{-5}	χ (m^3kg^{-1}x 10^{-5})	χ (m^3kg^{-1}x 10^{-7})	Depth (m)
1	mc27	nd	nd	nd	nd	nd	1.25
2	mc26	5.8	2.18	656.7	0.301238532	30.12385321	1.35
3	mc25	5.78	2.16	1396	0.646296296	64.62962963	1.75
4	mc24	7.01	3.39	1825	0.538348083	53.83480826	2.1
4	mc23	5.68	2.06	816	0.396116505	39.61165049	2.25
5	mc22	6.52	2.9	472.6	0.162965517	16.29655172	2.5
6	mc21	6.33	2.71	559.4	0.206420664	20.64206642	2.75
7	mc20	5.58	1.96	243.4	0.124183673	12.41836735	3.3
8	mc19	5.37	1.75	252.4	0.144228571	14.42285714	3.75
9	mc18	5.64	2.02	209.7	0.103811881	10.38118812	4.3
10	mc17	5.73	2.11	252.9	0.11985782	11.98578199	5.75
11	mc16	6.08	2.46	430.1	0.174837398	17.48373984	6.35
12	mc15	8.33	4.71	500.1	0.106178344	10.61783439	6.725
13	mc14	6.55	2.93	2715	0.92662116	92.66211604	7.25
14	mc13a	5.91	2.29	216.6	0.094585153	9.458515284	7.5
15	mc13b	6.54	2.92	492.8	0.168767123	16.87671233	7.65
16	mc12	7.26	3.64	573.4	0.157527473	15.75274725	7.85
17	mc11a	4.54	0.92	81.42	0.0885	8.85	8.25
19	mc11b	nd	nd	nd	nd	nd	8.40
18	mc10	7.2	3.58	673.4	0.188100559	18.81005587	8.85
19	mc9	5.57	1.95	419.3	0.215025641	21.5025641	9.15
20	mc8	4.86	1.24	115.2	0.092903226	9.290322581	9.45
21	mc7	4.65	1.03	392.6	0.381165049	38.11650485	9.9
22	mc6	4.96	1.34	285.2	0.212835821	21.28358209	10.2
23	mc5	4.82	1.2	263.3	0.219416667	21.94166667	10.45
24	mc4	5.89	2.27	588	0.259030837	25.9030837	10.75
25	mcHB	6.06	2.44	930.8	0.38147541	100.14754098	11
26	mc3	5.8	2.18	1770	0.811926606	81.19266055	11.35
27	mc2	5.47	1.85	653.3	0.353135135	35.31351351	11.65
28	mc1	5.35	1.73	930	0.537572254	53.75722543	11.85
29	rb24	nd	nd	nd	nd	nd	11.90
30	rb23	nd	nd	nd	nd	nd	11.95
31	rb22	6.36	2.74	1017	0.371167883	37.11678832	12
32	rb21	6.25	2.63	1359	0.516730038	51.6730038	12.75
33	rb20	6.02	2.4	1182	0.4925	49.25	13
34	rb19	6.51	2.89	1183	0.409342561	40.93425606	13.65
33	rb18	8.59	4.97	3039	0.611468813	61.14688129	14.05
34	rb17	5.92	2.3	1461	0.635217391	63.52173913	14.65
35	rb16	4.96	1.34	625	0.46641791	46.64179104	15.15
36	rb15	5.88	2.26	1367	0.604867257	60.48672566	15.65
37	rb14	6.43	2.81	1457	0.518505338	51.85053381	15.9
38	rb13	5.03	1.41	1204	0.853900709	85.39007092	16.25
39	rb12	5.19	1.57	946.9	0.603121019	60.31210191	16.5
40	rb11	6.94	3.32	1461	0.440060241	44.0060241	16.75

41	rb10	6.35	2.73	1354	0.495970696	49.5970696	17.15
42	rb9	6.02	2.4	498.4	0.207666667	20.76666667	17.5
43	rb8	6.54	2.92	1422	0.486986301	48.69863014	17.75
44	rb7	7.19	3.57	2361	0.661344538	66.13445378	18.15
45	rb6b	6.23	2.61	1068	0.409195402	40.91954023	18.45
46	rb6a	6.24	2.62	1128	0.430534351	43.05343511	18.65
47	rb5	6.39	2.77	1242	0.448375451	44.83754513	19.05
48	rb4	5.57	1.95	676.6	0.346974359	34.6974359	19.35
49	rb3	6.7	3.08	194.1	0.063019481	6.301948052	19.75
50	rb2	6.68	3.06	5854	1.913071895	191.3071895	20.1
51	rb1	7.03	3.41	623.8	0.182932551	18.29325513	20.6
52	rs39	5.54	1.92	1629	0.8484375	84.84375	21.5
53	rs38	5.59	1.97	1487	0.754822335	75.4822335	21.85
54	rs37	5.48	1.86	861.9	0.463387097	46.33870968	22.05
55	rs36	6.15	2.53	1489	0.588537549	58.85375494	22.3
56	rs35	5.53	1.91	1400	0.732984293	73.29842932	22.65
57	rs34	5.55	1.93	2440	1.264248705	126.4248705	23
58	rs33	8.5	4.88	2795	0.572745902	57.27459016	23.2
59	rs32	6.59	2.97	3738	1.258585859	125.8585859	23.3
60	rs31	5.51	1.89	3205	1.695767196	169.5767196	23.5
61	rs30	7.58	3.96	1063	0.268434343	26.84343434	23.65
62	rs29	5.32	1.7	2262	1.330588235	133.0588235	23.7
63	rs28	7.47	3.85	8604	2.234805195	223.4805195	23.85
64	rs27	7.79	4.17	10110	2.424460432	242.4460432	24
65	rs26	6.05	2.43	3294	1.355555556	135.5555556	24.1
66	rs25	6.74	3.12	947.5	0.303685897	30.36858974	24.35
67	rs24	5.09	1.47	1244	0.846258503	84.62585034	24.4
68	rs23	6.3	2.68	6562	2.448507463	244.8507463	24.75
69	rs22	5.56	1.94	1578	0.813402062	81.34020619	25.3
70	rs21	5.41	1.79	145.4	0.08122905	8.122905028	25.75
71	rs20	4.64	1.02	50.59	0.049598039	4.959803922	26.1
72	rs19	4.55	0.93	151.5	0.162903226	16.29032258	26.3
73	rs18	4.9	1.28	183.4	0.14328125	14.328125	26.65
74	lk10	7.02	3.4	1711	0.503235294	50.32352941	27.15
75	lk9	7.48	3.86	689.9	0.17873057	17.87305699	29.35
76	lk8	9.29	5.67	931.7	0.164320988	16.43209877	29.85
77	lk7	7.57	3.95	1234	0.312405063	31.24050633	30.45
78	lk6b	8.23	4.61	1533	0.332537961	33.2537961	30.85
79	lk6a	8.99	5.37	1497	0.27877095	27.87709497	31.05
80	lk5	8.41	4.79	1355	0.282881002	28.28810021	31.45
81	lk4	6.86	3.24	413.1	0.1275	12.75	31.75
82	lk3	7.08	3.46	177.3	0.051242775	5.124277457	32.15
83	lk2	6.08	2.46	811.7	0.32995935	32.99593496	32.85
84	rs17	4.59	0.97	823.6	0.849072165	84.90721649	32.85
85	rs16	4.73	1.11	258.1	0.232522523	23.25225225	33.25
86	rs15	4.83	1.21	344.9	0.285041322	28.50413223	33.5
87	rs14	5.06	1.44	370	0.256944444	25.69444444	33.7
88	rs13	5.45	1.83	54.95	0.030027322	3.00273224	33.8
89	rs12	4.36	0.74	46.1	0.062297297	6.22972973	33.95
90	rs11	5.67	2.05	95.79	0.046726829	4.672682927	34.05
91	rs10	4.44	0.82	32.86	0.040073171	4.007317073	34.2

92	rs9	5.02	1.4	47.9	0.034214286	3.421428571	34.3
93	rs8	4.43	0.81	42.6	0.052592593	5.259259259	34.45
94	rs7	5.96	2.34	151.3	0.06465812	6.465811966	34.6
95	rs6	4.5	0.88	33.74	0.038340909	3.834090909	34.85
96	rs5	4.24	0.62	28.27	0.045596774	4.559677419	35.1
97	rs4	6.03	2.41	40.8	0.016929461	1.692946058	35.3
98	rs3	5.24	1.62	23.62	0.014580247	1.458024691	35.45
99	rs2	6.66	3.04	39.69	0.013055921	1.305592105	35.6
100	rs1	6.06	2.44	26.34	0.010795082	1.079508197	35.85
101	z25	4.96	1.34	214.5	0.160074627	16.00746269	35.85
102	z24	4.84	1.22	149.8	0.122786885	12.27868852	36.45
103	3z	4.74	1.12	63.71	0.056883929	5.688392857	37.1
104	2z	4.46	0.84	85.53	0.101821429	10.18214286	37.9
105	zl	4.61	0.99	61.47	0.062090909	6.209090909	38.4
106	1z	5.52	1.9	229.9	0.121	12.1	38.6
107	zk	4.8	1.18	176.7	0.149745763	14.97457627	39.3
108	z23	6.54	2.92	950	0.325342466	32.53424658	39.9
109	z22	4.68	1.06	56.42	0.053226415	5.322641509	40.05
110	z21c	4.89	1.27	106.9	0.084173228	8.417322835	40.1
111	z21b	4.37	0.75	20.12	0.026826667	2.682666667	40.15
112	z21a	4.65	1.03	59.15	0.057427184	5.742718447	40.2
113	z21	5.05	1.43	49.72	0.034769231	3.476923077	40.25
114	z20	4.74	1.12	68.5	0.061160714	6.116071429	40.3
115	z19	4.71	1.09	80.63	0.073972477	7.397247706	40.45
116	z18	4.57	0.95	48.46	0.051010526	5.101052632	40.5
117	z17	4.41	0.79	42.15	0.05335443	5.335443038	40.65
118	z16	5.01	1.39	79.2	0.056978417	5.697841727	40.75
119	z15	4.84	1.22	113.8	0.093278689	9.327868852	40.9
120	z14	5.41	1.79	232.4	0.129832402	12.98324022	41.05
121	z13	5.29	1.67	137	0.082035928	8.203592814	41.15
122	z12	5.09	1.47	136.4	0.092789116	9.278911565	41.3
123	z11	5.24	1.62	258.2	0.159382716	15.9382716	41.5
124	z10	5.08	1.46	152	0.104109589	10.4109589	41.8
125	z9	4.77	1.15	162.2	0.141043478	14.10434783	42
126	z8	5.8	2.18	613.1	0.281238532	28.12385321	42.2
127	z7	4.98	1.36	202	0.148529412	14.85294118	42.45
128	z6	4.83	1.21	145.5	0.120247934	12.02479339	42.65
129	z5	5.43	1.81	261	0.144198895	14.4198895	42.75
130	z4	5.22	1.6	189.3	0.1183125	11.83125	42.85
131	z3	5.88	2.26	431.9	0.191106195	19.11061947	43.05
132	z2	4.87	1.25	417.1	0.33368	33.368	43.3
133	z1	5.24	1.62	223.4	0.137901235	13.79012346	43.65
134	zj	4.67	1.05	35.8	0.034095238	3.40952381	44.1
135	zi	5.61	1.99	1814	0.911557789	91.15577889	44.9
136	zh	4.57	0.95	100.8	0.106105263	10.61052632	45.1
137	zg	4.24	0.62	311.4	0.502258065	50.22580645	45.2
138	zf	9.48	5.86	133.1	0.022713311	2.271331058	45.4
139	ze	4.76	1.14	263.9	0.231491228	23.14912281	45.55
140	zd	5.73	2.11	144.9	0.068672986	6.867298578	45.7
141	zb	5.16	1.54	110.5	0.071753247	7.175324675	46
142	za	6.46	2.84	219.5	0.077288732	7.728873239	46.25

APPENDIX 9

SAMPLE DESCRIPTIONS, MINERALOGICAL ANALYSES, MAGNETIC SUSCEPTIBILITY MEASUREMENT RESULTS, STEREO MICROSCOPIC AND MICROMORPHOLOGICAL DESCRIPTIONS.

APPENDIX 9.1: MANONGA-WEMBERE VALLEY SECTION - SAMPLE DESCRIPTIONS, MAGNETIC SUSCEPTIBILITY MEASUREMENTS RESULTS, MINEROLOGICAL ANALYSES AND MICROMORPHOLOGICAL DESCRIPTIONS

APPENDIX 9.2: HOLILI GRITSTONE SECTION - PALEOSOL SAMPLE DESCRIPTIONS, STEREO MICROSCOPIC EXAMINATIONS AND MICROMORPHOLOGICAL DESCRIPTIONS.

APPENDIX 9.1: MANONGA WEMBERE (KININGINILA SECTION): SAMPLE DESCRIPTIONS, MAGNETIC SUSCEPTIBILITY MEASUREMENTS, MINEROLOGICAL ANALYSES AND MICROMORPHOLOGICAL DESCRIPTIONS.

A: FIELD DESCRIPTIONS

Sample No.	Thickness (cm)	Colour name /code	Description	Remarks
Mano6	100	Olive (5Y4/4)	Compact dense mudstone showing animal traces and biotarbation.	Mudstone
Mano3b	40	Reddish brown (5YR4/4)	Mottled clay	Paleosol
Mano3a	40	Upper – White (10YR8/2) Lower – Light red (2.5YR6/6)	Boundary between white clay and red paleosol.	Paleosol/clay boundary
Mano2	60	Red (2.5R5/6)	Massive mottled clay	Paleosol
Mano1	220	Reddish brown (2.5R5/4)	layered clay	Clay
Mano5	60	White (2.5Y8/2	Compact homogeneous silt clay sediments	Siltstone
Mano4	110	Reddish brown (2.5YR6/4)	Clay with carbonate concretions	Paleosol

B: MAGNETIC SUSCEPTIBILITY MEASUREMENTS

no	sample	Wgt-tot(g)	Wgt(g)	χ-tot	χ (m^3kg^{-1}) x 10^{-7}	χ (m3/kg) x 10^{-8}	Depth(m)
1	mano6	9.786	6.166	0.00119	1.92994	19.2994	1.5
2	mano3b	9.41	5.79	0.002107	3.63903	36.3903	3.5
3	mano3a	8.98	5.36	0.001011	1.88619	18.8619	3.9
4	mano2	9.18	5.56	0.9277	1,6685.3	16,685.30	5.3
5	mano1	9.55	5.93	0.001165	1.96459	19.6459	7.2
6	mano5	6.88	3.26	0.4002	1,2276.1	12,276.10	9.5
7	mano9	9.01	5.39	0.00109	2.02226	20.2226	11
8	mano4	9.22	5.6	0.8143	1,4541.1	14,541.10	13.8
9	mano8	8.88	5.26	0.00123	2.3384	23.384	15
10	mano7	12.43	8.81	0.00341	3.8706	38.706	16.4

C: INFRARED REFLECTANCE SPECTRA (PROFILES)

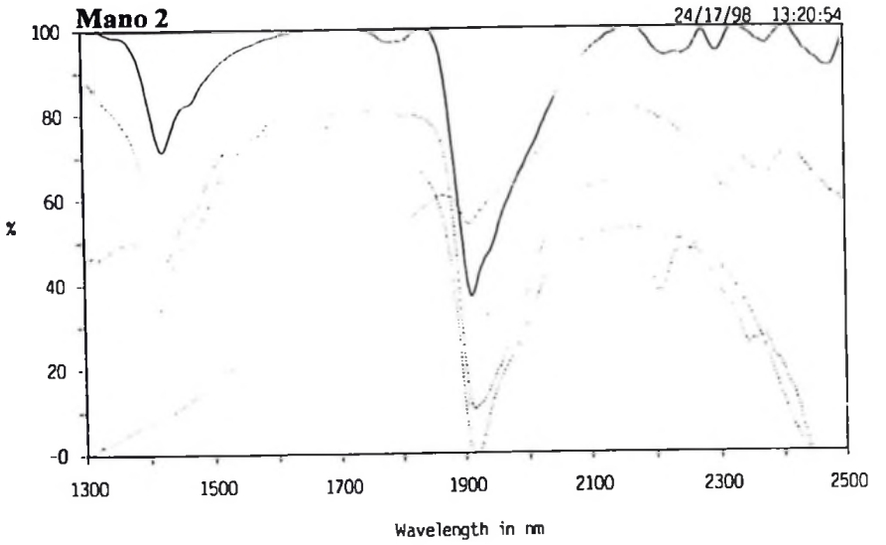

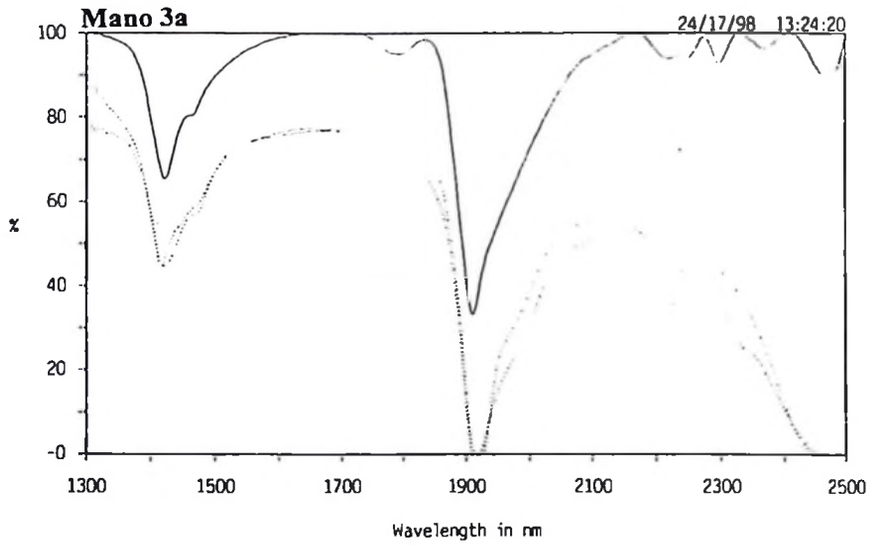

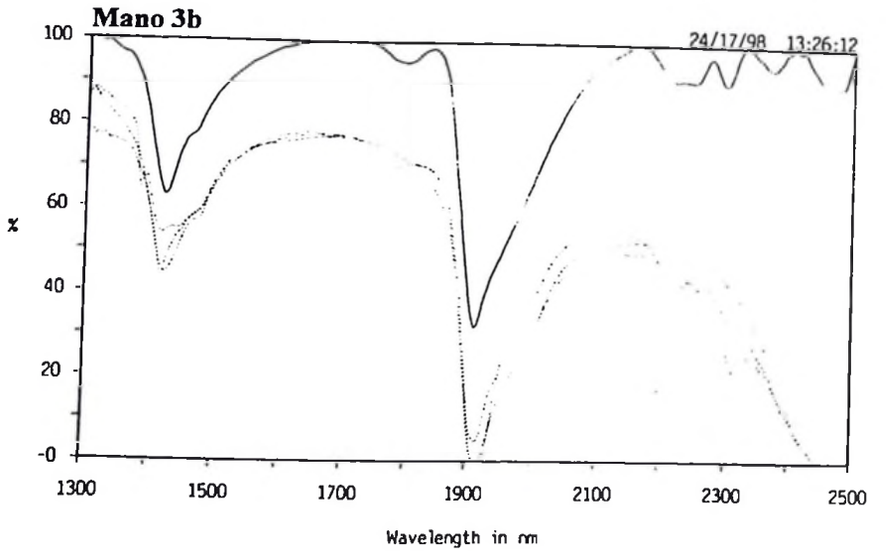

D: INFRARED SPECTROMETRY MEASUREMENTS

No	Sample	Carbonate IR(%)intensity	Clay minerals IR(%)intensity	Depth(m)	Plaeosol level	Minerals
1	mano6	17.32	15.31	1.5		
2	mano3b	15.98	8.65	3.5	GS1	Palygorskite, sepiolite, analcime, stilbite.
3	mano3a	20.65	11.31	3.9	GS1	Illite, Kaolinite, Halloysite gibbsite.
4	mano2	15.1	5.2	5.3	GS2 &GS3	Palygorskite, stilbite, Analcime
5	mano1	29.9	20.04	7.2		
6	mano5	25.98	17.32	9.5		
7	mano9	No data	No data	11		
8	mano4	33.97	21.98	13.8	GS4	Kaolinite, halloysite Stilbite, gibbsite
9	mano8	No data	No data	15		
10	mano7	No data	No data	16.4		

E: PALAEOSOL FIELD DESCRIPTIONS

Palaeosol	Depth/thickness (m)	Lithology	Description
GS0	0 – 0.55	Calcareous sediments	Present soil with present root activity
GS1	4.5 – 7	Clay	Light red (2.5YR6/6) showing red mottling.
GS2	8 – 8.5	Massive clay	Red (2.5YR5/6) showing gray mottling
GS3	8.5 – 9	Layered clay	Reddish brown (2.5R5/4) with gray mottling
GS4	18.4 – 19.6	Clay	Reddish brown (2.5YR6/4) with carbonate concretions.

F: STEREO MICROSCOPIC EXAMINATION OF PALAEOSOL HAND SPECIMENS.

Sample Manol

Microstructure: Layered clay

Groundmass:

- Basic components: (>600μm); quartz (5%) and localized transparent elongated minerals found in cavities (10%).
- Fine material: (<600μm), brown to red clay.
- Organic residues: Not observed.

Pedofeatures: Numerous animal activities about 30% porosity. Cavity faces coated by clay and partly by long neddlelike crystals.

Sample Mano3b – GS1

Microstructure: Layered clay.

Groundmass:

- Basic components: (>600μm); indistinguishable.
- Fine material: (<600μm), yellowish brown clay mixed with calcite.

Organic residues: Not observed.

Pedofeatures: Cavities created by animal activity about 30% porosity. Cavity faces coated by clay and partly by long neddlelike crystals.

Sample Mano3a – GS1
Microstructure: The boundary between clay and red palaeosol seems massive with some animal activity.
Groundmass:
- Basic components: (>300μm); Not observed.
- Fine material: (<300μm), Red brown clay.

Organic residues: Not observed.
Pedofeatures: Animal borrows by calcite and elongated minerals.

Sample Mano2 – GS2 and GS3
Microstructure: Massive and indurated clay sediments.
Groundmass:
- Basic components: (>300μm); no particles observed.
- Fine material: (<300μm), Red clay.

Organic residues: Not observed.
Pedofeatures: Cavities coated by yellowish clay

Sample Mano4 – GS4
Microstructure: Massive and indurated red clay.
Groundmass:
- Basic components: (>300μm); no particles observed.
- Fine material: (<300μm), Red clay.

Organic residues: Not observed.
Pedofeatures: Not observed.

G. MICROMORPHOLOGIC CHARACTERISTICS

Thin section No: Mano4 (GS4)
Microstructure
Relict granules and crumbs. Channels (40%) and some planes.
Groundmass..
Fabric:
C/F distribution limit at 10μm: No coarse material observed.
Basic component:
Coarse component (>10μm): No coarse materials observed.
Fine component, (<10μm): Consists of brown mass. Limpidity: cloudy.
organic material
Not observed.
Pedofeatures
Mn-Fe oxide nodules. Oriented laminated red (sometimes yellow) clay-coating fragments in the groundmass. Typic orieted homogeneous yellow clay coatings on channels sometimes juxtaposed with Fe-oxyhydrate hypocoating. Some zeolite? Mineral coating in pores.

Suggested palaeoenvironments:
The material is an accummulation of fragments of clay coatings probably rounded by short transport. It looks like a soil sediment of weathering clay developed on limestone.Wet palaeoclimates and environments (warm humid –Mediterranen type) during the Pliocene. (Clay illuviation dominate).

Thin section No: Mano2 (GS2)
Microstructure
Moderately developed sub-angular peds, (granule to crumbs??). The microstructure consists complex packing microstructure with channels and planes (30%).
Groungmass
Fabric:

C/F distribution limit at 10μm: Very rare coarse materials about 1/100 c/f ratio with a very-very open porphyric c/f related distribution.

Basic component:

Coarse component (>10μm): Very rare quartz grains (<1%).

Fine component, (<10μm): Consists of yellowish brown mass. The yellow zones are mainly clay illuviation (infills and coatings) with pockets (1mm size) of yellow fragmented clay. Limpidity: cloudy. And b-fabric: Undifferentiated (thicker parts) and speckled in thinner parts of the section.

Organic material

Not observed.

Pedofeatures

Reddish yellow strongly oriented homogeneous clay coatings in channels. Red strongly oriented homogeneous oriented clay coating and rare in-fillings in channels. Large (1–3mm) relic rounded sometimes elongated, pores (channels?) filled with fragmented oriented clay. There are also clay-coating fragments in the brownish yellow groundmass (seen in the thinner parts of the section). Empty channels (10%). Channels with typic Fe-Mn hydr(o)xide coatings (2%).

Suggested palaeoenvironments:

The material is also an accummulation of fragments of clay coatings probably rounded by short transport. In this case the clay coating fragments are coarser. It looks like soil sediment of weathering clay developed on limestone. Wet palaeoclimates and environments during the Lower Pleistocene as indicated by clay illuviation (clay coating fragments). Fe-Mn oxyhydrate coating indicate an aquic moisture regime (hydromorphism) during that time.

Thin section No: Mano3a (GS1)

Microstructure

A heterogeneous mass (rather an accummulation of laminated brownish red clay coating fragments) of brownish red clay with a channels microstructure. There are two sets of channels; empty channels and channels in-filled by dispersed light yellow clay.

Groundmass

Fabric:

C/F distribution limit at 10μm: No coarse material observed.

Basic component:

Coarse component (>10μm): No coarse material.

Fine component, (<10μm): Consists of two layered zones; Zone 1. Yellowish brown to red dominated by fragmented oriented clay fragments in a groundmass of amorphous clay hydrated Fe-hydroxides and Fe gels. Zone 2. Brownish yellow zone, which is mainly, dispersed clay masses. Limpidity: cloudy. And b-fabric: cloudy.

Organic material:

Not observed.

Pedofeatures

Channels with typic dark red to black Fe-Mn hydroxide hypocoatings around channels. Some channels in zone 1 are in-filled by materials of zone 2 (dispersed yellow clay material) groundmass. Large oriented microlaminated yellowish red clay coating fragments in zone 1 forming large part of the groundmass. Typic homogeneous red channel clay coatings in zone 2 (coatings probably derived from zone 1). Yellow Clay coating fragments in the groundmass of zone 2.

Suggested palaeoenvironments:

An insitu clay weathering. Warm humid (Mediterranean type) palaeoclimates and environments during the Lower Pleistocene as indicated by extensive clay illuviation (clay coating fragments) and Fe-hydroxide coating. A presence of a substancial hydromorphic regime.

APPENDIX 9.2: HOLILI SECTION: PALEOSOL SAMPLE DESCRIPTIONS, STEREO MICROSCOPIC EXAMINATIONS AND MICROMORPHOLOGICAL DESCRIPTIONS.

A: FIELD DESCRIPTION

Sample No.	Thickness (cm)	Colour name/code	Description	Remarks
96k4	300	Red (10R5/6)	Dense red paleosol intensively penetrated by root casts, channels and root lets	Red paleosol (Oxisol/Latosol)

B: STEREO MICROSCOPIC EXAMINATION

Sample 96K4 – Red palaeosol of Holili
Microstructure: Well developed sub-angular blocky structure
Groundmass:
- Basic components: (>600μm); indistinguishable.
- Fine material: (<600μm), red clay.

Organic residues: (1mm – 1cm) rootlets, root traces and twigs.
Pedofeatures: Rootlets and twigs encrusted by red material (Fe-hydroxides?).

C. MICROMORPHOLOGICAL CHARACTERISTICS

Thin section No: 96K4 –Holili palaeosol level.
Microstructure
Strongly developed granular microagregates. Some relict channels (20%) and rare planes.
Groungmass
Fabric:
C/F distribution limit at 10μm: c/f ratio is about 1/100 very open porphyric c/f related distribution.
Basic component:
Coarse component (>10μm): Rare altered and sometimes completely leached away pyroxene grains (<1%). Angular feldspar grains (<2%). Silt sized.
Fine component, (<10μm): Consists of yellowish to brownish red mass (clay and Fe-oxyhydrates). Limpidity: speckled. And b-fabric: undifferentiated.
Organic material
Not observed.
Pedofeatures
Channel and planes (relict pores) with Fe-oxyhydate coatings. Numerous impregnative Fe-Mn- oxide nodules (50%). Fragments of reddish yellow clay hypocoating (2%). There is an increasing Red to Dark red (Fe-hydroxides?) colour from one side of the section to the other. Pseudomorphs of mineral grains transformed into clay mass.

Suggested palaeoenvironments:
This is a strongly weathered material indicating wet (humid – warm) palaeoclimates and environments.

Thin section No: 96K2
Microstructure
No peds.
Groungmass
Fabric:
C/F distribution limit at 10μm: c/f ratio is about 3/1 closed porphyric c/f related distribution.

Basic component:

Coarse component (>10μm): 0.5mm-2mm pieces of volcanic tuff (>50%). Other coarse components are feldspars (20%), quartz (10%) and olivine crystals (2%). These particles are cemented by crystalline calcite.

Fine component, (<10μm): Translucent calcite mass. The calcite fills voids around mineral grains and rock fragments.

Organic material

Not observed.

Pedofeatures

Not observed

Suggested palaeoenvironments:

A volcanic calcareous gritstone deposited during a wet period (rain) where carbonate recystallised to form the cement. It known elsewhere that carbonate materials from carbonatite volcanic eruptions recystallises instantatly after eruption if the eruption takes place during a wet climate. This might have been the case of Holili eruption.